

H 24/3528

MONASH UNIVERSITY
THESIS ACCEPTED IN SATISFACTION OF THE
REQUIREMENTS FOR THE DEGREE OF
DOCTOR OF PHILOSOPHY

ON..... 4 April 2003

.....
✓ Sec. Research Graduate School Committee

Under the copyright Act 1968, this thesis must be used only under the normal conditions of scholarly fair dealing for the purposes of research, criticism or review. In particular no results or conclusions should be extracted from it, nor should it be copied or closely paraphrased in whole or in part without the written consent of the author. Proper written acknowledgement should be made for any assistance obtained from this thesis.

THE STRATIGRAPHY AND EVOLUTION OF
THE LATE CENOZOIC,
INTRA-PLATE WERRIBEE PLAINS
BASALTIC LAVA FLOW-FIELD,
NEWER VOLCANIC PROVINCE,
VICTORIA, AUSTRALIA

Alison Hare



Submitted for the Degree of Doctor of Philosophy

School of Geosciences

Monash University

September 2002

TABLE OF CONTENTS

ABSTRACT	VIII
STATEMENT	XI
ACKNOWLEDGEMENTS	XII
CHAPTER 1: INTRODUCTION	15
1.1 AIMS OF THE STUDY	15
1.2 PROJECT BACKGROUND	18
1.2.1 Geological Setting	18
<i>The Newer Volcanic Province</i>	<i>18</i>
<i>The Werribee Plains</i>	<i>19</i>
1.2.2 Intra-plate volcanism in eastern Australia	19
1.2.3 Geology of the Newer Volcanic Province	23
1.2.4 Basaltic lava flow fields	25
1.3 PREVIOUS WORK AND SIGNIFICANCE OF THIS STUDY	26
1.4 METHODS	28
1.5 THESIS OUTLINE	29
REFERENCES	30
CHAPTER 2: CHARACTERISING THE INTERIORS OF PAHOEHOE AND AA LAVAS: AN INVESTIGATION OF EMPLACEMENT AND CRYSTALLISATION PROCESSES	37
2.1 INTRODUCTION	37
2.2 METHODS	40
2.3 RESULTS	43
2.3.1 Identifying flow unit boundaries	43
2.3.2 Vesicle zonations	45
<i>Pahoehoe</i>	<i>45</i>
<i>Aa</i>	<i>50</i>
2.3.3 Petrographic textural variations through flow units	54
<i>Pahoehoe</i>	<i>56</i>

Aa	61
2.3.4 Geochemical variations through basalt flows	64
2.4 DISCUSSION	68
2.4.1 Vesicles and segregation veins	68
2.4.2 Petrographic textures	72
2.4.3 Geochemical variations	76
2.5 CONCLUSIONS	78
REFERENCES	79

CHAPTER 3: THE ROCK MAGNETISM AND PALAEOMAGNETISM OF THE BASALTS OF THE LATE CENOZOIC, INTRA-PLATE WERRIBEE PLAINS LAVA FLOW-FIELD, NEWER VOLCANIC PROVINCE, VICTORIA

3.1 INTRODUCTION	85
3.1.1 Background theory	85
<i>The Geomagnetic Field</i>	85
<i>Ferromagnetism of fine particles: single domain vs. multi-domain grains</i>	86
<i>Demagnetisation techniques</i>	89
3.2 METHODS	90
3.3 RESULTS	94
3.3.1 Thermal demagnetisation	94
3.3.2 AF demagnetisation	95
3.3.3 Rock magnetic studies	95
3.4 DISCUSSION	100
<i>Identifying palaeomagnetically unstable samples</i>	100
<i>Variations in inclination values through discrete flows</i>	103
3.5 CONCLUSIONS	104
REFERENCES	104

CHAPTER 4: THE STRATIGRAPHY, FACIES ARCHITECTURE AND ERUPTION FREQUENCY IN THE LATE CENOZOIC, INTRA-PLATE BASALTIC WERRIBEE PLAINS, NEWER VOLCANIC PROVINCE, VICTORIA

4.1 INTRODUCTION	107
------------------------	-----

4.2 METHODS	109
4.3 PHYSIOGRAPHY OF THE WERRIBEE PLAINS	110
4.4 AIRBORNE GEOPHYSICAL DATA	113
4.5 GEOPHYSICAL WELL LOG INTERPRETATION	116
4.6 VOLCANIC FACIES	118
4.6.1 Identifying flow unit and eruption package boundaries	118
4.6.2 Pahoehoe flow units	119
<i>Inflated (P-type) pahoehoe lobes</i>	119
<i>Spongy (S-type) pahoehoe lobes</i>	120
4.6.3 Pondered lavas	121
4.6.4 Aa	121
4.6.5 Transitional lavas	122
4.6.6 Scoria	122
4.7 INTER-FLOW SEDIMENTARY FACIES	124
4.8 NATURE OF THE BASAL BASALT CONTACT	126
4.9 DISTRIBUTION OF VOLCANIC AND SEDIMENTARY FACIES	127
4.10 GEOCHEMISTRY: IDENTIFYING GEOCHEMICALLY DISTINCT MAGMA BATCHES	135
4.11 PALAEOMAGNETIC RESULTS	139
4.11.1 Magnetostratigraphy	139
4.11.2 Secular variation	141
4.12 AGE CONSTRAINTS	142
4.13 PALAEO TOPOGRAPHY	143
4.14 STRATIGRAPHY	145
4.14.1 Producing a stratigraphic map of the surface of the Werribee Plains	145
4.14.2 Sub-surface stratigraphy: correlating eruption packages between drill holes	147
4.15 DISCUSSION	151
4.15.1 Palaeogeography	151
4.15.2 Change in geochemistry through sequence	153
4.15.3 Eruption frequency	153
4.16 CONCLUSIONS	154
REFERENCES	155

CHAPTER 5: THE PALAEOVOLCANOLOGY AND EVOLUTION OF THE LATE CENOZOIC, INTRA-PLATE BASALTIC WERRIBEE PLAINS, NEWER VOLCANIC PROVINCE, VICTORIA	161
5.1 INTRODUCTION	161
5.2 ERUPTION PROCESSES	161
5.2.1 Features of the eruption centres, and their distribution in the Werribee Plains	161
5.2.2 Eruption styles and durations	169
<i>Hawaiian fire-fountaining</i>	170
<i>Strombolian explosive eruptions</i>	173
5.3 EVOLUTION OF THE WERRIBEE PLAINS	174
5.3.1 Pre-existing palaeotopography and substrate geology	174
5.3.2 Commencement of volcanism	174
5.3.3 Eruption styles and resultant products	175
5.3.4 Lava types and factors controlling these	175
5.3.5 Lava dimensions	177
5.3.6 Controls on vent distribution, and is there evidence of migration of volcanism within the Werribee Plains?	178
5.3.7 Geochemistry and compositional trends through time	179
5.3.8 Eruption frequency and the likelihood of further volcanic activity in the Werribee Plains	179
5.3.9 Sedimentation: provenance, distribution and influences	180
5.4 THE WERRIBEE PLAINS: REPRESENTATIVE OF VOLCANISM IN THE NEWER VOLCANIC PROVINCE?	180
5.4.1 Eruption centres: types and dimensions	181
5.4.2 Volcanic facies and thickness of basaltic succession	182
5.4.3 Eruption frequency	183
5.5 PLAINS-BASALT VOLCANISM EXPLORED	183
5.5.1 Flood-basalt provinces	183
5.5.2 Monogenetic volcanic fields	184
<i>General features of plains-basalt lava fields</i>	186
5.5.3 Tectonic settings and stress regimes in intra-plate continental basaltic provinces	187
REFERENCES	189

CHAPTER 6: CONCLUSIONS AND DISCUSSION	195
6.1 MAJOR CONCLUSIONS OF THE STUDY	195
6.1.1 The interiors of pahoehoe and aa lava flows (Chapter 2)	195
6.1.2 The facies architecture and magnetostratigraphy of the Cenozoic, Werribee Plains basaltic lava flow-field (Chapters 3 & 4)	196
6.1.3 The palaeovolcanology and evolution of the Cenozoic, Werribee Plains basaltic lava flow-field (Chapter 5)	198
6.2 IMPLICATIONS OF THE STUDY AND FURTHER WORK	201
6.2.1 The interiors of pahoehoe and aa lava flows: emplacement and crystallisation processes of basaltic lava flows	201
6.2.2 The Newer Volcanic Province	203
6.2.3 Other basaltic provinces	204
6.2.4 Economic implications	206
REFERENCES	207
APPENDICES	211
A- X-RAY FLUORESCENCE (XRF) SAMPLE PREPARATION AND ANALYTICAL PROCEDURES	211
B- PETROGRAPHIC TEXTURAL MEASUREMENTS	214
C- XRF RESULTS: INTRA-FLOW GEOCHEMICAL VARIATIONS	223
D- PALAEOMAGNETIC INCLINATION RESULTS	226
E- ROCK MAGNETIC RESULTS	248
F- MAGNETIC SUSCEPTIBILITY (K) MEASUREMENTS	249
G- KÖNIGSBERGER RATIO (Q) CALCULATIONS AND IDENTIFICATION OF SPM-SD THRESHOLD GRAINS	256
H- GEOPHYSICAL WELL LOG INTERPRETATIONS	259
I- GEOCHEMICAL DATA FROM THE WERRIBEE PLAINS	273
J- PETROGRAPHIC RESULTS	281
K- SURFACE MAGNETIC POLARITY DATA	282
L- LIST OF PUBLICATIONS	282

ABSTRACT

The Late Cenozoic Newer Volcanic Province (NVP) is an intra-plate plains-basalt province. It is located in south-eastern Australia and covers an area greater than 15,000 km². It is dominated by broad, flat lava plains, which have been produced by a number of small monogenetic volcanoes (predominantly lava shields and scoria cones). Outcrop is scarce in the NVP due to the flat-lying nature of the lavas, extensive vegetation cover and limited erosional incision. For this reason, few stratigraphic and basic volcanic geological studies have been attempted. However, in the Werribee Plains, at the eastern end of the NVP, a network of drill holes provides an opportunity to establish a facies and time-stratigraphic architecture for at least part of the NVP. In this study the sub-surface basaltic sequence was explored, through the analysis of diamond drill core and geophysical wells from the Werribee Plains. A magnetostratigraphy was established, and the volcanic evolution of the Werribee Plains explored.

The interiors of the two end-member types of basaltic lava flows (pahoehoe and aa) were better characterised using data collected from the NVP and from Hawaii. Inflated P-type pahoehoe lobes were consistently observed to contain vesicular upper and lower margins surrounding a dense core, which commonly contains segregation material. Plagioclase grain-sizes consistently increase from the margins towards the centre of the pahoehoe lobes. These features are considered to reflect the endogenous growth mechanism of these lobes, which cool by conduction upon stagnation. In contrast, aa lavas were found to have vesicles dispersed throughout the flows, demonstrate uniform plagioclase grain-sizes, and have higher crystal number densities than the pahoehoe lavas. Autobrecciation of aa lavas involves a physical mixing process in which clasts and cooler material are entrained into the core of the flow. Based upon the results of this study, it appears that upon stagnation of an aa lava flow the majority of the flow has already crystallised. The interior of an aa lava is therefore unlikely to cool significantly more slowly than the margins (cf. pahoehoe flows). All of the basaltic lavas analysed were compositionally homogeneous through vertical compositional profiles, apart from local geochemical anomalies. The small geochemical anomalies have been attributed to locally variable phenocryst contents, and/or differences in the cooling histories of adjacent samples. Further work is required to better characterise the significance of these anomalies in terms of emplacement and crystallisation processes of the different lava types.

Volcanism in the Werribee Plains began during late stages of a eustatic regression at around 3.8 Ma. Eruptions commenced with the formation of eruptive fissures. Commonly,

there is evidence of a change in eruption style at the volcanic centres from explosive Strombolian, to Hawaiian fire-fountaining, to passive effusion of lava. The orientations of the eruptive fissure systems appear to be controlled to some extent by the orientation of pre-existing basement structures. Eruptions producing the lava shields lasted about 6 months on average, whereas scoria cone eruptions probably lasted days to weeks. Inflated pahoehoe lavas were the dominant volcanic facies produced in the Werribee Plains. Other lava facies identified include ponded lavas, S-type pahoehoe, transitional lavas, and a thick, distal aa lava facies. Both scoria cones and lava shields fed significant lava flows, and in each instance the flows are the same composition as the eruption centre they were produced at. There is no evidence of a systematic change in composition of the lavas with time. Similarly, there is no evidence of a broad shift in magma generation within the Werribee Plains over time. The products of twenty-seven eruptions were identified in the magnetostratigraphy within a restricted area of the plains (constrained by diamond drill hole distribution). In five out of nine of the drill holes analysed, a simple reverse polarity, normal, reverse stratigraphy is evident. Based upon available age constraints, these magnetic intervals occurred within the Gauss and Matuyama Chrons. Eruptions are inferred to have occurred on average approximately every 66,000 years, from the commencement of volcanism in this area (at around 3.2 Ma) until the most recent eruption (1.41 Ma). Despite relatively long repose periods between eruptions, there are relatively few inter-flow sediments preserved in the sequence. These are mostly from the Palaeozoic highlands. Minimal physical erosion of the lavas occurred, probably due to the shallow gradient of the Werribee Plains and the onset of arid climatic conditions in the late Tertiary period. Based upon the calculated eruption frequency (~66,000 years) and the amount of time that has passed since the most recent eruption (1.41 Ma), it is unlikely that the Werribee Plains will experience any further volcanic activity.

The relative proportion of different lava facies produced in plains-basalt provinces, and the dimensions of the lava flows are considered to reflect both the characteristically flat substrates of these continental provinces and the volumes of magma produced in an eruption. Plains-basalt lava flows are typically thinner than lavas produced in continental flood-basalt provinces, but thicker than those associated with large central volcanoes (eg. Hawaii and Mt. Etna). Pahoehoe lavas are the dominant lava facies produced in plains-basalt provinces, and aa lavas constitute only a small proportion of the total products. Significant differences exist between plains-basalt lava fields in terms of the type and size of eruption centres, the total volume of products, and the frequency of eruptions. These differences are considered to be related to the different tectonic settings of the provinces, and the resultant magmatic processes operating.

There is a time for everything,
and a season for every activity under heaven...

Ecclesiastes 3:1

STATEMENT

This thesis contains no material which has been accepted for the award of any other degree or diploma in any university or other institution, and to the best of my knowledge contains no material previously published or written by another person, except where due reference is made in the text.



13/9/02

Alison Hare

ACKNOWLEDGEMENTS

Firstly, I would like to acknowledge the help of my Supervisor, Ray Cas. He has been supportive of me throughout my PhD, and I am grateful for the guidance he has provided. Thanks also to the rest of the MONVOLC (Monash Volcanology) group, who have provided helpful feedback for me. In particular, I am grateful to Steve for the proofreading he did for me. Thanks to a number of people for helping me with my computer queries: Matt Purss for giving me a crash-course on the use of ER Mapper, Draga for teaching me about PageMaker, and Mary Jane who is always willing to help. Barbara Wagstaff from the Geography Department at Monash assisted me by analysing a sample to check its pollen content.

Thanks to Bob Musgrave for sharing his Palaeomag expertise and facilities with me. His help was invaluable, and I also appreciated his enthusiasm and his love of the work. Chris Gray provided a lot of geochemical and geochronological data and helped me to interpret it. I am grateful for the time and effort he put in to this project. He also gave advice about whether or not to pursue K-Ar dating of my samples, which again was a great help.

Thanks to Malcolm Wallace for letting us know about the geophysical well (and drill core) data in the first place. It opened up the way for me to study the lavas of the NVP, which had really been on my heart from the beginning. Malcolm helped with initial interpretations of the data, and gave computer software advice etc. Thanks to Wiltshire Geological Services who were generous enough to donate the digital geophysical well log data to us. Bernie Joyce shared his expertise and love of the NVP with me, particularly in regard to the application of airborne geophysical data, and I have appreciated it. Thanks to David Phillips for his help with the Ar dating. He and Asaf went out of their way to assist with the sample preparation, which was much appreciated.

A number of people from DNRE provided me with logistical support, particularly in accompanying me regularly to the core store. Thanks to Dee, Avi, and David. Thanks also to Allan Willocks for supplying me with the airborne geophysical data I needed.

I greatly appreciated the support and assistance of Jim Kauahikaua and the staff at the Hawaiian Volcano Observatory while I was in Hawaii. They were very generous in providing me with

accommodation, logistical support etc. Jim made sure I was able to visit the active lava field a number of times in my short stay, and took me on a helicopter flight. I learnt a lot and had a great time- thank you.

Closer to home, thanks to a number of companies who allowed me to visit their basalt quarries. The Boral staff were particularly helpful. They allowed me to work on the faces of the Deer Park Quarry, and also provided me with diamond drill core from the vicinity. Thanks also to CSR and Aerolite for providing me with access to the Werribee and Anakies quarries, respectively. Many landowners in the Werribee Plains were also generous in allowing me unlimited access to their properties, which was greatly appreciated.

Thanks to Caro, Em and Marty for their friendships and support throughout my PhD. I am thankful for the proofreading they did, along with Tim and Ben. I've missed having them around at uni in the last little while, but at the same time I've enjoyed getting to know David, Beccy, Katie and others better- sharing driving and having lunch together.

Mum and Dad were a lot more involved with this PhD in the first couple of years, before I got married, and I am grateful for their love and support. Finally, thanks to Ben for continually encouraging me to trust Jesus in everything. I've appreciated his prayers throughout my PhD, and I know that the Lord has answered them and been gracious to me, teaching me things that I could learn in no other way.

CORRECTIONS

- pp.viii Paragraph 2, 3rd line. Add "(pipe vesicle-bearing)" after "P-type".
- pp. ix Paragraph 1, 4th line. Change sentence "Eruptions producing ... to weeks." to "Based on calculations of the emplacement times of the lava flows, eruptions producing the lava shields lasted about 6 months on average. Scoria cone eruptions probably lasted days to weeks."
- pp.ix Paragraph 1, 5th bottom line. Remove "These are mostly from the Palaeozoic highlands."
- pp. ix Paragraph 2, 3rd line. Change "produced in an eruption" to "generated".
- pp.16 Fig. 1.1 Add to caption "Refer to Fig. 1.3b for locality map."
- pp.25 Paragraph 3, 4th line. Insert "are considered to" before "occur".
- pp.37 3rd bottom line. Change "and propagate by autobrecciation of the flow front" to "and autobrecciation occurs during emplacement".
- pp.40 Table 2.1 Change third column title to "Depth to tops of NVP flows (m)".
- pp.44 Fig. 2.4a Add "The lobe contains a thin NVZ, beneath which are pipe vesicles." after "...UVZ."
- pp.45 5th line. Change "channels" to "flows".
- pp.46 Table 2.2 Typos: remove space between apostrophe and "s" for HVZ's, VS's and VC's. Column 1: 2nd and 3rd bottom line in 1st section; column 2: 6th line and 2nd bottom line in 1st section.
- pp.46 Paragraph 2, 1st line. Add "(Table 2.2)" after "segregation structures".
- pp.54 Paragraph 2, 5th line. Add "otherwise mostly-" before "aa".
- pp.57 Paragraph 2, 5th line. Delete "other" before "groundmass minerals".
- pp.73 Paragraph 2, 7th bottom line. Change "It is important to note...the interiors of the flows." to "Although lava flows lose heat by radiation to the atmosphere (compared with dykes for example), pahoehoe flows also cool by conduction (eg. Hon *et al.* 1994), without physical mixing or convection. In this study, the average groundmass plagioclase size is larger in the interiors of the pahoehoe flows than the margins as expected, reflecting lower cooling rates in the interiors of the flows."
- pp.75 4th bottom line. Typo. Remove "n" from directly after "interval".
- pp.79 7th line. Add "margins of the" before "lava".
- pp.107 Paragraph 2, 3rd bottom line. Change "constructional volcanic features" to "preserved vent structures".
- pp.121 Paragraph 1, 4th line. Change the final sentences in the paragraph to "This facies is most commonly produced when the local topography is too steep for inflation to occur. Non-inflating, low aspect ratio spongy lobes are instead formed, and result in a general flattening out of the previously steep local topography."
- pp.121 Paragraph 2, 1st and 2nd lines. Delete "(analogous to lava lakes)" and "Helz 1987".
- pp.139 Paragraph 2, 4th line. Add "largely" before "unmodified".
- pp.141 Change final sentence of the page to "Secular variation is recorded here by a significant change in the average inclination of adjacent eruption packages. It is a helpful feature when correlating eruption packages from different drill holes that have been erupted in the same magnetostratigraphic interval (section 4.14.2, Fig. 4.16)."
- pp.157 Delete 5th reference: "Helz, R.T., 1987...."
- pp.166 Paragraph 2, 4th line. Add to beginning of sentence "With little outcrop and".
-

pp.169 Paragraph 2, 2nd bottom line. Add "Both eruption styles commonly occur in a given eruption. For example," before "At constant magma rise speeds..."

pp.170 Paragraph 1, 1st line. Change sentence to "This is one way of accounting for the common occurrence of spatter around the rims of scoria cone craters (Wood 1980), and the production of lava flows by both scoria cones and low shields."

pp.171 Paragraph 2, 5th bottom line. Change "errors...duration" to "variations of more than 25% in the estimated emplacement durations".

pp.171 Paragraph 2, 2nd bottom line. Change final sentence to "Variations of ~25% are also predicted when calculating the eruption durations of volcanoes in this study."

pp.177 Paragraph 2, 5th-9th bottom lines. Change "Indeed,...reaching there." to "Aa lavas were probably produced in the steeper terrain to the north of the field area, as the two southernmost drill holes have no record of aa flows. It seems likely that the lavas would have thickened upon reaching the flatter plains, thus producing exceptionally thick flows."

pp.184 Paragraph 1, 3rd line. Add "generally" before "considered".

pp.196 Paragraph 1, 2nd line. Add "partially" before "attributed".

pp.196 Paragraph 1, 6th bottom line. Change the second last sentence of the paragraph to "Once the lava begins to propagate by autobrecciation a physical mixing process occurs, involving entrainment of clasts and cooler material into the core of the flow."

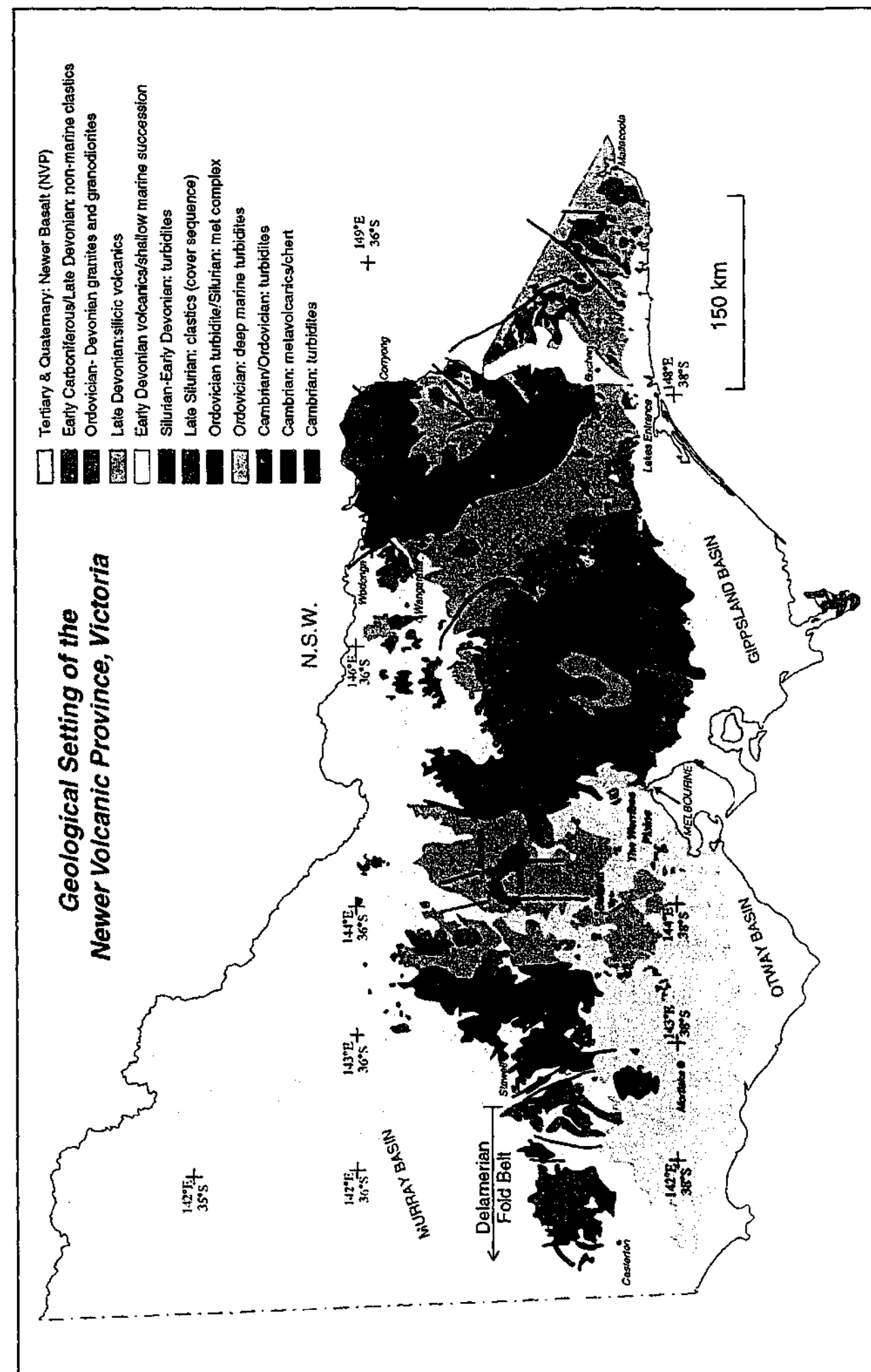
CHAPTER 1

INTRODUCTION

1.1 AIMS OF THE STUDY

The Newer Volcanic Province (NVP) is an intra-plate, continental plains-basalt province situated in south-eastern Australia (Fig. 1.1). It is one of only two volcanic provinces in Australia that is presently classified as active, and yet little is known about it. The NVP has an east-west trend extending west from Melbourne 330 km into South Australia, and covering an area of over 15,000 km² (Joyce 1975). The products range in age from 4.6 Ma-4.5 ka, and the volcanism is considered to be a continuation of the volcanic activity associated with rifting and the break-up of the super-continent Gondwana (Lister & Etheridge 1989, Price *et al.* 1997; section 1.2.2). Nearly 400 eruption points have been identified within the province, however it is dominated by flat basaltic lava plains, which are locally over 100 m thick (Joyce 1975). Much of the lava has been subjected to prolonged periods of weathering, vegetation is extensive, and erosional incision is limited. Due to the general lack of outcrop little is known about the basic volcanic geology of NVP, including volumes of eruptions, the types and distribution of products, and the frequency of eruptions. Few attempts have been made to put the radiometric dating of widely separated samples in the NVP (McDougall *et al.* 1966, Aziz-Ur-Rahman & McDougall 1972, Price *et al.* 1997) into a stratigraphic context (eg. Mitchell 1990, Price *et al.* 1997). A number of diamond drill holes and geophysical wells that penetrate the entire basaltic sequence are situated in the Werribee Plains, in the east of the NVP (Fig. 1.1). These provide a unique opportunity to explore the sub-surface geology of the NVP. In continental flood-basalt provinces, magnetostratigraphic studies have involved successfully correlating lava flows over hundreds of kilometres. Few stratigraphic studies have been completed in plains-basalt provinces, and indeed little is known about plains-basalt volcanism in general - a style of volcanism intermediate between continental flood-basalt volcanism and ocean island volcanism (section 1.2.4).

Much is known about the emplacement mechanisms and resultant surface morphologies of basaltic lavas, based upon observations of active lava flows in places such as Hawaii and Mt. Etna (eg. Peterson & Swanson 1974, Peterson & Tilling 1980, Guest *et al.* 1987, Lipman & Banks 1987, Kilburn & Lopes 1988, Calvari *et al.* 1994, Cashman *et al.* 1994, Hon *et al.* 1994, Peterson *et al.* 1994, Calvari & Pinkerton 1998, Kauahikaua *et al.*



1998, Cashman *et al.* 1999). Pahoehoe and aa lavas have been identified as end-members in a range of basaltic lava types: produced under different eruption and flow conditions (Macdonald 1953). Solidified pahoehoe and aa lava flows are distinguished from each other primarily by their different surface morphologies, although internal structures are known to differ as well. Until recently, few studies have characterised the interiors of solidified basalt flows, despite the fact that vertical sections through lavas are commonly all that are accessible in ancient terrains (eg. road cuttings, diamond drill core etc.). Vesiculation patterns through pahoehoe lobes have been well characterised and are understood in terms of emplacement processes (eg. Aubele *et al.* 1988, Wilmoth & Walker 1993, Cashman & Kauahikaua 1997). Few studies of the petrographic textural and geochemical variations through individual basaltic lava flows have been performed (Watkins *et al.* 1970, Siders & Elliot 1983, Katz 1997, Sharma *et al.* 2000), particularly with a view to characterising the differences between the interiors of pahoehoe and aa lavas.

The aims of this study therefore are:

- to characterise the internal vesiculation patterns, petrographic textural and compositional variations through basaltic lava flow units. In particular, inflated P-type pahoehoe lobes are to be compared with aa flows to better understand the emplacement and crystallisation processes of these two end-member lava types.
- to establish the facies architecture, and a magnetostratigraphy in a plains-basalt lava flow field in the eastern Newer Volcanic Province, the Werribee Plains.
- to explore the palaeovolcanology and evolution of the Werribee Plains, and to better characterise plains-basalt volcanism.

Fig. 1.1 (Facing page) Geological setting of the Newer Volcanic Province in Victoria. Note the broad expanse of the NVP, extending 330 km west of Melbourne (total extent not shown on this map). The area of particular interest in this study is the Werribee Plains, located in the east of the NVP (west of Melbourne).

1.2 PROJECT BACKGROUND

1.2.1 Geological Setting

The Newer Volcanic Province

The basement rocks in Victoria are the deformed remains of the Palaeozoic Lachlan Fold Belt, the southernmost super-terrane of the Tasman Orogenic Zone (Cas 1983, Gray 1988). This orogenic belt developed along the Gondwana continental margin in the Palaeozoic era. It has had a complex history, involving amalgamation and the interplay of crustal extension and compressional events from the beginning of the Cambrian to the Early Carboniferous period. The Lachlan Fold Belt in Victoria is dominated by a thick (2-5 km) and extensive (800 km present width) Cambrian-Ordovician-Devonian turbidite sequence, containing fault-bounded Cambrian greenstone slices, granitoid plutons and volcanic rocks throughout (Gray 1988). It is considered to represent both continental margin sediment-prism and back-arc basin sequences (Crawford *et al.* 1984, Gray 1988). The palaeogeography progressively changed from wholly submarine in the Cambrian and Ordovician to nearly wholly continental in the Late Devonian-Carboniferous, reflecting the progressive emergence of the orogen from the end-Ordovician onwards. Major compressional deformational events caused widespread regional deformation, with principal north-south structural trends predominating. Metamorphism up to amphibolite facies and regionally extensive granitoid plutonism also occurred.

Victoria remained tectonically stable from the Early Carboniferous until the Early Cretaceous period, when rifting associated with the break-up of Gondwana commenced along the southern margin of the continent (Müller *et al.* 2000). Rifting led to the formation of the Otway, Bass and Gippsland Basins along the southern margin of Victoria, the opening of the Southern Ocean between Australia and Antarctica, and the subsequent opening of the Tasman Sea to the east. Basaltic volcanism associated with, and post-dating, rifting was distributed across the state, although more widespread in the east (the Older Volcanics, Fig. 1.1). This phase of volcanism commenced 95 Ma and continued until 19 Ma (Day 1983). After the original continental rift-forming phase, all basins subsided thermally and isostatically and were transgressed by the sea (Cas *et al.* 1993). Further subsidence during the Tertiary period resulted in the formation of the Murray Basin, Port Phillip Basin, Ballan Graben and Western Port Basin, in which thick sedimentary sequences accumulated (Abele *et al.* 1988). Intermittent faulting occurred throughout the Tertiary period and tectonic movements were most intense in the Late Pliocene and Early Pleistocene epochs. These were responsible for uplift of the

Palaeozoic highlands bordering the sedimentary basins (Kosciusko uplift) (Abele *et al.* 1988). Basaltic volcanism commenced again in Victoria at 4.6 Ma (the Newer Volcanics) after a period of quiescence, marked only by minor felsic volcanics in the Macedon-Trentham area. Products of the renewed period of basaltic volcanic activity (4.6 Ma-4.5 ka) straddle the northern margin of the Otway Basin, the northwest margin of Port Phillip Basin, and the Palaeozoic basement of the Lachlan Fold Belt; Fig. 1.1 (Price *et al.* 1988). The Otway Basin has an east-west orientation that is subparallel to the original west-northwest rift trend (Hill *et al.* 1995). The east-west orientation of the Newer Volcanic Province is thought to reflect the influence of basement faults associated with rifting and the formation of the Otway Basin (Cas *et al.* 1993).

The Werribee Plains

The products of volcanism forming the Werribee Plains, in the east of the Newer Volcanic Province, overlie Tertiary aged sediments of the Port Phillip Basin; Fig. 1.2 (Abele *et al.* 1988, Holdgate *et al.* 2001). The Port Phillip Basin is a broad low-lying area between two major lineaments: the Rowsley and Selwyn faults, and formed due to subsidence towards the end of the Tertiary period (Abele *et al.* 1988). Sediments within the basin wedge out against the Palaeozoic basement to the north of the basin without notable faulting. These sediments range in age from Lower Cretaceous (the Otway Group), to Plio- Pleistocene (the Brighton Group) (Abele *et al.* 1988). The Brighton Group contains a lower marine unit (the Black Rock Sandstone), and an upper unit deposited in a terrestrial environment (the Red Bluff Sands). The basalts of the Werribee Plains disconformably overlie the Red Bluff Sands (Holdgate *et al.* 2002). The development of the Yarra and Werribee deltas during the Late Tertiary and Quaternary produced the present-day topography of Port Phillip. Recent sea-level and climatic changes have modified, but not greatly changed, the morphology (Holdgate *et al.* 2001).

1.2.2 Intra-plate volcanism in eastern Australia

Late Mesozoic to Quaternary volcanic rocks extend in a broken belt 4,400 km from Torres Strait in the north, along the eastern side of Australia, to eastern Victoria. Here the volcanic areas trend westwards into South Australia, and southwards into the Bass Basin and Tasmania; Fig. 1.3a (Johnson 1989). Three types of volcanoes, and associations thereof, have been identified in eastern Australia: central volcanoes, lava-fields, and leucitite suites (Wellman

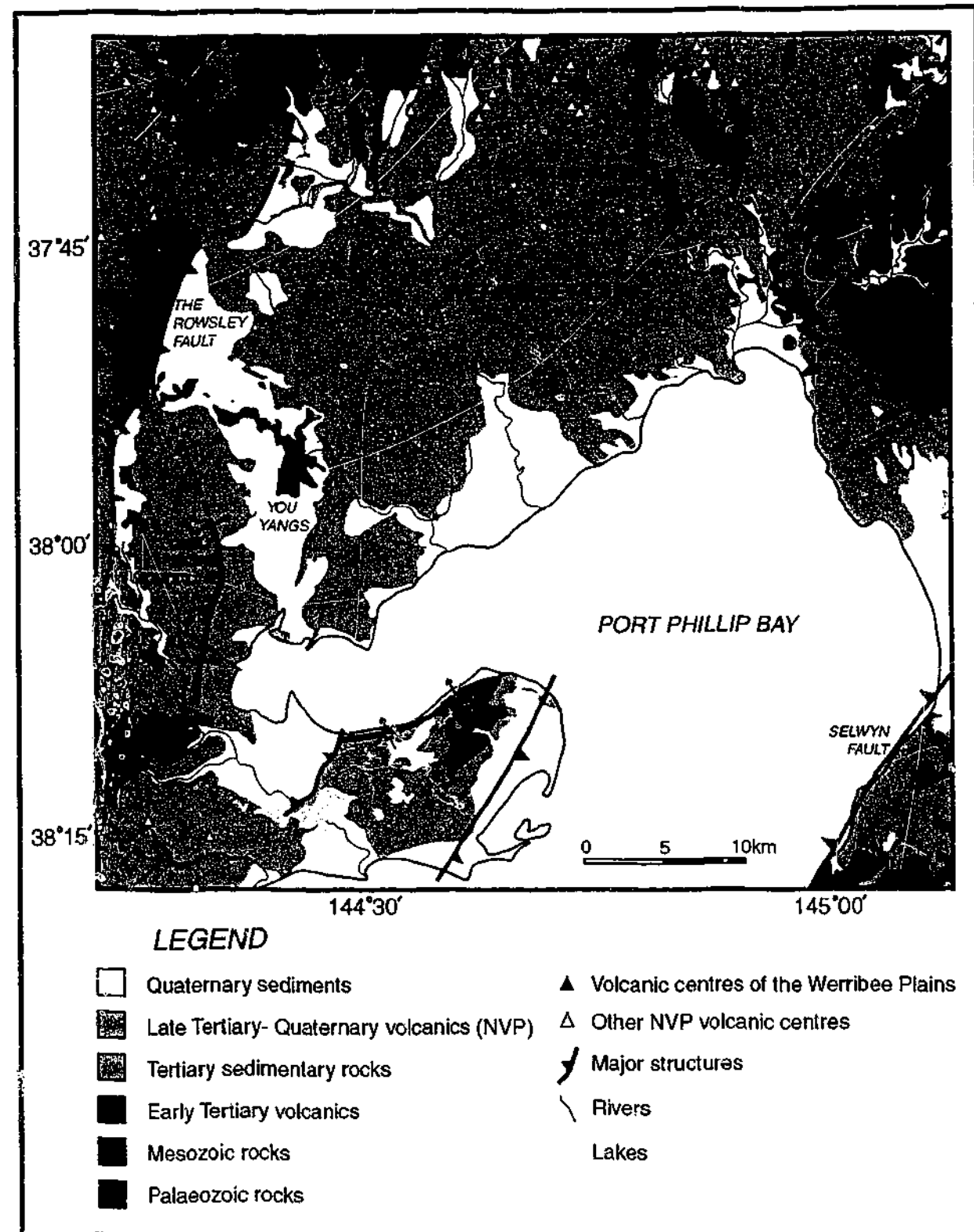


Fig. 1.2 Geological setting of the Werribee Plains, located in the east of the NVP (Fig. 1.1). The Werribee Plains are bounded by the Rowsley Fault in the west, the Maribyrnong River in the east, the highlands in the north, and the coast in the south (section 1.2.3).

& McDougall 1974). Central volcanoes produce predominantly basaltic lava flows from central vents, and have felsic lava flows and/or intrusions associated with them. The lava-fields are basaltic, and are characterised by numerous monogenetic point-source volcanoes feeding

extensive lava plains (eg. the Newer Volcanic Province). Leucitite suites are composed of high potassium intrusions and lavas that are petrologically and spatially distinct from all other volcanic areas in eastern Australia. The total-volume estimate produced by all of the eastern Australian volcanism is ~20,000 km³, consisting of ~9,000 km³ from the central volcanoes, and the remainder from the lava-fields (see Fig. 1.3b for the distribution of central volcanoes and lava-fields). The leucitite suite is volumetrically minor (Wellman & McDougall 1974).

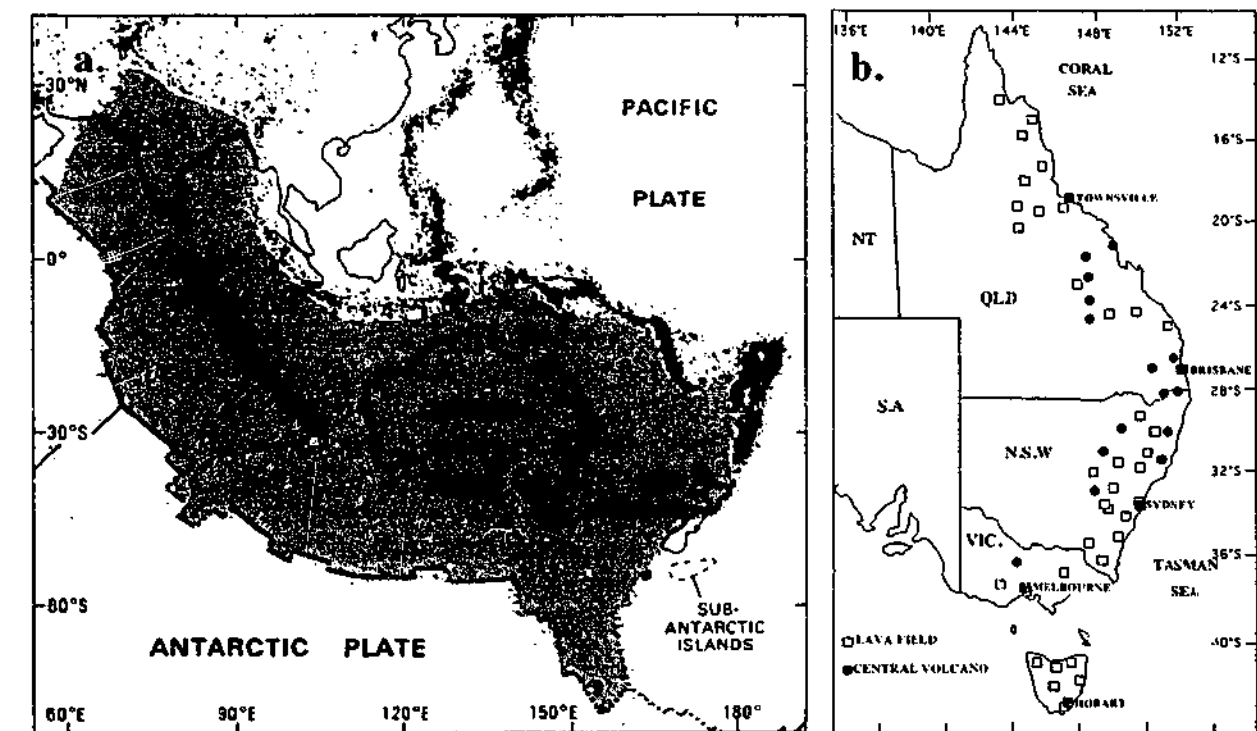


Fig. 1.3 The distribution of Late Mesozoic to Quaternary products of intra-plate volcanism (modified from Johnson (1989)). a. The Indo-Australian plate, showing the distribution of continental intra-plate volcanic areas of eastern Australia and New Zealand. Dots represent earthquakes defining margins of the plate. Intra-plate and New Zealand earthquake epicentres are omitted. b. The distribution of central volcano and lava-field provinces in eastern Australia.

The rate of volcanism is considered to have been relatively constant during the past 60 Myrs, although the central and lava-field types began their activity at different times (Wellman & McDougall 1974). The central-volcano magmatism began at about 35 Ma in Central Queensland, and volcanoes produced during this phase of activity are progressively younger towards the south (Duncan & McDougall 1989). The time progression of central-volcano magmatism is considered to reflect the northward drift of the Indo-Australian plate over a mantle plume (the Australian plume) or hot-spot. This plume is now possibly situated beneath the Bass Strait between the Australian continent and Tasmania (Wellman & McDougall

1974). In contrast, the age distribution of lava-field provinces does not show any relationship to the northward motion of the Australian plate (Duncan & McDougall 1989). The origin of the lava-field volcanism is incompletely resolved and alternative possibilities remain in interpretation (eg. Duncan & McDougall 1989). Some of the proposed models for the origin of the intra-plate volcanism in eastern Australia include: the presence of hot-spots or a series of these (hot-lines) beneath the Australian plate (Sutherland 1981, 1998); tension in the lithosphere due to erosional rebound of the Eastern Highlands (Stephenson & Lambeck 1985, Lambeck & Stephenson 1986); and thermal instability in the mantle due to the break-up of the super-continent Gondwana, considered to be responsible for the continuation of volcanism over the following tens of millions of years (Lister & Etheridge 1989, Price *et al.* 1997). It seems that no single model can account for all of the volcanism observed along the south-east and eastern margin of Australia.

The SKIPPY (seismic hopping) project has used arrivals of large earthquake events bordering Australia to define regions of higher and lower seismic *P* shear wave velocity within Australia's lithospheric mantle (Zielhuis & van der Hilst 1996). These areas of contrasting faster and slower seismic velocity have been interpreted as cooler and hotter mantle regions respectively (Sutherland 1998). Two of the largest slow regions in the SKIPPY results underlie areas of young volcanism and hot geotherms in western Victoria and North Queensland (O'Reilly & Griffin 1985, Sutherland *et al.* 1994), and there is evidence of anomalously hot mantle extending up much of the eastern coast of Australia (Sutherland 1998). Price *et al.* (1997) proposed that the intra-plate volcanism in eastern Australia is related to the break-up of Gondwana, resulting in thermal instability in the mantle, involving asthenospheric upwelling. This seems to be reasonable, considering the SKIPPY evidence of the present extent of the thermal anomalies, in relation to the distribution of volcanism, and the continental margin along which the break-up of Gondwana occurred. Issues that remain unresolved include: the relationship between volcanism and the uplift of the eastern highlands; the types of mantle thermal anomalies involved, whether single hotspot, multiple hotspot, or hotlines; and the exact nature of the stress fields under which the volcanism occurs, whether tensional or compressional relative to Australian plate dynamics (eg. Sutherland 1998). The last point is important considering that measurements of the present-day stress in south-eastern Australia are consistent with a compressional stress field (Denham *et al.* 1979). This is considered to have originated around 10 Ma, with completion of the northern margin collision (Veevers *et al.* 1991). The simplest explanation for the intra-plate volcanism in eastern Australia

is an extensive post-rifting thermal anomaly in the mantle, which has persisted since the break-up of the super-continent Gondwana, and has been responsible for intermittent volcanism from the Late Cretaceous period until Recent.

1.2.3 Geology of the Newer Volcanic Province

Nearly 400 eruption points have been identified in the NVP (Joyce 1975). These are characterised by low profile shield volcanoes, scoria cones, maars and tuff rings; Fig. 1.4. Although explosive centres are the most prominent geomorphic features, the total proportion of pyroclastic material in the NVP is estimated to be only 1% (Ollier & Joyce 1973). The Province has been subdivided into three sub-provinces based upon morphology; Fig. 1.4 (Joyce 1988). The Central Highlands sub-province in the north rests upon exposed Palaeozoic basement and contains the highest concentration of eruption centres (at least 250), as well as valley-confined lava flows, in basement-entrenched valleys. The Mt. Gambier sub-province in the west is separated from the rest of the NVP by 60-80 km of largely Recent sedimentary cover sequences (no volcanic outcrop). This sub-province contains clusters of scoria cones and maars, with minor lavas associated. The NVP is dominated by the flat basaltic lava plains of the Western Plains sub-province, reaching greater than 100 m thickness in places. Small central vent eruption centres are scattered through the plains (scoria cones, maars, lava shields and complex centres), locally aligned along inferred basement lineaments. The flat topography is in part a reflection of the flat depositional surface of the underlying Otway and Port Phillip Basin successions, but also the topography filling and blanketing nature of the lava flows. Also, significant weathering has occurred since emplacement, and intensive farming has obscured much of the lava plain geology. The area of study for this project within the Western Plains sub-province was chosen to be the Werribee Plains in the far east, as it has the greatest concentration of diamond drill holes, geophysical wells and quarries; permitting three dimensional analysis of the stratigraphy and facies architecture.

The Werribee Plains lava flow field is extensive (2,000 km²), covering the area between Melbourne, Geelong and Bacchus Marsh; Figs. 1.2 & 1.4 (Nicholls & Joyce 1989). The Werribee Plains are bounded by the Rowsley Fault in the west, the Maribyrnong River in the east, the highlands in the north, the coast in the south, and Cretaceous sediments in the vicinity of Geelong; Fig. 1.2 (Ollier & Joyce 1964). The surrounding highlands are topographically raised features (Fig. 4.1, Chapter 4), in sharp contrast with the lava plains, which are relatively flat, and gently slope towards the coast in the south-east. The basaltic lavas forming the

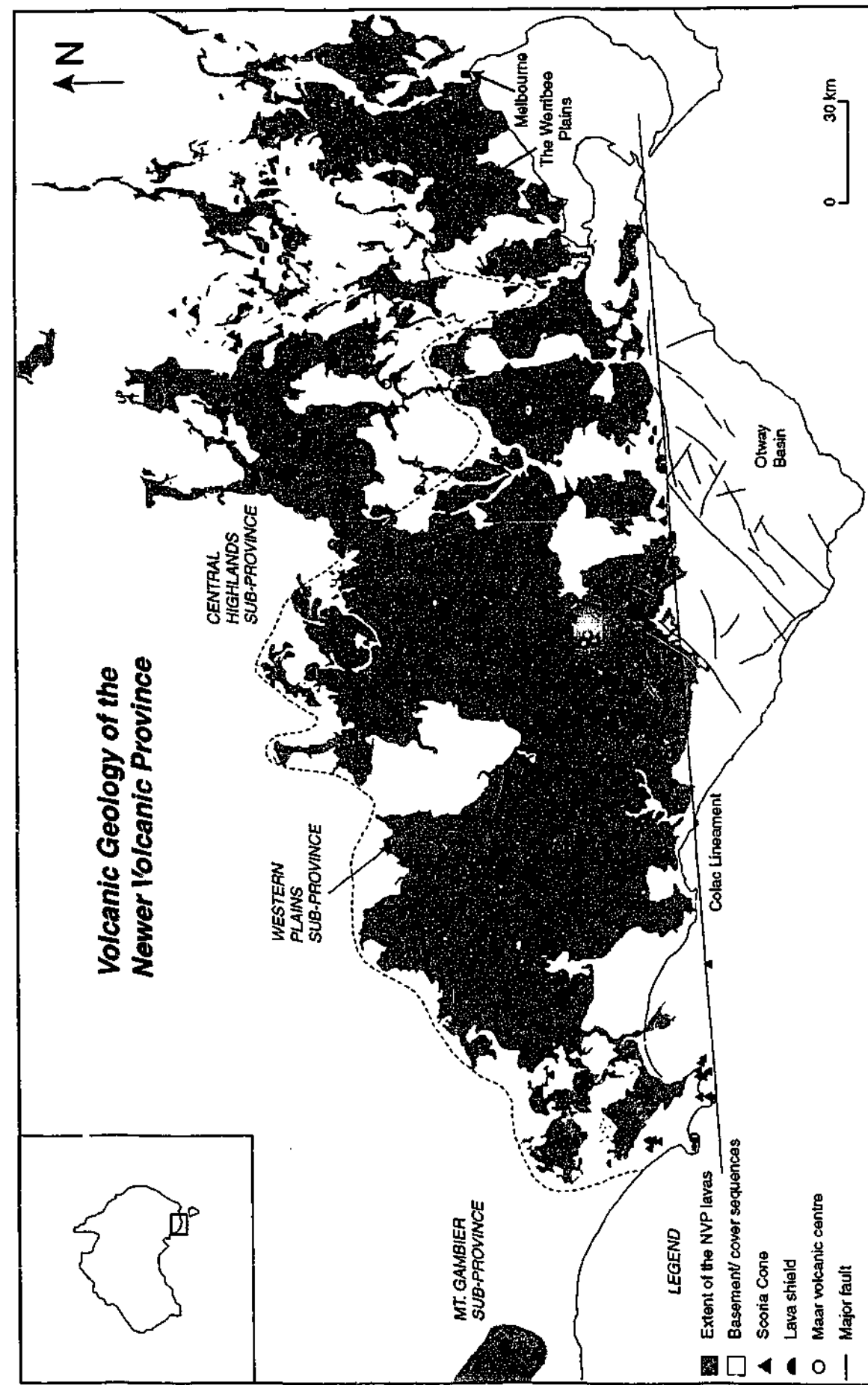


Fig. 1.4 The volcanic geology of the Newer Volcanic Province. The distribution of scoria cones, low profile shield volcanoes and maars, and the total extent of the products (modified from Joyce (1975)). The Western Plains sub-province is the most extensive sub-province, and contains the Werribee Plains in the east.

Werribee Plains are almost continuous in the area, broken only by outcropping granite of the Late Devonian You Yangs, and locally buried by Middle Pleistocene-Recent sediments. A number of small, point source eruption centres known to have fed the lavas have been recognised; both scoria cones and lava shield volcanoes. These volcanoes range from ~1.0 to 12.0 km in diameter, and are up to 120 m high. Previous radiometric dating work gives an age range of 1.41- 2.6 Ma for the basaltic succession of the Werribee Plains (McDougall *et al.* 1966, Aziz-Ur-Rahman & McDougall 1972, Price *et al.* 1997). Compositions of the lavas are tholeiitic, differentiates (olivine and quartz tholeiitic basalts and icelandites) and alkaline basalts (alkali basalts or mafic hawaiites) (Nicholls & Joyce 1989). The lavas from late eruption points are considered to be generally more alkaline (Nicholls & Joyce 1989).

1.2.4 Basaltic lava flow fields

The two main types of intra-plate continental basaltic provinces are monogenetic volcano fields and flood-basalt provinces (Walker 2000). Monogenetic fields contain a number of volcanic centres that erupt only once. The eruption centres are most commonly scoria cones and lava shields and may be clustered or widely dispersed within a volcanic field (Connor & Conway 2000). Plains-basalt provinces (eg. the Snake River Plain, U.S.A., (Greeley 1977, 1982a, b, Kutzt *et al.* 1992)) are a unique type of monogenetic volcano field, produced by a style of volcanism intermediate between continental flood-basalt volcanism and ocean island volcanism. The Newer Volcanic Province has been identified as a plains-basalt province (Cas 1989).

Flood-basalt provinces are characterised by very thick (15-50 m), regionally extensive (up to hundreds of km's long, 100 - 1,000+ km³), sheet-like lavas with low aspect ratios (eg. the Columbia River Plateau basalts, U.S.A., (Swanson *et al.* 1975, Camp *et al.* 1982, Hooper 1982, Reidel & Hooper 1989, Self *et al.* 1996, Thordarson & Self 1998)). Eruptions occur primarily from fissure vent systems and lavas are emplaced on slopes of up to 0.1%. The lavas tend to drown any pre-existing topography; forming a flat, plateau-like morphology without any evidence of sites of eruption. The total area of an individual continental flood-basalt province is up to ~500,000 km² (eg. the Deccan flood-basalt province, India (Subbarao & Sukheswala 1981)). Aa lavas have rarely been identified in these provinces. Similarly the total pyroclastic content is very low (Self *et al.* 1997). The sheet-like lavas have pahoehoe morphologies, and are now considered to have formed by endogenous growth (eg. Self *et al.* 1996, 1997, 1998, Thordarson & Self 1998, Bondre *et al.* submitted); much like Hawaiian

pahoehoe lavas (Hon *et al.* 1994).

The total size of plains-basalt provinces is an order of magnitude less than flood-basalt provinces, for example the NVP covers an area of 15,000 km², and the Pliocene-Quaternary basaltic provinces of northern Queensland cover an area of 23,000 km² (Joyce 1975, Stephenson 1989). The lava flows produced in plains-basalt provinces have the same long-term effect of flattening out the topography as in flood-basalt provinces, by preferentially filling topographic lows with valley-confined, small volume lavas (Greeley 1982a). However, unlike in flood-basalt provinces, point-source eruption centres are preserved throughout plains-basalt provinces, and the lava flows are significantly smaller volume than flood-basalt lavas. Lavas in plains-basalt provinces are similar in size and form to Hawaiian shield-forming lavas, and both pahoehoe and aa morphologies have been recognised in plains-basalt provinces. However, volcanic activity in ocean island volcanic systems (eg. Hawaii (Wentworth & Macdonald 1953, Macdonald 1967, Walker 1993)) is focussed around a central magma conduit system, in contrast to continental basaltic systems, which have regionally dispersed products. Pyroclastic deposits are minor in plains-basalt provinces, and soils and sediments may be intercalated with the flows.

1.3 PREVIOUS WORK AND SIGNIFICANCE OF THIS STUDY

Relatively few studies have used the interiors of solidified basaltic lava flows as a guide to emplacement and crystallisation processes. Vesicle zonation has been documented and characterised through different types of pahoehoe flows, particularly in Hawaii (eg. Aubele *et al.* 1988, Wilmoth & Walker 1993, Cashman & Kauahikaua 1997), and also through flood-basalts (eg. McMillan *et al.* 1987, 1989, Self *et al.* 1996, 1997, Thordarson & Self 1998). These studies have identified features that are useful in determining the mode of emplacement of the lava flows (eg. inflation vs. ponding in a topographic depression (Cashman & Kauahikaua 1997)). Textural zonation studies through individual flows have also been previously conducted on continental flood-basalts (eg. Long & Wood 1986, Degraff *et al.* 1989, Self *et al.* 1997, Thordarson & Self 1998) and lava flows in Hawaii (Katz 1997, Sharma *et al.* 2000). Few studies however, have explored the interior of aa flows (eg. Katz 1997), and how internal features reflect emplacement processes. Rowland & Walker (1987, 1988) compared variations in the phenocryst content in vertical sections through various types of basaltic lava flows, and interpreted these variations in terms of the different viscosities of the lavas. Others have compared the groundmasses of pahoehoe and aa flows (eg. Sato 1995, Cashman *et al.* 1999,

Polacci *et al.* 1999), however these studies have not addressed how the textures vary throughout individual flow units. Relatively few studies of the compositional variations through basalt flows have been performed (eg. Watkins *et al.* 1970, Siders & Elliot 1983), and these have not been interpreted in terms of emplacement processes. This study involves characterising the interiors of pahoehoe and aa flows by exploring vesiculation patterns, petrographic textural zonation and compositional variations throughout individual flows. It will be explored whether there are consistent, characterisable differences between the interiors of pahoehoe and aa lavas. If so, it will be investigated how these reflect differences in the emplacement and crystallisation processes of the two end-member basaltic lavas.

Previous studies of the Newer Volcanic Province have mainly concentrated on the geomorphology and physiography of the province (eg. Ollier & Joyce 1964, Ollier 1967, Joyce 1988, 1998), and the geochemistry of the products (eg. Irving & Green 1976, Frey *et al.* 1978, McDonough *et al.* 1985, Price *et al.* 1997, Vogel & Keays 1997) and incorporated xenoliths (eg. O'Reilly & Griffin 1985, 1988, Chen *et al.* 1989, Yaxley *et al.* 1991). Limited geochronological and palaeomagnetic studies have been performed (Green & Irving 1958, McDougall *et al.* 1966, Aziz-Ur-Rahman & McDougall 1972), and physical volcanological studies have focussed on the pyroclastic volcanic activity (eg. Edney 1987, Cas *et al.* 1993). In general, little is known about the sub-surface geology and stratigraphy of the NVP. Price *et al.* (1997) attempted to define a stratigraphy for the Western Plains sub-province (including the Werribee Plains) by combining radiometric dating work with Sr isotope analyses to subdivide it into discrete domains representing eruption units. Other work on the Werribee Plains includes an overview of the geology by Condon (1951), and a geological and geochemical study by Mitchell (1990). It has already been established that conventional mapping techniques are largely inappropriate in the NVP, due to the lack of outcrop. Instead, this study combines many data sets (including diamond drill hole logs, geophysical well logs, geochemistry, palaeomagnetic results, airborne geophysical images) to establish a magnetostratigraphy in the Werribee Plains. Many features of the volcanism will be explored, such as the nature, frequency and duration of eruptions, as well as the types and distribution of products.

Greeley (1982a) was the first to formalise the concept of plains-basalt volcanism with his study of the Snake River Plain, U.S.A. This province has subsequently been better characterised (eg. Kuntz *et al.* 1992, Reed *et al.* 1997). Other plains-basalt provinces include the Pliocene-Quaternary provinces of northern Queensland and the NVP in Australia. Much

is known about flood-basaltic volcanism and Hawaiian shield-forming eruptions, as previous studies have focussed on these end-member basaltic volcanic styles. On the other hand, relatively little is known about plains-basalt volcanism, including the overall facies architecture, and the frequency of lava flow forming events. Results of this study will be compared with the type locality, the Snake River Plain, U.S.A., and with other monogenetic volcanic fields from around the world to better characterise plains-basalt volcanism.

1.4 METHODS

- The interiors of basaltic lava flows were studied using data collected from the Werribee Plains of the NVP, and Hawaii. Refer to Chapter 2 for a more complete discussion on the methods employed in this part of the study. The distribution of vesicles (and segregation structures) within each flow unit identified was sketched and qualitatively described. The vesiculation patterns were quantified in selected pahoehoe and aa flows. Thin sections were made at regular intervals through some flows for petrographic textural analysis. Variations in the mineralogy and texture of the groundmass through the flows were systematically recorded, both qualitatively and quantitatively (by point-counting and taking multiple grain-size measurements). Bulk rock x-ray fluorescence (XRF) analyses were made in some flow units at positions corresponding to thin section samples. Some of the samples were analysed as fused disks for major and trace elements at Melbourne University, and some for major elements at the University of New South Wales (see Appendix A for more complete outline of methods). Pressed powder pellets were used for trace element analysis at the University of New South Wales (Appendix A).
- Two to three samples were taken from every flow unit identified in diamond drill core from the Werribee Plains for the palaeomagnetic studies (see Chapter 3 for details). Most samples were thermally demagnetised, and a small number were demagnetised using alternating-field (AF) techniques. It was possible to determine the inclination of the primary remanence for most samples. Twenty samples were selected for rock magnetic study (hysteresis and isothermal remanence experiments), in order to determine the dominant ferromagnetic grain type, and hence to assess how confidently the primary remanence could be identified.

- The characteristics and distribution of volcanic and sedimentary facies in the Werribee Plains were investigated by completing fieldwork, logging diamond drill core, interpreting geophysical well logs, and doing petrographic studies (Chapter 4). The products of discrete eruptions were identified (eruption packages) and correlated between drill holes to produce a magnetostratigraphy. This involved combining a number of data sets. For example, the extent of lava flows from the exposed eruption centres was investigated through analysis of airborne geophysical images and geochemical data. Samples were collected from eruption points, other field localities and drill core for bulk rock X-ray fluorescence spectroscopy (XRF analysis). Analysis for major element concentrations took place on fused glass disks at the University of New South Wales (Appendix A). One sample from drill core was chosen for $^{40}\text{Ar}/^{39}\text{Ar}$ dating. Sample preparation was done at Monash University; the rock was crushed and the feldspar phenocrysts separated out. The sample has been sent to be irradiated in position 5C of the Macmaster reactor in Canada, and will then be analysed using facilities in the Noble Gas Laboratory, School of Earth Sciences, the University of Melbourne. The analysis is yet to be completed.

1.5 THESIS OUTLINE

Each of the three main aims are addressed in a separate chapter of this thesis, and an additional chapter is included in which the palaeomagnetic results are presented. The internal features of pahoehoe and aa flows are investigated in Chapter 2, with a view to gaining a better understanding of the emplacement, cooling and crystallisation processes of basaltic lavas. The results of the palaeomagnetic and rock magnetic studies are presented and interpreted in Chapter 3, along with some background theory. These results are combined with additional data in Chapter 4 to produce a magnetostratigraphy. Also in Chapter 4, the types and distribution of volcanic and sedimentary facies in the Werribee Plains are investigated. The results of all of these chapters are combined with some further data in Chapter 5, and the palaeovolcanology and evolution of the Werribee Plains are explored. The Newer Volcanic Province is then compared with other intra-plate basaltic provinces, and plains-basalt volcanism is better characterised. Conclusions of the study and a discussion of the implications of the results are presented in Chapter 6.

REFERENCES

- Abele, C., Gloe, C.S., Hocking, J.B., Holdgate, G., Kenley, P.R., Lawrence, C.R., Ripper, D., Threlfall, W.F. & Bolger, P.F., 1988. Tertiary. In: *Geology of Victoria* (eds Douglas, J.G. & Ferguson, J.A.), pp. 251-350, Victorian Division, Geological Society of Australia Incorporated, Melbourne.
- Abele, J.C., Crumpler, L.S. & Elston, W.E., 1988. Vesicle zonation and vertical structure of basalt flows. *Journal of Volcanology and Geothermal Research*, **35**, 349-374.
- Aziz-Ur-Rahman & McDougall, I., 1972. Potassium-Argon ages on the Newer Volcanics of Victoria. *Royal Society of Victoria Proceedings*, **85**, 61-69.
- Bondre, N.R., Duraiswami, R. & Dole, G., submitted. Morphology and emplacement of flows from the western Deccan Volcanic Province, India. *Bulletin of Volcanology*.
- Calvari, S. & Pinkerton, H., 1998. Formation of lava tubes and extensive flow field during the 1991-1993 eruption of Mount Etna. *Journal of Geophysical Research*, **103**(B11), 27,291-27,301.
- Calvari, S., Coltelli, M., Neri, M., Pompilio, M. & Scribano, V., 1994. The 1991-1993 Etna eruption: chronology and lava flow-field evolution. *Acta Vulcanologica*, **4**, 1-14.
- Camp, V.E., Hooper, P.R., Swanson, D.A. & Wright, T.L., 1982. Columbia River basalt in Idaho: physical and chemical characteristics, flow distribution, and tectonic implications. In: *Cenozoic geology of Idaho*. (eds Bonnischen, B. & Breckenridge, R.M.), pp. 55-75, Idaho Bureau of Mines and Geology, Idaho.
- Cas, R.A.F., 1983. *Palaeogeographic and tectonic development of the Lachlan Fold Belt Southeastern Australia*. Geological Society of Australia, Sydney, 104 p.
- Cas, R.A.F., 1989. Physical Volcanology. In: *Intraplate Volcanism in Eastern Australia and New Zealand* (eds Johnson, R.W., Knutson, J. & Taylor, S.R.), pp. 55-87, Cambridge University Press, Cambridge.
- Cas, R.A.F., Simpson, C. & Sato, H., 1993. Excursion Guide: Newer Volcanic Province- processes and products of phreatomagmatic activity. In: *General Assembly IAVCEI*, Australian Geological Survey Organisation, Canberra, Australia, 94 p.
- Cashman, K.V. & Kauahikaua, J.P., 1997. Reevaluation of vesicle distributions in basaltic lava flows. *Geology*, **25**(5), 419-422.
- Cashman, K.V., Mangan, M.T. & Newman, S., 1994. Surface degassing and modifications to vesicle size distributions in active basalt flows. *Journal of Volcanology & Geothermal Research*, **61**, 45-68.
- Cashman, K.V., Thornber, C. & Kauahikaua, J.P., 1999. Cooling and crystallization of lava in open channels, and the transition of Pahoehoe Lava to 'A'a. *Bulletin of Volcanology*, **61**, 306-323.
- Chen, C.-Y., Frey, F.A. & Song, Y., 1989. Evolution of the upper mantle beneath southeast Australia: geochemical evidence from peridotite xenoliths in Mount Leura basanite. *Earth and Planetary*

- Science Letters*, **93**, 195-209.
- Condon, M.A., 1951. The geology of the lower Werribee River, Victoria. *Royal Society of Victoria Proceedings*, **63**, 1-24.
- Connor, C.B. & Conway, F.M., 2000. Basaltic volcanic fields. In: *Encyclopaedia of Volcanoes* (eds Sigurdsson, H., Houghton, B.F., McNutt, S.R., Rymer, H. & Stix, J.), pp. 331-343, Academic Press, San Diego.
- Crawford, A.J., Cameron, W.E. & Keays, R.R., 1984. The association beninite- low Ti andesite-tholeiite in the Heathcote Greenstone Belt, Victoria; ensimatic setting for the early Lachlan Fold Belt. *Australian Journal of Earth Sciences*, **31**, 161-175.
- Day, R.A., 1983. Petrology and geochemistry of the Older Volcanics of Victoria. *Unpub. PhD Thesis, Monash University, Melbourne*.
- Degraff, J.M., Long, P.E. & Aydin, A., 1989. Use of joint-growth directions and rock textures to infer thermal regimes during solidification of basaltic lava flows. *Journal of Volcanology and Geothermal Research*, **38**, 309-324.
- Denham, D., Alexander, L.G. & Worotnicki, G., 1979. Stresses in the Australian crust: evidence from earthquakes and in-situ stress measurements. *BMR Journal of Australian Geology and Geophysics*, **4**, 289-295.
- Duncan, R.A. & McDougall, I., 1989. Volcanic Time-Space Relationships. In: *Intraplate Volcanism in Eastern Australia and New Zealand* (eds Johnson, R.W., Knutson, J. & Taylor, S.R.), pp. 43-53, Cambridge University Press, Cambridge.
- Edney, W.J., 1987. Facies contrasts and their origins in scoria cones, maars and tuff rings of the Newer Volcanics Province, Western Victoria, Australia. *Unpub. Bachelor of Applied Science Thesis, Monash University, Melbourne*.
- Frey, F.A., Green, D.H. & Roy, S.D., 1978. Integrated models of basalt petrogenesis: a study of quartz tholeiites to olivine melilitites from southeastern Australia utilizing geochemical and experimental petrological data. *Journal of Petrology*, **19**, 463-513.
- Gray, D.R., 1988. Structure and Tectonics. In: *Geology of Victoria* (eds Douglas, J.G. & Ferguson, J.A.), pp. 1-36, Victorian Division, Geological Society of Australia, Melbourne.
- Greeley, R., 1977. Basaltic "Plains" volcanism. In: *Volcanism of the Eastern Snake River Plain, Idaho: A Comparative Planetary Geology Guidebook* (eds Greeley, R. & King, J.S.), pp. 23-44, NASA, Washington D.C.
- Greeley, R., 1982a. The Snake River Plain, Idaho: Representative of a new category of volcanism. *Journal of Geophysical Research*, **87**(B4), 2,705-2,712.
- Greeley, R., 1982b. The Style of Basaltic Volcanism in the Eastern Snake River Plain, Idaho. In: *Cenozoic geology of Idaho* (eds Bonnischen, B. & Breckenridge, R.M.), pp. 407-421, Idaho Bureau of Mines and Geology, Idaho.

- Green, R. & Irving, E., 1958. The palaeomagnetism of the Cainozoic basalts from Australia. *Royal Society of Victoria Proceedings*, **70**, 1-17.
- Guest, J.E., Kilburn, C.R.J., Pinkerton, H. & Duncan, A.M., 1987. The evolution of lava flow-fields: observations of the 1981 and 1983 eruptions of Mount Etna, Sicily. *Bulletin of Volcanology*, **49**, 527-540.
- Hill, K.A., Finlayson, D.M., Hill, K.C. & Cooper, G.T., 1995. Mesozoic tectonics of the Otway Basin region; the legacy of Gondwana and the active Pacific margin; a review and ongoing research. *The Australian Petroleum Exploration Association Journal*, **35**(1), 467-493.
- Holdgate, G.R., Guerin, B., Wallace, M.W. & Gallagher, S.J., 2001. Marine geology of Port Phillip, Victoria. *Australian Journal of Earth Sciences*, **48**, 439-455.
- Holdgate, G.R., Gallagher, S.J. & Wallace, M.W., 2002. Tertiary coal geology and stratigraphy of the Port Phillip Basin, Victoria. *Australian Journal of Earth Sciences*, **49**, 437-453.
- Hon, K., Kauahikaua, J., Denlinger, R. & Mackay, K., 1994. Emplacement and inflation of pahoehoe sheet flows: Observations and measurements of active lava flows on Kilauea Volcano, Hawaii. *Geological Society of America Bulletin*, **106**, 351-370.
- Hooper, P.R., 1982. The Columbia River basalts. *Science*, **215**, 1463-1468.
- Irving, A.J. & Green, D.H., 1976. Geochemistry and petrogenesis of the newer basalts of Victoria and South Australia. *Journal of the Geological Society of Australia*, **23**, 45-66.
- Johnson, R.W., 1989. Volcano distribution and classification. In: *Intraplate Volcanism in eastern Australia and New Zealand* (eds Johnson, R.W., Knutson, J. & Taylor, S.R.), pp. 7-12. Cambridge University Press, Cambridge.
- Joyce, E.B., 1975. Quaternary volcanism and tectonics in southeastern Australia. *Bulletin of the Royal Society of New Zealand*, **13**, 169-176.
- Joyce, E.B., 1988. Newer Volcanic Landforms. In: *Geology of Victoria* (eds Douglas, J.G. & Ferguson, J.A.), pp. 419-426, Victorian Division, Geological Society of Australia, Melbourne.
- Joyce, E.B., 1998. A new regolith map of the eastern Victorian volcanic plains, Victoria, Australia. In: *3rd Australian Regolith Conference: New approaches to an old continent* (eds Taylor, G. & Pain, C.), pp. 117-126, CRC LEME, Kalgoorlie, Western Australia.
- Katz, M.G., 1997. Patterns of lava flow coverage in drill cores. *Unpub. Master of Science Thesis, University of Oregon, Oregon*.
- Kauahikaua, J., Cashman, K.V., Mattox, T.N., Heliker, C.C., Hon, K.A., Mangan, M.T. & Thornber, C.R., 1998. Observations on basaltic streams in tubes from Kilauea Volcano, island of Hawai'i. *Journal of Geophysical Research*, **103**(B11), 27,303-27,323.
- Kilburn, C.R.J. & Lopes, R.M.C., 1988. The growth of aa lava flow fields on Mount Etna, Sicily. *Journal of Geophysical Research*, **93**(B12), 14,759-14,772.
- Kuntz, M.A., Covington, H.R. & Schorr, L.J., 1992. An overview of basaltic volcanism of the eastern

- Snake River Plain, Idaho. In: *Regional Geology of the Eastern Idaho and Western Wyoming: Geological Society of America Memoir 179*. (eds Link, P.K., Kuntz, M.A. & Platt, L.B.), pp. 227-267, The Geological Society of America, Inc., Boulder, Colorado.
- Lambeck, K. & Stephenson, R., 1986. The post-Palaeozoic uplift history of south-eastern Australia. *Australian Journal of Earth Sciences*, **33**, 253-270.
- Lipman, P.W. & Banks, N.G., 1987. Aa flow dynamics, Mauna Loa 1984. *U.S. Geological Survey Professional Paper 1350*, 1,527-1,565.
- Lister, G.S. & Etheridge, A., 1989. Detachment models for uplift and volcanism in the Eastern Highlands and their applications to the origins of passive margin mountains. In: *Intraplate Volcanism in Eastern Australia and New Zealand* (eds Johnson, R.W., Knutson, J. & Taylor, S.R.), pp. 297-313, Cambridge University Press, Cambridge.
- Long, P.E. & Wood, B.J., 1986. Structures, textures, and cooling histories of Columbia River basalt flows. *Geological Society of America Bulletin*, **97**, 1,144-1,155.
- Macdonald, G.A., 1953. Pahoehoe, aa and block lava. *American Journal of Science*, **251**, 169-191.
- Macdonald, G.A., 1967. Forms and structures of extrusive basaltic rocks. In: *Basalts. The Poldervaart treatise on rocks of basaltic composition* (eds Hess, H.H. & Poldervaart, A.), Interscience Publishers, New York, 1861 p.
- McDonough, W.F., McCulloch, M.T. & Sun, S.S., 1985. Isotopic and geochemical systematics in Tertiary-Recent basalts from southeastern Australia and implications for the evolution of the sub-continental lithosphere. *Geochimica et Cosmochimica Acta*, **49**, 2,051-2,067.
- McDougall, I., Allsopp, H.L. & Chamalaun, F.H., 1966. Isotopic dating of the Newer Volcanics of Victoria, Australia, and Geomagnetic Polarity Epochs. *Journal of Geophysical Research*, **71**(24), 6,107-6,118.
- McMillan, K., Cross, R.W. & Long, P.E., 1987. Two-stage vesiculation in the Cohasset flow of the Grande Ronde Basalt, south-central Washington. *Geology*, **15**, 809-812.
- McMillan, K., Long, P.E. & Cross, R.W., 1989. Vesiculation in Columbia River basalts. In: *Volcanism and tectonism in the Columbia River flood-basalt province: Boulder, Colorado* (eds Reidel, S.P. & Hooper, P.R.), pp. 157-167, Geological Society of America.
- Mitchell, M.M., 1990. The geology and geochemistry of the Werribee Plains, Newer Volcanics, Victoria. *Unpub. Honours thesis Thesis, La Trobe University, Melbourne*.
- Müller, R.D., Gaina, C. & Clark, S., 2000. Seafloor spreading around Australia. In: *Billion-year earth history of Australia and neighbours in Gondwanaland* (ed Veevers, J.J.), pp. 18-28, GEMOC Press, Sydney.
- Nicholls, I.A. & Joyce, E.B., 1989. Newer Volcanics. In: *Intraplate Volcanism in Eastern Australia and New Zealand* (eds Johnson, R.W., Knutson, J. & Taylor, S.R.), pp. 137-142, Cambridge University Press, Cambridge.

- Ollier, C.D., 1967. Landforms of the Newer Volcanic Province of Victoria. In: *Landform studies from Australia and New Guinea* (eds Jennings, J.N. & Mabbutt, J.A.), pp. 315-339, A.N.U. Press, Canberra.
- Ollier, C.D. & Joyce, E.B., 1964. Volcanic physiography of the western plains of Victoria. *Royal Society of Victoria Proceedings*, **77**, 357-376.
- Ollier, C.D. & Joyce, E.B., 1973. Geomorphology of the Western District volcanic plains, lakes and coastline. In: *Regional Guide to Victorian Geology* (eds McAndrew, J. & Marsden, M.A.H.), pp. 100-113, School of Geology, University of Melbourne, Melbourne.
- O'Reilly, S.Y. & Griffin, W.L., 1985. A xenolith-derived geotherm for southeastern Australia and its geographical implications. *Tectonophysics*, **111**, 41-63.
- O'Reilly, S.Y. & Griffin, W.L., 1988. Mantle metasomatism beneath western Victoria, Australia I: Metasomatic processes in Cr-diopside lherzolites. *Geochimica et Cosmochimica Acta*, **52**, 433-447.
- Peterson, D.W. & Swanson, D.A., 1974. Observed formation of lava tubes during 1970-1971 at Kilauea volcano, Hawaii. *Studies in speleology*, **2**(6), 209-222.
- Peterson, D.W. & Tilling, R.I., 1980. Transition of basaltic lava from pahoehoe to aa, Kilauea volcano, Hawaii: Field observations and key factors. *Journal of Volcanology and Geothermal Research*, **7**, 271-293.
- Peterson, D.W., Holcomb, R.T., Tilling, R.I. & Christiansen, R.L., 1994. Development of lava tubes in the light of observations at Mauna Ulu, Kilauea Volcano, Hawaii. *Bulletin of Volcanology*, **56**, 343-360.
- Polacci, M., Cashman, K.V. & Kauahikaua, J.P., 1999. Textural characterization of the pahoehoe-'a'a transition in Hawaiian basalt. *Bulletin of Volcanology*, **60**, 595-609.
- Price, R.C., Gray, C.M., Nicholls, I.A. & Day, A., 1988. Cainozoic Volcanic Rocks. In: *Geology of Victoria* (eds Douglas, J.G. & Ferguson, J.A.), pp. 439-451, Victorian Division, Geological Society of Australia, Melbourne.
- Price, R.C., Gray, C.M. & Frey, F.A., 1997. Strontium isotopic and trace element heterogeneity in the plains basalts of the Newer Volcanic Province, Victoria, Australia. *Geochimica et Cosmochimica Acta*, **61**(1), 171-192.
- Reed, M.F., Bartholomay, R.C. & Hughes, S.S., 1997. Geochemistry and stratigraphic correlation of basalt lavas beneath the Idaho Chemical Processing Plant, Idaho National Engineering Laboratory. *Environmental Geology*, **30**, 108-118.
- Reidel, S.P. & Hooper, P.R., 1989. Volcanism and tectonism in the Columbia River flood-basalt province: Boulder, Colorado. *Geological Society of America Special Paper* **239**, 386 p.
- Rowland, S.K. & Walker, G.P.L., 1987. Toothpaste lava: Characteristics and origin of a lava structural type transitional between pahoehoe and aa. *Bulletin of Volcanology*, **49**, 631-641.

- Rowland, S.K. & Walker, G.P.L., 1988. Mafic-crystal distributions, viscosities, and lava structures of some Hawaiian lava flows. *Journal of Volcanology and Geothermal Research*, **35**, 55-66.
- Sato, H., 1995. Textural differences between pahoehoe and aa lavas of Izu-Oshima volcano, Japan- an experimental study on population density of plagioclase. *Journal of Volcanology and Geothermal Research*, **66**, 101-113.
- Self, S., Thordarson, T., Keszthelyi, L., Walker, G.P.L., Hon, K., Murphy, M.T., Long, P. & Finnemore, S., 1996. A new model for the emplacement of Columbia River basalts as large, inflated pahoehoe lava flow fields. *Geophysical Research Letters*, **23**(19), 2,689-2,692.
- Self, S., Thordarson, T. & Keszthelyi, L., 1997. Emplacement of Continental Flood Basalt Lava Flows. In: *Large Igneous Provinces: Continental, Oceanic, and Planetary Flood Volcanism*. (eds Mahoney, J.J. & Coffin, M.), pp. 381-410, American Geophysical Union.
- Self, S., Keszthelyi, L. & Thordarson, T., 1998. The importance of pahoehoe. *Annual Review of Earth and Planetary Science*, **26**, 81-110.
- Sharma, K., Keszthelyi, L., Thornber, C. & Self, S., 2000. Variations in the cooling, crystallization textures and glass chemistry during emplacement of Kilauea pahoehoe lobes, as constrained by in situ field experiments. *Geological Society of America Abstracts with Programs*, **32**(7), A-395.
- Siders, M.A. & Elliot, D.H., 1983. Intraflow variability in the Kirkpatrick basalt, northern Victoria land, Antarctica. *Geological Society of America Abstracts with Programs*, **15**, 687.
- Stephenson, P.J., 1989. Northern Queensland. In: *Intraplate Volcanism in Eastern Australia and New Zealand* (ed Johnson, R.W.), pp. 89-97, Cambridge University Press, Cambridge.
- Stephenson, R. & Lambeck, K., 1985. Erosion-isostatic rebound models for uplift: an application to southeastern Australia. *Geophysical Journal of the Royal Astronomical Society*, **82**, 31-55.
- Subbarao, K.V. & Sukheswala, R.N., 1981. *Deccan Volcanism and Related Basalt Provinces in other parts of the World. Memoir- Geological Society of India*, **3**, Geological Society of India, Bangalore, 474 p.
- Sutherland, F.L., 1981. Migration in relation to possible tectonic and regional controls in eastern Australian volcanism. *Journal of Volcanology and Geothermal Research*, **9**, 181-213.
- Sutherland, F.L., 1998. Origin of north Queensland Cenozoic volcanism: Relationships to long lava flow basaltic fields, Australia. *Journal of Volcanology and Geothermal Research*, **103**(B11), 27,347-27,358.
- Sutherland, F.L., Raynor, L.R. & Pogson, R.E., 1994. Spinel to garnet lherzolite transition in relation to high temperature palaeogeotherms, eastern Australia. *Australian Journal of Earth Sciences*, **41**, 205-220.
- Swanson, D.A., Wright, J.H. & Helz, R.T., 1975. Linear vent systems and estimated rates of magma production and eruption of the Yakima basalt on the Columbia Plateau. *American Journal of*

Science, 275, 877-905.

- Thordarson, T. & Self, S., 1998. The Roza Member, Columbia River Basalt Group: A gigantic pahoehoe lava flow field formed by endogenous processes? *Journal of Geophysical Research*, 103(B11), 27,411-27,445.
- Veevers, J.J., Powell, C.M. & Roots, S.R., 1991. Review of seafloor spreading around Australia, I. Synthesis of the patterns of spreading. *Australian Journal of Earth Sciences*, 38, 373-389.
- Vogel, D.C. & Keays, R.R., 1997. The petrogenesis and platinum-group element geochemistry of the Newer Volcanic Province, Victoria, Australia. *Chemical Geology*, 136, 181-204.
- Walker, G.P.L., 1993. Basaltic-volcano systems. In: *Magmatic Processes and Plate Tectonics* (eds Prichard, H.M., Alabaster, T., Harris, N.B.W. & Neary, C.R.), pp. 3-38, Geological Society of America.
- Walker, G.P.L., 2000. Basaltic volcanoes and volcanic systems. In: *Encyclopaedia of Volcanoes* (eds Sigurdsson, H., Houghton, B.F., McNutt, S.R., Rymer, H. & Stix, J.), pp. 283-289, Academic Press, San Diego.
- Watkins, N.D., Gunn, B.M. & Coy-yll, R., 1970. Major and trace element variations during the initial cooling of an Icelandic lava. *American Journal of Science*, 268, 24-29.
- Wellman, P. & McDougall, I., 1974. Cainozoic igneous activity in eastern Australia. *Tectonophysics*, 23, 49-65.
- Wentworth, C.K. & Macdonald, G.A., 1953. Structures and forms of basaltic rocks in Hawaii. *U.S. Geological Survey Bulletin*, 994, 98 p.
- Wilmoth, R.A. & Walker, G.P.L., 1993. P-type and S-type pahoehoe: a study of vesicle distribution patterns in Hawaiian lava flows. *Journal of Volcanology and Geothermal Research*, 55, 129-142.
- Yaxley, G.M., Crawford, A.J. & Green, D.H., 1991. Evidence for carbonatite metasomatism in spinel peridotite xenoliths from western Victoria, Australia. *Earth and Planetary Science Letters*, 107, 305-317.
- Zielhuis, A. & van der Hilst, R.D., 1996. Upper-mantle shear velocity beneath eastern Australia: inversion of wave forms from SKIPPY portable arrays. *Geophysical Journal International*, 127, 1-16.
-

CHAPTER 2

CHARACTERISING THE INTERIORS OF PAHOEHOE AND AA LAVAS: AN INVESTIGATION OF EMPLACEMENT AND CRYSTALLISATION PROCESSES

2.1 INTRODUCTION

Unlike many geological processes, we are able to observe basaltic lavas actively erupting and being emplaced (Fig. 2.1). Active basalt lavas have therefore been widely studied, and much is known about the emplacement mechanisms and resultant surface morphologies of these lavas (eg. Macdonald 1953, Greeley 1987, Guest *et al.* 1987, Lipman & Banks 1987, Hon *et al.* 1994, Peterson *et al.* 1994, Calvari & Pinkerton 1998, Kauahikaua *et al.* 1998, Cashman *et al.* 1999). Two end-member types of basalt have been identified primarily based upon emplacement mechanisms: pahoehoe and aa. Pahoehoe lavas propagate by budding out from small toes at the flow front beneath chilled, smooth, low relief surface crusts. Aa lavas are generally emplaced at higher velocities than pahoehoe, and propagate by autobrecciation of the flow front. Talus from the cooled, broken surface crust is dumped over the flow front and falls to the base of the flow. The talus is overridden by lava outwelling from the fluid

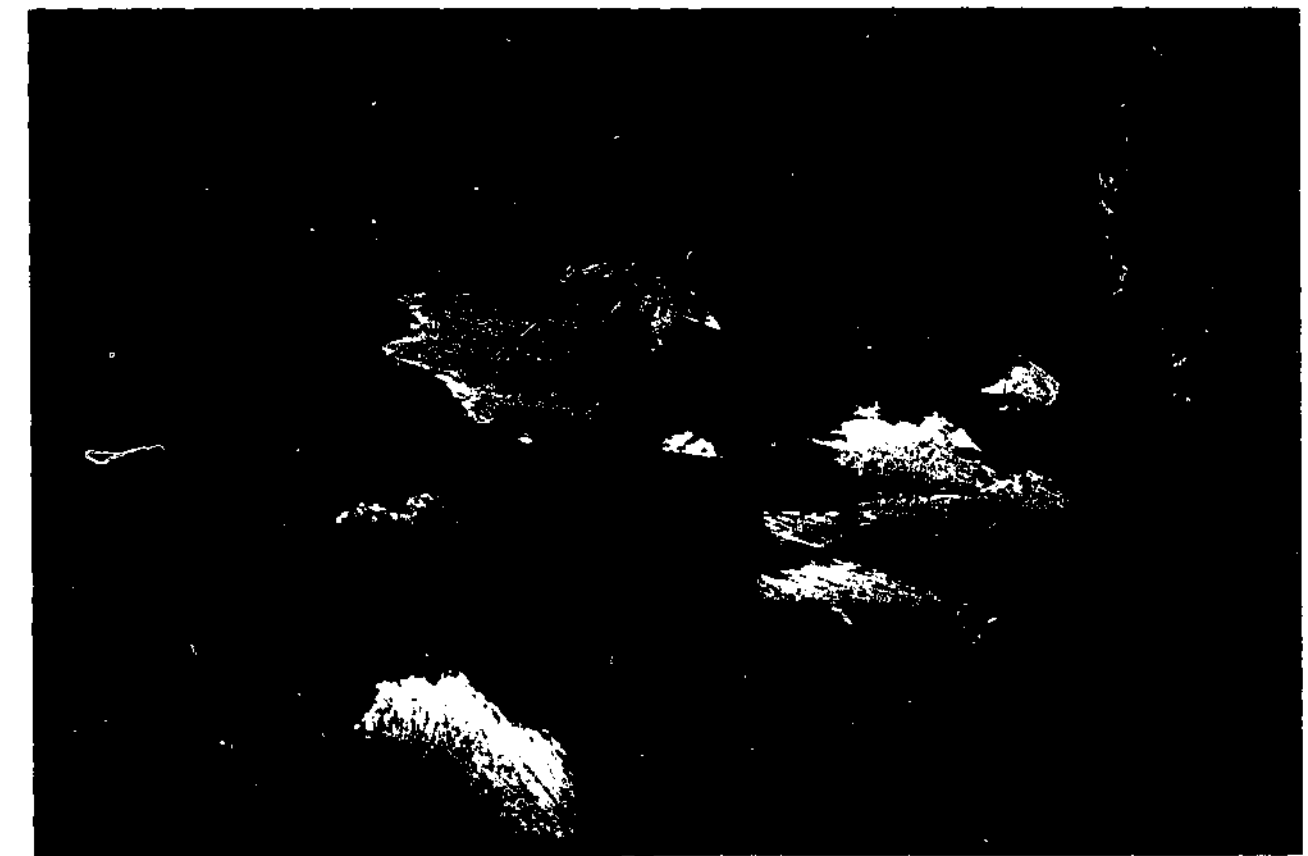


Fig. 2.1 Photograph of pahoehoe lava being emplaced on the island of Hawaii. Note the smooth to roopy morphology of the crust, which initially stretches plastically as more lava is injected beneath it.

inner core, thus producing a fragmented basal layer. Solidified pahoehoe and aa lava flows are primarily distinguished from each other by their different surface morphologies, although the internal structures are known to differ as well. Until recently, few studies have characterised the interiors of solidified basalt flows, despite the fact that commonly only vertical sections through lavas are accessible when studying ancient terrains (eg. road cuttings, diamond drill core etc.).

The internal vesicle distributions through solidified pahoehoe lobes have recently been documented and quantified, in order to understand more about emplacement and crystallisation processes (eg. Long & Wood 1986, Aubele *et al.* 1988, Wilmoth & Walker 1993, Self *et al.* 1996, Cashman & Kauahikaua 1997). Two main types of pahoehoe lobes have been identified on the basis of vesicle and crystal textures: S-type or "spongy" lobes, and P-type lobes (eg. Walker 1989, Wilmoth & Walker 1993). S-type lobes form with minimal inflation and contain spherical vesicles distributed throughout, with a higher concentration in the centre. P-type lobes consist of a dense interior (non-vesicular zone, NVZ or core) surrounded by more vesicular upper and lower margins (upper vesicular zone, UVZ and lower vesicular zone, LVZ), and they may contain pipe vesicles at the base; Fig. 2.2. They form either by inflation of the lobe beneath a chilled crust, or by ponding of the lava in a topographic depression. Vesicle zonation within P-type lobes have been characterised in

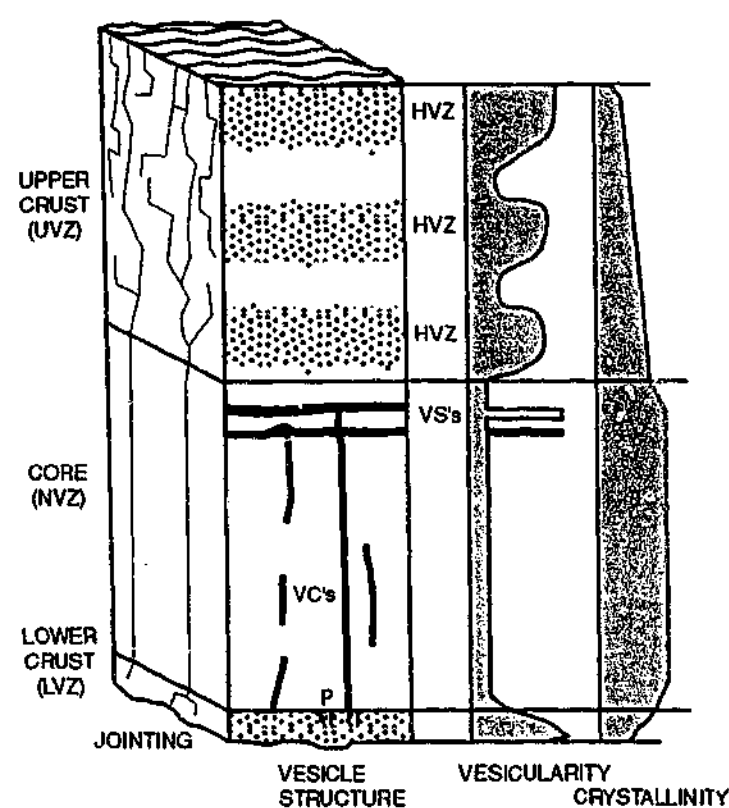


Fig. 2.2 Idealised schematic diagram of an inflated P-type pahoehoe lobe. The lobe is divided into three sections on the basis of vesicle structures, jointing and crystal texture, after Self *et al.* (1998). Abbreviations: UVZ- upper vesicular zone, NVZ- non-vesicular zone, LVZ- lower vesicular zone, HVZ- horizontal vesicle zone, VS- vesicle sheet, VC- vesicle cylinder, P- pipe vesicle (see Table 2.2).

order to distinguish between these mechanisms of formation (Hon *et al.* 1994, Self *et al.* 1996, Cashman & Kauahikaua 1997, Kauahikaua *et al.* 1998). Petrographic textures of pahoehoe and aa flows have previously been compared (Sato 1995, Cashman *et al.* 1999, Polacci *et al.* 1999), however little work has been done to characterise textural and compositional changes throughout individual basalt flows (eg. Watkins *et al.* 1970, Siders & Elliot 1983, Katz 1997, Sharma *et al.* 2000). This is surprising, considering that the textural and compositional zonation through Archaean komatiite lavas are well known (eg. Pyke *et al.* 1973, Arndt *et al.* 1977, Arndt 1986, Turner *et al.* 1986, Renner *et al.* 1994). In this study the vesiculation patterns, petrographic textural zonation and geochemical variations through selected lavas from the Newer Volcanic Province, Victoria and from Hawaii are investigated. In particular, P-type pahoehoe lobes that are considered to have formed by inflation are investigated and compared with aa flows. Inflated P-type pahoehoe lobes were chosen in preference to S-type lobes for this study, in order to gain a better understanding of the inflation process. The relationship of any identifiable petrographic textural and geochemical zonation with vesicle zonation and surface features is investigated. The characterisation of the interiors of inflated P-type pahoehoe lobes and aa flows will lead to a better understanding of the processes occurring beneath the chilled lava crusts, which are not observable in active lava flows.

Much of the data for this study was collected from diamond drill core, taken from the Werribee Plains of the Newer Volcanic Province (NVP) (see Chapter 1, Fig. 2.3a). There are obvious limitations associated with drill core analysis, particularly in a sequence that has experienced prolonged periods of quiescence and weathering throughout its history (Chapter 4). Positive identification of flow unit boundaries is difficult, the morphology of flow tops can be hard to discern, and it is impossible to assess the geometry of flows and lateral variations in vesiculation patterns within flows. Fieldwork was carried out in Hawaii to supplement the data set (Fig. 2.3b). Although the composition of the Hawaiian and NVP basalts are quite different (oceanic tholeiites cf. predominantly continental alkalic basalts), the general processes associated with the emplacement and crystallisation are considered to be comparable. Samples in Hawaii were preferentially collected from outcrops of both historical and recent pahoehoe and aa lavas for which the emplacement history is known, in order to characterise the vesiculation and petrographic textures. These results are compared with and complement the results of the NVP basalt study.

2.2 METHODS

Diamond drill holes in the Werribee Plains have intersected up to 110 m basalt, and only the top 5-25 m of each hole contain lavas that were fed by the exposed eruption centres (Fig. 2.3a). Each of the NVP flows analysed here are labelled according to drill hole name, followed by a letter to distinguish between the different flows from a single drill hole (Table 2.1). See Chapter 4 for a more complete discussion on the stratigraphy of the lavas. More than 50 P-type pahoehoe lobes considered to have formed by inflation, and seven aa flows were identified in diamond drill core (see Table 2.1 for list of flows analysed). Hawaiian samples were collected from road cuttings and cliff exposures (Fig. 2.3b). Two aa lava flows exposed in road cuttings were studied: one from the 1868 eruption of Mauna Loa, and an associated S-type pahoehoe lobe (eg. Silliman & Dana 1868, Lockwood & Lipman 1987), and one from the 1955 eruption of the east rift zone of Kilauea (eg. Macdonald & Eaton 1964). Three inflated P-type pahoehoe lobes were investigated: two prehistoric flows from within the Hawaii Volcanoes National Park and one lobe exposed in the sea cliff at Kalapana from the 1990-1991 eruption of the east rift zone of Kilauea (eg. Heliker *et al.* 1998). The pre-historic flows are considered to have been erupted from within the vicinity of Kilauea caldera between 200-750 years B.P. and 400-750 years B.P. respectively (Wolfe & Morris

Table 2.1 List of all flows analysed in this study, and the depths of the flows in drill core.

	Flow name	Depth of NVP flows (m)	Vesicularity quantified	Petrography	Geochemistry
NVP pahoehoe lobes	DER7A	63.5	Y		
	KOR15A	9.0	Y	Y	Y
	KOR15B	28.5	Y	Y	Y
	KOR15C	35.0	Y		
	KOR16A	4.5	Y	Y	
	KOR16B	15.5	Y		
	PYW7A	15.5	Y		
	PYW7B	23.0	Y		
	PYW7C	46.0	Y		
	TAR12A	17.0	Y		
TAR12B	27.5	Y			
NVP aa flows	DER7B	37.0	Y	Y	Y
	KOR15D	55.5	Y		
	KOR16C	36.0	Y		
Hawaiian pahoehoe lobes	HAW-CCD		Y	Y	Y
	HAW-HPR		Y	Y	
	HAW-KAL		Y	Y	
	HAW-MAU1		Y	Y	
Hawaiian aa flows	HAW-HWY 1		Y		
	2		Y		
	3		Y	Y	Y
	HAW-MAU2		Y	Y	

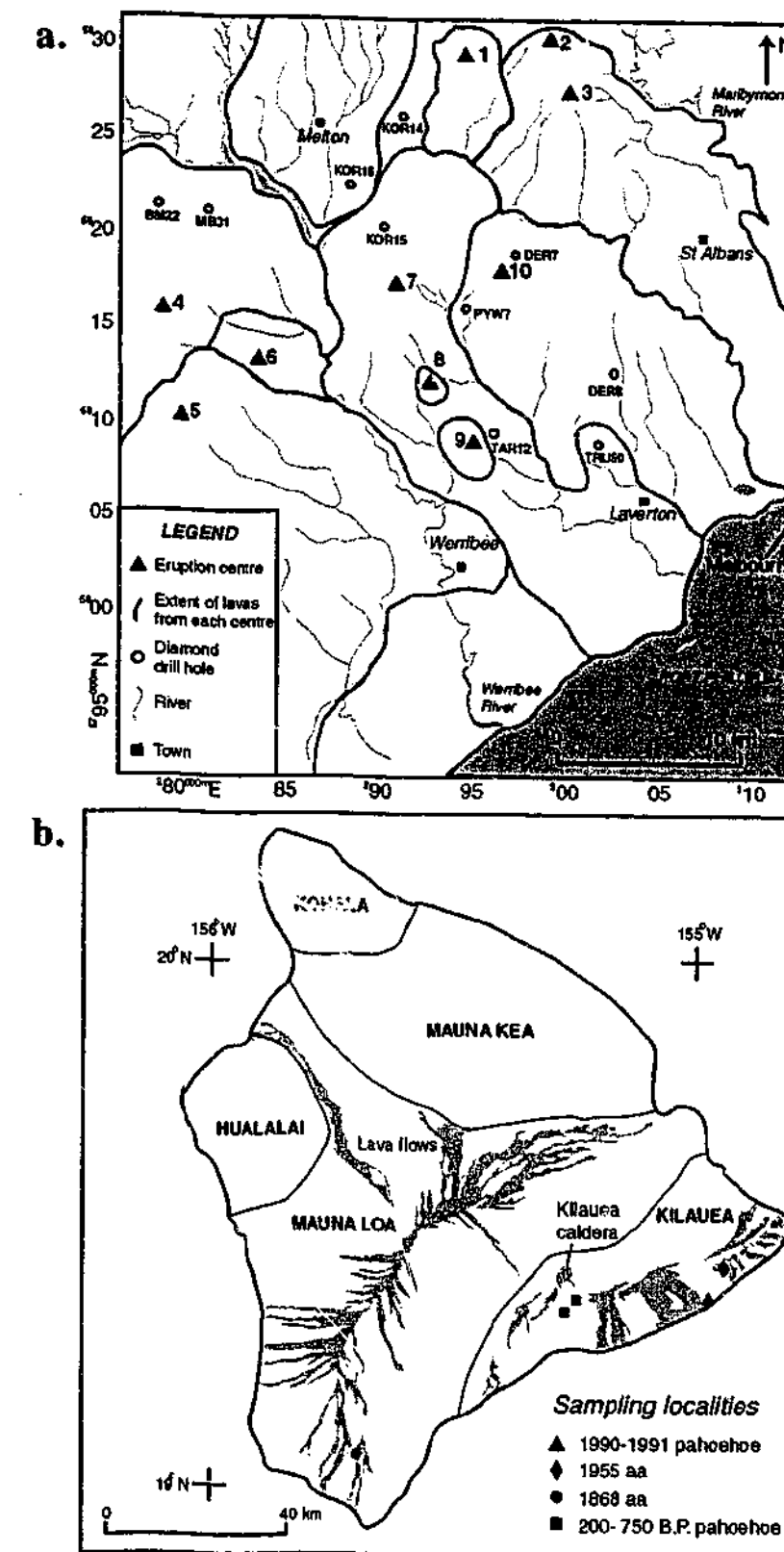


Fig. 2.3 Sampling locality diagrams. a. The diamond drill hole distribution in the Werribee Plains in relation to the exposed volcanic centres: 1- Mt. Kororoit, 2- Ryan's Hill, 3- Stony Hill, 4- Spring Hill, 5- One Tree Hill, 6- Green Hill, 7- Mt. Cottrell, 8- Greek Hill, 9- Black Hill, 10- Mt. Atkinson. See Chapter 1 for the location of the Werribee Plains. The extent of the lava flows from each centre is constrained by the stratigraphic studies (Chapter 4). b. Five major volcanoes make up the island of Hawaii. The distribution of historic lava flows from Mauna Loa and Kilauea are shown, with the sampling localities. Two prehistoric lava flows were sampled, and although they are considered to have been erupted from within the vicinity of Kilauea caldera, their extent is poorly constrained and not shown.

1996). The Hawaiian flows are all labelled with a prefix HAW- to distinguish them from flows from the NVP (eg. Table 2.1).

Flow units were identified (section 2.3.1) and the distribution of vesicles and segregation structures within each flow unit was sketched and qualitatively described. The vesicle distribution was quantified in selected flow units that were considered to be complete (ie. lacked evidence of significant weathering and/or erosion). A transparent, plastic grid was overlain on the core, and point counting yielded the total vesicle area fraction (%). The total number of vesicles within the grid area (divided by the area) gave the number density. The mean diameter of the ten largest vesicles yielded the maximum vesicle size (mm). Thin sections were made at regular intervals through selected complete pahoehoe and aa flow units, and petrographic textures analysed. For reasons given in section 2.3.3 this study focuses on groundmass textures. Variations in the mineralogy and texture of the groundmass through the flows were systematically recorded, both qualitatively and quantitatively. Point counting (400 counts per section) gave the overall proportion of each of the groundmass minerals, volcanic glass, phenocrysts and vesicles in each section. The average grain-size of each groundmass mineral was determined by the mean of the measurements of 16 grains of a particular mineral per section (using the cross-hairs). The longest dimension of each mineral was measured. The methods used to quantify vesicularity, mineral sizes and mineral proportions were repeated multiple times on a given sample to test reproducibility. Relative errors were determined (shown as error bars on relevant figures) based upon the standard deviation from the mean value obtained from multiple counts. Areal number densities (N_a) of all groundmass minerals (ie. the number of crystals per unit area) were calculated by combining the grain-size and mineral abundance data according to:

$$N_a = \phi / \pi r^2 \quad 2.1$$

OR
$$N_a = \phi / l * w \quad 2.2$$

where ϕ is the area fraction of the mineral in the groundmass (normalised for vesicle-free rocks) and r is the average radius of the grain, assuming equant grain shapes. To calculate N_a for plagioclase laths and elongate opaque rods equation 2.2 was used, where l and w are the average length and width respectively of a mineral. Bulk rock x-ray fluorescence (XRF) analyses were made in some flow units at positions corresponding to thin section samples. Some of the samples were analysed as fused disks for major and trace elements at Melbourne

University, and some for major elements at the University of New South Wales (see Appendix A for outline of methods). Pressed powder pellets were used for trace element analysis at the University of New South Wales (Appendix A). Geochemical analyses were repeated multiple times on the same fusion buttons for each of two samples in order to check the relative precision of the analytical technique. Acceptable error levels for all geochemical analyses are fixed values of 0.1% for SiO_2 , 0.05% for the remainder of the major elements, and trace elements have an error of 1% of a given trace element value.

2.3 RESULTS

2.3.1 Identifying flow unit boundaries

The smallest coherent package of lava is a lobe (Self *et al.* 1998). This term is synonymous with flow unit or vesiculation unit: a package of lava that has experienced a unique cooling history. Pahoehoe flow units contain upper and lower chilled margins, in which vesicles are the smallest. Inwards there is a general increase in vesicle size (Wilmoth & Walker 1993). Although pahoehoe flow tops may contain ropy structures these are relatively low relief, and in a sequence of pahoehoe lobes the contact between each is generally planar, and identifiable by the presence of chilled margins and vesicle zonations as described. Identifying the contacts between pahoehoe flow units was relatively straightforward in the outcrops observed in Hawaii, using these criteria (Fig. 2.4a). The flow units studied are generally the uppermost lobe within a sequence, are lobate in vertical section, and aspect ratios (Vertical/Horizontal) range from 0.20-0.40. The glassy chilled margins are preserved to a limited extent in the lavas of the NVP, and contacts between flow units are identified by the vesicle zonations: an abrupt change in size, shape and overall vesicularity. This often occurs as a general decrease in vesicle size with depth overlying a sharp, planar contact with the drill core containing a general increase in vesicle size locally. For the scope of this study pahoehoe flow units that have a planar, conformable upper contact are considered to be complete, even when the chilled margin is not preserved. Each flow unit studied petrographically occurs in the centre of a package of lobes (3-5 lobes), 20-30 m thick. Pahoehoe flow units exposed in outcrop in the Werribee Plains (in quarries) generally have a sheet-like morphology, and the average aspect ratio is calculated to be less than 0.20.

The crusts of aa lava flows consist of 'jumbles of rough, clinkery and spinose fragments' (Williams & McBirney 1979), produced through autobrecciation during emplacement. The lava fragments that make up both the irregular upper and basal crusts

The upper crust always grades down into a dense lava core, which overlies a basal fragmental layer. The upper and lower fragmental crusts each range in thickness from 10's of centimetres to metres. Individual aa lobes were identified in Hawaii by the presence of their dense lava cores. The aspect ratios (V/H) of the aa lobes studied are 0.07-0.10, and these values are less than the aspect ratios of pahoehoe lobes because the aa channels are significantly wider than the pahoehoe lobes (45-70 m cf. 5-10 m). In drill core aa flows are identified by the presence of upper and lower fragmental zones of clinkery clasts around a dense core. Each of them are bounded above and below by paleosoils. No aa flows have been identified in outcrop in the Werrabee Plains, hence it is not possible to constrain lateral dimensions of the flows identified in drill core.

2.3.2 Vesicle zonation

Pahoehoe

The vesiculation trends of a number of inflated P-type pahoehoe lobes have been quantified (Fig. 2.6). All of the lobes can be subdivided into an UVZ, NVZ and LVZ (Table 2.2). The vesicles in the UVZ are generally spherical to slightly irregular in shape, and they are not commonly interconnected. Although there are large variations in size and proportion of vesicles within a given UVZ, locally the vesiculation patterns are relatively homogeneous (Fig. 2.5a). Generally the lobes demonstrate a decrease in overall vesicularity and number density towards the base of the UVZ, and a small increase in vesicle size. A striking feature that occurs in about half of the flow units observed is the presence of horizontal vesicle trains toward the base of the UVZ, and these have not previously been documented. Vesicle trains occur as either (i) a spherical vesicle outline with a sub-horizontal elongate tail trailing behind it (a void up to a few cm long) or (ii) a series of slightly elongate vesicles in a line, commonly interconnected (Fig. 2.5b). Zones of vesicle trains range from ~0.1-2 m in thickness. The zones contain numerous vesicle trains, as well as isolated spherical vesicles and diktytaxitic voids.

Although zones of vesicle trains commonly occur at the base of the UVZ there are some cases where they overlie a zone of spherical vesicles within the UVZ (eg. KOR15A) and in one instance vesicle trains are observed at the top of the LVZ (HAW-HPR, Fig. 2.6). The contact between the vesicle trains and underlying spherical vesicles within the UVZ is relatively sharp in a broad sense, however it is locally gradational, and interpreted to represent a horizontal vesicle zone (HVZ). HVZ's are more easily identifiable in outcrop than drill

Table 2.2 List of terms used throughout the chapter and corresponding definitions (Shelley 1993, Self et al. 1998, Thordarson & Self 1998).

Terms and Abbreviations	Definition
<i>Vesiculation patterns</i>	
UVZ	Upper vesicular zone- corresponds to the upper crust of P-type pahoehoe lobes (Fig. 2.2).
NVZ	Non-vesicular zone- corresponds to the core or centre of P-type pahoehoe lobes.
LVZ	Lower vesicular zone- corresponds to the lower crust of P-type pahoehoe lobes.
HVZ	Horizontal vesicle zone. May occur within the upper crust of inflated P-type pahoehoe lobes. HVZ's are discrete zones of increased vesicularity, and have gradational contacts.
(Horizontal) vesicle trains	Generally are located at or towards the base of the upper crust of inflated P-type pahoehoe lobes. The trains occur as a series of commonly interconnected, spherical to elongate vesicles (generally horizontally oriented).
Pipe vesicles	Occur in the lower crust of some inflated P-type pahoehoe lobes. Roughly cylindrical pipes of near-vertical orientation that are hollow.
Segregation material (including VS's & VC's)	Commonly vesicular, coarsely crystalline material that is typically found in the core of P-type pahoehoe lobes. Segregation material occurs in a variety of geometries (veins, vesicles, sheets (VS's), cylinders (VC's)), but characteristically has sharp contacts with the surrounding basalt.
<i>Petrographic textures</i>	
Porphyritic	Phenocrysts set in a finer-grained groundmass.
Trachytic	The alignment of feldspar laths in volcanic rocks due to laminar flow.
Intergranular	Equant clinopyroxene grains occur interstitial to a plagioclase lath network.
Ophitic	Large clinopyroxene grains are intergrown with and partially to completely enclose plagioclase laths.
Sub-ophitic	Some degree of intergrowth of clinopyroxene and plagioclase is exhibited, yet not a complete enclosing of plagioclase by the clinopyroxene.

core, due to their laterally continuous nature. In outcrop, thin laterally continuous zones of increased vesicularity or locally increased vesicle size were often observed, however these may easily be overlooked in drill core. In drill core changes in size of vesicles are generally observed to be gradational, although this is difficult to illustrate (Fig. 2.6). The base of the UVZ is marked by a decrease in vesicularity, although there is rarely a sharp contact. The normalised UVZ thicknesses of the lobes (ie. UVZ thickness/total flow thickness) range from 0.27-0.75, and average 0.50.

Segregation structures are present in most of these lobes, and are commonly sub-horizontal at the top of the NVZ, and occur as vertical vesicle cylinders at depth in some instances. The segregation veins are thin, vesicular veins generally of more coarsely crystalline material, containing sharp contacts with the surrounding basalt. The veins range from less than 1 to 10 cm thick, and vesicle cylinders have been observed in drill core and outcrop to be

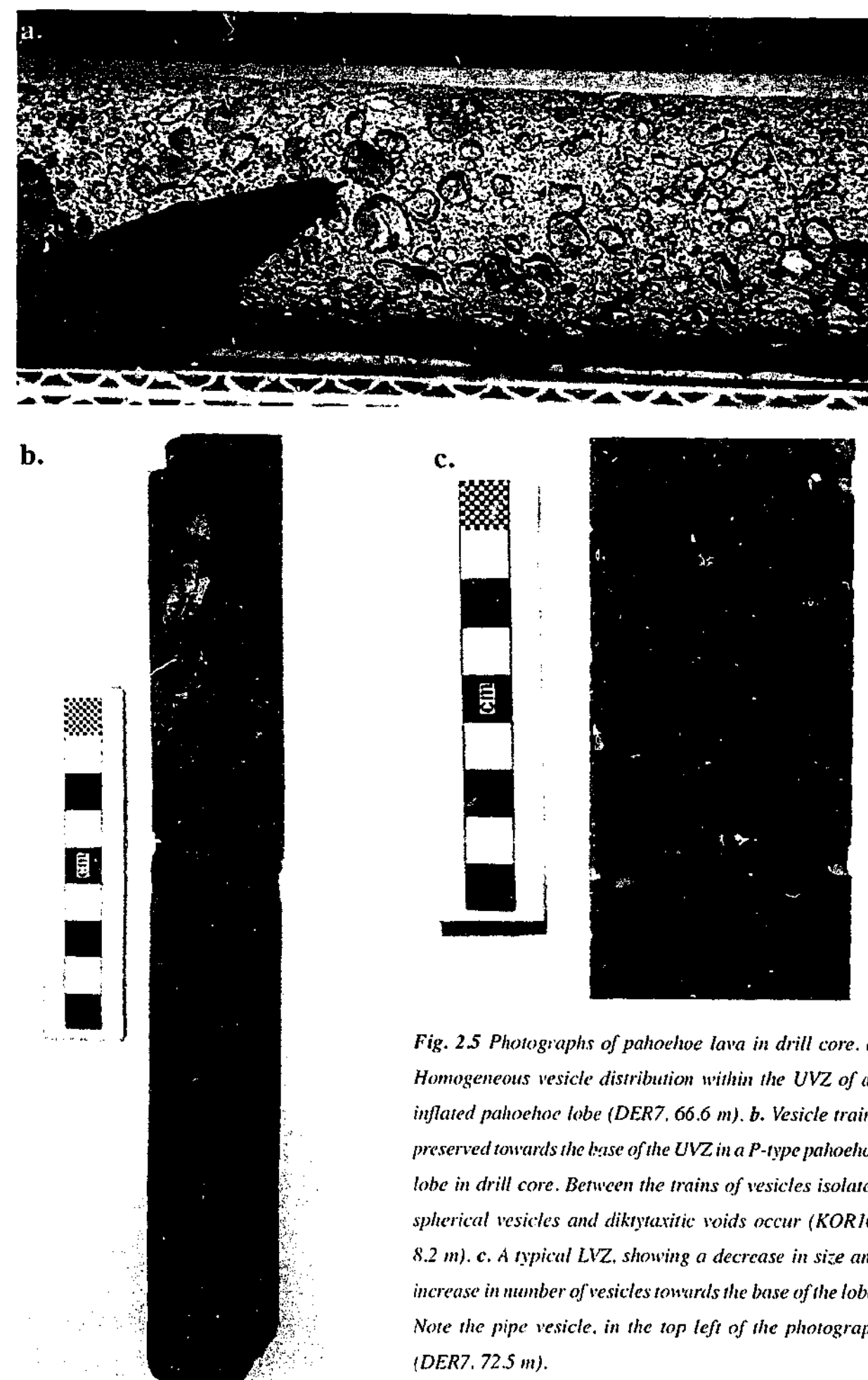


Fig. 2.5 Photographs of pahoehoe lava in drill core. a. Homogeneous vesicle distribution within the UVZ of an inflated pahoehoe lobe (DER7, 66.6 m). b. Vesicle trains preserved towards the base of the UVZ in a P-type pahoehoe lobe in drill core. Between the trains of vesicles isolated spherical vesicles and diktytaxitic voids occur (KOR16, 8.2 m). c. A typical LVZ, showing a decrease in size and increase in number of vesicles towards the base of the lobe. Note the pipe vesicle, in the top left of the photograph (DER7, 72.5 m).

well over 1 m long. The geometries of these structures are not very well constrained in drill core. The contact between the NVZ and LVZ is generally gradational, with a few stray vesicles trapped in the core of the flow. The LVZ ranges from 0.1-0.6 m thick, and averages 0.3 m thick. It generally contains very small, spherical vesicles at the base, which become larger with height (Fig. 2.5c). Larger vesicles commonly range from irregular shapes to diagonally elongate and are sparsely distributed above the base of the flow. Pipe vesicles are vertically elongate voids that are more than ~10 cm long (although an incomplete section may be intersected by the drill core), and these are contained within the LVZ of some flow units (Fig. 2.5c). The distribution of both the size of vesicles and overall vesicularity in the LVZ is generally more heterogeneous than the distribution in the UVZ.

Aa

The aa flows observed occur as relatively thin flows from Hawaii (less than ~5 m), and thick flows from the NVP (more than 10 m) (Fig. 2.8). The Hawaiian flows are more vesicular than those from the NVP which are predominantly non-vesicular, although isolated vesicles occur throughout the flows. The relative thicknesses and vesicularity of aa flows are considered to be related in part to their proximity to vent (Lipman & Banks 1987, Rowland & Walker 1988, Walker 1993). Both of the aa flows from Hawaii are proximal to vent, occurring within 5 km (Fig. 2.3b), whereas for reasons discussed in Chapters 4 & 5 the NVP aa flows are considered to represent a distal facies (probably greater than 10 km from vent). Despite this, similarities were observed between the aa flows analysed. The Hawaiian flows were easily identified as aa in outcrop, due to the clinkery upper and lower surfaces separating a dense core. Both flows studied have eyewitness accounts and have been subsequently studied (eg. Silliman & Dana 1868, Macdonald & Eaton 1964, Polacci *et al.* 1999). Clinkery material is variably agglutinated to the core base, so the base of the flow has irregular relief. Material from the base is commonly entrained into the interior. The aa flows were more difficult to identify in drill core. All three flows identified have palaeosoils developed over the flow, and only one has retained at least some of the clinkery upper fragments (Fig. 2.7a). The main defining feature which is present in all flows is a small rubbly, clinkery zone at the base of the flow. The fragments within this zone generally show evidence of autobrecciation so as to distinguish them from weathered basalt clasts. The clinkery clasts generally have rough, spinose surfaces, and may have a spatter-like appearance. The basal zones constitute a small proportion of the flow, compared with the Hawaiian flows observed, however in each instance they are

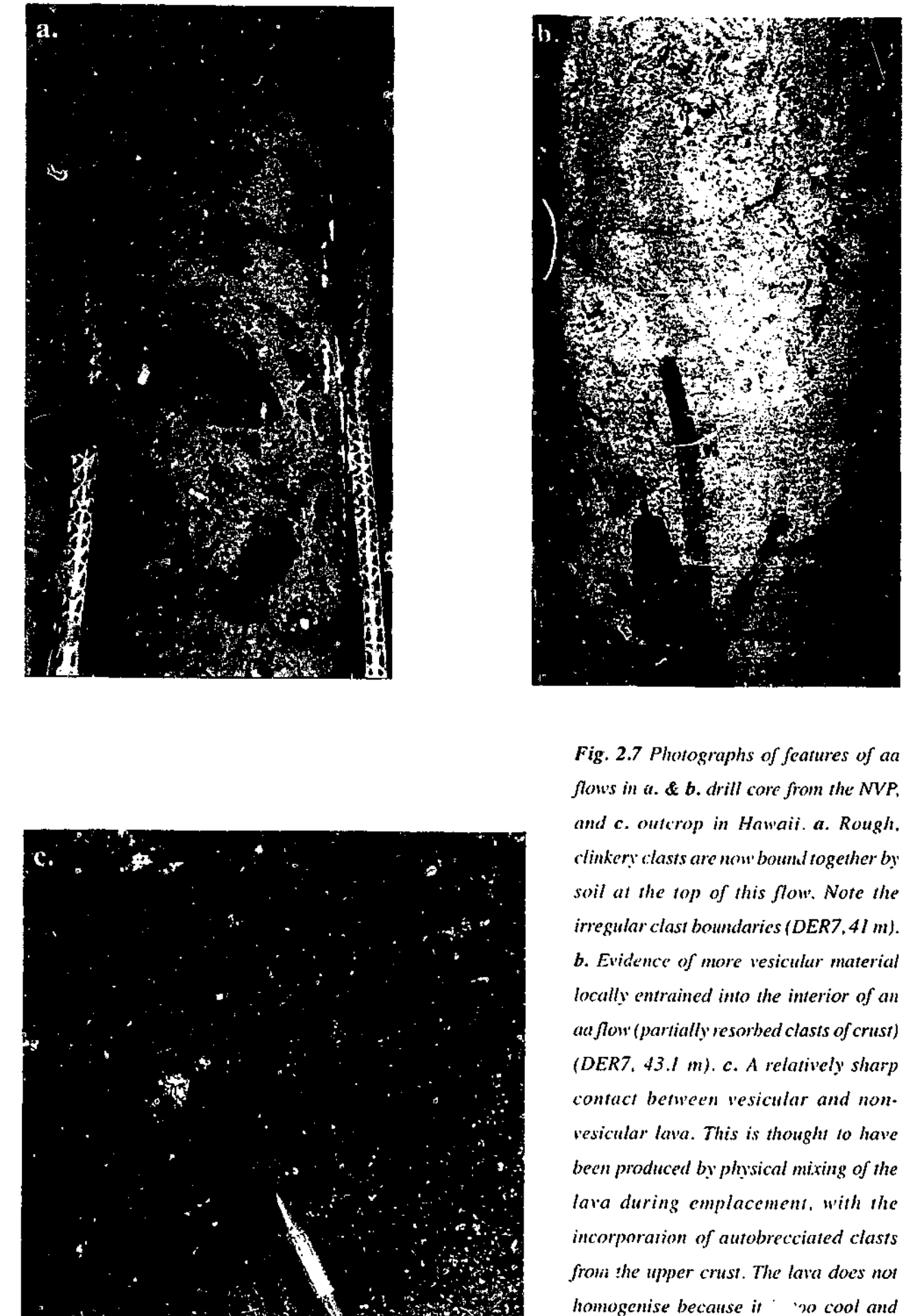


Fig. 2.7 Photographs of features of aa flows in a. & b. drill core from the NVP, and c. outcrop in Hawaii. a. Rough, clinkery clasts are now bound together by soil at the top of this flow. Note the irregular clast boundaries (DER7, 41 m). b. Evidence of more vesicular material locally entrained into the interior of an aa flow (partially resorbed clasts of crust) (DER7, 43.1 m). c. A relatively sharp contact between vesicular and non-vesicular lava. This is thought to have been produced by physical mixing of the lava during emplacement, with the incorporation of autobrecciated clasts from the upper crust. The lava does not homogenise because it is too cool and viscous (HAW-MAU2 and cutting, correct way up).

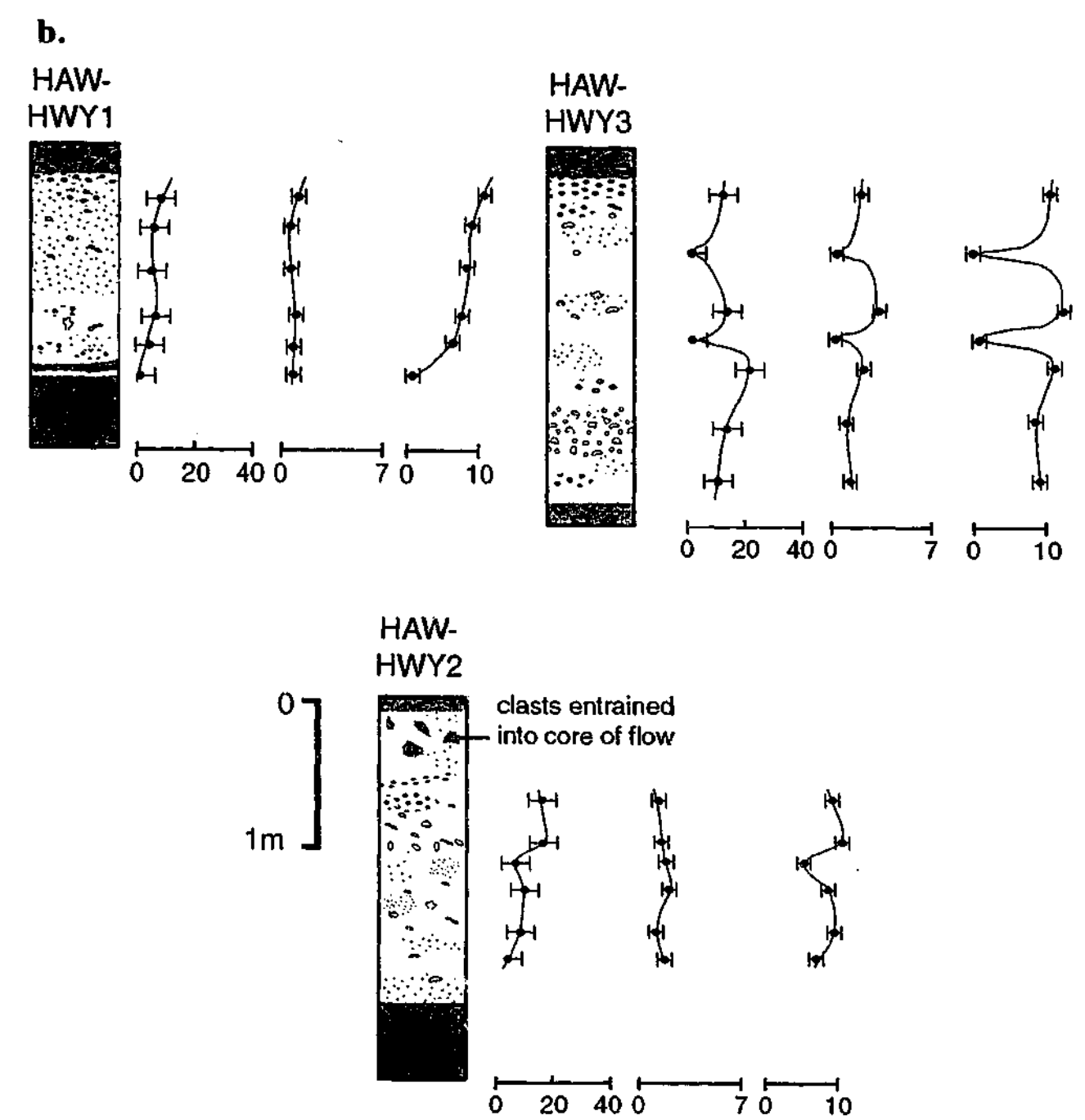
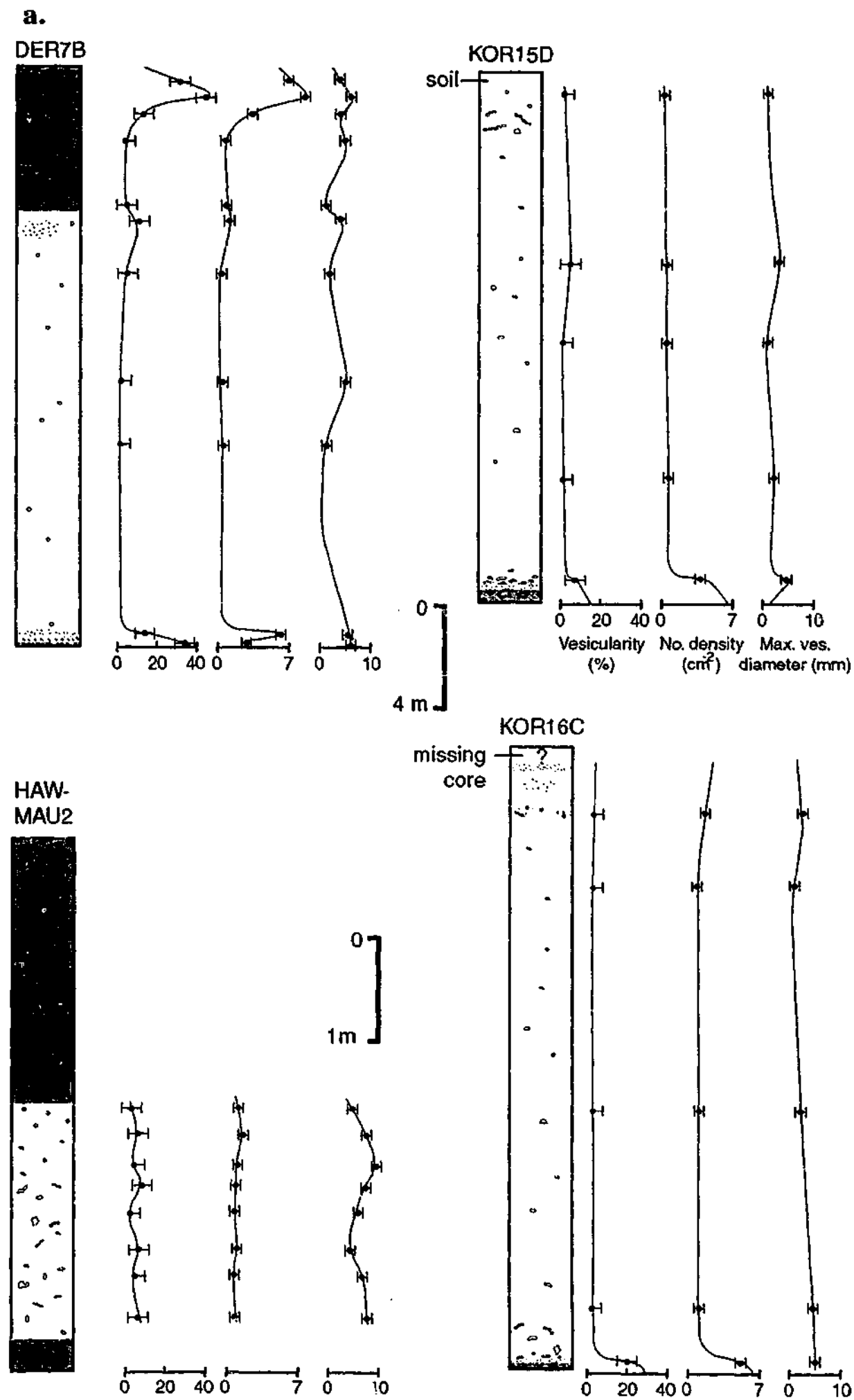


Fig. 2.8 Graphic logs of representative aa flows from a. the NVP and Hawaii, and b. Hawaii, with vesicle zonation trends quantified. Note the heterogeneous vesicle distributions throughout the flows compared with the pahoehoe lobes (Fig. 2.6). Again, the lobes are drawn at different scales in a. & b., and HAW-MAU2 is different again. Refer to Fig. 2.6 for legend.

~0.2-0.5 m thick. Near the tops of the cores of the thick NVP flows locally there are vesicular patches, with relatively sharp contacts with the surrounding core. These pseudo-clastic textures are interpreted to be evidence of the entrainment of more vesicular material into the cores of the flows, rather than being trapped gas bubbles rising from within the core (Fig. 2.7b).

Vesicles, where present in the dense cores of aa flows, are heterogeneously distributed. Unlike P-type pahoehoe lobes, aa flows lack a tripartite zonation; vesicles are distributed

randomly throughout the flows. There are commonly relatively sharp contacts between vesicular and dense basalt (Fig. 2.7c), and within some coarsely vesicular zones there are patches of very finely vesicular material. Locally the vesicular portions may have a spongy appearance, with numerous small round vesicles between large, irregular shaped vesicles (often elongate and rarely spherical). This bimodal size distribution is not uncommon in the aa flows observed (cf. relatively homogeneous size distribution in pahoehoe flows). Bands of vesicles that are elongate and sub-parallel preserve the local direction of motion of the lava prior to solidification. These are not to be confused with vesicle trains observed in pahoehoe lobes. The elongate vesicles observed in aa flows are discrete, sheared bubbles cf. a series of these in the pahoehoe lobes, and they lack the interstitial spherical bubbles and diktytaxitic voids. Often a 'swirly', concentric arrangement of bubbles is preserved suggesting either irregular, non-laminar flow conditions, or the ductile folding of laminar flow layers. These patterns are in stark contrast to the continuous, linear horizontal vesicular zones preserved in pahoehoe flow units. Even in the very thick flows there is no evidence of any post-emplacment bubble rise. Unlike most of the P-type pahoehoe lobes there is no evidence of any segregation veins in the aa flows.

2.3.3 Petrographic textural variations through flow units

Six pahoehoe flow units inferred to have formed by inflation were sampled for petrographic studies, three from the NVP (~6.5-11 m thick) and three from Hawaii (~1-2.5 m thick), Table 2.1, Fig. 2.9. Three aa flows have been studied petrographically, one from the NVP (~22 m thick) and two from Hawaii (~2.5-3 m thick), Table 2.1, Fig. 2.11. A small pahoehoe S-type lobe associated with the aa flow from the Mauna Loa 1868 eruption was also analysed (~0.4 m thick). The aim of this study is to investigate cooling and crystallisation processes that occur in basaltic lavas during and after emplacement. Phenocrysts characteristically are formed prior to eruption, and the size, mineralogy and abundance of phenocrysts in a lava flow is a function of the pre-eruptive history of the magma (eg. Ho & Garcia 1988, Baker *et al.* 1996, Garcia 1996, Kuritani 1999). The flows studied here contain widely varying phenocryst populations, making it difficult to compare them. Although the phenocrysts would have had some effect on the cooling rates of the lavas, the groundmasses of the lavas are considered to have preserved a more complete cooling history. Variations in the abundance of phenocrysts through the flows are documented in section 2.3.4, and the major focus in this section is the differences in groundmass textures. Phenocrysts are

distinguished from the groundmass minerals as they are commonly euhedral to subhedral, are generally significantly larger than the groundmass, and are not intergrown with other minerals. Qualitatively, the sizes of phenocrysts were not observed to vary substantially or systematically throughout individual lobes.

Each of the Hawaiian lava flows and one of the NVP lavas (KOR16A) sampled are tholeiitic in composition, and the remainder that underwent petrographic studies are alkalic. All samples (apart from chilled margins) are dominated by plagioclase laths, and contain clinopyroxene and opaque phases. Where olivine or orthopyroxene minerals are present in the groundmass they are generally an equivalent size to the clinopyroxene, and occur in relatively minor quantities. For simplicity these minerals are thus included with clinopyroxene hereafter. Variations in size and proportion of the groundmass minerals are quantified (Figs. 2.8 & 2.10), and some groundmass textural features are documented. The relationship between the groundmass plagioclase and clinopyroxene is documented as intergranular (I), ophitic (O), or sub-ophitic (S-O) (Table 2.2, Figs. 2.8 & 2.10). It is important to note that no distinction is made in this classification about the glass content of the groundmass: these textural terms are only used to describe the relationship between plagioclase and clinopyroxene. Variations in the glass content are shown graphically, and in some instances the original volcanic glass has devitrified or been altered. Dusty zones containing very fine opaques occur interstitial to plagioclase laths in some pahoehoe samples, and are interpreted to once have been volcanic glass. In these cases opaques that have crystallised directly from the melt are distinguishable from the other opaques as they are coarser, and are not confined to the interstices, but extend and interact with other minerals (Fig. 2.10c). Opaque minerals in basalts occur as suboctahedral, tabular grains or elongate rods and needles. The morphology and overall orientation of the opaque minerals in each sample are documented on the graphs showing the variations in mineral abundances.

The deduction of the true 3-D grain-size distribution from measurements on 2D sections are problematic because (i) larger grains are statistically more likely to be sampled by the thin section than smaller grains, and (ii) thin sectioning will produce a complete spectrum of lengths ranging from the true grain dimension to infinitesimally small dimensions. These two effects have been found in most distributions to cancel each other out, producing distributions in 2-D that are representative of the true 3-D distribution (Jerram 1996). See section 2.2 for error calculation methods. The mineral abundances are given as the proportion of each mineral within the groundmass (phenocrysts and vesicles are not included).

Pahoehoe

The pahoehoe lavas studied consistently demonstrate a smooth change in grain-size of all groundmass minerals, coarsening towards the centre of the flows and fining towards the margins (Fig. 2.9). See Appendix B for all petrographic measurements, and the positions and names of the individual samples within the flows. Of all the minerals clinopyroxene demonstrates the most dramatic change in grain-size, as observed in the thicker flows from the NVP. Grain-size variations are not as marked in the thinner Hawaiian flows studied, however the margins consistently contain finer minerals than the interiors. Although the minerals in the core of the lobes are coarser than those in the upper and lower crusts, interestingly no sharp change in grain-size is observed at the UVZ-NVZ boundary, distinguishing between the upper crust and the core of the flows (cf. komatiites; see Chapter 6). This suggests that perhaps the cooling regime at the base of the crust and top of the core of the flow are similar, and that no other processes occur during emplacement and crystallisation to modify the morphology of the crystals of these two zones. The minerals in the interiors of the thicker flows from the NVP are coarser than those in the Hawaiian flows observed, however there is not a consistent relationship between flow thickness and grain-size (ie. KOR15B is the thinnest of the NVP pahoehoe flows studied, yet contains the coarsest minerals.)

The pahoehoe flows are texturally variable both within a single flow, and between different flows (Fig. 2.9). All flows contain phenocrysts throughout; marginal samples are all porphyritic, demonstrating a significant difference in grain-size of the phenocrysts and groundmass minerals, and some samples from the interiors of the flows are porphyritic and some are not. Groundmass textures are broadly homogeneous within a given sample; the sizes of each mineral are generally fairly even, and apart from locally aligned plagioclase laths (locally trachytic zones), minerals are generally randomly oriented. While the local trachytic zones are not a dominant feature within a given sample, they occur at all intervals through the pahoehoe flows, and in fact are one of the most consistent features observed (Fig. 2.10a). All of the Hawaiian pahoehoe flows observed are sub-ophitic throughout (Fig. 2.10c & d). In contrast, the NVP pahoehoe flows vary from containing intergranular groundmass textures throughout (KOR15A, Fig. 2.10a), to ophitic- sub-ophitic textures throughout (KOR15B, Fig. 2.10b), to having a combination of all three textures (KOR16A). Rods and needles are the dominant opaque mineral morphology observed within the pahoehoe flows, and these are commonly randomly oriented. In some cases the rods occur parallel to each other locally (Fig. 2.10c). Each of the Hawaiian flows contain sets of parallel opaque rods in

the interiors, and although all the NVP flows show some evidence of this feature it is much more rarely observed. Interestingly, these sets of parallel opaque minerals are not necessarily parallel to a locally trachytic texture, suggesting the minerals were not necessarily aligned during flow, but may have crystallised in these orientations (see section 2.4.2). Tabular, suboctahedral grains are observed at the margins of some of the flows and also in the interiors (NVZ's) of the two thickest flows studied (KOR15A and KOR16A).

The tholeiitic flows contain a consistently higher glass content than the flows that are alkalic in composition. At least one chilled margin has been sampled from most flows, and the glass content decreases dramatically from the chilled margin into the interior of each flow. Corresponding to the decrease in glass content is a sharp increase in the content of the other groundmass minerals. In the thinner Hawaiian flows the concentration of each of the groundmass minerals is fairly constant throughout each of the interiors. In the thicker NVP flows there is a gradual increase in the plagioclase content towards the centre of the flow, a corresponding decrease in the opaque mineral content, and the clinopyroxene content fluctuates but is generally fairly constant.

Five out of six of the inflated pahoehoe flows sampled contain segregation veins (ie. late-stage, residual melt crystallised to form veins within the NVZ, with sharp contacts with the surrounding basalt) (Fig. 2.6). Thin sections were made of three of these veins (from KOR16A, KOR15B & HAW-CCD). Each of the segregation veins contain minerals that are significantly more coarse grained than those in the surrounding groundmass. Elongate opaque rods and needles are abundant in each of them, and in one vein these occur in parallel sets that appear to cross-cut all other minerals. Glass is a dominant feature in one of the veins, whereas another is well crystallised and contains a sub-ophitic texture. The other vein is intermediate between these two and locally contains very fine-grained opaque-rich portions, particularly around the vesicles, however it also contains coarse, elongate plagioclase and pyroxene. All of the veins have phenocrysts incorporated within, and contain abundant relatively large vesicles, compared with the surrounding non-vesicular groundmass. The margins of the veins generally appear sharp mesoscopically (except for the vein in HAW-CCD) however microscopically the contact between the vein and surrounding groundmass minerals is always locally diffuse. Segregation vesicles (ie. late-stage, residual melt crystallised within vesicles) are also common in these flows and again five out of six of the inflated pahoehoe flows contain these in the UVZ. Four of the LVZ's contain segregation vesicles as does the interior of the S-type lobe sampled (HAW-MAU1). Segregation vesicles are characteristically opaque-

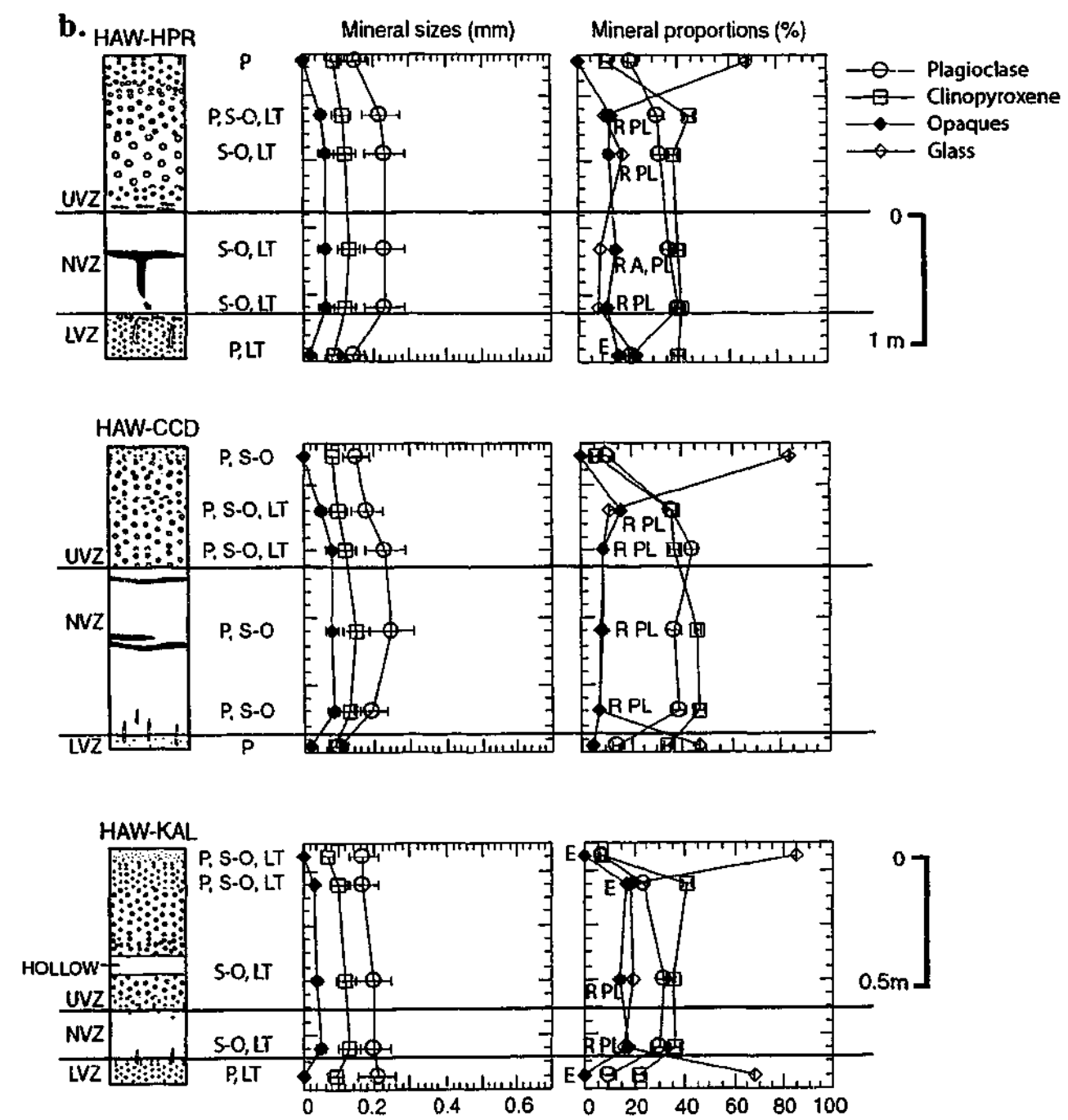
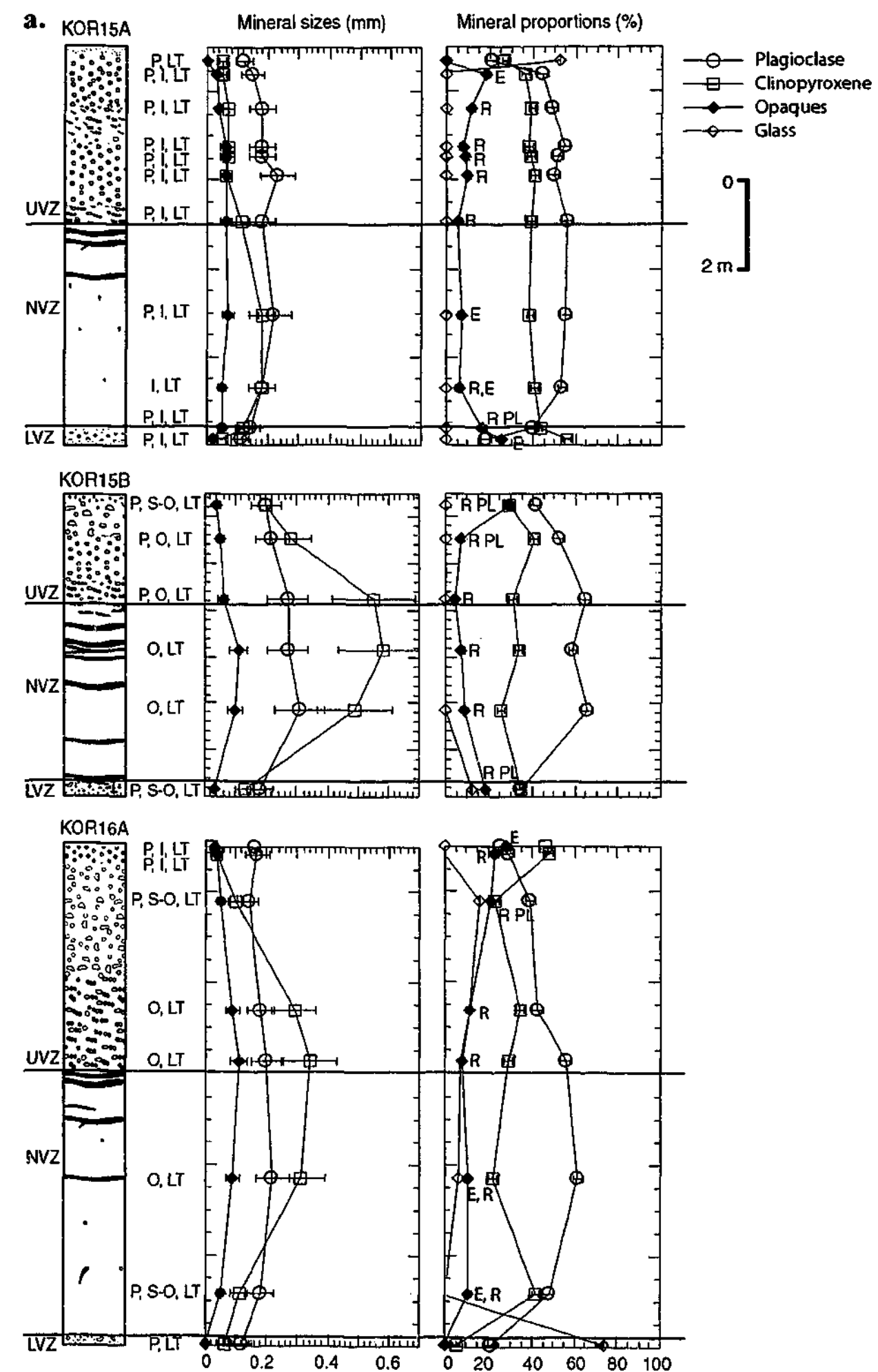


Fig. 2.9 Variations in grain-size and mineral abundances are shown beside graphic logs of pahoehoe flows from a. the NVP, and b. Hawaii. Textural characteristics of each sample are given: P-porphyrritic, I-intergranular, SO-sub-ophitic, O-ophitic, T-trachytic, LT-locally trachytic. Adjacent to the opaque grain abundances, the dominant morphology of the opaques in that sample is given: E-equant, tabular or R-rods, needles, and where the distribution through the groundmass is not random, it is given as: A-aligned or P-parallel. See text for further discussion.

rich. The opaques may be coarse, elongate rods or fine-grained and disseminated. Similarly the other minerals associated (plagioclase and pyroxene) may be coarser or finer than the surrounding groundmass, however high aspect ratio, skeletal morphologies are common. Glass is present in some cases. The segregation material may completely infill a vesicle, or may just line the margin and extend into the groundmass (Fig. 2.10d). The contact between the segregation material and the groundmass ranges from very sharp to diffuse.

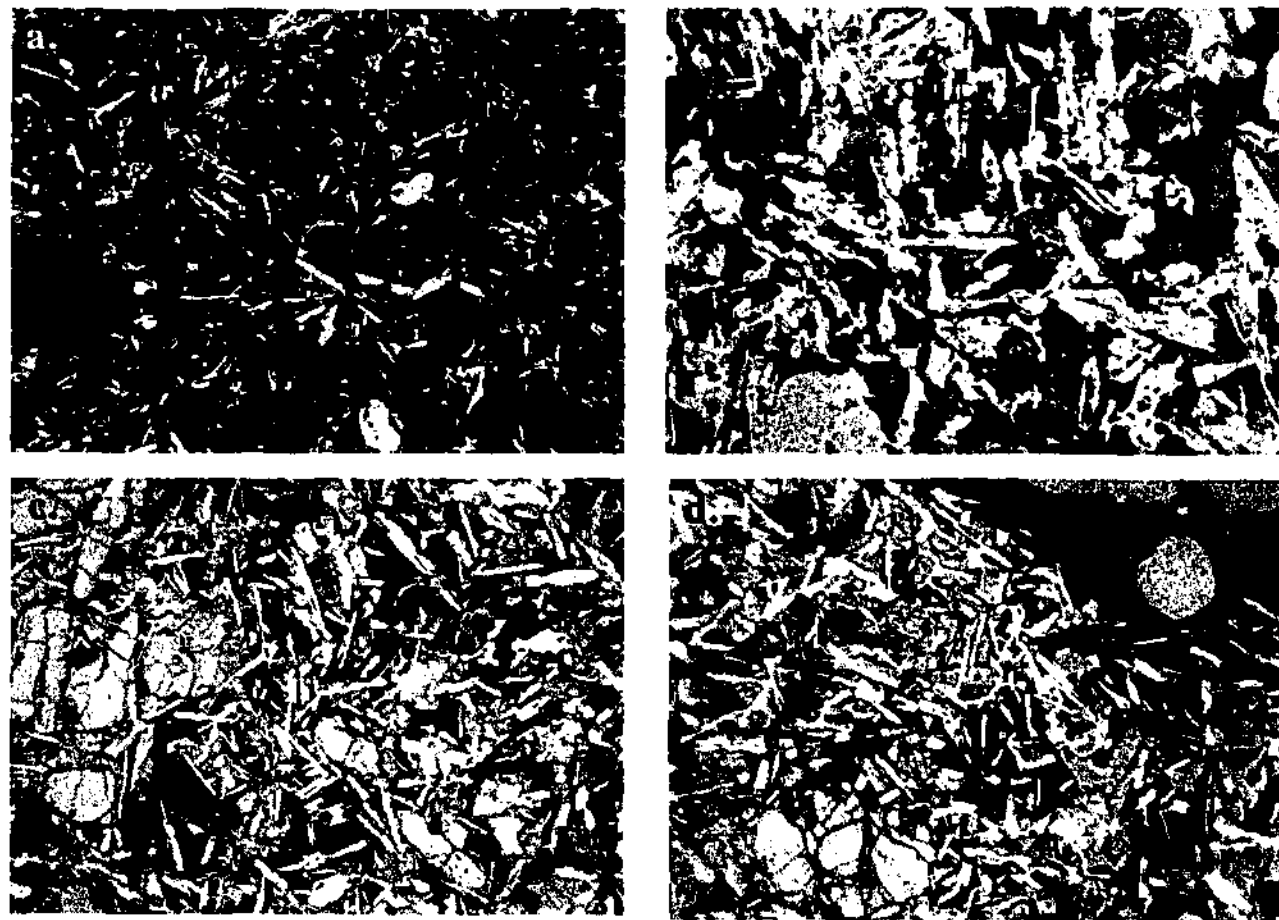


Fig. 2.10 Textural photomicrographs of representative pahoehoe textures observed. The field of view for all photos is 2.5 mm. a. Intergranular pahoehoe, containing fine clinopyroxene and opaques interstitial to a plagioclase lath network. Note that the texture is locally trachytic (K1503, crossed polars- XPL). b. Ophitic pahoehoe texture, with intergrown plagioclase and pyroxene grains. Small microphenocrysts and elongate opaque rods are also dispersed throughout (K1515, plane polarised light- PPL). c. Sub-ophitic pahoehoe groundmass, with some evidence of plagioclase and pyroxene intergrowth. Opaque rods are locally parallel, and can be distinguished from the dark, dusty zones in the groundmass interstices, that were once volcanic glass (CCD2, PPL). d. Sub-ophitic pahoehoe groundmass, with part of a large pyroxene phenocryst evident in the bottom left corner. The top right of the photo is the margin of a segregation vesicle, characteristically opaque-rich, and in this case very fine-grained (HPR2, PPL).

Aa

Unlike the grain-size variation trends in pahoehoe flows, the aa lavas exhibit remarkably constant grain-sizes throughout each of the flows (Fig. 2.11). The one exception is the thick aa flow from the NVP, which has much coarser grained clinopyroxene in the interior of the core than the margins. Apart from this, plagioclase laths are consistently the coarsest mineral in each flow, opaques are the finest, clinopyroxene grains are intermediate in size between the two, and each of these minerals is a constant size throughout (within error). All samples from the aa flows are porphyritic, containing large phenocrysts in a much more fine-grained groundmass. Groundmass textures are more heterogeneous than textures in pahoehoe samples, particularly local grain-size variations (Fig. 2.12c & d). Domains of material that are more fine-grained than the rest of the groundmass have been located in the core of each of the flows. The domains vary in shape and size, however they all tend to have diffuse contacts with the surrounding groundmass minerals. The contacts between the finer material and the remaining groundmass are not planar but irregular, and suggest a degree of mixing or fluidal interaction between the two. These domains are interpreted to have cooled more rapidly than the surrounding core (closer to the surface for example), and subsequently have been entrained and incorporated during emplacement. They are not considered to be discrete clasts, as they do not have sharp contacts with the rest of the groundmass, nor are they glassy like the clinkery clasts observed. These domains occur throughout HAW-MAU2, near the top of HAW-HWY, and at the top and base of DER7B (up to 2.2 m beneath the base of the upper clinkery crust).

The thick aa flow from the NVP contains trachytic textures throughout (Fig. 2.12b), and the other flows locally contain trachytic textures at various positions throughout. Both of the Hawaiian flows have intergranular textures throughout, with no sign of plagioclase and pyroxene intergrowth (Fig. 2.12c & d). The thick NVP flow on the other hand contains a variety of textures, ranging from intergranular and sub-ophitic near the margins and partly into the interior, to ophitic in two of the samples in the core of the flow (Fig. 2.12b). One feature characteristic of all aa flows observed, and different to the pahoehoe flows is that suboctahedral tabular opaque grains are the dominant opaque morphology throughout. In only two samples are rods dominant, however clearly there is not a notable change in grain-size in these instances. In both of the Hawaiian flows studied there are places where the opaques are locally aligned. There may be up to ~10 grains that are touching, and just slightly offset from each other so that it can be seen that they are discrete grains (Fig. 2.12c & d).

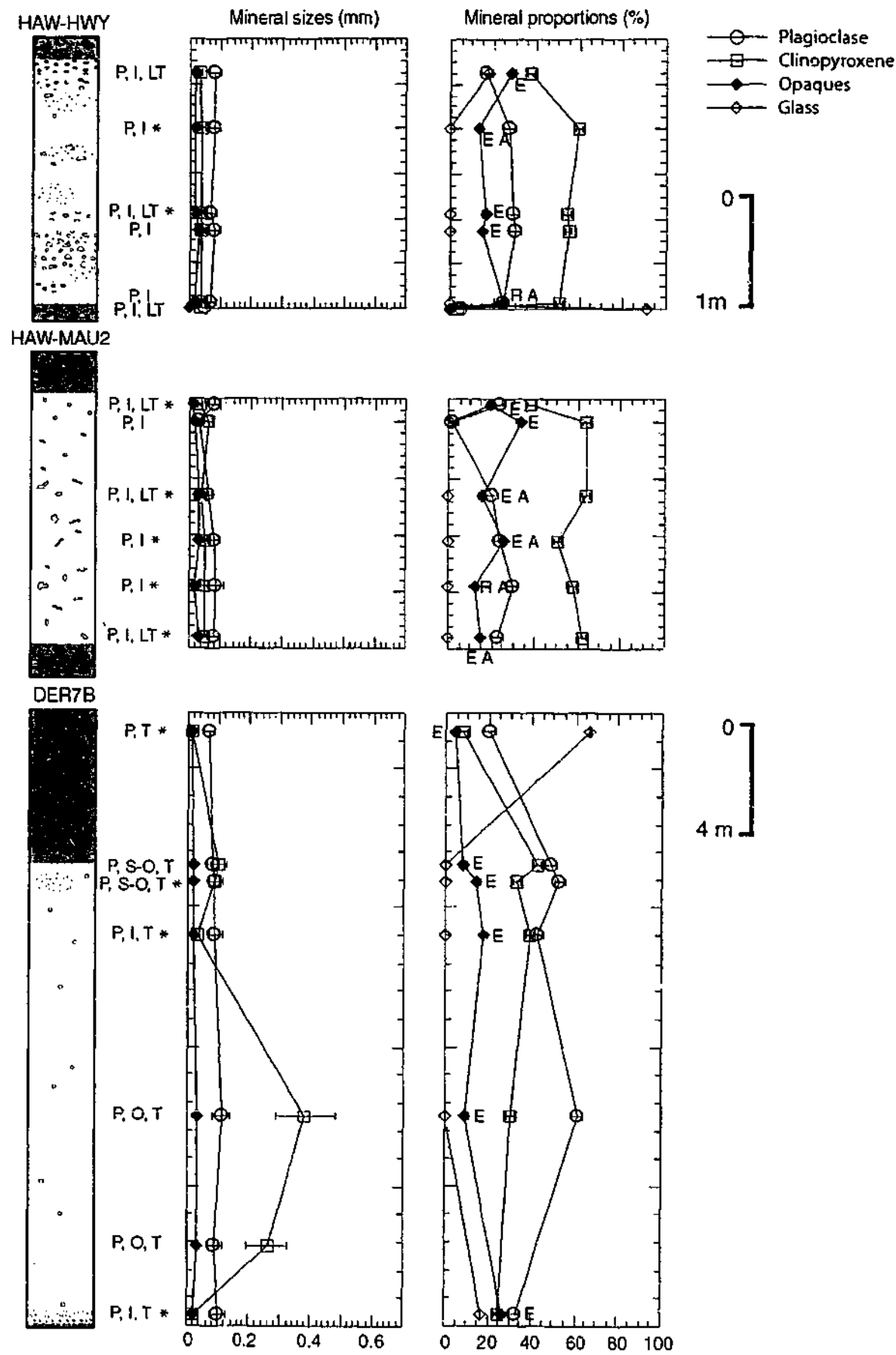


Fig. 2.11 Variations in grain-size and mineral abundances are shown beside graphic logs of selected aa flows. See Fig. 2.9 and caption for explanation of abbreviations. Note: * represents evidence of entrained material into the core of the flow.

The clinkery clasts sampled are generally dominated by glass (Fig. 2.12a), and some of the samples that are marginal to the core of the flows contain up to 20% glass. This is not as much as is present in the chilled margins of the pahoehoe flows (more than 50% glass), and notably no glass was observed within the interiors of any of the aa flows, which appear to have fully crystallised. Again, as glass content decreases there is an increase in the proportion of the other minerals. The proportion of minerals remains approximately constant throughout each of the thinner Hawaiian aa flows. It is difficult to define a trend in the variation of mineral abundances through the thicker NVP aa flow. Variations are not smooth as they are in the thicker pahoehoe flows, which is noteworthy in itself. A larger data set is required to

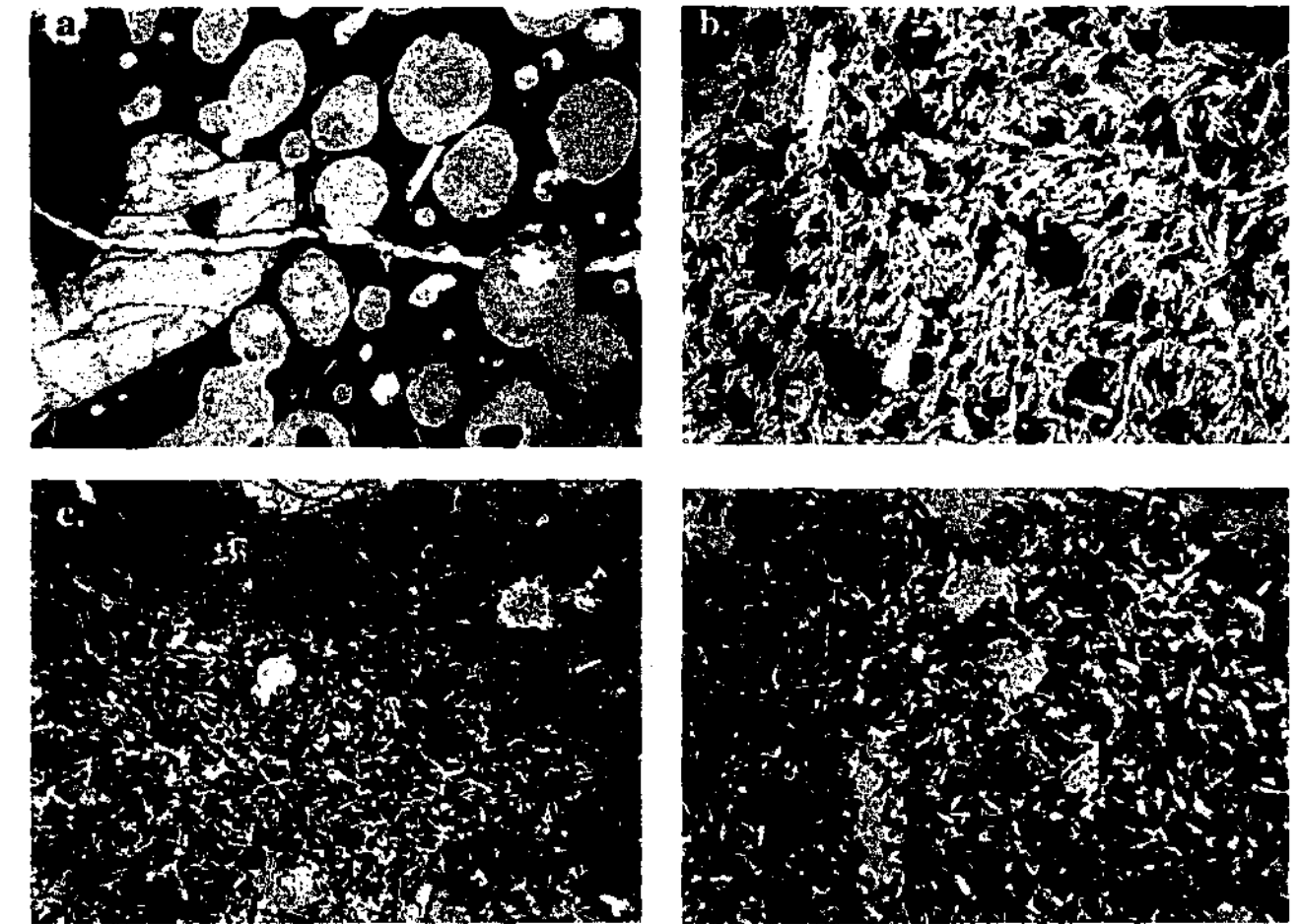


Fig. 2.12 Textural photomicrographs of representative aa textures observed. Again, the field of view for all photos is 2.5 mm. a. Glassy, clinkery clast from the top of an aa flow. A fracture extends across the width of the photo, connecting vesicles and cross-cutting the large phenocryst (DE707, PPL). b. Ophitic aa groundmass from the core of a flow. Note the texture is broadly trachytic (sub-vertical fabric in photograph), and dark patches represent oxidised phenocrysts and tubular opaque minerals (DE711, PPL). c. Intergranular aa groundmass, showing a diffuse change in grain-size, with finer, entrained material in the top right of the photo. Note that the tabular, equant opaques commonly occur aligned together (MAU10, PPL). d. As in photo c, this contains a diffuse change in grain-size, with the finer, entrained material on the left (MAUS, PPL).

determine whether this is characteristic of all thick aa flows or not, but some implications will be drawn below.

Although no segregation veins were observed in any of the aa flows, the two Hawaiian flows sampled contain segregation vesicles. These occur towards the top, centre and base of the flows. Like the segregation vesicles observed in the pahoehoe flows, these are all opaque-rich and in each case they are more coarse-grained than the surrounding groundmass. The shapes of the segregation vesicles range from rounded to irregular-shaped, and the margins range from sharp to diffuse. The opaque minerals are consistently elongate, and occur with plagioclase, pyroxene ± glass. There is no evidence of segregation material in the thick aa flow from the NVP. Thin, elongate fractures occur in each of the aa flows and are not observed in any of the pahoehoe flows. The fractures are located at the top of HAW-MAU2, the base of HAW-HWY and at all intervals within HAW-DER7B. They may locally connect vesicles or be separate from them, and commonly the fractures appear to be oriented sub-parallel to each other. The margins of the fractures are parallel to each other, but rarely planar. They have wavy, irregular, locally scalloped margins, and in the NVP flows are infilled with zeolites. Commonly the fractures cross-cut phenocrysts (Fig. 2.12a), and may locally offset the fractured portions of the crystals. The fractures become wider towards the centre of the thick NVP aa flow (up to ~0.4 mm wide) and apparently more abundant.

2.3.4 Geochemical variations through basalt flows

Three P-type pahoehoe lobes have been analysed for major and trace element concentrations (two from the NVP and one from Hawaii), and two aa flows (one from the NVP and one from Hawaii). Regardless of the composition of the flow (ie. tholeiitic or alkalic) the purpose of this exercise is to look at *relative* changes in composition throughout each lava flow. A useful way to compare the variation in elements of widely different concentrations is to calculate the coefficients of variation (CV's) of the various elements within a flow. The coefficient of variation is the standard deviation expressed as a percentage of the mean value (eg. Watkins *et al.* 1970). The CV's of the major and selected trace elements were calculated, and almost without exception SiO₂ was found to have the lowest value (generally less than 1). For this reason, and because of its very different concentration to the other major elements (Appendix C), SiO₂ was not included in the geochemical plots. All other major elements were plotted except where the total concentration is less than 0.5%. Trace elements were selected that are known to be strongly partitioned into the major minerals in basalt (Ni, Co,

Cr, V and Sr), and also two elements that are known to be incompatible (Ce and Rb) (Rollinson 1993). The variation in phenocryst content (normalised to a vesicle-free basis) through the lobes is shown adjacent to the geochemical plots.

In each of the P-type pahoehoe lobes, MgO shows the greatest variation (Fig. 2.13). The CV for MgO is consistently more than 10 compared with all other major elements, which generally yield values of less than 5. In the thin Hawaiian flow (HAW-CCD), the large range in MgO concentrations is attributed to two anomalous samples; there is a sharp drop in concentration in the second sample from the top (CCD2) compared with the rest of the flow, and a less dramatic decrease at the base of the flow (CCD6). The rest of the flow is fairly homogeneous with respect to MgO. The two anomalous samples also demonstrate a noticeable decrease in Fe₂O₃, Cr and Ni, and an increase in Al₂O₃, CaO and Sr. Corresponding to these geochemical anomalies, CCD2 and CCD6 have significantly lower phenocryst contents than the rest of the flow. The phenocryst population in this lobe consists of ortho- and clinopyroxenes and olivine, and it is proposed that the relative depletion and enrichment of the elements described here can be accounted for by the lower phenocryst content in these samples compared with the rest of the flow, and the higher relative groundmass (particularly plagioclase) proportion. In addition, CCD2 contains a number of segregation vesicles, and is therefore enriched in opaque minerals (Fig. 2.9b) and incompatible elements (Ce). In contrast to this lobe, the trends in MgO variation within the thicker flows from the NVP appear to be independent of all other elements. In one lobe the maximum MgO value corresponds to the maximum phenocryst concentration at the base of the NVZ (KOR15B). It appears likely that these two maxima may be related, although it is unclear why no other elements are affected by the increased phenocryst content. In the other lobe (KOR15A), maximum MgO concentrations correspond to *minimum* phenocryst values in the NVZ. At the margins of the flow where MgO values are the lowest, Ni demonstrates a sharp increase in concentration (CV is ~25). Ni partitions strongly into magnetite (Rollinson 1993), and it is considered that the high Ni contents reflect the high groundmass opaque (and glass) contents at the margins of KOR15A (Fig. 2.9a). The corresponding decrease in MgO at the margins would in this case reflect the lower relative proportion of olivine and pyroxene. As the flow is relatively homogeneous through the interior, it is proposed that the changes in geochemistry of the marginal samples may be attributed to different cooling rates producing different composition rocks.

The two aa lava flows analysed demonstrate very different geochemical trends. Despite

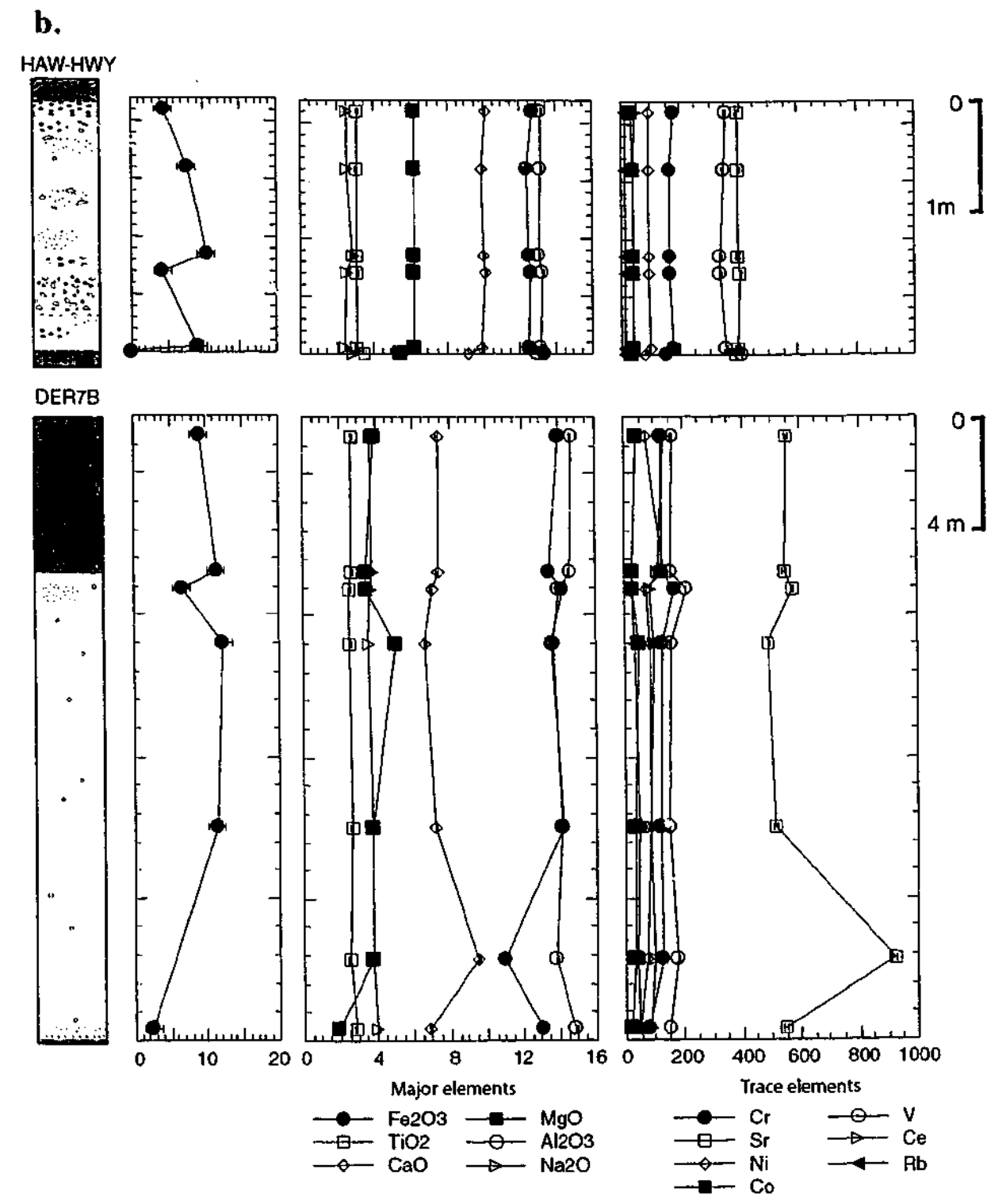
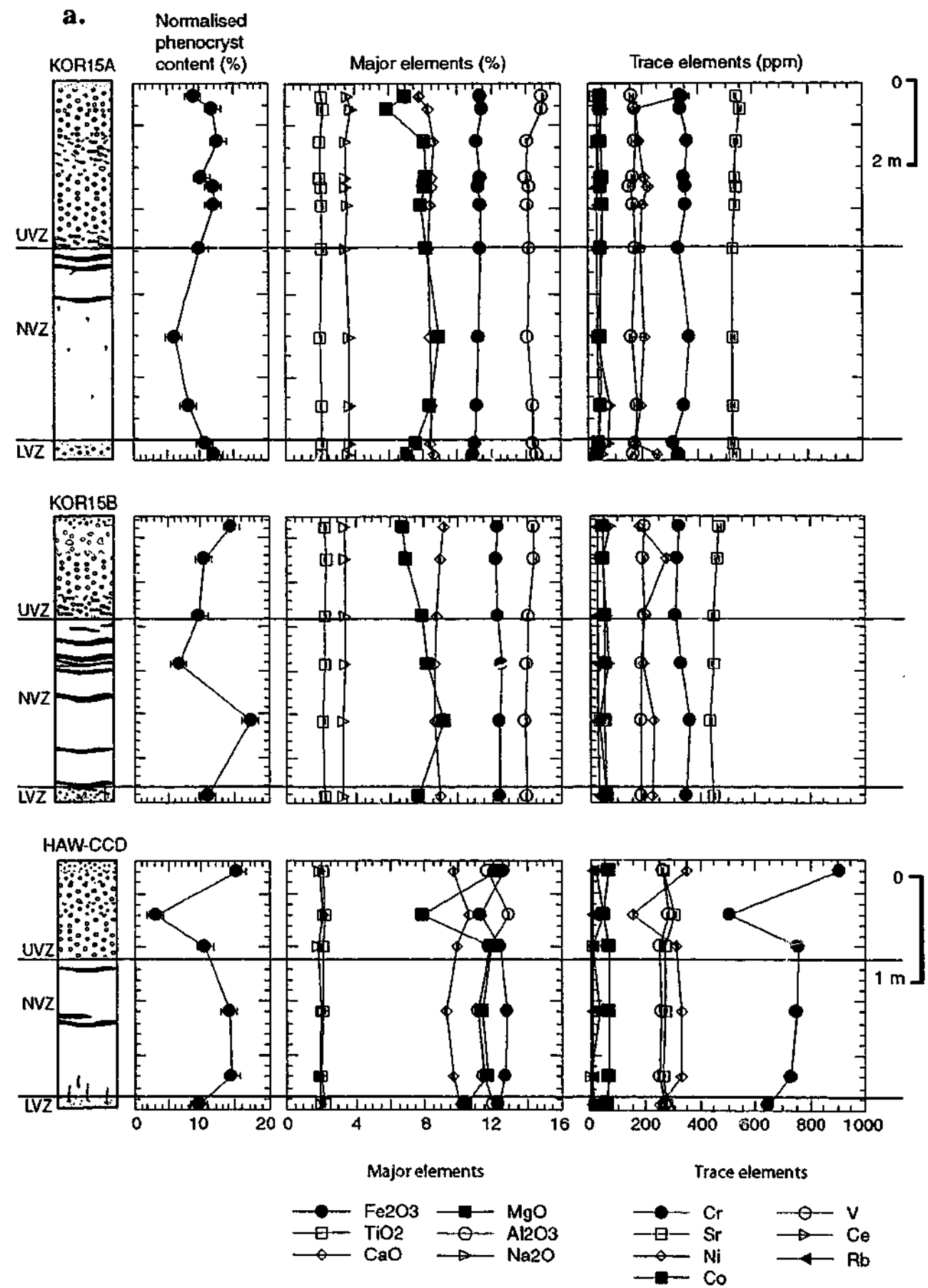


Fig. 2.13 Major and trace element concentrations are plotted against position in the flow for selected a. pahoehoe and b. aa flows. Normalised phenocryst concentrations are also shown (although sample DER7B-6 was not point-counted because it is pervasively altered). Note the different scales of the various logs.

the variable phenocryst content in the thinner Hawaiian aa flow (HAW-HWY), it appears to be geochemically homogeneous throughout. The only sample to vary in concentration is the lowermost sample (HWY6), a basal clinkery clast with a high glass content (Fig. 2.11). CV's for all elements are less than 10 for this flow. In contrast DER7B demonstrates a higher

degree of variability in concentration throughout the flow, and 5 elements have CV's greater than 20. Three samples appear to have anomalous concentrations in certain elements: the fourth top sample, and the two lowermost samples (DE710, DE712 and DE713 respectively). Sample DE713 has a particularly low phenocryst content, and this appears to be reflected by a decrease in MgO, Cr and Ni. A more dramatic change in concentration occurs in sample DE712. Unfortunately this sample has been substantially altered and therefore was not point counted. For this reason the phenocryst content is unknown. There is a dramatic decrease in Fe₂O₃, and a corresponding increase in CaO and Sr. It is not clear whether this is due to a relative change in the phenocryst or groundmass content or composition. Sample DE710 has a high MgO content, but demonstrates no significant variation in other elements or phenocryst content compared with the rest of the flow. There is evidence that this sample contains material entrained into the core of the flow (Fig. 2.11), and this might account for the difference in concentration compared with adjacent samples, due to the different cooling histories (see section 2.4.3).

2.4 DISCUSSION

2.4.1 Vesicles and segregation veins

Many of the differences between pahoehoe and aa flows observed in this study have previously been identified and explained in terms of emplacement processes (Table 2.3). Upon eruption, the external margins of pahoehoe lavas cool almost instantaneously, forming smooth low relief crusts beneath which molten lava is fed (Macdonald 1953). Pahoehoe sheet flows (or inflated P-type lobes) are produced by the radial spreading of pahoehoe toes on shallow slopes and the coalescence of the surface crust, forming a continuous sheet under which molten lava is fed (Hon *et al.* 1994). Steady inward growth and thickening of the upper and lower crusts occurs around a constant fluid layer or interior tube of freshly supplied lava, which is ~1 m thick in Hawaiian flows (Hon *et al.* 1994). Some gas bubbles within the molten interior lava are trapped at the flow base (LVZ), but most rise to the top of the tube basalt layer, are initially trapped beneath, and on further cooling are incorporated within the upper crust (UVZ), leaving a dense core (NVZ). These bubbles are not generally subjected to significant shear stresses, hence vesicles are generally discrete and spherical, and locally the distribution is homogeneous (Aubele *et al.* 1988, Wilmoth & Walker 1993, Self *et al.* 1996, Cashman & Kauahikaua 1997). Segregation veins form because incompatible elements (Fe, Mn, Ti, Na, K, P) including volatiles (H₂O, CO₂) are concentrated in the residual melt during

crystallisation of the NVZ (Goff 1996). These periodically rise as buoyant diapirs and spread out at the base of the semi-solidified crust. They are preserved as vertical vesicle cylinders and horizontal vesicle sheets (collectively called segregation veins here for simplicity) in the NVZ.

A large proportion of P-type pahoehoe lobes were observed to contain horizontal vesicle trains, and these have not been previously documented. Although these do not directly help to distinguish between pahoehoe and aa flows, they are considered to be a useful feature for distinguishing between inflated and ponded pahoehoe lobes. Identifying the emplacement mechanism of P-type lobes in ancient sequences has implications about the paleoslope: inflation only occurs on gentle slopes, less than 2° (Hon *et al.* 1994, Cashman & Kauahikaua 1997). Vesicle trains are interpreted here to reflect the final stages of lava movement in inflated flows. They generally occur towards the base of the UVZ. As the lava begins to stagnate and crystallise in the interior of the lobe, it becomes more viscous, has higher yield strength and is more resistant to closure behind migrating gas bubbles. Although lava movement is minimal, it is proposed that some horizontal flowage is occurring at this point, recorded by the horizontal vesicle trains. One would not expect to observe horizontal vesicle trains in ponded lavas, because the vesiculation pattern is dominated by post-emplacement bubble rise, and there is no horizontal component of motion of the lava during solidification. Horizontal vesicle trains are suggested to complement the criteria previously identified for distinguishing between these flows (Cashman & Kauahikaua 1997). The vesicle trains are particularly useful in ancient sequences where a lobe may not be completely preserved/exposed (thus the normalised UVZ thickness is meaningless). Also, in drill core it is difficult to characterise and quantify changes in vesicularity with depth, and to identify horizontal vesicle zones from such a limited perspective of a lobe. Horizontal vesicle trains are readily identifiable in drill core, however.

The interiors of aa flows reflect to some extent the unique emplacement mechanism compared with pahoehoe lavas. The rough, clinkery crust is produced by autobrecciation, and clasts from the upper crust may be entrained into the core, or fall to the base of the flow during flow advance (Macdonald 1953, Lipman & Banks 1987, Kilburn 1990, Crisp *et al.* 1994). It is considered that the lava undergoes autobrecciation because the viscosity or yield strength of the lava beneath the crust is too high for it to flow between the torn-apart portions of lava to heal the tear (Rowland & Walker 1990). Thus the exteriors of the autobrecciated clasts are characteristically rough, as the viscous lava that is torn apart retains an irregular, rough outline. It appears that gas bubbles are not able to migrate significantly during

Table 2.3 Summary of differences observed in this study between the interiors of 1. P-type pahoehoe lobes, and 2. aa flows. The fourth column in the table lists where these features have previously been documented.

General feature	1. Pahoehoe this study	2. Aa this study	Previously documented
Flow thickness (see Chapter 5)	Range of thicknesses observed: average NVP P-type pahoehoe lobe is ~7.5 m, average thickness of Hawaiian pahoehoe lobe sampled is 1.8 m	NVP aa flows are significantly thicker than pahoehoe lobes: average 22.5 m thick	
Flow-top, base morphology	Relatively smooth and low relief	Crusts consist of rough, clinkery clasts	1. & 2. Macdonald 1953, Kilburn 1990 and others
Incorporation of autobrecciated clasts into core of flow	Absent	Partially resorbed autobrecciated clasts and associated material occur near the top and base of the cores of the flows	2. Lipman & Banks 1987, Crisp & Baloga 1994
Vesiculation patterns	Lobes are subdivided into UVZ, NVZ & LVZ	Vesicles are dispersed throughout the core	1. Aubele <i>et al.</i> 1988, Wilmoth & Walker 1993, Self <i>et al.</i> 1996, Cashman & Kauahikaua 1997
	Vesicles are generally spherical, and distribution is locally homogeneous	Vesiculation patterns are heterogeneous: they consist of a range of shapes and sizes locally	1. As above. 2. Katz 1997, Polacci & Papale 1997, Cashman <i>et al.</i> 1999, Polacci <i>et al.</i> 1999
	Generally more vesicular than aa flows	Generally less vesicular than pahoehoe flows	1. & 2. Lipman & Banks 1987, Polacci <i>et al.</i> 1999
	Vesicles are generally discrete and are not interconnected	Vesicles are commonly interconnected (apparent microscopically)	1. Cashman & Kauahikaua 1997 2. Cashman <i>et al.</i> 1999
	May contain horizontal vesicle trains towards the base of the UVZ	'Vesicle trains' are not confined to a particular part of the flow, and they lack associated spherical vesicles	
Segregation material	Segregation veins are common	No segregation veins were observed	1. Puffer & Harter 1993, Hon <i>et al.</i> 1994, Goff 1996, Self <i>et al.</i> 1996, 1997, Thordarson & Self 1998, Caroff <i>et al.</i> 2000
	Segregation vesicles are relatively common in the UVZ and LVZ	Segregation vesicles were observed in the thin aa flows (~2.5 m thick)	1. Anderson <i>et al.</i> 1984 2. Katz 1997
Fractures (as per text)	Absent	Present in all flows	

Groundmass grain-sizes	Generally relatively coarse-grained	Generally relatively fine-grained	1. & 2. Katz 1997
	Smooth change in grain-size: general coarsening towards centre of flow	Grain-size generally constant throughout (except for clinopyroxene in the thick aa flow)	
Interstitial groundmass glass	Tholeiitic pahoehoe lavas contain volcanic glass in interstices between plagioclase laths throughout (less in interior than chilled margin samples)	Volcanic glass content is high in the clinkery clasts, relatively low in marginal core samples, and evidently absent in interiors of aa flows	1. Long & Wood 1986, Degraff <i>et al.</i> 1989
Mineral abundance variations	Thicker flows (NVP) contain a general increase in plagioclase and decrease in opaques towards the centre of flows. No systematic variation in the clinopyroxene content was observed.	Constant mineral proportions were observed throughout the thinner aa flows, and fluctuating abundances were observed in the thick aa flow (no smooth trend identifiable).	
Number densities of groundmass minerals	Crystal number densities are generally low. Average areal plagioclase number densities: $5.6 \times 10^3 \text{ mm}^{-2}$	Crystal number densities relatively high. Average plagioclase number densities: $2.8 \times 10^4 \text{ mm}^{-2}$	1. & 2. Sato 1995, Katz 1997, Cashman <i>et al.</i> 1999
Textural features: phenocrysts	Consistently porphyritic at lobe margins, but not necessarily porphyritic in the interior	Consistently porphyritic throughout	
Textural features: groundmass	Broadly homogeneous groundmass texture	Locally heterogeneous groundmass texture, with sharp changes in grain-size common	
Opaque mineral morphology and distribution	Rods and needles are dominant; they are randomly distributed, or in parallel sets.	Tabular grains are dominant throughout; they are generally randomly distributed but sometimes locally aligned	
Geochemical variations	Predominantly geochemically homogeneous throughout all flows	Generally homogeneous or locally heterogeneous composition. No consistent trends apparent	1. Siders & Elliot 1983, Fleming <i>et al.</i> 1992, Bates <i>et al.</i> 1998
	Thicker flows demonstrate an increase in MgO towards flow centres.	No significant increase in MgO towards flow centres was observed.	

emplacement due to the high viscosity or yield strength of the lava. Although aa flows are generally less vesicular than pahoehoe flows (Lipman & Banks 1987, Polacci *et al.* 1999), vesicles have been observed to be distributed throughout the cores (Fig. 2.8). This is in stark contrast to P-type pahoehoe lobes, which characteristically have a dense core due to the unhindered rise of gas bubbles. Vesicles are generally irregular shapes, interconnected to a high degree, and their distribution is heterogenous (Katz 1997, Polacci & Papale 1997, Cashman *et al.* 1999, Polacci *et al.* 1999), again reflecting the fact that the lava is more viscous (higher crystallinity), and less able to homogenise. The higher viscosity of the aa lava is considered to be a more likely explanation for the difference in the vesicularity patterns between aa and pahoehoe flows than the higher strain rates in aa flows (Polacci *et al.* 1999). No segregation veins were observed within aa flows, but segregation vesicles were observed. Again it is proposed that either the lava is too viscous for the residual melt (enriched in incompatible elements and volatiles) to propagate through the surrounding crystal mush as it does in pahoehoe flows, or aa lavas are significantly depleted in volatiles (reflected in the lower vesicle concentration). The presence of fractures in all aa flows observed might represent an alternative mechanism to segregation veins for explaining the release of built-up gas pressure during the crystallisation of more viscous lava. The fractures locally break apart and off-set phenocrysts, suggesting they are brittle features and form with substantial shear stress. Although aa flows are more viscous than pahoehoe, they are also commonly described as being higher velocity flows. This is probably in part due to the fact that aa lava flows are considered to most commonly form when eruption rates are high (eg. Macdonald 1953, Rowland & Walker 1990). The high discharge rates of the lava flows result in high imposed stresses on the flow fronts, which can cause disruption and autobrecciation of the crusts (eg. Kilburn 1990). This will subsequently expose the cores of the flows, resulting in higher cooling rates in the interiors of these flows, thus increasing the viscosity of the lava.

2.4.2 Petrographic textures

Pahoehoe and aa lavas have previously been recognised to have different petrographic textures. In particular, aa lavas have been observed to contain significantly higher groundmass crystal number densities than pahoehoe lavas (Sato 1995, Katz 1997, Cashman *et al.* 1999, Polacci *et al.* 1999). Sato (1995) observed that the number density of groundmass plagioclase differed by about two orders of magnitude between *surface samples* of the two different lavas. The high crystal number densities in aa flows have been attributed either to higher

cooling (and crystal nucleation) rates in proximal aa channels (Katz 1997, Cashman *et al.* 1999, Polacci *et al.* 1999), or to a higher degree of undercooling prior to degassing and eruption than pahoehoe lavas (Sato 1995). It is important to note that most of these studies have involved studying surface samples, and Katz (1997) is the only one to also look at the petrographic textures in the interiors of these flows. The focus of this study is to compare the rock textures throughout the different lava flows, which provides information about relative cooling rates in the range of crystallisation (Degraff *et al.* 1989). In this study groundmass plagioclase number densities were observed to differ by only one order of magnitude between pahoehoe and aa flows, and it is considered that this is because the values compared are the means of the number densities of the entire flows. Furthermore, number densities are dependent on the relative proportion of a mineral, which can be highly variable between flows with different compositions. The average groundmass grain-size data is therefore considered to be better for general comparisons between flows.

Although few studies have involved documenting textural variations through basaltic lava flows (eg. Long & Wood 1986, Degraff *et al.* 1989, Sharma *et al.* 2000), groundmass grain-size and number density variations through bodies of magma cooled by conduction are well constrained, due to studies and subsequent numerical modelling of dykes (eg. Winkler 1949, Ikeda 1977), lava lakes (Moore & Evans 1967, Kirkpatrick 1977, Wright & Okamura 1977, Cashman & Marsh 1988) and laboratory experiments (Lofgren 1977, Grove 1978, Walker *et al.* 1978, Lofgren *et al.* 1979). Specifically, the cooling rate of the lava affects plagioclase crystallisation and growth in a systematic, predictable way (Cashman 1993). In general, crystal sizes increase and crystal number densities decrease with decreasing cooling rates. It is important to note that of the flows examined in this study, this holds only for pahoehoe flows, which cool by simple conduction without convection or mixing (eg. Hon *et al.* 1994). As expected, the cooling rates in the interiors of the pahoehoe flows studied are significantly lower than the margins, as the average groundmass plagioclase size is larger in the interiors of the flows. This effect is particularly evident in the thicker pahoehoe flows from the NVP, and similarly it has been found that the peak grain-size in dykes increases with increasing dyke width (Ikeda 1977).

Based upon observations of active aa flows we know that they do not cool by simple conduction, but instead consist of a single advancing core and an overriding layer of cooler material. The core is assumed to be thermally well mixed, and entrainment of semi-solid surface crust material into the core occurs due to physical mixing in the flow (Crisp &

Baloga 1994). Entrained crustal material was observed in all aa flows, commonly with the margins partially resorbed, and represented by locally sharp changes in vesicularity or groundmass grain-sizes. The physical mixing process serves to enhance the rate of crystal nucleation, so that it is greater than can be explained by rapid cooling by conduction alone (Emerson 1926, Kouchi *et al.* 1986, Cashman *et al.* 1999). In spite of evidence that physical mixing occurs during emplacement, it is generally considered that aa flow interiors, or the cores of aa flows cool slowly (Cashman *et al.* 1999). This is based upon sampling break-outs from flow interiors, as these commonly have transitional pahoehoe surface morphologies and nearly constant temperatures (eg. Neal *et al.* 1988, Calvari & Pinkerton 1998, 1999). Average plagioclase grain-size trends through aa flows from this study suggest that even upon stagnation and final solidification of the lava flows, their interiors did not cool more slowly by conduction, as there is no evidence of increased grain-size towards the centre of the core. Instead, the average length of plagioclase laths is surprisingly constant, even through the thick NVP aa flow (the core is ~15 m thick), and textures do not resemble those observed in relatively slow-cooling pahoehoe lobes.

An alternative explanation for the consistent plagioclase grain-sizes observed throughout the aa flows, assuming the interiors did cool slowly, is that plagioclase growth rates (and nucleation rates) decrease with increasing crystallisation (Cashman & Marsh 1988). It is now well established that aa flows have higher crystallinities than pahoehoe during emplacement (Cashman *et al.* 1999, Polacci *et al.* 1999). However, this explanation does not seem likely, as the number density of groundmass plagioclase laths in the pahoehoe break-out (HAW-MAU1) from the aa channel (HAW-MAU2) sampled in this study, is on average an order of magnitude lower than the aa flow. The plagioclase laths demonstrate an increase in size towards the centre of the lobe, suggesting that unlike the aa flow, it cooled by simple conduction and the cooling rate was lower in the centre of the lobe. If the growth rate of the plagioclase were affected by the higher degree of crystallisation in the aa lava, the break-out would be expected to reflect this also. Thus, based upon the results of this study, it appears that the interiors of aa flows may not necessarily cool slowly, but instead high plagioclase number densities throughout, and constant grain-sizes reflect the physical mixing process that serves to enhance heat loss. Further work is required to determine how representative these results are of all aa flows, because if the interiors do cool quickly as has been suggested here, it is difficult to explain how inflation of aa lavas can occur (eg. Calvari & Pinkerton 1998, 1999).

The morphology of the opaque minerals tends to be unique to the different flow types. Unlike previous studies of flood basalt flows which have identified cruciform or octahedral Fe-Ti oxide phenocrysts in slow-cooling portions, and feathery, dendritic crystals in the more rapid cooling parts of the flow (eg. Long & Wood 1986, Degraff *et al.* 1989, Thordarson & Self 1998), dominant morphologies observed in this study are rod-shaped and tabular. Rod-shaped grains occur toward the centre of pahoehoe flows, suggesting they form at relatively slow cooling rates (but not as slow as in the flood basalts, which have large, tabular phenocrysts). Fine, tabular grains occur throughout aa flows (Fig. 2.11) and at the margins of the thinner pahoehoe lobes (Fig. 2.9), reflecting higher cooling rates, higher nucleation rates and lower crystal growth rates than the interiors of pahoehoe flows. This supports the hypothesis that the interiors of aa flows do not cool slowly, as previously has been suggested (eg. Cashman *et al.* 1999). The parallel nature of sets of rod-shaped grains in pahoehoe flows may be due to heterogeneous nucleation of the opaques (ie. on a pre-existing substrate). Commonly the pre-existing substrate appears to have been an olivine or pyroxene phenocryst, and the opaque grains are considered to have grown perpendicular to the phenocryst, into the interstitial melt. They are not necessarily oriented parallel to any trachytic texture present, suggesting they crystallised after the lava had stagnated. In aa flows the tabular opaque grains are locally aligned, and this is considered to have occurred during emplacement in a similar way to the alignment of plagioclase laths, producing a trachytic texture. These textural features are again interpreted to reflect the higher relative cooling rates of aa lavas.

It has been observed that no characteristic textural progression is unique to either flow type, apart from a trend in the size of the minerals, which coarsen inwards in pahoehoe lobes. Pahoehoe lobes range from intergranular throughout, to ophitic throughout to a combination of the two textures within a lobe. Similarly, different combinations of these textures were observed in the aa flows. This is in part related to the different pre-eruption and emplacement histories of the different flows prior to stagnation and final crystallisation, eg. the degree of undercooling prior to eruption (Lofgren 1980, and others). These differences may affect the order of crystallisation of the phases, which in turn may influence the crystallisation behaviour of a particular phase through availability of heterogeneous nucleation sites and rate of cooling through the crystallisation interval (Cashman 1993). Note also that the degree of alignment of plagioclase laths is not consistently a reflection of the emplacement style. The aa flows studied are not consistently trachytic throughout, as one might expect due to the higher viscosities of the lava and higher strain rates (eg. Peterson & Tilling 1980).

2.4.3 Geochemical variations

The basaltic lavas have generally been found to be chemically homogeneous, however anomalous concentrations of some elements occur locally within each of the flows. These variations are most pronounced in the thick aa flow from the NVP (DER7B), which demonstrates the highest CV's for elements within this flow. The anomalies have been attributed to (i) anomalous phenocryst contents (eg. HAW-CCD, KOR15B and DER7B), or (ii) material with a different cooling history to adjacent samples (eg. KOR15A, DER7B and HAW-HWY). There is no evidence that the chemistry of the magma feeding the lavas changed progressively with time. If this were the case, one would anticipate that the margins of the inflated lobes would be similar in composition, with a progressive change through the UVZ with depth, and a different composition NVZ. This is not observed in any of the lobes, and any changes in geochemistry of the magma that may have occurred are considered to be below the detection limit of this study. All variations in geochemistry within the lobes are interpreted in terms of in-flow and post-flow processes (physical and thermo-chemical).

(i) The most convincing example of the geochemistry reflecting the relative phenocryst content occurs in HAW-CCD (section 2.3.4). The second top sample in the flow is clearly depleted in phenocrysts compared with the rest of the flow, and this is the only flow analysed in which such a dramatic depletion occurs. The lower phenocryst content is considered to be related to an increase in segregation material compared with adjacent samples. The uppermost sample in the flow is very glassy, reflecting fast cooling upon contact with the air. The second sample was able to cool more slowly because of the insulating crust that formed above it, but more importantly because it was sampled from within a small vesicle zone, or horizontal vesicle zone (HVZ) (Fig. 2.13). HVZ's have previously been documented within the UVZ of inflated lobes, and occur as thin bands of increased vesicularity, representing pause events during the inflation process, due to hiatuses in magma supply (Cashman & Kauahikaua 1997). Increased vesiculation is triggered by the temporary loss in pressure within the lobe, during a pause in magma supply. Microscopically it is suggested that HVZ's may be characterised by a low phenocryst content because the decrease in pressure within the flow allows phenocrysts to settle (eg. Rowland & Walker 1987, 1988). A high proportion of segregation material may also be expected, as the pause in lava supply and inflation allows crystallisation to proceed to a greater extent than it would otherwise, and allows the residual melt to segregate to some degree, forming segregation vesicles. HVZ's are more easily recognised in outcrop than drill core, and each of the Hawaiian lobes analysed have evidence of at least 2 pause events in

magma supply during formation of the lobes (eg. Fig. 2.6b). In KOR15A there is evidence of a pause in magma supply during inflation. The zone of horizontal vesicle trains within the UVZ overlies another zone of spherical vesicles, considered to represent temporary stagnation of lava within the lobe followed by the injection of a fresh pulse of lava (Fig. 2.6a). No samples within this lobe show evidence of significant phenocryst depletion, nor increased segregation material. Either the sampling spacing was too wide to identify these features, or their presence may depend on the relative viscosity (and temperature) of the lava, the distance it has travelled from vent, and the consistency in phenocryst content of the supplied lava.

Enrichment of phenocrysts towards the base of the NVZ has previously been described in terms of crystal settling (Rowland & Walker 1987, 1988). This possibly occurred in KOR15B, although MgO appears to have been the only element affected by it. Again, to confirm whether or not crystal settling has occurred within the inflated pahoehoe lobes more samples are required (particularly in the NVZ's). The thick aa flow (DER7B) has variable phenocryst contents throughout the flow, and this can be attributed to the emplacement process, involving variably mixed core material, and thus unevenly distributed phenocrysts.

(ii) The margins of KOR15A are clearly enriched in opaque minerals compared with the interior of the flow (Fig. 2.9a). This is reflected in the geochemistry as an increase in Ni and decrease in MgO (reflecting the relative depletion of olivine and pyroxene) at the flow margins (Fig. 2.13a). In fact, a number of the pahoehoe lobes analysed demonstrate increased opaque mineral contents at the margins, and a decrease in groundmass plagioclase (Fig. 2.9). Similarly it appears that adjacent aa lava samples that have undergone different cooling histories contain different proportions of minerals (Fig. 2.11), and have different compositions (Fig. 2.13b). In particular, the fourth top sample and the sample at the base of the flow, both of which contain entrained material, are enriched in opaques and depleted in plagioclase compared with adjacent samples (Fig. 2.11). It is proposed here that the increased opaque content is due to a delay in plagioclase nucleation, as a result of the high cooling rates experienced by marginal/entrained samples (eg. Gibb 1974). In fact, it has been documented that plagioclase can reverse its order of appearance (with ilmenite for example) during crystallisation, because of its reluctance to nucleate at very high cooling rates (Walker *et al.* 1976). This may explain why there is a relative increase in groundmass plagioclase content into the interiors of the P-type pahoehoe lobes analysed, as the cooling rate of the lava decreases inwards (Fig. 2.9).

2.5 CONCLUSIONS

- This study has involved characterising the vesiculation patterns, petrographic textural zonations, and compositional variations through the interiors of basalt lava flows (in particular, inflated P-type pahoehoe lobes and aa flows). Proximal and distal facies of each type of lava were sampled, and alkalic and tholeiitic lavas were compared. General trends have been identified which can be tested and refined with further work.
- P-type pahoehoe lobes were observed to consistently contain dense, non-vesicular cores, and many contain segregation veins. In contrast, vesicles are dispersed throughout aa lavas, and no segregation veins were observed. These features are considered to be related to the differences in viscosity between the two lava types. Vesicles (and any segregation material) are prevented from rising through more viscous aa lava flows.
- Petrographic textural zonations were found to be different in pahoehoe and aa flows. Plagioclase grain-sizes consistently increase towards the centres of P-type pahoehoe lobes, indicating slower cooling in the interiors than the margins. Aa flows demonstrate consistently uniform plagioclase grain-sizes throughout all flows analysed; they are always smaller than plagioclase grains in pahoehoe flows, but more numerous, thus resulting in higher plagioclase number densities than pahoehoe flows. This is considered to be a result of the physical mixing process that occurs during emplacement of aa flows, which enhances crystal nucleation rates throughout the flow. Importantly, it appears that the interiors of aa flows may not cool slowly by conduction (cf. pahoehoe flows).
- Pahoehoe and aa flows were found to be compositionally homogeneous, apart from local anomalies. These anomalies have been attributed to locally variable phenocryst contents, and/or differences in the cooling histories of adjacent samples. In order to expand upon these results, a similar type of study could be pursued with closer sampling spacing. The regularity of 'anomalies' through the flows could then be evaluated and the different flow types compared.

- The distinctive emplacement style of aa lavas (and resulting surface morphology and internal structure) can be attributed to the higher viscosity of these lavas compared with pahoehoe lavas. The higher viscosity is due to the higher crystallinity of these lavas, possibly due to a greater degree of undercooling prior to eruption. For aa lavas that have changed from pahoehoe, the higher viscosity (and crystallinity) is related to the degree of cooling that has occurred during emplacement. Once a threshold viscosity has been reached, the lava will begin to autobrecciate and propagate as aa. This threshold viscosity is not a unique value, but is related to the rate of shear strain of the lava, which is influenced by the velocity of the lava flow (related to volumetric flow rate, slope of the substrate, local topographic irregularities etc.). Once the lava begins to propagate by autobrecciation it no longer cools by conduction, but is dominated by a physical mixing process involving entrainment of clasts and cooler material into the core of the flow.

REFERENCES

- Anderson, A.T.J., Swihart, G.H., Artioli, G. & Geiger, C.A., 1984. Segregation vesicles, gas filter pressing, and igneous differentiation. *Journal of Geology*, **92**, 55-72.
- Arndt, N.T., 1986. Differentiation of komatiite flows. *Journal of Petrology*, **27**(2), 279-301.
- Arndt, N.T., Naldrett, A.J. & Pyke, D.R., 1977. Komatiitic and Iron-rich Tholeiitic Lavas of Munro Township, Northeast Ontario. *Journal of Petrology*, **18**, 319-369.
- Aubele, J.C., Crumpler, L.S. & Elston, W.E., 1988. Vesicle zonation and vertical structure of basalt flows. *Journal of Volcanology and Geothermal Research*, **35**, 349-374.
- Baker, M.B., Alves, S. & Stolper, E.M., 1996. Petrography and petrology of the Hawaii Scientific Drilling Project lavas: Inferences from olivine phenocryst abundances and compositions. *Journal of Geophysical Research*, **101**(B5), 11,715-11,727.
- Bates, D.L., McCurry, M., Ingram, J.C. & Cortez, M.M., 1998. Meso-Scale Chemical and Textural Variations within an Eastern Snake River Plain Basalt Flow: Implications for Heterogeneous Chemical Interaction with Trichloroethylene. *Eos*, **79**(17), S364.
- Calvari, S. & Pinkerton, H., 1998. Formation of lava tubes and extensive flow field during the 1991-1993 eruption of Mount Etna. *Journal of Geophysical Research*, **103**(B11), 27,291-27,301.
- Calvari, S. & Pinkerton, H., 1999. Lava tube morphology on Etna and evidence for lava flow emplacement mechanisms. *Journal of Volcanology and Geothermal Research*, **90**, 263-280.
- Caroff, M., Maury, R.C., Cotten, J. & Clément, J.-P., 2000. Segregation structures in vapor-differentiated basaltic flows. *Bulletin of Volcanology*, **62**, 171-187.

- Cashman, K.V., 1993. Relationship between plagioclase crystallization and cooling rate in basaltic melts. *Contributions to Mineralogy and Petrology*, **113**, 126-142.
- Cashman, K.V. & Kauahikaua, J.P., 1997. Reevaluation of vesicle distributions in basaltic lava flows. *Geology*, **25**(5), 419-422.
- Cashman, K.V. & Marsh, B.D., 1988. Crystal size distribution (CSD) in rocks and the kinetics and dynamics of crystallization II: Makaopuhi lava lake. *Contributions to Mineralogy and Petrology*, **99**, 292-305.
- Cashman, K.V., Thornber, C. & Kauahikaua, J.P., 1999. Cooling and crystallization of lava in open channels, and the transition of Pahoehoe Lava to 'A'a. *Bulletin of Volcanology*, **61**, 306-323.
- Crisp, J. & Baloga, S., 1994. Influence of crystallization and entrainment of cooler material on the emplacement of basaltic aa lava flows. *Journal of Geophysical Research*, **99**(B6), 11,819-11,831.
- Crisp, J., Cashman, K.V., Bonini, J.A., Hougén, S.B. & Pieri, D.C., 1994. Crystallization history of the 1984 Mauna Loa lava flow. *Journal of Geophysical Research*, **99**(B4), 7177-7198.
- Degraff, J.M., Long, P.E. & Aydin, A., 1989. Use of joint-growth directions and rock textures to infer thermal regimes during solidification of basaltic lava flows. *Journal of Volcanology and Geothermal Research*, **38**, 309-324.
- Emerson, O.H., 1926. The formation of aa and pahoehoe. *American Journal of Science*, **12**, 1-9.
- Fleming, T.H., Elliot, D.H., Jones, L.M., Bowman, J.R. & Siders, M.A., 1992. Chemical and isotopic variations in an iron-rich lava flow from the Kirkpatrick Basalt, north Victoria Land, Antarctica: implications for low-temperature alteration. *Contributions to Mineralogy and Petrology*, **111**, 440-457.
- Garcia, M.O., 1996. Petrography and olivine and glass chemistry of lavas from the Hawaii Scientific Drilling Project. *Journal of Geophysical Research*, **101**(B5), 11,701-11,713.
- Gibb, F.G.F., 1974. Supercooling and the crystallization of plagioclase from a basaltic magma. *Mineralogical Magazine*, **39**, 641-653.
- Goff, F., 1996. Vesicle cylinders in vapor-differentiated basalt flows. *Journal of Volcanology and Geothermal Research*, **71**, 167-185.
- Greeley, R., 1987. The role of lava tubes in Hawaiian volcanoes. *U.S. Geological Survey Professional Paper 1350*, 1,589-1,602.
- Grove, T.L., 1978. Cooling histories of Lunar 24 very low Ti (VLT) ferrobaltaltes: an experimental study. *Proceedings of Lunar and Planetary Science Conference*, **9**, 565-584.
- Guest, J.E., Kilburn, C.R.J., Pinkerton, H. & Duncan, A.M., 1987. The evolution of lava flow-fields: observations of the 1981 and 1983 eruptions of Mount Etna, Sicily. *Bulletin of Volcanology*, **49**, 527-540.
- Heliker, C.C., Mangan, M.T., Mattox, T.N., Kauahikaua, J.P. & Helz, R.T., 1998. The character of

- long-term eruptions: inferences from episodes 50-53 of the Pu'u 'O'o-Kupaianaha eruption of Kilauea Volcano. *Bulletin of Volcanology*, **59**, 381-393.
- Ho, R.A. & Garcia, M.O., 1988. Origin of differentiated lavas at Kilauea Volcano, Hawaii: Implications from the 1955 eruption. *Bulletin of Volcanology*, **50**, 35-46.
- Hon, K., Kauahikaua, J., Denlinger, R. & Mackay, K., 1994. Emplacement and inflation of pahoehoe sheet flows: Observations and measurements of active lava flows on Kilauea Volcano, Hawaii. *Geological Society of America Bulletin*, **106**, 351-370.
- Ikeda, Y., 1977. Grain size of plagioclase of the basaltic andesite dikes, Iritono, central Abukuma plateau. *Canadian Journal of Earth Sciences*, **14**, 1860-1866.
- Jerram, D.A., 1996. The development and application of detailed textural analysis techniques: a case study- the origin of komatiite cumulates. *Unpub. Doctor of Philosophy Thesis, University of Liverpool*.
- Katz, M.G., 1997. Patterns of lava flow coverage in drill cores. *Unpub. Master of Science Thesis, University of Oregon, Oregon*.
- Kauahikaua, J., Cashman, K.V., Mattox, T.N., Heliker, C.C., Hon, K.A., Mangan, M.T. & Thornber, C.R., 1998. Observations on basaltic streams in tubes from Kilauea Volcano, island of Hawai'i. *Journal of Geophysical Research*, **103**(B11), 27,303-27,323.
- Kilburn, C., 1990. Surfaces of Aa Flow-Fields on Mount Etna, Sicily: Morphology, Rheology, Crystallization and Scaling Phenomena. In: *Lava Flows and Domes. Emplacement Mechanisms and Hazard Implications* (ed Fink, J.H.), pp. 129-156, Springer-Verlag, Berlin.
- Kirkpatrick, R.J., 1977. Nucleation and growth of plagioclase, Makaopuhi and Alae lava lakes, Kilauea Volcano, Hawaii. *Geological Society of America Bulletin*, **88**, 78-84.
- Kouchi, A., Tsuchiyama, A. & Sunagawa, I., 1986. Effect of stirring on crystallization kinetics of basalt: texture and element partitioning. *Contributions to Mineralogy and Petrology*, **93**, 429-438.
- Kuritani, T., 1999. Phenocryst crystallization during ascent of alkali basalt magma at Rishiri Volcano, northern Japan. *Journal of Volcanology and Geothermal Research*, **88**, 77-97.
- Lipman, P.W. & Banks, N.G., 1987. Aa flow dynamics, Mauna Loa 1984. *U.S. Geological Survey Professional Paper 1350*, 1,527-1,565.
- Lockwood, J.P. & Lipman, P.W., 1987. Holocene eruptive history of Mauna Loa Volcano. *US Geological Survey Professional Paper 1350*, 509-535.
- Lofgren, G.E., 1977. Dynamic crystallization experiments bearing on the origin of textures in impact-generated liquids. *Proceedings of Lunar and Planetary Science Conference*, **8**, 2079-2095.
- Lofgren, G.E., 1980. Experimental studies on the dynamic crystallization of silicate melts. In: *Physics of magmatic processes* (ed Hargraves, R.B.), pp. 487-551, Princeton University Press, New Jersey.

- Lofgren, G.E., Grove, T.L., Brown, R.W. & Smith, D.P., 1979. Comparison of dynamic crystallization techniques on Apollo 15 quartz normative basalts. *Proceedings of Lunar and Planetary Science Conference*, **10**, 423-438.
- Long, P.E. & Wood, B.J., 1986. Structures, textures, and cooling histories of Columbia River basalt flows. *Geological Society of America Bulletin*, **97**, 1,144-1,155.
- Macdonald, G.A., 1953. Pahoehoe, aa and block lava. *American Journal of Science*, **251**, 169-191.
- Macdonald, G.A. & Eaton, J.P., 1964. Hawaiian volcanoes during 1955. *U.S. Geological Survey Bulletin*, **1171**, 1-170.
- Moore, J.G. & Evans, B.W., 1967. The role of olivine in the crystallisation of the prehistoric Makaopuhi lava lake, Hawaii. *Contributions to Mineralogy and Petrology*, **15**, 202-223.
- Neal, C.A., Duggan, T.J., Wolfe, E.W. & Brandt, E.L., 1988. Lava samples, temperatures, and compositions. *U.S. Geological Survey Professional Paper*, **1463**, 99-126.
- Peterson, D.W. & Tilling, R.J., 1980. Transition of basaltic lava from pahoehoe to aa, Kilauea volcano, Hawaii: Field observations and key factors. *Journal of Volcanology and Geothermal Research*, **7**, 271-293.
- Peterson, D.W., Holcomb, R.T., Tilling, R.I. & Christiansen, R.L., 1994. Development of lava tubes in the light of observations at Mauna Ulu, Kilauea Volcano, Hawaii. *Bulletin of Volcanology*, **56**, 343-360.
- Polacci, M. & Papale, P., 1997. The evolution of lava flows from ephemeral vents at Mount Etna: Insights from vesicle distribution and morphological studies. *Journal of Volcanology and Geothermal Research*, **76**, 1-17.
- Polacci, M., Cashman, K.V. & Kauahikaua, J.P., 1999. Textural characterization of the pahoehoe-'a'a transition in Hawaiian basalt. *Bulletin of Volcanology*, **60**, 595-609.
- Puffer, J.H. & Horter, D.L., 1993. Origin of pegmatitic segregation veins within flood basalts. *Geological Society of America Bulletin*, **105**, 738-748.
- Pyke, D.R., Naldrett, A.J. & Eckstrand, A.R., 1973. Archaean ultramafic flows in Munro Township, Ontario. *Geological Society of America Bulletin*, **84**, 955-978.
- Renner, R., Nisbet, E.G., Cheadle, M.J., Arndt, N.T., Bickle, M.J. & Cameron, W.E., 1994. Komatiite Flows from the Reliance Formation, Belingwe Belt, Zimbabwe: I. Petrography and Mineralogy. *Journal of Petrology*, **35**, 361-400.
- Rollinson, H.R., 1993. *Using geochemical data: evaluation, presentation, interpretation*. Longman Group Limited, Essex, 352 p.
- Rowland, S.K. & Walker, G.P.L., 1987. Toothpaste lava: Characteristics and origin of a lava structural type transitional between pahoehoe and aa. *Bulletin of Volcanology*, **49**, 631-641.
- Rowland, S.K. & Walker, G.P.L., 1988. Mafic-crystal distributions, viscosities, and lava structures of some Hawaiian lava flows. *Journal of Volcanology & Geothermal Research*, **35**, 55-66.

- Rowland, S.K. & Walker, G.P.L., 1990. Pahoehoe and aa in Hawaii: volumetric flow rate controls the lava structure. *Bulletin of Volcanology*, **52**, 615-628.
- Sato, H., 1995. Textural differences between pahoehoe and aa lavas of Izu-Oshima volcano, Japan- an experimental study on population density of plagioclase. *Journal of Volcanology and Geothermal Research*, **66**, 101-113.
- Self, S., Thordarson, T., Keszthelyi, L., Walker, G.P.L., Hon, K., Murphy, M.T., Long, P. & Finnemore, S., 1996. A new model for the emplacement of Columbia River basalts as large, inflated pahoehoe lava flow fields. *Geophysical Research Letters*, **23**(19), 2,689-2,692.
- Self, S., Thordarson, T. & Keszthelyi, L., 1997. Emplacement of Continental Flood Basalt Lava Flows. In: *Large Igneous Provinces: Continental, Oceanic, and Planetary Flood Volcanism*. (eds Mahoney, J.J. & Coffin, M.), pp. 381-410, American Geophysical Union.
- Self, S., Keszthelyi, L. & Thordarson, T., 1998. The importance of pahoehoe. *Annual Review of Earth and Planetary Science*, **26**, 81-110.
- Sharma, K., Keszthelyi, L., Thornber, C. & Self, S., 2000. Variations in the cooling, crystallization textures and glass chemistry during emplacement of Kilauea pahoehoe lobes, as constrained by in situ field experiments. *Geological Society of America Abstracts with Programs*, **32**(7), A-395.
- Shelley, D., 1993. *Igneous and metamorphic rocks under the microscope: classification, textures, microstructures and mineral preferred orientations*. Chapman and Hall, London, 445 p.
- Siders, M.A. & Elliot, D.H., 1983. Intraflow variability in the Kirkpatrick basalt, northern Victoria land, Antarctica. *Geological Society of America Abstracts with Programs*, **15**, 687.
- Silliman, B. & Dana, J.D., 1868. Recent Eruption of Mauna Loa and Kilauea, Hawaii. *The American Journal of Science and Arts*, **46**, 105-123.
- Thordarson, T. & Self, S., 1998. The Roza Member, Columbia River Basalt Group: A gigantic pahoehoe lava flow field formed by endogenous processes? *Journal of Geophysical Research*, **103**(B11), 27,411-27,445.
- Walker, D., Kirkpatrick, R.J., Longhi, J. & Hays, J.F., 1976. Crystallization history of lunar picrite basalt sample 12002: phase equilibria and cooling-rate studies. *Geological Society of America Bulletin*, **87**, 646-656.
- Walker, D., Powell, M.A., Lofgren, G.E. & Hays, J.F., 1978. Dynamic crystallization of a eucritic basalt. *Proceedings of Lunar and Planetary Science Conference*, **9**, 1369-1391.
- Walker, G.P.L., 1989. Spongy pahoehoe in Hawaii: a study of vesicle-distribution patterns in basalt and their significance. *Bulletin of Volcanology*, **53**, 546-558.
- Walker, G.P.L., 1993. Basaltic-volcano systems. In: *Magmatic Processes and Plate Tectonics* (eds Prichard, H.M., Alabaster, T., Harris, N.B.W. & Neary, C.R.), pp. 3-38, Geological Society of America.

- Watkins, N.D., Gunn, B.M. & Coy-yll, R., 1970. Major and trace element variations during the initial cooling of an Icelandic lava. *American Journal of Science*, **268**, 24-29.
- Williams, H. & McBirney, A.R., 1979. *Volcanology*. Freeman Cooper, San Francisco, 397 p.
- Wilmoth, R.A. & Walker, G.P.L., 1993. P-type and S-type pahoehoe: a study of vesicle distribution patterns in Hawaiian lava flows. *Journal of Volcanology and Geothermal Research*, **55**, 129-142.
- Winkler, H.G.F., 1949. Crystallization of basaltic magmas as recorded by variation in crystal size in dikes. *Mineralogical Magazine*, **28**, 557-574.
- Wolfe, E.W. & Morris, J., 1996. Geologic Map of the Island of Hawaii. Miscellaneous Investigations Series Map, U.S. Geological Survey.
- Wright, T.L. & Okamura, R.T., 1977. Cooling and crystallization of tholeiitic basalt, 1965 Makaopuhi lava lake, Hawaii. *U.S. Geological Survey Professional Paper 1004*, 78 p.

CHAPTER 3

THE ROCK MAGNETISM AND PALAEOMAGNETISM OF THE BASALTS OF THE LATE CENOZOIC, INTRA-PLATE WERRIBEE PLAINS LAVA FLOW-FIELD, NEWER VOLCANIC PROVINCE, VICTORIA

3.1 INTRODUCTION

Magnetostratigraphic studies involve organising strata systematically into identifiable units based on stratigraphic variations in their magnetisation directions (see Chapter 4). Only a few studies have previously been done on the palaeomagnetism and rock magnetism of basalts from the Newer Volcanic Province (eg. Green & Irving 1958, Parry 1960, Mumme 1963, Hurren 1998), and this study is the first attempt to establish a magnetostratigraphy in the NVP. Determining the magnetic polarity, or direction of magnetisation of the rocks, involves isolating the magnetisation acquired during emplacement of the lavas, termed the primary remanent magnetisation (remanence) from secondary remanent magnetisation. In this chapter the background theory and representative results of the palaeomagnetic studies for this project are given. In some samples the primary remanent magnetisation was not identifiable because these samples were found to be palaeomagnetically unstable. The reasons why these samples are unstable are explored here, with a view to identifying and discarding the results of any other unreliable samples. Finally, variations in inclination results through individual lava flows are briefly explored in order to assess how representative the results of one to two samples per flow are of the direction of the magnetic field during lava emplacement.

3.1.1 Background theory

The Geomagnetic Field

Generation of the geomagnetic field occurs within the Earth's fluid outer core, where the magnetohydrodynamic features of convection cells, rotational shear, and flux trapping serve to produce a self-exciting dynamo (Butler 1992). The essential elements of this self-exciting dynamo are: (i) a moving electrical conductor (Fe-Ni alloy in core), (ii) an initial magnetic field, (iii) reinforcement of the original magnetic field by interaction between the magnetic field and the conductor, and (iv) energy supplied to overcome electrical resistivity losses (Butler 1992). It is a positive feedback system: an electrical current is produced by the initial magnetic field, which produces a magnetic moment, thus reinforcing it. The dominant

portion of the Earth's geomagnetic field has the form of a dipole field, currently inclined at $\sim 11^\circ$ to the rotational axis. The time-averaged model used for the Earth's magnetic field is a geocentric axial dipole (GAD): a magnetic field produced by a single magnetic dipole at the centre of the Earth and aligned with the rotation axis. In a GAD, where geographic and magnetic poles coincide, the inclination of the field increases from -90° at the geographic/magnetic south pole to $+90^\circ$ at the geographic/magnetic north pole. Lines of equal inclination should be parallel to lines of latitude and, for a GAD, the declination (angle from geographic north to horizontal component) is 0° everywhere.

However, in the present geomagnetic field there are deviations from the simple GAD model. For example, the geographic and magnetic poles do not coincide, nor are the magnetic poles completely antipodal. Furthermore, the direction and magnitude of the geomagnetic field change with time, partially attributed to fluid eddy currents within the core near the core-mantle boundary. Changes with periods between 1 and 10^5 years constitute geomagnetic secular variation (Butler 1992). On longer time scales (10^4 - 10^8 years (Butler 1992)), the dipolar geomagnetic field has been observed to switch polarity, i.e. a 180° change in the declination (bearing) of the geomagnetic field at all points, and a change in the sign of the angle of inclination (magnetic dip). In the last 45 Myr the mean interval between reversals has been ~ 0.4 Myr and the duration of a polarity switch event may be up to several thousand years (Jacobs 1984). Secular variation and reversals of the geomagnetic field form the basis of magnetostratigraphic studies, as volcanic rocks commonly retain a record of the Earth's magnetic field direction at the time of emplacement, and rocks with a similar record may be correlated.

Ferromagnetism of fine particles: single domain vs. multi-domain grains

Rocks contain assemblages of fine-grained ferromagnetic minerals dispersed within a matrix of diamagnetic and paramagnetic minerals. Ferromagnetic minerals (eg. titanomagnetite, titanohematite) are unique in that they are able to retain a magnetisation from an applied magnetic field upon removal of the field. Palaeomagnetic studies utilise this record of the primary remanent magnetisation of rocks (i.e. the direction of magnetisation of the geomagnetic field at the time of emplacement). This discussion on ferromagnetism of fine particles is largely taken from Butler (1992). Basically, ferromagnetic particles seek the configuration of their magnetisation that minimises their total energy. Magnetisation is most easily achieved along certain crystallographic directions, called magnetocrystalline easy

directions. If a grain is elongate however, magnetostrictive energy (shape anisotropy) will dominate, so that the grain will magnetise along its long axis. When a rock is magnetised, magnetic forces cause parallel or anti-parallel alignments of electron spin along the easy axes of grains. The magnetostatic forces are increased because of the attraction of the poles of individual grains to one another.

In order to minimise the total energy, formation of magnetic domains occurs within some particles. This decreases magnetostatic energy because the percentage of the grain's surface covered by magnetic charges is reduced and charges of opposite signs are adjacent rather than separated. Domains are separated by domain walls, which have both finite energy and finite width. The rock acquires its overall magnetisation by the sum of all the individual grain/domain orientations. Grains that contain several domains are referred to as multi-domain (MD). With decreasing grain size, the number of domains are reduced until grains become single domain (SD). The single-domain threshold grain size depends on a number of factors including grain shape and saturation magnetisation (see below). It is important to be able to differentiate between the different grain types when doing palaeomagnetic work, as their magnetic properties are very different. SD grains for example are more efficient carriers of remanent magnetisation than MD grains. Pseudo-single domain (PSD) grains are intermediate between SD and MD grains. They contain a small number of domains, can have substantial magnetic moment, and are potentially important carriers of remanent magnetism. Superparamagnetic grains (SPM) are fine-grained ferromagnetic minerals. Remanent magnetisation in an assemblage of these grains is unstable; the remanence will decay to zero very soon after removal of the magnetising field, hence SPM grains are unsuitable for palaeomagnetic studies.

A hysteresis loop (the path of magnetisation as a function of the applied field) is shown in Fig. 3.1 for a rock whose ferromagnetic population is dominated by SD grains. Magnetisation of individual ferromagnetic particles (lower-case symbols) adds vectorially to yield the net magnetisation for the sample (upper-case), which is the parameter measured in the hysteresis experiment. Application of the initial magnetising field leads to net magnetisation acquired parallel to the field along the path 0-1-2. As the field is applied, j_s of each SD grain begins to rotate toward the applied magnetic field. The sample reaches its saturation magnetisation, J_s , once all the grains have j_s aligned with the field, if the applied field is increased to a sufficient level. The saturation magnetisation of a sample depends (nearly) linearly on concentration of the ferromagnetic mineral. Reduction of the magnetising field

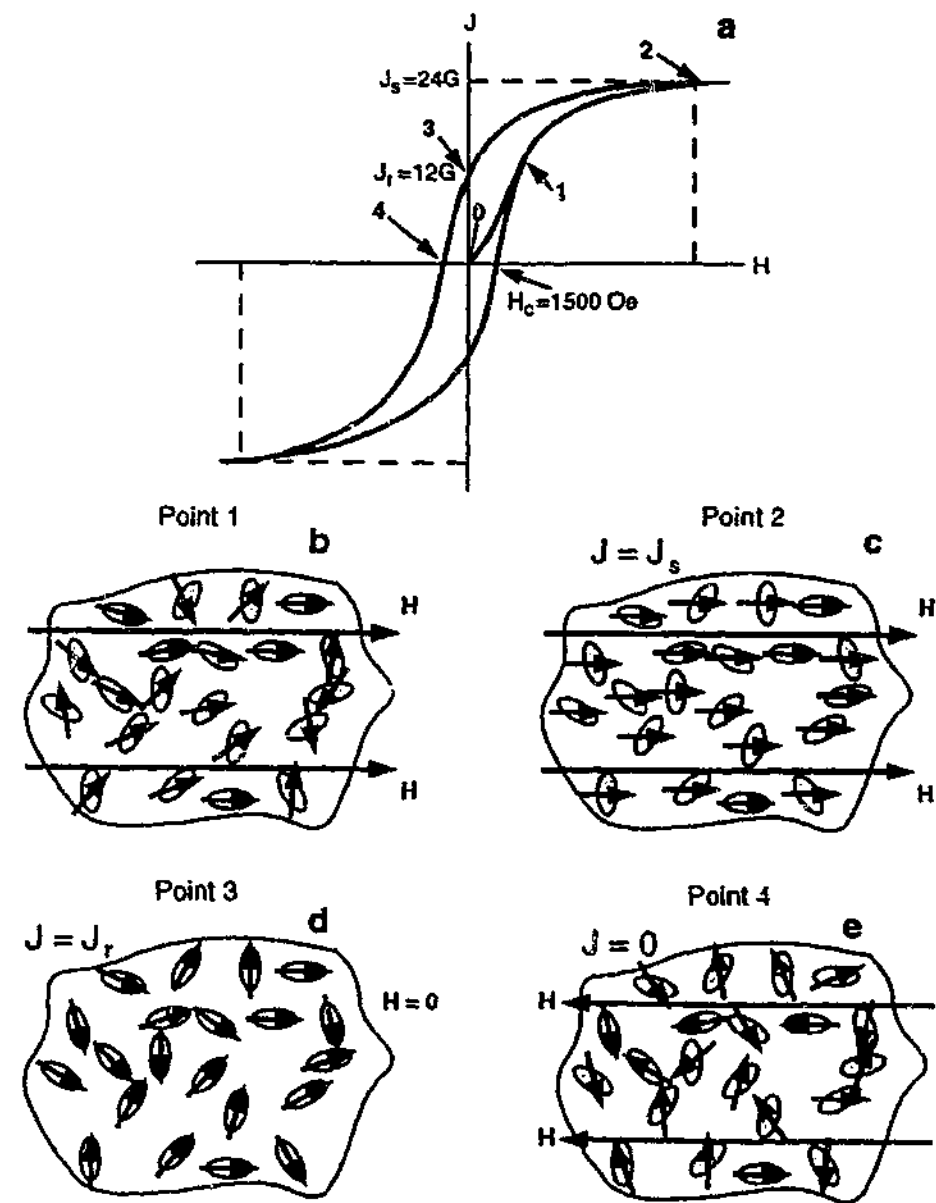


Fig. 3.1a. Hysteresis loop for synthetic sample containing 5% by volume of dispersed elongate SD magnetite particles. Note the significance of shape anisotropy of the elongate grains here (magnetostrictive energy), rather than magnetocrystalline energy. The saturation magnetisation of the sample is J_s , the remanent magnetisation of the sample is J_r , and the bulk coercive force is H_c . b. Magnetisation directions within SD grains at point 1 on hysteresis loop. Stippled ovals are schematic representations of elongate SD magnetite grains; arrows indicate directions of j_i for each SD grain. H is the magnetising field, and note that j_i of each grain is rotating toward H . c. Magnetisation directions within SD grains at point 2 on hysteresis loop. Sample is at saturation magnetisation J_s , and note that j_i of every grain is aligned with H . d. Magnetisation directions within SD grains at point 3 on hysteresis loop. The magnetising field has been removed, and sample magnetisation is remanent magnetisation J_r . Note that j_i of each grain has rotated back to the long axis closest to the saturating magnetic field, which was directed toward the right. e. Magnetisation directions within SD grains at point 4 on hysteresis loop. The sample has magnetisation $J = 0$. Note that j_i of every grain has been slightly rotated toward the magnetising field H (now directed toward the left). After Butler (1992).

causes J to decrease along the path 2-3. After removal of the magnetising field, a remanent magnetisation J_r remains. To force J back to zero, a magnetic field must be applied in the opposite direction to the original field. J decreases along the path 3-4, and the magnetic field required to drive J to zero is the bulk coercive force, H_c . H_c depends on energy balances within the individual SD grains, h_c and not on the concentration of the ferromagnetic mineral. The hysteresis loop is completed by driving the sample to saturation in the negative direction, then cycling back to saturation in the positive direction.

Application of a magnetic field to a MD grain produces preferential growth of domains with magnetisation parallel to the field. If the applied field is sufficiently strong, domain walls are destroyed, and magnetisation reaches saturation. On removal of the magnetising field, domains reform and move back toward their original positions. Due to lattice imperfections and internal strains domain walls settle in energy minima near their initial positions, and a small remanent magnetisation results. Coercive forces of MD grains are low however, as only a small magnetic field is required to drive the domain walls back to the zero moment positions. Furthermore, magnetisation of MD particles tends to decay with time, thus explaining why they are less effective recorders of palaeomagnetism than SD grains.

Demagnetisation techniques

The remanent magnetisation present in a volcanic rock sample prior to laboratory treatment is typically composed of primary and secondary remanence components. The most thermodynamically stable component in a sample is termed the 'characteristic remanence'. Generally, this will be the primary remanence. Recognition and erasure of the secondary remanence by partial demagnetisation techniques is the major goal of palaeomagnetic laboratory work. Secondary remanence can result from chemical changes affecting the ferromagnetic minerals (eg. Verhoogen 1962), subsequent heating and cooling (partial thermoremanence, pTRM), long-term exposure to the geomagnetic field subsequent to rock formation (viscous remanence, VRM) or lightning strikes (Butler 1992). Three basic forms of primary remanence are thermoremanence, chemical remanence and detrital remanence. Basalts retain a thermoremanent magnetisation, which is produced by cooling from above the magnetic blocking temperature in the presence of a magnetic field. At surface temperatures this may be stable over geologic time. Two partial demagnetisation techniques have been developed to isolate the primary remanence: thermal demagnetisation and alternating-field (AF) demagnetisation.

The procedure for step-wise thermal demagnetisation involves heating a specimen to an elevated temperature (T_{demag}) below the blocking temperature of the constituent ferromagnetic minerals, then cooling to room temperature in zero magnetic field. The blocking temperature (T_B), which is characteristic of the particular ferromagnetic mineral is the temperature beyond which the grains become paramagnetic in nature, and do not retain a remanent magnetisation (Butler 1992). In general, grains which carry a viscous remanence also tend to have low T_B . As a sample is heated, the magnetisation of all grains for which $T_B \leq T_{demag}$ is randomised. The effect of a viscous remanence can therefore be randomised, and the primary remanence isolated. The Curie temperature of a mineral is higher than its blocking temperature, and grains behave superparamagnetically between these two temperatures (ie. do not retain a stable remanence). AF demagnetisation techniques involve exposing a specimen to an alternating magnetic field. The waveform of the alternating magnetic field is a sinusoid with linear decrease in magnitude with time. By constantly switching the direction of the applied magnetic field, the magnetisation of grains with $h_c \leq H_{AF}$ (the maximum amplitude of the applied magnetic field) tend to cancel each other out, as they point in opposite directions (Butler 1992). The secondary remanence is predominantly carried by grains which have lower h_c values than the primary remanent component, thus allowing isolation of the primary remanence.

3.2 METHODS

Samples were collected from diamond drill core from the Werribee Plains (Fig. 3.2). Two to three samples were taken from every flow unit identified for the demagnetisation experiments (180 samples, Fig. 3.3). Rock that exhibited the least effects of oxidation and/or alteration was preferentially sampled, commonly near flow margins. Material with fractures, cracks, and large vesicles were avoided. Moderately long segments of core (> 30 cm) were preferentially sampled, and it was checked that the core fitted snugly with the surrounding pieces (ie. the orientation was correct). Approximately 10 cm long half-core samples were taken, and a line was drawn down the central axis of each sample. The central axis of the core represents the way down (the z axis), as the drill holes are vertical. The half-core segments were press-drilled to produce 2.5 cm diameter cylinders (2.1 cm long). Orientation markings and sample numbers were added with heat-proof paint for samples undergoing thermal demagnetisation.

Both thermal and AF demagnetisation are step-wise techniques, and have common

features. After calibrating a Molspin "Minispin" spinner magnetometer with a sample of known magnetic moment, the natural remanent magnetisation (NRM) or undemagnetised remanence of each sample in a batch (~15 samples) was measured (eg. Piper 1987). Samples were then demagnetised, the demagnetised remanence was measured, the demagnetisation step increased, the samples remeasured, and so on. Thermal demagnetisation involved heating the samples in a MMTD (Magnetic Measurements Thermal Demagnetiser) shielded furnace to progressively higher temperatures, holding them for 25 minutes at each heating stage, before cooling to room temperature (and analysing) in magnetic field-free space. The increments of heating were 50°C steps beginning at 100°C, up to 500°C. Between 500°C and 600°C the increments of heating were reduced to 25°C. The dominant carrier of remanent magnetism in basalts is generally found to be titanomagnetite (Petersen 1976, Herzog *et al.* 1988), with a Curie temperature of around 580°C (Butler 1992). For this reason the maximum temperature the samples were heated to was 600°C. The magnetic susceptibility of each sample within a batch was measured with a Bartington MS2 system after the remanence measurement in each demagnetisation step, prior to the next stage of heating. This machine operates at two frequencies: high (4.6 kHz) and low frequency (0.46 kHz). At the NRM stage, both high and low frequency measurements were taken, and thereafter only low frequency measurements. Each sample was demagnetised separately when doing AF demagnetisation. Demagnetisation was conducted in a Molspin AF demagnetiser, where the sample was exposed to an alternating magnetic field, which decreased in magnitude with time. The first field applied was 5 mT, and then the sample was subsequently subjected to higher alternating magnetic fields at 5 mT intervals up to 60 mT. The magnetic susceptibility of each sample was measured at the NRM stage only (both high and low frequency measurements).

Twenty samples were carefully selected for rock magnetic study, in order to determine the dominant ferromagnetic grain type (SD, PSD, MD or SPM), and hence to assess how confidently the primary remanence could be identified. The primary remanence was confidently identified in ten samples, and ten were significantly overprinted by a secondary remanence. Samples for hysteresis and isothermal remanence studies were prepared by being crushed to a coarse sand size. A split of the crushed sample (~0.3 g) was put into small (1 cm³) syringes. Hysteresis loops and coercivity of remanence (H_{cr}) were measured with a Molspin NUVO vibrating sample magnetometer. In hysteresis, the specimen was subjected to an applied field produced by a dipolar electromagnet. The specimen was vibrated, the net magnetisation of the specimen (remanence and induction) produced an oscillating magnetic field, which

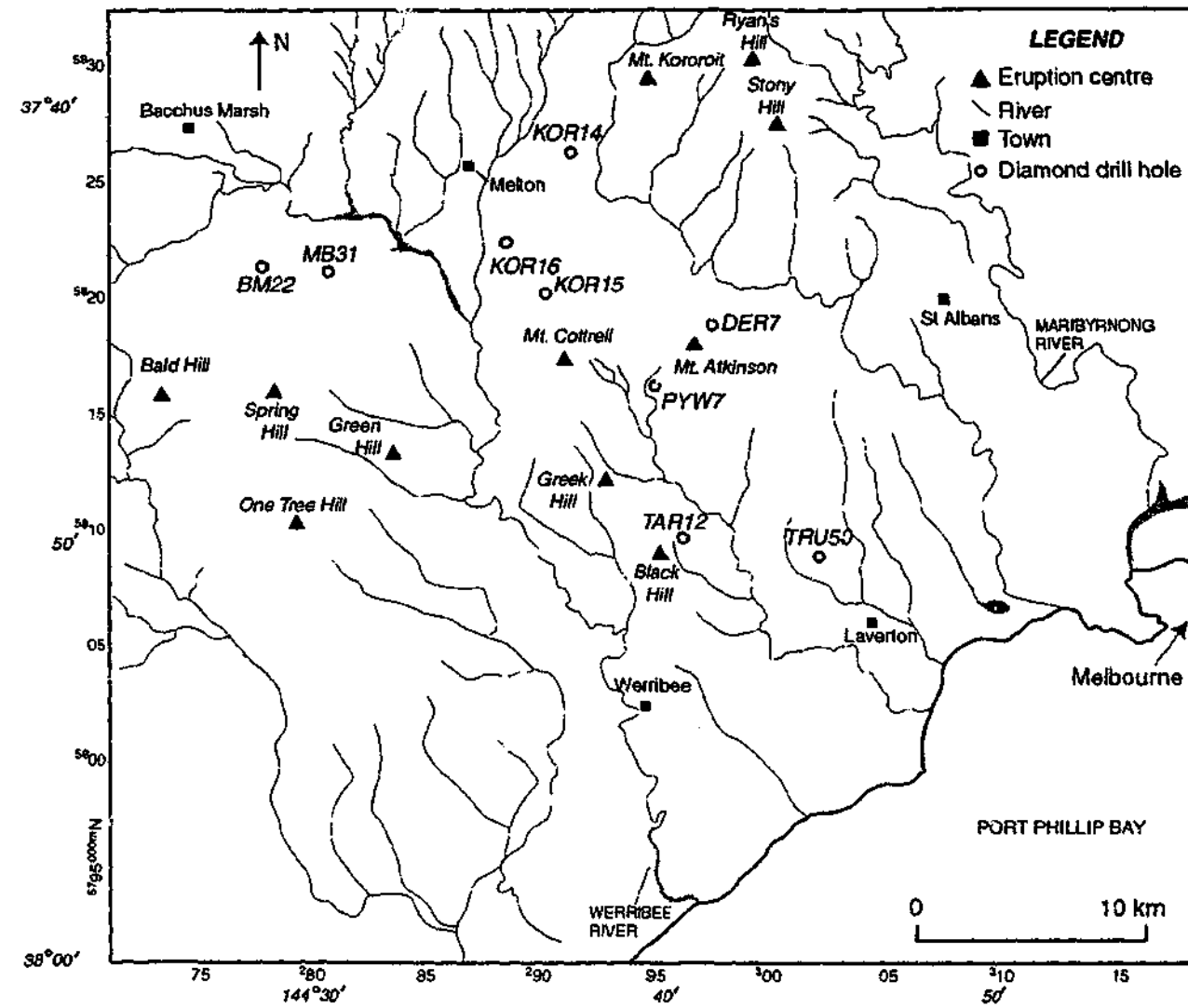


Fig. 3.2 The distribution of diamond drill holes in relation to the eruption centres exposed in the Werribee Plains. Samples for palaeomagnetic studies were collected from almost every flow unit identified (Fig. 3.3).

produced an alternating current in a detector coil. The applied field was initially set at 1000 mT (exceeding saturation for magnetite), and the magnetisation measured. The applied field was then reduced incrementally until it reached zero, with the resulting magnetisation measured at each step. The applied field was then increased stepwise in the opposite direction, until it reached 1000 mT, decreased again to zero, and increased from zero to 1000 mT in steps in the original direction (magnetisation again was measured at each step). H_c was determined by imparting a saturation remanence at 1000 mT. The applied field was then switched off, and the remanence measured in the absence of induction. The polarity of the applied field was reversed, and the sample was subjected to a progressively stronger applied field, beginning at 10 mT (the practical minimum limit of the vibrating sample magnetometer). After each step the applied field was again switched off, and the remanence measured. H_c is defined by the interpolated value of the applied field at which the remanence becomes zero.

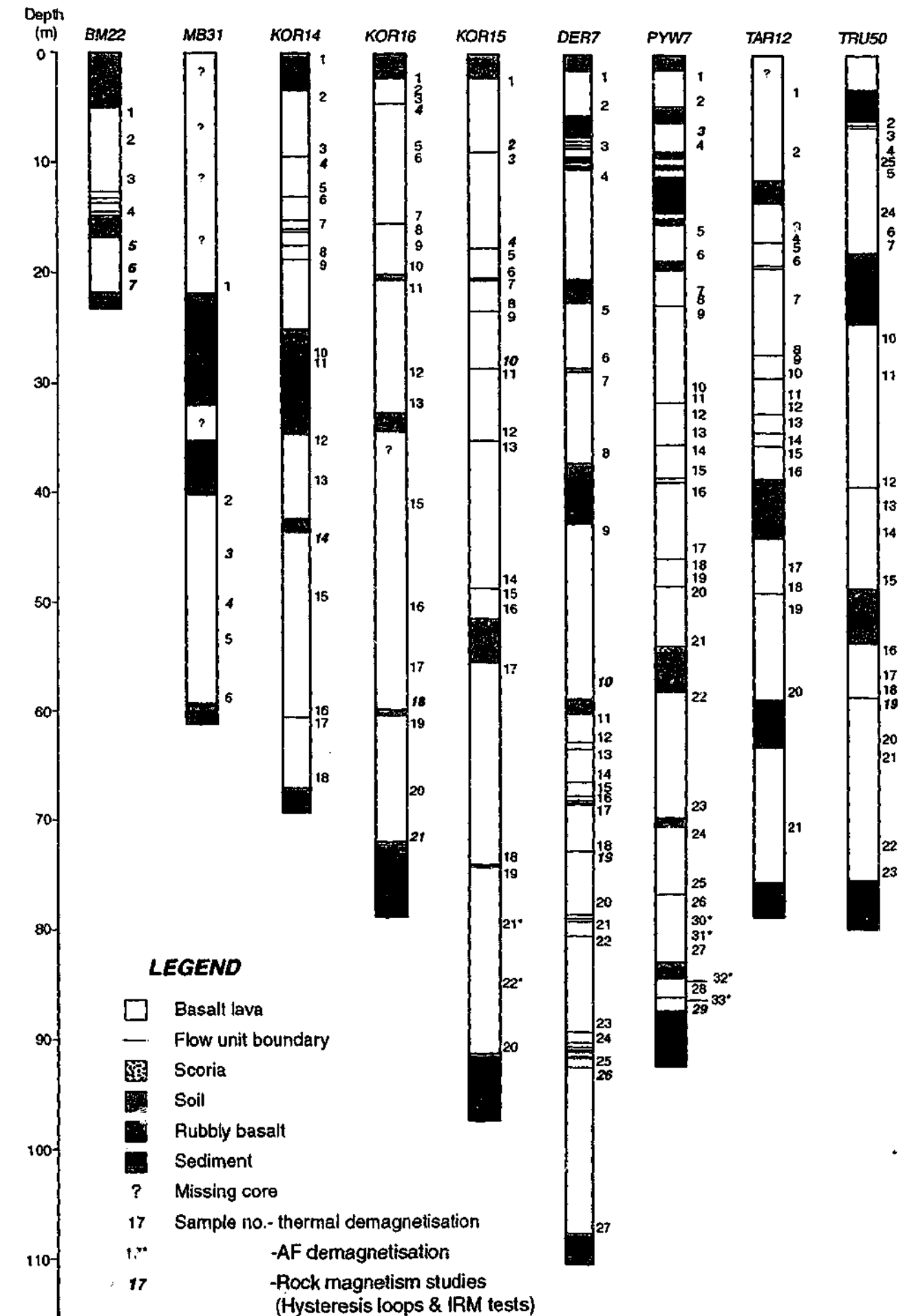


Fig. 3.3 Positions of samples taken for palaeomagnetic and rock magnetic studies. Samples were taken near the margins and in some instances through the interiors of almost every flow unit identified in drill core.

3.3 RESULTS

3.3.1 Thermal demagnetisation

Analysis of demagnetisation data was aided by the use of Zijderveld and Equal Area plots. Zijderveld plots are vector component diagrams that display the progressive changes in both direction and magnitude of remanence (Zijderveld 1967). The base of the remanence vector at each demagnetisation step is placed at the origin of a Cartesian coordinate system, and the tip of the vector is projected onto orthogonal horizontal and vertical planes. These are shown as superimposed plots sharing a common axis, either the North-South or East-West axis, as appropriate. The distance of each data point from the origin is proportional to the intensity of the remanence vector projected onto that plane. Ideally, if the remanence consists of two components, two linear sets of data points will be plotted. The trajectory of the set of demagnetisation steps representing the primary remanence component projects toward the origin (Butler 1992). This is important to observe, as it indicates that a single vector with constant direction is being removed, and that the low stability remanence component has successfully been removed. Principal component analysis was used to determine the direction of the line of best fit through the data points of interest (eg. Kirschvink 1980). The origin was used as a separate data point, along with the points selected and considered to represent a single magnetic component projecting towards the origin (Figs. 3.4 & 3.5). The software "PaleoMag" automatically calculated the direction of the line of best fit for the selected points, as well as a maximum angular deviation to provide a quantitative measure of the precision. Equal Area plots are spherical projections, produced by projecting onto a hemisphere the tips of the vectors of magnetisation removed at each demagnetisation interval. If two components of magnetisation are present in a sample, two discrete clusters of points would be expected (if their stability spectra are distinct).

The primary remanent magnetisation was identified in the majority of samples, commonly in the demagnetisation steps from ~525-600°C (Appendix D). This confirms that the dominant carrier of the remanent magnetisation is titanomagnetite with a Curie temperature of around 580°C. These data points form a straight line on the Zijderveld plot, passing through the origin. Based upon the Zijderveld plots, samples can be subdivided into three main groups: (1) those which have not been significantly overprinted, and the primary remanence is clearly identifiable, (2) those which have been overprinted, yet the primary remanence is identifiable, and (3) those which have been overprinted and the primary remanence is not identifiable (Appendix D). The majority of samples fall into group (1) (Fig. 3.4a). Equal Area plots for

group (1) samples consist of a single cluster of points, indicating a constant orientation of magnetisation throughout the demagnetisation process (Fig. 3.4b). A Zijderveld plot characteristic for group (2) samples, in which two distinct magnetic components have been identified, is shown in Fig. 3.4c. Secondary overprints may be partial thermal remanent magnetisation, produced by reheating the rock to a temperature below the blocking temperature of the constituent ferromagnetic minerals (section 3.1.1). This may occur by thermal conduction from an overlying lava flow that was emplaced at a later time. Alternatively, the overprint may be viscous in origin, acquired subsequent to emplacement by prolonged exposure to the geomagnetic field. A VRM will always be normal polarity, so if an overprint has positive inclination it is probably a partial thermal remanent magnetisation (Fig. 3.4c). For the purpose of this study it was not vital to distinguish between the two; it was more important that they were identified and removed, regardless of origin. It was not always possible to identify the primary remanence, and in these cases (group (3)) both the Zijderveld and Equal Area plots were found to be irregular (Fig. 3.5a & b). The magnetisation in these samples was too weak at the higher demagnetisation levels, and a linear progression was not identified. The secondary remanence component was considered to be dominant, and these samples were disregarded from the magnetostratigraphic studies, although the polarity of each was recorded.

3.3.2 AF demagnetisation

Zijderveld and Equal Area plots were also used to present the results of AF demagnetisation experiments. Instead of the data points representing heating stages, they represent increments of the applied magnetic field. Results are not dissimilar to those obtained using the thermal method, but more magnetisation was generally removed at the lower demagnetisation intervals with the AF technique (Fig. 3.5c). This meant that it was more difficult to identify the primary remanence in some instances, as the magnetic response was relatively weak. The primary remanence component was generally removed and identified in the interval 35-60 mT (ie. over six demagnetisation intervals compared with four in the thermal demagnetisation experiments.) It is difficult to make sound comparisons between the two techniques, as few AF experiments were performed.

3.3.3 Rock magnetic studies

Rock magnetic studies involved running hysteresis loops and doing Isothermal Remanence (IRM) tests on selected samples once the majority of samples had been

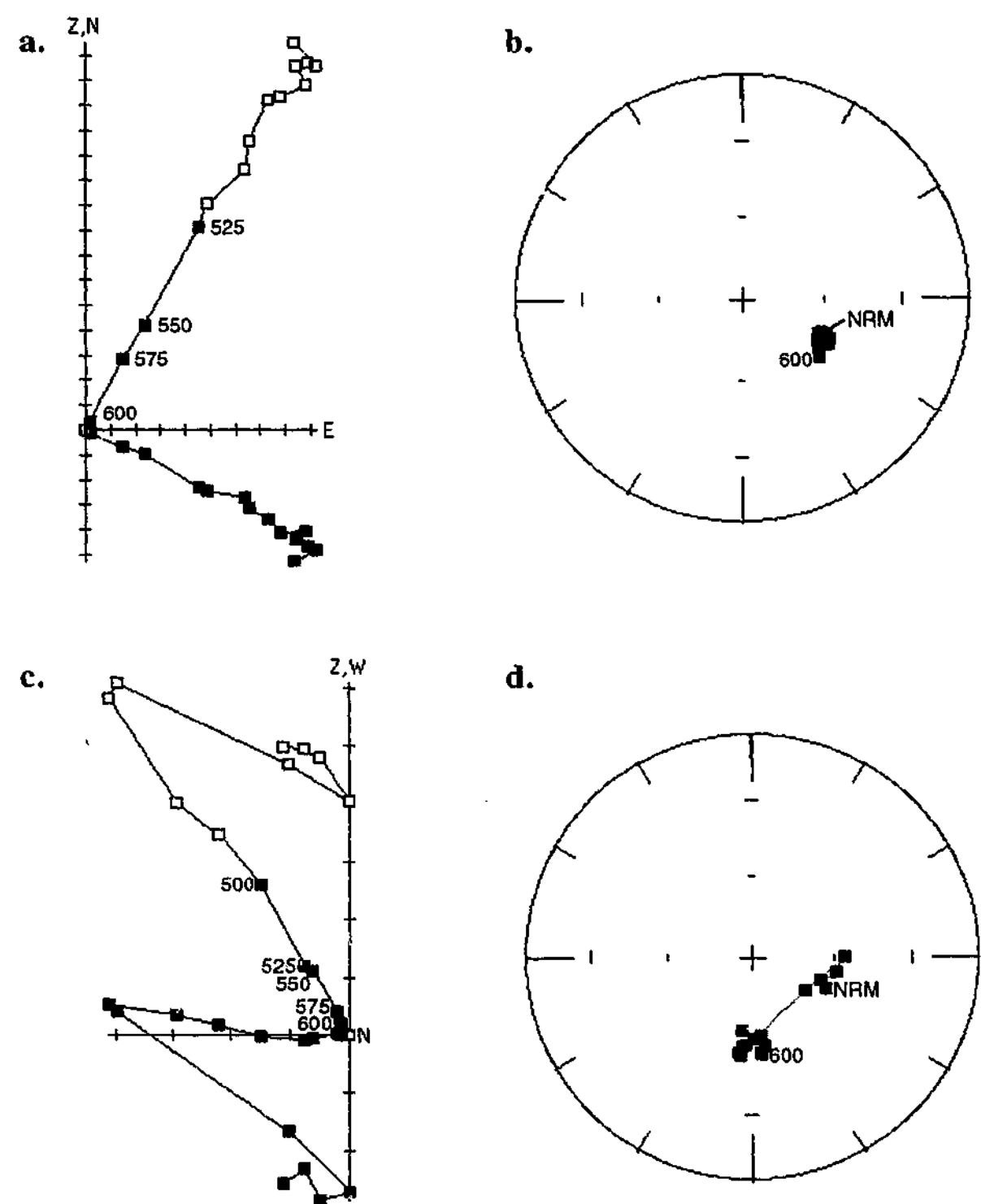


Fig. 3.4 Representative Zijderveld plots and equal area stereographic plots for a. & b. group (1) and c. & d. group (2) samples. Zijderveld plots: greyed squares are projection on the N-S vertical plane, solid black squares are projection on a horizontal plane, north to the right. Stereographic plots: greyed squares are projection on upper hemisphere; solid black squares are projection on lower hemisphere. All plots are shown as geographic coordinates, and each division on the Zijderveld plots is a. 10^{-4} emu and c. 10^{-5} emu. a. & b. Sample PYW7-17 has not been substantially overprinted, as only one component of magnetisation dominates. The inclination was calculated as -57.9° . c. & d. Two components of magnetisation are identified in sample BM22-5. The secondary overprinting component is reversed polarity, while the inclination of the primary remanent magnetisation is -60.1° . This is not particularly uncommon.

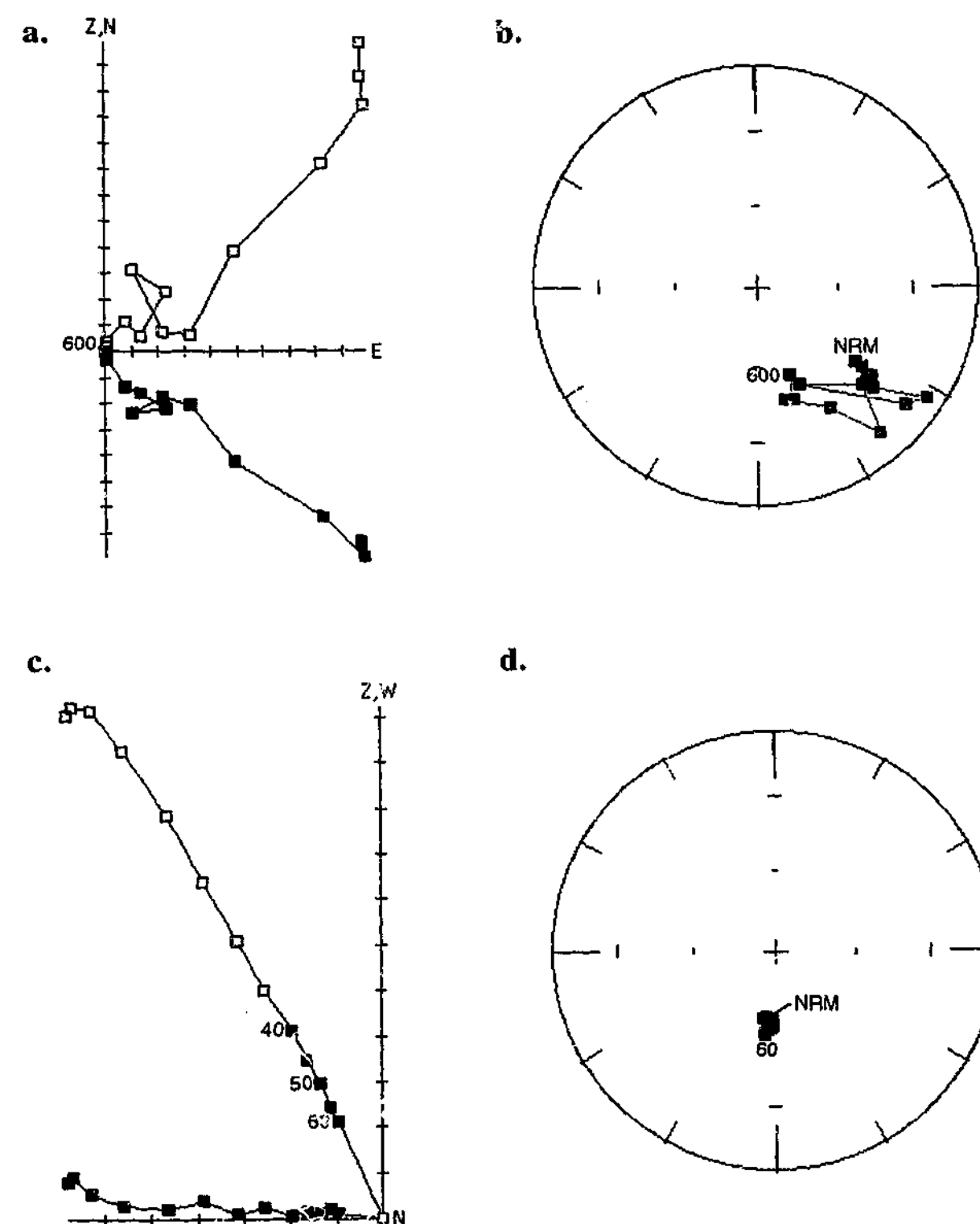


Fig. 3.5 Representative Zijderveld plots and equal area plots for a. & b. group (3) and c. & d. AF demagnetised samples. Refer to Fig. 3.4 for explanation of symbols on Zijderveld and stereographic plots. Each division on the Zijderveld plots is a. 10^{-4} emu and c. 10^{-5} emu. a. & b. The primary remanent magnetisation was not able to be identified for sample MB31-4. Note the large proportion of demagnetisation that occurred at the lower temperatures. Also note the irregular path of demagnetisation, as shown on the equal area projection. c. & d. The primary remanence is identified over the interval 40-60 mT for sample PYW7-32, as a linear projection toward the origin (-61.7°).

demagnetised. A representative group of samples were chosen from most drill holes, from various positions within flows, and from each of the three groups identified above (Fig. 3.3). Hysteresis loops were run on all of these samples (eg. Fig. 3.6). The curves produced consist

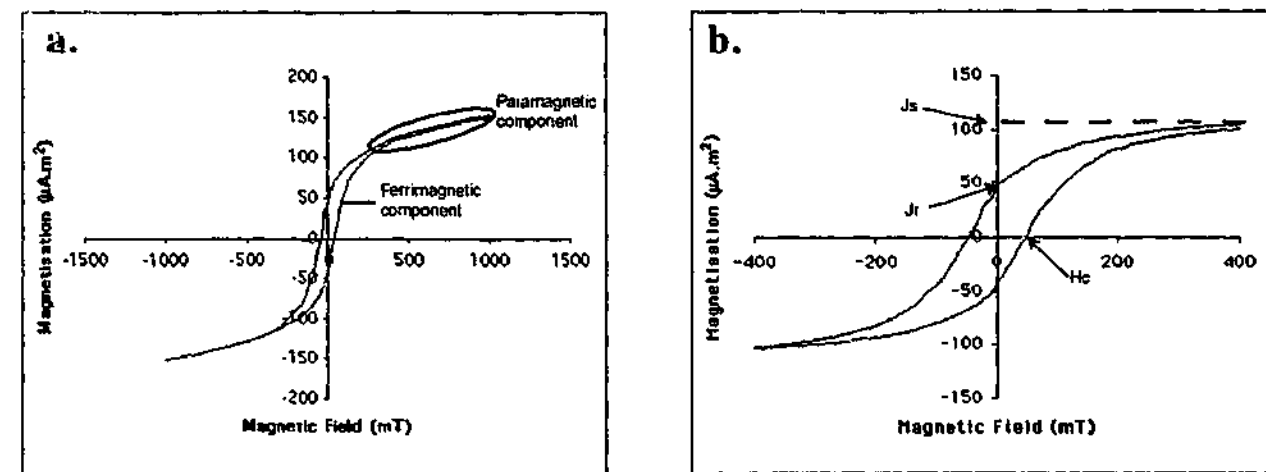


Fig. 3.6a. The results of a representative hysteresis loop for sample KOR16-4 prior to b. removal of the paramagnetic component. Values of interest from this graph are the saturation magnetisation (J_s), which is the maximum value of magnetisation, at which the graph plateaus; the saturation remanent magnetisation (J_r) which is the point at which the graph crosses the y axis, ie. the magnetisation retained after the magnetic field is removed; and the coercivity (H_c) which is the point the graph crosses the x axis - the back-field required so that the induced magnetisation (in the reversed direction) and the surviving remanence add up to zero.

of a paramagnetic component in addition to the ferromagnetic component. Paramagnets do not support a remanence and do not saturate, so the paramagnetic contribution takes the form of a straight line through the origin, with a slope determined by the paramagnetic part of the susceptibility. This is superimposed on the ferromagnetic contribution, which forms an open loop around the origin of the hysteresis plot, and saturates above about 300 mT. The curves were modified by removing the paramagnetic component of the magnetisation and correcting for calibration. These results were used along with the coercivity of remanence to construct a Day plot (Day *et al.* 1977) and a Bradshaw & Thompson plot (Bradshaw & Thompson 1985, Fig. 3.7). The coercivity of remanence was obtained by doing IRM tests (section 3.2, Appendix E). The Day plot defines *theoretical* fields for different domain states of the dominant ferromagnetic grains present in each sample. This is based upon experimental studies of the magnetisation and coercivity ratios for random assemblages of non-interacting magnetic grains of various grain sizes (Day *et al.* 1977). The Bradshaw & Thompson plot has been constructed based upon *empirical* observations. This explains why samples plot in different fields on the two graphs (section 3.4).

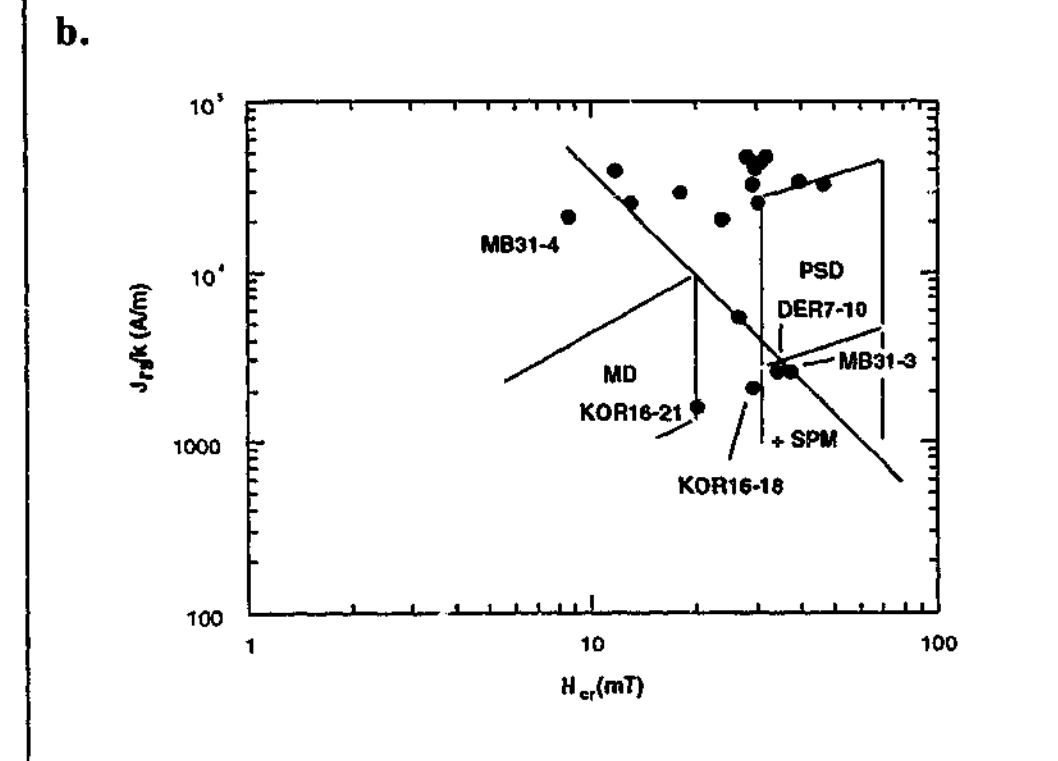
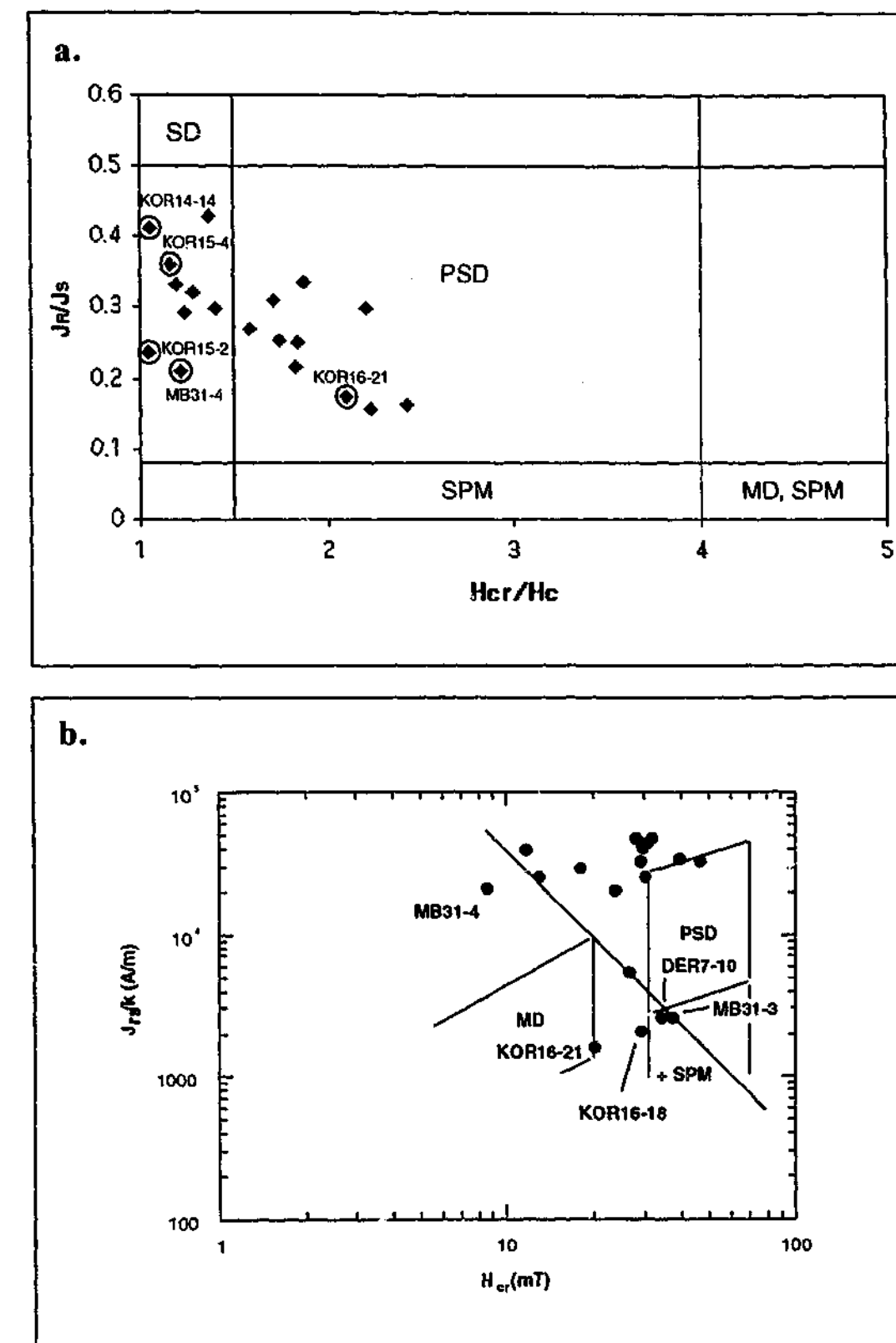


Fig. 3.7a A Day plot (Day *et al.* 1977), constructed using the data collected in the rock magnetic experiments as outlined. All samples plot in a band extending between the theoretical fields for pure PSD and SD assemblages, suggesting that they are dominated by a mixture of PSD and SD grains. They are therefore potentially efficient carriers of remanent magnetisation. The primary remanence was not identified for the circled and labelled samples (group 3)). b. A Bradshaw & Thompson plot (Bradshaw & Thompson 1985). Most of the samples plot between the PSD and MD grain fields, and the samples labelled have been discarded from this study (section 3.4).

3.4 DISCUSSION

Identifying palaeomagnetically unstable samples

The results of the demagnetisation experiments have been subdivided into three groups based upon Zijdeveld and Equal Area plot interpretations (section 3.3.1). Group (3) samples (16 in total) do not have an identifiable primary remanent magnetisation. One aim of this discussion is to investigate why these samples have not retained an identifiable primary remanence, and to identify additional samples with unreliable results. The group (3) samples may have been significantly overprinted by a subsequent chemical remanent (eg. oxidation), thermoremanent (pTRM), viscous remanent (VRM), and/or isothermal remanent (lightning strikes) magnetisation. A VRM is likely to affect the very fine-grained population (on the threshold between superparamagnetic and SD), and the coarser grained MD grains.

It is possible to quantify to some extent the degree a sample has been magnetically overprinted by calculating the Königsberger ratio, Q (equations 3.1-3.4). This gives an indication of the relative proportion of induced and remanent magnetisation present in a sample (Dunlop & Özdemir 1997).

$$Q = J_r / J_i \quad 3.1$$

where J_r is the remanent magnetisation and J_i is the induced magnetisation in a field of 50,000 nT.

$$J_i = kH; B = \mu_0 H \quad 3.2, 3.3$$

where k is the susceptibility (Appendix F), H is the magnetic field strength, B is magnetic induction, and μ_0 is the permeability of free space ($4\pi \cdot 10^{-7} \text{ Hm}^{-1}$). Combining these equations, we find that:

$$Q = \frac{J_{NRM} [Am^{-1}]}{k \times 5 \cdot 10^{-5} [T]} \times 4\pi \cdot 10^{-7} [Hm^{-1}] \quad 3.4$$

where J_{NRM} is the remanent magnetisation measured prior to demagnetisation. For high values of Q (greater than 1) the magnetisation in a sample is dominated by the primary remanent magnetisation, and the sample is considered to be stable and a good recorder of the ancient

magnetic field (Jacobs 1987). For example, Q values for SD magnetite are usually more than 10 (Dunlop & Özdemir 1997). Rocks with low Q values (less than 1) have weak remanent magnetisations relative to their induction, and are dominated by induced magnetisation. The mean value of Q calculated for all the palaeomagnetic samples in this study was 10.7 ± 1.7 (Appendix G). Thus, in general, the samples have retained a strong remanent magnetisation. Samples with Q values less than 2 are considered to have unreliable inclination values for this study, as the primary remanence is either unidentifiable, or very weak and inconsistent. Ten of the group (3) samples (~2/3) were found to have Q values less than 2. Four additional samples (TRU50-13, KOR15-22, PYW7-27 & PYW7-31) were found to have Q values less than 2, even though a weak primary remanent magnetisation was identified in each of these samples. The inclination values of these samples have been discarded from the magnetostratigraphic studies as the magnetisation was considered to be too weak to be reliable. The samples that have been discarded (group (3) and/or Q less than 2) are palaeomagnetically unstable. They are considered to have either a significant proportion of (a) very fine-grained minerals at the superparamagnetic (SPM)-SD grain threshold, or (b) MD grains (section 3.1.1).

(a) Fine-grained magnetite may occur at the SPM-SD grain threshold, and these grains retain a remanence upon removal of a magnetising field, however the remanence quickly decays to zero. Based upon the rock magnetic study, a number of samples potentially may contain SPM-SD threshold grains (Fig. 3.7). On the Day plot some samples occur close to the boundary between PSD and SPM, and on the Bradshaw & Thompson plot three samples occur in or near the SPM grain field. An independent test was carried out on all samples to identify the samples that are dominated by SPM-SD threshold grains. It has been consistently observed that there is a loss in susceptibility in SPM-SD threshold dominated samples when measured at high frequency as compared to low frequency on the Bartington MS2 susceptibility meter (Maher 1988, section 3.2). At the higher frequency some of the ultra-fine SPM grains (in the size range near the SPM-SD boundary) 'block in', thus no longer contributing as SPM but as SD grains (Stephenson 1971). This results in the values of high frequency susceptibility to be proportionally lower than low frequency values. The difference between the two can be expressed as a percentage loss in susceptibility according to:

$$(LF-HF)/LF \times 100 \quad 3.5$$

where LF is the low frequency susceptibility and HF is the high frequency susceptibility.

Equation 3.5 was calculated for all samples (Appendix G). In general, where the value yielded exceeds 5%, the sample is considered to be dominated by SPM-SD grains (eg. Özdemir & Banerjee 1982, Dearing *et al.* 1985). Only three samples were found to have values marginally over 5% (KOR14-4, KOR15-15 and TRU50-3). For each of these samples Q was more than 2 and a primary remanent magnetisation was considered to have been identified. The inclination values for these samples were retained for the magnetostratigraphic studies. No group (3) samples had values calculated to be more than 5%, hence no samples in this study are considered to be dominated by SPM-SD threshold grains.

(b) A sample may have a significant proportion of MD magnetite grains either because the SD and PSD grains have been oxidised subsequent to emplacement leaving predominantly MD grains (eg. Verhoogen 1962), or the grains were originally large (eg. flow centre). High and/or low temperature oxidation of ferromagnetic grains subsequent to emplacement changes their magnetic properties (eg. Verhoogen 1962). The majority of samples that have been discarded with Q values less than 2, and/or are in group (3) occur at or near the base of the basaltic sequence. It is considered that they experienced high levels of groundwater interaction, due to their close proximity to the more porous underlying sediments and, more particularly, due to their location adjacent to the contact which is considered to have been a permeability boundary and zone of preferential fluid flow. Samples that were taken from the centres of flows (in the first sample batch) generally yielded very weak to non-identifiable remanent magnetisations, probably because the ferromagnetic grains are larger in the centres of flows (slower cooling) and multi-domain. MD grains are less effective recorders of palaeomagnetism than SD grains (section 3.1.1). The centres were avoided for sampling thereafter where possible.

The Bradshaw & Thompson plot appears to be more useful than the Day plot for identifying samples dominated by MD grains in this study. All samples that underwent rock magnetic studies plotted in the PSD grain field, or between the PSD and SD fields on the Day plot, suggesting they all have properties favourable for retaining a remanent magnetisation. However, a primary remanence could not be identified in five of the samples (group (3)). In contrast, only one sample occurs in the PSD field on the Bradshaw & Thompson plot. Most appear to be transitional between PSD and MD, with high values of saturation remanent magnetisation normalised for susceptibility (J_r/k), but low coercivity of remanence values (H_{cr}). A similar, although more marked phenomenon, was observed in samples from the Older Volcanics of Victoria (Sawyer 2001) and interpreted to be due to pinning of domain walls in MD grains. When a MD grain has imperfections in the lattice (eg. exsolution lamellae) these

imperfections may prevent the migration of domain walls. This leads to a deviation from classic MD grain behaviour, and results in the persistence of an overprinting remanence to higher demagnetisation temperatures than anticipated. The temperatures required to isolate and remove this remanence are more like those required to remove the primary remanence, therefore making it impossible to isolate the inclination of the primary remanence. Hence, samples dominated by MD grains with pinned domain walls may have high Q values, will have high values of saturation remanent magnetisation normalised for susceptibility (and therefore plot in the PSD grain field on the Day plot), but will not have an identifiable primary remanence. A diagonal line has been drawn on the Bradshaw & Thompson plot, based upon observations, beneath which the (viscous) overprint is considered to have been too large for the primary remanence to have been identified (Sawyer 2001). These samples have been discarded from the magnetostratigraphic studies.

A final cause of overprinting of primary TRM is lightning. Lightning strikes may penetrate up to several metres below the surface as well as horizontally through the sequence (N. Opdyke pers. comm.). They result in a complete overprinting of the primary remanent magnetisation. When this occurs the rock has a characteristically high remanent magnetisation intensity (an order of magnitude higher than adjacent samples) and a complex demagnetisation path. None of the samples from group (3) are considered to have been struck by lightning, however two other samples (PYW7-3 & PYW7-4) might possibly have been. Sample number PYW7-4, in particular has a very high remanence intensity and an anomalously high Q value. Although the Zijderveld plots do not demonstrate particularly complex demagnetisation paths, the inclination values for the two samples are very low and variable (21.5° & -8.5°). For these reasons they are not considered to be primary remanent magnetisations. These samples have been discarded from the magnetostratigraphic studies.

Variations in inclination values through discrete flows

Three flows (two from TRU50 and one from KOR16) had more than three samples taken with identifiable primary remanent magnetisations (Fig. 3.3, Appendix D). The standard error in the mean inclination value for each flow ranged from 0.2 to 2.6° . These relatively small errors are similar to other studies that have looked at variations in magnetic properties and remanent magnetisations through lava flows (eg. Petersen 1976, Herzog *et al.* 1988). Variations in inclination within most of the flows analysed in these studies were considered to be "small and statistical" (Herzog *et al.* 1988). The small variations in inclination values

within a flow in this study are considered to be due to a combination of any or all of the following potential errors: deviations from vertical drilling of the diamond drill holes, inaccuracies occurring during sub-sampling (eg. drill core not cut exactly in half, non-perpendicular press drilling etc.), and random analytical errors.

3.5 CONCLUSIONS

- Almost every flow unit identified in diamond drill core was sampled for palaeomagnetic studies (180 samples). All samples were demagnetised, and the primary remanent magnetisation (the inclination of the geomagnetic field during emplacement of the lavas) was identified in most samples. It was not possible to identify the primary remanence in some samples (24 in total), and these were discarded from the magnetostratigraphic studies.
- The samples discarded are considered to have been significantly overprinted subsequent to emplacement, either by a partial thermoremanent, chemical remanent, viscous, or isothermal remanent magnetisation. These samples were found to be dominated by MD grains with pinned domain walls. The secondary overprinting magnetisation thus persisted to high demagnetisation levels, preventing isolation of the primary remanence.
- It is considered that the primary remanent magnetisation of two samples per flow is representative of the inclination of the magnetic field during emplacement of that lava flow.

REFERENCES

- Bradshaw, R.H.W. & Thompson, R., 1985. The use of magnetic measurements to investigate the mineralogy of some Icelandic lake sediments and to study catchment processes. *Boreas*, **14**, 203-215.
- Butler, R.F., 1992. *Paleomagnetism: Magnetic Domains to Geologic Terranes*. Blackwell Science Ltd., Boston, 319 p.
- Day, R., Fuller, M. & Schmidt, V.A., 1977. Hysteresis Properties of titanomagnetites: grain size and compositional dependence. *Physics of the Earth and Planetary Interiors*, **13**, 260-267.
- Dearing, J.A., Maher, B.A. & Oldfield, F., 1985. Geomorphological linkages between soils and sediments: the role of magnetic measurements. In: *Geomorphology and Soils* (eds Richards,

- K.S., Arnett, R. & Ellis, S.), pp. 245-266, George Allen & Unwin, London.
- Dunlop, D.J. & Özdemir, Ö., 1997. *Rock Magnetism: Fundamentals and frontiers*. Cambridge University Press, New York, 573 p.
- Green, R. & Irving, E., 1958. The palaeomagnetism of the Cainozoic basalts from Australia. *Royal Society of Victoria Proceedings*, **70**, 1-17.
- Herzog, M., Böhnell, H., Kohnen, H. & Negendank, J.F.W., 1988. Variation of magnetic properties and oxidation state of titanomagnetites within selected alkali-basalt flows of the Eifel-Area, Germany. *Journal of Geophysics*, **62**, 180-192.
- Hurren, R.J., 1998. The Lateral Variation of Magnetisation in Tertiary Near Surface Basalts, Victoria. *Unpub. Honours Thesis, University of Melbourne, Melbourne*.
- Jacobs, J.A., 1984. *Reversals of the Earth's Magnetic Field*. Adam Hilger Ltd., Bristol, Great Britain, 230 p.
- Jacobs, J.A., 1987. *Geomagnetism*. Academic Press, Orlando, 627 p.
- Kirschvink, J.L., 1980. The least-squares line and plane and the analysis of palaeomagnetic data. *Geophysical Journal of the Royal Astronomical Society*, **62**, 699-718.
- Maher, B.A., 1988. Magnetic properties of some synthetic sub-micron magnetites. *Geophysical Journal*, **94**, 83-96.
- Mumme, W.G., 1963. Thermal and Alternating Magnetic Field Demagnetization Experiments on Cainozoic Basalts from Victoria, Australia. *Geophysical Journal International*, **7**, 314-327.
- Özdemir, Ö. & Banerjee, S.K., 1982. A preliminary magnetic study of soil samples from west-central Minnesota. *Earth and Planetary Science Letters*, **59**, 393-403.
- Parry, L.G., 1960. Thermomagnetic Properties of Basalt from the Newer Volcanics of Victoria, Australia. *Journal of Geophysical Research*, **65**(8), 2,425-2,428.
- Petersen, N., 1976. Notes on the Variation of Magnetization within Basalt Lava Flows and Dikes. *Pure and Applied Geophysics*, **114**, 177-195.
- Piper, J.D.A., 1987. *Palaeomagnetism and the Continental Crust*. Open University Press, 433 p.
- Sawyer, M., 2001. A new palaeomagnetic pole from the mid-late Eocene Older Volcanics. *Unpub. Honours Thesis, La Trobe University, Melbourne*.
- Stephenson, A., 1971. Single domain grain distributions. 1. A method for the determination of single domain size distributions. *Physics of the Earth and Planetary Interior*, **4**, 353-360.
- Verhoogen, J., 1962. Oxidation of Iron-Titanium Oxides in Igneous Rocks. *Journal of Geology*, **70**, 168-181.
- Zijderveld, J.D.A., 1967. A.C. demagnetisation of rocks: Analysis of results. In: *Methods in Palaeomagnetism* (eds Collinson, D.W., Creer, K.M. & Runcom, S.K.), pp. 254-286, Elsevier, Amsterdam.

CHAPTER 4

THE STRATIGRAPHY, FACIES ARCHITECTURE AND ERUPTION FREQUENCY IN THE LATE CENOZOIC, INTRA-PLATE BASALTIC WERRIBEE PLAINS, NEWER VOLCANIC PROVINCE, VICTORIA

4.1 INTRODUCTION

In basaltic terrains stratigraphic studies have largely been confined to Continental Flood Basalt provinces (eg. Swanson *et al.* 1975, Swanson *et al.* 1979, Camp *et al.* 1982, Hooper 1982, Bailey 1989, Landon & Long 1989, Reidel *et al.* 1989, Wells *et al.* 1989, Ho *et al.* 1996, Self *et al.* 1996, 1997, Thordarson & Self 1998, Marsh *et al.* 2001). Lava flows have been shown to be correlatable over hundreds of kilometres, based upon geochemistry and magnetostratigraphic studies. Less common have been stratigraphic studies in smaller, monogenetic basaltic volcanic fields (eg. Greeley 1982a, b, Tanaka *et al.* 1986, Böhnel *et al.* 1987, Condit *et al.* 1989, Kuntz *et al.* 1992, Müller-Sohnius 1993, Condit & Connor 1996, Reed *et al.* 1997). In the Newer Volcanic Province, for example we have little idea about the frequency and volume of eruptions, the distribution of products (pyroclastic vs. effusive), the lava flow types (pahoehoe vs. aa) and their dimensions, and even the thickness of the basaltic pile is poorly constrained. We know little about the repose periods between eruptions: was sedimentation widespread, and to what extent were the volcanic products eroded and redeposited? What did the NVP (and more particularly the Werribee Plains) look like prior to the commencement of volcanism, and what effect did the palaeotopography have on the distribution of volcanic products? Some of these issues will begin to be addressed in this chapter, as a stratigraphy of the Werribee Plains, NVP is established. They will be expanded on in Chapter 5, and the NVP will be compared with other basaltic provinces, with the intention of better characterising plains-basalt volcanism.

The volcanic products of the Newer Volcanic Province have previously been subdivided into two major groupings, based upon geomorphology and composition (eg. Price *et al.* 1988). The lava plains are considered to be dominantly tholeiitic or chemically transitional, and the constructional volcanic features (scoria cones, maars, tuff rings, and lava shields) are dominantly alkalic. The constructional volcanic features are considered to be younger than most of the lava flows covering the western plains (Price *et al.* 1988). For this reason it has been assumed that there has been a broad change in the composition of the magmas producing

the Newer Volcanic Province with time, from predominantly tholeiitic to more alkalic. Previous stratigraphic studies of the Werribee Plains in particular, have been restricted to sampling and mapping the limited surface outcrops (eg. Condon 1951, Mitchell 1990, Price *et al.* 1997). Condon (1951) identified two main phases of volcanic activity in the Plains: earlier volcanism through fissure eruptions producing sheet flows, and later activity producing 'tongue-flows' from central vents. Through the development and application of radiometric dating techniques it has been shown that the Werribee Plains evolved through more than two phases of volcanism (McDougall *et al.* 1966, Aziz-Ur-Rahman & McDougall 1972, Price *et al.* 1997). By combining the K-Ar ages with Sr isotopic data and other information, Price *et al.* (1997) were able to identify six domains within the Werribee Plains, each considered to consist of single flows or related groups of flows from discrete volcanic centres (ie. eruption packages). This study was done over the whole of the Western Plains sub-province of the NVP, hence details such as identifying eruption centres within the domains was not investigated. Mitchell (1990) did a more focussed study of the geology of the Werribee Plains, including much of this geochemical data. Mitchell did field mapping, detailed petrological studies and additional whole rock geochemical analyses at most of the eruption centres to characterise the products of each. Due to lack of outcrop however, many inferences were made, and she was unable to constrain features such as the types and dimensions of lava flows produced by the various centres.

In this study it is possible to look at the basaltic sequence sub-surface, as continuous core from a number of diamond drill holes that penetrate through the whole basalt pile are available. The characteristics and distribution of volcanic and sedimentary facies are investigated, to better understand the interplay between volcanism and sedimentation, and the palaeogeography of the Werribee Plains. The extent to which the identified eruption packages can be correlated between drill holes to produce a magnetostratigraphy will be investigated, by combining a number of data sets. For example, airborne geophysical images and geochemical data from surface samples will be analysed to investigate the extent of lava flows from the exposed eruption centres, and thus to aid in making these sub-surface correlations. Our present understanding of geochemically distinct lava plains and constructional features in the NVP will be assessed, and the stratigraphy established will provide an ideal framework for further studies investigating broad changes in magma chemistry with time. Once a magnetostratigraphy has been produced, a minimum eruption frequency can be calculated for the Werribee Plains, based upon the age constraints identified.

4.2 METHODS

Volcanic and sedimentary facies were identified, characterised, and their distribution documented through fieldwork, logging diamond drill core, interpreting geophysical well logs, and petrographic studies. Fieldwork was limited to areas with exposed outcrop, which included the eruption centres, road cuttings, river banks and quarries. Core was logged from nine diamond drill holes that have the contact with the underlying Red Bluff Sands preserved (up to 110 m long), as well as four shorter holes through the top part of the basalt sequence. In addition to logging the distribution of volcanic and sedimentary facies, flow unit and eruption package boundaries were identified where possible. Digital data was supplied for >35 geophysical wells in the Werribee Plains by Wiltshire Geological Services, and the corresponding diamond drill core is preserved for two of these wells. The physical properties measured in the well logs are the resistivity, bulk density and radiometric (gamma ray) response of the rock. The range of characteristic values of these parameters for the different lithologies (ie. basalt, sediments and paleosols) was identified in the holes that contained both well logs and diamond drill core, so allowing geophysical well log facies to be calibrated against actual rock intervals. These results were applied to all holes containing only well logs. The contact with the underlying Red Bluff Sands was identified in each well log and the local thickness of the volcanic sequence (including inter-flow sediments) determined. Combining this with the diamond drill hole data, the general shape of the palaeotopography of the Werribee Plains prior to volcanism was deduced (taking into account the present topography).

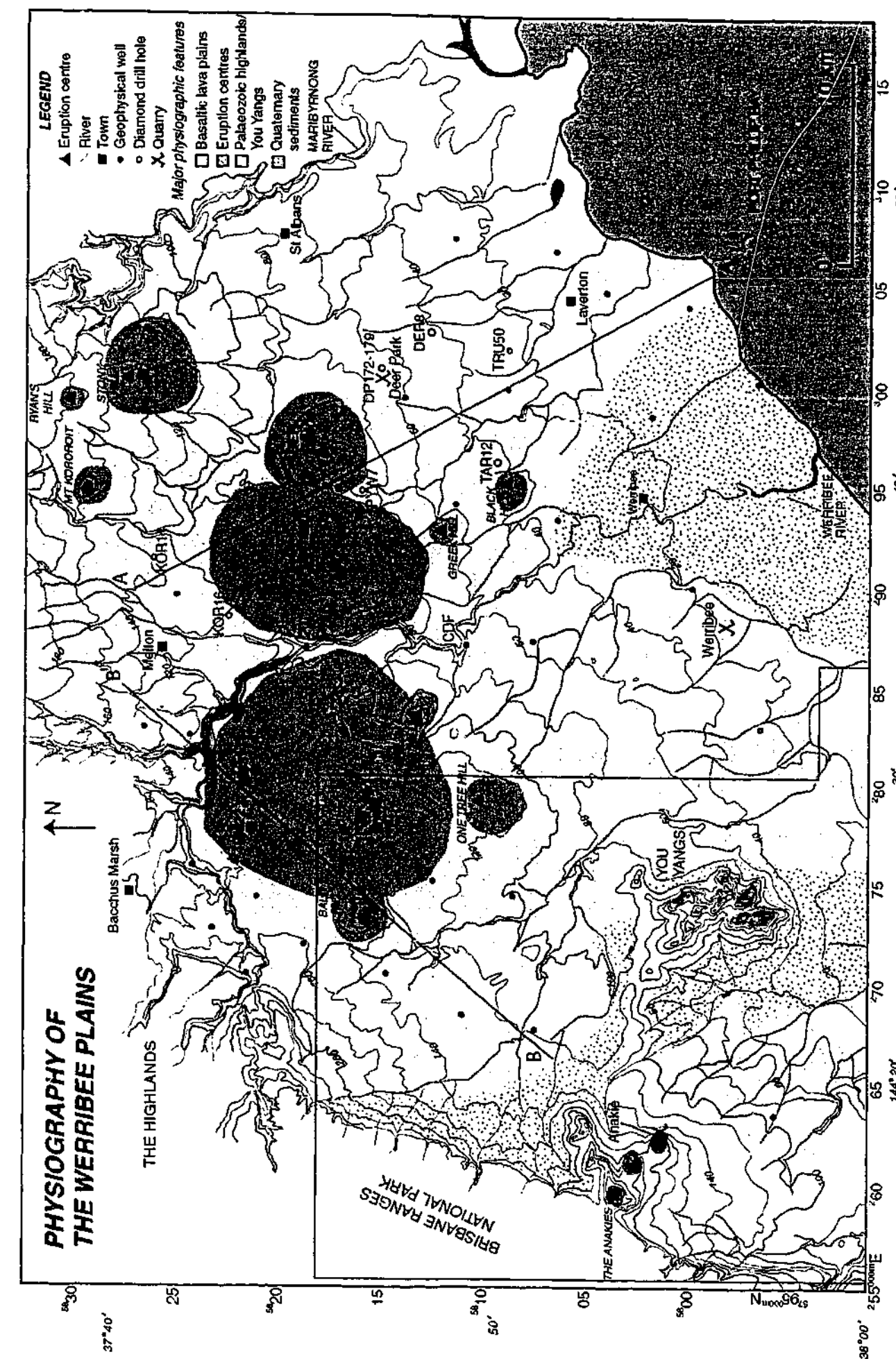
The primary remanent magnetisation of each lava flow identified in drill core was determined by step-wise thermal demagnetisation at Latrobe University. As the core was only vertically oriented, only the inclination of the primary remanence was determined. Two to three samples per flow unit identified in drill core were analysed. For more details about the palaeomagnetic methods see Chapter 3. Samples were collected from eruption points and selected lavas from drill core and fieldwork for bulk rock X-ray fluorescence spectroscopy (XRF analysis). Samples were analysed for major element concentrations on fused glass disks at the University of New South Wales (see Appendix A for methods). Data previously collected from a number of the eruption centres and surrounds (Mitchell 1990), and from grab sampling a grid of ~5 km² spacing over the Plains (Price *et al.* 1997, Gray unpubl. data) was also available. These samples were analysed at Latrobe University by XRF on fused glass disks (for major elements) and pressed powder pellets (for trace elements). Precision for major elements is better than $\pm 0.5\%$.

One sample from drill core was chosen for $^{40}\text{Ar}/^{39}\text{Ar}$ dating, for reasons discussed in section 4.12. This sample (~10 cm long piece of ~3 cm diameter half core) was crushed and the feldspar phenocrysts were separated out by magnetic and heavy liquid separation techniques. The feldspar was extracted in the 2.58 micron fraction using TBE (tetrabromoethane) adjusted with acetone at Monash University. The sample was run through a Franz magnetic separator several times to improve the concentrate purity. Approximately 10% of the remaining material was calcite from amygdalae and veins within the basalt. The calcite grains were characteristically white, opaque grains, and the plagioclase grains were colourless and transparent. This was confirmed by using the electron microprobe at Melbourne University on representative grains of the two types. The calcite grains were dissolved in 0.1 M nitric acid. Composite grains (feldspar phenocrysts with other minerals still attached), and feldspar phenocrysts with large glassy inclusions were separated from the sample by hand, yielding ~500 mg of pure feldspar grains. This sample will be irradiated in position 5C of the McMaster reactor in Canada and then analysed using facilities in the Noble Gas Laboratory, School of Earth Sciences, the University of Melbourne.

4.3 PHYSIOGRAPHY OF THE WERRIBEE PLAINS

The Werribee Plains are bordered to the north and west by the Palaeozoic highlands (Fig. 1.2). In the west the contact is marked by the Rowsley Fault, and there is a corresponding sharp change in topographic relief, with the uplifted highlands sitting significantly higher than the Plains. In the north the change in topography is more subtle, and the Plains gently rise away from the coast in the south-east (Fig. 4.1). The Palaeozoic granitic You Yangs are exposed in the south-west of the Plains, around which the basaltic lavas forming the Plains have been diverted. The eastern boundary of the Werribee Plains is the Maribyrnong River, and the map in Fig. 4.1 does not extend beyond this. The Werribee River flows south through the centre of the field area, and has down-cut into the basaltic lava pile, exposing up to 10 m of lavas locally. The smaller creeks and rivers throughout the Plains have not incised deeply enough to expose any outcrop. An alluvial fan from the Werribee River has locally buried some of the volcanic products.

Fig. 4.1 (Facing page) The major physiographic features of the Werribee Plains. Eruption centres are generally small topographic features distributed throughout the Plains, which gently slope towards the coast in the south-east. The distribution of diamond drill holes, geophysical wells, and quarries are shown, as well as Cobbleticks Ford (CDF). The location of the northern part of the available airborne geophysical images is given as a light grey box, and the lines for cross-sections A-A' and B-B' (Figs. 4.14 & 4.16) are shown.



Twelve eruption centres have previously been recognised in the Werribee Plains (Table 4.1; Ollier & Joyce 1964, Mitchell 1990). The eruption centres are typically relatively small volume scoria cones and lava shields that have been extensively weathered and vegetated (eg. Fig. 4.2). The heights and exposed lateral dimensions of the individual centres were determined from topographic maps, based upon their extent as topographically raised features above the surrounding plains (Fig. 4.1). The average slopes of their exposed flanks was calculated (Table 4.1). In general the only outcrop preserved at each of these topographic highs consists of spatter, variably agglutinated and locally producing clastogenic lavas (see Chapter 5 for a fuller discussion on the eruption centres). The extent of the lavas fed by each centre cannot be determined by conventional mapping techniques, due to a lack of outcrop. In all but one of the outcrop localities of this study, pahoehoe sheet flows are exposed (section 4.6.2), and it is impossible in outcrop to distinguish which eruption centre they were fed from. Rarely do the products have distinctive phenocryst assemblages to aid in distinguishing between them, as has previously been noted (Price *et al.* 1997).

Table 4.1 Characteristics of the major eruption centres in the Werribee Plains, their exposed dimensions and morphologies. Grid references are for the Bacchus Marsh (BM) and Melbourne (ME) 1: 100 000 map sheets.

Eruption centre	Grid reference	Height (m)	Diameter: E-W x N-S (km)	Average slope of volcano's flanks (°)	Classification
The Anakies	BM597032	120 (W)	1.2 x 1.0	6.0	Three scoria cones (West, Middle and East)
	BM610022	100 (M)	1.1 x 1.1	5.0	
	BM623009	80 (E)	0.9 x 1.0	5.0	
Mt Atkinson	ME959185	60	4.5 x 4.5	1.0	Low shield
Bald Hill	BM730158	80	3.0 x 3.0	1.5	Low shield
Black Hill	ME948095	15	1.5 x 1.5	0.5	Low shield
Mt Cottrell	ME905177	100	7.5 x 10.0	0.5	Low shield
Greek Hill	ME925125	30	1.0 x 1.0	2.0	Scoria cone
Green Hill	ME830135	60	2.0 x 1.5	2.0	Low shield
Mt Kororoit	ME936298	90	2.0 x 1.5	3.0	Scoria cone
One Tree Hill	BM788104	25	3.5 x 3.0	0.5	Low shield
Ryan's Hill	ME982308	40	1.0 x 1.0	2.5	Scoria cone
Spring Hill	BM778162	90	12.5 x 12.0	0.5	Low shield
Stony Hill	ME991285	60	4.5 x 4.5	1.0	Low shield



Fig. 4.2 Photograph of Bald Hill, a low shield in the Werribee Plains. Note the lack of outcrop, and the broad, flat lava plains at the base of the shield.

4.4 AIRBORNE GEOPHYSICAL DATA

Remote sensing techniques were investigated to aid with mapping, including aerial photograph interpretation, and airborne magnetics and radiometrics image analysis. Aerial photographs were found to be particularly useful in characterising the morphology of, and mapping the eruption centres (Chapter 5), however it is difficult to identify lava flows due to the extensive soil and vegetation cover, and the flat-lying nature of the lavas. Airborne geophysical data for the majority of the Werribee Plains was collected by Geoscience Australia (formerly called the Australian Geological Survey Organisation, AGSO) only at broad (1500 m) line spacing, due to the close proximity of the plains to Melbourne. Unfortunately the resolution of these images is too poor to be able to distinguish anything but very large features (eg. the Werribee Delta, Port Phillip Bay), and the extent of the lavas is difficult to discern. Data flown at 200 m line spacing (grid cell size 50 m²) was available for the very west of the field area from the Department of Natural Resources and Environment (DNRE). These images were viewed with the intention of identifying the extent of lava flows from the different eruption centres (Fig. 4.3).

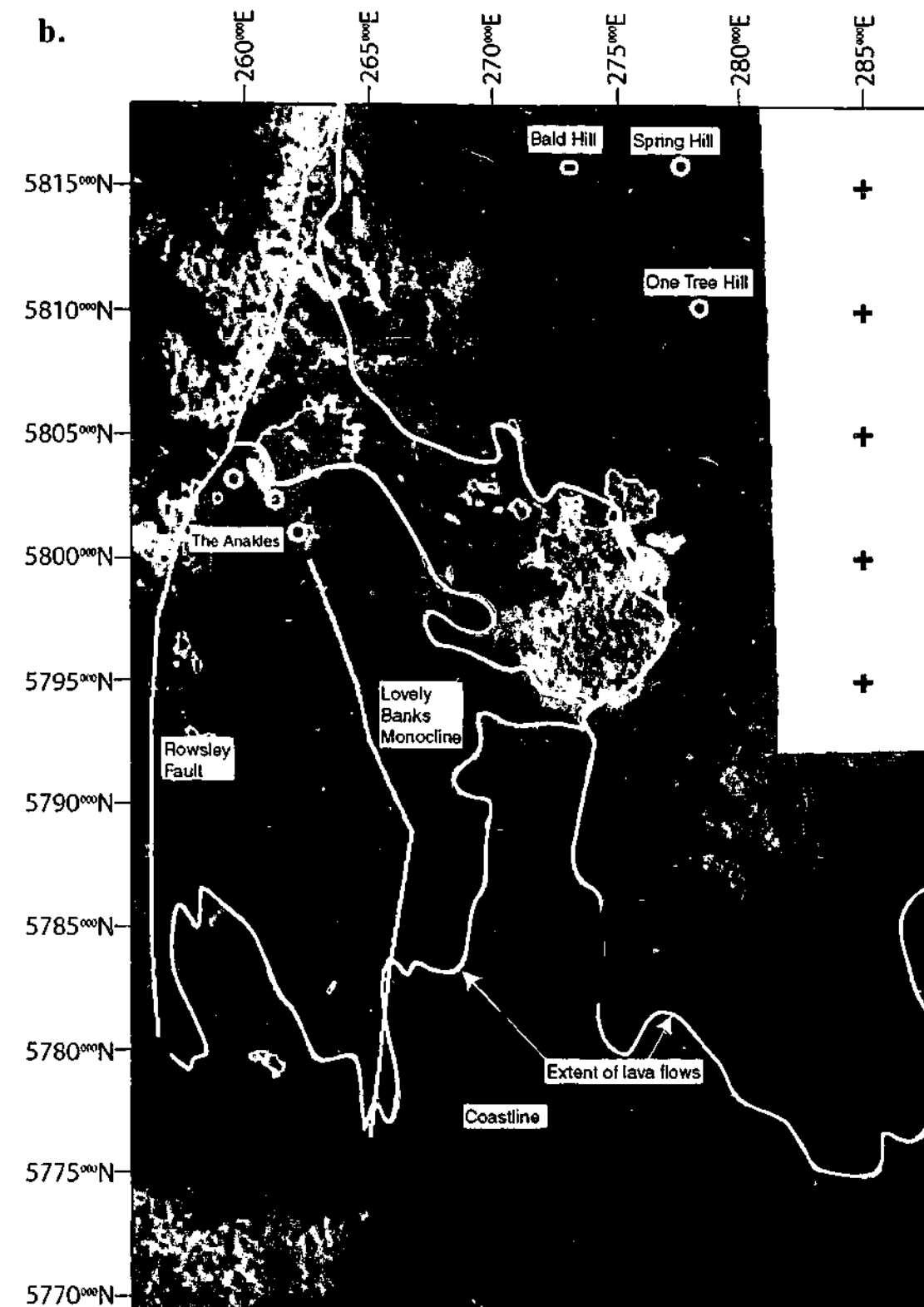
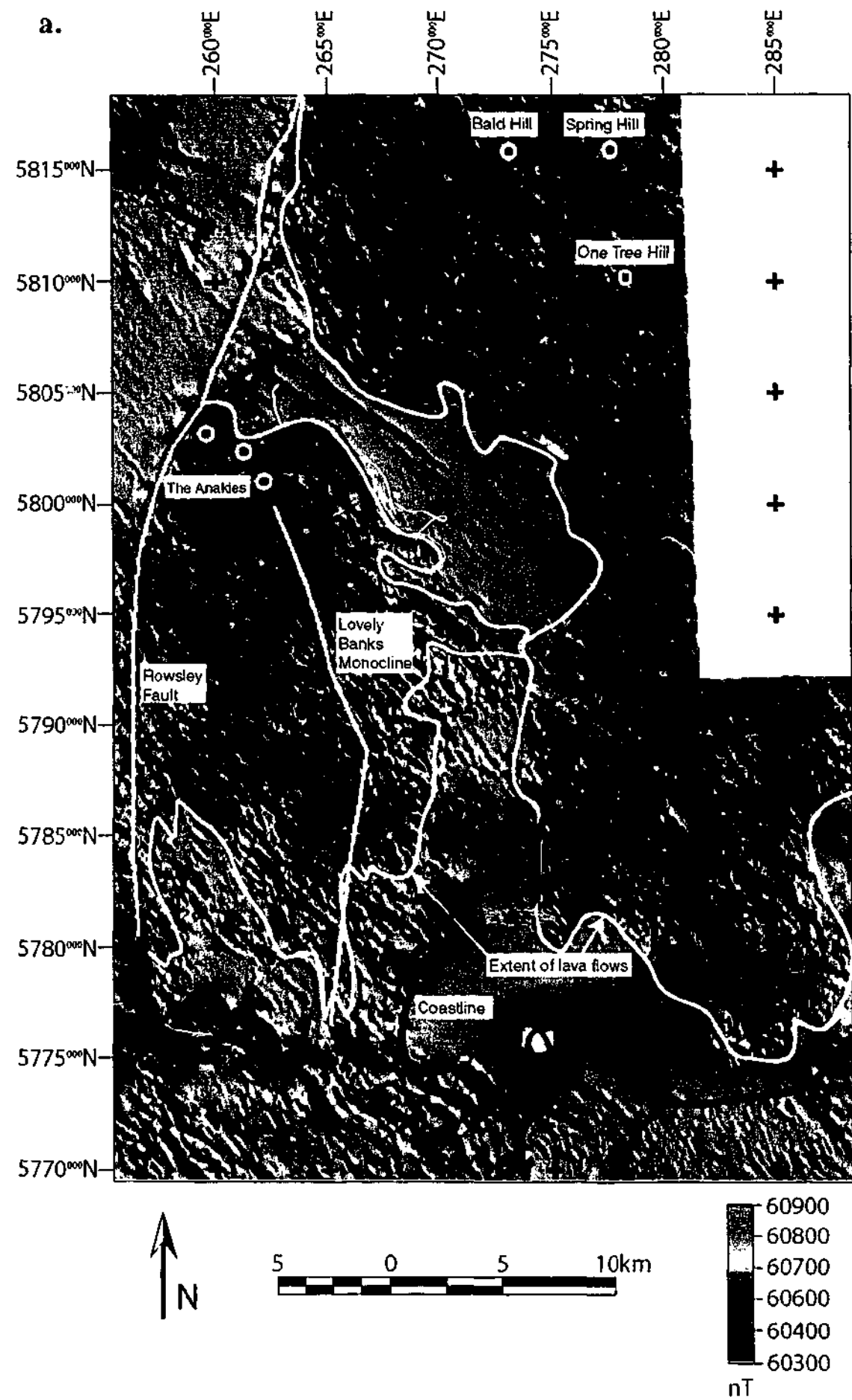


Fig. 4.3 Airborne geophysical images from the west of the Werribee Plains (see Fig. 4.1 for location). Data was collected at 200 m line spacing and grid cell size is 50 m². Data was not available for the top right hand corner of the images. **a** Total magnetic intensity (TMI) sun-shaded, pseudocolour image with gaussian equalisation. Sun shading is 45° elevation and 45° azimuth. The bright red circle marks the position of Pt. Henry, to the east of Geelong. **b** Corresponding pseudocolour K radiometrics image with a gaussian equalised distribution. Dark blue represents 0.05 equivalent % K, red is 3.4%, with green, orange and yellow representing intermediate values. The images have been annotated, and the features of interest highlighted, including the eruption centres and extent of the lavas fed from them.

The broad extent of the lavas in this area is discernible based on their magnetic response (Fig. 4.3a). They are more magnetic than the surrounding lithologies, and have a more complex, textured response. The eruption centres in the images include Bald Hill, Spring Hill, One Tree Hill and the Anakies. Lavas fed from the northern centres are diverted by the Devonian aged granitic You Yang Hills, and are bounded to the west by the Rowsley Fault and the uplifted Palaeozoic highlands. The lavas to the east of the You Yangs extend almost as far as the Bellarine Peninsula, and do not appear to have interacted with water in Port Phillip Bay. The location of the Anakies appears to have been controlled, in part at least by the Lovely Banks Monocline. It has previously been shown that different aged lavas from the NVP have unique radiometric responses due to the different weathering histories (Dickson & Scott 1991). Weathering results in up to 50% loss of K, and a gain in U and Th. The radiometric response also reflects the original composition of the lava, particularly the K content. The radiometrics image shows the measured K content (equivalent % K) of the top ~3-30 cm of the ground (Fig. 4.3b). Unfortunately it was not possible to distinguish between the lavas from different centres, as the radiometric responses of the lavas were too similar. This in itself is significant, suggesting that the eruption centres are of similar ages and have experienced similar weathering histories. As the Anakies are physically separate from the other centres, the extent of lavas from these cones was identified. Lavas have extended up to ~25 km away, however again the lavas fed from the discrete cones were not able to be isolated.

4.5 GEOPHYSICAL WELL LOG INTERPRETATION

The geophysical well data was analysed to investigate the potential of identifying volcanic facies and discrete eruption packages within the basalt (section 4.6), to characterise the distribution of inter-flow sediments in the sequence (section 4.7), and to produce a map of the palaeotopography prior to volcanism, by determining the total thickness of basalt (and inter-flow sediments) in each of the holes (section 4.13). Firstly, the geophysical response of each lithology was characterised using two diamond drill holes (BM22 and MB31) that have corresponding geophysical well logs (Fig. 4.4). The geophysical response of the Red Bluff Sands underlying the basalt was found to be almost identical to that of any interflow sedimentary rocks and palaeosols within the sequence. All of these units are low density (<~2.3 g cm⁻³), have low resistivity (<~80-90 Ohm.m) and a high radiometric response (> 70). The gamma ray response was measured with reference to the American Petroleum Institute standard (GAPI). Coherent basalt has a very different response, and is characteristically high

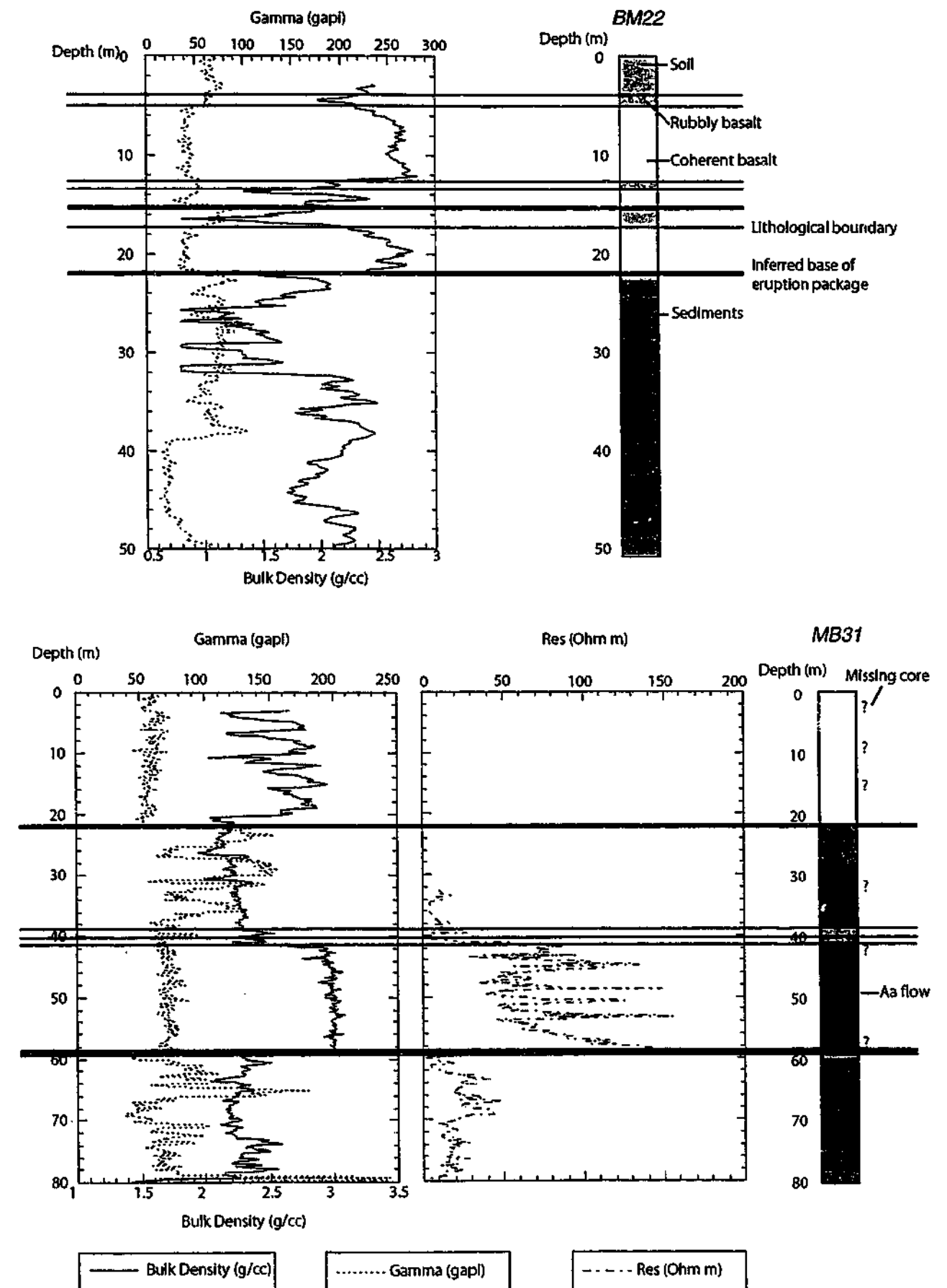


Fig. 4.4 Graphic logs and corresponding geophysical well logs for diamond drill holes BM22 and MB31. Threshold values for each geophysical parameter were identified to distinguish between sediments and palaeosols, and basalt (see text). Volcanic facies have been identified based upon the geophysical response where possible (section 4.6).

density, has a high resistivity and low radiometric response. Rubbly basalt (either produced through weathering, autobrecciation, or possibly the drilling process) has intermediate density and resistivity values, and a low radiometric content. The contact between the basalt and underlying Red Bluff Sands unit is generally sharp, and was easily identified on the well logs lacking associated diamond drill core (Appendix H). Because the geophysical response of sediments and palaeosoils are difficult to distinguish between, a threshold thickness of ≥ 5 m was chosen to identify the inter-flow sediments in the well logs. The low bulk density of the sediments compared with basalt is the most reliable criterion for identifying them in the well logs, as the radiometric responses were found to be more variable. Although the gamma ray content is generally higher for sediments than basalt, high K basalts (eg. from the Anakies (Irving & Green 1976), well log ANA8003, Appendix H) have a particularly high radiometric response, and thick units inferred to be sediments sometimes have low radiometric responses (eg. MOU8007, Appendix H).

4.6 VOLCANIC FACIES

4.6.1 Identifying flow unit and eruption package boundaries

Lava flow unit boundaries were identified in diamond drill core by the presence of any or all of these features: (i) significant weathering of basalt and/or soil formation, suggesting a significant time break between adjacent flows; (ii) a sharp change in vesicularity; or (iii) the presence of clinkery, autobrecciated clasts, indicating an aa flow margin (Chapter 2), Fig. 4.8. Eruption packages (the products of discrete eruptions) were identified within the sequence by evidence of a significant time break between adjacent packages of flows. Again, this may take the form of oxidised, rubbly basalt or palaeosoil development at the top of a package, and/or a change in polarity in the sequence (where the sign of the inclination of more than one sample differs from the underlying or overlying samples; section 4.11.1). In the geophysical well logs boundaries between eruption packages were inferred by the presence of thin palaeosoil horizons, rubbly basalt, or interflow sediments (eg. Figs. 4.4, 4.9, Appendix H). It is not considered to be a completely reliable technique to identify eruption packages in this way, as the magnetic polarity is not recorded in the well logs. Also, many rubbly basalt intervals that are recorded in the well logs do not necessarily represent a significant time break between adjacent lava flows, but instead may be attributed to the drilling process for example. An attempt has been made to identify all eruption packages in the well logs (Fig. 4.10, Appendix H), however it is considered to be an approximation only.

In Chapter 2 the interiors of inflated pahoehoe lobes and aa lava flows were better characterised in drill core and outcrop, and features characteristic of the different lava types were documented. Four additional volcanic facies have been identified in drill core and outcrop in the Werribee Plains: S-type (or spongy) pahoehoe lobes, ponded lava flows, transitional lava flows and scoria. Each facies have unique characteristics that can be interpreted in terms of the physical emplacement processes. The criteria used to differentiate between facies are described below and shown graphically in the drill core logs (Fig. 4.8). Locally inflated P-type pahoehoe lobes and aa flows were identified in the geophysical well logs, as described below.

4.6.2 Pahoehoe flow units

Pahoehoe flow units contain planar, chilled margins (\pm ropes) with very small spherical vesicles preserved just within the margins. The vesicles characteristically increase in size towards the interior of the lobe at both the top and basal margins (Wilmoth & Walker 1993). Two main types of pahoehoe lobes have been identified on the basis of vesicle distribution: S-type or "spongy" lobes, and P-type lobes, which may contain pipe vesicles at the base (Walker 1989, Wilmoth & Walker 1993). S-type lobes form with minimal inflation, and contain spherical vesicles distributed throughout, with a higher concentration in the centre. The general characteristics of P-type lobes are a dense interior (non-vesicular zone- NVZ) surrounded by more vesicular upper and lower margins (upper vesicular zone- UVZ and lower vesicular zone- LVZ). They form either by inflation of the lobe beneath a chilled crust, or by ponding of the lava in a topographic depression. Lobes that have formed by inflation typically (i) have thicker normalised UVZ's than ponded lavas (the UVZ constitutes 40-60% of the total lobe thickness); (ii) demonstrate an overall increase in vesicle size and decrease in vesicularity in the UVZ with depth; (iii) may have horizontal vesicle zones (HVZ's) in the UVZ; and (iv) may contain pipe vesicles in the LVZ' (Hon *et al.* 1994, Self *et al.* 1996, Cashman & Kauahikaua 1997; Self *et al.* 1998). The presence of vesicle trains at or towards the base of the UVZ has also been recognised in this study to be unique to lavas that have formed by inflation (see Chapter 2).

Inflated (P-type) pahoehoe lobes

Vesicles within the UVZ of pahoehoe lobes that are considered to have formed by inflation in this study, are generally sub-spherical and locally evenly distributed. The tops of

some lobes have been removed by weathering and erosion, and the UVZ in these flows is therefore only partially preserved. The normalised UVZ thickness, and progressions in vesicularity within the UVZ are not useful criteria to use in these instances to distinguish inflated lobes from ponded lavas. Instead, HVZ's and vesicle trains that have been identified locally within the UVZ's of these flows indicate the flows have formed by inflation. The NVZ's of P-type pahoehoe lobes were observed to differ from the dense cores of aa flows, as the pahoehoe lobes commonly contain segregation material (vesicle cylinders and vesicle sheets (eg. Goff 1996)) and generally lack other vesicles. The LVZ is consistently ~0.3 m thick regardless of the lobe thickness and some contain pipe vesicles, another feature characteristic of flows that have formed by inflation. Inflated pahoehoe lobes identified in drill core range in thickness from 1.2 to 17.1 m (average ~7.5 m) and in outcrop occur as wide, low aspect ratio lobate to sheet-like structures (Fig. 4.5a). In general, pahoehoe sheet flows which are totally exposed vary from 1.5-3 m in thickness and widths vary from 10-30 m. Of the thicker flows, where the tops and/or bases are not preserved or exposed the widths are generally 50-100 m. Flow thicknesses quoted are minimum estimates of the original flow thicknesses, and include any weathered basalt or palaeosoils developed above the flows. In one instance a feature resembling a large lava tube or elongate tumulus was observed in the field (extending southward from the eastern Anakie scoria cone). Although there is no outcrop preserved, this tube is slightly raised up above the surface of the plains, and is considered to have developed over time within an inflated sheet flow system, as a preferential pathway for the lava. This is the only example of a tumulus or tube observed in the Werribee Plains. In geophysical well logs inflated P-type lobes were identified by their unique geophysical responses compared with the other volcanic facies. The lower half of inflated pahoehoe lobes are denser and have higher resistivity values than the top half of these lobes (corresponding to the NVZ and UVZ respectively). The transition between the two zones generally appears to be gradational in terms of density changes, with a general decrease in density towards the top of the flow, before an abrupt increase in density (and resistivity) at the base of the overlying lobe (Fig. 4.9b).

Spongy (S-type) pahoehoe lobes

Although single S-type lobes are commonly associated with inflated lobes (small break-outs or toes that have not inflated), locally multiple spongy lobes occur together. In these instances they occur as a discrete package of small lobes, and are considered to represent

a unique facies. Six examples of this have been observed in drill core (four in DER7, one in BM22, and one in KOR14, Fig. 4.8). Individual lobes in these packages range in thickness from 0.1-2.1 m and average ~0.5 m, and entire packages range in thickness from 2.0-5.5 m and average 3.0 m. The spongy lobes are considered to represent flattening out of the local topography. This facies is produced when the local topography is too steep for inflation to occur, and instead non-inflating, low aspect ratio spongy lobes are formed.

4.6.3 Ponded lavas

Ponded lava flows (analogous to lava lakes) contain abundant segregation material (Helz 1987, Puffer & Horter 1993). This enables ponded lavas to be distinguished from aa flows, as aa lavas lack segregation veins in the cores of the flows. Mostly ponded lavas are distinguished from inflated lobes using negative criteria: they lack pipe vesicles in the LVZ, vesicle trains and HVZ's. Five ponded lava flows have been identified with particularly thin or absent UVZ's, a lack of features that are diagnostic of the inflation process, and they generally contain abundant segregation material. The ponded lavas range in thickness from 6.0-17.3 m, and average 11.0 m.

4.6.4 Aa

Aa lava flows contain clinkery, autobrecciated clasts at the top and base, surrounding a dense core eg. (Williams & McBirney 1979). Unfortunately due to subsequent weathering after emplacement, or incomplete recovery of the drill core these clasts are not always preserved, so identification of the flow boundary and facies type involves looking at other features of the flow. The clinkery clasts at the margins of these flows are sometimes entrained into the core of the flows during emplacement (Crisp & Baloga 1994), and preserved in drill core. This helps to distinguish aa flows from pahoehoe flows, which rarely entrain any material. Vesicles were sparsely dispersed throughout the cores of flows observed; they had irregular shapes and their distribution was heterogeneous. The aa flows identified all lack segregation material in the cores of the flows (cf. many thick pahoehoe flows, Chapter 2). Vesicle cylinders have previously only been observed in relatively low viscosity pahoehoe flows (Goff 1996). Seven aa flows have been identified in drill core, ranging in thickness from 15.3-31.7 m and average 22.5 m. No aa flows were observed in outcrop, hence the dimensions of the channels could not be ascertained. The geophysical well logs of aa flows demonstrate consistently high density and resistivity values throughout the cores of these thick flows, beneath a rubbly

basalt zone and/or palaeosoil (eg. Fig. 4.4b).

4.6.5 Transitional lavas

These lavas contain features characteristic of both aa and pahoehoe (eg. Katz 1997). Commonly the top margin of a transitional lava flow was observed to contain rubbly, clinkery material, and yet the coherent interior could be subdivided into an UVZ, NVZ and LVZ. The basal margins locally contained clinkery clasts, however they were also observed to form a planar contact with the underlying lobe/palaeosoil horizon. Some of the transitional lavas contain segregation material in the cores of the flows. Locally the vesiculation patterns within the UVZ are quite irregular, with barren patches adjacent to more vesicular basalt, however generally the vesiculation is fairly homogeneous. The thickness of individual lobes ranges from ~3.5-11.5 m and average 7.3 m thickness. In outcrop the transitional lava flows occur as vast sheets, separated by clinkery, rubbly zones, considered to be channel levees or tube margins (Fig. 4.5b). The rubbly zones range from 4-8 m wide and occupy the entire height of the quarry faces (~5 m). Channel/tube widths range from ~65-120 m. Katz (1997) interpreted the transitional flows to be thin, vesicular aa flows, however they are considered here to either represent aa lava flows that later became inflated (eg. Calvari & Pinkerton 1998), or pahoehoe flows that have become autobrecciated behind the flow-front (eg. Keszthelyi 2002). In the latter case these types of flows have been called rubbly pahoehoe, and differ from the transitional lavas observed in this study as the disrupted fragments at the tops of rubbly pahoehoe flows are variably broken pahoehoe toes and are *not* clinkery in nature (Keszthelyi 2002). Further work is required to understand how the transitional lavas observed in this study were emplaced.

4.6.6 Scoria

Scoria has been observed in three drill holes (MB31, BM22 and PYW7). The intervals of scoria are relatively thin (0.1-0.6 m) and small clasts are preserved within these (1-1.5 cm diameter). The small, vesicular scoria clasts are bound together by calcrete and/or clay material. In each instance they overlie a soil horizon and are directly overlain by a sequence of lava flows. They are interpreted to represent the preliminary stages of an eruption prior to burial by the lavas.

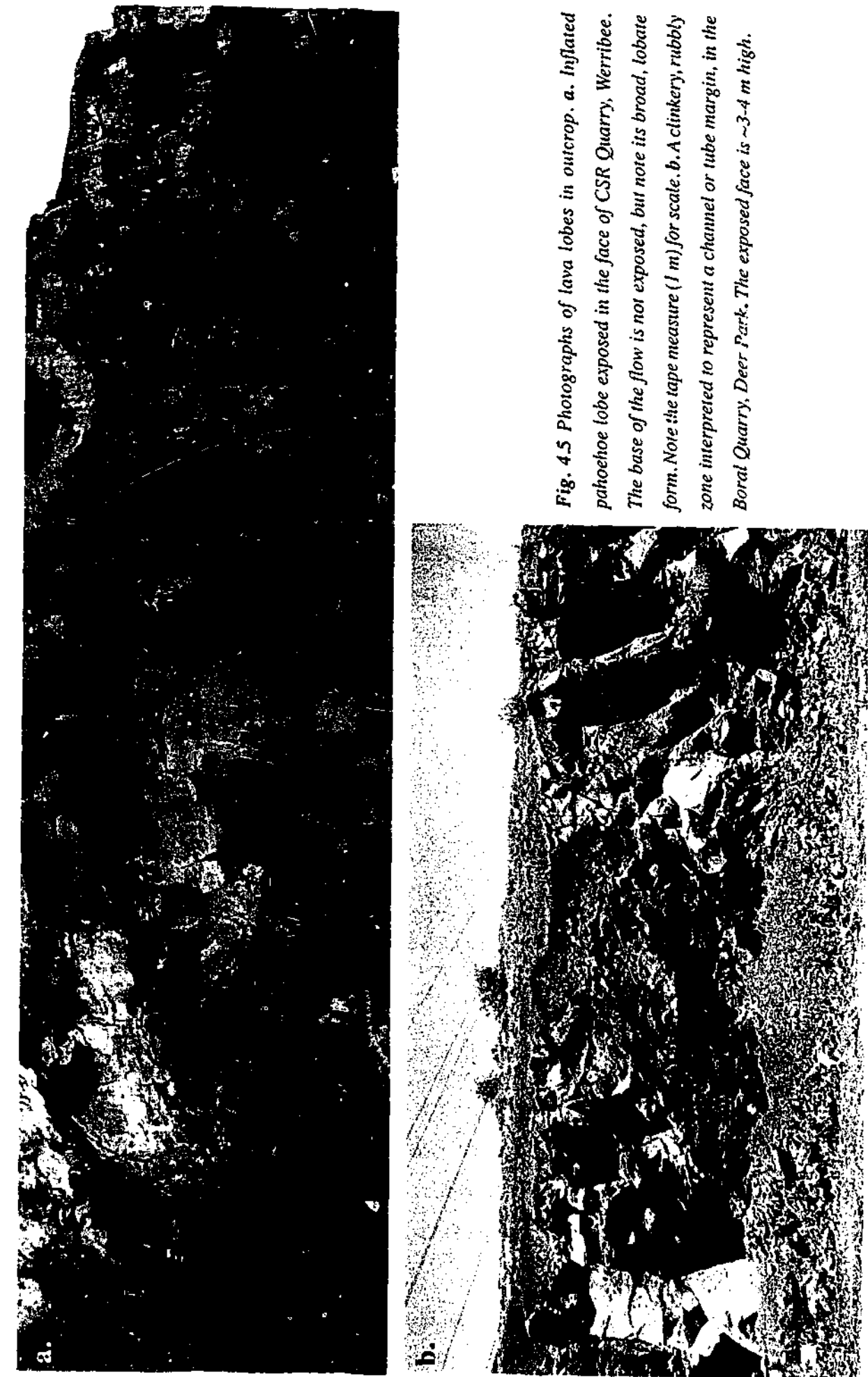


Fig. 4.5 Photographs of lava lobes in outcrop. *a.* Inflated pahoehoe lobe exposed in the face of CSR Quarry, Werrisbee. The base of the flow is not exposed, but note its broad, lobate form. Note the tape measure (1 m) for scale. *b.* A clinkery, rubbly zone interpreted to represent a channel or tube margin, in the Borral Quarry, Deer Park. The exposed face is ~3-4 m high.

4.7 INTER-FLOW SEDIMENTARY FACIES

The general features of the inter-flow sediments observed in the Werribee Plains are described based upon their limited occurrence in drill core and outcrop. Only two diamond drill holes have inter-flow sediments preserved (MB31 and TAR12) and sediments are also preserved in outcrop at Cobbledecks Ford (CDF, Fig. 4.1) between eruption packages. The overall distribution of sediments in the Plains is better recorded by the geophysical wells, a number of which have evidence of inter-flow sediments (section 4.9). The interflow sediments in MB31 comprise three upward-fining sequences, ranging in grain-size from gravels to mudstones (Fig. 4.8h). The lower two packages are separated from the top sequence by a palaeosol, and palaeosols are also located above and below the entire sedimentary interval. The gravel at the base of the sedimentary package is moderately well sorted, containing clasts averaging ~1.5 cm. It contains sub-rounded to well-rounded quartz grains and red, oxidised meta-sandstone clasts, and angular basalt clasts. The gravel lens higher in the sequence lacks basalt clasts, and consists predominantly of sub-rounded, coarse (average ~3 cm) quartz grains and minor meta-sandstone lithic clasts. The sandstone unit is clast-supported, consisting mainly of well-sorted quartz grains, set in a clay matrix. The grains vary from angular to sub-rounded, and are generally equant. Many of the quartz grains have undulose extinction, suggesting they are low-grade metamorphic in origin. Lithic clasts are more rare in the sandstone, and are generally very fine-grained with a distinct foliation, interpreted to be metapelites. It is difficult to distinguish the grain types in the mudstone, due to its fine-grained nature. Like the sandstone it appears that the main grain type is quartz, and these are generally sub-angular and dispersed throughout. Within the matrix there are some opaque and clay minerals. No basaltic lithic clasts are observed in either the sandstone or mudstone facies.

The inter-flow sediments preserved in TAR12 overlie a ~3 m thick interval of heavily weathered basalt (altered with abundant calcrete). The sediments are red-brown and sandy at the top, becoming more silty and muddy with depth. The overlying basalt flow has a sub-planar contact with the sediments. The base of the flow is not completely smooth, but this is probably due to local irregularities in the substrate. The sandstone consists predominantly of quartz, in a matrix-supported rock. The sample is relatively poorly sorted, containing a range of grain-sizes within a very fine matrix containing clay minerals. The quartz grains are generally sub-rounded to rounded, have undulose extinction and the grains are commonly fractured. The matrix and some of the quartz grains are locally oxidised and iron-stained. No lithic

clasts were observed in these sediments

At Cobbledecks Ford the inter-flow sediments also overlie a weathered interval of basalt. The sequence contains thin, planar siltstone and sandstone laminae with abrupt changes in proportions of different grain types (Fig. 4.6). The dominant grains are altered (buff-coloured) scoria clasts, basaltic lithic clasts and quartz. The scoria and basaltic clasts generally occur together, with some quartz grains scattered amongst them. There are also laminae that consist predominantly of quartz, and the contacts between adjacent laminae are generally very sharp (Fig. 4.6). Individual laminae are from ~5-40 cm thick, and the grain-size fluctuates throughout the sequence. The scoria clasts are highly vesicular, and are sub-rounded to irregular shapes. It appears that the original shapes have not been greatly modified through transport (Fig. 4.6). The basaltic lithic clasts are generally non-vesicular and textures within these vary from ophitic to intergranular, and some are trachytic. The clasts are generally sub-rounded to rounded. Clasts are locally moderately well-sorted by mass, but not by size, and they are considered to have been hydraulically sorted. This feature, combined with the presence of ubiquitous quartz grains throughout the sequence suggest a fluvial emplacement mechanism, rather than air-fall scoria deposits. Quartz grains in the quartz-rich facies are sub-angular to sub-rounded and occur within a matrix-supported rock.

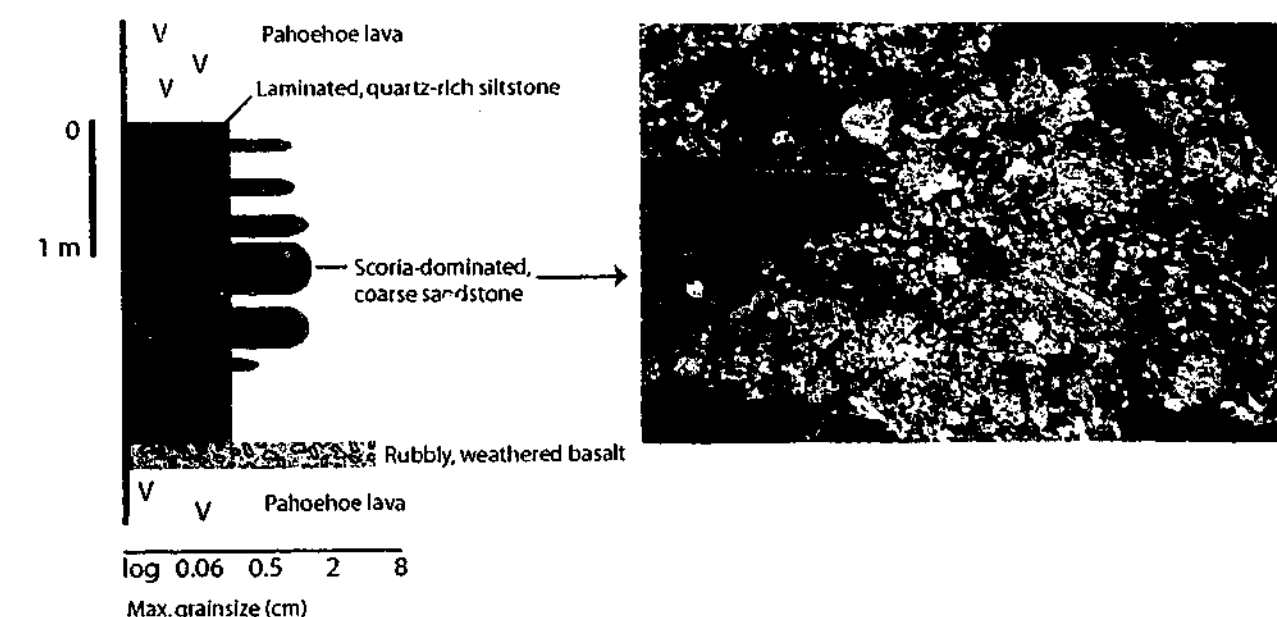


Fig. 4.6 Stratigraphic log of the inter-flow sediments preserved at Cobbledecks Ford, with a photograph of the coarse sandstone facies, containing abundant altered scoria clasts. Note the locally variable grain-sizes in the unit, a result of hydraulic sorting.

4.8 NATURE OF THE BASAL BASALT CONTACT

The sediments that occur directly beneath the basalt are typically siltstones and sandstones of continental origin, called the Red Bluff Sands (Abele *et al.* 1988). In diamond drill core from three holes to the north of the field area (KOR14, BM22 and MB31; Figs. 4.1 & 4.8), the basaltic lava has a planar contact with palaeosoils, which have developed above the sediments, indicating a period of weathering and erosion between the cessation of sedimentation and the onset of volcanism. Planar contacts between the lowermost basalt flows and underlying sediments are preserved in two drill holes (KOR15 & KOR16). One drill hole, slightly further south of these shows some evidence of interaction between the basalt and sediments (DER7, Fig. 4.7). The base of the flow is not planar, but has an irregular fluidal outline, with very localised inter-fingering of the basalt and sediment, indicating the sediments were unconsolidated and probably wet at the time of emplacement of the basalt. This lowermost basalt flow is 15 m thick, has a regular vesicle zonation at its base, and there is no evidence of the development of pillow lavas or hyaloclastite. Directly beneath the contact the sediments are homogeneous, grey mudstones. It appears that the sediments were waterlogged at the time of emplacement of the lavas, resulting in some downward intrusion or loading of lava and perhaps fluidisation mobilisation of sediments. The two southernmost



Fig. 4.7 Photograph of the contact between the base of the lowermost vesicular basalt flow (dark) and the underlying Red Bluff Sands (light grey; 107.5 m) in drill hole DER7. Note the fluidal nature of the basalt and the inter-fingering between the basalt and sediments. Up stratigraphy towards top of page.

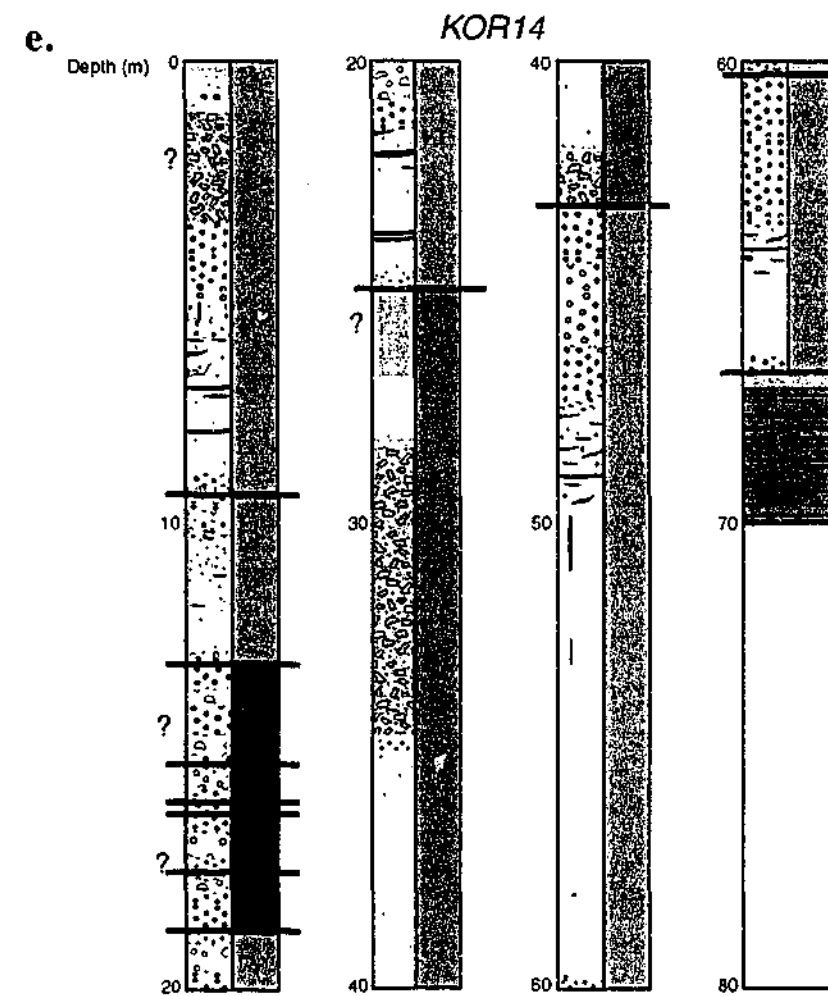
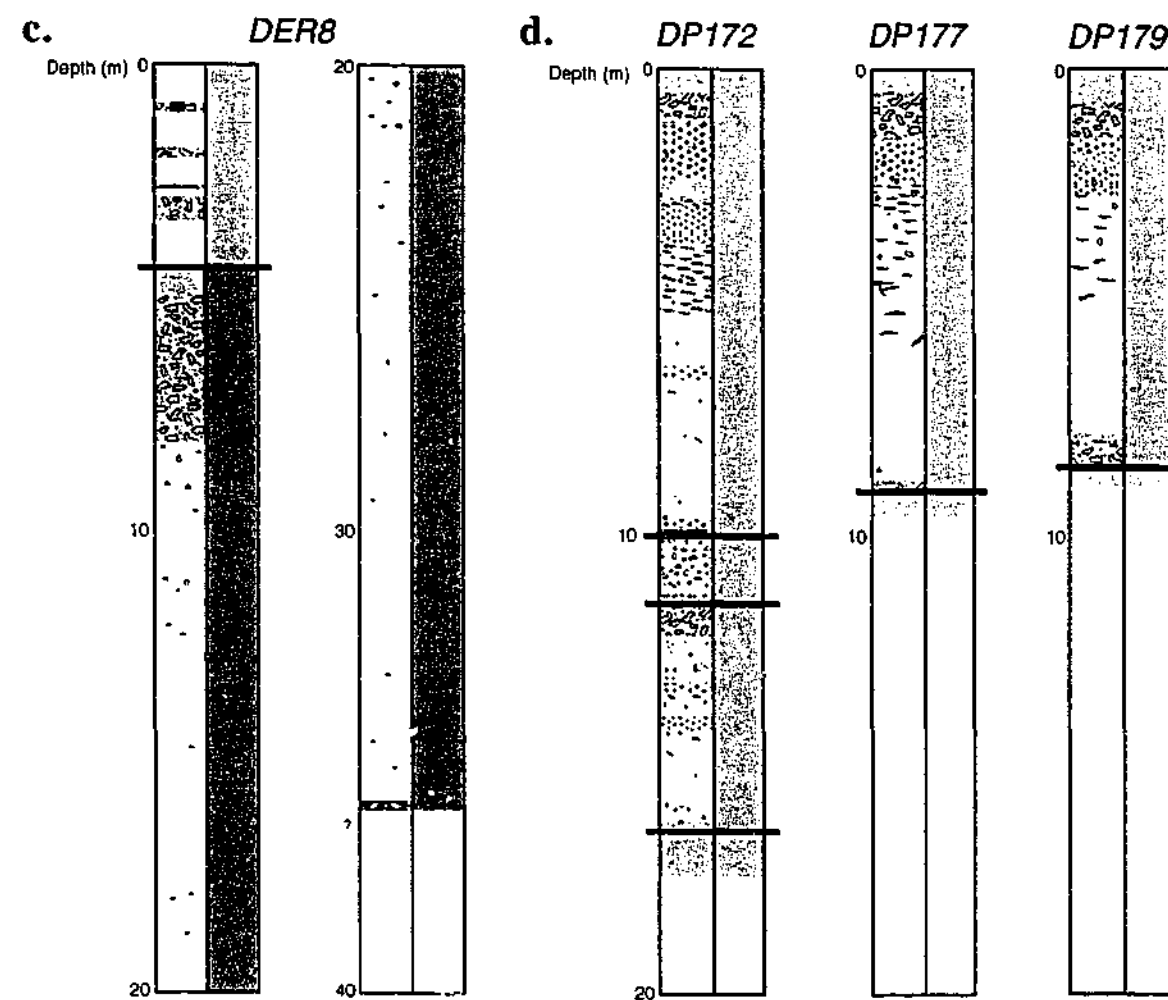
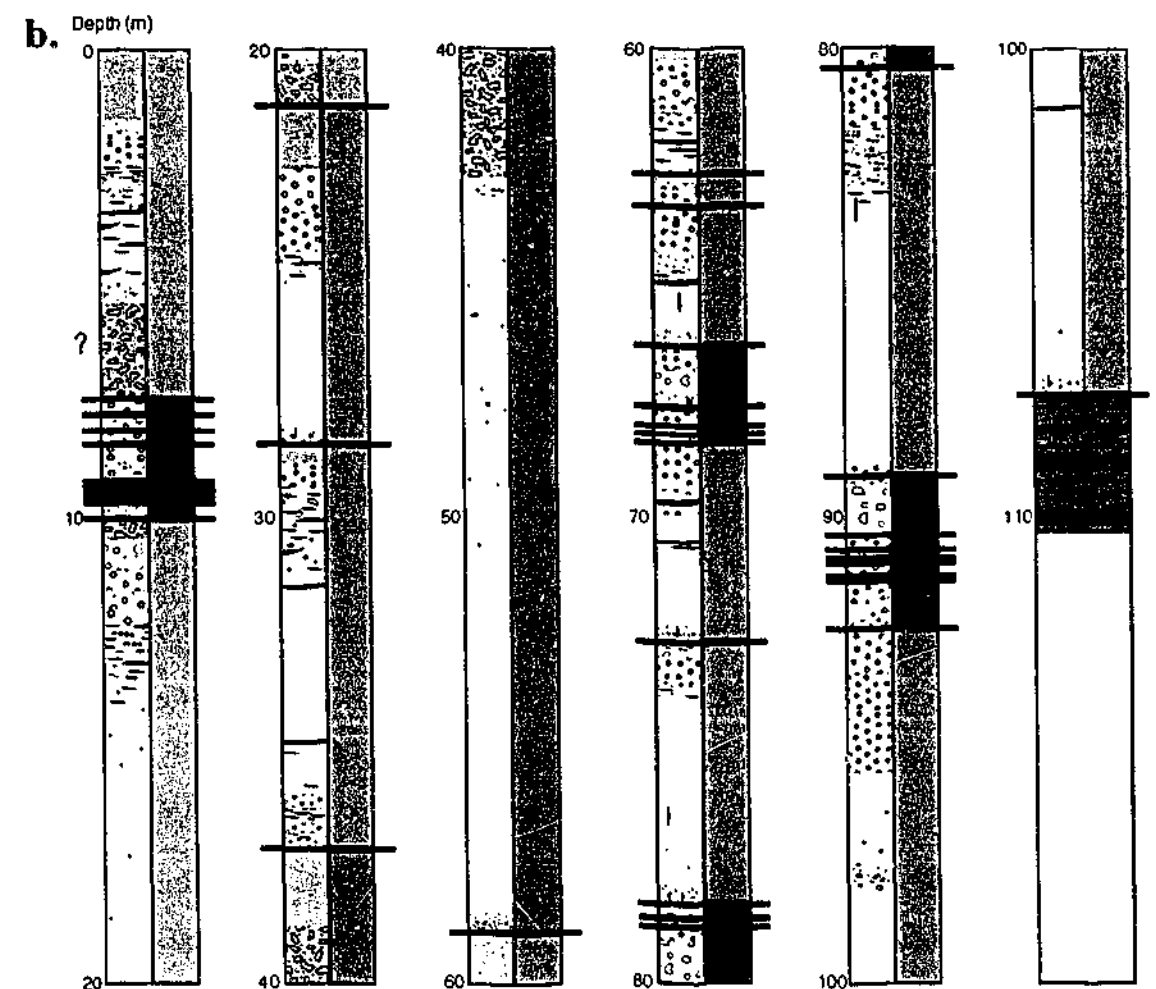
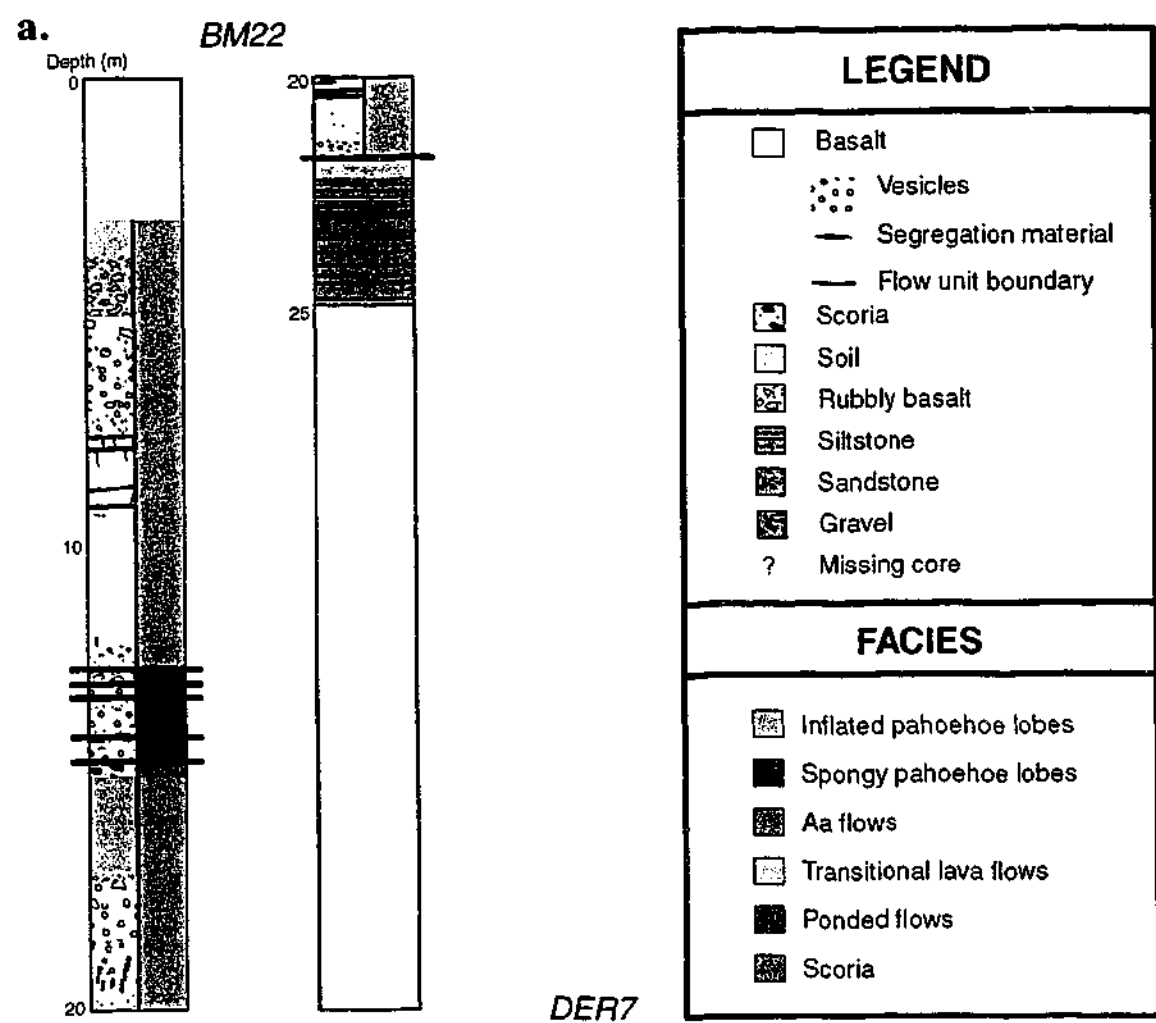
drill holes (TAR12 & TRU50) contain hyaloclastites at the contact between the basalt and sediments. In each case only a small zone of hyaloclastite has been preserved (up to ~10 cm thick), consisting of angular basalt fragments in a dark, altered matrix. Again, the lava flows at the base of these holes are ~15 m thick, and there is no evidence of pillow lavas. It is

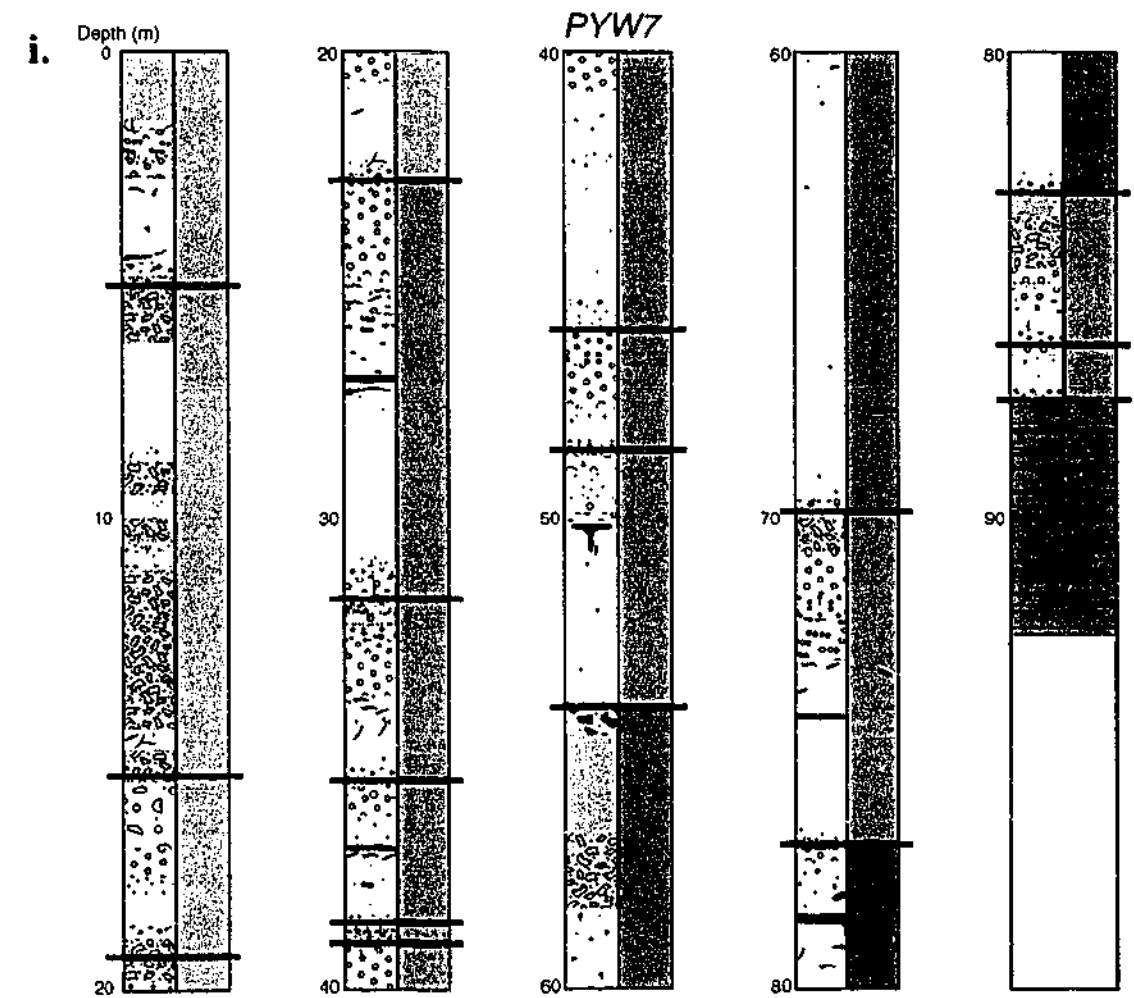
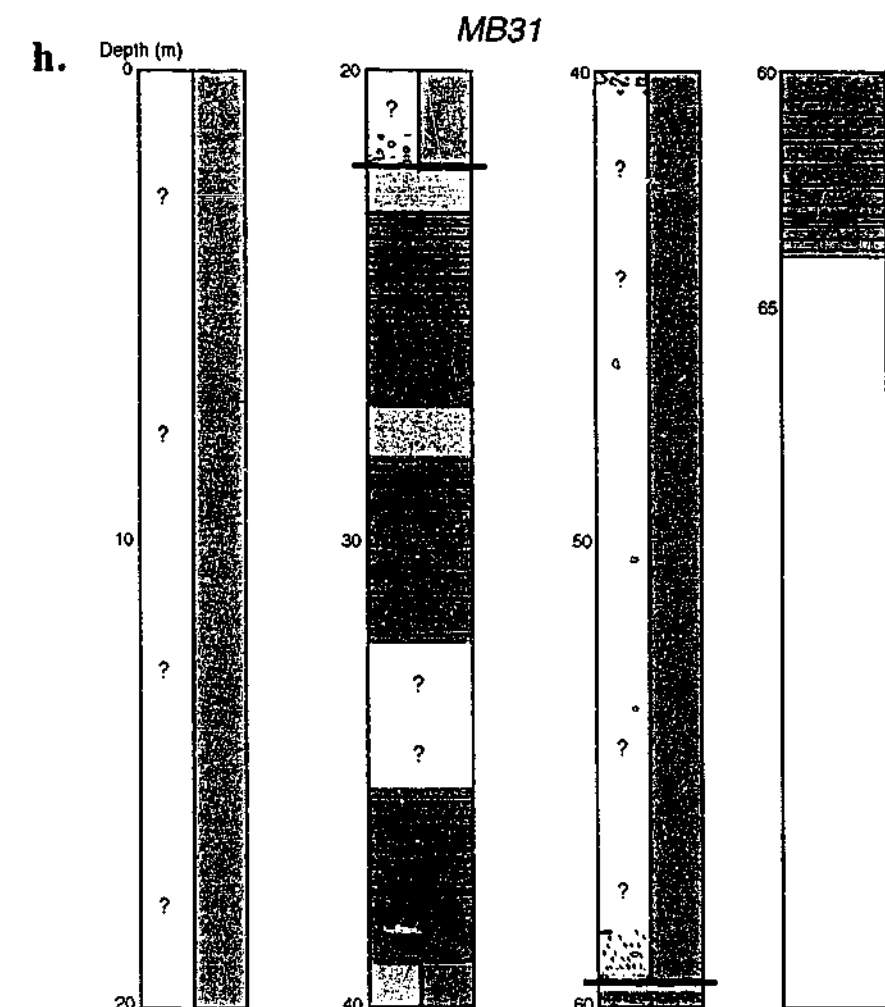
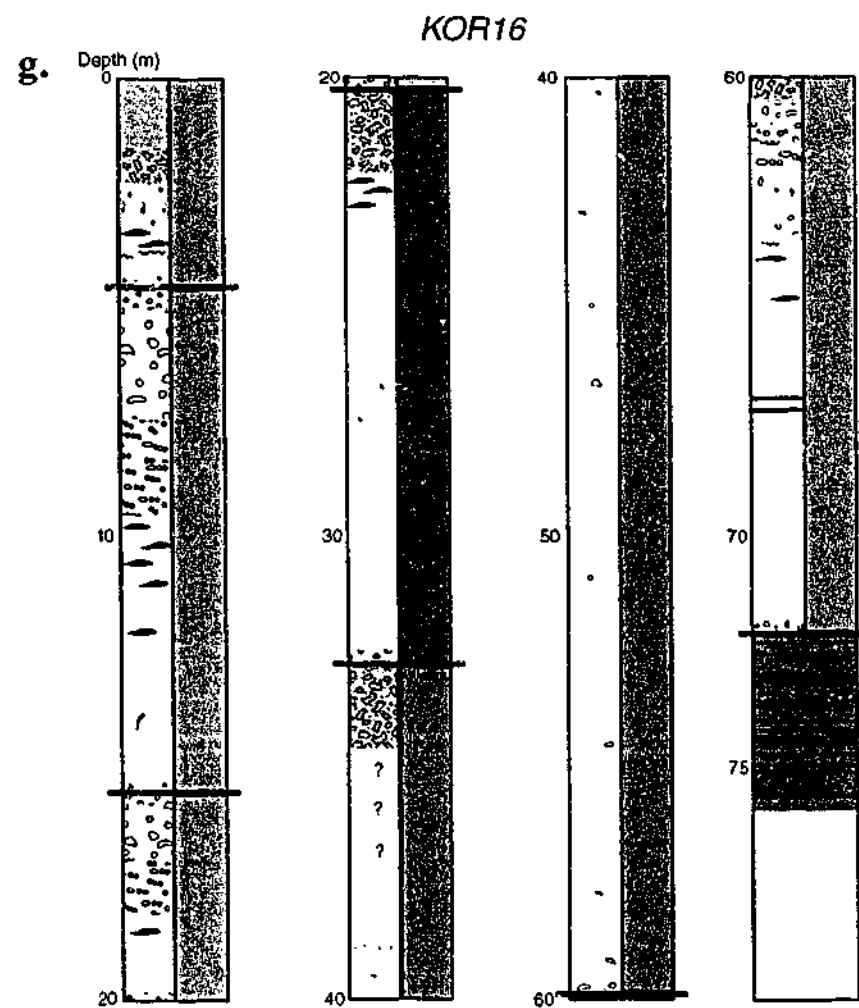
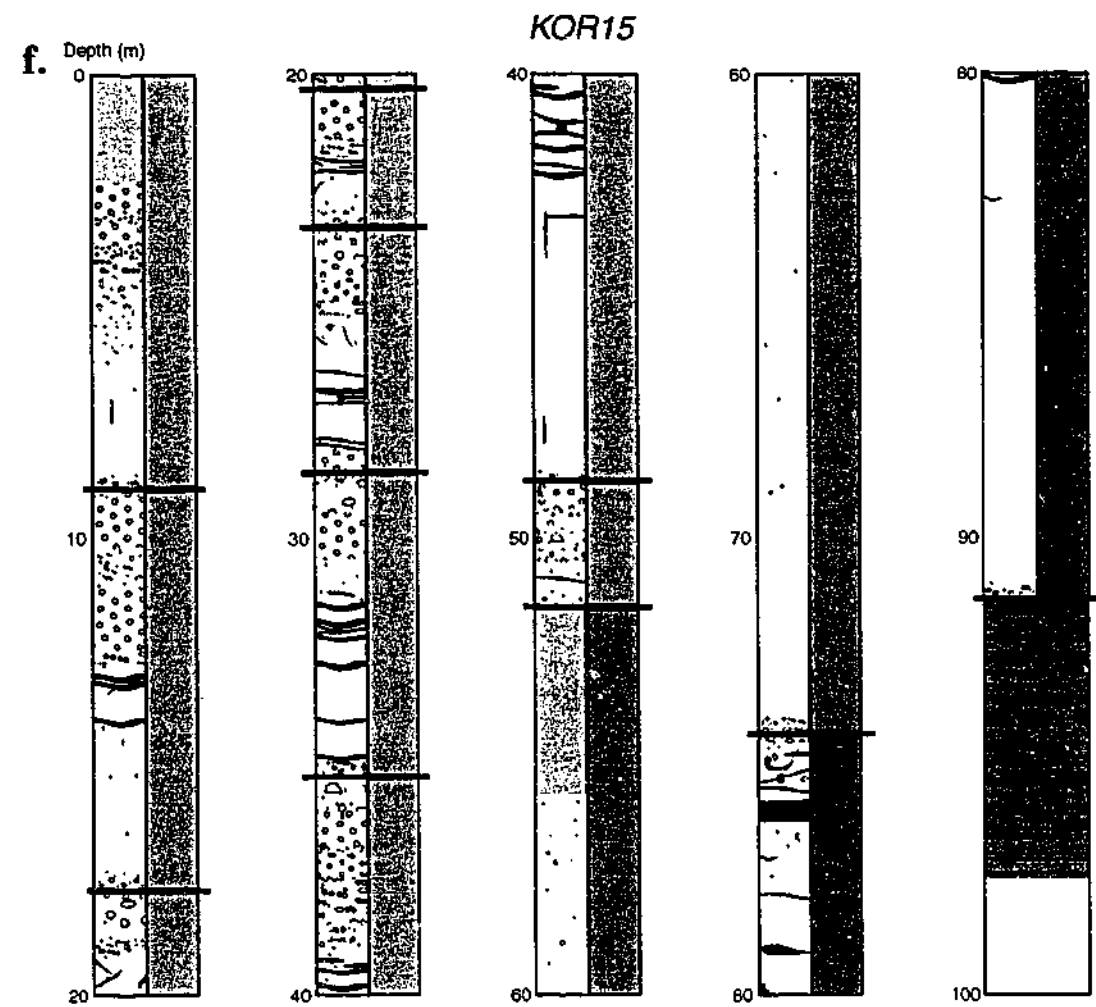
proposed that the lavas were emplaced into very shallow water, which caused localised quench fragmentation of the lava at the base of the flows, and the water was evaporated or displaced by this. In some of the holes (KOR14, MB31, KOR15) the soil horizon or sandstone directly underlying the basalt have been baked within ~10 cm of the contact, reflected by a change in colour and higher degree of consolidation of the underlying material. This suggests that the underlying material was hard and dry at the time of emplacement of the lavas, resulting in efficient heat transferral. One drill hole (PYW7) has core missing at the contact, so the relationship between the basalts and sediments is unknown here.

4.9 DISTRIBUTION OF VOLCANIC AND SEDIMENTARY FACIES

The inferred distribution of volcanic facies for all diamond drill holes logged in this study is shown with the graphic logs (Fig. 4.8). Inflated pahoehoe lobes represent the dominant lava facies observed in drill core, comprising ~65% of all flow units logged. Eruption packages are observed in drill core to typically consist either of a single inflated pahoehoe lobe; several inflated lobes stacked together; or several inflated lobes with intervening packages of S-type pahoehoe lobes. Aa flows, transitional, and ponded lavas occur less commonly throughout the sequence. Volcanic facies have been identified, where possible from the geophysical well logs (Fig. 4.9). The distribution of volcanic facies and inter-flow sediments in the Werribee Plains is shown in Fig. 4.10. Transitional lavas were only identified at the top of the stratigraphy, and are inferred to have been erupted from Mt. Atkinson (Fig. 4.15). Lavas from geophysical wells within this vicinity that do not have responses characteristic of aa or inflated pahoehoe lavas have been classified as transitional lavas. Aa lavas are only observed at depth in the sequence, and are confined to the north of the field area. Based upon the thicknesses and the generally non-vesicular nature of the aa flows, they are all considered to represent a distal aa facies (eg. Lipman & Banks 1987, Rowland & Walker 1988, Walker 1993). They are considered to have been fed by eruption centres to the north, and as they reached the relatively flat area of the Werribee Plains began to thicken (see Chapter 5). Thus the aa flows are not considered to be correlatable with any of the pahoehoe flows in drill core. The transitional lavas again are a unique facies and are not considered to be correlatable with the pahoehoe flows. P-type and S-type pahoehoe and ponded lavas are all considered to be correlatable.

Within the sequence of basalts in the Werribee Plains there is evidence that sedimentation occurred relatively locally, almost entirely in the north-west of the field area (Figs. 4.10 & 4.11; Appendix H). Sixteen geophysical well logs have recorded the presence





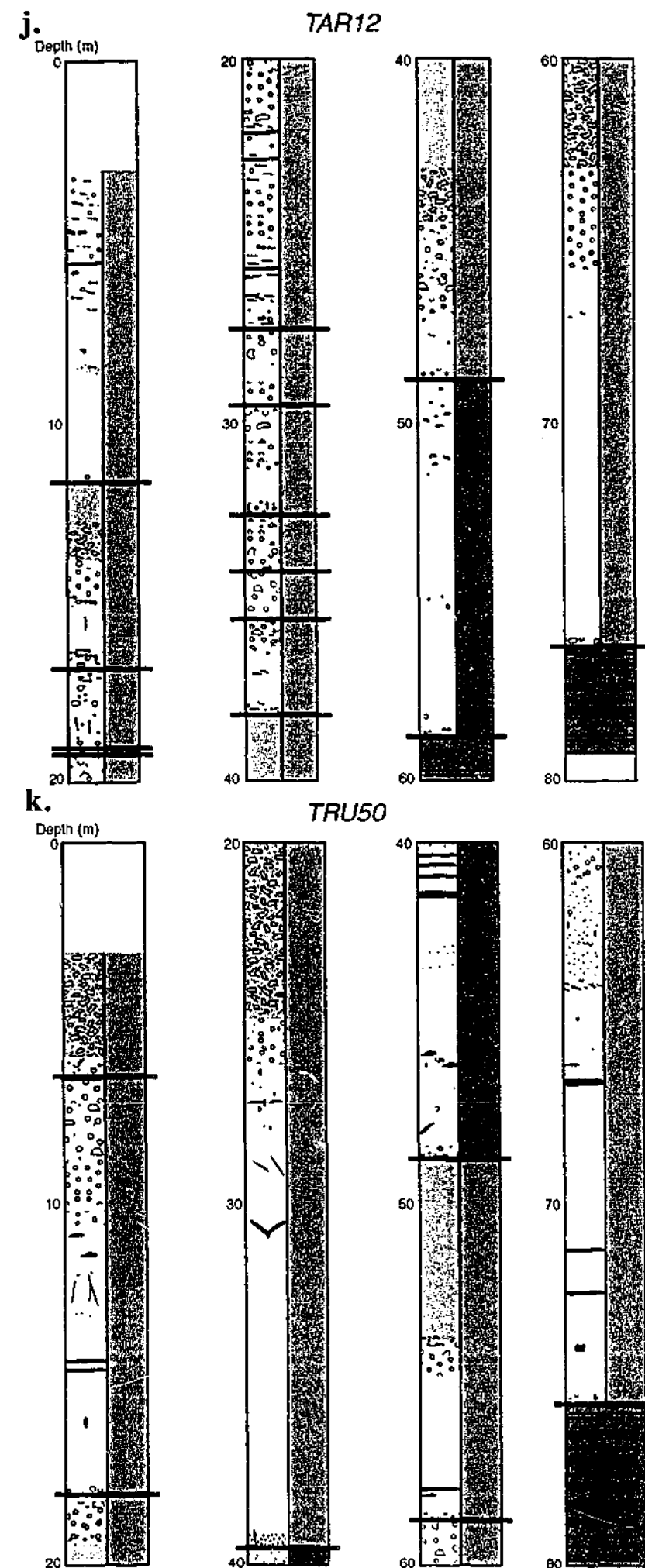


Fig. 4.8 Graphic logs showing the distribution of lava flow units and identified volcanic facies as identified in diamond drill core. Note that flow unit boundaries are commonly identified by a sharp change in vesicularity. The sequence is dominated by inflated pahoehoe lobes, which represent ~65% of all flow units logged. Refer to a. for legend.

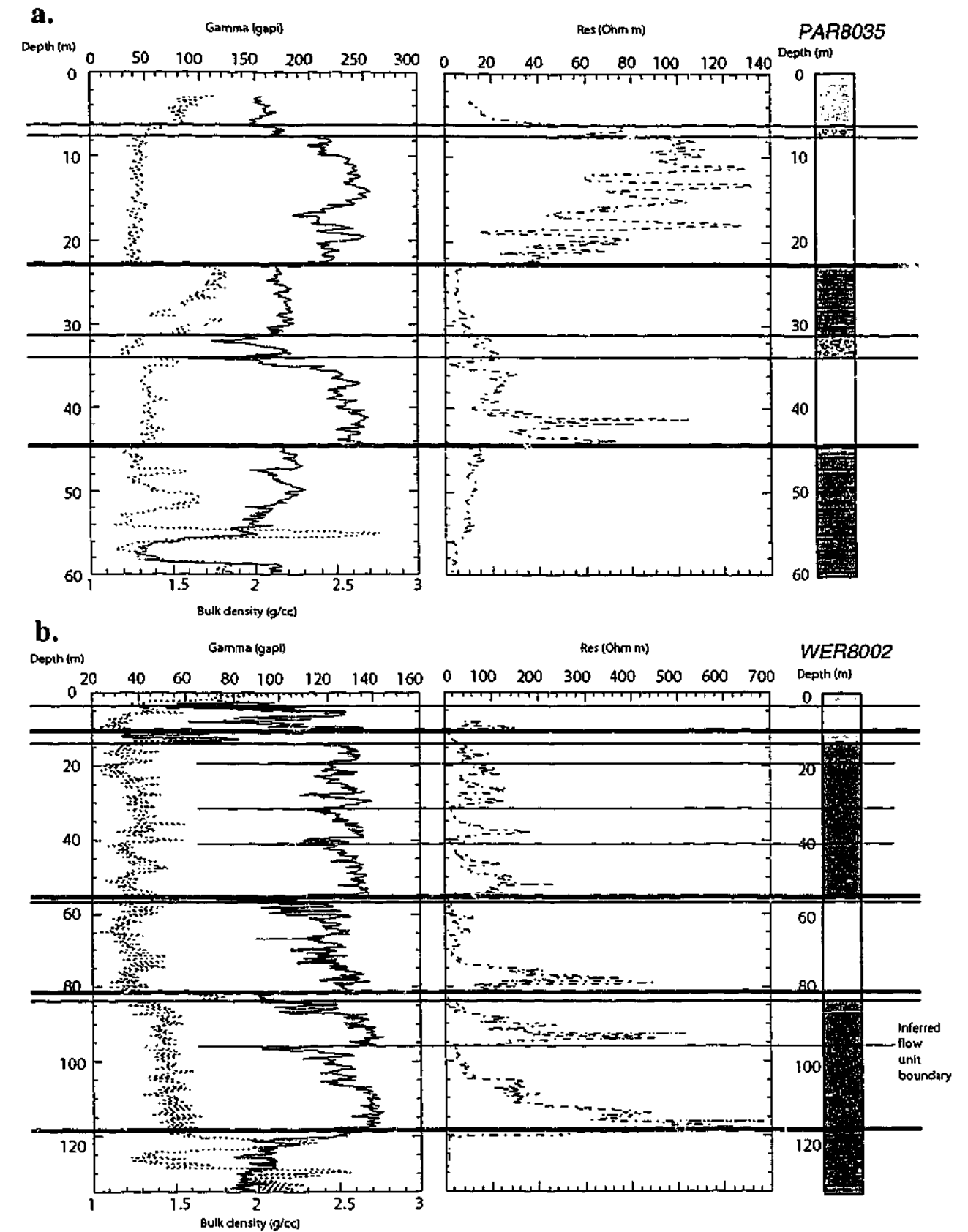


Fig. 4.9 Representative geophysical well logs and corresponding inferred graphic logs for a. PAR8035 and b. WER8002. Of particular importance is the contact between the basalt and underlying sediments, which is identified by a relatively sharp increase in gamma ray content and decrease in bulk density and resistivity. Interflow sediments occur in PAR8035, and inflated pahoehoe lava lobes have been identified in WER8002. Refer to Fig. 4.4 for explanation of symbols, and Fig. 4.8a for volcanic facies legend.

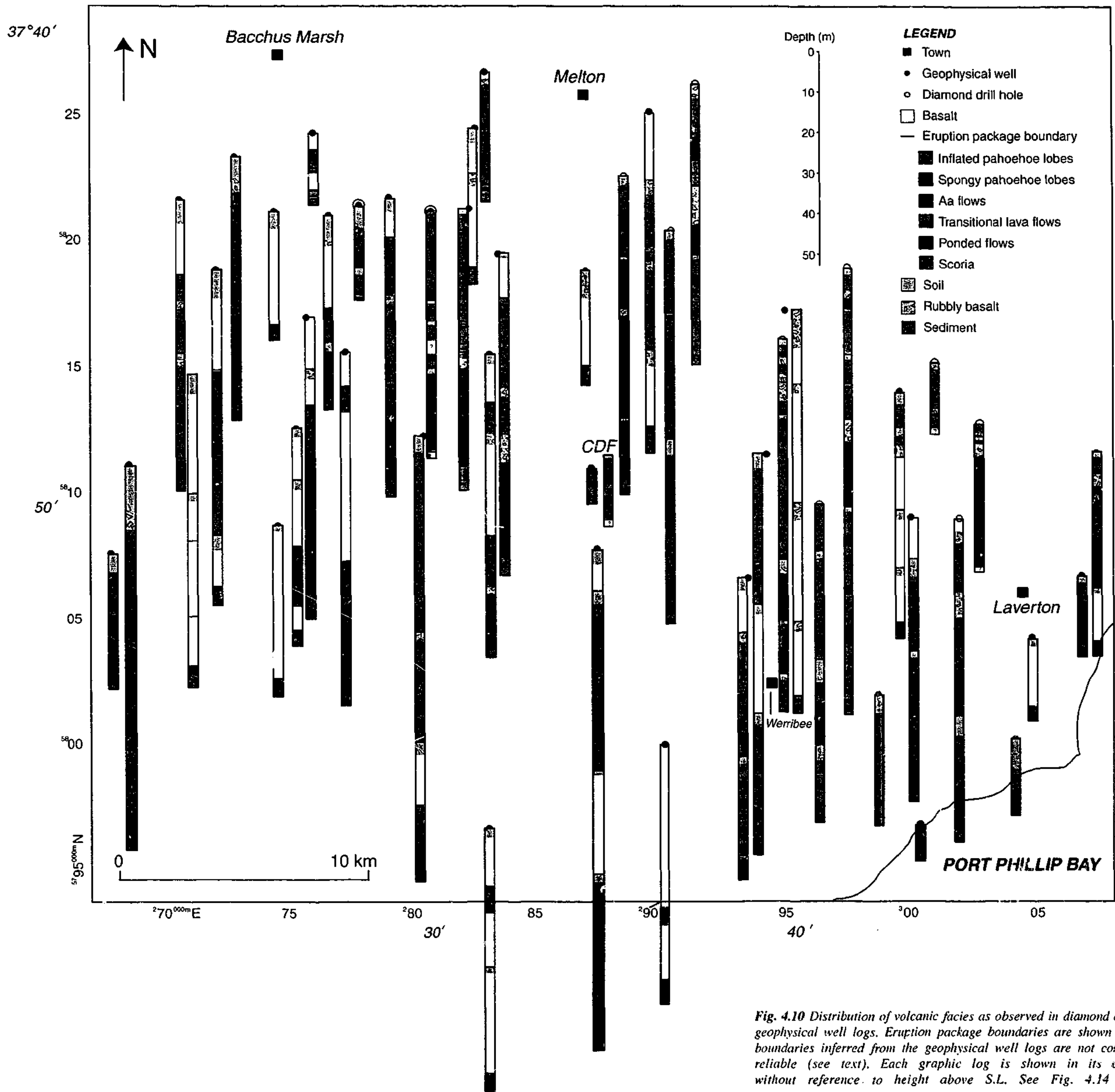


Fig. 4.10 Distribution of volcanic facies as observed in diamond drill core, or inferred from geophysical well logs. Eruption package boundaries are shown (section 4.6.1), although boundaries inferred from the geophysical well logs are not considered to be completely reliable (see text). Each graphic log is shown in its correct spatial location, without reference to height above S.L. See Fig. 4.14 for drill hole names.

of discrete packages of sediments between the basalt flows, in addition to the drill core and outcrop localities described (section 4.7). The sedimentary packages identified range from 5-30 m thick in GOR8007 and PAR8034 respectively, and the average cumulative thickness is ~12.5 m. In most of these instances only one horizon of sediments was observed within a well log, however three holes contain two horizons (MOO8005, PAR8036 & PAR8040) and one hole contains three (MOO8006), each occurring between lava flows.

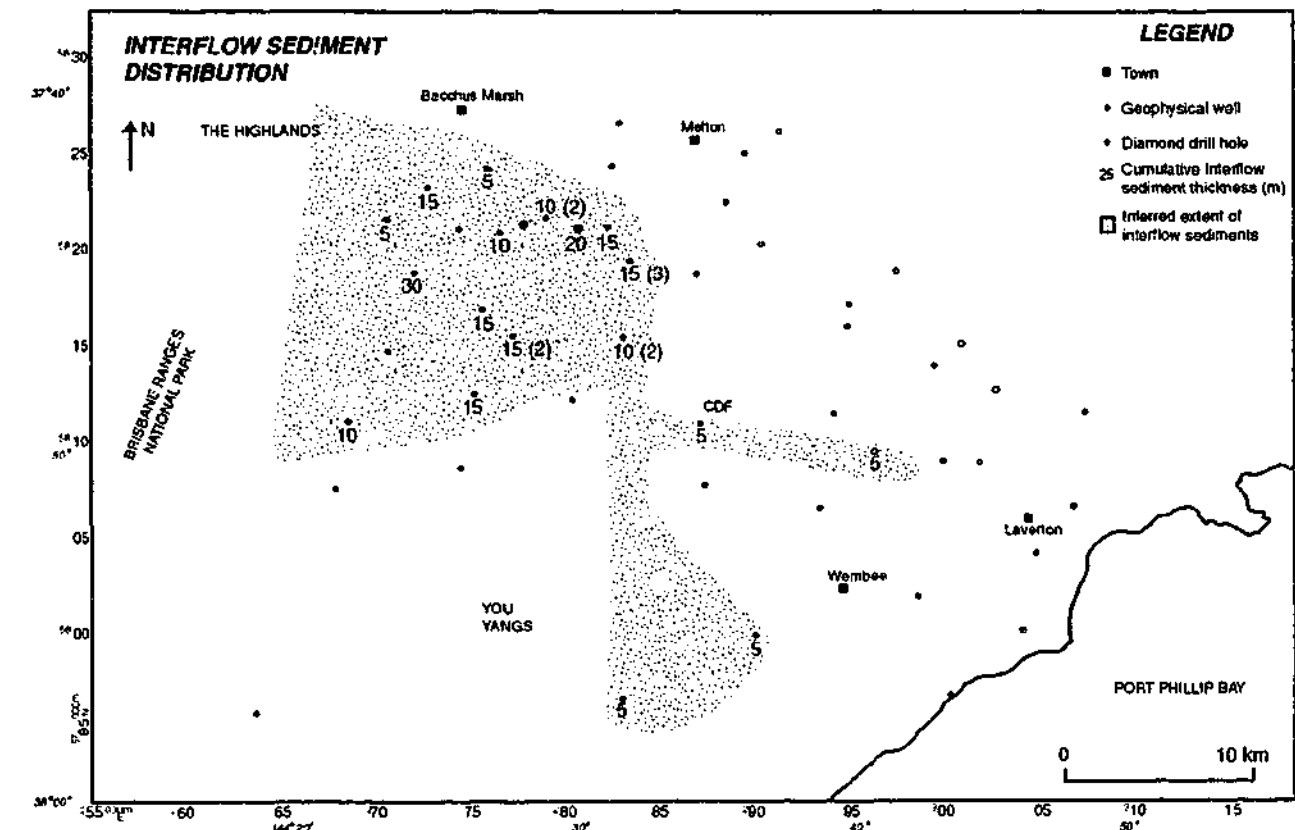


Fig. 4.11 The total cumulative thickness of inter-flow sediments are shown (to the nearest 5 metres) where they have been identified within the basalt pile. In each instance only one sedimentary horizon was identified, except where specified in brackets next to the thickness. Note that generally the sediments occur in the north-west corner of the field area, adjacent to the highlands, although interpretations are limited by drill hole coverage.

4.10 GEOCHEMISTRY: IDENTIFYING GEOCHEMICALLY DISTINCT MAGMA BATCHES

Whole rock geochemical data from more than 80 samples exposed at the surface of the Werribee Plains and 10 sub-surface samples has been analysed (eg. Table 4.2, Appendix I). Previous geochemical studies in the NVP have focussed on petrogenetic processes (eg. Irving & Green 1976, Frey *et al.* 1978, McDonough *et al.* 1985, Price *et al.* 1997, Vogel & Keays 1997), hence these will not be explored here. Instead, the geochemical data is used as a stratigraphic tool in this study, to distinguish between products of different eruptions. Intra-

Table 4.2 Representative whole rock major element geochemical analyses for samples from the Werribee Plains. Source of data: ¹ this study; ² C. Gray unpublished data; ³ Mitchell (1990). Other analyses are included in Appendix I. CIPW norm. classification abbreviations: H- Hawaiite, TR- transitional, T- tholeiite, QT- quartz tholeiite, BI- basaltic icelandite.

Sample no.	T50A ¹	BLK ¹	9 ²	200 ²	LTU9619 ³
Rock type	BI	T	TR	T	QT
Location	DDH TRU50 (29.9 m)	Black Hill	Mt. Atkinson apron	Ryan's Hill/ Stony Hill apron	Mt. Kororoit
SiO ₂	52.55	51.19	48.82	51.77	50.28
TiO ₂	1.68	1.97	2.13	1.69	2.51
Al ₂ O ₃	13.78	13.81	13.41	13.78	14.61
Fe (total)	10.65	11.24	11.03	10.38	13.34
MnO	0.17	0.21	0.16	0.16	0.18
MgO	8.1	7.18	8.90	8.30	4.92
CaO	8.18	8.47	8.45	8.25	7.14
Na ₂ O	2.87	3.38	3.48	3.10	3.38
K ₂ O	0.85	1.21	1.48	0.79	1.75
P ₂ O ₅	0.28	0.47	0.45	0.29	1.25
H ₂ O ⁺			0.71	0.64	0.45
H ₂ O ⁻			0.51	0.38	0.18
CO ₂			0.62	0.06	0.04
Total	100.12	100.17	100.15	99.52	100.02
⁸⁷ Sr/ ⁸⁶ Sr			0.70443	0.70546	

flow chemical variations in basalts are relatively minor (Chapter 2), hence one sample per flow is considered to be representative of the chemistry of the flow and eruption package. The CIPW normative compositions have been used to classify rocks as alkali basalts (0-5% normative nepheline), transitional (6-10% normative hypersthene), and tholeiitic (more than 10% normative hypersthene) (Price *et al.* 1997). The CIPW norm. calculation was made assuming anhydrous compositions and an Fe₂O₃/FeO ratio of 0.2. The tholeiitic rocks have been subdivided according to SiO₂ abundance and the presence of quartz in the CIPW norm. Tholeiitic rocks with SiO₂ more than 52% are termed basaltic icelandites, whereas those with

SiO₂ less than 52% are tholeiites, or if they contain normative quartz are quartz tholeiites. Some samples that were not analysed geochemically were classified as being alkalic or tholeiitic petrographically (Appendix J). Aa lavas were found to be too fine-grained to identify the composition petrographically. The groundmass of pahoehoe lavas is generally more coarse-grained however (see Chapter 2), and alkalic basalts have a fully crystallised groundmass, while tholeiites have glassy mesostasis preserved interstitial to the plagioclase lath network.

It is widely believed that alkalic rocks (hawaiites and transitional compositions) and tholeiitic rocks are produced by magmas subject to different degrees of partial melting (eg. Frey *et al.* 1978). It is also argued however, that the two broadly different magma types instead are sourced from different parts of a chemically inhomogeneous mantle (Price *et al.* 1997). Whatever the reason for the chemical differences, alkalic magmas cannot be derived from olivine tholeiite magmas by near surface fractionation because there is a thermal barrier shown by the simple system silica-albite-nepheline, as well as by more complex systems at one atmosphere (White 1995). Furthermore, there is a correlation of increasing ⁸⁷Sr/⁸⁶Sr isotopic ratio and silica content within the products of the Newer Volcanic Province, with hawaiites tending to have the lowest and basaltic icelandites the highest values (Price *et al.* 1988). This again suggests that alkalic and tholeiitic magmas are genetically unrelated, and it therefore follows that upon eruption, fractionation of tholeiitic lavas will not produce alkalic basalts.

Major element abundances were investigated to identify any unique chemical subtypes within the tholeiitic and alkalic rocks. This is a common method that has been used in other basaltic provinces, to identify chemically distinct magma batches, in order to establish a stratigraphy (Bailey 1989, Landon & Long 1989, Reidel *et al.* 1989, Reed *et al.* 1997). Major element abundances in the rocks from the NVP are not considered to have been greatly affected by weathering and alteration processes, whereas Ba, Y and the rare-earth elements have been shown to be mobile (Price *et al.* 1991). The hawaiites and transitional lavas (alkalic basalts) were found to be chemically homogeneous, and no subdivisions were made within these samples (Fig. 4.12a-e). In addition to the geochemical plots shown, incompatible major element oxide plots (K₂O vs. TiO₂) were constructed to see if samples from the different centres could be distinguished. There was considerable overlap in the results of the products from the different centres, and again no clear distinctions could be made. One sub-group was identified within the tholeiites, hereafter referred to as Group I tholeiites (Fig. 4.12a-e). These samples are enriched compared with the other tholeiites in TiO₂ (>2.5%), K₂O (>1.5%), and FeO (total >12.5%), and depleted in MgO (<6%) and CaO (<7.5%). A sample is included in

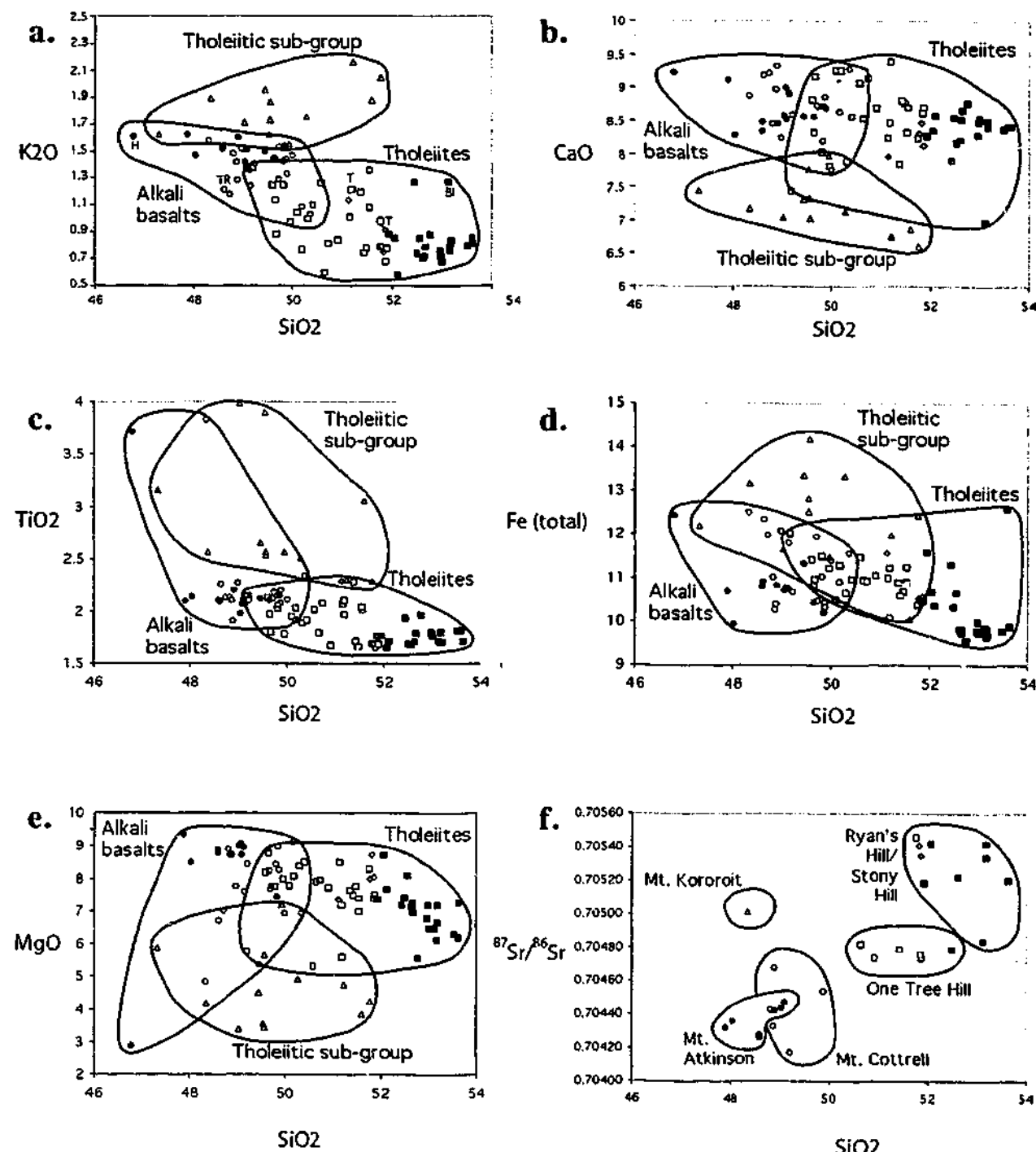


Fig. 4.12a-e. Major element plots for all samples analysed in the Werribee Plains. The samples have been classified according to the CIPW norm classification scheme, and the tholeiitic and alkalic lavas grouped together. A geochemically distinctive tholeiitic group has been identified and plotted separately to the other tholeiitic samples (Group I tholeiites- Δ). Symbols are as follows: Hawaiites- \bullet , Transitional- \circ , Tholeiites- \square , Quartz tholeiites- \diamond , basaltic icelandites- \blacksquare . f. $^{87}\text{Sr}/^{86}\text{Sr}$ ratios plotted for a limited number of samples. The products of different eruption centres have been inferred and grouped together.

this sub-type if it contains three or more of these parameters listed. The sub-surface distribution of inferred chemical sub-types is shown in Fig. 4.13, and the surface distribution in Fig. 4.15.

In addition to major element abundances, initial $^{87}\text{Sr}/^{86}\text{Sr}$ isotopic ratios were investigated to differentiate between lavas from different centres. Sr isotopic ratios have previously been found to be powerful tracers of genetic relationships amongst the basalts because they are unmodified by geochemical fractionation and weathering, and vary greatly within the NVP (Price *et al.* 1988). Although no new data was collected in this study due to time constraints and cost, existing data (Price *et al.* 1997) has been analysed and samples from different eruption centres grouped together where possible (Fig. 4.12f). Again, there appears to be some overlap between the products of the alkalic eruption centres. The spread of sample points of the lavas inferred to have been fed from Mt. Cottrell in particular, suggest it is an isotopically complex source. The samples have been grouped here based upon proximity to the eruption centres and topographic constraints. The tholeiitic centres analysed each have fairly distinctive isotopic signatures.

4.11 PALAEOMAGNETIC RESULTS

4.11.1 Magnetostratigraphy

Magnetostratigraphic studies involve organising strata systematically into identifiable units based on stratigraphic variations in their magnetisation directions (Butler 1992). The inclination of the primary remanent magnetisation was identified in most lava flow units in drill core (Chapter 3; Fig. 4.13). In a small amount of samples the primary remanence was not identified, as these samples are palaeomagnetically unstable. Although the inclination of the primary remanence for these samples was not determined, the polarity of the magnetic field during lava emplacement was recorded. In addition to the data collected in this study, magnetic polarity data was available for selected outcrop localities (N. Opdyke, unpubl. data and Hurren 1998, Appendix K). Magnetostratigraphic units were identified within the sequence as intervals of constant polarity (Fig. 4.13). Some samples are considered to have been upside down in the core trays, as the polarity of these discrete samples differ from all the others within a magnetostratigraphic interval. The inclination values in these cases are retained, however the sign is changed. In order to establish a magnetostratigraphy within this sequence a simple assumption is made that all major reversals of the magnetic field during volcanic activity are recorded by the remanent magnetisation of the lavas (ie. eruptions were relatively continuous, and no major reversals were missed). This is reasonable, given that the eruption

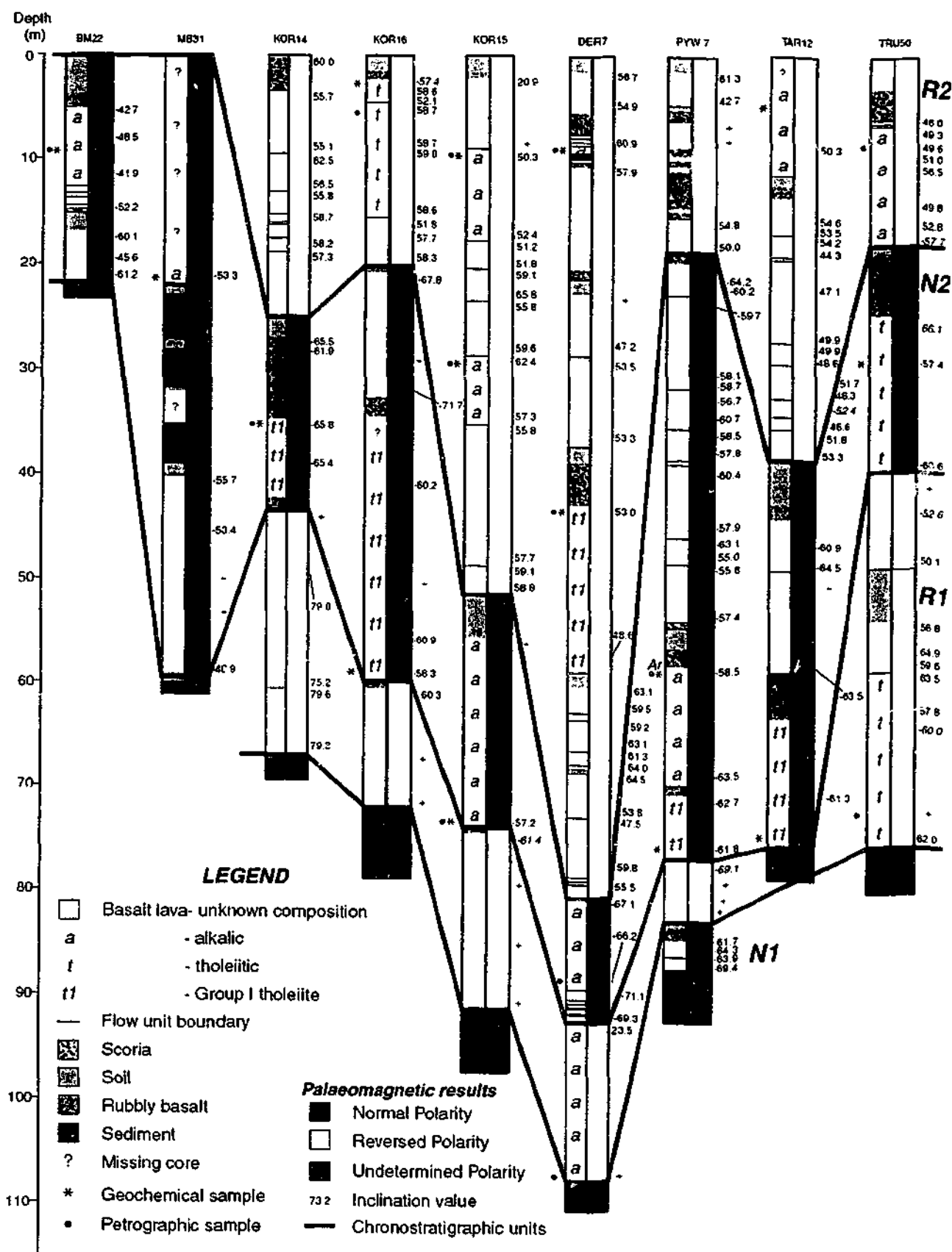


Fig. 4.13 Palaeomagnetic results: inclination values are next to graphic logs. Where it was not possible to determine the absolute value, just the sign of the polarity is recorded. The inclinations of samples that are considered to have been inverted in the core trays are italicised. A simple magnetostratigraphy is established, with boundaries between identified chronostratigraphic units shown. Geochemical results for flows that have been analysed (XRF) or examined petrographically are shown in the left-hand column of each graphic log (section 4.10). The position of the sample chosen from PYW7 for ⁴⁰Ar/³⁹Ar dating (section 4.12) is shown (Ar).

frequency in other continental basaltic fields ranges from one eruption every 2 ka in the Eifel field, Germany, to one eruption every 15 ka in the Columbia River flood basalt field, U.S.A. (Schmincke *et al.* 1983, Tanaka *et al.* 1986, Bailey 1989, Condit & Connor 1996, Conway *et al.* 1998).

In five out of nine of the diamond drill holes analysed, a simple reverse polarity, normal, reverse stratigraphy is evident, and this is considered to be correlatable between each of these holes (Fig. 4.13). The magnetostratigraphic units are labelled following the scheme adopted by Swanson *et al.* (1979) for the Columbia River basalts (ie. N₁, and R₁ are the oldest normal and reverse polarity intervals etc.). Although the eruption packages contained within these units may not be genetically related, the magnetostratigraphic units represent discrete periods of time within which all lavas preserved in the interval were emplaced. In drill hole PYW7 an additional normal polarity interval is preserved at the base of the sequence, and this is considered to represent the oldest lavas intersected by the drill holes. TAR12 is not considered to have had lavas emplaced in this location during the earliest reverse polarity interval, and only one normal polarity interval is preserved in both BM22 and MB31.

4.11.2 Secular variation

The average inclination was determined for each eruption package (the mean), and the standard deviation and standard error (Appendix D). This is an approximation only, as this technique does not take into account the declination of the magnetic field, because the samples are not oriented horizontally (eg. McFadden & Reid 1982). For the scope of this study this technique is adequate. Some eruption packages do not have enough samples within them to calculate the standard deviation of the inclination for that package (eg. some consist of a single flow). The average of the standard errors for the sequence is ~3.5° and this value was used in these instances. Within identified eruption packages variations in inclination are generally observed to be relatively small, especially when compared with the amplitude of the variation between adjacent eruption packages (up to ~10°). Secular variations in the geomagnetic field are changes in the direction and magnitude of the field, and occur on the order of every 1-10⁵ years (Butler 1992). Secular variation is recorded here by a significant change in the average inclination of an eruption package, and aids in correlating eruption packages from different drill holes that have been erupted in the same magnetostratigraphic interval (section 4.14.2, Fig. 4.16).

4.12 AGE CONSTRAINTS

Previous K-Ar radiometric dating studies have yielded an age range for surface samples of the Werribee Plains of 1.41-2.6 Ma (McDougall *et al.* 1966, Aziz-Ur-Rahman & McDougall 1972, Price *et al.* 1997, Gray unpubl. data; Fig. 4.15). Two of the dates obtained are from lavas considered to have been fed by Mt. Cottrell and Mt. Atkinson, the products of which have been intersected in a number of the drill holes. This yields upper age constraints for the magnetostratigraphy of 1.41 ± 0.02 Ma and 2.24 ± 0.03 Ma. The upper reverse polarity interval labeled R₂ (Fig. 4.13) therefore actually contains lavas erupted in two different magnetic polarity periods (Table 4.3, Fig. 4.16). The assumption that all magnetic field reversals are recorded within the sequence still may hold, although the complete stratigraphy is clearly not recorded in each drill hole. To confirm that the inferred correlations are correct, and that all major reversals are recorded within the sequence, lower age constraints for the magnetostratigraphy were investigated.

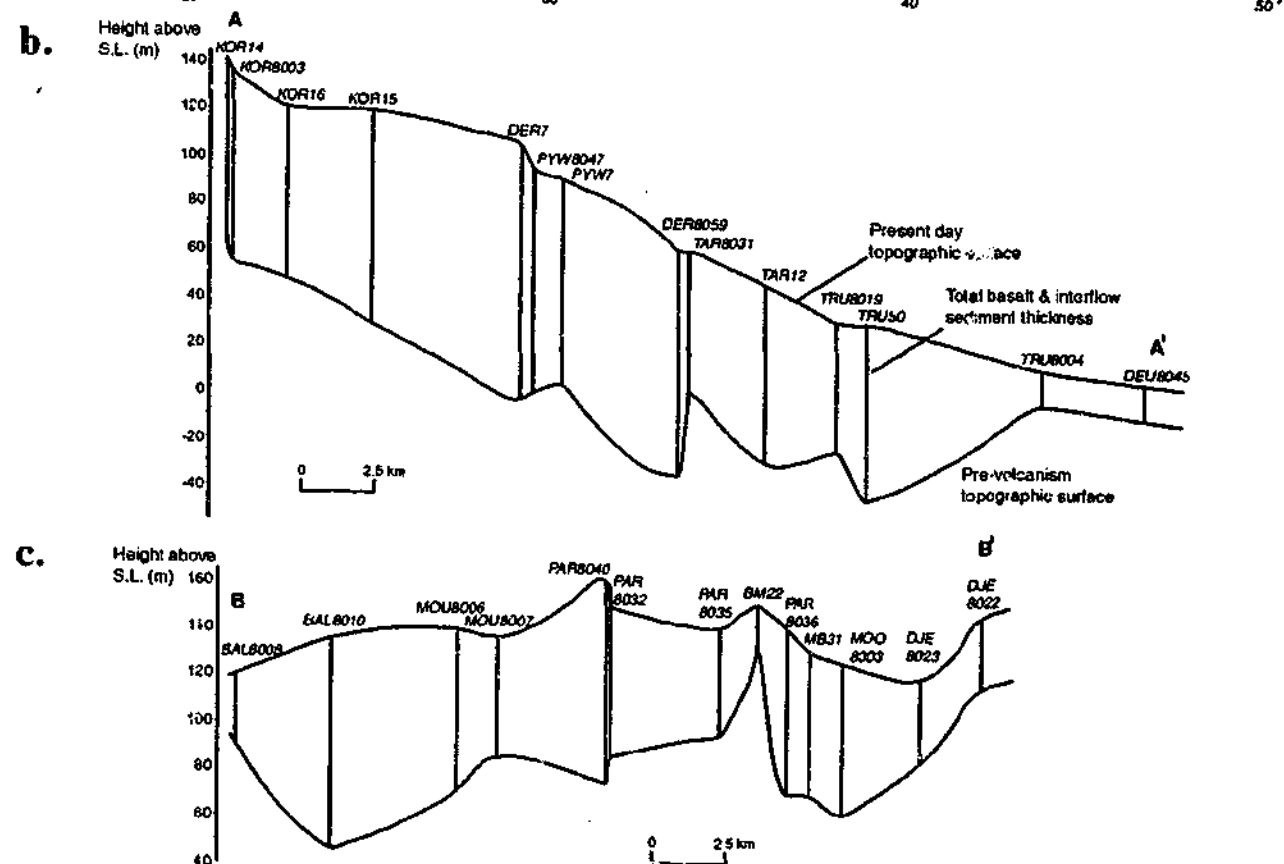
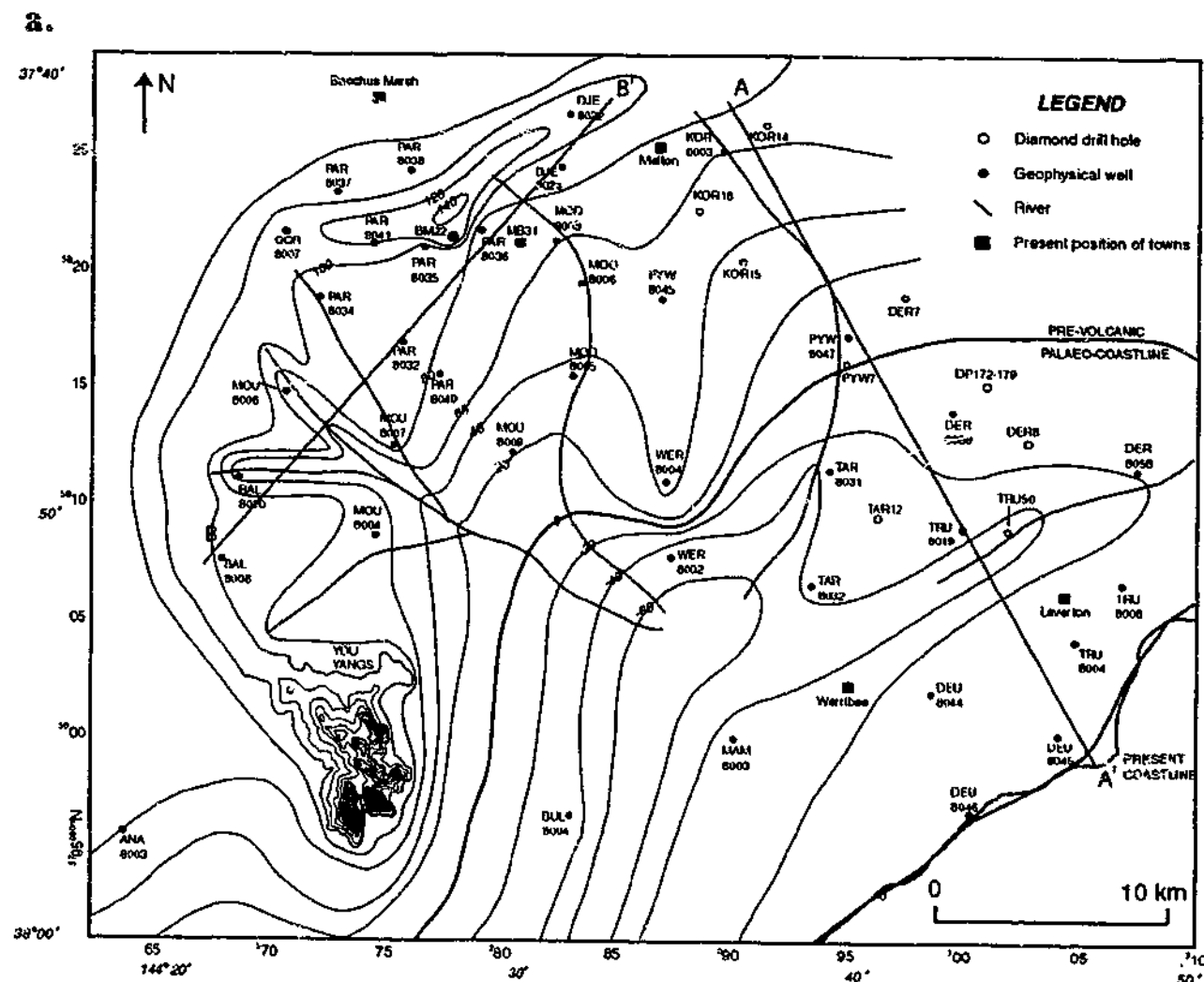
Thin sections were made of some of the least altered samples at or toward the base of the sequence, with a view to doing whole rock K-Ar dating on them. Unfortunately they were all too altered to attempt dating (C. Gray pers. comm.). The groundmass commonly contained smectite and zeolites, any interstitial glassy mesostasis was altered beyond recognition and amygdales were abundant. Plagioclase phenocrysts are relatively rare in the basalts of this study (eg. Appendix J), however one sample that occurs towards the base of the sequence (Fig. 4.13) has large, unaltered plagioclase phenocrysts, and was considered suitable for ⁴⁰Ar/³⁹Ar dating (D. Phillips pers. comm.). The possibility of doing radiometric dating was largely ruled out earlier in the course of this study, due to what was considered to be pervasive alteration of the basalts at depth in the sequence. This sample with plagioclase phenocrysts was discovered fairly late, is presently being irradiated, and unfortunately the results are therefore not yet available. The sample occurs in the N₂ chronostratigraphic unit, and two magnetic polarity intervals are recorded beneath this in the sequence. The age will give a better constraint on the timing of commencement of volcanism. Other dating techniques were also explored, however these rocks are either too young for the technique to work without copious amounts of sample (eg. SHRIMP dating of baddeleyite), or too old (eg. carbon dating or thermoluminescent dating of interflow or basal sediments), the constituent minerals are too small (eg. fission track dating of apatite grains), or the appropriate minerals were lacking (eg. the zircons are considered to be inherited, C. Gray pers. comm.). The basal sediments are commonly oxidised and iron-stained, and are generally not considered to be likely to contain

any organic material including pollen. One sample was found at the base of drill hole DER7 that is remarkably unaltered. It is a clean, light grey to buff-coloured siltstone that was analysed in the Geography Department for its pollen content. Palynological studies in western Victoria have identified some distinctive pollen assemblages in the late Tertiary period (B. Wagstaff pers. comm.). Unfortunately the sample was found to be completely barren in terms of organic material and could not be dated in this way either.

Although the age of the underlying sediments is not well constrained, it is known approximately. The Brighton Group consists of the Black Rock Sandstone and the overlying Red Bluff Sands and has been traced beneath the basalts of the Werribee Plains in bore holes (Kenley 1967). The marine Black Rock Sandstone unit ranges in age from Uppermost Miocene to at least the Lower Pliocene (Abele *et al.* 1988). Towards the end of the Lower Pliocene a marine regression occurred (Abele *et al.* 1988) resulting in continental deposition of the Red Bluff Sands. This is considered to have been a eustatic sea level fall, as it corresponds to the timing of an event identified by Haq *et al.* (1987) at 3.8 Ma. There is evidence that the area of study was in the midst of a marine regression when volcanism commenced (section 4.15.1), hence a lower age limit for the commencement of volcanism is ~3.8 Ma, towards the end of the Lower Pliocene.

4.13 PALAEO TOPOGRAPHY

A contour map of the palaeotopography prior to volcanism was produced using the geophysical well and diamond drill core data (Fig. 4.14a). This map was produced by subtracting the total basalt (and inter-flow sediment) thickness in each hole from the present topography, assuming that, locally earth movements have been minimal since volcanic activity commenced. There is no evidence to suggest otherwise. There are however, some minor problems and limitations associated with reconstructing the palaeotopography. Firstly, the map of the palaeotopography shows the elevation of the underlying sediments prior to volcanism, however the basalt was not all erupted simultaneously across the Plains. Based upon the map produced, and previous work (Kenley 1967), the Werribee Plains appears to have been a dynamic environment prior to volcanism: rivers were dissecting the landscape, and sedimentation was widespread. In spite of this, the amount of interflow sediments observed within the basalt pile was minimal (section 4.9). It is considered that the amount of sedimentation or erosion occurring subsequent to the commencement of volcanism was not enough to substantially alter the topography, and the map produced gives the general shape



of the landscape. Details of the map were constrained by the spacing of the drill holes, which were generally kilometres apart. Again, only the broad picture can be obtained and inferences were made between the holes. Finally, earth movements associated with the Kosciusko uplift were occurring contemporaneously with the volcanism, and culminated in the Late Pliocene-Early Pleistocene (Abele *et al.* 1988). Although this must be taken into consideration, it is impossible to quantify the amount of movement that has occurred. It is assumed that any movements affected the whole area, as there is no evidence of localised faulting within the Plains.

The present slope towards the coast in the south-east is reflected in the palaeotopography, however the palaeo-coastline was situated ~20 km north-west of its present position (Fig. 4.14a). A prominent ridge is situated in the north-west corner of the field area, and there is also evidence of a N-S trending ridge in the centre of the area. It appears that the land was heavily dissected by fluvial systems, and these are considered to have fed into a more major tributary flowing south, adjacent to the You Yangs. Two cross-sections (A-A' and B-B') through the basaltic sequence were constructed (Fig. 4.14b; refer to Figs. 4.1 & 4.14a for location of the sections). All drill holes within ~3 km either side of the section lines are included in the cross-sections. The basalts appear to have filled in pre-existing valleys and depressions and have smoothed out the overall topography.

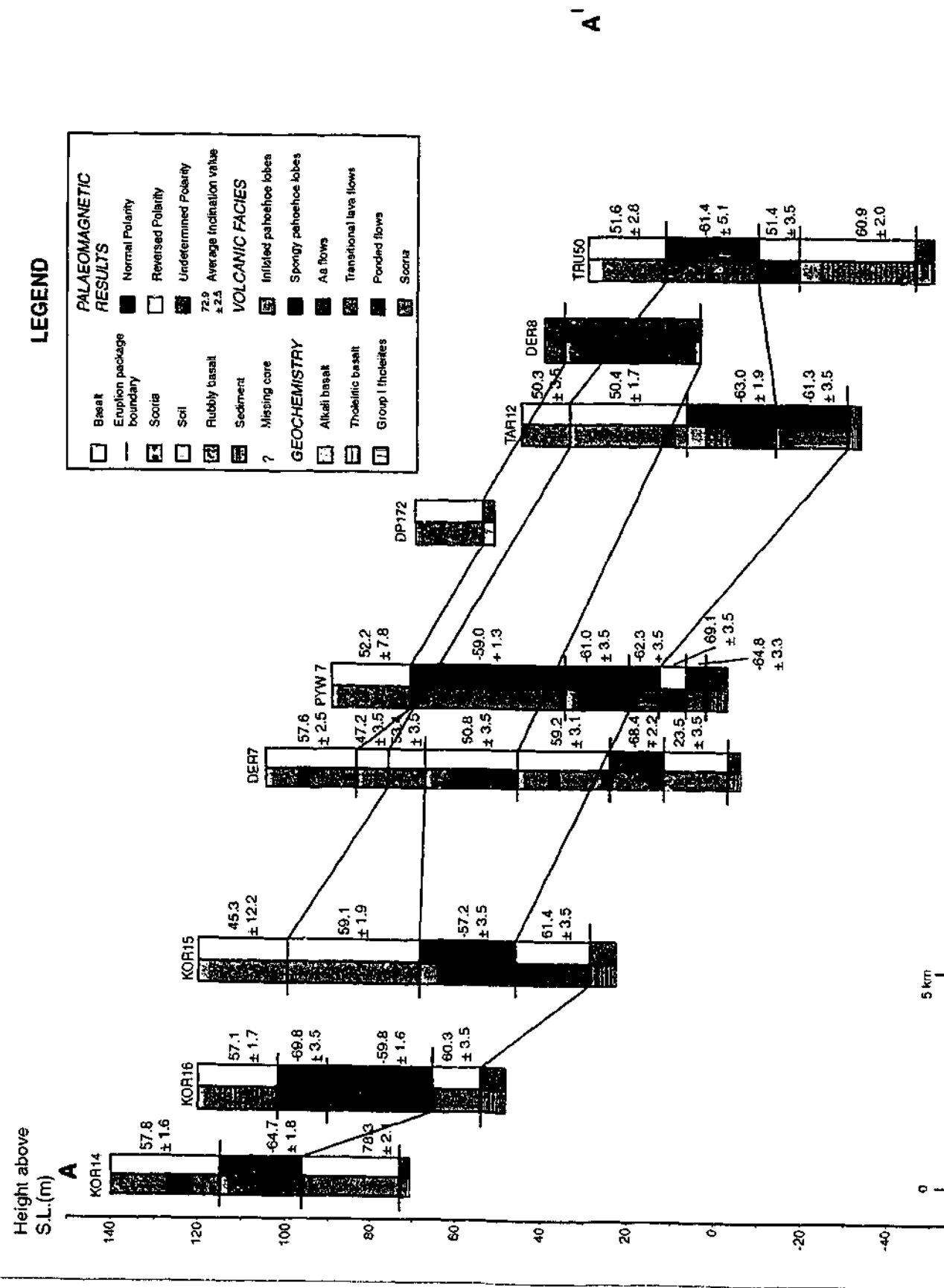
4.14 STRATIGRAPHY

4.14.1 Producing a stratigraphic map of the surface of the Werribee Plains

Combining the geochemical data with other information (available K-Ar ages, magnetic polarity data, airborne geophysical data and the present topography), the extent of lavas fed from the different centres, and boundaries between eruption packages have been inferred (Fig. 4.15). The central and western cone of the Anakies are hawaiites, and the eastern cone is nepheline mugearite in composition (Irving & Green 1976). Four samples from Spring Hill are borderline tholeiites, containing just over 10% normative hypersthene. They are isotopically similar to the other Spring Hill samples (C. Gray pers. comm.) and have therefore been grouped here with the alkalic lavas. One Tree Hill has been inferred to have fed significant

Fig. 4.14 (Facing page) a. Map of the palaeotopography prior to volcanism (20 m contour line spacing). Note that the area was not as flat as it is today, but there is evidence of ridges, and rivers dissected the landscape. b. & c. Schematic cross-sections through the basalt pile (see Fig. 4.1 and above for position of sections). Note the vertical scale is exaggerated.

Fig. 4.16 Magnetostratigraphy for the east of the Werribee Plains. Drill holes are shown at their present elevation above S.L. and have been projected to the cross-section line A-A' (Fig. 4.1). The average inclination values calculated for each eruption package are adjacent to the logs. Correlations of eruption packages between drill holes (solid black lines) were made using the criteria discussed in the text, and are listed in Table 4.3.

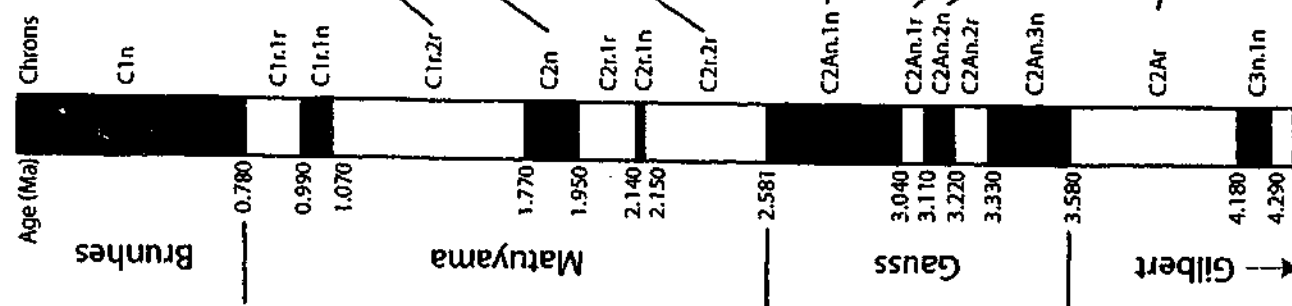


be reasonably separated in terms of palaeotopography, other drill holes and likely lengths of flows (sections 4.13, 4.14.1). Although the locations of the eruption centres are not always known, palaeotopographical considerations can discount making correlations between holes that would require the lava to flow down and then uphill. It is not considered reasonable to correlate eruption packages between two holes that have one directly in between that has no evidence of the eruption. All of the drill holes in the magnetostratigraphy lie within ~20 km of each other, which is less than the maximum preserved extent of lavas from an eruption centre at the surface (section 4.14.1). Eruption packages can therefore potentially be correlated between any of the drill holes, depending on the other parameters previously listed.

In addition to the eruptions identified in Fig. 4.16, the relative timing of some more eruptions that occurred in the Werribee Plains have been constrained and added to the stratigraphy (Table 4.3). The products of the Spring Hill eruption overlie inter-flow sediments in a number of drill holes (Figs. 4.10, 4.15). This eruption is considered to have diverted the pre-existing drainage to the north and east (forming the present Werribee River), and thus is considered to have post-dated the eruption of Mt. Cottrell. The products of the Spring Hill eruption are normal polarity (as recorded by drill holes BM22 & MB31; Fig. 4.13), and as it is inferred to have post-dated the eruption of Mt. Cottrell, the Spring Hill eruption must have occurred in the Matuyama Chron (Table 4.3). An eruption package is preserved in each of the drill holes BM22 and MB31 beneath the Spring Hill eruption, and these are considered to be part of the N2 magnetostratigraphic interval (Fig. 4.13), and occurred some time in the Gaussian Chron (Table 4.3). The upper eruption package preserved at CDF (overlying a package of inter-flow sediments, Fig. 4.6) has been inferred to have been erupted from One Tree Hill based upon geochemistry, magnetic polarity and topographic constraints. In Table 4.3, the eruptions that occurred within each magnetostratigraphic interval are listed chronologically wherever possible (eg. if two eruptions are recorded in the same drill hole the older eruption is listed lower in the table). Commonly however, there is no way of identifying the relative timing of the eruptions, without more comprehensive radiometric dating. Bald Hill, Greek Hill, Green Hill and the Anakies are the only exposed eruption centres in the Werribee Plains that are not included in the stratigraphy in Table 4.3, because we have no constraint on the relative timing of the eruptions.

Table 4.3 Every eruption identified in the magnetostratigraphy is listed (a total of 27 eruptions). Within an interval of constant polarity eruptions are listed in the correct relative order where possible (ie. where 2 or more eruptions are intersected by 1 drill hole). The magnetic polarity time scale is shown on the left (Cande & Kent 1995). Abbreviations: A-alkalic, tholeiitic, Gr T- Group I tholeiites.

No. eruptions identified	Eruption centres	Drill holes/outcrop	Products	Composition	Average inclination	Age (Ma)
2	Mt. Atkinson	DER7, PYW7, DP172, DER8	Transitional	A	54.9 ± 4.3	1.41
1	One Tree Hill	CDF	Pahoehoe	T	+47.7 ± 4.7	1.62-1.66
7	Spring Hill Mt. Cottrell	BM22, MB31 KOR15, DER7, TAR12, TRU50	Pahoehoe	A	49.1 ± 4.3	2.24
		KOR14	Pahoehoe	A	57.8 ± 1.6	
		KOR16	Pahoehoe	T	57.1 ± 1.7	
		KOR15, DER7	Pahoehoe	A	58.2 ± 2.0	
		DER7, DER8	Aa	GrIT	50.8 ± 3.5	
		TAR12	Pahoehoe	T	50.4 ± 1.7	
		DER7	Pahoehoe	T	59.2 ± 3.1	
10	Ryan's Hill/ Stony Hill	TRU50, TAR12	Pahoehoe, Ponded lava	T	-62.2 ± 2.6	2.5-2.6
		BM22	Pahoehoe		-55.6 ± 10.1	
		MB31	Aa		-52.7 ± 4.0	
		KOR16	Ponded lava	GrIT	-69.8 ± 3.5	
		KOR14, KOR16	Aa		-62.6 ± 2.3	
		PYW7	Pahoehoe		-59.0 ± 1.3	
		KOR15, PYW7	Scoria	A	-59.7 ± 3.8	
		PYW7, TAR12	Pahoehoe	GrIT	-61.9 ± 0.8	
		DER7	Pahoehoe	A	-68.4 ± 2.2	
6		KOR14	Pahoehoe		78.3 ± 2.1	
		KOR16, KOR15	Pahoehoe		60.9 ± 3.5	
		DER7	Pahoehoe	A	23.5 ± 3.5	
		PYW7	Ponded lava		69.1 ± 3.5	
		TRU50	Ponded lava		51.4 ± 3.5	
		TRU50	Pahoehoe	T	60.9 ± 2.0	
1		PYW7	Pahoehoe		-64.8 ± 3.3	
Black Rock Sandstone- Red Bluff Sands eustatic sea level fall event						
						3.8



4.15 DISCUSSION

4.15.1 Palaeogeography

Based upon observations made in drill core (section 4.8), the airborne magnetic image (section 4.4), and the palaeotopography (section 4.13), the area is interpreted to have been in the midst of a marine regression at the onset of volcanism. There is evidence of only very shallow water in the deepest parts of the basin (in drill holes TAR12 & TRU50). It is interesting to note however, that there appears to be a progression from north to south of increasing 'wetness' of the underlying sediments. The drill holes to the north of the field area have well developed soil horizons above the basal sediments, and the southern holes have small amounts of hyaloclastite. Volcanism may thus have commenced right at the end of, or relatively soon after the marine regression, or it may just be a function of the local topography, with some drill holes located on palaeo-ridges and others in palaeo-valleys. Uplift of the Palaeozoic highlands to the north and west of the field area was probably initiated as early as the middle Miocene, and culminated in the Late Pliocene-Early Pleistocene (Abele *et al.* 1988). Therefore, although uplift was still continuing during volcanism, there would have been substantial topographic relief to the north and west of the Werribee Plains prior to volcanic activity. Rivers were actively dissecting the landscape, producing valleys and relatively high relief ridges (Fig. 4.14). Although the topography prior to volcanism was not as subdued as it is now, it must have been relatively flat for inflation of the pahoehoe flows to have occurred (inflation is restricted to slopes of less than 2° (Hon *et al.* 1994, Cashman & Kauahikaua 1997)). Inflated pahoehoe lavas constitute the dominant lava facies, and occur at the base of the sequence in all but one diamond drill hole (Fig. 4.16). Most of the rivers would have originated in the highlands, supplying sediment from the highlands south and south-east into a valley draining south-south-west into the sea.

This is consistent with observations of the interflow sediments, made in drill core and outcrop (section 4.7). Apart from minor basaltic lithic clasts in the gravel at the base of the sediment package in MB31, there is no evidence of any basaltic input to the sediments in this hole or TAR12. Instead, the quartz and meta-sedimentary clasts are considered to have been derived from the uplifted Palaeozoic highlands. In MB31 the upward-fining point-bar sequences are the products of a meandering river system. Periods of low flow are shown by the presence of soil horizons, as the river migrated laterally. The sediment supply recorded at CDF is different to elsewhere within the Plains, as there is significant volcanic material preserved. The sequence is interpreted to represent over-bank flood deposits from a meandering

river. The individual beds are formed in discrete flooding events, and the change in grain types is a reflection of the bed-load at the time of flooding. The volcanic material is considered here to have been derived from Mt. Cottrell, Spring Hill, or possibly Green Hill all of which are centres to the north and are considered to have erupted prior to the One Tree Hill eruption preserved at CDF (Table 4.3). Scoria is often produced during the early stages of a basaltic eruption (Chapter 5), and the unconsolidated clasts would be readily eroded and transported, particularly during rain fall. Similarly the outer crust of pahoehoe lavas tends to spall off during eruption, and again immediately following eruption would be easily eroded. It appears that this material was periodically fed (possibly during rainy periods) into a river that was already transporting material from the highlands.

Two interesting features of the sedimentary record within the basaltic succession are: (i) that the interflow sediments are concentrated in the north-west of the field area, and (ii) there is very little evidence of volcanic material within the sediments. (i) The focus of sedimentation in the north-west of the field area may be because uplift of the highlands was concentrated in the west rather than the north during this time (along the Rowsley Fault for example), and east to south-easterly flowing rivers were supplying quartz-rich sediment between eruptions. There is evidence of a N-S trending ridge in the centre of the field area, in the map of the palaeotopography (Fig. 4.14), and this is considered to have diverted the rivers south, thus accounting for the general lack of inter-flow sediments in the east of the field area. (ii) Although there is evidence of substantial time-breaks between eruptions (thick paleosoil horizons locally), only one occurrence of basaltic material in the interflow sediments was observed (CDF, Fig. 4.6). In the Early Pliocene the climate in southeastern Australia was humid, and deep pallid, kaolinitic weathering profiles were common (Joyce 1998). However, by the Late Pliocene the area was arid, and shallow weathering profiles developed. The dramatic change in climatic conditions are thought to be due to a major global cooling event which occurred at the end of the Miocene (Kemp 1978), or during the Middle Pliocene at 3.4-3.2 Ma (White 1994). It has also been argued that the onset of aridity was due to other causes, and occurred as late as 2.5 Ma (Bowler 1982). Although the timing and cause is not well resolved, it appears that the area was arid during the entire period of volcanism (and subsequently) in the Werribee Plains. There is evidence of a general lack of erosion and sedimentation of the basaltic products between eruptions, and relatively shallow weathering profiles are observed.

4.15.2 Change in geochemistry through sequence

Although the data is incomplete in its coverage, there are no clear trends evident in terms of a widespread change in composition of magmas with time in the stratigraphy (Fig. 4.16). Group I tholeiitic lavas occur in a number of drill holes, and have been emplaced over at least 2 magnetic polarity intervals. Although these samples have been classified as tholeiites using the CIPW norm. classification scheme, they plot as alkalic basalts on a Macdonald-Katsura diagram (ie. total alkalis vs. SiO_2 , (Mitchell 1990)). Only one sample within the Group I tholeiites has been analysed for the $^{87}\text{Sr}/^{86}\text{Sr}$ isotopic ratio (sample 92), and this is anomalously radiogenic for a tholeiite (Fig. 4.12f). It is inferred that crystal fractionation occurred in a high-level magma chamber to produce this distinctive composition (Mitchell 1990), and this is rarely seen in the NVP (C. Gray pers. comm.). The Group I tholeiites are therefore considered to have been fed from a common magma chamber, and although it is beyond the scope of this project, this has implications for the residence time of magmas in magma chambers, and the petrogenesis of these basalts. Previously it has been considered that the basaltic plains of the NVP are dominantly tholeiitic (Price *et al.* 1988), however this is clearly not the case in the Werribee Plains. Disregarding the unique Group I tholeiites, more alkalic basalts have been identified than tholeiites in the sub-surface, and both lava types have been erupted in all major polarity intervals identified. The only scoria cones in the Werribee Plains that are alkalic are the Anakies, and the other three cones are tholeiitic in composition. The magnetostratigraphy identified in this study provides an ideal framework for further, more complete petrogenetic studies of the basalts of the NVP than have been previously attempted.

4.15.3 Eruption frequency

Twenty-seven discrete eruptions have been identified in the magnetostratigraphy, the products of which occur in the Werribee Plains (Table 4.3). Based upon other studies in similar provinces (eg. Greeley 1982a, Kuntz *et al.* 1992, Stephenson *et al.* 1998) and the size of the exposed eruption points, all eruption centres are considered to be monogenetic (ie. erupted only once). Therefore there are a number of buried eruption centres within the plains, as well as volcanoes that occur outside the boundaries of the Plains that have fed material into the area. The majority of eruptions appear to have been small volume, as the products of almost two thirds of the eruptions identified are preserved in one drill hole only. This raises the issue of whether there are in fact more genetically related eruption packages that have not

been correlated between drill holes due to limited data. Although this is a possibility, it is clear that even very closely spaced drill holes can preserve very different eruptive histories, eg. DER7 & PYW7 (Figs. 4.1, 4.13, 4.16). These two drill holes are located ~4 km apart and at the onset of volcanism the substrate would have been at a similar elevation in both places (Fig. 4.14). Very different thicknesses of lava accumulated at different times in the two holes, thus emphasising that as well as infilling topographic depressions, the basalt lavas form constructional features which may serve as obstacles or topographic barriers to the products of succeeding eruptions. Based upon these observations and other constraints (section 4.14), it seems reasonable to assume that all eruption packages within the magnetostratigraphy that are related have been identified.

Based upon the age constraints identified and the assumption that all major reversals of the earth's magnetic field are recorded in the sequence (section 4.12, Table 4.3), the 27 identified eruptions occurred between ~3.2 and 1.41 Ma. This gives an eruption frequency of one eruption every ~66,000 years. Although this is the same order of magnitude as studies in other basaltic, monogenetic volcanic fields (Schmincke *et al.* 1983, Tanaka *et al.* 1986, Bailey 1989, Condit & Connor 1996, Conway *et al.* 1998), it suggests that eruptions have occurred less frequently in the Werribee Plains than other provinces. This may be attributed to the limited data analysed, and the likelihood that many other eruptions occurred that have not been identified. However, the Werribee Plains is but a small part of the larger Newer Volcanic Province. If the frequency of eruptions within the entire NVP were being investigated, volcanism was occurring in many other places contemporaneously with activity in the Werribee Plains and thus the frequency of eruptions would have been greater over the whole province (see Chapter 5).

4.16 CONCLUSIONS

- Volcanism began during late stages of the 3.8 Ma eustatic regression.
- The products of twenty-seven eruptions identified in the Werribee Plains have been incorporated into a magnetostratigraphy.
- Although most eruptions appear to have been small volume (the products intersected by only one drill hole), both scoria cones and lava shields have been observed to have

fed significant lava flows. In each instance the flows are the same composition as the eruption centre that fed them, and no trend was identified in terms of a broad change in composition of the lavas with time. Tholeiitic and alkalic basalts are intercalated throughout the history of the succession. Further work is required to confirm this.

- Eruptions are inferred to have occurred approximately every 66,000 years on average, from the commencement of volcanism (~3.2 Ma) to the most recent eruption of Mt. Atkinson (1.41 Ma). Despite relatively long repose periods between eruptions, only one occurrence of basaltic interflow sediments was observed, probably due to the onset of arid climatic conditions in the late Tertiary.
- Prior to volcanism in the Werribee Plains, continental fluvial erosion and sedimentation was occurring in the area, producing local topographic highs and lows. Significant topographic relief probably already existed particularly to the west of the field area (uplift of the highlands along the Rowsley Fault), and sediments were being transported into the plains by easterly flowing rivers, throughout the volcanic activity.
- Inflated pahoehoe lavas are the dominant volcanic facies produced in the eruptions, and the cumulative result of the lavas of the many eruptions is a general smoothing out of the topography. The present topography of the Werribee is relatively flat, punctuated only by the eruption centres that are exposed.

REFERENCES

- Abele, C., Gloe, C.S., Hocking, J.B., Holdgate, G., Kenley, P.R., Lawrence, C.R., Ripper, D., Threlfall, W.F. & Bolger, P.F., 1988. Tertiary. in: *Geology of Victoria* (eds Douglas, J.G. & Ferguson, J.A.), pp. 251-350, Victorian Division, Geological Society of Australia Incorporated, Melbourne.
- Aziz-Ur-Rahman & McDougall, I., 1972. Potassium-Argon ages on the Newer Volcanics of Victoria. *Royal Society of Victoria Proceedings*, 85, 61-69.
- Bailey, M.M., 1989. Revisions to stratigraphic nomenclature of the Picture Gorge Basalt Subgroup, Columbia River Basalt Group. *Geological Society of America Special Paper* 239, 67-84.
- Böhm, H., Reisman, N., Jäger, G., Haverkamp, U., Negendank, J.F.W. & Schmincke, H.-U., 1987. Paleomagnetic investigation of Quaternary West Eifel volcanics (Germany): indication for

- increased volcanic activity during geomagnetic excursion/ event? *Journal of Geophysics*, **62**, 50-61.
- Bowler, J.M., 1982. Aridity in the late Tertiary and Quaternary of Australia. In: *Evolution of the Flora and Fauna of Arid Australia* (eds Barker, W.R. & Greenslade, P.J.M.), pp. 35-45, Peacock Publications, Frewville.
- Butler, R.F., 1992. *Paleomagnetism: Magnetic Domains to Geologic Terranes*. Blackwell Science Ltd., Boston, 319 p.
- Calvari, S. & Pinkerton, H., 1998. Formation of lava tubes and extensive flow field during the 1991-1993 eruption of Mount Etna. *Journal of Geophysical Research*, **103**(B11), 27,291-27,301.
- Camp, V.E., Hooper, P.R., Swanson, D.A. & Wright, T.L., 1982. Columbia River basalt in Idaho: physical and chemical characteristics, flow distribution, and tectonic implications. In: *Cenozoic geology of Idaho*. (eds Bonnischen, B. & Breckenridge, R.M.), pp. 55-75. Idaho Bureau of Mines and Geology, Idaho.
- Cande, S.C. & Kent, D.V., 1995. Revised calibration of the geomagnetic polarity timescale for the Late Cretaceous and Cenozoic. *Journal of Geophysical Research*, **100**, 6,093-6,095.
- Cashman, K.V. & Kauahikaua, J.P., 1997. Reevaluation of vesicle distributions in basaltic lava flows. *Geology*, **25**(5), 419-422.
- Condit, C.D. & Connor, C.B., 1996. Recurrence rates of volcanism in basaltic volcanic fields: An example from the Springerville volcanic field, Arizona. *Geological Society of America Bulletin*, **108**, 1225-1241.
- Condit, C., Crumpler, L.S., Aubele, J.C. & Elston, W.E., 1989. Patterns of Volcanism along the Southern Margin of the Colorado Plateau: The Springerville Field. *Journal of Geophysical Research*, **94**(B6), 7,975-7,986.
- Condon, M.A., 1951. The geology of the lower Werribee River, Victoria. *Royal Society of Victoria Proceedings*, **63**, 1-24.
- Conway, F.M., Connor, C.B., Hill, B.E., Condit, C.D., Mullaney, K. & Hall, C.M., 1998. Recurrence rates of basaltic volcanism in SP cluster, San Francisco volcanic field, Arizona. *Geology*, **26**(7), 655-658.
- Crisp, J. & Baloga, S., 1994. Influence of crystallization and entrainment of cooler material on the emplacement of basaltic aa lava flows. *Journal of Geophysical Research*, **99**(B6), 11,819-11,831.
- Dickson, B.L. & Scott, K.M., 1991. Radioelement distributions in soils and rocks from the Newer Volcanics, south-west Victoria. *AMIRA Unpub. Report*, **216R**, 31 p.
- Frey, F.A., Green, D.H. & Roy, S.D., 1978. Integrated models of basalt petrogenesis: a study of quartz tholeiites to olivine melilitites from southeastern Australia utilizing geochemical and experimental petrological data. *Journal of Petrology*, **19**, 463-513.

- Goff, F., 1996. Vesicle cylinders in vapor-differentiated basalt flows. *Journal of Volcanology and Geothermal Research*, **71**, 167-185.
- Greeley, R., 1982a. The Snake River Plain, Idaho: Representative of a new category of volcanism. *Journal of Geophysical Research*, **87**(B4), 2,705-2,712.
- Greeley, R., 1982b. The Style of Basaltic Volcanism in the Eastern Snake River Plain, Idaho. In: *Cenozoic geology of Idaho* (eds Bonnischen, B. & Breckenridge, R.M.), pp. 407-421, Idaho Bureau of Mines and Geology, Idaho.
- Haq, B.U., Hardenbol, J. & Vail, P.R., 1987. Chronology of Fluctuating Sea Levels Since the Triassic. *Science*, **235**, 1156-1167.
- Helz, R.T., 1987. Differentiation behaviour of Kilauea Iki lava lake, Kilauea Volcano, Hawaii: An overview of past and current work. In: *Magmatic Processes: Physicochemical Principles* (ed Mysen, B.O.), pp. 241-258, The Geochemical Society.
- Ho, A., Cashman, K.V. & Reidel, S.P., 1996. Physical Characteristics of Two Columbia River Basalt Group Flows. *Eos*, **77**(46), F824.
- Hon, K., Kauahikaua, J., Denlinger, R. & Mackay, K., 1994. Emplacement and inflation of pahoehoe sheet flows: Observations and measurements of active lava flows on Kilauea Volcano, Hawaii. *Geological Society of America Bulletin*, **106**, 351-370.
- Hooper, P.R., 1982. The Columbia River basalts. *Science*, **215**, 1463-1468.
- Hurren, R.J., 1998. The Lateral Variation of Magnetisation in Tertiary Near Surface Basalts, Victoria. *Unpub. Honours Thesis, University of Melbourne, Melbourne*.
- Irving, A.J. & Green, D.H., 1976. Geochemistry and petrogenesis of the newer basalts of Victoria and South Australia. *Journal of the Geological Society of Australia*, **23**, 45-66.
- Joyce, E.B., 1998. A new regolith map of the eastern Victorian volcanic plains, Victoria, Australia. In: *3rd Australian Regolith Conference: New approaches to an old continent* (eds Taylor, G. & Pain, C.), pp. 117-126, CRC LEME, Kalgoorlie, Western Australia.
- Katz, M.G., 1997. Patterns of lava flow coverage in drill cores. *Unpub. Master of Science Thesis, University of Oregon, Oregon*.
- Kemp, E.M., 1978. Tertiary climatic evolution and vegetation history in the southeast Indian Ocean region. *Palaeogeography, Palaeoclimatology, Palaeoecology*, **24**, 169-208.
- Kenley, P.R., 1967. Tertiary. In: *Geology of the Melbourne district, Victoria* (ed Kenley, P.R.), pp. 33-46, Mines Department, Melbourne, Victoria, Australia, Melbourne.
- Keszthelyi, L., 2002. Classification of the mafic lava flows from ODP Leg 183. *Proceedings of the Ocean Drilling Program, Scientific Results* **183**, 1-28.
- Kuntz, M.A., Covington, H.R. & Schorr, L.J., 1992. An overview of basaltic volcanism of the eastern Snake River Plain, Idaho. In: *Regional Geology of the Eastern Idaho and Western Wyoming: Geological Society of America Memoir 179*. (eds Link, P.K., Kuntz, M.A. & Platt, L.B.), pp.

- 227-267, The Geological Society of America, Inc., Boulder, Colorado.
- Landon, R.D. & Long, P.E., 1989. Detailed stratigraphy of the N₂ Grande Ronde Basalt, Columbia River Basalt Group, in the central Columbia Plateau. *Geological Society of America Special Paper 239*, 55-66.
- Lipman, P.W. & Banks, N.G., 1987. Aa flow dynamics, Mauna Loa 1984. *U.S. Geological Survey Professional Paper 1350*, 1,527-1,565.
- Marsh, J.S., Ewart, A., Milner, S.C., Duncan, A.R. & Miller, R.M., 2001. The Etendeka Igneous Province: magma types and their stratigraphic distribution with implications for the evolution of the Paran-Etendeka flood basalt province. *Bulletin of Volcanology*, **62**, 464-486.
- McDonough, W.F., McCulloch, M.T. & Sun, S.S., 1985. Isotopic and geochemical systematics in Tertiary-Recent basalts from southeastern Australia and implications for the evolution of the sub-continental lithosphere. *Geochimica et Cosmochimica Acta*, **49**, 2,051-2,067.
- McDougall, I., Allsopp, H.L. & Chamalaun, F.H., 1966. Isotopic dating of the Newer Volcanics of Victoria, Australia, and Geomagnetic Polarity Epochs. *Journal of Geophysical Research*, **71**(24), 6,107-6,118.
- McFadden, P.L. & Reid, A.B., 1982. Analysis of palaeomagnetic inclination data. *Geophysical Journal of the Royal Astronomical Society*, **69**, 307-319.
- Mitchell, M.M., 1990. The geology and geochemistry of the Werribee Plains, Newer Volcanics, Victoria. *Unpub. Honours thesis Thesis, La Trobe University, Bundoora*.
- Müller-Sohnius, D., 1993. Variation on a 36-Ma-old theme: length, intensity and rhythm of volcanism. A record from the Hoheifel (Germany). *Journal of Volcanology and Geothermal Research*, **55**, 261-270.
- Ollier, C.D. & Joyce, E.B., 1964. Volcanic physiography of the western plains of Victoria. *Royal Society of Victoria Proceedings*, **77**, 357-376.
- Price, R.C., Gray, C.M., Nicholls, I.A. & Day, A., 1988. Cainozoic Volcanic Rocks. In: *Geology of Victoria* (eds Douglas, J.G. & Ferguson, J.A.), pp. 439-451, Victorian Division, Geological Society of Australia, Melbourne.
- Price, R.C., Gray, C.M., Wilson, R.E., Frey, F.A. & Taylor, S.R., 1991. The effect of weathering on rare-earth element, Y and Ba abundances in Tertiary basalts from southeastern Australia. *Chemical Geology*, **93**, 245-265.
- Price, R.C., Gray, C.M. & Frey, F.A., 1997. Strontium isotopic and trace element heterogeneity in the plains basalts of the Newer Volcanic Province, Victoria, Australia. *Geochimica et Cosmochimica Acta*, **61**(1), 171-192.
- Puffer, J.H. & Horter, D.L., 1993. Origin of pegmatitic segregation veins within flood basalts. *Geological Society of America Bulletin*, **105**, 738-748.
- Reed, M.F., Bartholomay, R.C. & Hughes, S.S., 1997. Geochemistry and stratigraphic correlation of

- basalt lavas beneath the Idaho Chemical Processing Plant, Idaho National Engineering Laboratory. *Environmental Geology*, **30**, 108-118.
- Reidel, S.P., Tolan, T.L., Hooper, P.R., Beeson, M.H., Fecht, K.R., Bentley, R.D. & Anderson, J.L., 1989. The Grande Ronde Basalt, Columbia River Basalt Group; Stratigraphic descriptions and correlations in Washington, Oregon, and Idaho. *Geological Society of America Special Paper 239*, 21-53.
- Rowland, S.K. & Walker, G.P.L., 1988. Mafic-crystal distributions, viscosities, and lava structures of some Hawaiian lava flows. *Journal of Volcanology and Geothermal Research*, **35**, 55-66.
- Schmincke, H.-U., Lorenz, V. & Seck, H.A., 1983. The Quaternary Eifel volcanic fields. In: *Plateau Uplift; the Rhenish shield; a case history* (eds Fuchs, K., von Gehlen, K., Maelzer, H., Murawski, H. & Semmel, A.), pp. 139-150, Springer-Verlag, Berlin.
- Self, S., Thordarson, T., Keszthelyi, L., Walker, G.P.L., Hon, K., Murphy, M.T., Long, P. & Finnemore, S., 1996. A new model for the emplacement of Columbia River basalts as large, inflated pahoehoe lava flow fields. *Geophysical Research Letters*, **23**(19), 2,689-2,692.
- Self, S., Thordarson, T. & Keszthelyi, L., 1997. Emplacement of Continental Flood Basalt Lava Flows. In: *Large Igneous Provinces: Continental, Oceanic, and Planetary Flood Volcanism*. (eds Mahoney, J.J. & Coffin, M.), pp. 381-410, American Geophysical Union.
- Self, S., Keszthelyi, L. & Thordarson, T., 1998. The importance of pahoehoe. *Annual Review of Earth and Planetary Science*, **26**, 81-110.
- Stephenson, P.J., Burch-Johnston, A.T., Stanton, D. & Whitehead, P.W., 1998. Three long lava flows in north Queensland. *Journal of Geophysical Research*, **103**(B11), 27,359-27,370.
- Swanson, D.A., Wright, J.H. & Helz, R.T., 1975. Linear vent systems and estimated rates of magma production and eruption of the Yakima basalt on the Columbia Plateau. *American Journal of Science*, **275**, 877-905.
- Swanson, D.A., Wright, T.L., Hooper, P.R. & Bentley, R.D., 1979. Revisions in stratigraphic nomenclature of the Columbia River Basalt Group. *U.S. Geological Survey Bulletin*, **1457-G**, 59.
- Tanaka, K.L., Shoemaker, E.M., Ulrich, G.E. & Wolfe, E.W., 1986. Migration of volcanism in the San Francisco volcanic field, Arizona. *Geological Society of America Bulletin*, **97**, 129-141.
- Thordarson, T. & Self, S., 1998. The Roza Member, Columbia River Basalt Group: A gigantic pahoehoe lava flow field formed by endogenous processes? *Journal of Geophysical Research*, **103**(B11), 27,411-27,445.
- Vogel, D.C. & Keays, R.R., 1997. The petrogenesis and platinum-group element geochemistry of the Newer Volcanic Province, Victoria, Australia. *Chemical Geology*, **136**, 181-204.
- Walker, G.P.L., 1989. Spongy pahoehoe in Hawaii: a study of vesicle-distribution patterns in basalt and their significance. *Bulletin of Volcanology*, **53**, 546-558.

- Walker, G.P.L., 1993. Basaltic-volcano systems. In: *Magmatic Processes and Plate Tectonics* (eds Prichard, H.M., Alabaster, T., Harris, N.B.W. & Neary, C.R.), pp. 3-38, Geological Society of America.
- Wells, R.E., Simpson, R.W., Bentley, R.D., Beeson, M.H., Mangan, M.T. & Wright, T.L., 1989. Correlation of Miocene flows of the Columbia River Basalt Group from the central Columbia River Plateau to the coast of Oregon and Washington. *Geological Society of America Special Paper 239*, 113-129.
- White, A.J.R., 1995. *Igneous rocks simplified*. Unpub. book, Melbourne University, Melbourne, 250 p.
- White, M.E., 1994. *After the Greening- the Browning of Australia*. Kangaroo Press, Kenthurst, NSW, 288 p.
- Williams, H. & McBirney, A.R., 1979. *Volcanology*. Freeman Cooper, San Francisco, 397 p.
- Wilmoth, R.A. & Walker, G.P.L., 1993. P-type and S-type pahoehoe: a study of vesicle distribution patterns in Hawaiian lava flows. *Journal of Volcanology and Geothermal Research*, **55**, 129-142.

CHAPTER 5

THE PALAEOVOLCANOLOGY AND EVOLUTION OF THE LATE CENOZOIC, INTRA-PLATE BASALTIC WERRIBEE PLAINS, NEWER VOLCANIC PROVINCE, VICTORIA

5.1 INTRODUCTION

This chapter ties together much of the work of the previous chapters, in order to investigate the overall evolution of the Werribee Plains. The eruption centres are better characterised and eruption processes discussed. Combining this with the study of basaltic lava emplacement processes (Chapter 2) and stratigraphic work (Chapter 4), the main characteristics of the eruptions, repose periods, and general evolution of this lava flow-field are discussed. Issues such as controls on the vent distribution in the Werribee Plains, and the likelihood of further volcanic activity are investigated. The degree to which volcanism in the Werribee Plains is representative of the entire Newer Volcanic Province (NVP) is explored. And finally, the results of this study are used to better characterise plains-basalt volcanism, by comparing the NVP with other plains-basalt provinces. Major differences between plains-basalt provinces and other intra-plate continental basaltic fields (flood-basalt provinces and scoria-dominated fields) are highlighted, and the different tectonic settings in which they are produced are discussed.

5.2 ERUPTION PROCESSES

5.2.1 Features of the eruption centres, and their distribution in the Werribee Plains

A variety of basaltic volcanic landforms exist, including scoria cones, lava shields, lava cones, spatter cones, maars, tuff rings and lava fields, the final form depending on the dominant eruption style. Eruption centres in the Werribee Plains lava flow-field are low (lava) shields and scoria cones, and sometimes spatter cones are associated with them (Fig. 5.1, Table 5.1). By definition, low shields have slopes of $\sim 0.5^\circ$ and are typically ~ 15 km in diameter (eg. Greeley 1982a, Fig. 5.2). These are distinguished from large lava shields such as those which occur in Hawaii and Iceland, primarily based upon their smaller sizes (Hawaiian shields are up to ~ 100 km diameter), but also on their lower profiles (other shields have slopes up to 10° (Cas & Wright 1987)). The low shields presently exposed in the Werribee Plains range in maximum dimension from 1.5-12.5 km (Table 4.1, Chapter 4). In contrast to lava shields, the

Table 5.1 Characteristics of the eruption centres of the Werribee Plains. See Table 4.1 (Chapter 4) for eruption centre dimensions, calculated slopes and grid references.

Eruption centre	Morphology	Crater features	Evidence of eruptive fissure system	Preserved products, inferred extent of lava flows, and other features
<i>The Anakies</i>	Three scoria cones: West, Middle and East (Fig. 5.3)	W: a moderately deep depression is preserved at the summit. The crater rim appears to be breached in the W. M: not preserved E: not preserved	Three volcanoes aligned NW-SE along the Lovely Banks Monocline; 3.5 km apart. Considered to be too far apart to have been erupted from a single eruptive fissure (section 5.2.1).	Scoria is the dominant product exposed at these centres (eg. Fig. 5.3). A large lava tube/elongate tumulus extends southward from the E cone, and is inferred to have fed lavas to the S. Each centre is inferred to have fed significant lava flows predominantly to the S (Fig. 5.1).
<i>Mt Atkinson</i>	Low-angle lava shield	No crater preserved	Summit of volcano is a flat, ~E-W trending ridge, inferred to reflect the trend of the original eruptive fissure.	Products include variably welded spatter and clastogenic lavas near summit, and transitional lava flows. Lava flows were fed in all directions to form the shield, and extend further south beyond base of shield (Figs. 5.1 & 5.5).
<i>Bald Hill</i>	Lava shield	Crater does not appear to have been preserved	Apparently symmetrical: no evidence of fissure system	Unable to have access to the summit, and therefore no products observed. Lavas are inferred to have flowed in all directions, and probably not far beyond the shield.
<i>Black Hill</i>	Low shield	No crater preserved	Little outcrop, no clear trend identified	Limited welded spatter preserved at summit. Lava flows fed in all directions, but most have subsequently been buried by the products of Mt. Cottrell.
<i>Mt Cottrell</i>	Flat-topped, immature lava shield	Crater is preserved as a small topographic depression; walls breached in the north-west (Fig. 5.2b).	~Symmetrical: no evidence of fissure system	Welded spatter is preserved in beds dipping in towards the centre of the crater (Fig. 5.2b). The slope beneath the breached portion of crater lacks outcrop, is smooth and convex upward compared with the other slopes. Lava is considered to have been fed through here, building up the shield to the north, and also flowing to the south, beyond the limit of the shield. Inflated P-type pahoehoe flows are the dominant product (Chapter 4).
<i>Greek Hill</i>	Scoria cone	No depression, but crater outline is preserved by the trend of welded spatter beds (dipping in towards centre of crater). Crater rim breached in north-west.	The crater and overall volcano outline are slightly elongate NW-SE: perhaps reflecting trend of original fissure?	Limited scoria exposed; predominantly welded spatter at summit. E side of volcano is topographically raised cf. the W (due to lavas burying/breaking through built-up spatter in W). Limited lavas inferred to have initially been fed to north-west, and then diverted south (down-slope).

<i>Green Hill</i>	Broad, flat-topped lava shield	Significant arcuate, topographic depression preserved. Crater rim breached in the south-east.	No evidence of eruptive fissure system	Limited welded spatter preserved at summit. Lavas predominantly fed towards the south-east.
<i>Mt Kororoit</i>	Scoria cone and associated spatter cones and ramparts	Small topographic depression preserved, and outline also defined by welded spatter beds. Crater wall breached in the south-east.	Spatter ramparts and spatter cones occur to the north-east and south-east (respectively) of Mt. Kororoit. Inferred to have been fed by ~N-S trending eruptive fissure system (Fig. 5.4a).	Scoria and variably welded spatter are preserved at the summit and on the volcano's flanks. The south-east slope is smooth, convex, contains little outcrop and lava is considered to have been fed out of the breached crater to the south-east. Lava generally flowed to the S, and aa flows considered to have been fed from Kororoit are preserved beneath the products of Mt. Cottrell.
<i>One Tree Hill</i>	Low shield	Little outcrop: no evidence of crater	No trend identified	A significant volume of lava is considered to have been fed to the south and south-east of One Tree Hill, beyond the base of the low profile shield.
<i>Ryan's Hill</i>	Scoria cone	No crater preserved	Apparently symmetrical: no evidence of fissure system	Welded spatter and clastogenic lavas preserved at summit. Lavas inferred to have been fed to south, but extent uncertain (same composition as Stony Hill lavas).
<i>Spring Hill</i>	Low shield	No summit crater preserved	Summit consists of ENE-WSW trending ridge, considered to reflect trend of original eruptive fissure. The majority of welded spatter on the northern flank is oriented ENE-WSW also.	Welded spatter is preserved at the summit and scoria from this centre is preserved in two diamond drill holes (BM22 & MB31). The volcano fed inflated P-type pahoehoe flows in all directions, producing a broad shield. Other small eruption centres are associated with Spring Hill: poor outcrop, but appear to be more low shields.
<i>Stony Hill</i>	Low shield	Crater does not appear to have been preserved	Apparently symmetrical: no evidence of fissure system	A significant volume of lava is considered to have been fed to the south-east, extending well beyond the base of the shield.

flanks of scoria cones are initially ~30° (angle of repose (Wood 1980)), although this angle is commonly modified due to subsequent weathering and erosion. The scoria cones preserved in the Werribee Plains presently have slopes of less than 10°, and the mean scoria cone diameter is 1.2 km.

Outcrop is preserved to different extents at the various eruption centres, and generally consists of variably welded spatter and clastogenic lavas. The primary flattening plane of the

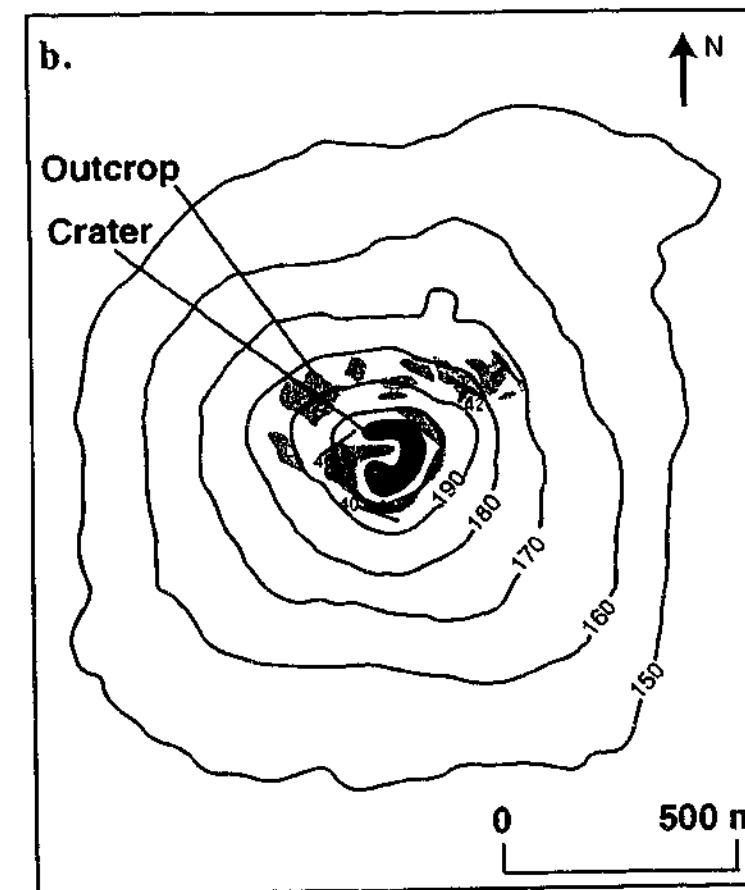
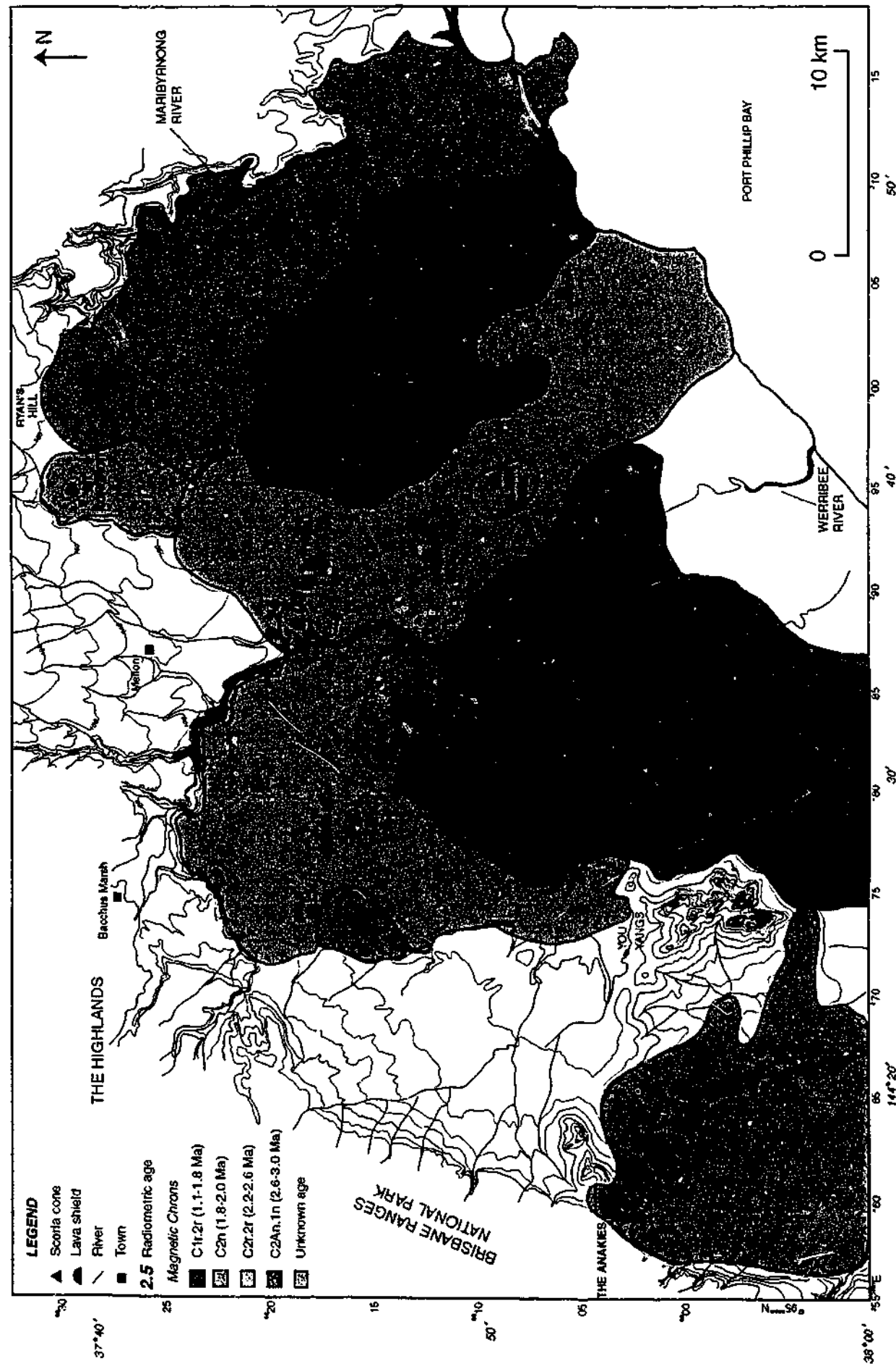


Fig. 5.2a. Photograph of Spring Hill, a low shield. Note the low angle of the flanks of the volcano, which is typical of the low shields in the Werribee Plains. b. Map of Mt. Cottrell, showing the distribution of outcrop at the summit. The low shield appears to have been built up by lava flows in all directions (it is symmetrical), and note the breached crater rim in the north-west. Strike and dip measurements are of welded spatter 'beds'.

Fig. 5.1 (Facing page) Geological map of the Werribee Plains showing the inferred extent of lava flows from each of the exposed scoria cones and lava shields, based upon work presented in Chapter 4. The products have been grouped into the magnetic Chrons (Cande & Kent 1995) in which eruptions are considered to have occurred, based upon the magnetostratigraphy.

welded spatter has been locally preserved, and these spatter beds have a measurable strike and dip. The spatter beds tend to dip in towards the centre of the crater (eg. Fig. 5.2b), due to agglutination of the spatter to the crater walls during low-level fire-fountaining. Even when outcrop is minimal and no topographic depression has been preserved, the outline of the crater may still be determined (eg. Greek Hill). Crater rims of both low shields and scoria cones are commonly breached (Table 5.1) and both types of volcanoes are considered to have fed lava flows (eg. Chapter 4, Figs. 5.1 & 5.5). Outcrop is exposed in the eastern cone of the Anakies due to scoria quarrying. The sequence is unremarkable, consisting of weakly stratified, moderately well sorted scoria clasts, with larger blocks and bombs sporadically distributed throughout (Fig. 5.3). No welded horizons or finer ash layers were observed. There is no evidence of pauses during this eruption, and it is difficult to comment on whether there were pauses in other eruptions in the Werribee Plains, due to lack of outcrop. The trends of eruptive fissure systems have been inferred at a number of centres due to (i) crater and/or volcano elongation (Wood 1980, Kuntz *et al.* 1992), or (ii) aligned spatter cones and ramparts (Table 5.1). In most cases however, it is considered that the lavas produced by the centres in addition to subsequent weathering and vegetation growth, have buried any evidence of the original fissure system. Aligned spatter cones and ramparts have only been observed in one instance, at Mt. Kororoit (Fig. 5.4). The fissure system is considered to have been linear, trending ~N-S. The spatter ramparts to the north-east of the scoria cone are ~3-5 m high, and contain evidence of being built up through fire-fountaining. The welded spatter clasts appear to have accumulated progressively, and are draped over each other (Fig. 5.4b).

A number of the eruption centres appear to be aligned at a larger scale. The Anakies, for example, lie on the NW-SE trending Lovely Banks Monocline (see Chapter 4), and other possible alignments include Greek Hill & Black Hill (NW-SE); Bald Hill, Spring Hill, Mt. Cottrell & Mt. Atkinson (~E-W); and Ryan's Hill & Stony Hill (~N-S); Fig. 5.1. Without using univariate and multivariate statistical methods to correctly identify the alignments (eg. Connor *et al.* 1992), these observations are largely subjective. Each of these alignments is not considered to represent a single eruptive fissure, but numerous discrete fissures that were produced because the ascending magmas exploited pre-existing structures (eg. Connor *et al.* 1992, Conway *et al.* 1997). The scoria cones of the Anakies are the most closely spaced volcanoes aligned, and they are up to 4 km apart. In the Eastern Snake River Plain where volcanoes are substantially larger than are observed here (section 5.5.2), eruptive fissure zones are generally less than 3 km long (Kuntz *et al.* 1992). Large basement structures studied

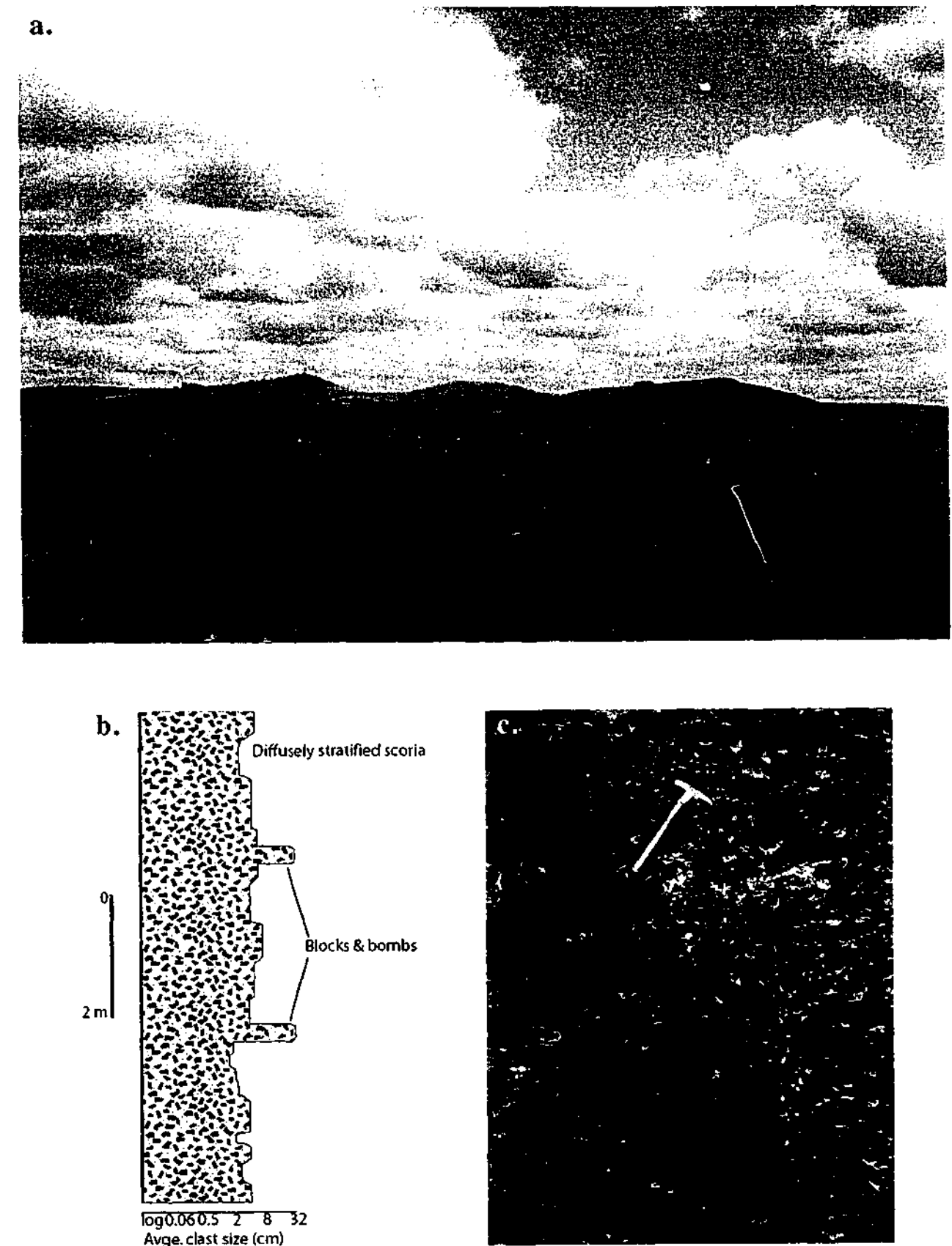


Fig. 5.3a. Photograph of the three scoria cones of the Anakies. Note the very different morphology of the scoria cones to the low shields (eg. Fig. 5.2a). b. Representative stratigraphic log of the scoria sequence exposed in the eastern flank of the easternmost cone. c. Note the relatively homogeneous nature of the scoria deposits, broken up only by few larger bombs and blocks.

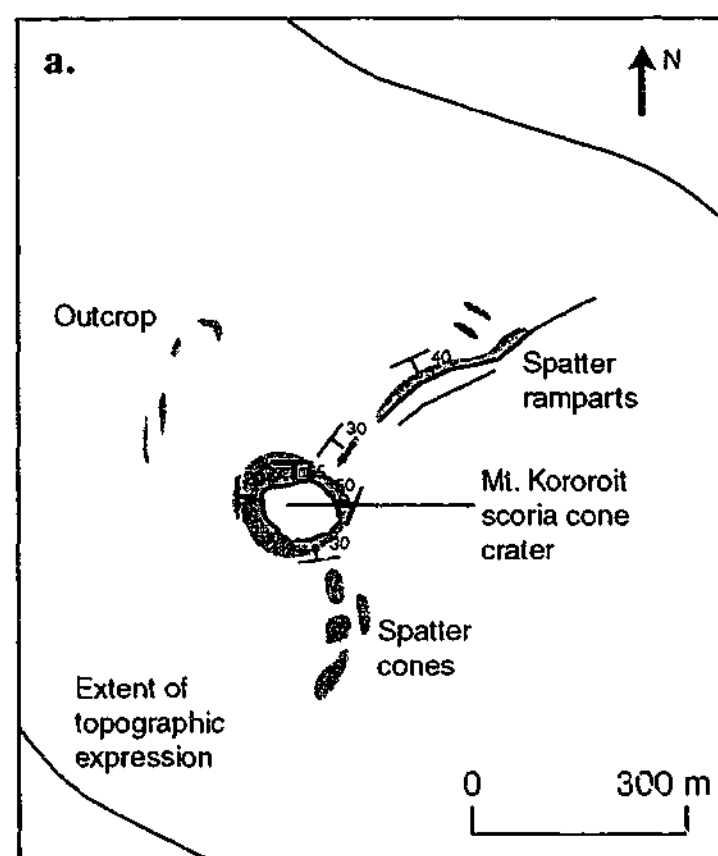


Fig. 5.4a. Aerial photograph interpretation of Mt. Kororoit. The spatter ramparts to the north of the Mt. Kororoit scoria cone are aligned with spatter cones to the south, suggesting the eruptive fissure system was ~N-S trending.
b. Photograph of the spatter ramparts at Mt. Kororoit, consisting of welded basaltic spatter draped on top of each other. Note the bag at the base of the outcrop for scale.

in other basaltic fields have hosted numerous volcanic events over periods of up to 1 Myr, sometimes the products of which are geochemically heterogeneous along the length of the structure (Conway *et al.* 1997). The parallel nature of the Lovely Banks Monocline with the alignment of Greek Hill & Black Hill (NW) suggest this is a local structural trend. Four volcanoes are aligned ~E-W, which is the general orientation of the entire Newer Volcanic Province, thought to reflect the influence of basement faults associated with rifting and the formation of the Otway Basin (Cas *et al.* 1993, Hill *et al.* 1995). The trend of fissure system orientation (Mt. Kororoit) and volcano alignment (Ryan's Hill & Stony Hill) in the north of the Werribee Plains, at the border of the Central Highlands sub-province of the NVP is ~N-S. This is considered to reflect the dominant N-S trend of the underlying Palaeozoic rocks of the Melbourne Zone of the Lachlan Fold Belt (Gray 1988).

5.2.2 Eruption styles and durations

The basaltic volcanic products of the Werribee Plains were produced through a combination of Strombolian and Hawaiian fire-fountaining eruptions, commonly followed by passive effusion of lava. Strombolian explosive activity is characterised by a series of closely spaced explosions, resulting in the ejection of vesicular, scoriaceous material forming cinder or scoria cones (Blackburn *et al.* 1976). Hawaiian fire-fountaining eruptions typically have high (tens to hundreds of metres) incandescent lava fountains (Parfitt 1998), out of which spatter clasts are ejected, falling with ballistic trajectories. Although many basaltic eruptions initiate with fire-fountaining, this commonly diminishes after several days, resulting in passive effusion of lava (Kuntz *et al.* 1992), sometimes producing lava shields. The main control on the type of basaltic eruption is the magma rise speed, and to a lesser extent the volatile content of the magma (Parfitt & Wilson 1995). Hawaiian fire-fountaining eruptions are produced at high magma rise speeds, in which little bubble coalescence occurs upon ascent, and instead the magma disrupts at a relatively deep level and high pressure (Parfitt & Wilson 1995). Subsequent rise of the disrupted gas-pyroclast mixture leads to considerable gas expansion, resulting in high eruption velocities producing high fountains. At low magma rise speeds bubble coalescence occurs upon ascent, and large bubbles are lost from the system. A pond of lava forms in the vent, and the bursting of the large bubbles at the surface of the pond gives rise to classic Strombolian activity; intermittent explosions and relatively low eruption column heights (Blackburn *et al.* 1976). At constant magma rise speeds, a reduction in gas content of the magma through time results in the transition from Strombolian to Hawaiian

style eruptions, and then to passive effusion of vesicular lava (Parfitt & Wilson 1995). This explains why spatter is commonly observed around the rims of scoria cone craters (Wood 1980), and why both scoria cones and low shields have been observed to have fed significant lava flows. All scoria cones observed in the Werribee Plains (except the Anakies) have evidence of welded spatter preserved at their summits, and all without exception are inferred to have fed lava flows (Table 5.1, Fig. 5.1). Similarly, spatter is preserved at most lava shields, and again all are considered to have subsequently fed lava flows.

Hawaiian fire-fountaining

The main stages of Hawaiian fissure-fed eruptions are listed based upon previous work in Hawaii (eg. Wentworth & Macdonald 1953, Swanson *et al.* 1979, Holcomb 1987, Peterson & Moore 1987, Wolfe *et al.* 1987, Parfitt & Wilson 1995, Parfitt 1998, Parfitt & Wilson 1999), which has largely been summarised by Kuntz *et al.* (1992). Although the rates of the volcanic processes may differ from other basaltic provinces, general features of the processes are considered to be universal. Hawaiian fissure-fed eruptions generally proceed through four distinct stages. (i) The ground cracks and there is local steam and fume activity. Fissuring is followed by lava fountains, which extend for several hundred metres, and erupt to heights of up to 500 m. Spatter ramparts typically form along both sides of erupting fissures, and fine tephra is deposited at distances up to 10 km downwind. Lava flows form by accumulation and welding of the hot pyroclasts, and cover areas less than 5 km². (ii) After several days the erupting fissure system diminishes in length, and lava fountains become localised along short segments of fissure. Spatter cones (or scoria cones if there is a reduction in magma rise speed) may form over the earlier ramparts. Diminished fountaining is typically followed by quiet, more voluminous outpouring of lava. Surface-fed pahoehoe or tube-fed flows are produced if eruption rates are fairly high. Small lava cones or shields may be produced during the latter parts of this stage. (iii) During long-lived eruptions lava fountaining diminishes and is followed by quiet, prolonged, voluminous outpouring of lava for periods of months to years, producing a large lava cone or shield volcano. Lava cone or shield summits commonly have a crater elongated parallel to the underlying feeder fissure. Lava flow-fields produced during this stage may extend beyond the limits of the lava shields they are fed from. (iv) Few volcanoes experience the fourth stage in the evolution of basaltic eruptions (eg. Mauna Loa, Mauna Kea). This stage results from eruptions that take place over thousands to millions of years from a central vent area and volcanic rift zones, producing a large, polygenetic shield

volcano.

The low shields of the Werribee Plains are considered to have been produced during stages (i)-(iii) of the sequence outlined above. Most eruptions producing the low shields are not considered to have been long-lived, but probably lasted a number of weeks to months, because of the relatively small size of both the shields and lava flows. In order to better estimate the duration of the eruptions, the emplacement times of the lava flows were investigated. Most of the lava shields in the Plains are considered to have fed inflated pahoehoe lavas (Chapter 4). In Hawaii an equation has been formulated that gives the time taken for a pahoehoe lava flow to inflate, based upon the preserved thickness of the crust (Hon *et al.* 1994).

$$C = 0.079 t^{0.5} \quad 5.1$$

where C is the crust thickness (m) and t is the time (hr). This equation has been applied to the Columbia River flood-basalt lavas, U.S.A., and errors of more than 25% in the estimated duration have been predicted (Self *et al.* 1997). This is despite significant differences in the amounts of rainfall in Hawaii and western U.S.A., and the thermal properties (heat capacity, diffusivity, latent heat of crystallisation) of the different lavas. Errors of ~25% are therefore predicted when calculating the eruption durations of the volcanoes of the Werribee Plains.

The upper vesicular zone (UVZ) of an inflated pahoehoe flow represents the extent of the upper crust (C) during active inflation of the lobe (Chapter 2). To estimate the duration of active inflation of a lobe, the UVZ thickness is used in equation 5.1. Once the lava supply is cut off from a lobe it ceases inflating, stagnates and solidifies. Within an eruption package consisting of multiple stacked inflated pahoehoe lobes, it is considered that inflation of the overlying lobes will only occur once the underlying lavas have stagnated (eg. Self *et al.* 1997). Therefore, ideally the most complete record of lobes produced by a volcano is analysed to estimate its eruption duration. The inflation times calculated for the successive lobes in the eruption package is summed. This gives a minimum estimate of the eruption duration, as it assumes that each of the overlying lobes were emplaced immediately after the lower lobes stopped inflating, and also the UVZ of the upper lobe may not be completely preserved. Mt. Cottrell is considered to have fed the uppermost eruption package preserved in diamond drill hole KOR15 (Chapter 4). This eruption package is ~20 m thick and consists of 3 inflated pahoehoe lobes. The sum of the inflation times calculated for these lobes is 357 days, therefore the eruption of Mt. Cottrell is considered to have lasted for a minimum of ~one year \pm 3

Table 5.2 Calculated durations of volcanic eruptions in the Werribee Plains, which produced inflated pahoehoe lobes, based upon diamond drill hole data. Calculations are based upon the known cooling rates of inflated pahoehoe lobes in Hawaii (Hon et al. 1994), using the preserved thickness of the upper crust (UVZ). The results are minimum estimates, to the nearest day (see text).

Eruption centre	Diamond drill hole	No. lobes in eruption package	Upper crust (UVZ) thickness (m)	Calculated inflation time for lobe (days)	Total time of eruption (days)
Spring Hill	BM22	1	7.7	396	396
?	BM22	1	4.0	107	107
Mt. Cottrell	DER7	1	3.2	66	66
?	DER7	1	1.0	7	7
?	DER7	4	2.7, 1.4, 0.9, 1.0	47, 13, 5, 7	72
?	DER7	1	2.1	29	29
?	DER7	1	3.1	64	64
?	KOR14	3	5.3, 1.9, 2.8	188, 24, 52	264
?	KOR14	2	4.1, 3.3	112, 73	185
Mt. Cottrell	KOR15	3	6.1, 3.8, 1.4	248, 96, 13	357
?	KOR15	5	1.4, 1.8, 2.6, 3.7, 1.8	13, 22, 45, 91, 22	193
?	KOR16	3	2.3, 5.0, 2.0	35, 167, 27	229
?	KOR16	1	3.8	94	94
?	PYW7	7	2, 3.2, 1.8, 0.8, 1.9, 1.5, 1.5	27, 68, 22, 4, 24, 15, 15	175
?	PYW7	1	3.0	60	60
?	PYW7	2	2.3, 0.4	35, 1	36
Mt. Cottrell	TAR12	1	5.6	209	209
Black Hill	TAR12	6	3.0, 1.0, 2.2, 1.0, 2.3, 0.6	60, 7, 32, 7, 35, 2	143
?	TAR12	1	5.8	225	225
Mt. Cottrell	TRU50	2	3.3, 4.0	73, 107	180
Ryan's Hill/ Stony Hill	TRU50	1	8.1	438	438
?	TRU50	2	6.1, 5.5	248, 202	450
Overall Average					181

months. Although the error seems quite substantial, it gives a general idea of the relatively short time frame of the eruption durations expected for these volcanoes. The eruption duration was calculated for each eruption package consisting of inflated pahoehoe lobes observed in drill core (Table 5.2). The average eruption duration of all the volcanoes producing inflated pahoehoe flows in the Werribee Plains was found to be ~6 months. For some reason in the Werribee Plains the magma supply stopped before centres had grown very large.

Strombolian explosive eruptions

Based upon data from 910 scoria cones from around the world, the median and mean basal diameters are 0.8 km and 0.9 km respectively (Wood 1980). These are similar dimensions to the cones observed in this study, and the processes involved in their formation are considered to be analogous. Cone growth can be divided into three phases: (i) the height increases rapidly, (ii) the height increases at a slower rate, and (iii) the cone height changes only slightly and lava extrusion dominates over pyroclastic activity (Wood 1980). Eruptions commence with the opening of fissures and weak venting of gases, followed within hours by intense eruptions of large amounts of juvenile pyroclastic material. The initial explosions are nearly continuous (1 explosion/1-2 sec) and cones reach near their final heights within a few days (ie. stage (i)), after which the explosion frequency and intensity decrease and lava flows are the main eruptive product. Fifty percent of observed cinder cone eruptions last less than 30 days, and 95% are over in one year or less (compared with the average shield volcano in the Werribee Plains, which was calculated to have erupted for ~6 months; Table 5.2). Generally, products accumulate around circular vents, but an eruption may occur along a fissure and not immediately become localised to a single vent, resulting in the construction of an elongate cone (eg. Greek Hill). Commonly the cones eject pyroclastic material beyond the cone itself, and sometimes the resultant distal mantling layer of fine scoria and ash is volumetrically much greater than the products making up the scoria cone. Two drill holes approximately 6 km from Spring Hill for example, have preserved scoria, inferred to have been from that eruption centre (BM22 & MB31, Chapter 4). This is the only evidence that Strombolian explosive activity occurred at Spring Hill. The eruption style is considered to have rapidly changed to Hawaiian fire-fountaining, preventing the construction of a scoria cone there. The total volume of lava flows is commonly greater than the volume of the cone as well (eg. the Anakies). Thus, although scoria cones are the most visible results of many eruptions, they commonly represent the least significant fraction of the entire ash and lava output of an eruption (Wood 1980).

5.3 EVOLUTION OF THE WERRIBEE PLAINS

5.3.1 Pre-existing palaeotopography and substrate geology

The Werribee Plains are contained within the Port Phillip Basin, a Tertiary depression bounded to the west and east by the Rowsley and Selwyn faults respectively (Chapter 1). A thick sedimentary sequence accumulated in the Port Phillip Basin during the Tertiary period, the uppermost unit being the continental Red Bluff Sands of the Brighton Group (Abele *et al.* 1988). The Red Bluff Sands are composed of clay, sand and gravel; they are occasionally cross-bedded and variably iron-stained. They contain fossil wood, other plant remains and freshwater sponge spicules, and the base of the unit is regarded as Pliocene in age (Abele *et al.* 1988). The pre-volcanic substrate in the vicinity of the Werribee Plains was relatively flat, gently sloping towards the south-east, however significantly more dissected than it is today by the drainage systems. Rivers from the topographically raised Palaeozoic highlands to the north and west were fed into a major tributary, which drained towards the south (Chapter 4). The area of interest was in the midst of a marine regression at the commencement of volcanism. The substrate onto which lavas, from some of the earliest eruptions, were emplaced was up to 50 m below sea level, and yet there is evidence of only minor interaction between the lavas and water. Airborne magnetic images show that lavas extended off-shore to the south, almost as far as the Bellarine Peninsula without any evidence of interaction with water (Chapter 4). The basalts of the Werribee Plains disconformably overlie the Moorabool Viaduct Formation (considered to be equivalent to the Brighton Group (Abele *et al.* 1988)), covering the onshore Port Phillip Basin between Melbourne and Geelong (Holdgate *et al.* 2002).

5.3.2 Commencement of volcanism

The marine regression that was taking place at the commencement of volcanism in the Werribee Plains is considered to have been eustatic in nature, at ~3.8 Ma (Haq *et al.* 1987). There is evidence that volcanism commenced relatively soon after the onset of the regression, as the substrate demonstrates an increase in 'wetness' beneath the volcanic products from north to south (Chapter 4). The products of the earliest eruption identified in the magnetostratigraphy are preserved in one drill hole (PYW7), located close to the centre of the Werribee Plains (eg. Fig. 4.1, Chapter 4). This eruption is considered to have occurred in the Gaussian Chron (probably between 3.11-3.22 Ma (Cande & Kent 1995), Chapter 4). Earlier eruptions may have occurred that were not intersected by the drill holes analysed, and there is no evidence why the first eruption might have occurred in this location. It has been

proposed that the volcanic activity producing the Newer Volcanic Province is just the most recent expression of basaltic volcanism, which has occurred intermittently in south-eastern Australia from the Late Cretaceous to Recent (Lister & Etheridge 1989, Price *et al.* 1997). The volcanism is considered to be related to the break-up of the Gondwana supercontinent (Chapter 1). Extension associated with the continental break-up is considered to have initiated thermal instability in the mantle, involving asthenospheric upwelling (probably a number of hotspots) which is thought to be responsible for the continuation of volcanism over the following tens of millions of years (Price *et al.* 1997).

5.3.3 Eruption styles and resultant products

Each eruption is considered to have commenced with the formation of an eruptive fissure system. Upon formation of an eruptive fissure, each eruption commenced with either Strombolian explosive activity or Hawaiian fire-fountaining, depending largely on the magma rise speed, and to a lesser extent on the volatile content of the magma (Parfitt & Wilson 1995). At constant magma rise speeds, a reduction in gas content of the magma through time results in the transition from Strombolian to Hawaiian style eruptions, to passive effusion of vesicular lava (Parfitt & Wilson 1995). This sequence of events is considered to have occurred at a number of the eruption centres in the Werribee Plains. Following the initial formation of a scoria cone, the summit craters are subsequently rimmed by welded spatter, and finally the lavas breach a crater wall and propagate away from the volcano (eg. Mt. Kororoit, Greek Hill, Ryan's Hill). The larger shield volcanoes are considered to have commenced eruptions with Hawaiian fire-fountaining, followed by a period of passive outpouring of lava. The duration of volcanic activity at the different centres varied from days (for the more short-lived, scoria cone producing eruptions) to several months. The average low shield is considered to have erupted for about 6 months. Volumetrically, basaltic lavas are the dominant products of the volcanic eruptions in the Werribee Plains (eg. Fig. 5.5).

5.3.4 Lava types and factors controlling these

Inflated pahoehoe lavas are the dominant lava facies produced by the eruption centres. These lavas thicken by inflation of a lobe beneath its chilled crust, on gentle slopes of less than 2°, (Hon *et al.* 1994, Cashman & Kauahikaua 1997). They have distinctive internal characteristics, and can be distinguished from flows that have formed by other mechanisms (Chapter 2). Eruption packages identified in drill core commonly consist of a series of stacked

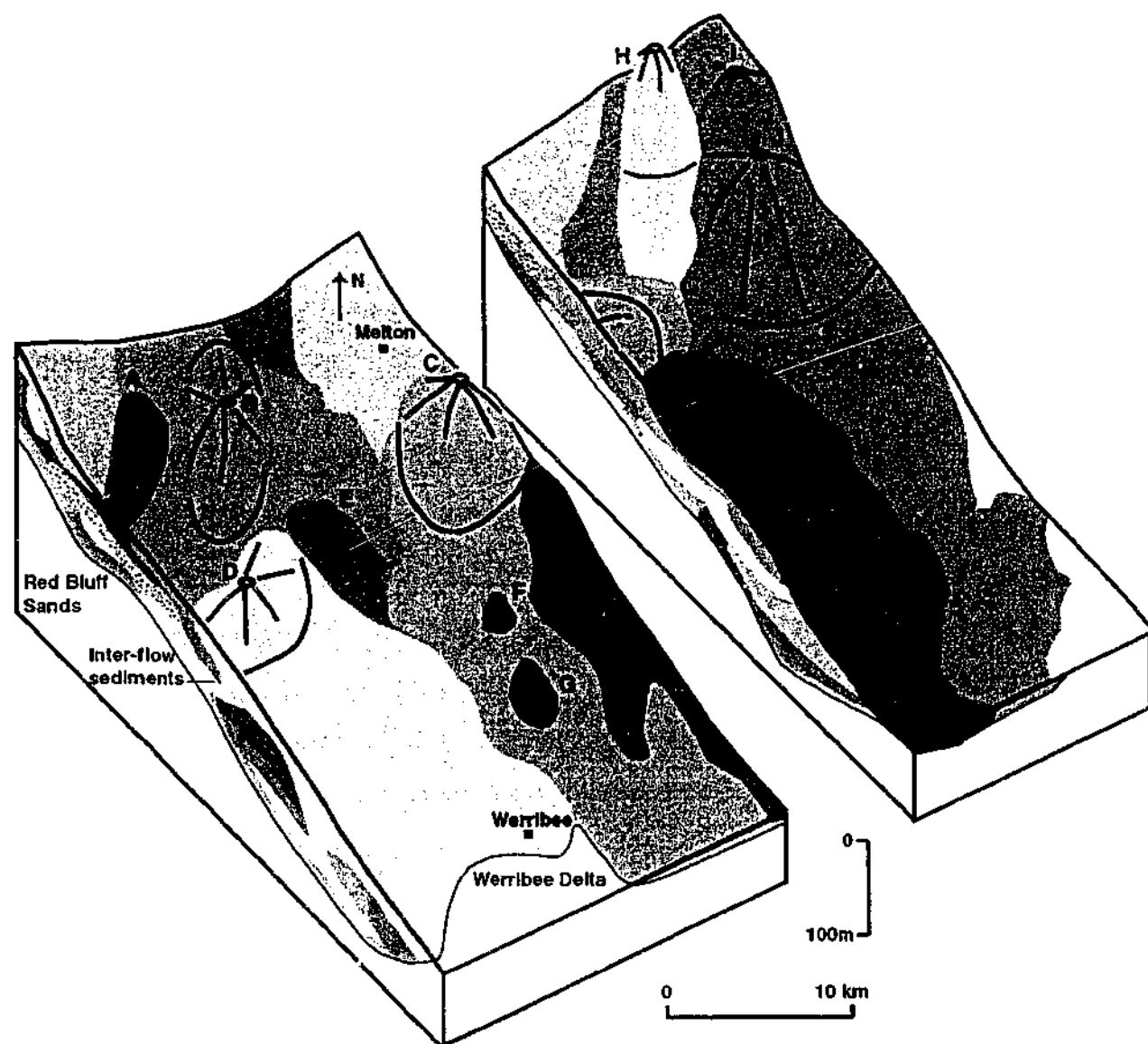


Fig. 5.5 Schematic split block diagram of the Werribee Plains lava-flow field. The extent of the products from each of the eruption centres (A- Bald Hill, B- Spring Hill, C- Mt. Cottrell, D- One Tree Hill, E- Green Hill, F- Greek Hill, G- Black Hill, H- Mt. Kororoit, I- Ryan's Hill, J- Stony Hill, K- Mt. Atkinson) is shown. Aa lavas are shown by a stippled pattern and pahoehoe lavas are plain. Lavas from eruption centres that are not exposed, or are not within the Plains are various shades of grey. Each colour represents a single eruption package- generally either a collection of pahoehoe lobes or a single aa flow. Note that inter-flow sediments only occur in the west of the field area, and the vertical scale is exaggerated.

inflated pahoehoe lobes, sometimes with S-type pahoehoe lobes in between, inferred to represent a smoothing out of the local topography. It is considered that inflated pahoehoe lavas were the dominant products due primarily to the flat nature of the substrate. These lavas are not considered to have travelled extensively laterally, either due to the shallow gradients, or the flow-fronts encountering some sort of topographic barrier (such as the products of an earlier eruption). Instead, break-outs of lava would have occurred from within earlier lobes closer to the source (eg. Hon *et al.* 1994), resulting in the building up of the lava fields

vertically. Ponding of lavas in topographic depressions was rarely observed in the sequence, however there is evidence of the lavas infilling irregularities and smoothing out the topography. In drill hole TAR12 for example, a ponded lava occurs directly above a thin sedimentary package (the lava is inferred to have ponded in a small valley), and directly overlying this is an inflated pahoehoe lobe from the same eruption.

The aa lavas identified within the sequence are all considered to represent a thickened, distal facies (due to the thickness of the flows and general lack of vesicles, Chapter 4). Aa lavas have not previously been recognised or documented in the NVP (Cas 1989a), none are exposed at the surface of the Werribee Plains, and of the 27 eruptions identified in the magnetostratigraphy, only four produced aa lavas. Although a number of factors may have contributed to aa flows being produced (eg. a higher degree of undercooling of the magma prior to eruption (Sato 1995), relatively steep terrain (Lipman & Banks 1987), a higher magma discharge rate (Rowland & Walker 1990), or a higher magmatic SiO_2 content (Kuntz *et al.* 1992)), it seems that the most important of these was the slope of the substrate. Indeed, it seems likely that the exceptional thicknesses of these flows are also a function of the slope, as they would have thickened upon reaching the flatter plains. The two southernmost drill holes are furthest from the Highlands sub-province, and these have no record of aa flows reaching there. Only one transitional lava type was observed in the sequence and it is not clear why. The composition of the lava is similar to other alkalic centres (eg. the adjacent Mt. Cottrell), and the terrain is not likely to have been substantially different to what it is today. Possibly the magma was significantly undercooled prior to eruption, as evidenced by higher crystallinity lavas, and/ or the eruption rate was initially higher than at the other centres.

5.3.5 Lava dimensions

The average thickness of the pahoehoe flow units (both S-type and P-type lobes) observed in drill core in this study is 4.7 m (see section 5.5.2 for comparison with lavas in other basaltic provinces). In outcrop they vary from lobate to more sheet-like morphologies, and individual inflated P-type lobes are up to 50-100 m wide. Aa flows were observed to be much thicker than pahoehoe lobes, ranging from 15.3-31.7 m thick, and averaging 22.5 m. No aa flows are exposed at the surface of the Werribee Plains. Eruption packages, commonly containing a number of lobes average ~10-20 m in thickness. It was difficult to constrain how the thicknesses of these packages vary with distance from the source, however they are clearly variable, as there is evidence of the lavas infilling and locally smoothing out the topography.

Lavas flowed up to ~25 km from individual eruption centres, however commonly the products of a given eruption were more localised, and were intersected by only one diamond drill hole (Chapter 4).

5.3.6 Controls on vent distribution, and is there evidence of migration of volcanism within the Werribee Plains?

The orientation of the eruptive fissure systems appear to be controlled to some extent by the orientation of pre-existing basement structures. In a number of instances volcanoes are aligned, even though they are considered to have erupted at different times. The Anakies for example are aligned along the NW-SE trending Lovely Banks Monocline. Large basement structures studied in other basaltic fields have hosted numerous volcanic events over periods of up to 1 Myr (Conway *et al.* 1997). Three dominant alignment trends were identified in the Werribee Plains: NW-SE (considered to be a local structural trend), E-W (considered to reflect structures associated with rifting and the break-up of Gondwana), and N-S (reflecting the underlying Palaeozoic structural trend in the north of the Plains).

The relative (and absolute) timing of eruptions of most of the exposed eruption centres in the Werribee Plains has been constrained (Chapter 4, Fig. 5.1). The eruption centres are considered to be monogenetic (i.e. erupted only once). The earliest eruption of an exposed centre occurred at Ryan's Hill/ Stony Hill in the far east of the Plains (2.5-2.6 Ma (McDougall *et al.* 1966)). The products of fifteen eruptions that occurred prior to the eruption of this centre are preserved in drill core in the magnetostratigraphy. These were all fed either by buried centres, or by volcanoes that are beyond the boundaries of the Werribee Plains (eg. in the Central Highlands sub-province, Fig. 5.5). It was not possible to identify the source volcanoes of these eruptions. For this reason it is difficult to comment on whether there has been a broad shift in magma generation within the Werribee Plains with time, such as has been identified in the San Francisco and Springerville intra-plate basaltic provinces (Tanaka *et al.* 1986, Crumpler *et al.* 1994). The surface geology really only gives a very limited perspective of the overall volcanic evolution of the Plains. Based upon what is known of the exposed centres, there is a general migration of volcanism to the west with time, from Ryan's Hill/ Stony Hill to Mt. Cottrell, Kororoit and Black Hill, to Spring Hill and finally to One Tree Hill (Fig. 5.1). The youngest eruption preserved however, is at Mt. Atkinson, which is situated in the east of the Werribee Plains. Further work is required to clarify this, however based upon the present results it appears that lava flow-fields were built up randomly throughout

the Plains, their positions constrained only by pre-existing basement structures.

5.3.7 Geochemistry and compositional trends through time

A fundamental finding of this study is that the lavas producing the Werribee Plains are the same composition as the eruption centres they were fed from (Chapter 4). It is not possible therefore, to distinguish geochemically between plains basalts and the basalts that form constructional features, as suggested, for example, by Price *et al.* (1988). It has previously been considered that the lava plains of the NVP are dominantly tholeiitic compared with the constructional features which are dominantly alkalic and generally younger than the plains lavas (Price *et al.* 1988). The scoria cones and shields exposed at the surface of the Werribee Plains were produced by both alkalic and tholeiitic magmas, and all eruption centres fed lavas of the same composition as the centre. More alkalic basalts have been identified than tholeiites in the sub-surface (disregarding the unique Group I tholeiites), and both lava types have been erupted in all major polarity intervals identified. No broad change in composition of the eruptions with time was identified, and instead the production of the different types of magma appears to be random throughout the sequence (Chapter 4). The alkalic and tholeiitic magmas of the NVP are considered to be genetically unrelated; they are produced either by different degrees of partial melting (eg. Frey *et al.* 1978), or are sourced from different regions of a chemically inhomogeneous mantle (Price *et al.* 1997). Based upon the results of this study, alkalic and tholeiitic magmas were generated randomly during the volcanism, rather than there being a broad shift towards alkalic magma generation with time, as previously thought. It is beyond the scope of this project to explore the petrogenesis of the basalts, however further work may involve exploring the significance of this random distribution.

5.3.8 Eruption frequency and the likelihood of further volcanic activity in the Werribee Plains

Based upon the age constraints identified and the assumption that all major reversals of the earth's magnetic field are recorded in the sequence, the 27 eruptions identified in the magnetostratigraphy occurred between ~3.2 and 1.41 Ma (Chapter 4). This gives an average eruption frequency of one eruption every 66,000 years in the Werribee Plains. This is considered to be a minimum estimate, as the magnetostratigraphy was established for a relatively small part of the Plains (constrained by the diamond drill hole distribution), and it is likely that many other eruptions occurred that have not been identified. Based upon time-segmented

analysis (Table 5.3), eruptions appear to have occurred less frequently with time in the Werribee Plains. In order to look at the progressive change in frequency with time, the eruption frequency was calculated for each magnetic polarity interval in which eruptions occurred. The frequency changed from one eruption approximately every 12 kyrs, to one every 46 kyrs, to one every 61 kyrs, and finally to one every 180 kyrs. It therefore appears that the repose time between eruptions has been gradually increasing, and possibly the rate of magma generation and supply decreasing. This observation needs to be treated cautiously however, as there were clearly other eruptions occurring simultaneously both in the Werribee Plains and in the rest of the NVP, and this is a limited data set. Based upon the calculated overall average eruption frequency in the Werribee Plains (one eruption every 66,000 years), and the timing of the most recent eruption (1.41 Ma), one would not expect further volcanic activity to occur in the Plains. Even when we take into account the apparent decrease in eruption frequency with time (Table 5.3), it does not seem likely that further activity will occur, as too long an interval has passed since the most recent eruption.

Table 5.3 The eruption frequency is calculated separately for each magnetic interval in which eruptions occurred in the Werribee Plains, based upon the established magnetostratigraphy (Chapter 4). The age ranges of some of the magnetic Chrons has been modified based upon known radiometric ages for the eruptions (McDougall et al. 1966, Aziz-Ur-Rahman & McDougall 1972, Price et al. 1997).

Magnetic Chron	Age (Ma)	No. of eruptions	Eruption frequency (1 eruption/ x kyrs)
C1r.2r	1.41-1.77	2	180
C2n	1.77-1.95	1	?
C2r.2r	2.15-2.58	7	61
C2An.1n	2.58-3.04	10	46
C2An.1r	3.04-3.11	6	12
C2An.2n	3.11-3.22	1	?

5.3.9 Sedimentation: provenance, distribution and influences

Within the basaltic sequence of the Werribee Plains there are few inter-flow sediments, and these are largely confined to the NW of the Plains. Sediment supply was predominantly from the topographically raised Palaeozoic highlands to the north and west of the field area. A N-S trending ridge which was present in the centre of the Werribee Plains prior to volcanism is considered to have prevented the sediments from being transported to the east of the Plains throughout the period of volcanic activity (Chapter 4). Basaltic input into the sediments was

extremely rare, and where it did occur it is inferred to have been transported soon after the eruption. These sediments contain scoria and small basalt lava fragments (from the spalling off of lava flows). Reworking and redeposition of this unconsolidated material would have occurred during heavy rainfall, and physical erosion of the lavas is not considered to have occurred to a great extent. The general lack of physical erosion can in part be attributed to the shallow gradient of the Werribee Plains, and also to the climate during volcanism, which was dry and arid in the late Tertiary period to early Quaternary (Bowler 1982). Shallow weathering profiles are typical of this period in south-eastern Australia. In contrast, the early Pliocene was humid, and deep pallid, kaolinitic weathering profiles were common (Joyce 1998). Chemical weathering of the basaltic lavas would have been the dominant process occurring in the repose periods between eruptions, and relatively large volumes of rock would have been removed in solution, in surface and groundwaters (eg. Cas 1989a).

5.4 THE WERRIBEE PLAINS: REPRESENTATIVE OF VOLCANISM IN THE NEWER VOLCANIC PROVINCE?

This study has focussed on a relatively small part of the Newer Volcanic Province (approximately 10% by area). In order to use the results of this study to make comparisons with other basaltic provinces, the degree to which the Werribee Plains are representative of volcanism in the entire NVP is investigated.

5.4.1 Eruption centres: types and dimensions

The dimensions of the eruption centres in the Werribee Plains (Chapter 4) are considered to be typical of the dimensions of scoria cones and lava shields throughout the NVP. The majority of volcanoes in the NVP are less than 300 ft (~100 m) above their bases (Ollier & Joyce 1964), the lava shields have exposed maximum dimensions of 4-5 km (Cas *et al.* 1993), and the scoria cones are from 1-1.5 km in diameter (Joyce 1988). It is therefore considered that the eruption processes would have been comparable, and durations of eruptions would have been of the same order of magnitude across the entire Province. The NVP has been sub-divided into three sub-provinces (Chapter 1), and the types and distribution of volcanic centres varies between (and within) these sub-provinces. This is largely due to the differences in substrate geology and topography. Phreatomagmatic centres (maar volcanoes and tuff rings) are largely confined to the southern half of the Western Plains sub-province and the Mt. Gambier sub-province. This is primarily due to the existence of aquifers in the

underlying Tertiary Otway Basin succession (Joyce 1975), and the Oligocene-Miocene Gambier Limestone (Cas *et al.* 1993) respectively. The Brighton Group of the Port Phillip Basin is the substrate onto which the Werribee Plains lavas were erupted. It consists of ferruginous clays and sands (Abele *et al.* 1988), and is not considered to host significant aquifers. Likewise the Palaeozoic basement rocks to the north (beneath the Central Highlands sub-province) are composed largely of granites and metasediments, and these are unlikely to host significant aquifers. Evidence of phreatomagmatic activity is therefore almost completely lacking in these places. The Central Highlands sub-province contains the highest density of preserved eruption centres (250 of the 400 identified centres in a relatively small area, (Joyce 1975)). About 75% of the exposed scoria cones of the NVP, and more than 80% of the lava shields are located in the Central Highlands sub-province (Nicholls & Joyce 1989). This sub-province occurs in a dissected upland region consisting largely of Palaeozoic meta-sediments and granites. The higher number density of eruption centres may be due to better preservation and exposure of the centres, as a result of lavas not subsequently burying them as occurs in the flatter, Western Plains sub-province. Alternatively the Central Highlands sub-province may have experienced more eruptions than elsewhere in the NVP due to a higher degree of magma generation beneath this zone. Further work, including magnetostratigraphic studies combined with additional radiometric dating, may help to clarify this point. The Mt. Gambier sub-province, dominated by scoria cones and maars, contains very few lava shields (Cas *et al.* 1993). The lack of lava shields reflects the smaller volumes of magma feeding these eruptions than elsewhere, although it is not known why this is the case. Further work could involve investigating whether this is a trend that has developed in the more recent eruptions (2 Ma-4.6 ka Mt. Gambier sub-province, Nicholls & Joyce 1989), compared with the earlier volcanic activity (such as in the Werribee Plains (~3.2-1.41 Ma), where many lava shields were generated).

5.4.2 Volcanic facies and thickness of basaltic succession

The range of volcanic facies produced at the eruption centres in the Werribee Plains, the lengths and thicknesses of the lava flows, and the total thickness of the basaltic sequence (average of 45 drill holes) are considered to be representative of the Western Plains sub-province. There is no evidence of phreatomagmatic volcanism in the Werribee Plains however, and this is common in the south of the sub-province. The distribution of volcanic products in the Central Highlands sub-province is considered to be different to that observed in the Werribee

Plains due to the difference in substrate (higher topographic relief, Palaeozoic basement). The production of aa lava flows is considered to generally be confined to this sub-province (section 5.3.4), and few inflated pahoehoe lavas would be expected due to the steeper slopes. Due to the irregular, hilly topography, many valley-confined flows have been documented (Cas *et al.* 1993), and the total thickness of the basaltic succession is difficult to estimate without more detailed studies (although it is likely to be less on average than the thickness of the Plains sub-province). The Mt. Gambier sub-province is considered to differ substantially to the Werribee Plains as relatively few lava flows have been identified (Cas *et al.* 1993); the eruptions experienced here were typically smaller volume than the eruptions in the Werribee Plains.

5.4.3 Eruption frequency

The eruption frequency calculated for the Werribee Plains is considered to be a minimum value for the entire NVP (one eruption every 66,000 years). A number of eruptions were occurring elsewhere in the province contemporaneously with the volcanism in the Werribee Plains (eg. Price *et al.* 1997), even as far west as Warrnambool. As a simple illustration of this, activity in the NVP proper commenced 4.6 Ma (Price *et al.* 1988). Over 400 volcanoes are known in the Province (Joyce 1975), suggesting that an eruption occurred on average every 11,500 years, and this does not take into account buried centres. The Werribee Plains may thus have an anomalously low eruption frequency relative to the entire NVP. Further work is required to determine how many other eruptions were occurring, the products of which are no longer exposed, and/or haven't been dated.

5.5 PLAINS-BASALT VOLCANISM EXPLORED

5.5.1 Flood-basalt provinces

The two main types of intra-plate continental basaltic provinces are monogenetic volcano fields and flood-basalt provinces (Chapter 1, (Walker 2000)). Eruptions in flood-basalt provinces occur primarily from fissure vent systems and lavas are emplaced on slopes of $\leq 0.1\%$. The lavas tend to drown any pre-existing topography, so forming a flat, plateau-like morphology, without any evidence of sites of eruption. Huge volumes of magma are generated in these systems, and individual flood-basalt provinces have estimated volumes of up to 1 million km³, and cover areas of up to 500,000 km² (eg. the Deccan flood-basalt province, India (Bondre *et al.* submitted)). Aa lavas have rarely been identified in these

provinces, and similarly the total pyroclastic content is very low (Self *et al.* 1997). Instead, flood-basalt provinces are dominated by sheet-like lavas with pahoehoe morphologies, which are considered to have formed by endogenous growth (eg. Self *et al.* 1996, 1997, 1998, Thordarson & Self 1998), much like Hawaiian pahoehoe lavas (Hon *et al.* 1994). The best known example of a flood-basalt province is the Columbia River Plateau basalt system, U.S.A. (Swanson *et al.* 1975, Camp *et al.* 1982, Hooper 1982, Reidel & Hooper 1989, Self *et al.* 1996). Other flood-basalt provinces, including the Deccan Volcanic Province, India (Subbarao & Sukheswala 1981, Beane *et al.* 1986, Khadri *et al.* 1988, Duraiswami *et al.* 2001, Bondre *et al.* submitted), the mid-Tertiary Ethiopian-Yemen plateaux (eg. Mohr 1983), and the Jurassic Karoo in South Africa (Bristow & Saggerson 1983) are less well known.

5.5.2 Monogenetic volcanic fields

Monogenetic volcanic fields contain a number of volcanic centres that erupt only once. The eruption centres are most commonly scoria cones and lava shields and may be clustered, or widely dispersed within a volcanic field (Connor & Conway 2000). The main characteristics of selected intra-plate monogenetic basaltic volcanic fields from around the world are summarised in Table 5.4. Monogenetic basaltic lava fields can be sub-divided into two groups. (1) The smaller provinces are dominated by scoria cones (eg. Auckland, Auvergne, Eifel, San Francisco, Springerville). These provinces have high eruption centre densities, and are made up of frequent, relatively short-lived, small volume (generally less than 0.1 km³ (Crumpler *et al.* 1994)) eruptions. (2) The ESRP and the Australian volcanic provinces are plains-basalt provinces, produced by a style of volcanism intermediate between continental flood-basalt volcanism and ocean island volcanism (Chapter 1). These provinces are significantly larger volumetrically than the scoria cone provinces, and contain many more lava shields and lava cones. The size and types of eruption centres produced in monogenetic basaltic fields is largely a function of the volume of magma supplied for each eruption. The plains-basalt fields are characterised by larger volume eruptions, allowing the construction of lava plains between the eruption centres. The eruption centres are preserved as topographic highs throughout the field.

Table 5.4 (Facing page) A comparison of some of the main features of selected intra-plate, continental basaltic lava fields from around the world, based upon previous work (Böhnel *et al.* 1982, Greeley 1982a, b, Böhnel *et al.* 1987, Joyce 1988, Smith 1989, Stephenson 1989, Kuntz *et al.* 1992, Crumpler *et al.* 1994, de Góer *et al.* 1994, Condit & Connor 1996, Conway *et al.* 1997, Stephenson *et al.* 1998), and work from this study.

Basaltic Province	Total basalt areal extent and thickness	No. eruption centres	Eruption centre dimensions, morphologies & relative proportions	Facies distribution (effusive, pyroclastic)	Period of main volcanic activity, and eruption frequency
Newer Volcanic Province, Victoria, Australia	15,000 km ² , av. thickness <60 m	~400	~50% scoria cones- av. 1.3 km ² , 55 m high; ~40% low shields- av. 12 km ² , 65 m high; ~10% maars & tuff rings- av. 1-2 km diameter	Predominantly effusive (>95% by volume of drill core logged consisted of lava flows).	4.6 Ma-4.5 ka, min. freq.: 1/11,500 yrs
Northern Queensland Cenozoic basaltic province, Australia	~23,000 km ² , av. thickness 30 m	>300	Low angle lava cones- eg. 0.16 km ² , 40 m high, shield volcanoes, scoria cones and few maars	"very limited pyroclastic activity" (Stephenson <i>et al.</i> 1998)	Main activity: 44 Ma-Holocene, but individual lava fields span <10 Myr. Up to 1 Myr dormancy between eruptions
Auckland intra-plate volcanic province, New Zealand	~350 km ²	>130	Mostly scoria cones and tuff rings, and few lava cones	In Auckland City lava field >70% of eruptive centres are predominantly phreatomagmatic.	1,56 Ma-1200 A.D.
Chaîne des Puys, Auvergne, France	~120 km ²	~75	Mostly scoria cones- av. 100-200 m high, 1.5 km diameter; maars- 100 m-1 km diameter; trachyandesitic complexes	Predominantly pyroclastic: lavas generated by the volcanoes not extensive enough to form a lava flow-field.	70-6 ka
Eifel, Germany West	600 km ²	240	~70% scoria cones (half fed lava flows); 30% maars & tuff rings	Pyroclastic products dominant	Main activity: 0.7-0.01 Ma
East		70			0.7 Ma-present
San Francisco field, Arizona, U.S.A.	4,800 km ² , av. thickness 100 m	>600	600 cinder cones commonly feeding lava flows; 8 major silicic centres	Lavas dominant by volume	~6 Ma-1,065 A.D.
Springerville volcanic field, Arizona, U.S.A.	3,000 km ² , av. thickness >90 m; up to 300 m thick where vent density is highest	>400	Mostly cinder cones- up to several hundred metres relief, av. 1.0 km diameter; 2 shield volcanoes; 5 maars; 4 fissure vents; several spatter mounds	Mostly lava flows: pyroclastic material ~10% of total volume	Main activity 2.1-0.3 Ma; freq.: 1/3,000 yrs
Eastern Snake River Plain (ESRP), Idaho, U.S.A.	20,000 km ² , av. thickness 1-2 km	~8,000 lava shields	Lava shields- av. 100-400 km ² ; lava cones- 1-50 km ² , 10-30 m high; scoria cones- 1 km ² , 100 m high; and tuff cones	90% volume of products: pahoehoe flows from lava shields. Aa flows, fissure-type eruptions and scoria cones: minor	Volcanism commenced 10 Ma; freq: 1/1,000 yrs >95% of surface contains products < 730 ka

General features of plains-basalt lava fields

Significant differences exist between the plains-basalt lava fields identified in Table 5.4 (the Australian provinces and the Eastern Snake River Plain, ESRP), in terms of the types and sizes of eruption centres, the overall volume of products in the different provinces, and the frequency of eruptions. These differences are considered to be related to the different tectonic settings of the provinces, and the resultant magmatic processes operating (section 5.5.3). Importantly, each of these lava fields are characterised by numerous monogenetic, point-source eruption centres which have fed significant lava flows. The lava flows have progressively built up lava plains between the eruption centres, and similarities exist between the different provinces in terms of the distribution and dimensions of the lava facies.

In the ESRP and the NVP pahoehoe lavas are the dominant lava facies produced. They constitute 90% of the volume of products in the ESRP (Kuntz *et al.* 1992), and approximately 70% of all flow units logged in drill core from the Werribee Plains. The average combined thickness of S-type and P-type pahoehoe flow units in the NVP is ~4.5 m. Flow units from the ESRP are a similar thickness (average 1-5 m (Greeley 1982a)), and eruption packages in the two provinces range from ~20 m to more than 35 m in thickness. Lava flows of shield volcanoes in the ESRP extend up to 30 km from their vents (Kuntz *et al.* 1992), and this order of magnitude has also been observed in the Werribee Plains (Chapter 4). These pahoehoe lobe dimensions are thicker on average than pahoehoe lobes in Hawaii, and thinner than pahoehoe lobes from the Columbia River Flood Basalt Province. In Hawaii pahoehoe flow units range from 0.1-5 m thick, averaging 0.5 m (Wilmoth & Walker 1993). The main reason for the significant difference in the average thickness of the pahoehoe lobes in Hawaii and the plains-basalt provinces is considered to be the slope of the substrate. The slopes of the Hawaiian volcanoes are relatively steep, compared with the flat plains in the continental provinces studied. Thus in Hawaii inflation of the lobes is restricted to the coastal plains, and on average thinner lobes are produced. In addition, there may have been a bias in data collection in Hawaii to include mainly the thinner flows that are presently exposed. In contrast, pahoehoe flows from the Columbia River Flood Basalt Province are commonly 10-100 m thick (Thordarson & Self 1998). The Roza Member is a single eruption package and ranges in thickness from 11.5-67 m, averaging 36 m. Individual lobes are 0.4-52 m thick, and average 16.7 m (Thordarson & Self 1998). The thickness of these lobes are a reflection of the total volume of magma generated and erupted, and this eruption alone covered an area of 40,300 km² (almost three times the area of the NVP).

Aa flows are less common in plains-basalt provinces. Aa flows observed in the NVP range from 15.3-31.7 m thick, and average 22.5 m. They are slightly thinner in the ESRP, where they are commonly 5-15 m thick, although up to 50 m where ponded (Kuntz *et al.* 1992). This may be due to the inferred sampling bias in the NVP, as only the thick, distal facies is considered to have been observed in the Werribee Plains (section 5.4.2). Aa flows in the ESRP may be several kilometres wide, and several tens of kilometres long. Again it is considered that thicker flows on average are produced in continental plains-basalt provinces than in other basaltic fields due to the relatively flat topography. In Hawaii, the average aa flow thickness is 6 m, and the maximum thickness is 24 m, based upon results of the Hawaiian Scientific Drilling Program (Cashman *et al.* 1996). At Mt. Etna the thicknesses of historic aa flows range from 1.5-22 m, and most are 8-11 m (Kilburn 1988). In a number of aa-producing eruptions, it has been observed that as the slope of the substrate flattens out away from the vent, the more distal facies is able to thicken and spread laterally, and commonly it is significantly thicker than the proximal facies (eg. Guest *et al.* 1987, Lipman & Banks 1987, Rowland & Walker 1988, Walker 1993). The distal facies in these instances is commonly greater than 10 m thick. In plains-basalt provinces where the vents may be closer to the surrounding plains, a facies that has similar characteristics to the distal facies in Hawaii or at Mt. Etna may be more abundant, and in fact may be more characteristic of aa flows in these provinces. Aa lavas have rarely been identified in continental flood-basalt provinces (Self *et al.* 1997). This may be due to the lack of elevated topography in the vent region, which is considered to contribute to the formation of aa lavas rather than pahoehoe, by resulting in higher volumetric flow rates of the lavas (Rowland & Walker 1990).

5.5.3 Tectonic settings and stress regimes in intra-plate continental basaltic provinces

Intra-plate continental volcanism is found in three main tectonic settings (Cas 1989b). (1) Rifting or newly rifted continents. Examples include the East African Rift system (eg. Mohr 1983), the Deccan Traps (Subbarao & Sukheswala 1981), and Karoo volcanism (Bristow & Saggerson 1983). Volcanism in this tectonic setting takes place under the influence of an extensional lithospheric stress field. There are two distinct types of volcanism associated with this tectonic setting. First, flood-basalt volcanism affects areas marginal to and beyond the rift. Second, where a narrow rift is well developed such as in East Africa, bimodal volcanism occurs within the rift valley.

(2) Basin-and-range provinces. The type example in the western United States is inland from, and closely associated with an active plate margin, the major transcurrent-transform San Andreas fault system (Cas 1989b). Different hypotheses for the origin of the extension and volcanism associated with the Basin and Range province include the transtensional effects of the San Andreas fault system, the effects of a subducted segment of the East Pacific spreading ridge underneath the North American continent, and continental backarc spreading (eg. Eaton 1982). Volcanism associated with the Basin and Range province includes flood-basalt volcanism (the Columbia River Plateau), plains-basalt volcanism (the Snake River Plain), scoria cone-dominated fields (the Springerville and San Francisco fields) and central-volcano type volcanism. Each of these volcanic province types are considered to have been produced as a result of regional extensional strain, which causes elevation of mantle isotherms, with adiabatic upwelling and melting of the mantle (eg. Fitton *et al.* 1988). The Northland and Auckland volcanic provinces in New Zealand are in an area of possible extension around and behind the present arc system of the North Island (eg. Walcott 1984). There may be some similarities with the setting of basin-and-range related volcanism, including the fact that the arc system to the east of the Northland-Auckland province is within the influence of the transcurrent-transform plate margin of the Alpine Fault (Cas 1989b). However, the scale of volcanism is greatly different, and basin-and-range style horst-and-graben topography is absent.

(3) Intra-plate continental volcanism well away from the influence of active plate margins. Two types of volcanism can be recognised in this category. First are the lines of volcanoes believed to be related to the passage of lithosphere over some form of mantle hotspot or hotline (eg. central-volcano magmatism in eastern Australia (Wellman & McDougall 1974), Chapter 1). Second is the volcanism that develops on the uplifted flanks of some rifted continental margins after periods of rifting and sea-floor spreading. The Newer Volcanic Province and other dominantly mafic, lava-field type volcanic provinces in eastern Australia are considered to be related to post-rifting uplift (Cas 1989b, Chapter 1). The rise of magma through the crust is facilitated most readily by the existence of an extensional stress field in the lithosphere (Shaw 1980). Rifting associated with the break-up of Gondwana commenced in the early Cretaceous (Müller *et al.* 2000), however since around 10 Ma (Sutherland 1998) the stress field in south-eastern Australia has been compressional (Denham *et al.* 1979). It is, as yet, unresolved how the NVP could form entirely within a compressional stress regime, and this is a recommended area for further work.

REFERENCES

- Abele, C., Gloc, C.S., Hocking, J.B., Holdgate, G., Kenley, P.R., Lawrence, C.R., Ripper, D., Threlfall, W.F. & Bolger, P.F., 1988. Tertiary. In: *Geology of Victoria* (eds Douglas, J.G. & Ferguson, J.A.), pp. 251-350, Victorian Division, Geological Society of Australia Incorporated, Melbourne.
- Aziz-Ur-Rahman & McDougall, I., 1972. Potassium-Argon ages on the Newer Volcanics of Victoria. *Royal Society of Victoria Proceedings*, **85**, 61-69.
- Beane, J.E., Turner, C.A., Hooper, P.R., Subbarao, K.V. & Walsh, J.N., 1986. Stratigraphy, composition and form of the Deccan Basalts, Western Ghats, India. *Bulletin of Volcanology*, **48**, 61-83.
- Blackburn, E.A., Wilson, L. & Sparks, R.S.J., 1976. Mechanisms and dynamics of strombolian activity. *Journal of the Geological Society of London*, **132**, 429-440.
- Böhnel, H., Kohnen, H., Negendank, J. & Schmincke, H.-U., 1982. Paleomagnetism of Quaternary volcanics of the East-Eifel, Germany. *Journal of Geophysics*, **51**, 29-37.
- Böhnel, H., Reisman, N., Jäger, G., Haverkamp, U., Negendank, J.F.W. & Schmincke, H.-U., 1987. Paleomagnetic investigation of Quaternary West Eifel volcanics (Germany): indication for increased volcanic activity during geomagnetic excursion/event? *Journal of Geophysics*, **62**, 50-61.
- Bondre, N.R., Duraiswami, R. & Dole, G., submitted. Morphology and emplacement of flows from the western Deccan Volcanic Province, India. *Bulletin of Volcanology*.
- Bowler, J.M., 1982. Aridity in the late Tertiary and Quaternary of Australia. In: *Evolution of the Flora and Fauna of Arid Australia* (eds Barker, W.R. & Greenslade, P.J.M.), pp. 35-45, Peacock Publications, Frewville.
- Bristow, J.W. & Saggerson, E.P., 1983. A review of Karoo vulcanicity in southern Africa. *Bulletin of Volcanology*, **46**, 135-159.
- Camp, V.E., Hooper, P.R., Swanson, D.A. & Wright, T.L., 1982. Columbia River basalt in Idaho: physical and chemical characteristics, flow distribution, and tectonic implications. In: *Cenozoic geology of Idaho* (eds Bonnischen, B. & Breckenridge, R.M.), pp. 55-75, Idaho Bureau of Mines and Geology, Idaho.
- Cande, S.C. & Kent, D.V., 1995. Revised calibration of the geomagnetic polarity timescale for the Late Cretaceous and Cenozoic. *Journal of Geophysical Research*, **100**, 6,093-6,095.
- Cas, R.A.F., 1989a. Physical Volcanology. In: *Intraplate Volcanism in eastern Australia and New Zealand* (eds Johnson, R.W., Knutson, J. & Taylor, S.R.), pp. 55-87, Cambridge University Press, Cambridge.
- Cas, R.A.F., 1989b. Regional Influences on Magma Emplacement. In: *Intraplate volcanism in eastern Australia and New Zealand* (eds Johnson, R.W., Knutson, J. & Taylor, S.R.), pp. 40-42, Cambridge University Press, Cambridge.

- Cas, R.A.F. & Wright, J.V., 1987. *Volcanic Successions: Modern and Ancient*. Allen and Unwin, London.
- Cas, R., Simpson, C. & Sato, H., 1993. Excursion Guide: Newer Volcanic Province- processes and products of phreatomagmatic activity. In: *General Assembly IAVCEI*, Australian Geological Survey Organisation, Canberra, Australia, 94 p.
- Cashman, K.V. & Kauahikaua, J.P., 1997. Reevaluation of vesicle distributions in basaltic lava flows. *Geology*, **25**(5), 419-422.
- Cashman, K.V., Katz, M.G. & Ho, A., 1996. Flow textures in LIPs - A Key to Flow Emplacement? *Eos*, **77**(46), F846.
- Condit, C.D. & Connor, C.B., 1996. Recurrence rates of volcanism in basaltic volcanic fields: An example from the Springerville volcanic field, Arizona. *Geological Society of America Bulletin*, **108**, 1225-1241.
- Connor, C.B., Condit, C.D., Crumpler, L.S. & Aubele, J.C., 1992. Evidence of Regional Structural Controls on Vent Distribution: Springerville Volcanic Field, Arizona. *Journal of Geophysical Research*, **97**(B9), 12,349-12,359.
- Connor, C.B. & Conway, F.M., 2000. Basaltic volcanic fields. In: *Encyclopaedia of Volcanoes* (eds Sigurdsson, H., Houghton, B.F., McNutt, S.R., Rymer, H. & Stix, J.), pp. 331-343, Academic Press, San Diego.
- Conway, F.M., Ferrill, D.A., Hall, C.M., Morris, A.P., Stamatakos, J.A., Connor, C.B., Halliday, A.N. & Condit, C., 1997. Timing of basaltic volcanism along the Mesa Butte Fault in the San Francisco Volcanic Field, Arizona, from $^{40}\text{Ar}/^{39}\text{Ar}$ dates: Implications for longevity of cinder cone alignments. *Journal of Geophysical Research*, **102**(B1), 815-824.
- Crumpler, L.S., Aubele, J.C. & Condit, C.D., 1994. Volcanoes and neotectonic characteristics of the Springerville Volcanic Field, Arizona. In: *Mogollon Slope: Socorro, New Mexico Geological Society Guidebook* (eds Chamberlain, R.M., Kues, B.S., Cather, S.M., Barker, J.M. & McIntosh, W.C.), pp. 147-164, New Mexico Geological Society.
- de Gøer, A., Bovin, P., Camus, G., Gourgaud, A., Kieffer, G., Mergoil, J. & Vincent, P., 1994. *Volcanology of the Chaîne des Puys*. Parc Naturel Régional des Volcans d'Auvergne, Aydat, 127 p.
- Denham, D., Alexander, L.G. & Worotnicki, G., 1979. Stresses in the Australian crust: evidence from earthquakes and in-situ stress measurements. *BMR Journal of Australian Geology and Geophysics*, **4**, 289-295.
- Duraiswami, R., Bondre, N.R., Dole, G., Phadnis, V.M. & Kale, V.S., 2001. Tumuli and associated features from the western Deccan Volcanic Province, India. *Bulletin of Volcanology*, **63**, 435-442.
- Eaton, G.P., 1982. The Basin and Range province: origin and tectonic significance. *Annual Review of*

- Earth and Planetary Science*, **10**, 409-440.
- Fitton, J.G., James, D., Kempton, P.D., Ormerod, D.S. & Leeman, W.P., 1988. The role of lithospheric mantle in the generation of Late Cenezoic basic magmas in the western United States. *Journal of Petrology* (Special Lithosphere Issue), 331-349.
- Frey, F.A., Green, D.H. & Roy, S.D., 1978. Integrated models of basalt petrogenesis: a study of quartz tholeiites to olivine melilitites from southeastern Australia utilizing geochemical and experimental petrological data. *Journal of Petrology*, **19**, 463-513.
- Gray, D.R., 1988. Structure and Tectonics. In: *Geology of Victoria* (eds Douglas, J.G. & Ferguson, J.A.), pp. 1-36, Victoria Division, Geological Society of Australia, Melbourne.
- Greeley, R., 1982a. The Snake River Plain, Idaho: Representative of a new category of volcanism. *Journal of Geophysical Research*, **87**(B4), 2,705-2,712.
- Greeley, R., 1982b. The Style of Basaltic Volcanism in the Eastern Snake River Plain, Idaho. In: *Cenozoic geology of Idaho* (eds Bonnischen, B. & Breckenridge, R.M.), pp. 407-421, Idaho Bureau of Mines and Geology, Idaho.
- Guest, J.E., Kilburn, C.R.J., Pinkerton, H. & Duncan, A.M., 1987. The evolution of lava flow-fields: observations of the 1981 and 1983 eruptions of Mount Etna, Sicily. *Bulletin of Volcanology*, **49**, 527-540.
- Haq, B.U., Hardenbol, J. & Vail, P.R., 1987. Chronology of Fluctuating Sea Levels Since the Triassic. *Science*, **235**, 1156-1167.
- Hill, K.A., Finlayson, D.M., Hill, K.C. & Cooper, G.T., 1995. Mesozoic tectonics of the Otway Basin region: the legacy of Gondwana and the active Pacific margin; a review and ongoing research. *The Australian Petroleum Exploration Association Journal*, **35**(1), 467-493.
- Holcomb, R.T., 1987. Eruptive history and long-term behavior of Kilauea Volcano. *U.S. Geological Survey Professional Paper*, **1350**, 261-350.
- Holdgate, G.R., Gallagher, S.J. & Wallace, M.W., 2002. Tertiary coal geology and stratigraphy of the Port Phillip Basin, Victoria. *Australian Journal of Earth Sciences*, **49**, 437-453.
- Hon, K., Kauahikaua, J., Denlinger, R. & Mackay, K., 1994. Emplacement and inflation of pahoehoe sheet flows: Observations and measurements of active lava flows on Kilauea Volcano, Hawaii. *Geological Society of America Bulletin*, **106**, 351-370.
- Hooper, P.R., 1982. The Columbia River basalts. *Science*, **215**, 1463-1468.
- Joyce, E.B., 1975. Quaternary volcanism and tectonics in southeastern Australia. *Bulletin of the Royal Society of New Zealand*, **13**, 169-176.
- Joyce, E.B., 1988. Newer Volcanic Landforms. In: *Geology of Victoria* (eds Douglas, J.G. & Ferguson, J.A.), pp. 419-426, Victorian Division, Geological Society of Australia, Melbourne.
- Joyce, E.B., 1998. A new regolith map of the eastern Victorian volcanic plains, Victoria, Australia. In: *3rd Australian Regolith Conference: New approaches to an old continent* (eds Taylor, G. &

- Pain, C.), pp. 117-126, CRC LEME, Kalgoorlie, Western Australia.
- Khadri, S.F.R., Subbarao, K.V., Hooper, P.R. & Walsh, J.N., 1988. Stratigraphy of Thakurwadi Formation, Western Deccan Basalt Province, India. *Memoirs of the Geological Society of India*, **10**, 281-304.
- Kilburn, C.R.J.L., R.M.C., 1988. The growth of aa lava flow fields on Mount Etna, Sicily. *Journal of Geophysical Research*, **93**(B12), 14,759-14,772.
- Kuntz, M.A., Covington, H.R. & Schorr, L.J., 1992. An overview of basaltic volcanism of the eastern Snake River Plain, Idaho. In: *Regional Geology of the Eastern Idaho and Western Wyoming: Geological Society of America Memoir 179*. (eds Link, P.K., Kuntz, M.A. & Platt, L.B.), pp. 227-267, The Geological Society of America, Boulder, Colorado.
- Lipman, P.W. & Banks, N.G., 1987. Aa flow dynamics, Mauna Loa 1984. *U.S. Geological Survey Professional Paper*, **1350**, 1,527-1,565.
- Lister, G.S. & Etheridge, M.A., 1989. Detachment models for uplift and volcanism in the Eastern Highlands and their applications to the origins of passive margin mountains. In: *Intraplate Volcanism in Eastern Australia and New Zealand* (eds Johnson, R.W., Knutson, J. & Taylor, S.R.), pp. 297-313, Cambridge University Press, Cambridge.
- McDougall, I., Allsopp, H.L. & Chamalaun, F.H., 1966. Isotopic dating of the Newer Volcanics of Victoria, Australia, and Geomagnetic Polarity Epochs. *Journal of Geophysical Research*, **71**(24), 6,107-6,118.
- Mohr, P.A., 1983. Ethiopian flood basalt province. *Nature*, **303**, 577-584.
- Müller, R.D., Gaina, C. & Clark, S., 2000. Seafloor spreading around Australia. In: *Billion-year earth history of Australia and neighbours in Gondwanaland* (ed Veevers, J.J.), pp. 18-28, GEMOC Press, Sydney.
- Nicholls, I.A. & Joyce, E.B., 1989. Newer Volcanics. In: *Intraplate Volcanism in Eastern Australia and New Zealand* (eds Johnson, R.W., Knutson, J. & Taylor, S.R.), pp. 137-142, Cambridge University Press, Cambridge.
- Ollier, C.D. & Joyce, E.B., 1964. Volcanic physiography of the western plains of Victoria. *Royal Society of Victoria Proceedings*, **77**, 357-376.
- Parfitt, E.A., 1998. A study of clast size distribution, ash deposition and fragmentation in a Hawaiian-style volcanic eruption. *Journal of Volcanology and Geothermal Research*, **84**, 197-208.
- Parfitt, E.A. & Wilson, L., 1995. Explosive volcanic eruptions-IX. The transition between Hawaiian-style lava fountaining and Strombolian explosive activity. *Geophysical Journal International*, **121**, 226-232.
- Parfitt, E.A. & Wilson, L., 1999. A Plinian treatment of fallout from Hawaiian lava fountains. *Journal of Volcanology and Geothermal Research*, **88**, 67-75.
- Peterson, D.W. & Moore, R.B., 1987. Geologic history and evolution of concepts, Island of Hawaii.

- U.S. Geological Survey Professional Paper*, **1350**, 149-190.
- Price, R.C., Gray, C.M., Nicholls, I.A. & Day, A., 1988. Cainozoic Volcanic Rocks. In: *Geology of Victoria* (eds Douglas, J.G. & Ferguson, J.A.), pp. 439-451, Victorian Division, Geological Society of Australia, Melbourne.
- Price, R.C., Gray, C.M. & Frey, F.A., 1997. Strontium isotopic and trace element heterogeneity in the plains basalts of the Newer Volcanic Province, Victoria, Australia. *Geochimica et Cosmochimica Acta*, **61**(1), 171-192.
- Reidel, S.P. & Hooper, P.R., 1989. Volcanism and tectonism in the Columbia River flood-basalt province: Boulder, Colorado. *Geological Society of America Special Paper* **239**, 386 p.
- Rowland, S.K. & Walker, G.P.L., 1988. Mafic-crystal distributions, viscosities, and lava structures of some Hawaiian lava flows. *Journal of Volcanology and Geothermal Research*, **35**, 55-66.
- Rowland, S.K. & Walker, G.P.L., 1990. Pahoehoe and aa in Hawaii: volumetric flow rate controls the lava structure. *Bulletin of Volcanology*, **52**, 615-628.
- Sato, H., 1995. Textural differences between pahoehoe and aa lavas of Izu-Oshima volcano, Japan- an experimental study on population density of plagioclase. *Journal of Volcanology and Geothermal Research*, **66**, 101-113.
- Self, S., Thordarson, T., Keszthelyi, L., Walker, G.P.L., Hon, K., Murphy, M.T., Long, P. & Finnemore, S., 1996. A new model for the emplacement of Columbia River basalts as large, inflated pahoehoe lava flow fields. *Geophysical Research Letters*, **23**(19), 2,689-2,692.
- Self, S., Thordarson, T. & Keszthelyi, L., 1997. Emplacement of Continental Flood Basalt Lava Flows. In: *Large Igneous Provinces: Continental, Oceanic, and Planetary Flood Volcanism*. (eds Mahoney, J.J. & Coffin, M.), pp. 381-410, American Geophysical Union.
- Self, S., Keszthelyi, L. & Thordarson, T., 1998. The importance of pahoehoe. *Annual Review of Earth and Planetary Science*, **26**, 81-110.
- Shaw, H.R., 1980. The fracture mechanisms of magma transport from the mantle to the surface. In: *Physics of Magmatic Processes* (ed Hargraves, R.B.), pp. 201-254, Princeton University Press, New Jersey.
- Smith, I.E.M., 1989. New Zealand Intraplate Volcanism- North Island. In: *Intraplate Volcanism in Eastern Australia and New Zealand* (ed Johnson, R.W.), pp. 157-162, Cambridge University Press, Cambridge.
- Stephenson, P.J., 1989. East Australian Volcanic Geology- Northern Queensland. In: *Intraplate Volcanism in Eastern Australia and New Zealand* (ed Johnson, R.W.), pp. 89-97, Cambridge University Press, Cambridge.
- Stephenson, P.J., Burch-Johnston, A.T., Stanton, D. & Whitehead, P.W., 1998. Three long lava flows in north Queensland. *Journal of Geophysical Research*, **103**(B11), 27,359-27,370.
- Subbarao, K.V. & Sukhwala, R.N., 1981. *Deccan Volcanism and Related Basalt Provinces in other*

- parts of the World. *Memoir- Geological Society of India*, 3, Geological Society of India, Bangalore, 474 p.
- Sutherland, F., 1998. Origin of north Queensland Cenozoic volcanism: Relationships to long lava flow basaltic fields, Australia. *Journal of Volcanology and Geothermal Research*, 103(B11), 27,347-27,358.
- Swanson, D.A., Wright, J.H. & Helz, R.T., 1975. Linear vent systems and estimated rates of magma production and eruption of the Yakima basalt on the Columbia Plateau. *American Journal of Science*, 275, 877-905.
- Swanson, D.A., Duffield, W.A., Jackson, D.B. & Peterson, D.W., 1979. Chronological narrative of the 1969-71 Mauna Ulu eruption of Kilauea Volcano, Hawaii. *U.S. Geological Survey Professional Paper*, 1056, 55 p.
- Tanaka, K.L., Shoemaker, E.M., Ulrich, G.E. & Wolfe, E.W., 1986. Migration of volcanism in the San Francisco volcanic field, Arizona. *Geological Society of America Bulletin*, 97, 129-141.
- Thordarson, T. & Self, S., 1998. The Roza Member, Columbia River Basalt Group: A gigantic pahoehoe lava flow field formed by endogenous processes? *Journal of Geophysical Research*, 103(B11), 27,411-27,445.
- Walcott, R.I., 1984. Reconstruction of the New Zealand region for the Neogene. *Palaeogeography, Palaeoclimatology, Palaeoecology*, 46, 217-231.
- Walker, G.P.L., 1993. Basaltic-volcano systems. In: *Magmatic Processes and Plate Tectonics* (eds Prichard, H.M., Alabaster, T., Harris, N.B.W. & Neary, C.R.), pp. 3-38, Geological Society of America.
- Walker, G.P.L., 2000. Basaltic volcanoes and volcanic systems. In: *Encyclopaedia of Volcanoes* (eds Sigurdsson, H., Houghton, B.F., McNutt, S.R., Rymer, H. & Stix, J.), pp. 283-289, Academic Press, San Diego.
- Wellman, P. & McDougall, I., 1974. Cainozoic igneous activity in eastern Australia. *Tectonophysics*, 23, 49-65.
- Wentworth, C.K. & Macdonald, G.A., 1953. Structures and forms of basaltic rocks in Hawaii. *U.S. Geological Survey Bulletin*, 994, 98 p.
- Wilmoth, R.A. & Walker, G.P.L., 1993. P-type and S-type pahoehoe: a study of vesicle distribution patterns in Hawaiian lava flows. *Journal of Volcanology and Geothermal Research*, 55, 129-142.
- Wolfe, E.W., Garcia, M.O., Jackson, D.B., Koyanagi, R.Y., Neal, C.A. & Okamura, A.T., 1987. The Puu Oo eruption of Kilauea Volcano, episodes 1-20, January 3, 1983, to June 8, 1984. *U.S. Geological Survey Professional Paper*, 1350, 471-508.
- Wood, C.A., 1980. Morphometric evolution of cinder cones. *Journal of Volcanology and Geothermal Research*, 7, 387-413.

CHAPTER 6

CONCLUSIONS AND DISCUSSION

6.1 MAJOR CONCLUSIONS OF THE STUDY

6.1.1 The interiors of pahoehoe and aa lava flows (Chapter 2)

- P-type pahoehoe lobes were observed to consistently contain dense, non-vesicular cores, and many contain segregation veins. In contrast, vesicles are dispersed throughout aa lavas, and no segregation veins were observed. These features are considered to be related to the differences in viscosity between the two lava types. Vesicles (and any segregation material) are prevented from rising through more viscous aa lava flows.
- Petrographic textural zonations were found to be different in pahoehoe and aa flows. Variations in the size of groundmass plagioclase laths through individual flows gives information about the relative cooling rates throughout the flows. Plagioclase grain-sizes consistently increase towards the centre of P-type pahoehoe lobes, reflecting a lower cooling rate in the interior than the margins. Aa flows demonstrate consistently uniform plagioclase grain-sizes throughout all flows analysed; they are always smaller than plagioclase grains in pahoehoe flows, but more numerous, thus resulting in higher plagioclase number densities than pahoehoe flows. This is considered to be due to the physical mixing process that occurs during emplacement of aa flows, which enhances cooling and crystal nucleation rates throughout the flow.
- Pahoehoe and aa flows were found to be compositionally homogeneous through vertical compositional profiles, apart from local geochemical anomalies. The small geochemical anomalies have been attributed to locally variable phenocryst contents, and/or differences in the cooling histories of adjacent samples. The cooling rate of the lava affects the order of nucleation of the constituent minerals, which is locally reflected in the geochemistry by a relative depletion or enrichment of certain elements. Further work is required to better characterise the significance of these anomalies in terms of emplacement and crystallisation processes of the different lavas.

- The distinctive emplacement style of aa lavas, and the resulting surface morphology and internal structure, can be attributed to the higher viscosity of these lavas compared with pahoehoe lavas. The higher viscosity is probably related to the higher crystallinity of these lavas, either upon eruption (due to a higher degree of undercooling prior to eruption), or that has developed during cooling and emplacement of the lava (resulting in the transition from pahoehoe to aa). Once a threshold viscosity has been reached, the lava will begin to autobrecciate and propagate as aa. This threshold viscosity is not a unique value, but is related to the rate of shear strain of the lava, which is influenced by the velocity of the lava flow (related to volumetric flow rate, slope of the substrate, local topographic irregularities etc.). Aa lavas are commonly higher velocity flows than pahoehoe, and this is considered to be related to the generally high discharge rates of aa-forming eruptions (Macdonald 1953, Rowland & Walker 1990). Once the lava begins to propagate by autobrecciation, it no longer cools by conduction, but is dominated by a physical mixing process, involving entrainment of clasts and cooler material into the core of the flow. Based upon observed vesiculation patterns and petrographic textural zonations in this study, it appears that upon stagnation of an aa lava flow, the majority of the flow has already crystallised, and the interior of the flow may not cool significantly more slowly than the margins (cf. pahoehoe flows).

6.1.2 The facies architecture and magnetostratigraphy of the Cenozoic, Werribee Plains basaltic lava flow-field (Chapters 3 & 4)

- Inflated pahoehoe lavas are the dominant volcanic facies present in the Werribee Plains, constituting ~65% of all flow units logged in diamond drill core. These flow units are ~7.5 m thick on average, and the abundance of this facies has implications for both the palaeotopography prior to volcanism, and the evolution of the Plains, as inflation of pahoehoe lava flows only occurs on gentle slopes, less than 2° (Cashman & Kauahikaua 1997). Other lava facies identified include S-type pahoehoe flows, ponded lavas, distal facies aa flows and transitional lava flows. These appear to be randomly dispersed throughout the sequence.
- Sedimentation within the Werribee Plains during volcanism was almost entirely restricted to the north-west of the field area. The sediments are mainly composed of

Palaeozoic bedrock from the elevated highlands to the north and west. Sediments were prevented from being transported to the east of the field area due to the presence of a ~N-S trending palaeo-ridge in the centre of the area. This ridge was identified, by compiling a map of the palaeotopography prior to volcanism. There is very little evidence of volcanic material within the inter-flow sediments due to limited weathering and erosion of the basalt between eruptions, as a result of the onset of arid climatic conditions in the late Tertiary.

- The primary remanent magnetisation (the inclination of the geomagnetic field during emplacement of the lavas) was identified by demagnetisation experiments in most lava flow units identified in diamond drill core. Some samples were discarded from the magnetostratigraphic study, as they were palaeomagnetically unstable. These samples were found to be dominated by multi-domain grains with pinned domain walls. The secondary overprinting magnetisation thus persisted to high demagnetisation levels, preventing isolation of the primary remanence. It is considered that the primary remanent magnetisation of two samples per flow is representative of the inclination of the magnetic field during emplacement of that lava flow.
- In five out of nine of the diamond drill holes analysed, a simple reverse polarity, normal, reverse stratigraphy is evident, and this is considered to be correlatable between each of these holes. Based upon available age constraints (eg. previously obtained K-Ar radiometric ages), these magnetic intervals occur within the Gauss and Matuyama Chrons. In one drill hole (PYW7) an additional normal polarity interval is preserved at the base of the sequence, and this is considered to represent the oldest lavas intersected by the drill holes. It corresponds to the C2An.2n Chron, which occurred between 3.11 and 3.22 Ma (Cande & Kent 1995).
- The products of twenty-seven eruptions have been identified in the magnetostratigraphy, which was established for a relatively small part of the Werribee Plains, the area of which was constrained by the diamond drill hole distribution. Eruption packages considered to be correlatable between drill holes have the same magnetic polarity; are close to within error limits of the average inclination value of

that package; are geochemically and petrographically similar; are the same, or related volcanic facies allowing for topographic constraints; and are reasonably separated in terms of palaeotopography, other drill holes and likely lengths of flows (based upon airborne magnetic and radiometric images, and surface geochemistry).

- A minimum eruption frequency for the Werribee Plains was calculated to be one eruption every 66,000 years, from the commencement of volcanism (~3.2 Ma) to the most recent eruption of Mt. Atkinson (1.41 Ma). Other eruptions are known to have occurred within the Plains, however due to a lack of age constraints they are not included in this stratigraphy.
- The sub-surface basalts of the Werribee Plains are difficult to date. The lavas that occur at depth in the sequence are pervasively altered, probably due to groundwater interaction and are unsuitable for K-Ar dating, the technique which has conventionally been used to date the products of the NVP (eg. McDougall *et al.* 1966, Aziz-Ur-Rahman & McDougall 1972, Price *et al.* 1997). Many different dating techniques were explored, and $^{40}\text{Ar}/^{39}\text{Ar}$ dating of plagioclase phenocrysts extracted from the basalt was found to be the most suitable technique. Few of the lavas have plagioclase phenocrysts, so only one sample was available for dating at a late stage in the study, and unfortunately the results are not yet available.

6.1.3 The palaeovolcanology and evolution of the Cenozoic, Werribee Plains basaltic lava flow-field (Chapter 5)

- Prior to volcanism in the Werribee Plains, continental fluvial erosion and sedimentation was occurring in the area, producing local topographic highs and lows. Significant topographic relief probably already existed particularly to the west of the field area, due to uplift of the highlands along the Rowsley Fault (Kosciusko uplift). The final stage of uplift is considered to have begun in the middle Miocene (Wellman 1974). Sediments were transported from the highlands into the Werribee Plains by easterly flowing rivers throughout the volcanic activity.
- Volcanism in the Werribee Plains began during late stages of the 3.8 Ma eustatic

regression. All eruptions are considered to have commenced with the opening of an eruptive fissure. The eruption centres are monogenetic, small volume scoria cones and low lava shields produced by Strombolian explosive eruptions and Hawaiian fire-fountaining (respectively). This was commonly followed by a period of passive outpouring of lava. Scoria cone eruptions probably lasted days to weeks, whereas the lava shields were calculated to erupt for several months on average, based upon the rates of inflation of P-type pahoehoe lobes.

- Although most eruptions appear to have been small volume (the products intersected by only one drill hole), both scoria cones and lava shields have been observed to have fed significant lava flows. In each instance the flows are the same composition as the eruption centre that fed them, and no trend was identified in terms of a broad change in composition of the lavas with time, contrary to previous generalisations for the NVP (eg. Price *et al.* 1988). Tholeiitic and alkalic basalts are intercalated throughout the history of the succession.
- Within the Werribee Plains there is no evidence of a general geographical shift in magma generation with time. Relatively small lava flow-fields appear to have progressively built up in a random distribution in the Plains. There is evidence that in some cases the distribution of volcanoes was controlled by preferential magma rise along pre-existing basement structures.
- Aa lavas have not previously been recognised in the NVP (Cas 1989), however they were identified in drill core in this study. The aa flows are anomalously thick (average 22.5 m thick), are restricted to the north of the field area, and are considered to have been produced by volcanoes in the Central Highlands sub-province. They were probably initially produced as a result of the steeper terrain in the highlands, and thickened upon reaching the flatter topography of the Werribee Plains.
- The cumulative result of the lavas of the many eruptions was a general smoothing out of the topography. The present topography of the Werribee Plains is relatively flat, punctuated only by the positive relief-eruption centres that are exposed. The landscape

has therefore changed from one marked by erosional downcutting, to the positive relief constructional landscape resulting from volcanism. Limited recent erosion is beginning to re-establish erosional landforms.

- The NVP is intermediate in terms of size of individual eruption centres, and total volume of products between small volume continental basaltic fields (eg. Auckland, Auvergne, Eifel, San Francisco, Springerville) and large volume fields (the Eastern Snake River Plain). The main control on the type of lava-field produced is considered to be the volume of magma generated for each eruption. On average, plains-basalt lava fields have greater volumes of lava produced for each eruption than other monogenetic basaltic fields. This results in the construction of lava plains in between the eruption centres. The volume of magma generated during volcanism is related to the tectonic setting and prevailing stress field in which the volcanism is occurring.
- The average pahoehoe and aa flow thicknesses in plains-basalt provinces were found to be significantly thicker than flows in Hawaii and at Mt. Etna, and thinner than flows in continental flood basalt provinces. The greater thickness of continental flood basalt lavas is considered to reflect the significantly greater volumes and rates of the eruptions. The main control on flow thickness elsewhere appears to be the slope of the substrate. Lavas are able to thicken in plains-basalt provinces on the gently sloping plains, either by endogenous growth or by lateral spreading and thickening of the flow-front of aa flows. The slopes of the flanks of large shields and stratovolcanoes prevent thickening of the lavas from occurring to the same extent, resulting in thinner lavas on average, apparently regardless of the volume of the eruption.
- A minimum eruption frequency for the NVP (one eruption every 11,500 years) appears to be substantially less than eruption frequencies in other continental basaltic provinces. Further work is required to explore why this may be the case.

6.2 IMPLICATIONS OF THE STUDY AND FURTHER WORK

6.2.1 The interiors of pahoehoe and aa lava flows: emplacement and crystallisation processes of basaltic lava flows

The study of the interiors of basaltic lavas has been useful in better characterising the different end-member lava types. The presence of vesicle trains towards the base of the UVZ of P-type pahoehoe lobes for example, was found to be unique to lavas that have formed by inflation. These can potentially be used in conjunction with other criteria to distinguish between lavas that have formed by inflation and lavas that have ponded in a topographic depression (eg. Cashman & Kauahikaua 1997). Vesicle trains are considered to be a valuable identifier of these flows in ancient terrains, where weathering and erosion has occurred and the normalised UVZ has been modified; and in diamond drill core, where horizontal vesicle zones are less easily identifiable than in outcrop. Identifying pahoehoe flows that have formed by inflation has implications for the slope of the substrate, as they only form on slopes of $<2^\circ$ (Hon *et al.* 1994, Cashman & Kauahikaua 1997). Again, this may be of particular interest in ancient terrains, when exploring the palaeogeography for example. Criteria were identified to distinguish between pahoehoe and aa lavas in drill core and petrographically. Although some of these criteria have already been recognised, this is a more comprehensive study than has previously been performed, particularly in terms of recognising variations in textures and vesicle zonations throughout individual flows. Generalisations have been made about the interiors of pahoehoe and aa flows that can be applied in other basaltic provinces to explore the distribution of volcanic facies, and to gain a better understanding of the evolution of the lava fields.

The most useful textural parameter used to compare pahoehoe and aa flows was found to be the groundmass plagioclase grain-sizes. Although it has previously been recognised that aa flows have higher plagioclase groundmass number densities than pahoehoe flows (eg. Sato 1995, Cashman *et al.* 1999, Polacci *et al.* 1999), these observations were based upon analysing surface samples of the flows. This is the first attempt to compare trends in groundmass grain-sizes and number densities throughout individual pahoehoe and aa flows. The results suggest that contrary to our present understanding of aa flows, the interiors may not cool slowly by conduction (eg. Cashman *et al.* 1999). It was beneficial to do this comprehensive study of all groundmass textural features in the different lava flows, however unfortunately due to time constraints, relatively few flows were studied petrographically. In order to check whether the trends identified are consistent or not among pahoehoe and aa flows, it would be

valuable to study many more flows. Further work should concentrate on trends in groundmass plagioclase grain-size variations through the flows. This seems to give the best indication of the relative cooling rates. In addition, it would be interesting to do a more detailed study of the geochemistry of the flows by increasing the number of samples taken per flow. The flows analysed were found to be generally compositionally homogeneous, however local anomalies were identified which would be interesting to explore. Combining this geochemical study with analysis of the phenocryst content for example, may give insight into crystal settling processes within the lava flows (eg. Rowland & Walker 1987, 1988). It would also be useful to combine the results of vertical compositional and textural profiles with microprobe studies of the compositions of the different minerals, to see how these vary through the lava flows.

Despite the fact that ultramafic komatiite lavas are restricted to Archaean and Proterozoic terrains and are commonly metamorphosed and poly-deformed, the internal textural and compositional zonations within these lavas have been well constrained (eg. Pyke *et al.* 1973, Arndt *et al.* 1977, Arndt 1986, Renner *et al.* 1994, Grove *et al.* 1997). Different types of komatiites have been identified, however the lavas are classically subdivided into an upper spinifex A zone (low MgO), and a lower cumulate B zone (high MgO) (Pyke *et al.* 1973). This study has confirmed that basaltic lavas do not demonstrate such marked textural and compositional variations through individual flows. The main reason for the internal differences between komatiites and basalts is considered to be the different viscosities of these two lava types. Komatiite lava viscosities are considered to have ranged from 0.1-10 Pa s, and basalt viscosities are generally more than 50 Pa s (Huppert *et al.* 1984). The difference in the viscosities of the lavas is related to the different eruption temperatures and initial compositions. Komatiites erupted at around 1400-1700°C with MgO contents of 18-35%, whereas the hottest basalts erupt at 1200°C and have MgO contents of less than 10-12% (Arndt & Nisbet 1982). At the lower temperatures at which basalts are being emplaced, the growth of abundant microlites is likely to increase the relative viscosity of the lava (compared with komatiites), and prevent significant crystal settling. On the other hand, crystals that have formed prior to eruption and during emplacement of komatiite lavas (eg. Jerram *et al.* submitted) are considered to settle with relative ease through the low viscosity lavas, resulting in texturally and chemically distinct zones. This effect is enhanced by the density differences of the crystals that form in the two types of lavas. Komatiites are dominated by olivines, which are more dense than the plagioclase laths that constitute the bulk of the groundmass in basalts. Furthermore, preserved komatiite lavas were emplaced in subaqueous environments,

resulting in higher cooling differentials from the margins of the flows than those experienced by subaerial basalts. This is considered to have contributed to the formation of quench spinifex textures in komatiites (eg. Lofgren 1980, Shore & Fowler 1999).

6.2.2 The Newer Volcanic Province

Much of the previous work within the Newer Volcanic Province has been very focussed in terms of using a single discipline to investigate or describe an aspect of the geology (eg. using geochemistry or geochronology or geomorphology). Price *et al.* (1997) were the first to begin compiling existing geochemical and geochronological data, and combined it with new data to investigate the entire Western Plains sub-province. Due to the large scale of the area being investigated, and the primary interest of the Price *et al.* (1997) study being petrogenetic processes, the stratigraphic domains identified were not put into a volcanic context, in terms of identifying the eruption centres from which the lavas were fed. This study goes a step further, by taking an inter-disciplinary approach to the investigation of a relatively small area within the NVP, the Werribee Plains. Existing data sets (airborne geophysical data, geochemical data for surface samples, geophysical well data, radiometric ages) were interpreted/analysed and combined with new data collected in this study (from diamond drill core logging, fieldwork, petrographic studies, geochemistry, palaeomagnetic studies, radiometric dating), and a magnetostratigraphy established. Importantly, it is the first time that the limited surface data has been combined with sub-surface data, to put the surface results into some sort of context. This stratigraphy was used to investigate the palaeovolcanology and evolution of the Werribee Plains, and to make general comments about plains-basalt volcanism, and the formation of the NVP.

The main interest of many studies of the NVP has been the geochemistry and petrogenesis of the magmas (eg. Edwards 1938, Irving & Green 1976, Frey *et al.* 1978, McDonough *et al.* 1985, Price *et al.* 1997, Vogel & Keays 1997). Based upon these studies, it is widely accepted that the lava plains of the NVP are dominantly tholeiitic or chemically transitional, and the volcanic centres, or constructional volcanic features are dominantly alkalic (Price *et al.* 1988). It is also considered that the constructional volcanic features are younger than most of the lava flows covering the western plains (Price *et al.* 1988). These two assumptions have formed the basis for petrogenetic models, which ultimately aim to understand and explain the processes involved in the intra-plate volcanism. In this study, it was found that the volcanic centres are both alkalic and tholeiitic in composition, and more importantly

perhaps, that the centres (both scoria cones and lava shields) feed the lavas that form the lava plains. Thus it is unreasonable to conclude that the plains are largely a different age and composition to the eruption centres. Furthermore, based upon this study there does not appear to have been a broad change in composition of magmas with time, but instead tholeiitic and alkalic lavas are intercalated throughout the stratigraphy.

The stratigraphy established in the Werribee Plains provides an ideal framework in which further petrogenetic studies can be undertaken. By applying this integrated methodological approach to other areas of the NVP, existing radiometric ages can also be put into a stratigraphic context. A significant finding of this study is that there are many buried eruption centres in the Werribee Plains (and therefore probably elsewhere in the Newer Volcanic Province), and the sub-surface geology is very complex. In the past, conclusions have been drawn about trends in volcanism in the NVP based upon limited surface radiometric ages (eg. Joyce 1975). Further geochronological studies interpreted in terms of the stratigraphy would be useful for gaining a better understanding of the evolution of the NVP, and of the processes operating in plains-basalt provinces. Issues such as whether there has been a major shift in the locus of magma generation with time could be addressed, and better estimates of the eruption frequency in this plains-basalt province obtained. More geochronological studies on sub-surface samples would be beneficial. However, until new techniques are developed, this will be limited to the relatively small proportion of lavas that contain plagioclase phenocrysts (for $^{40}\text{Ar}/^{39}\text{Ar}$ dating).

6.2.3 Other basaltic provinces

The techniques developed in this study could well be applied to other basaltic provinces, so as to better understand their evolution. As has previously been mentioned, the characterisation of the internal features of the different volcanic facies, particularly in drill core can be readily applied to other basaltic terrains. The distribution of lava facies is commonly overlooked when describing the geology of a basaltic province (eg. it has not been properly addressed before in the NVP), however it can provide insight into emplacement processes, the palaeotopography, and the general evolution of a field. Although a great deal of understanding can be gained from studying the surfaces of basaltic provinces that are well exposed, it is invaluable to be able to link this with sub-surface data, such as from drill core. Geophysical well logs are a tool which also could potentially be of more use in basaltic terrains. It has been demonstrated in this study that the geophysical response of basalt is

distinctive, and it was therefore straightforward to map the extent of basalt beneath the surface of the Werribee Plains. In some instances volcanic facies were identified within the basaltic sequence (aa lavas and packages of pahoehoe flows), based upon their known internal characteristics and resulting geophysical responses. Further work is recommended to refine this technique, particularly where both diamond drill core and geophysical wells are available. In terrains where exposure is not so good (such as the NVP), airborne geophysical data sets were found to be useful in mapping the extent of lava flows. Further work is again recommended to develop the interpretation of these images, particularly isolating the products of different centres using radiometric images.

The palaeomagnetic studies were a fundamental part of being able to establish a stratigraphy in the Werribee Plains. Establishing magnetostratigraphies in other parts of the NVP, and other basaltic terrains is considered to be worthwhile in order to gain a better understanding of these provinces. A degree of trial and error was involved in terms of methods used in the palaeomagnetic studies here, as there is little information in the literature about similar studies. Some recommendations for further studies in basaltic terrains based upon the work in this study are listed. Firstly, it was found that it was best to sample close to flow boundaries, while avoiding the very margins of the flows and any oxidised material. Sampling the centres of flows should be avoided, as the titanomagnetites were found to be coarse-grained (multi-domain), and it was difficult to isolate a primary remanent magnetisation in these samples. A useful exercise prior to commencing demagnetisation, would be to calculate the Königsberger ratio (Q) for all samples. This gives a rough indication of the relative proportion of induced and remanent magnetisation present in a sample (Dunlop & Özdemir 1997), and simply involves measuring the remanent magnetisation prior to demagnetisation and the magnetic susceptibility. In this study all samples with Q values less than 2 were discarded from the magnetostratigraphic studies, however it would save time if these were discarded prior to demagnetising the samples. Although more time-consuming than the AF demagnetisation technique, thermal demagnetisation tended to yield more reliable results. This is particularly important when making correlations based upon secular variations, and this technique is recommended for future studies.

Ideally, it would have been useful if the diamond drill holes were spaced more closely together in this study, however we had no control of this. The products of a number of eruptions were intersected by only one drill hole, suggesting that there were many other eruptions that occurred in the vicinity of the magnetostratigraphy, that were not incorporated. For this reason,

the eruption frequency calculated was a minimum estimate. It is significantly lower than the frequency calculated for the entire NVP, based upon the number of exposed eruption centres and the known time interval over which volcanism has been occurring (Chapter 5). It is difficult to know how to address this problem, because increasing the sampling spacing at the surface of a province like this would not help, as there are many buried eruption centres. Determining the eruption frequency based upon a magnetostratigraphy would tend to work better in continental flood basalt provinces, where the eruption packages are regionally correlatable, and the products of most (if not all) eruptions are included.

6.2.4 Economic implications

The basalt of the Werribee Plains (and elsewhere in the NVP) has been fairly extensively quarried for building materials and crushed rock for a variety of uses. In 1995 nine million tonnes of basalt were extracted from the area immediately north and west of Melbourne (Olshina & Jiricek 1996). The demand is still very high for basalt with high mechanical strength, i.e. unaltered, non-vesicular basalt. Inflated pahoehoe flows are the dominant lava facies in the Werribee Plains, however the UVZ (upper vesicular zone) of each of these lobes comprises about 50% the lobe, and this material is not as mechanically strong as non-vesicular basalt. Aa lava flows have not previously been recognised in the NVP, and within the Werribee Plains they were not observed at the surface. A number of sub-surface aa lavas were identified however, and each is considered to represent a thick (average ~22 m), very weakly vesicular, distal facies. In one drill hole an aa lava flow was located within a few metres of the surface (DER8). Aa lavas such as this one, that are located close to the surface and are not significantly weathered and altered, could potentially provide an excellent source of high mechanical strength basalt. Aa flows in the ESRP, another plains-basalt province are up to several kilometres wide, and several tens of kilometres long (Kuntz *et al.* 1992). It is recommended that the aa flows, identified using the criteria recognised in this study, be an exploration target for companies in the basalt extraction industry.

REFERENCES

- Arndt, N.T., 1986. Differentiation of komatiite flows. *Journal of Petrology*, **27**(2), 279-301.
- Arndt, N.T., Naldrett, A.J. & Pyke, D.R., 1977. Komatiitic and Iron-rich Tholeiitic Lavas of Munro Township, Northeast Ontario. *Journal of Petrology*, **18**, 319-369.
- Arndt, N.T. & Nisbet, E.G., 1982. What is a komatiite? In: *Komatiites* (eds Arndt, N.T. & Nisbet, E.G.), pp. 19-27, George Allen & Unwin, London.
- Aziz-Ur-Rahman & McDougall, I., 1972. Potassium-Argon ages on the Newer Volcanics of Victoria. *Royal Society of Victoria Proceedings*, **85**, 61-69.
- Cande, S.C. & Kent, D.V., 1995. Revised calibration of the geomagnetic polarity timescale for the Late Cretaceous and Cenozoic. *Journal of Geophysical Research*, **100**, 6,093-6,095.
- Cas, R.A.F., 1989. Physical Volcanology. In: *Intraplate Volcanism in Eastern Australia and New Zealand* (eds Johnson, R.W., Knutson, J. & Taylor, S.R.), pp. 55-87, Cambridge University Press, Cambridge.
- Cashman, K.V. & Kauahikaua, J.P., 1997. Reevaluation of vesicle distributions in basaltic lava flows. *Geology*, **25**(5), 419-422.
- Cashman, K.V., Thornber, C. & Kauahikaua, J.P., 1999. Cooling and crystallization of lava in open channels, and the transition of Pahoehoe Lava to 'A'a. *Bulletin of Volcanology*, **61**, 306-323.
- Dunlop, D.J. & Özdemir, Ö., 1997. *Rock Magnetism: Fundamentals and frontiers*. Cambridge University Press, Cambridge, 573 p.
- Edwards, A.B., 1938. The Tertiary volcanic rocks of central Victoria. *Journal of the Geological Society of London*, **94**, 243-320.
- Frey, F.A., Green, D.H. & Roy, S.D., 1978. Integrated models of basalt petrogenesis: a study of quartz tholeiites to olivine melilitites from southeastern Australia utilizing geochemical and experimental petrological data. *Journal of Petrology*, **19**, 463-513.
- Grove, T.L., de Wit, M.J. & Dann, J.C., 1997. Komatiites from the Komati type section, Barberton South Africa. In: *Greenstone belts* (eds de Wit, M.J. & Ashwal, L.D.) *Oxford Monographs on Geology and Geophysics*, pp. 438-453, Oxford University Press, New York.
- Hon, K., Kauahikaua, J., Denlinger, R. & Mackay, K., 1994. Emplacement and inflation of pahoehoe sheet flows: Observations and measurements of active lava flows on Kilauea Volcano, Hawaii. *Geological Society of America Bulletin*, **106**, 351-370.
- Huppert, H.E., Sparks, R.S.J., Turner, J.S. & Arndt, N.T., 1984. Emplacement and cooling of komatiite lavas. *Nature*, **309**, 19-22.
- Irving, A.J. & Green, D.H., 1976. Geochemistry and petrogenesis of the newer basalts of Victoria and South Australia. *Journal of the Geological Society of Australia*, **23**, 45-66.
- Jerram, D.A., Cheadle, M.J. & Philpotts, A.R., submitted. Quantifying the building blocks of igneous rocks: Are clustered crystal frameworks the foundation? *Journal of Petrology*.

- Joyce, E.B., 1975. Quaternary volcanism and tectonics in southeastern Australia. *Bulletin of the Royal Society of New Zealand*, **13**, 169-176.
- Kuntz, M.A., Covington, H.R. & Schorr, L.J., 1992. An overview of basaltic volcanism of the eastern Snake River Plain, Idaho. In: *Regional Geology of the Eastern Idaho and Western Wyoming: Geological Society of America Memoir 179*. (eds Link, P.K., Kuntz, M.A. & Platt, L.B.), pp. 227-267. The Geological Society of America, Inc., Boulder, Colorado.
- Lofgren, G.E., 1980. Experimental studies on the dynamic crystallization of silicate melts. In: *Physics of magmatic processes* (ed Hargraves, R.B.), pp. 487-551, Princeton University Press, New Jersey.
- Macdonald, G.A., 1953. Pahoehoe, aa and block lava. *American Journal of Science*, **251**, 169-191.
- McDonough, W.F., McCulloch, M.T. & Sun, S.S., 1985. Isotopic and geochemical systematics in Tertiary-Recent basalts from southeastern Australia and implications for the evolution of the sub-continental lithosphere. *Geochimica et Cosmochimica Acta*, **49**, 2,051-2,067.
- McDougall, I., Allsopp, H.L. & Chamalaun, F.H., 1966. Isotopic dating of the Newer Volcanics of Victoria, Australia, and Geomagnetic Polarity Epochs. *Journal of Geophysical Research*, **71**(24), 6,107-6,118.
- Olshina, A. & Jiricek, F., 1996. Melbourne Supply Area: Extractive Industry Interest Areas. *Unpublished Report 1996/1*, Geological Survey of Victoria, Melbourne.
- Polacci, M., Cashman, K.V. & Kauahikaua, J.P., 1999. Textural characterization of the pahoehoe-'a'a transition in Hawaiian basalt. *Bulletin of Volcanology*, **60**, 595-609.
- Price, R.C., Gray, C.M., Nicholls, I.A. & Day, A., 1988. Cainozoic Volcanic Rocks. In: *Geology of Victoria* (eds Douglas, J.G. & Ferguson, J.A.), pp. 439-451. Victorian Division, Geological Society of Australia, Melbourne.
- Price, R.C., Gray, C.M. & Frey, F.A., 1997. Strontium isotopic and trace element heterogeneity in the plains basalts of the Newer Volcanic Province, Victoria, Australia. *Geochimica et Cosmochimica Acta*, **61**(1), 171-192.
- Pyke, D.R., Naldrett, A.J. & Eckstrand, A.R., 1973. Archaean ultramafic flows in Munro Township, Ontario. *Geological Society of America Bulletin*, **84**, 955-978.
- Renner, R., Nisbet, E.G., Cheadle, M.J., Arndt, N.T., Bickle, M.J. & Cameron, W.E., 1994. Komatiite Flows from the Reliance Formation, Belingwe Belt, Zimbabwe: I. Petrography and Mineralogy. *Journal of Petrology*, **35**, 361-400.
- Rowland, S.K. & Walker, G.P.L., 1987. Toothpaste lava: Characteristics and origin of a lava structural type transitional between pahoehoe and aa. *Bulletin of Volcanology*, **49**, 631-641.
- Rowland, S.K. & Walker, G.P.L., 1988. Mafic-crystal distributions, viscosities, and lava structures of some Hawaiian lava flows. *Journal of Volcanology and Geothermal Research*, **35**, 55-66.
- Rowland, S.K. & Walker, G.P.L., 1990. Pahoehoe and aa in Hawaii: volumetric flow rate controls the

- lava structure. *Bulletin of Volcanology*, **52**, 615-628.
- Sato, H., 1995. Textural differences between pahoehoe and aa lavas of Izu-Oshima volcano, Japan - an experimental study on population density of plagioclase. *Journal of Volcanology and Geothermal Research*, **66**, 101-113.
- Shore, M. & Fowler, A.D., 1999. The origin of spinifex texture in komatiites. *Nature*, **397**, 691-693.
- Vogel, D.C. & Keays, R.R., 1997. The petrogenesis and platinum-group element geochemistry of the Newer Volcanic Province, Victoria, Australia. *Chemical Geology*, **136**, 181-204.
- Wellman, P., 1974. Potassium-argon ages on the Cainozoic volcanic rocks of eastern Victoria, Australia. *Journal of the Geological Society of Australia*, **21**, 359-368.

APPENDIX A

X-RAY FLUORESCENCE (XRF) SAMPLE PREPARATION AND ANALYTICAL PROCEDURES

At Monash University rock samples were crushed in a steel jaw crusher to small (~1-2 cm) chips. Samples were then powdered in soft Fe ringmills for 2 minutes, or until the samples had the consistency of fine talcum powder.

The University of Melbourne

Sample preparation procedure

Both major and trace elements were analysed on a single 5:1 lithium metaborate: rock powder fused bead. For each analysis 1.0 g of rock powder was weighed into a glass mixing jar with 5.0 g of pure lithium metaborate, additional ammonium nitrate oxidant, and mixed well. Fusion to 1000°C in platinum-gold crucibles was conducted in a Bradway furnace. Samples were weighed, loss on ignition (LOI) was calculated, and the samples were re-melted before final casting in graphite moulds. The technique used to prepare the glass discs is a modification of that described by Haukka & Thomas (1977) and Thomas & Haukka (1978).

Analytical equipment and corrections

A Siemens SRS3000 sequential X-ray fluorescence spectrophotometer was used for the analyses, driven by hardware and software. X-rays were generated by a Rh-anode tube, diffracted using LiF100, LiF110, OVO55 and PET crystals, and detected by either or both scintillation or argon flow count detectors. Each element analysis was fully corrected for line interference and matrix effects of all the other analysed elements. Matrix corrections were determined by duplicate preparation of 64 certified reference and spec-pure synthetic samples, and using the Lachance-Traill algorithm provided by the Siemens empirical alpha correction programme Spectra3000. The alphas used were dominantly theoretical and experimental with provision for regression based alphas (eg. for LOI).

Accuracy and precision

For every batch of analyses, one DCB-1 in-house standard basalt, and one CGD-1 in-house standard granite were analysed. This allowed for calculation of accuracy. Also, for every 20

samples at least one sample was repeated. This provided a measure of the reproducibility or precision of the analytical procedure. Machine drift was monitored for, and corrected, by the routine running of a commercial monitor sample containing appropriate levels of all elements of interest. Generally the major oxides have a detection limit of 0.01 % and a relative accuracy of 0.5 % by the fused glass disc method, while the figures for the trace elements are 2-10 ppm and 5 % respectively.

The University of New South Wales

Sample preparation: Major elements

Glass sample buttons were prepared using ~4.5g flux, 0.84g of powdered sample and 0.06g ammonium nitrate. The fusion mixture used for fluxing samples was the Sigma X-ray Flux (Norrish Formula) marketed by David Brown Scientific, Osborne Park, Western Australia. It is composed of lithium tetraborate (47 % by weight), lithium carbonate (36.6 %) and lanthanum oxide (16.4 %). For each sample, the mixture was heated in a platinum-gold crucible for 15 minutes at 1050°C until the specimen had dissolved and effervescence ceased. The melt was poured into a graphite disc, and held on a hot plate at ~220°C. An aluminium plunger was brought down gently to mould and quench the melt. For further details refer to the study by Norrish & Hutton (1969). The LOI figures used in the matrix correction calculations to derive "as-received" concentrations were determined by heating a portion of each sample at 1050°C for ~2 hours.

Trace elements

Pressed powder pellets were made to analyse the trace elements. For each analysis, ~10 g of dried, finely crushed sample was mixed intimately with ~1.5 mls of 2.5 % ELVANOL solution (PVA), a liquid binder. This was compounded into an aluminium cup, then dried overnight at ~30-40°C. The prepared pellets were labelled and stored in a dessicator until analysis occurred.

Analytical Equipment

A Philips PW2400 X-ray fluorescence spectrophotometer was used for the analyses, with a Rh end-window tube. Data was processed using "SUPERQ" software.

Relative errors

Relative accuracy is less than 1 % for all major elements. For trace elements, precision and accuracy tests are not done on routine samples, however control standards of known concentration are run frequently with batches of samples to assess the reliability of the results. With careful analysis, relative errors are ~1 to 5% with 95% confidence at 100ppm and higher concentrations. At lower levels, the relative errors increase and will have a value equal to two-thirds of the lower limit of detection (LLD) at that level.

REFERENCES

- Haukka, M.T. & Thomas, I.L., 1977. Total X-ray fluorescence analysis of geological samples using a low-dilution lithium metaborate fusion method. Matrix corrections for major elements. *X-ray Spectrometry*, **6**(4), 204.
- Norrish, K. & Hutton, J.T., 1969. An accurate X-ray spectrographic method for the analysis of a wide range of geological samples. *Geochimica et Cosmochimica Acta*, **33**, 431-453.
- Thomas, I.L. & Haukka, M.T., 1978. XRF determination of trace and major elements using a single-fused disc. *Chemical Geology*, **21**, 39-50.

Category	Item	MAU01	MAU02	MAU03	MAU04	Mean values	MAU05	MAU06	MAU07	MAU08	MAU09	MAU10	Mean values	HWY01	HWY02	HWY03	HWY04	HWY05	HWY06	Mean values
HAW-MAU1	MAU01	0.05	24.66	42.03	0.11	0.02	5.50	5.33	15.67											
	MAU02	0.15	37.50	45.18	0.18	0.02	9.00	16.84	37.00											
	MAU03	0.35	27.50	38.33	0.19	0.03	6.33	13.36	30.20											
	MAU04	0.60	20.00	37.56	0.15	0.02	7.50	2.00	6.02											
	Mean values		27.42	40.77	0.16	0.02	7.08	9.38	22.22											
HAW-MAU2	MAU05	2.55	26.50	31.18	0.08	0.01	8.00	13.75	23.50											
	MAU06	2.70	16.00	17.98	0.03	0.01	3.00	1.25	2.10											
	MAU07	3.35	22.00	23.49	0.06	0.01	6.00	14.66	20.45											
	MAU08	3.75	25.33	27.33	0.08	0.01	8.00	16.00	23.76											
	MAU09	4.15	16.33	21.87	0.09	0.01	9.00	17.33	29.71											
MAU10	4.60	32.00	34.78	0.08	0.01	8.00	13.66	22.77												
Mean values		23.03	26.10	0.07	0.01	7.00	12.78	20.38												
HAW-HWY	HWY01	0.25	3.50	4.49	0.08	0.01	8.00	12.37	16.60											
	HWY02	0.75	6.00	7.64	0.08	0.01	8.00	19.75	27.24											
	HWY03	1.50	8.00	10.39	0.07	0.02	3.50	20.25	29.35											
	HWY04	1.65	3.25	4.29	0.08	0.02	4.00	22.00	30.34											
	HWY05	2.30	7.50	9.15	0.07	0.01	7.00	18.25	24.50											
	HWY06	2.35	0.00	0.00	0.05	0.02	2.50	4.33	5.20											
	Mean values		4.71	5.99	0.07	0.02	5.50	16.16	22.20											

Category	Item	K1501 U	K1502 U	K1503 U	K1504 U	K1505 U	K1506 U	K1507 U	K1508 N	K1509 N	K1510 L	K1511 L	Mean values	K1512 U	K1513 U	K1514 U	K1515 N	K1516 N	K1517 L	Mean values	K1601 U	K1602 U	K1603 U	K1604 U	K1605 U	K1606 N	K1607 N	K1608 L	Mean values
KOR15A	K1501 U	5.81E+03	4.84E+07	0.05	17.75	27.00	1.37E+04	2.75E+08	0.00																				
	K1502 U	7.42E+03	4.95E+07	0.05	24.70	36.65	1.87E+04	3.73E+08	0.03																				
	K1503 U	6.77E+03	3.76E+07	0.07	30.70	39.36	1.02E+04	1.46E+08	0.04																				
	K1504 U	7.58E+03	4.21E+07	0.07	30.00	37.83	9.83E+03	1.40E+08	0.06																				
	K1505 U	4.76E+03	2.65E+07	0.07	31.00	39.29	1.02E+04	1.46E+08	0.06																				
	K1506 U	7.15E+03	3.11E+07	0.06	32.00	40.51	1.43E+04	2.39E+08	0.06																				
	K1507 U	6.20E+03	3.45E+07	0.11	32.70	38.61	4.06E+03	3.69E+07	0.06																				
	K1508 N	6.22E+03	2.83E+07	0.18	34.00	38.51	1.51E+03	8.41E+06	0.07																				
	K1509 N	5.94E+03	3.30E+07	0.18	36.30	40.65	1.60E+03	8.87E+06	0.05																				
	K1510 L	9.47E+03	6.76E+07	0.12	31.70	43.01	3.80E+03	3.17E+07	0.05																				
	K1511 L	8.56E+03	7.79E+07	0.05	38.30	55.51	2.83E+04	5.65E+08	0.02																				
	Mean values	6.90E+03	4.33E+07	0.09	30.83	39.72	1.06E+04	1.79E+08	0.05																				
	KOR15B	K1512 U	3.45E+03	1.72E+07	0.20	21.00	29.68	9.45E+02	4.72E+06	0.04																			
K1513 U		3.41E+03	1.55E+07	0.28	30.50	40.50	6.58E+02	2.35E+06	0.05																				
K1514 U		3.42E+03	1.27E+07	0.55	25.80	30.90	1.30E+02	2.36E+05	0.06																				
K1515 N		2.72E+03	1.01E+07	0.58	29.00	33.92	1.28E+02	2.21E+05	0.11																				
K1516 N		3.03E+03	9.78E+06	0.49	19.25	25.58	1.36E+02	2.77E+05	0.10																				
K1517 L		3.81E+03	2.12E+07	0.13	20.65	34.70	2.61E+03	2.01E+07	0.03																				
Mean values		3.31E+03	1.44E+07	0.37	24.37	32.55	7.68E+02	4.65E+06	0.07																				
KOR16A		K1601 U	5.37E+03	3.36E+07	0.02	32.75	45.64	1.45E+05	7.26E+09	0.03																			
		K1602 U	5.71E+03	3.36E+07	0.04	30.25	47.64	3.79E+04	9.48E+08	0.04																			
		K1603 U	7.02E+03	5.01E+07	0.10	16.08	23.30	2.97E+03	2.97E+07	0.05																			
		K1604 U	7.87E+03	4.37E+07	0.29	25.27	34.50	5.22E+02	1.80E+06	0.09																			
		K1605 U	5.55E+03	2.78E+07	0.34	20.88	29.00	3.19E+02	9.39E+05	0.11																			
		K1606 N	9.31E+03	4.23E+07	0.31	16.13	22.00	2.91E+02	9.40E+05	0.09																			
	K1607 N	4.39E+03	2.44E+07	0.11	34.66	41.76	4.39E+03	3.99E+07	0.05																				
	K1608 L	8.88E+03	7.40E+07	0.06	3.66	5.57	1.97E+03	3.28E+07	0.00																				
Mean values	4.42E+03	2.47E+07	0.25	24.62	34.76	2.71E+04	1.18E+09	0.06																					

		U.S. Dollars (\$ Mil)	Normalized Data (%)	U.S. Dollars (\$ Mil)	Normalized Data (%)	U.S. Dollars (\$ Mil)	Normalized Data (%)
KOR15A	K1501 U	0.00	0.00	0.00E+00	34.25	52.09	65.75
	K1502 U	0.01	18.87	6.29E+04	0.00	0.00	67.30
	K1503 U	0.01	11.92	2.98E+04	0.00	0.00	78.00
	K1504 U	0.01	7.57	1.26E+04	0.00	0.00	79.30
	K1505 U	0.01	9.25	1.54E+04	0.00	0.00	79.00
	K1506 U	0.01	10.13	1.69E+04	0.00	0.00	79.00
	K1507 U	0.01	5.55	9.25E+03	0.00	0.00	84.70
	K1508 N	0.01	6.80	9.71E+03	0.00	0.00	88.30
	K1509 N	0.01	5.94	1.19E+04	0.00	0.00	89.30
	K1510 L	0.01	17.23	3.45E+04	0.00	0.00	73.60
	K1511 L	0.01	25.65	1.28E+05	0.00	0.00	69.00
	Mean values	0.01	10.81	3.01E+04	3.11	4.74	77.57
KOR15B	K1512 U	0.01	20.50	7.25E+04	0.00	0.00	71.00
	K1513 U	0.01	5.30	1.41E+04	0.00	0.00	75.30
	K1514 U	0.01	3.70	7.39E+03	0.00	0.00	83.50
	K1515 N	0.01	6.20	6.59E+03	0.00	0.00	85.50
	K1516 N	0.01	6.50	8.64E+03	0.00	0.00	75.30
	K1517 L	0.01	11.31	6.34E+04	7.14	11.96	59.50
	Mean values	0.01	8.92	2.88E+04	1.19	1.99	75.02
KOR16A	K1601 U	0.01	20.50	9.52E+04	0.00	0.00	71.75
	K1602 U	0.01	14.75	5.81E+04	0.00	0.00	63.50
	K1603 U	0.01	14.72	4.27E+04	11.07	16.04	69.00
	K1604 U	0.01	8.25	1.25E+04	8.59	11.73	73.25
	K1605 U	0.01	5.74	7.25E+03	5.41	7.51	72.00
	K1606 N	0.01	7.64	1.16E+04	4.51	6.16	73.34
	K1607 N	0.01	9.00	2.17E+04	0.00	0.00	83.00
	K1608 L	0.00	0.00	0.00E+00	48.00	73.06	65.70
	Mean values	0.01	11.84	4.33E+04	2.77	4.28	71.37

		U.S. Dollars (\$ Mil)	Normalized Data (%)	U.S. Dollars (\$ Mil)	Normalized Data (%)	U.S. Dollars (\$ Mil)	Normalized Data (%)
DER7B	DE707	2.36	4.90	6.24E+04	31.99	66.66	48.00
	DE708	7.00	8.23	2.62E+04	0.00	0.00	85.01
	DE709	13.00	14.55	4.63E+04	0.00	0.00	89.35
	DE710	13.66	18.13	5.77E+04	0.00	0.00	75.34
	DE711	7.33	9.12	1.29E+04	0.00	0.00	80.34
	DE712						
	DE713	20.48	26.25	8.36E+04	13.00	16.67	78.00
	Mean values	10.64	13.53	4.82E+04	7.50	13.89	76.01
HAW-CCD	CCD01 U	0.00	0.00	0.00E+00	52.33	83.49	62.68
	CCD02 U	0.01	12.41	3.20E+04	8.83	11.39	77.50
	CCD03 U	0.01	7.15	1.16E+04	7.15	9.29	77.00
	CCD04 N	0.01	6.44	1.06E+04	6.08	8.03	75.67
	CCD05 N	0.01	5.24	7.79E+03	5.24	7.01	74.68
	CCD06 L	1.75	4.09	2.05E+04	20.01	46.81	42.75
	Mean values	5.50	7.49	1.38E+04	16.61	27.67	68.38
HAW-HPR	HPR01 U	0.00	0.00	0.00E+00	44.00	67.68	65.01
	HPR02 U	0.01	13.31	2.66E+04	7.33	10.25	71.50
	HPR03 U	0.01	10.00	2.03E+04	14.33	17.41	82.34
	HPR04 N	0.01	12.33	2.45E+04	7.66	9.12	84.01
	HPR05 N	0.01	10.28	1.98E+04	6.85	7.90	86.68
	HPR06 L	0.01	12.11	7.97E+04	17.15	22.57	76.00
	Mean values	9.04	11.32	2.85E+04	16.22	22.49	77.59
HAW-KAL	KAL01 U	0.00	0.00	0.00E+00	52.66	84.94	62.00
	KAL02 U	0.01	11.32	5.64E+04	12.66	18.90	67.00
	KAL03 U	0.01	10.00	3.59E+04	13.32	19.11	69.75
	KAL04 N	0.01	15.00	3.54E+04	13.72	16.24	84.68
	KAL05 L	0.00	0.00	0.00E+00	46.25	68.27	67.75
	Mean values	7.26	9.79	2.55E+04	27.72	41.49	70.24

	Fe (%)	Al (%)	Si (%)	Ca (%)	Mg (%)	Na (%)	Normalised Glass (%)	Cr (%)	Normalised Glass (%)	Grinding Loss (%)	Vestibles %
HAW-MAU1	MAU01	0.00	0.00	0.00E+00	24.66	72.51	34.01	41.33			
	MAU02	0.01	5.47	6.02E+04	6.32	13.89	45.50	17.00			
	MAU03	0.01	5.75	3.25E+04	8.23	18.64	44.25	28.25			
	MAU04	0.00	0.00	0.00E+00	28.26	84.97	33.25	46.75			
	Mean values	0.01	2.81	2.32E+04	16.87	47.50	39.25	33.33			
HAW-MAU2	MAU05	11.23	19.21	2.45E+05	11.23	19.21	58.50	15.00			
	MAU06	19.88	33.54	1.07E+05	0.37	0.62	73.00	11.00			
	MAU07	11.33	15.81	2.24E+04	0.00	0.00	71.67	6.33			
	MAU08	17.33	25.74	3.64E+04	0.00	0.00	67.34	7.33			
	MAU09	7.33	12.56	4.00E+04	0.00	0.00	58.34	25.33			
	MAU10	9.00	15.00	2.12E+04	0.00	0.00	60.00	8.00			
	Mean values	12.68	20.31	7.86E+04	1.93	3.31	64.81	12.17			
HAW-HWY	HWY01	21.28	28.56	9.09E+04	13.04	17.50	74.50	22.00			
	HWY02	9.75	13.45	4.28E+04	0.00	0.00	72.50	21.50			
	HWY03	11.50	16.67	5.31E+04	0.00	0.00	69.00	23.00			
	HWY04	11.00	15.17	2.15E+04	0.00	0.00	72.50	24.25			
	HWY05	18.75	25.17	8.01E+04	0.00	0.00	74.50	18.00			
	HWY06	0.00	0.00	5.77E+04	76.33	91.59	83.34	16.66			
	Mean values	12.05	16.50	5.77E+04	14.90	18.18	74.39	20.90			

APPENDIX C XRF RESULTS: INTRA-FLOW GEOCHEMICAL VARIATIONS

	Fe (%)	Al (%)	Si (%)	Ca (%)	Mg (%)	Na (%)	Normalised Glass (%)	Cr (%)	Normalised Glass (%)	Grinding Loss (%)	Vestibles %
Fe2O3 (%)	11.41	11.48	11.18	11.41	11.26	11.34	11.34	11.34	11.24	11.11	10.92
MnO (%)	0.13	0.16	0.15	0.15	0.15	0.15	0.15	0.15	0.15	0.15	0.12
TiO2 (%)	2.11	2.17	2.05	2.04	2.06	2.13	2.13	2.13	2.03	2.07	2.07
CaO (%)	7.77	8.29	8.66	8.53	8.53	8.45	8.45	8.45	8.46	8.49	8.63
K2O (%)	1.47	1.45	1.34	1.33	1.36	1.40	1.40	1.40	1.33	1.39	1.44
SO3 (%)	0.00	0.03	0.00	0.18	0.00	0.03	0.03	0.03	0.00	0.00	0.00
P2O5 (%)	0.44	0.48	0.45	0.44	0.45	0.45	0.45	0.45	0.45	0.44	0.41
SiO2 (%)	50.00	49.85	48.98	49.23	49.23	49.32	49.32	49.32	49.53	49.91	49.82
Al2O3 (%)	14.97	14.93	14.08	14.01	14.19	14.14	14.21	14.21	14.11	14.38	14.59
MgO (%)	6.95	5.93	8.13	8.20	8.13	7.91	8.21	8.21	8.98	8.40	7.03
Na2O (%)	3.53	3.84	3.46	3.50	3.52	3.54	3.46	3.46	3.65	3.73	3.59
V (ppm)	156	170	168	163	154	163	170	170	160	176	165
Cr (ppm)	335	333	360	352	354	354	329	347	369	347	331
Co (ppm)	48	49	46	56	47	54	44	48	44	48	35
Ni (ppm)	351	174	186	203	214	198	192	188	203	188	170
Cu (ppm)	94	132	60	129	49	167	149	48	43	48	60
Zn (ppm)	105	115	109	109	110	115	114	110	110	106	110
Ga (ppm)	31	29	24	29	29	32	33	26	27	26	31
Ba (ppm)	401	427	394	388	425	395	379	378	370	408	401
La (ppm)	34	57	44	35	10	32	67	64	31	64	34
Ce (ppm)	29	56	34	38	44	52	55	55	32	82	51
Nd (ppm)	26	29	15	16	34	18	31	32	20	40	31
Nb (ppm)	31	32	31	29	31	30	32	31	32	31	32
Zr (ppm)	176	180	169	168	171	177	177	172	167	181	175
Y (ppm)	26	24	22	23	23	24	24	24	23	24	25
Sr (ppm)	537	555	540	536	537	536	524	524	525	527	535
Rb (ppm)	36	35	32	32	32	36	33	37	34	37	36
U (ppm)	7	7	3	7	7	6	10	11	12	11	7
Pb (ppm)	11	11	1	0	9	1	3	8	5	7	11
Th (ppm)	7	9	5	9	11	12	6	9	8	9	8
Ph											
Sc (ppm)	21	25	31	32	32	33	28	33	22	28	32
F (%)	0	0	0	0	0	0	0	0	0	0	0
Cl (ppm)	85	99	79	68	99	123	98	170	123	139	89
As (ppm)	0	0	0	0	0	0	0	0	0	0	0
Sb (ppm)	0	0	0	0	0	0	0	0	0	0	0
Sn (ppm)	0	0	0	0	0	0	0	0	0	0	0
Mo (ppm)	0	0	0	0	0	0	0	0	0	0	0
Bi (ppm)	0	0	0	0	0	0	0	0	0	0	0
loi	1.08	0.97	1.11	0.47	0.65	0.42	0.39	-0.47	-0.52	0.30	1.08
F correction	0.00	0.00	0.00	0.00	0.00	0.00	0.00	0.00	0.00	0.00	0.00
Total	100.11	99.83	99.83	99.73	99.77	99.54	99.64	99.85	99.65	100.08	99.94

	12.34	12.24	12.36	12.55	12.46	12.45	13.97	13.44	14.20	13.55	14.18	10.97	13.09
Fe2O3 (%)	12.34	12.24	12.36	12.55	12.46	12.45	13.97	13.44	14.20	13.55	14.18	10.97	13.09
MnO (%)	0.16	0.16	0.16	0.16	0.16	0.17	0.18	0.14	0.17	0.14	0.21	0.16	0.20
TiO2 (%)	2.26	2.31	2.23	2.26	2.12	2.22	2.68	2.67	2.56	2.55	2.61	2.50	2.82
CaO (%)	9.19	8.92	8.73	8.60	8.61	8.92	7.34	7.34	7.04	6.68	7.19	9.51	6.87
K2O (%)	1.21	1.23	1.17	1.21	1.11	1.19	1.71	1.70	1.73	1.75	1.83	1.86	2.04
SO3 (%)	0.00	0.00	0.01	0.00	0.00	0.00	0.00	0.00	0.00	0.00	0.00	0.00	0.00
P2O5 (%)	0.43	0.41	0.39	0.42	0.37	0.39	1.44	1.41	1.31	1.32	1.32	1.36	1.66
SiO2 (%)	48.63	49.49	49.18	49.26	48.98	48.98	48.73	49.16	49.57	49.18	47.99	48.09	49.65
Al2O3 (%)	14.38	14.43	14.07	14.03	13.94	13.97	14.70	14.59	13.98	13.72	14.11	13.83	14.89
MgO (%)	6.72	6.98	7.91	8.17	9.13	7.67	3.93	3.43	3.46	5.04	3.78	3.78	1.86
Na2O (%)	3.39	3.40	3.37	3.38	3.27	3.23	3.67	3.81	3.67	3.59	3.80	3.84	4.04
V (ppm)	197	194	198	187	183	186	163	160	210	156	149	181	153
Cr (ppm)	325	315	307	332	365	347	128	124	171	127	117	123	80
Co (ppm)	48	49	56	53	53	59	42	29	27	48	32	35	22
Ni (ppm)	175	279	191	190	233	226	71	130	71	88	83	71	46
Cu (ppm)	70	104	111	73	51	74	42	45	29	43	31	31	39
Zn (ppm)	119	117	118	124	121	114	152	156	156	153	140	140	156
Ga (ppm)	27	31	32	27	28	28	31	33	25	26	31	25	32
Ba (ppm)	280	321	309	321	282	280	515	517	581	432	449	479	478
La (ppm)	20	31	50	30	35	0	51	18	34	72	34	28	28
Ce (ppm)	74	47	61	69	32	58	132	112	87	96	83	98	88
Nd (ppm)	31	25	33	17	12	35	74	49	44	56	44	41	41
Nb (ppm)	27	28	26	27	25	26	49	46	44	44	43	44	55
Zr (ppm)	175	176	167	176	157	170	295	291	262	273	283	280	320
Y (ppm)	26	29	25	27	23	27	43	40	37	37	36	38	44
Sr (ppm)	468	462	447	446	437	450	555	547	576	489	513	920	546
Rb (ppm)	27	25	27	27	25	30	41	39	29	34	44	39	47
U (ppm)	4	8	8	10	6	9	8	6	0	7	9	0	7
Pb (ppm)	8	7	5	5	0	4	1	5	7	0	4	7	8
Th (ppm)	7	9	6	11	5	6	10	9	4	10	9	4	11
Rn													
Sc (ppm)	35	39	37	32	30	26	31	27	31	33	31	27	27
F (%)	0	0	0	0	0	0	0	0	0	0	0	0	0
Cl (ppm)	89	86	87	83	92	86	114	103	0	116	116	0	99
As (ppm)	0	0	0	0	0	0	0	0	0	0	0	0	0
Sb (ppm)	0	0	0	0	0	0	0	0	0	0	0	0	0
Sn (ppm)	0	0	0	0	0	0	0	0	0	0	0	0	0
Mo (ppm)	0	0	0	0	0	0	0	0	0	0	0	0	0
Bi (ppm)	0	0	0	0	0	0	0	0	0	0	0	0	0
loi	1.07	0.09	0.14	-0.09	-0.16	0.49	1.15	1.50		2.17	2.40		2.14
F correction	0.00	0.00	0.00	0.00	0.00	0.00	0.00	0.00		0.00	0.00		0.00
Total	100.00	99.90	99.95	100.18	100.21	99.90	99.75	99.44	99.63	99.92	99.65	100.53	99.49

	12.70	12.46	12.53	12.62	12.51	13.32	12.66	11.30	12.42	12.85	12.71	12.35
Fe2O3 (%)	12.70	12.46	12.53	12.62	12.51	13.32	12.66	11.30	12.42	12.85	12.71	12.35
MnO (%)	0.16	0.17	0.17	0.17	0.17	0.18	0.18	0.16	0.17	0.17	0.18	0.17
TiO2 (%)	3.08	3.01	3.05	3.10	3.05	3.51	2.06	2.25	2.06	2.14	2.05	2.21
CaO (%)	10.06	9.91	10.01	10.14	9.94	9.17	9.71	10.59	9.94	9.26	9.64	10.09
K2O (%)	0.68	0.66	0.69	0.67	0.65	0.75	0.32	0.36	0.31	0.41	0.31	0.34
SO3 (%)	0.00	0.00	0.15	0.00	0.00	0.00	0.04	0.05	0.00	0.01	0.00	0.00
P2O5 (%)	0.35	0.34	0.34	0.35	0.34	0.42	0.21	0.21	0.20	0.24	0.19	0.22
SiO2 (%)	51.51	51.13	50.97	52.04	51.19	52.03	50.61	51.87	50.41	50.76	51.23	51.64
Al2O3 (%)	13.18	13.18	13.08	13.31	13.19	12.92	11.70	12.95	11.82	11.16	11.50	12.05
MgO (%)	6.24	6.24	6.21	6.25	6.25	5.46	12.21	7.88	11.88	11.33	11.66	10.44
Na2O (%)	2.50	2.55	2.85	2.55	2.47	2.80	1.89	2.10	1.81	2.03	1.86	1.96
V (ppm)	355	346	336	339	356	411	262	281	252	256	250	271
Cr (ppm)	176	165	168	168	179	152	905	510	760	748	730	642
Co (ppm)	36	38	37	39	37	31	68	45	65	65	67	57
Ni (ppm)	91	93	92	92	96	77	348	151	312	328	327	252
Cu (ppm)	124	129	113	117	121	128	88	101	79	100	76	104
Zn (ppm)	112	110	103	106	111	127	101	95	96	104	97	101
Ga (ppm)	23	23	22	23	22	24	18	20	18	18	17	19
Ba (ppm)	155	171	164	173	168	198	69	75	86	97	89	83
La (ppm)												
Ce (ppm)	49	41	42	40	40	39	19	44	10	32	1	15
Nd (ppm)												
Nb (ppm)	17	18	17	17	16	19	7	8	7	9	7	8
Zr (ppm)	186	188	185	189	187	222	109	123	109	132	108	118
Y (ppm)	34	32	33	34	33	40	24	26	23	28	23	25
Sr (ppm)	393	397	395	404	395	389	261	305	269	268	263	275
Rb (ppm)	15	15	15	16	15	16	9	10	7	9	8	8
U (ppm)	0	0	0	0	0	0	0	0	0	0	0	0
Pb (ppm)	4	4	5	5	5	5	5	4	4	5	4	4
Th (ppm)	1	0	0	1	0	0	0	0	0	0	0	0
Rn												
Sc (ppm)												
F (%)												
Cl (ppm)	0	0	0	0	0	0	0	0	0	0	0	0
As (ppm)	0	0	0	0	0	0	0	0	0	0	0	0
Sb (ppm)	0	0	0	0	0	0	0	0	0	0	0	0
Sn (ppm)	6	2	0	0	4	5	0	0	0	0	2	4
Mo (ppm)	0	1	3	2	3	2	2	1	0	1	1	1
Bi (ppm)												
loi												
F correction												
Total	100.45	99.67	100.05	101.20	99.75	100.55	101.59	99.12	101.02	100.35	101.33	101.47

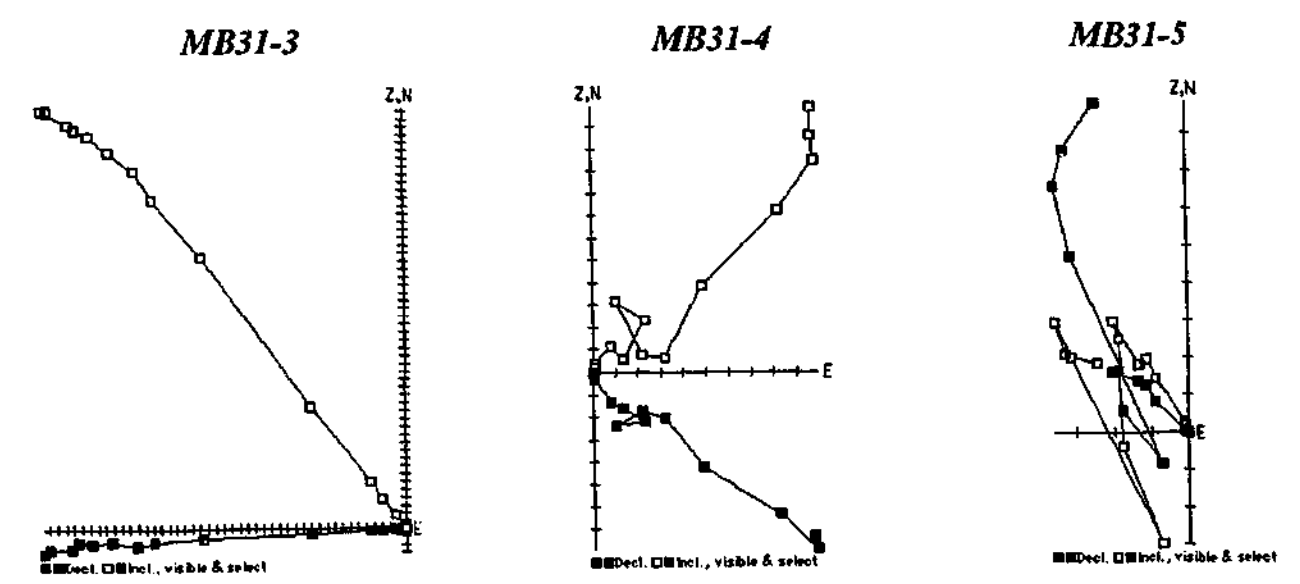
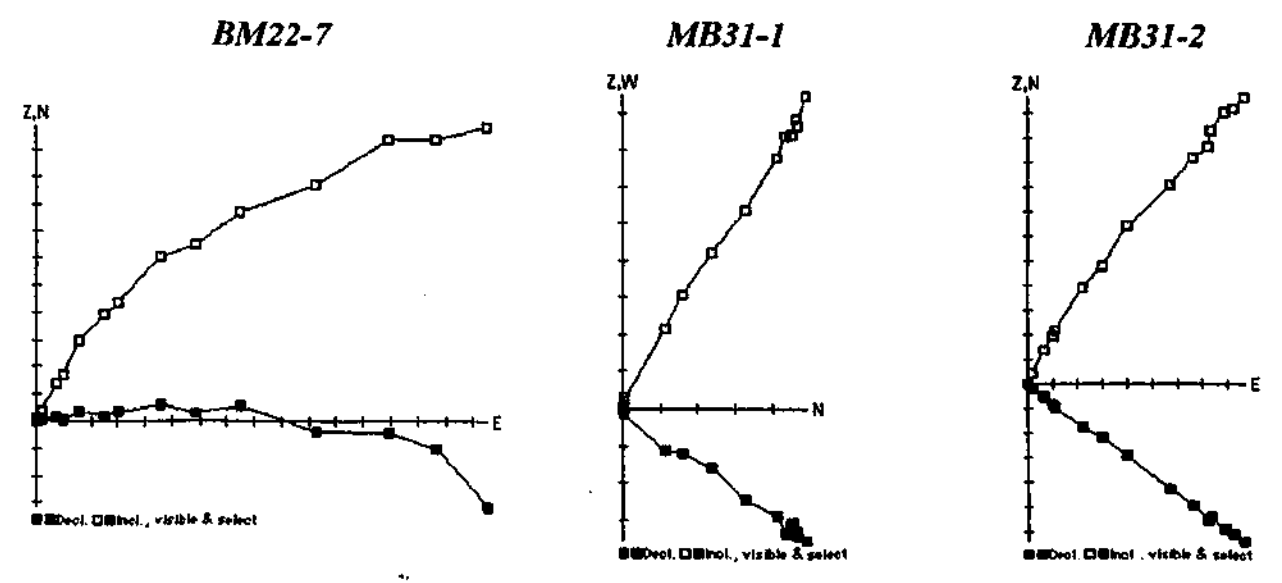
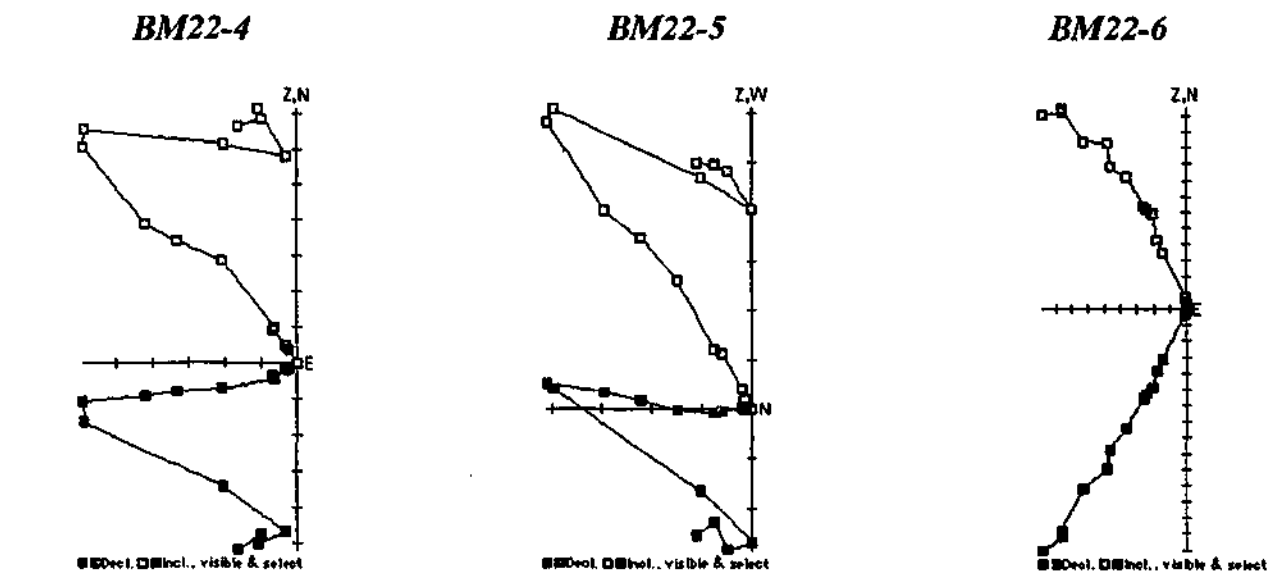
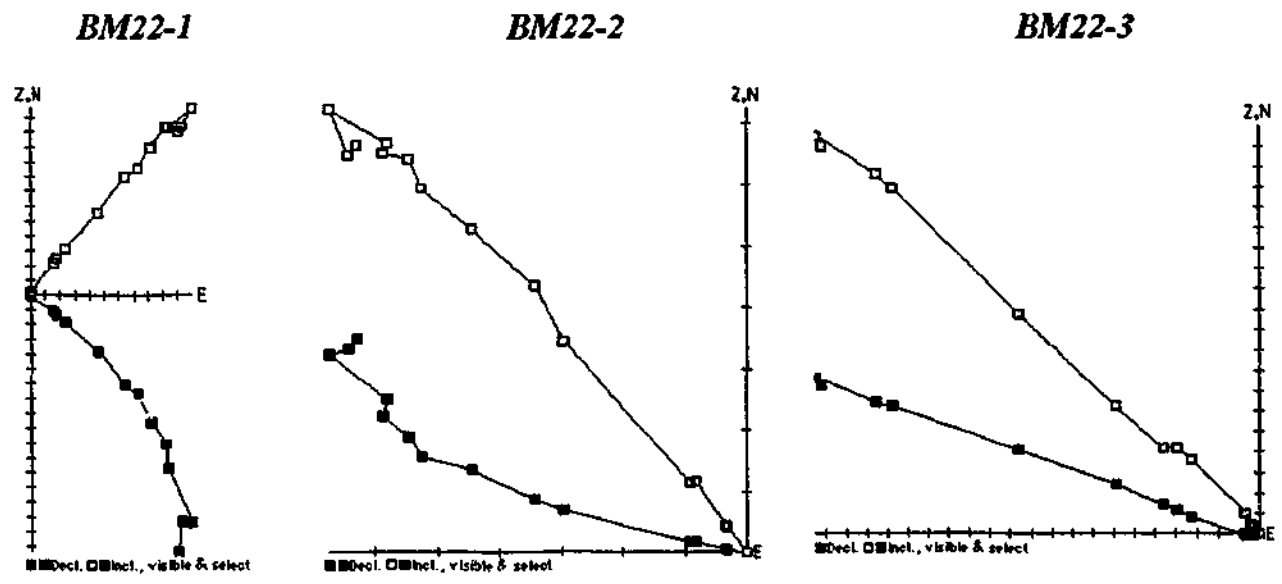
APPENDIX D

PALAEOMAGNETIC INCLINATION RESULTS

All Zijderveld plots constructed in this study are presented on the following pages. The inclination values determined from the plots are given in the Table below. Group (3) samples are represented by a ?; other samples that have been discarded from the magnetostratigraphic study are in bold type (*Q* values less than 2, or struck by lightning); and samples considered to have been upside-down are italicised. The average inclination values, standard deviations (S.D.) and standard errors (S.E.) for entire eruption packages are on the facing page.

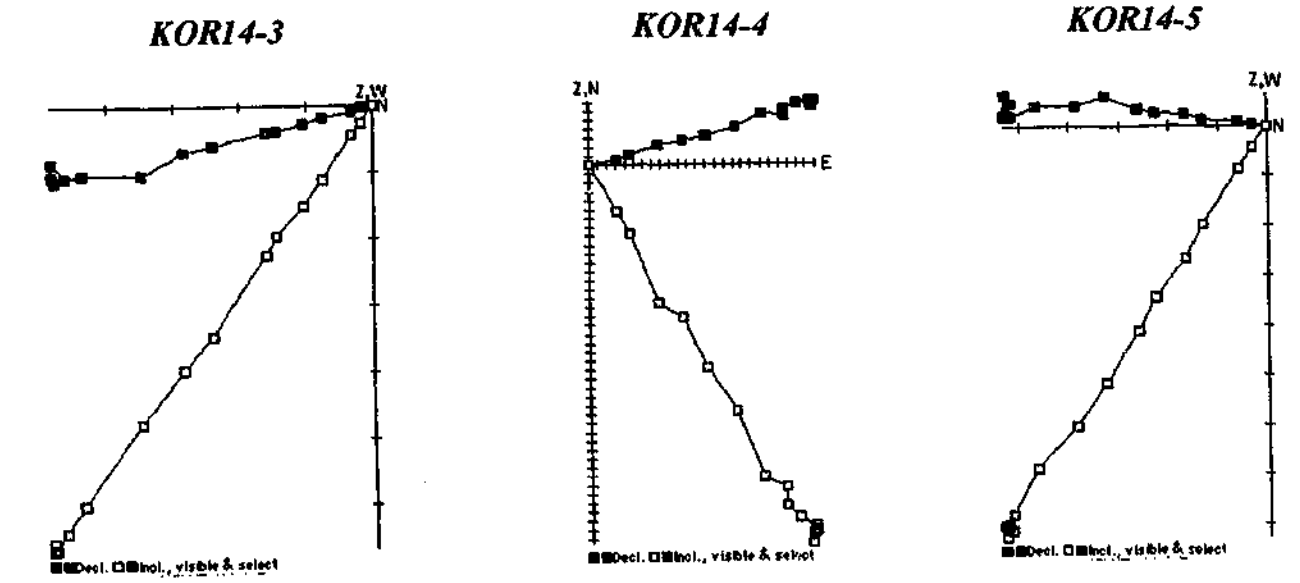
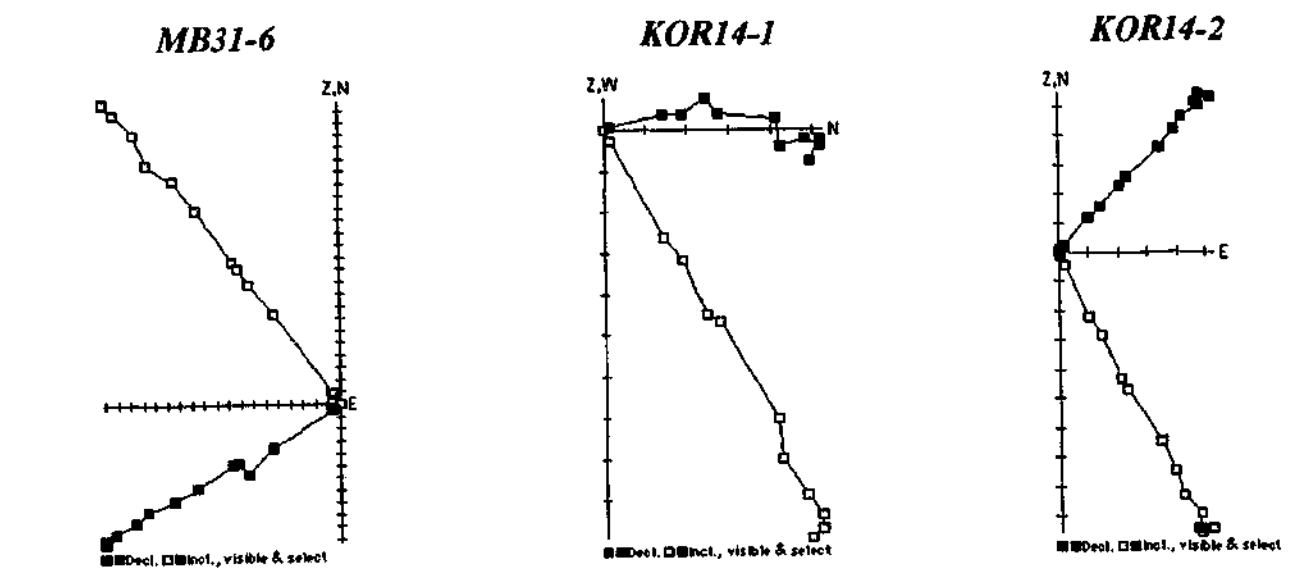
Sample no.	BM22	MB31	KOR14	KOR16	KOR15	DER7	PYW7	TAR12	TRU50
1	-42.7	-53.3	60.0	-57.4	20.9	56.7	61.3	?	
2	-48.5	-55.7	55.7	58.6	?	54.9	42.7	50.3	46.0
3	-41.9	-53.4	55.1	52.1	50.3	60.9	21.5	54.6	49.3
4	-52.2	?	62.5	58.7	52.4	57.9	-8.5	53.5	49.6
5	-60.1	-48.2	56.5	58.7	51.2	?	54.8	54.2	56.5
6	-45.6	-48.9	55.8	59.0	51.8	47.2	50.0	44.3	52.8
7	-61.2		58.7	58.6	59.1	53.5	-64.2	47.1	-57.7
8			58.2	51.8	65.8	53.3	-60.2	49.9	
9			57.3	57.7	55.8	53.0	-59.7	49.9	
10			-65.5	58.3	59.6	48.6	-58.1	48.6	66.1
11			-61.9	-67.8	62.4	63.1	-58.7	51.7	-57.4
12			-65.8	?	57.3	59.5	-56.7	48.3	-60.6
13			-65.4	-71.7	55.8	59.2	-60.7	-52.4	58.7
14			?		57.7	63.1	-58.5	46.6	-52.6
15			79.0	-60.2	59.1	61.3	-57.8	51.8	50.1
16			75.2	?	58.8	64.0	-60.4	53.3	58.8
17			79.6	-60.9	?	64.5	-57.9	-60.9	64.9
18			79.3	-58.3	-57.2	53.8	-63.1	-64.5	59.6
19				60.3	-61.4	47.5	55.0	?	63.5
20				?	?	59.8	-55.8	-63.5	57.8
21				74.8	?	55.5	-57.4	-61.3	-60.0
22					76.5	-67.1	-58.5		?
23						-66.2	-63.5		62.0
24						-71.1	-62.7		49.8
25						-69.3	-61.8		51.0
26						23.5	-69.1		
27						?	72.6		
28							-64.3		
29							-69.4		
30							?		
31							77.1		
32							-61.7		
33							-63.9		

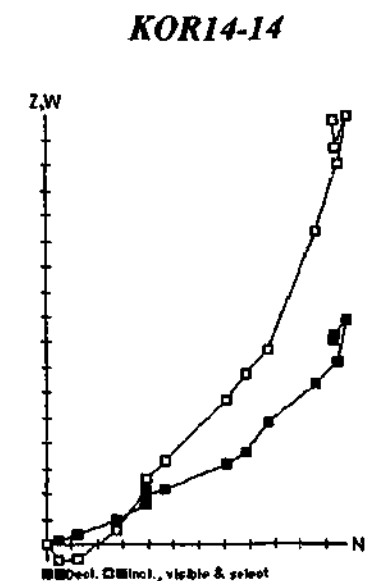
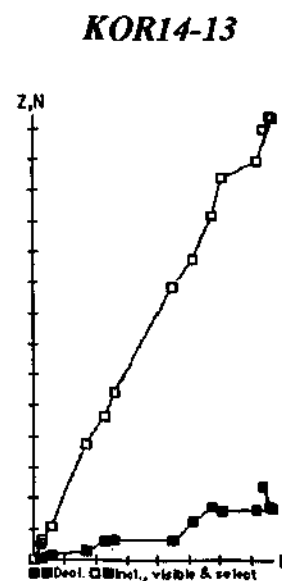
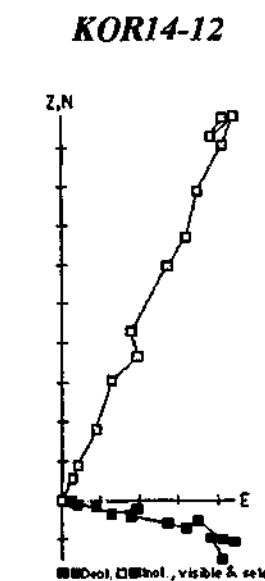
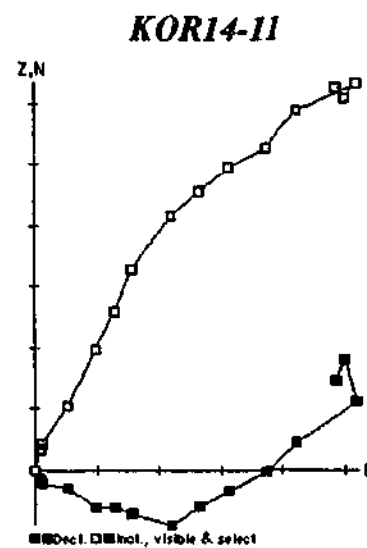
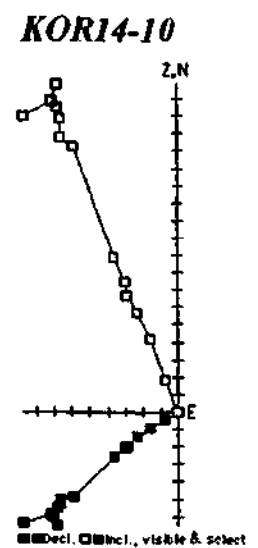
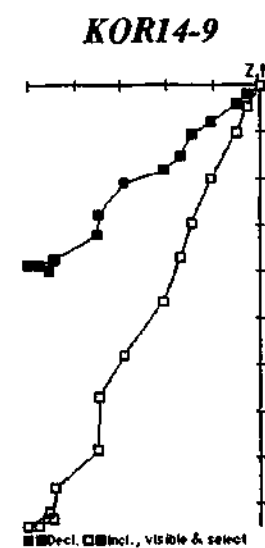
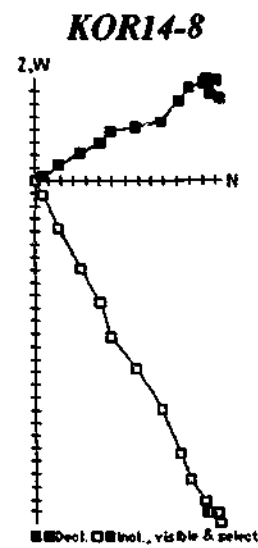
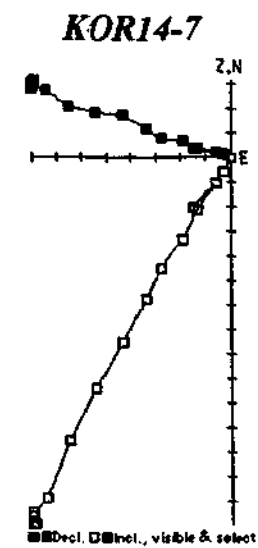
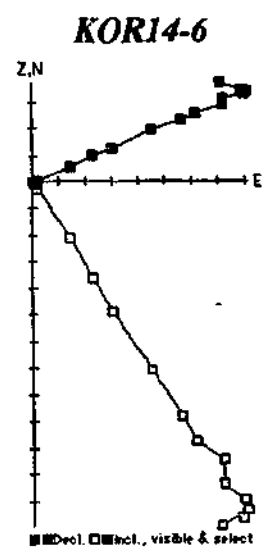
Eruption Package no.	BM22	MB31	KOR14	KOR16	KOR15	DER7	PYW7	TAR12	TRU50
I-	-46.3	-53.3	57.8	57.1	45.3	57.6	52.2	50.3	51.6
Average									
S.D.	4.9		2.4	2.8	13.7	2.5	7.8		3.9
S.E.	4.9		1.6	1.7	12.2	2.5	7.8		2.8
II	-55.6	-52.7	-64.7	-69.8	59.1	47.2	-59.0	50.4	-61.4
	8.7	3.5	1.8		3.0		2.5	3.1	4.4
	10.1	4.0	1.8		1.9		1.3	1.7	5.1
III			78.3	-59.8	-57.2	53.4	-61.0	-63.0	51.4
			2.1	1.3				1.9	
			2.1	1.6				1.9	
IV				60.3	61.4	50.8	-62.3	-61.3	60.9
									2.6
									2.0
V						59.2	-69.1		
						5.2			
						3.1			
VI						-68.4	-64.8		
						2.2	3.3		
						2.2	3.3		
VII						23.5			



? Group (3)

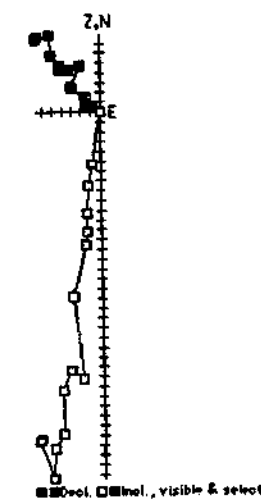
? Q<2



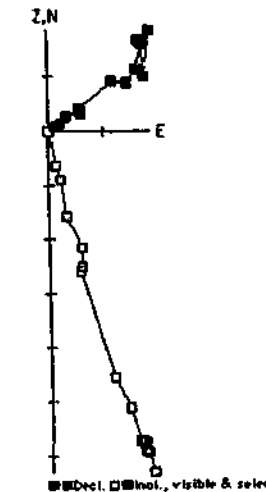


? Group (3)

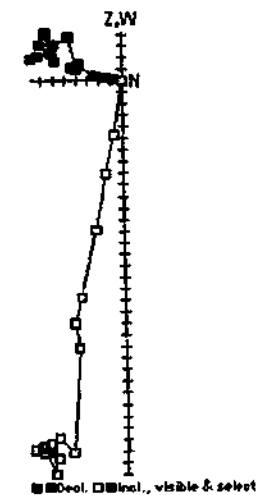
KOR14-15



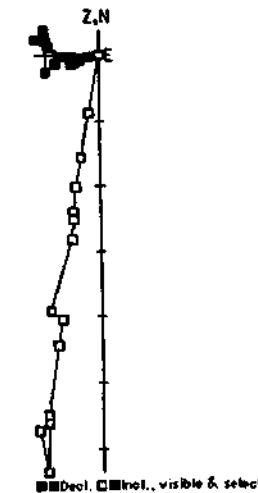
KOR14-16



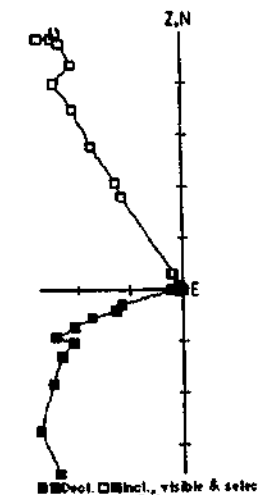
KOR14-17



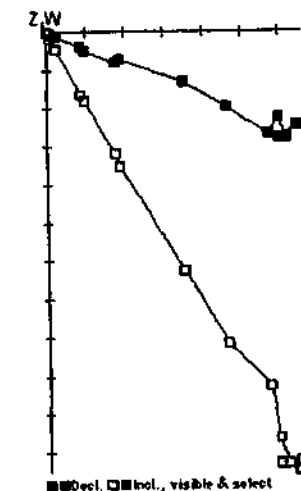
KOR14-18



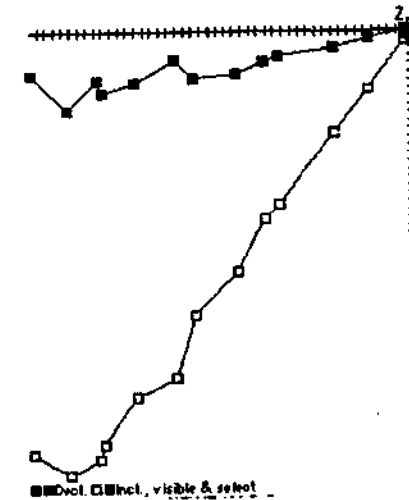
KOR16-1



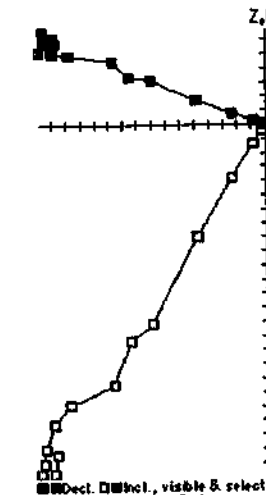
KOR16-2



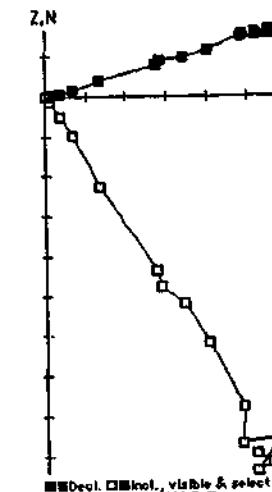
KOR16-3



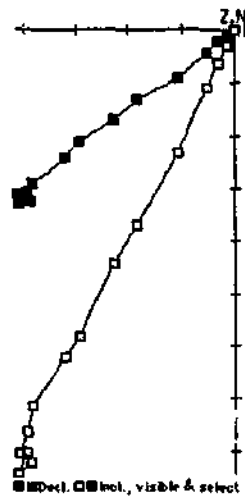
KOR16-4



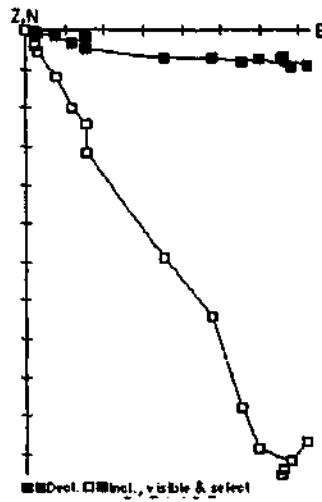
KOR16-5



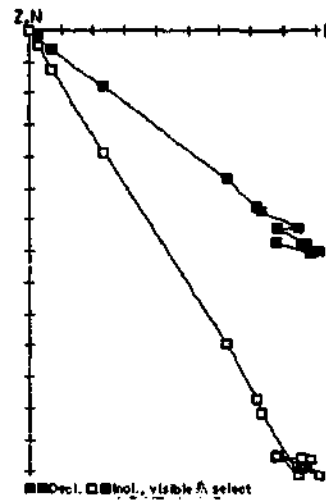
KOR16-6



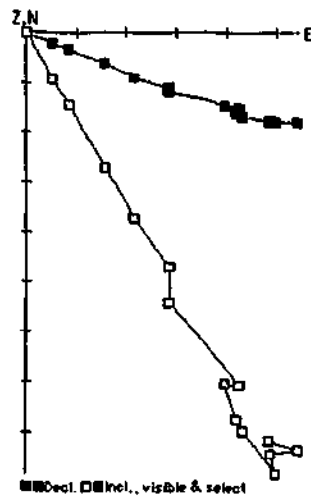
KOR16-7



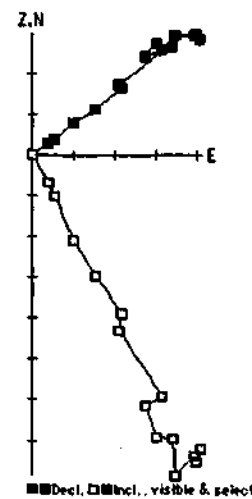
KOR16-8



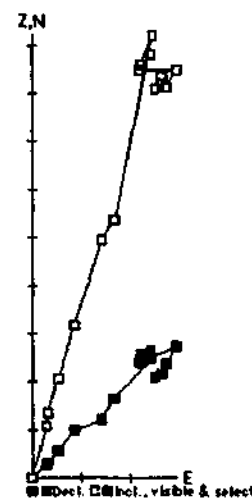
KOR16-9



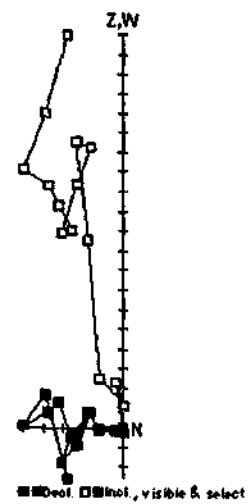
KOR16-10



KOR16-11

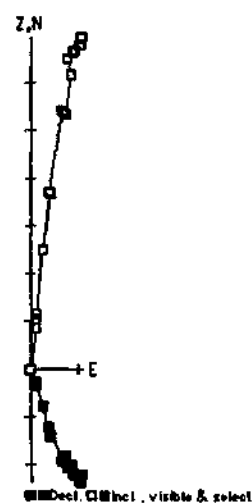


KOR16-12

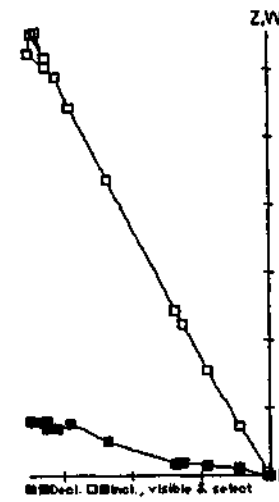


? Group (3)

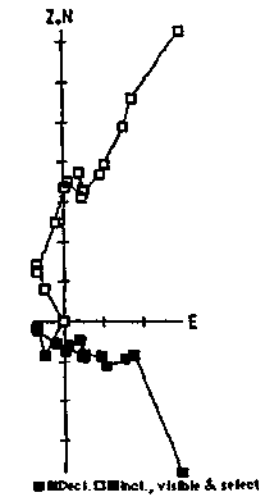
KOR16-13



KOR16-15

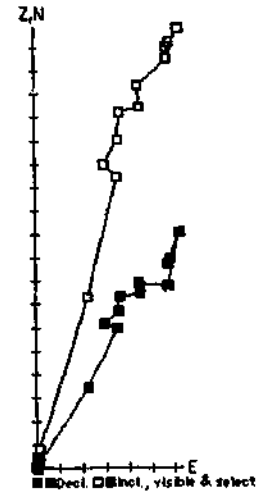


KOR16-16

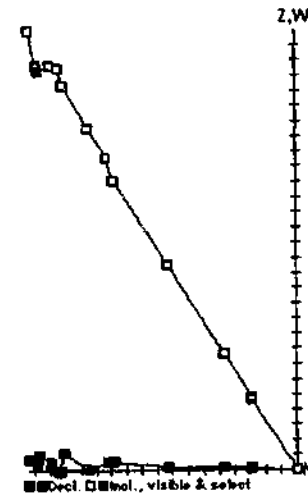


? Group (3)

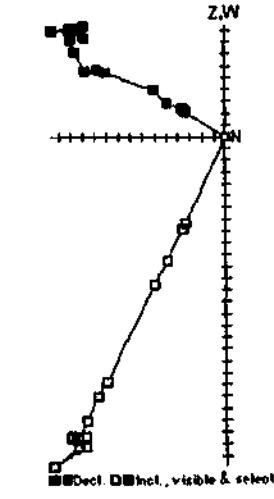
KOR16-17



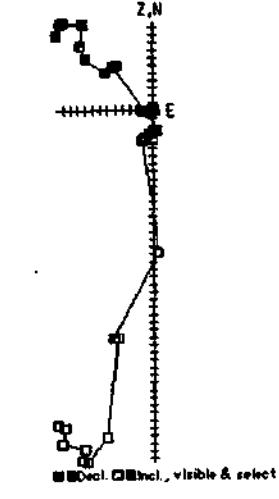
KOR16-18



KOR16-19

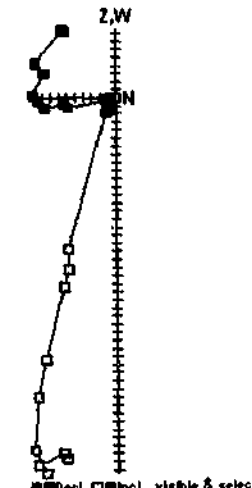


KOR16-20



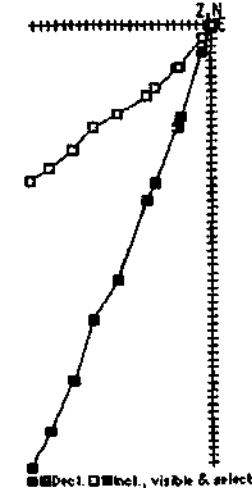
? Group (3)

KOR16-21

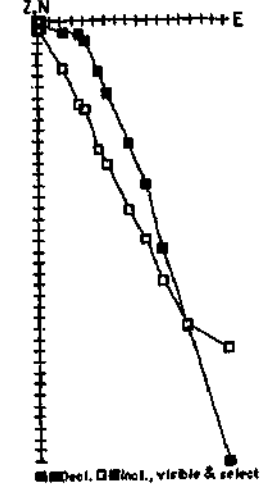


? Q<2

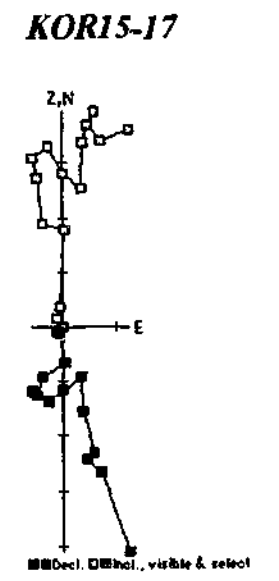
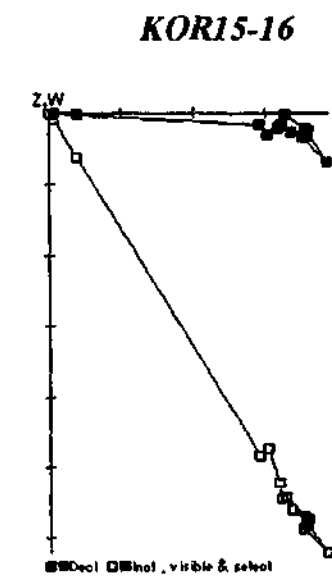
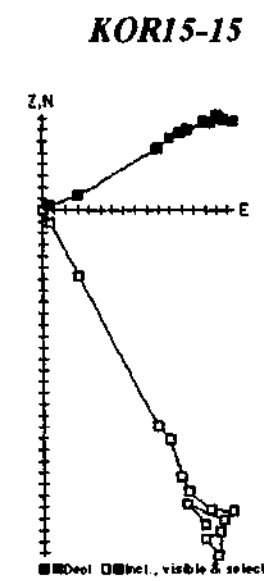
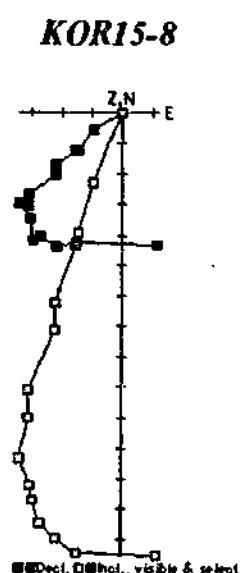
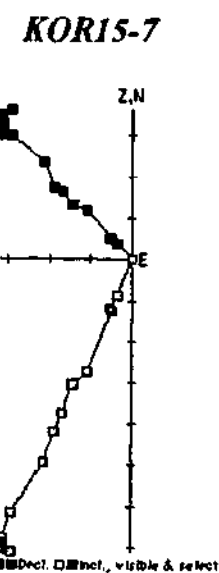
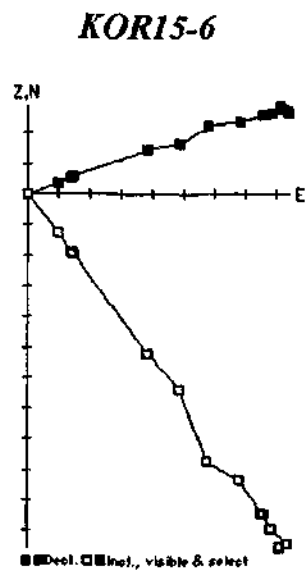
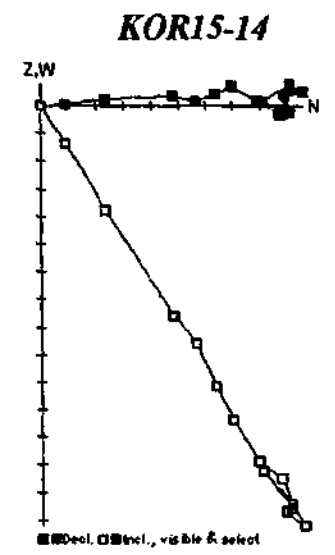
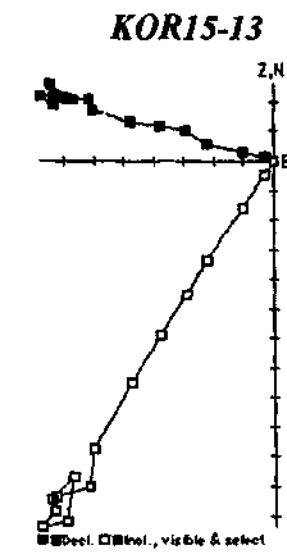
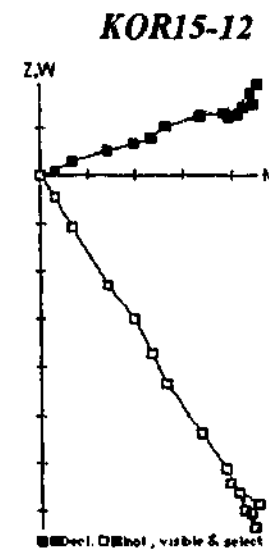
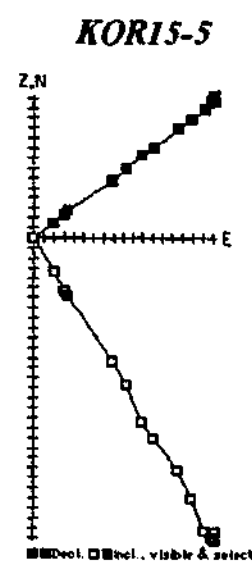
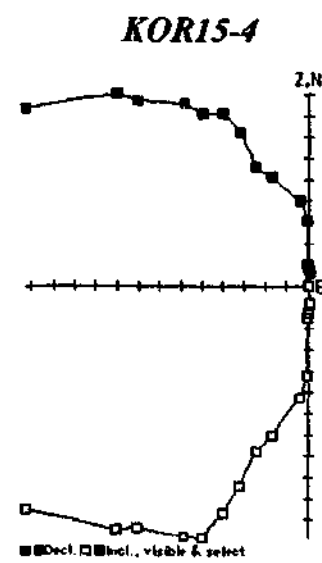
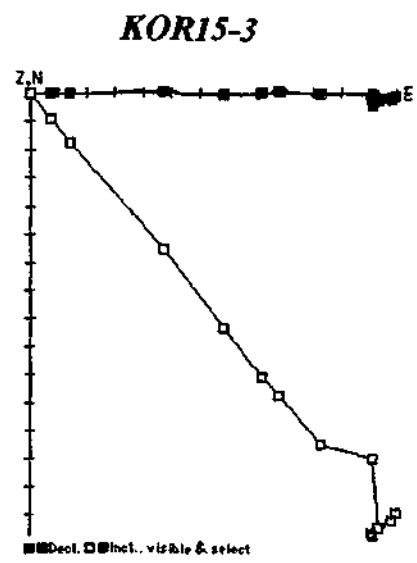
KOR15-1



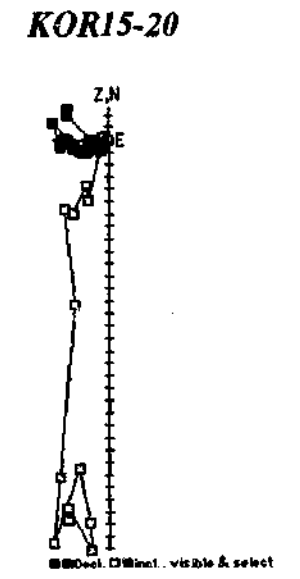
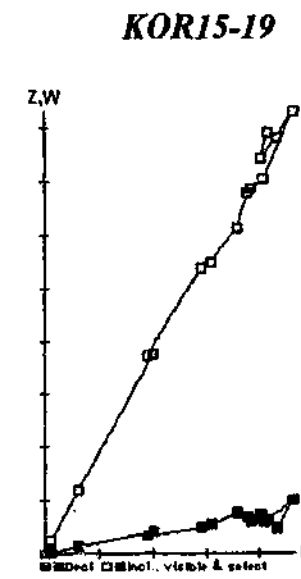
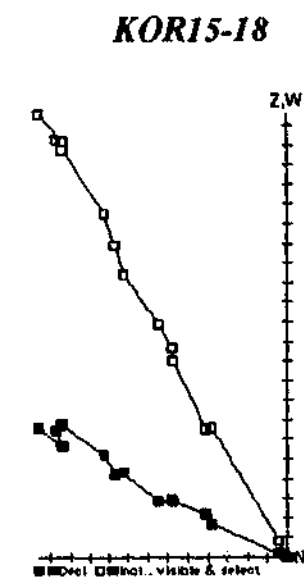
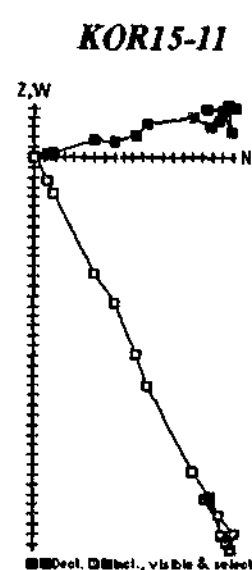
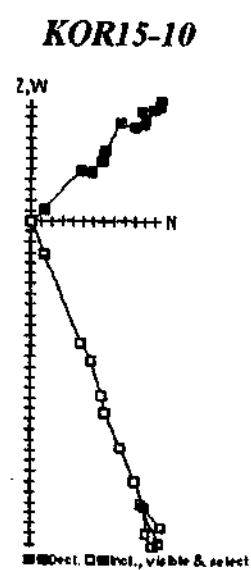
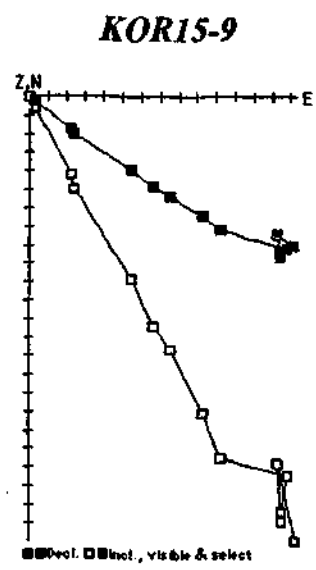
KOR15-2



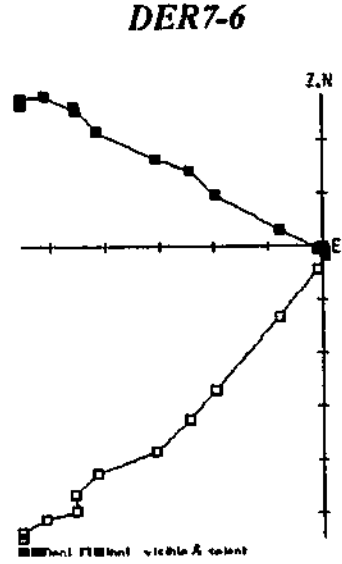
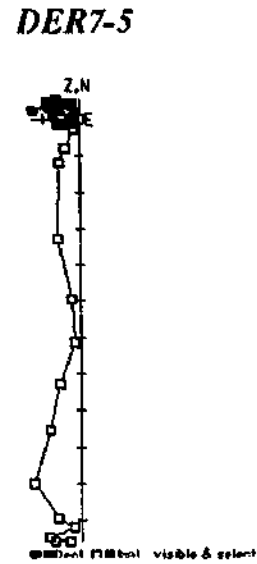
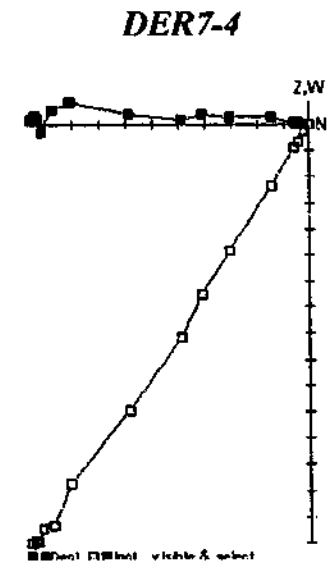
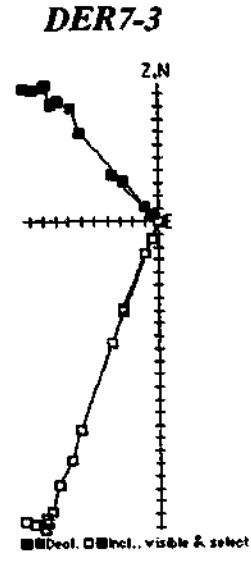
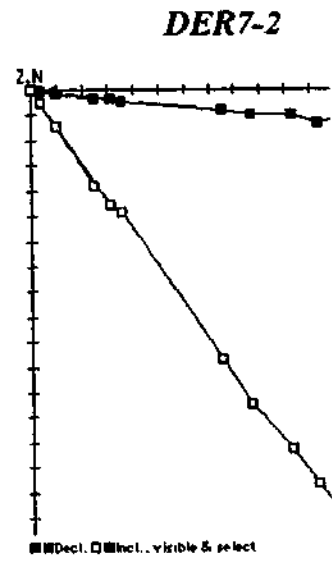
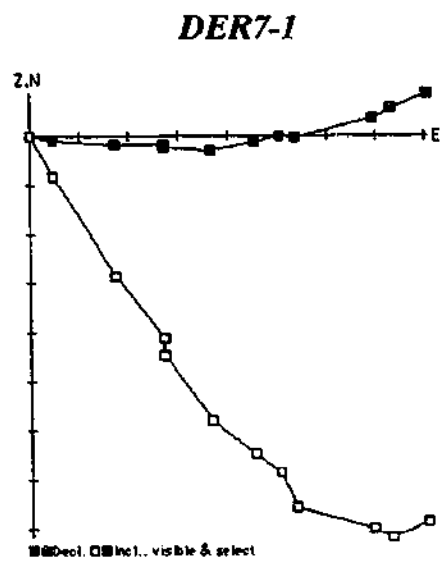
? Group (3)



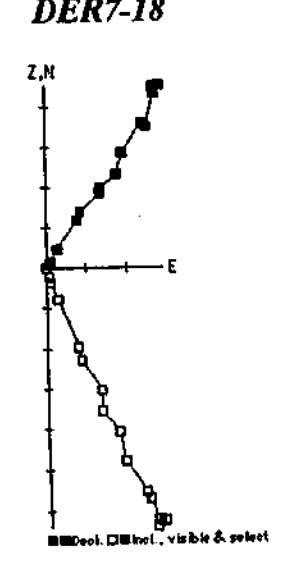
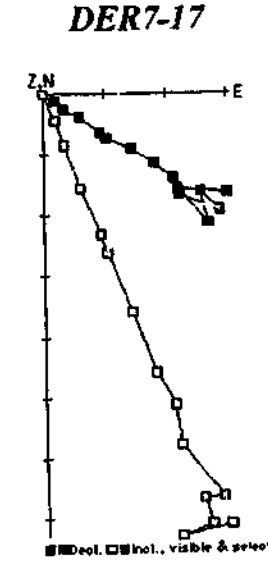
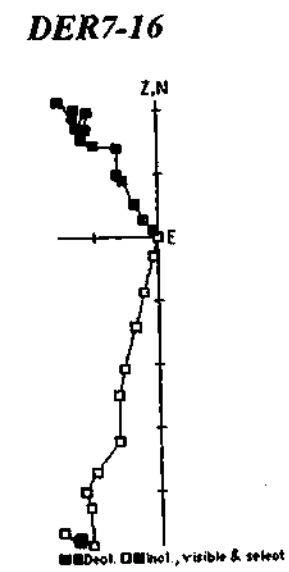
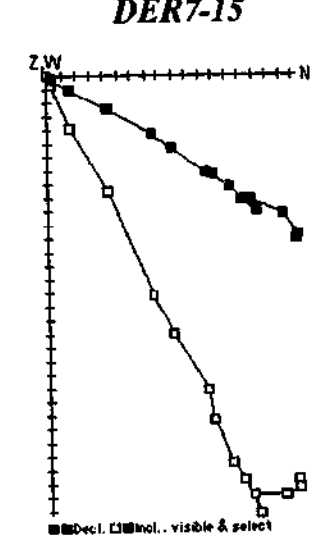
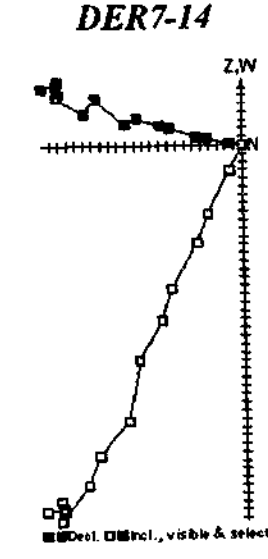
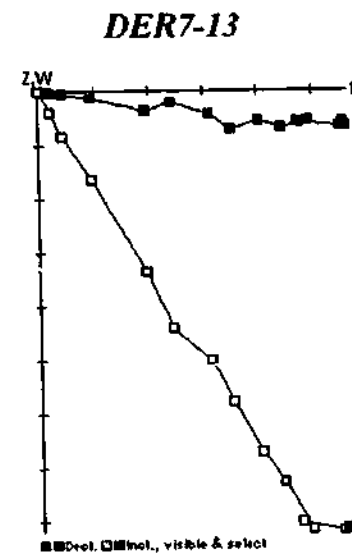
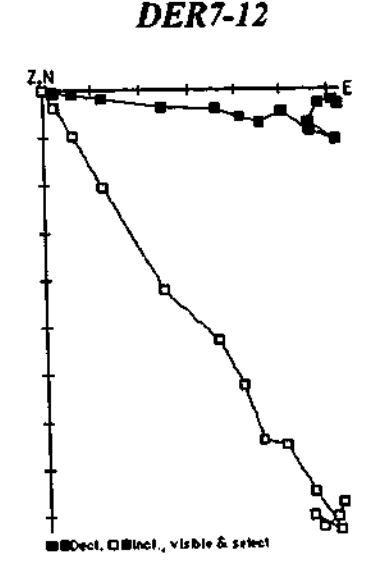
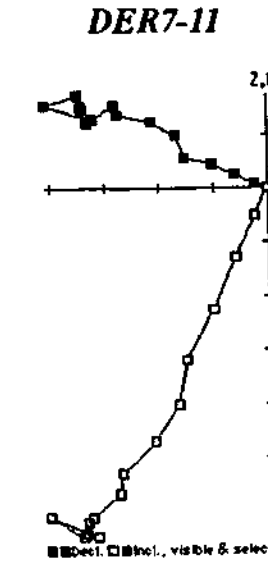
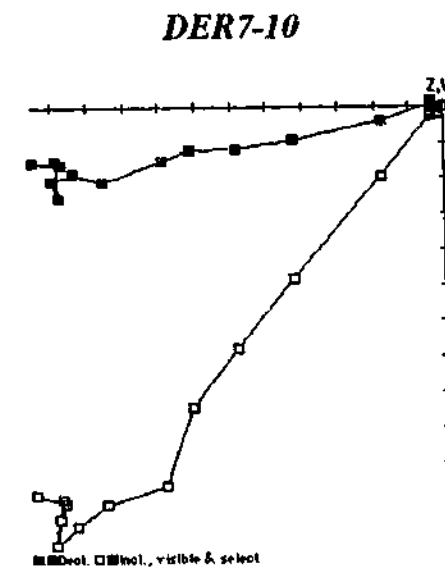
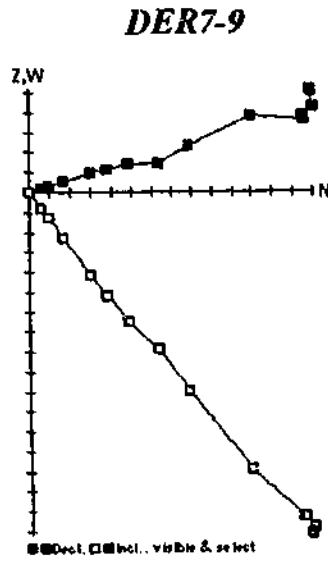
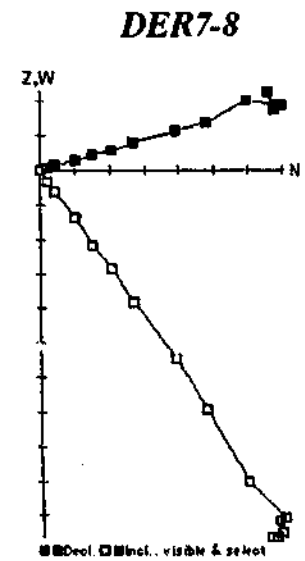
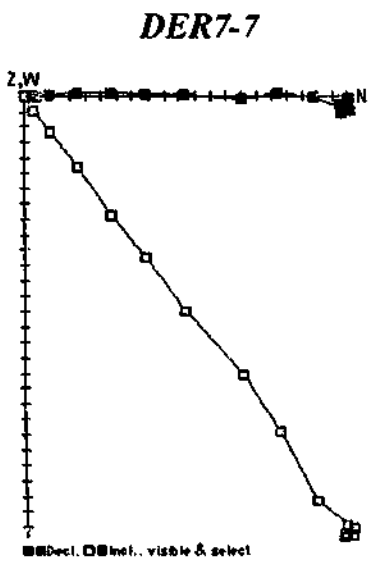
? Group (3)

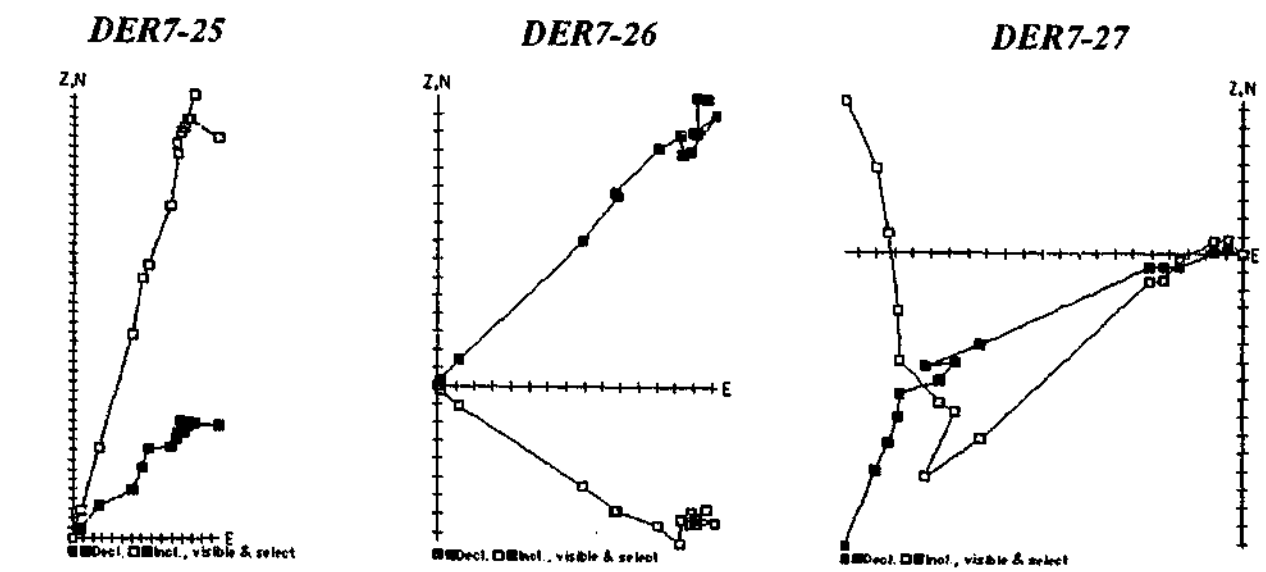
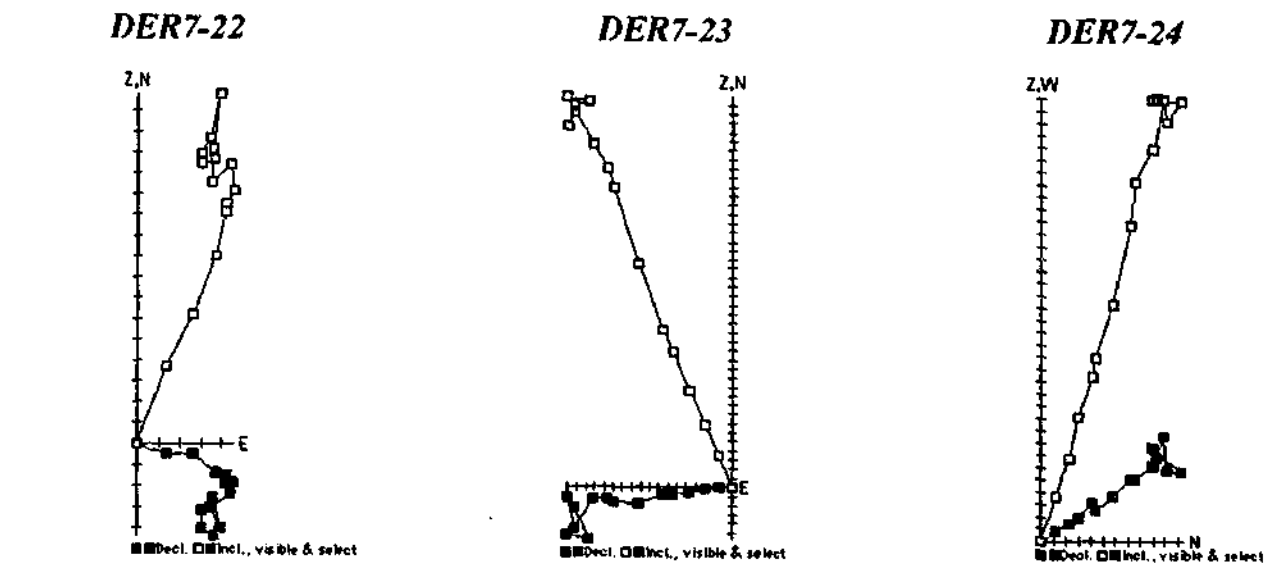
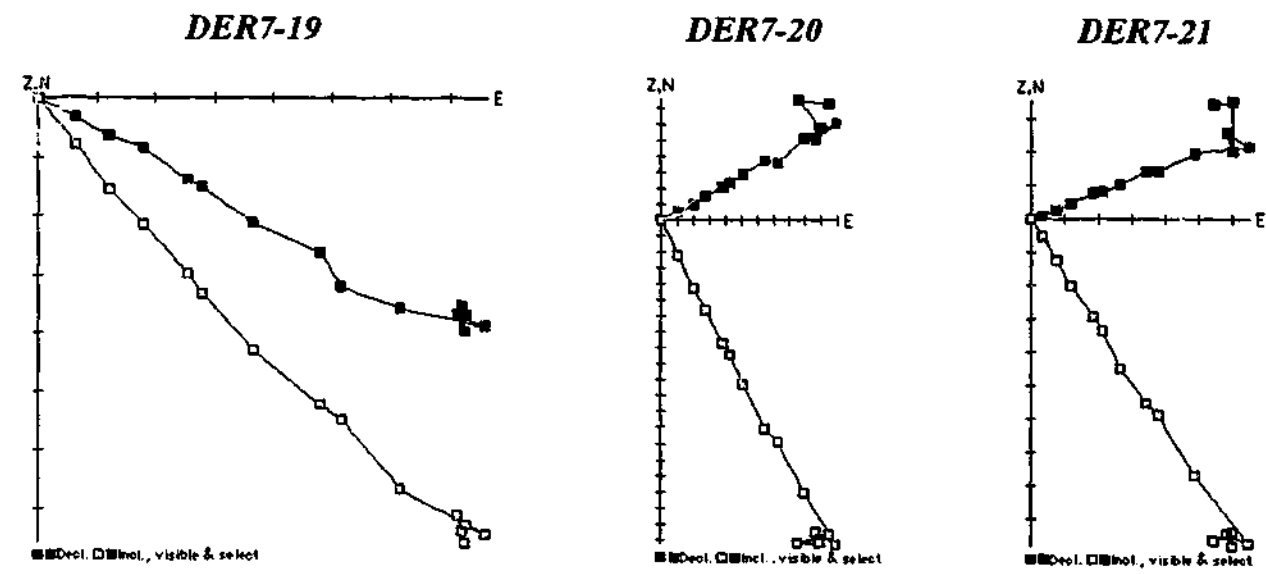


? Group (3)

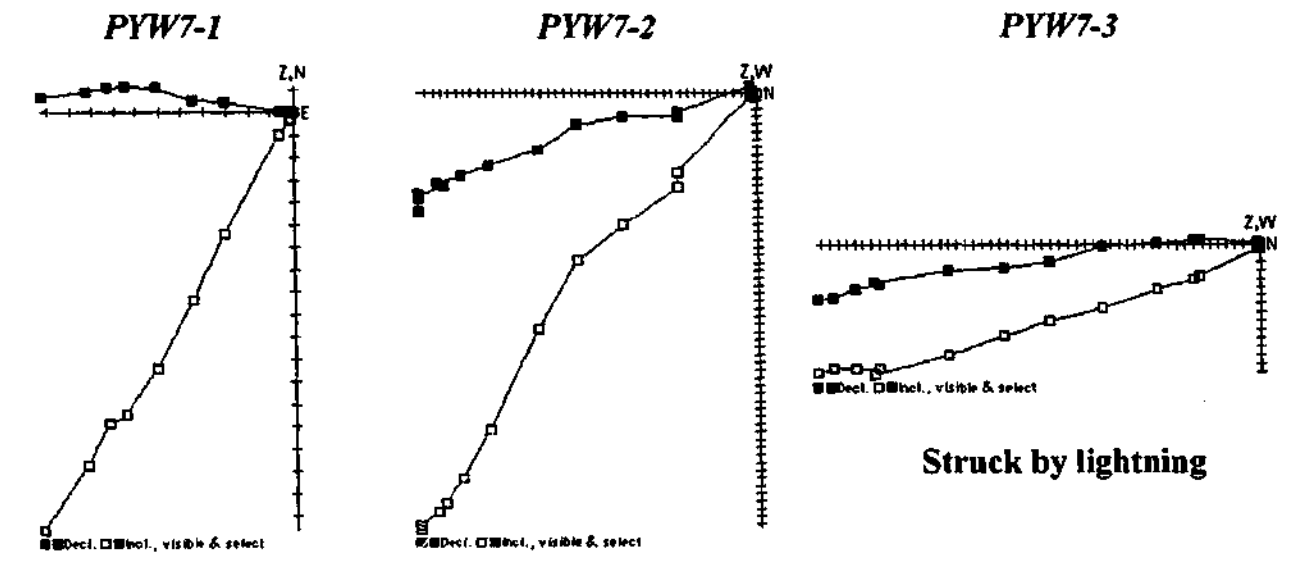


? Group (3)

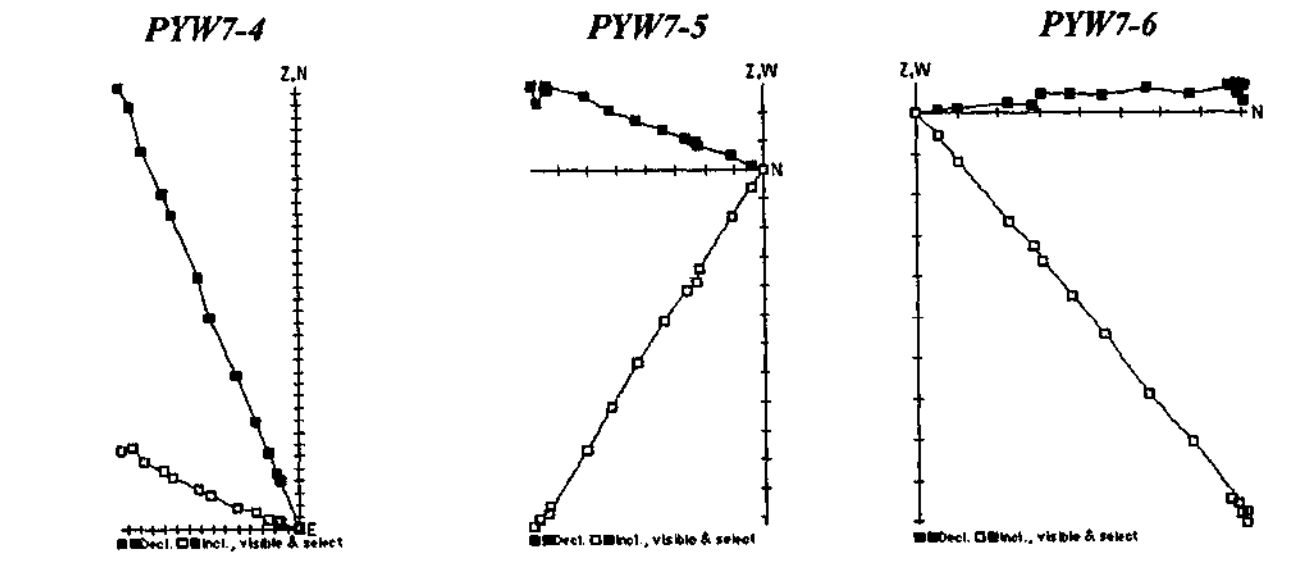




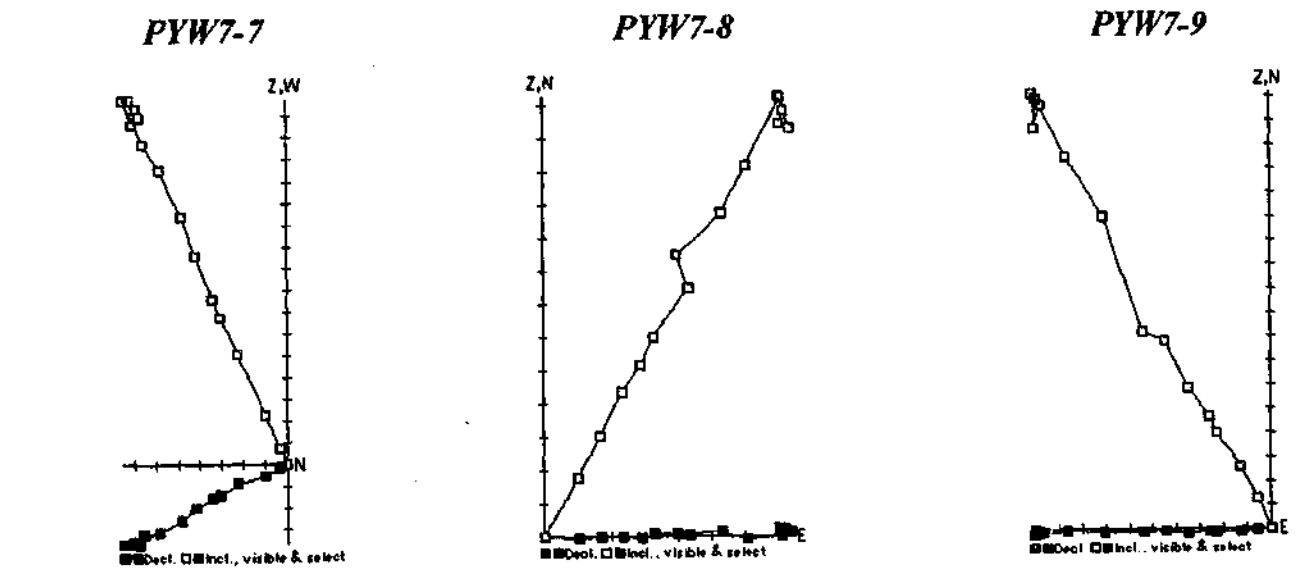
? Group (3)



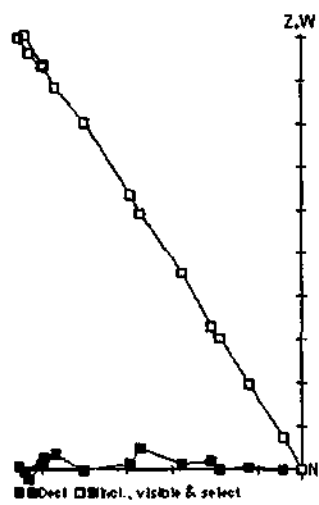
Struck by lightning



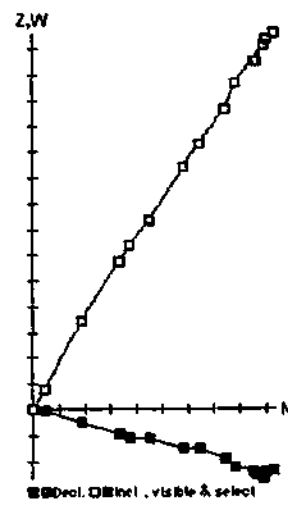
Struck by lightning



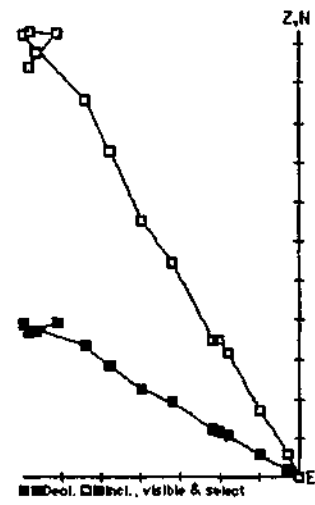
PYW7-10



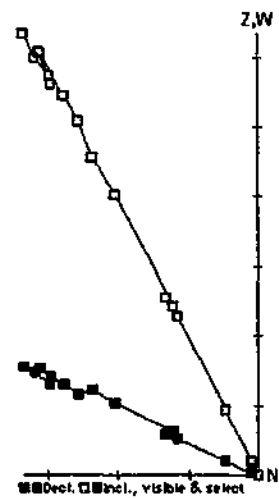
PYW7-11



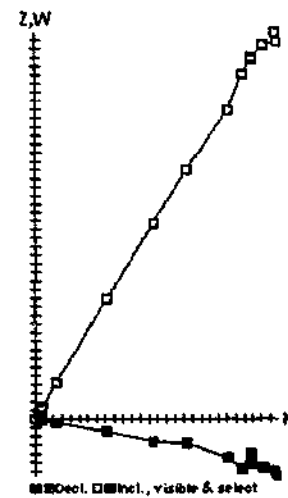
PYW7-12



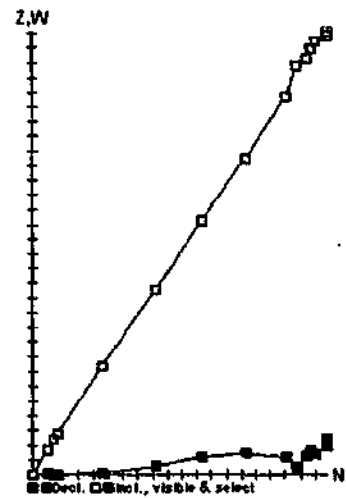
PYW7-13



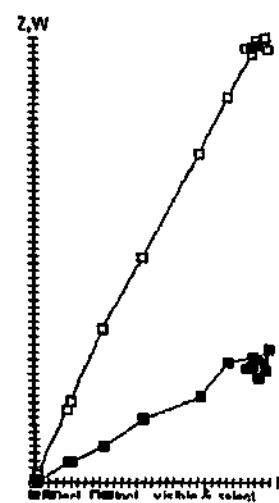
PYW7-14



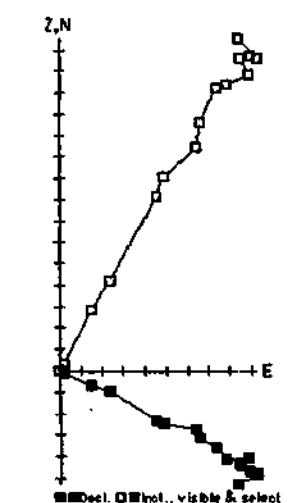
PYW7-15



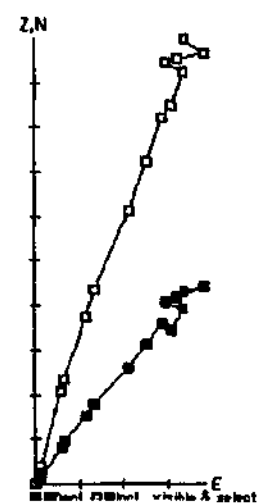
PYW7-16



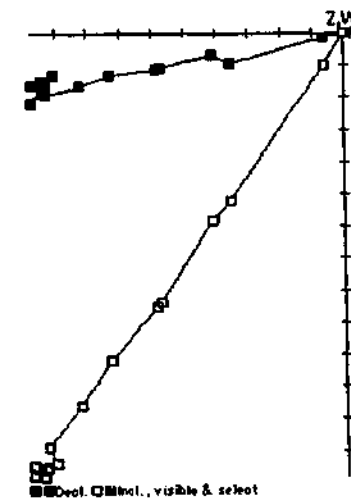
PYW7-17



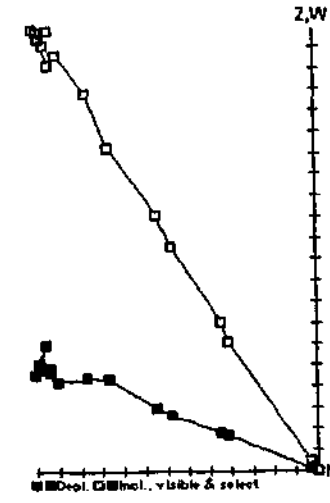
PYW7-18



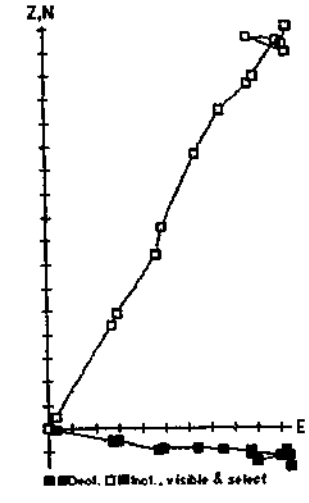
PYW7-19



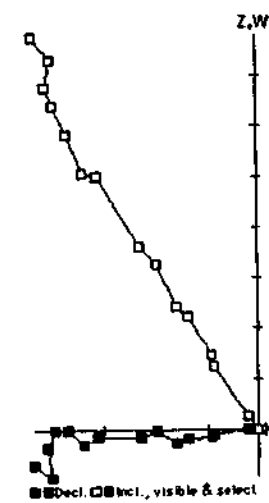
PYW7-20



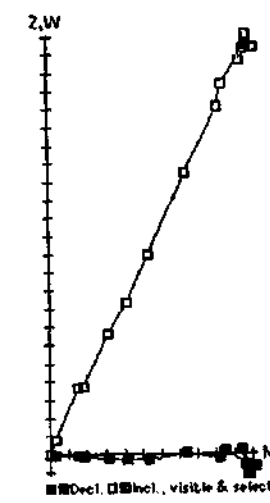
PYW7-21



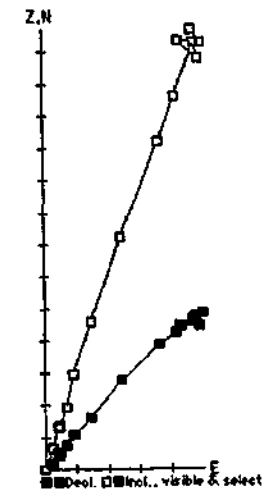
PYW7-22



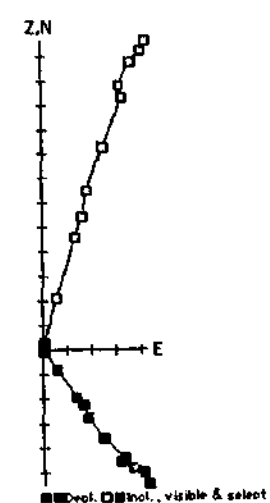
PYW7-23



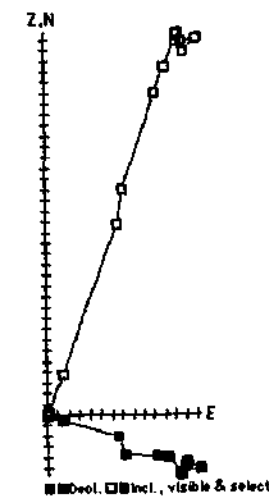
PYW7-24



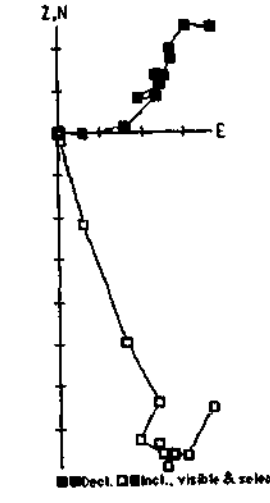
PYW7-25



PYW7-26

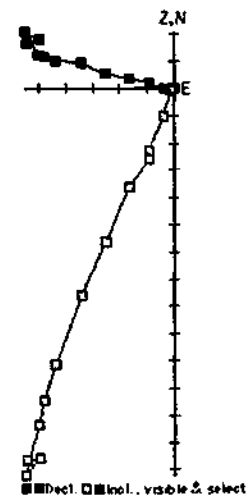


PYW7-27

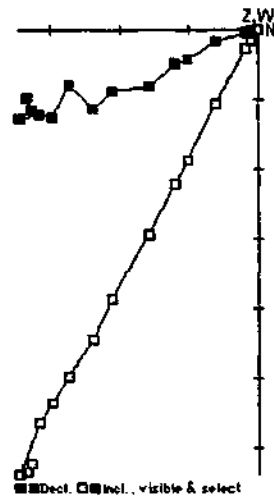


? Q-2

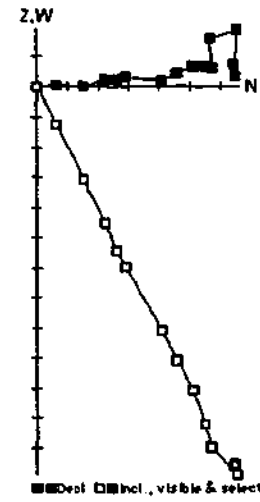
TRU50-17



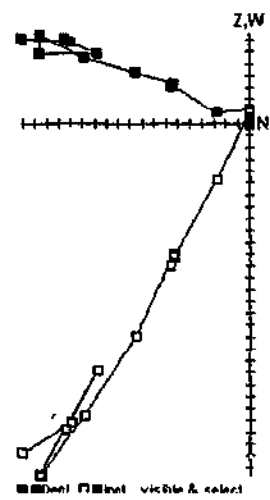
TRU50-18



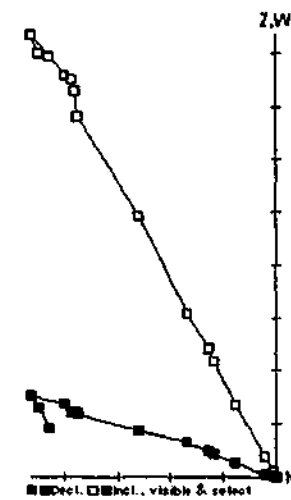
TRU50-19



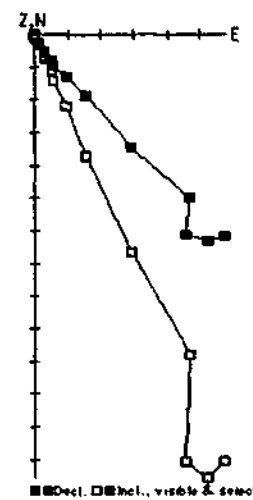
TRU50-20



TRU50-21

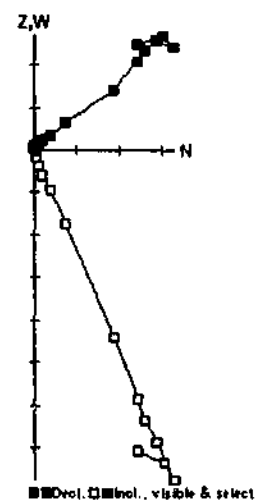


TRU50-22

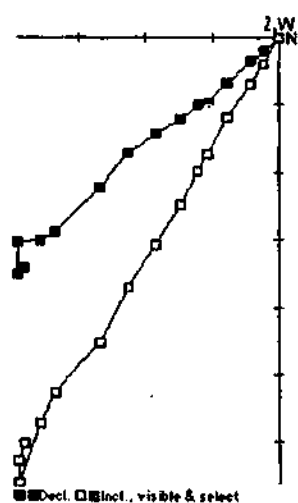


? Group (3)

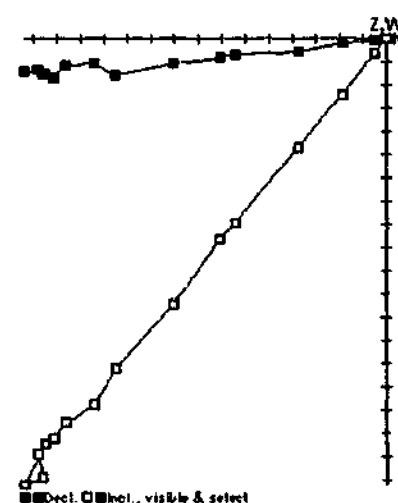
TRU50-23



TRU50-24

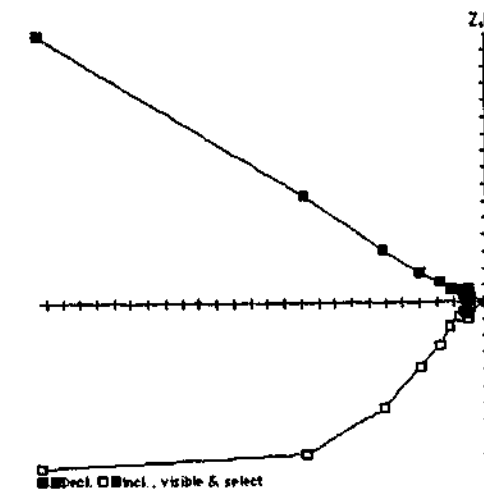


TRU50-25



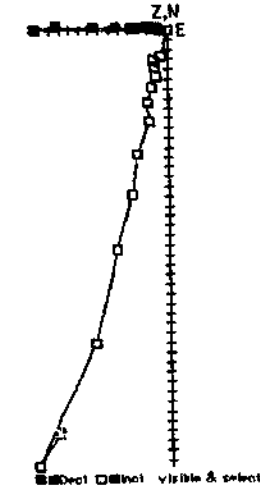
AF DEMAGNETISED SAMPLES

KOR15-21



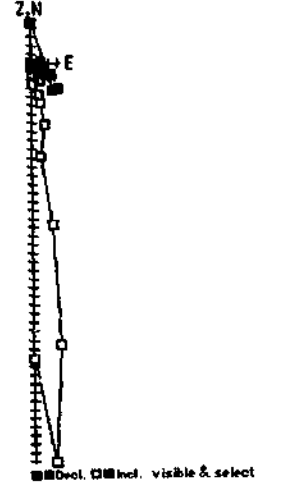
? Group (3)

KOR15-22



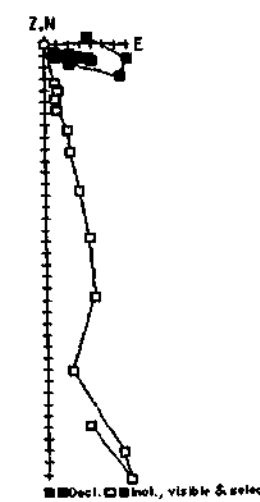
? Q<2

PYW7-30



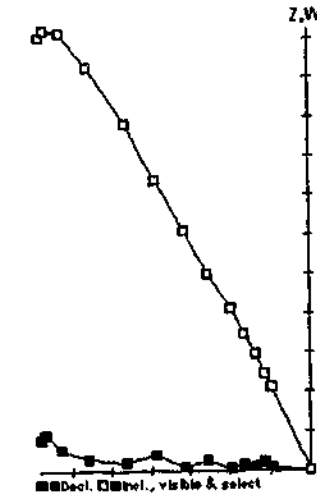
? Group (3)

PYW7-31

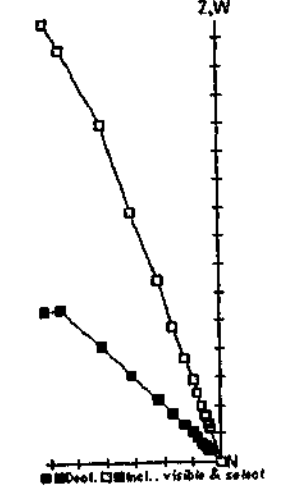


? Q<2

PYW7-32



PYW7-33



APPENDIX E ROCK MAGNETIC RESULTS

BM22-5	67.5	22.6	15.5	29.0	0.3348	1.8710	0.0250	0.23	681
BM22-6	44.5	13.0	14.5	18.0	0.2921	1.2414	0.0301	0.26	382
BM22-7	25.0	8.0	9.0	11.5	0.3200	1.2778	0.0331	0.27	173
DER7-10	24.5	4.0	14.0	34.0	0.1633	2.4286	0.0041	0.24	1445
DER7-19	60.5	18.0	20.0	28.0	0.2975	1.4000	0.0309	0.22	398
DER7-26	90.0	22.5	16.0	29.5	0.2500	1.8438	0.0344	0.25	504
KOR14-14	59.5	24.5	35.5	37.5	0.4118	1.0563	0.0300	0.25	208
KOR14-4	38.5	11.5	21.0	46.5	0.2987	2.2143	0.0304	0.24	336
KOR15-10	129.0	35.0	19.0	30.0	0.2713	1.5789	0.0396	0.27	1174
KOR15-2	118.0	28.0	12.5	13.0	0.2373	1.0400	0.0372	0.26	967
KOR15-3	24.5	9.0	31.0	26.5	0.3673	0.8548	0.0055	0.24	1553
KOR15-4	87.5	31.5	27.0	31.5	0.3600	1.1667	0.0349	0.23	650
KOR16-21	14.5	2.5	9.5	20.0	0.1724	2.1053	0.0032	0.25	1393
KOR16-18	22.5	3.5	13.0	29.0	0.1556	2.2308	0.0038	0.26	1449
KOR16-4	104.5	45.0	48.0	65.5	0.4306	1.3646	0.0467	0.27	242
MB31-3	34.5	7.5	20.5	37.5	0.2174	1.8293	0.0055	0.26	2478
MB31-4	142.5	30.0	7.0	8.5	0.2105	1.2143	0.0383	0.26	1238
PYW7-29	71.0	18.0	13.5	23.5	0.2535	1.7407	0.0287	0.27	746
PYW7-3	96.0	32.0	25.5	30.5	0.3333	1.1961	0.0327	0.21	790
TRU50-19	37.0	11.5	23.0	39.5	0.3108	1.7174	0.0292	0.23	339

mass cylinders: 23 g

APPENDIX F MAGNETIC SUSCEPTIBILITY (K) MEASUREMENTS

NRM (LF)	1217	470	1048	633	681	382	173	380	5377	2478	1238
NRM (HF)	1208	465	1038	627	677	380	172	377	5319	2468	1227
100 (LF)	1253	476	1073	647	696	408	192	385	5550	2488	1327
150	1322	494	1200	723	773	464	193	426	5801	2572	1486
200	1387	509	1319	770	830	470	194	466	6032	2640	1566
250	1401	510	1362	747	799	482	202	467	6097	2644	1609
300	1417	512	1424	628	674	511	231	497	6156	2634	1673
350	1427	513	1374	603	638	537	306	500	6389	2649	2131
400	1433	510	1362	839	791	538	538	567	6578	2650	3831
450	1384	507	1365	1921	1584	560	724	599	6326	2629	4705
500	1281	499	1351	2193	1956	538	709	574	6023	2637	4589
525	1239	492	1215	1989	1926	502	615	472	5342	2638	3929
550	1205	482	1201	1916	1835	483	561	450	5224	2642	3128
575	934	479	1105	1419	1427	425	442	412	4990	2607	2801
600	899	474	1068	1158	1064	371	405	332	4431	2531	2065
600 (HF)	878	458	1044	1120	1033	359	400	322	4404	2488	2048
NRM (LF)	2098	1569	304	327	425	545	202	242	509	1950	312
NRM (HF)	2079	1571	304	324	426	527	203	241	507	1910	306
100 (LF)	2165	1620	325	336	450	557	208	248	524	1981	319
150	2227	1679	370	356	468	589	222	263	584	2050	330
200	2273	1735	381	367	475	615	235	279	614	2130	336
250	2343	1776	401	378	492	641	246	289	636	2192	328
300	2614	1789	411	385	505	661	260	301	624	2213	328
350	3663	1780	443	378	523	662	254	292	575	2243	318
400	5291	1846	489	384	541	659	251	287	536	2233	320
450	5513	1854	520	388	557	661	243	283	530	2248	333
500	5038	1866	515	375	534	640	232	271	518	2195	335
525	4346	1834	400	351	479	587	226	264	513	2177	337
550	3172	1625	397	340	444	528	224	258	474	2105	336
575	2983	1638	205	313	385	483	216	250	425	1980	330
600	2602	1633	179	293	359	441	207	244	376	1868	331
600 (HF)	2599	1604	170	282	353	410	198	236	368	1812	313

NRM (LF)	545	429	741	1820	278	1715	2548	2058	1449	854	631	1393
NRM (HF)	540	425	737	1790	272	1703	2498	2043	1442	839	621	1396
100 (LF)	551	433	797	1842	282	1722	2590	2075	1462	881	641	1428
150	566	440	806	1957	288	1743	2613	2067	1489	929	667	1497
200	584	445	799	2129	296	1770	2608	2085	1517	999	683	1507
250	594	444	856	2222	294	1786	2634	2103	1520	990	678	1528
300	605	452	956	2232	301	1805	2618	2143	1498	977	686	1457
350	605	447	1123	2115	302	1806	2627	2171	1506	952	658	1406
400	601	442	1213	2022	302	1834	2502	2246	1477	944	693	1766
450	617	455	1366	1700	327	1844	2163	2299	1456	936	733	1860
500	613	456	1328	1644	334	1866	2177	2317	1449	927	786	1859
525	606	451	1140	1442	368	1864	2032	2424	1405	872	750	1307
550	573	440	910	1220	379	1972	1726	2649	1348	845	719	1267
575	486	416	796	1157	370	1998	1718	2743	1282	809	684	1256
600	445	403	723	1128	364	2050	1693	2761	1269	796	653	1227
600 (HF)	431	391	736	1093	351	2031	1557	2713	1232	759	631	1209
NRM (LF)	2704	1994	341	336	348	406	613	513	404	396	404	1131
NRM (HF)	2655	1969	339	318	344	400	610	508	401	390	401	1123
100 (LF)	2792	2027	348	336	350	413	623	515	411	394	413	1167
150	2952	2184	381	341	366	464	680	548	434	403	462	1300
200	3158	2565	405	341	394	500	728	575	459	414	500	1384
250	3258	2724	416	354	403	520	782	592	471	426	509	1435
300	3225	2742	382	350	378	504	757	579	446	418	478	1446
350	3177	2772	367	348	371	538	741	571	445	409	516	1550
400	3088	2687	371	357	359	536	677	550	422	410	520	1594
450	2854	2308	373	354	344	568	706	547	420	419	588	1824
500	2782	2190	369	354	338	591	788	520	410	426	776	1795
525	2593	1806	357	355	323	593	776	481	399	425	564	1841
550	2402	1566	344	356	303	573	732	449	371	425	529	1793
575	2074	1182	327	349	265	504	639	416	336	415	454	1637
600	1832	980	316	333	224	404	490	370	295	402	378	1210
600 (HF)	1809	953	309	310	217	392	481	362	284	397	370	1209

NRM (LF)	1313	208	227	712	1468	227	555	967	1553	650	377	258
NRM (HF)	1305	205	232	696	1457	229	551	957	1537	649	373	257
100 (LF)	1321	216	232	724	1496	219	577	1004	1536	655	381	262
150	1361	235	255	741	1534	231	632	1106	1765	676	399	277
200	1389	262	269	743	1619	253	651	1131	1939	696	412	283
250	1383	260	256	709	1598	258	655	1149	2032	698	416	283
300	1380	229	236	716	1634	228	702	1230	2190	701	421	284
350	1400	224	241	672	1721	212	684	1231	2161	693	412	280
400	1388	204	233	608	1691	195	700	1276	2146	689	413	279
450	1356	180	266	559	1659	181	701	1262	2111	664	404	272
500	1862	841	705	853	2643	802	564	1145	1985	648	386	262
525	1321	175	251	518	1595	174	487	1046	1821	635	368	254
550	1331	163	260	488	1562	170	490	1009	1668	614	339	220
575	1331	154	248	452	1435	176	442	842	1423	591	332	213
600	1314	138	245	400	1345	167	455	861	1267	559	313	198
600 (HF)	1303	136	249	393	1330	165	446	851	1249	556	311	195
NRM (LF)	519	782	1174	716	1562	1779	878	660	797	7334	498	676
NRM (HF)	512	776	1158	698	1547	1760	870	625	786	7329	495	671
100 (LF)	521	784	1183	721	1581	1790	883	664	801	7353	510	699
150	545	869	1243	742	1674	1881	908	693	826	1410	577	815
200	551	893	1278	757	1773	2023	920	699	830	1420	600	873
250	555	904	1299	766	1838	2095	922	698	828	1465	626	941
300	557	881	1313	772	1857	2122	910	684	836	1655	628	1031
350	545	844	1317	778	1873	2142	899	693	856	1660	634	1086
400	543	784	1302	800	1862	2091	883	703	865	1600	714	1719
450	536	762	1275	794	1822	1968	869	714	863	1661	801	3186
500	524	689	1240	776	1795	1862	841	705	853	1643	802	3367
525	509	616	1168	738	1731	1764	810	693	886	1624	796	3672
550	483	589	1138	705	1639	1620	767	682	897	1624	772	3677
575	470	505	1044	639	1499	1463	726	652	976	1624	724	3165
600	450	493	1023	611	1367	1262	653	621	1010	1618	624	842
600 (HF)	441	488	1006	606	1356	1233	647	584	972	1626	429	794

NRM (LF)	522	1300	1148	343	509	297	449	232	1725	1445	252	265	364
NRM (HF)	524	1283	1139	337	493	296	447	231	1704	1444	246	264	358
100 (LF)	537	1310	1162	345	515	311	458	237	1770	1451	256	271	370
150	557	1336	1179	363	525	347	474	254	1942	1474	261	279	372
200	568	1382	1231	378	539	379	496	275	2043	1479	267	289	373
250	548	1329	1176	369	526	349	489	263	1968	1527	262	280	364
300	586	1377	1217	387	540	385	522	290	2161	1496	282	288	371
350	593	1365	1202	386	525	379	537	291	2045	1600	271	284	364
400	585	1316	1161	373	516	385	540	303	1995	1729	271	280	360
450	585	1236	1132	370	542	457	542	344	2100	1779	260	269	352
500	552	1113	1000	355	549	461	522	346	2136	1735	251	265	341
525	546	1104	995	323	551	464	492	340	2077	1735	247	259	326
550	527	1061	961	297	494	428	457	325	1987	1675	239	254	312
575	495	967	910	286	452	365	431	296	1862	1651	235	243	295
600	459	919	851	276	411	290	413	257	1619	1581	210	231	271
600 (HF)	455	913	850	270	390	285	406	254	1616	1595	204	228	270
NRM (LF)	207	1520	186	261	369	398	629	348	173	806	1076	488	504
NRM (HF)	201	1485	182	260	374	385	625	348	173	802	1055	466	501
100 (LF)	207	1494	186	264	362	393	622	361	173	808	1099	470	516
150	208	1507	187	280	392	412	710	405	198	875	1149	499	538
200	212	1537	193	306	425	450	782	456	218	939	1222	495	541
250	212	1509	194	292	416	443	790	461	208	938	1194	490	527
300	222	1571	193	302	456	448	841	487	222	975	1199	512	574
350	241	1570	192	296	462	423	745	450	193	930	1174	486	581
400	262	1495	194	282	457	419	744	406	188	891	1161	474	640
450	242	1372	188	276	451	413	694	400	180	877	1070	454	977
500	247	1335	185	267	452	388	628	400	192	839	981	416	2009
525	224	1234	187	262	457	379	594	383	497	793	923	402	2137
550	215	1122	182	247	443	375	555	357	494	790	876	374	2202
575	206	1041	173	227	401	352	513	321	182	734	797	355	2155
600	175	884	158	200	331	318	456	274	150	718	695	327	1978
600 (HF)	174	900	152	196	326	322	444	281	150	693	672	319	1950

NRM (LF)	701	268	338	790	860	302	538	597	483	607	1678	1744	1403
NRM (HF)	705	265	338	786	860	298	526	592	480	597	1647	1727	1394
100 (LF)	699	277	351	798	896	304	538	600	488	611	1680	1765	1413
150	709	309	399	844	1098	327	577	669	518	687	1795	1883	1573
200	725	314	420	866	1153	342	605	718	547	733	1919	1991	1720
250	722	319	409	871	1122	346	611	721	560	753	2055	2114	1812
300	789	380	419	883	1174	348	615	726	555	762	2092	2181	1835
350	813	456	496	877	1315	334	614	727	532	736	2170	2247	1766
400	841	510	772	906	1841	326	616	782	517	697	2225	2299	1644
450	948	482	998	923	2373	315	637	873	517	693	2203	2311	1541
500	1173	412	1042	876	2186	313	663	1018	510	667	2066	2134	1273
525	1379	420	1037	832	1962	310	663	1068	484	609	1859	1995	1209
550	1519	428	1036	836	1896	310	656	1068	467	604	1825	1964	1190
575	1883	426	811	762	1413	283	588	954	434	531	1694	1760	1057
600	2525	401	625	717	1001	153	504	766	405	464	1534	1461	906
600 (HF)	2490	394	609	709	993	243	484	749	393	450	1494	1441	904
NRM (LF)	1467	1739	1551	2062	1619	349	658	294	604	442	1025	464	241
NRM (HF)	1452	1720	1539	2058	1604	343	652	288	602	443	1019	464	243
100 (LF)	1476	1757	1563	2097	1629	352	666	297	609	453	1019	470	248
150	1570	1824	1614	2126	1631	361	680	303	610	464	1050	501	261
200	1616	1892	1713	2266	1660	371	701	308	615	487	1065	526	267
250	1591	1845	1707	2253	1682	362	702	297	620	472	1061	542	269
300	1557	1833	1667	2235	1715	359	699	293	629	481	1066	555	347
350	1546	1820	1620	2209	1795	359	679	285	640	469	1070	530	536
400	1552	1837	1651	2277	1945	365	668	286	673	576	1122	568	649
450	1520	1818	1647	2301	1986	359	655	287	686	840	1138	642	595
500	1551	1780	1636	2321	2070	352	633	283	706	935	1141	702	515
525	1533	1711	1619	2211	2096	362	620	277	851	973	1213	676	449
550	1545	1641	1609	2105	2110	371	606	275	982	964	1275	640	410
575	1540	1599	1573	1993	2143	379	597	274	1042	947	1293	620	411
600	1538	1564	1540	1742	2330	412	532	255	1499	600	1334	505	373
600 (HF)	1500	1539	1519	1717	2274	393	520	245	1426	588	1302	491	366

NRM (LF)	719	1484	525	746	878	1003	535	1045	558	771	2230	1378	1245
NRM (HF)	718	1475	520	736	?	?	?	?	?	?	?	?	?
100 (LF)	724	1480	536	756	896	1019	546	1075	566	785	2270	1393	1262
150	738	1541	559	781	9330	1051	564	1173	610	816	2316	1428	1291
200	757	1513	569	796	924	1055	567	1215	626	839	2241	1406	1310
250	779	1525	564	828	958	1093	584	1335	667	838	2241	1450	1330
300	813	1556	679	989	958	1075	577	1315	666	742	2198	1577	1367
350	903	1626	795	1124	953	1071	572	1255	638	757	2250	1989	1428
400	920	1675	1101	1376	921	1055	568	1206	609	953	2246	2812	1514
450	839	1576	983	1341	894	1088	578	1400	597	1546	2305	3106	1552
500	779	1443	1105	1216	857	1074	559	1485	555	1878	2260	2899	1518
525	625	1177	1047	1111	819	1085	551	1440	545	1911	2318	2266	1437
550	608	887	958	967	807	1059	542	1369	512	1710	2276	2046	1362
575	600	908	806	940	752	1023	483	1171	465	1391	2232	1650	1250
600	594	976	736	992	749	1020	466	885	453	997	2168	1516	1206
600 (HF)	581	971	709	954	739	996	451	876	441	963	2144	1497	1182
NRM (LF)	1145	748	798	795	1554	551	758	2223	935	1423	1029	339	632
NRM (HF)	?	?	799	791	1574	563	756	2204	930	1400	1026	334	623
100 (LF)	1155	753	816	807	1574	554	764	2263	955	1463	1067	343	641
150	1180	771	834	852	1611	563	781	2412	992	1515	1120	353	765
200	1185	773	826	837	1613	562	781	2383	984	1453	1092	356	837
250	1211	801	845	853	1685	569	793	2468	1016	1210	1107	352	867
300	1220	803	876	883	1671	574	797	2474	1037	1645	1154	348	771
350	1250	817	963	925	1688	578	822	2406	1021	1688	1101	342	699
400	1242	824	1031	977	1733	592	888	2482	1091	1822	1295	330	852
450	1271	958	1008	969	1702	596	958	2451	1262	1813	1779	327	1066
500	1239	1036	978	1014	1602	713	1346	2324	1368	1845	1774	1774	1035
525	1257	1167	943	1065	1565	801	1436	2211	1355	1875	1720	1720	990
550	1228	1289	906	1176	1433	960	1530	2035	1293	1820	1439	1439	790
575	1247	1395	907	1308	1345	1015	1615	1921	1226	1688	1206	1206	557
600	1249	1508	873	1404	1236	1082	1718	1748	1048	1531	932	932	379
600 (HF)	1228	1452	859	1351	1220	1024	1665	1725	1033	1488	913	913	360

NRM (LF)	192	190	363	238	418	363	292	424	561	892	606	243	411
NRM (HF)	182	187	361	234	416	362	290	417	554	881	598	239	406
100 (LF)	192	192	368	239	425	366	298	445	550	891	610	246	416
150	197	198	398	244	463	383	318	471	569	942	631	255	432
200	196	202	416	245	497	381	307	462	580	964	637	262	441
250	201	205	430	247	516	399	317	481	578	971	645	269	449
300	202	206	419	249	478	425	336	499	573	966	637	296	475
350	199	199	395	255	427	454	444	620	565	971	607	311	501
400	203	203	376	266	408	488	608	779	557	950	583	321	482
450	205	204	372	276	620	554	690	918	550	931	543	553	566
500	205	203	354	273	819	586	628	899	524	890	495	736	664
525	204	201	328	318	836	600	549	836	503	812	490	763	690
550	200	197	316	453	792	606	482	751	491	770	450	775	691
575	198	195	306	668	633	602	430	661	470	725	324	602	608
600	195	186	332	812	466	562	389	619	445	665	256	436	478
600 (HF)	179	178	323	754	455	548	380	618	430	643	244	411	457
NRM (LF)	339	149	344	189	212	233	267	1103	679	1296	741	358	642
NRM (HF)	337	144	343	187	210	229	258	1096	673	1290	729	352	645
100 (LF)	342	149	353	200	218	235	273						
150	351	152	372	218	232	253	283						
200	357	155	380	225	235	262	286						
250	361	160	379	229	222	267	289						
300	378	167	419	254	256	263	288						
350	392	197	498	362	299	255	286						
400	388	296	546	587	291	261	292						
450	412	1452	511	792	445	260	296						
500	468	1964	482	832	861	264	302						
525	479	1978	442	805	1052	257	302						
550	471	1887	449	790	1174	239	298						
575	418	1648	437	731	1099	212	292						
600	316	1323	387	657	849	187	280						
600 (HF)	306	1271	378	637	835	179	265						

APPENDIX G

KÖNIGSBERGER RATIO (Q) CALCULATIONS AND

IDENTIFICATION OF SPM-SD THRESHOLD GRAINS

Sample no.	J (NRM)	NRM (S.I.)	K (S.I.)	Q	K ₁ (CF)	K ₂ (CF)	Q ₁ (CF)
BM22-1	1.10E+03	1.10	1.22E-02	2.49	1217	1208	0.74
2	2.21E+03	2.21	4.70E-03	13.00	470	465	1.06
3	2.78E+03	2.78	1.05E-02	7.33	1048	1038	0.95
4	1.92E+03	1.92	6.33E-03	8.38	633	627	0.95
5	5.72E+02	0.57	6.81E-03	2.32	681	677	0.59
6	2.12E+03	2.12	3.82E-03	15.33	382	380	0.52
7	2.00E+03	2.00	1.73E-03	31.94	173	172	0.58
MB31-1	9.73E+02	0.97	3.90E-03	7.08	380	377	0.79
2	1.59E+04	15.90	5.36E-02	8.18	5377	5319	1.08
3	7.03E+03	7.03	2.48E-02	7.84	2478	2468	0.40
4	1.70E+03	1.70	1.24E-02	3.80	1238	1227	0.89
5	9.33E+02	0.93	2.10E-02	1.23	2098	2079	0.91
6	3.32E+03	3.32	1.57E-02	5.84	1569	1571	-0.13
KOR14-1	1.09E+04	10.90	2.70E-02	11.14	2704	2655	1.81
2	1.20E+04	12.02	1.99E-02	16.66	1994	1969	1.25
3	8.26E+02	0.83	3.41E-03	6.70	341	339	0.59
4	4.86E+02	0.49	3.36E-03	4.00	336	318	5.36
5	9.63E+02	0.96	3.48E-03	7.65	348	344	1.15
6	1.52E+03	1.52	4.06E-03	10.33	406	400	1.48
7	1.72E+03	1.72	6.13E-03	7.75	613	610	0.49
8	3.07E+03	3.07	5.13E-03	16.53	513	508	0.97
9	1.13E+03	1.13	4.04E-03	7.74	404	401	0.74
10	2.02E+03	2.02	3.96E-03	14.11	396	390	1.52
11	8.06E+02	0.81	4.04E-03	5.52	404	401	0.74
12	1.07E+03	1.07	1.13E-02	2.62	1131	1123	0.71
13	1.64E+03	1.64	1.31E-02	3.46	1313	1305	0.61
14	2.18E+02	0.22	2.08E-03	2.89	208	205	1.44
15	3.50E+02	0.35	2.27E-03	4.26	227	232	-2.20
16	6.17E+02	0.62	7.12E-03	2.40	712	696	2.25
17	3.29E+03	3.29	1.47E-02	6.19	1468	1457	0.75
18	5.81E+02	0.58	2.27E-03	7.07	227	229	-0.88
KOR16-1	6.58E+02	0.66	3.04E-03	5.98	304	304	0.00
2	1.31E+03	1.31	3.27E-03	11.05	327	324	0.92
3	7.01E+02	0.70	4.25E-03	4.56	425	426	-0.24
4	2.82E+03	2.82	5.45E-03	14.31	545	527	3.30
5	1.05E+03	1.05	2.02E-03	14.42	202	203	-0.50
6	9.51E+02	0.95	2.42E-03	10.87	242	241	0.41
7	1.29E+03	1.29	5.09E-03	7.01	509	507	0.39
8	1.70E+04	17.04	1.95E-02	24.15	1950	1910	2.05
9	9.66E+02	0.97	3.12E-03	8.56	312	306	1.92
10	8.71E+02	0.87	5.45E-03	4.42	545	540	0.92
11	8.73E+02	0.87	4.29E-03	5.63	429	425	0.93
12	2.04E+02	0.20	7.41E-03	0.76	741	737	0.54
13	7.05E+03	7.05	1.82E-02	10.71	1820	1790	1.65
15	7.40E+03	7.40	1.72E-02	11.93	1715	1703	0.70
16	8.74E+02	0.87	2.55E-02	0.95	2548	2498	1.96
17	2.12E+03	2.12	2.06E-02	2.85	2058	2043	0.73
18	3.16E+03	3.16	1.45E-02	6.03	1449	1442	0.48
19	2.92E+03	2.92	8.54E-03	9.46	854	839	1.76
20	4.47E+02	0.45	6.31E-03	1.96	631	621	1.58
21	4.58E+02	0.46	1.39E-02	0.91	1393	1396	-0.22

Sample no.	J (NRM)	NRM (S.I.)	K (S.I.)	Q	K ₁ (CF)	K ₂ (CF)	Q ₁ (CF)
KOR15-1	6.87E+03	6.87	5.55E-03	34.23	555	551	0.72
2	5.29E+03	5.29	9.67E-03	15.12	967	957	1.03
3	1.99E+04	19.87	1.55E-02	35.36	1553	1537	1.03
4	1.89E+03	1.89	6.50E-03	8.03	650	649	0.15
5	3.78E+03	3.78	7.60E-03	13.75	760	754	0.79
6	1.44E+03	1.44	3.77E-03	10.58	377	373	1.06
7	8.48E+02	0.85	2.58E-03	9.09	258	257	0.39
8	1.52E+03	1.52	5.19E-03	8.11	519	512	1.35
9	2.90E+03	2.90	7.82E-03	10.25	782	776	0.77
10	3.39E+03	3.39	1.17E-02	7.99	1174	1158	1.36
11	4.39E+03	4.33	7.16E-03	16.73	716	698	2.51
12	8.45E+03	8.45	1.56E-02	14.95	1562	1547	0.96
13	1.39E+04	13.88	1.78E-02	21.57	1779	1760	1.07
14	1.72E+03	1.72	8.78E-03	5.40	878	870	0.91
15	3.18E+03	3.18	6.60E-03	13.34	660	625	5.30
16	6.78E+03	6.78	7.97E-03	23.51	797	786	1.38
17	5.61E+02	0.56	7.33E-02	0.21	7334	7329	0.07
18	2.67E+03	2.67	4.98E-03	14.80	498	495	0.60
19	8.97E+02	0.90	2.24E-03	11.07	224	218	2.68
20	3.09E+02	0.31	6.76E-03	1.26	676	671	0.74
21	4.94E+02	0.49	1.10E-02	1.24	1103	1096	0.63
22	4.29E+02	0.43	6.79E-03	1.75	679	673	0.88
DER7-1	1.10E+03	1.10	5.22E-03	5.81	522	524	-0.38
2	2.21E+03	2.21	1.30E-02	4.70	1300	1283	1.31
3	2.78E+03	2.78	1.15E-02	6.69	1148	1139	0.78
4	1.92E+03	1.92	3.43E-03	15.46	343	337	1.75
5	1.16E+03	1.16	5.09E-03	6.27	509	493	3.14
6	8.19E+02	0.82	2.97E-03	7.62	297	296	0.34
7	3.51E+03	3.51	4.49E-03	21.62	449	447	0.45
8	1.27E+03	1.27	2.32E-03	15.17	232	231	0.43
9	2.27E+03	2.27	1.73E-02	3.64	1725	1704	1.22
10	1.59E+03	1.59	1.45E-02	3.04	1445	1444	0.07
11	7.30E+02	0.73	2.52E-03	8.01	252	246	2.38
12	1.07E+03	1.07	2.65E-03	11.17	265	264	0.38
13	9.93E+02	0.99	3.64E-03	7.54	364	358	1.65
14	5.06E+02	0.51	2.07E-03	6.76	207	201	2.90
15	3.69E+03	3.69	1.52E-02	6.70	1520	1485	2.30
16	5.36E+02	0.54	1.86E-03	7.97	186	182	2.15
17	7.87E+02	0.79	2.61E-03	8.33	261	260	0.38
18	8.24E+02	0.82	3.69E-03	6.17	369	374	-1.36
19	1.09E+03	1.09	3.98E-03	7.59	398	385	3.27
20	2.34E+03	2.34	6.29E-03	10.27	629	625	0.64
21	1.16E+03	1.16	3.48E-03	9.19	348	348	0.00
22	1.48E+02	0.15	1.73E-03	2.36	173	173	0.00
23	4.69E+03	4.69	8.06E-03	16.08	806	802	0.50
24	3780.72	3.78	1.08E-02	9.71	1076	1055	1.95
25	4592.51	4.59	4.88E-03	26.01	488	466	4.51
26	2263.20	2.26	5.04E-03	12.41	504	501	0.60
27	282.75	0.28	7.01E-03	1.11	701	705	-0.57

Sample no.	J (NEM)	NRM (S.I)	K (S.I)	Q	F (LF)	F (HF)	LINE-HOLE (G)
PYW7-1	2.18E+03	2.18	2.68E-03	22.45	268	265	1.12
2	7.27E+02	0.73	3.38E-03	5.95	338	338	0.00
3	5.50E+03	5.50	7.90E-03	19.23	790	786	0.51
4	3.98E+04	39.76	8.60E-03	127.76	860	860	0.00
5	1.49E+03	1.49	3.02E-03	13.60	302	298	1.32
6	1.29E+03	1.29	5.38E-03	6.61	538	526	2.23
7	1.86E+03	1.86	5.97E-03	8.59	597	592	0.84
8	1.50E+03	1.50	4.83E-03	8.59	483	480	0.62
9	2.07E+03	2.07	6.07E-03	9.43	607	597	1.65
10	1.19E+04	11.86	1.68E-02	19.54	1678	1647	1.85
11	1.74E+04	17.37	1.74E-02	27.52	1744	1727	0.97
12	1.37E+04	13.72	1.40E-02	27.02	1403	1394	0.64
13	7.34E+03	7.34	1.47E-02	13.82	1467	1452	1.02
14	5.29E+03	5.29	1.74E-02	8.41	1739	1720	1.09
15	3.61E+03	3.61	1.55E-02	6.43	1551	1533	1.16
16	7.06E+03	7.06	2.06E-02	9.46	2062	2058	0.19
17	1.84E+03	1.84	1.62E-02	3.15	1619	1604	0.93
18	1.14E+03	1.14	3.49E-03	9.06	349	343	1.72
19	1.68E+03	1.68	6.58E-03	7.07	658	652	0.91
20	2.50E+03	2.50	2.94E-03	23.53	294	288	2.04
21	2.01E+03	2.01	6.04E-03	9.18	604	602	0.33
22	8.93E+02	0.89	4.42E-03	5.58	442	443	-0.23
23	2.55E+03	2.55	1.03E-02	6.88	1025	1019	0.59
24	1.52E+03	1.52	4.64E-03	9.05	464	464	0.00
25	1.44E+03	1.44	2.41E-03	16.54	241	243	-0.83
26	3.73E+03	3.73	7.19E-03	14.32	719	716	0.14
27	7.89E+02	0.79	1.48E-02	1.47	1484	1475	0.61
28	2.03E+03	2.03	5.25E-03	10.69	525	520	0.95
29	2.53E+03	2.53	7.46E-03	9.39	746	736	1.34
30	3.46E+02	0.35	1.30E-02	0.74	1296	1290	0.46
31	3.30E+02	0.33	7.41E-03	1.23	741	729	1.62
32	1.30E+03	1.30	3.58E-03	10.02	358	352	1.68
33	1.76E+03	1.76	6.42E-03	7.57	642	645	-0.47
TAR12-1	2.52E+03	2.52	8.78E-03	7.92	878	Not measured	N/A
2	3.50E+03	3.50	1.00E-02	9.64	1003	"	N/A
3	2.09E+03	2.09	5.35E-03	10.78	535	"	N/A
4	3.66E+03	3.66	1.05E-02	9.69	1045	"	N/A
5	4.07E+03	4.07	5.58E-03	20.16	558	"	N/A
6	3.53E+03	3.53	7.71E-03	12.64	771	"	N/A
7	1.58E+04	15.84	2.23E-02	19.63	2230	"	N/A
8	1.81E+03	1.81	1.38E-02	3.64	1378	"	N/A
9	2.43E+03	2.43	1.25E-02	5.40	1245	"	N/A
10	2.76E+03	2.76	1.15E-02	6.66	1145	"	N/A
11	1.53E+03	1.53	7.48E-03	5.66	748	"	N/A
12	2.34E+03	2.34	7.98E-03	8.11	798	799	-0.13
13	2.15E+03	2.15	7.95E-03	7.47	795	791	0.50
14	4.57E+03	4.57	1.55E-02	8.12	1554	1574	-1.29
15	1.71E+03	1.71	5.51E-03	8.55	551	563	-2.18
16	1.68E+03	1.68	7.58E-03	6.11	758	756	0.26
17	1.34E+04	13.45	2.22E-02	16.71	2223	2204	0.85
18	1.60E+03	1.60	9.35E-03	4.72	935	930	0.53
19	1.54E+03	1.54	1.42E-02	3.00	1423	1400	1.62
20	2.16E+03	2.16	1.03E-02	5.79	1029	1026	0.29
21	1.18E+03	1.18	3.39E-03	9.61	339	334	1.47

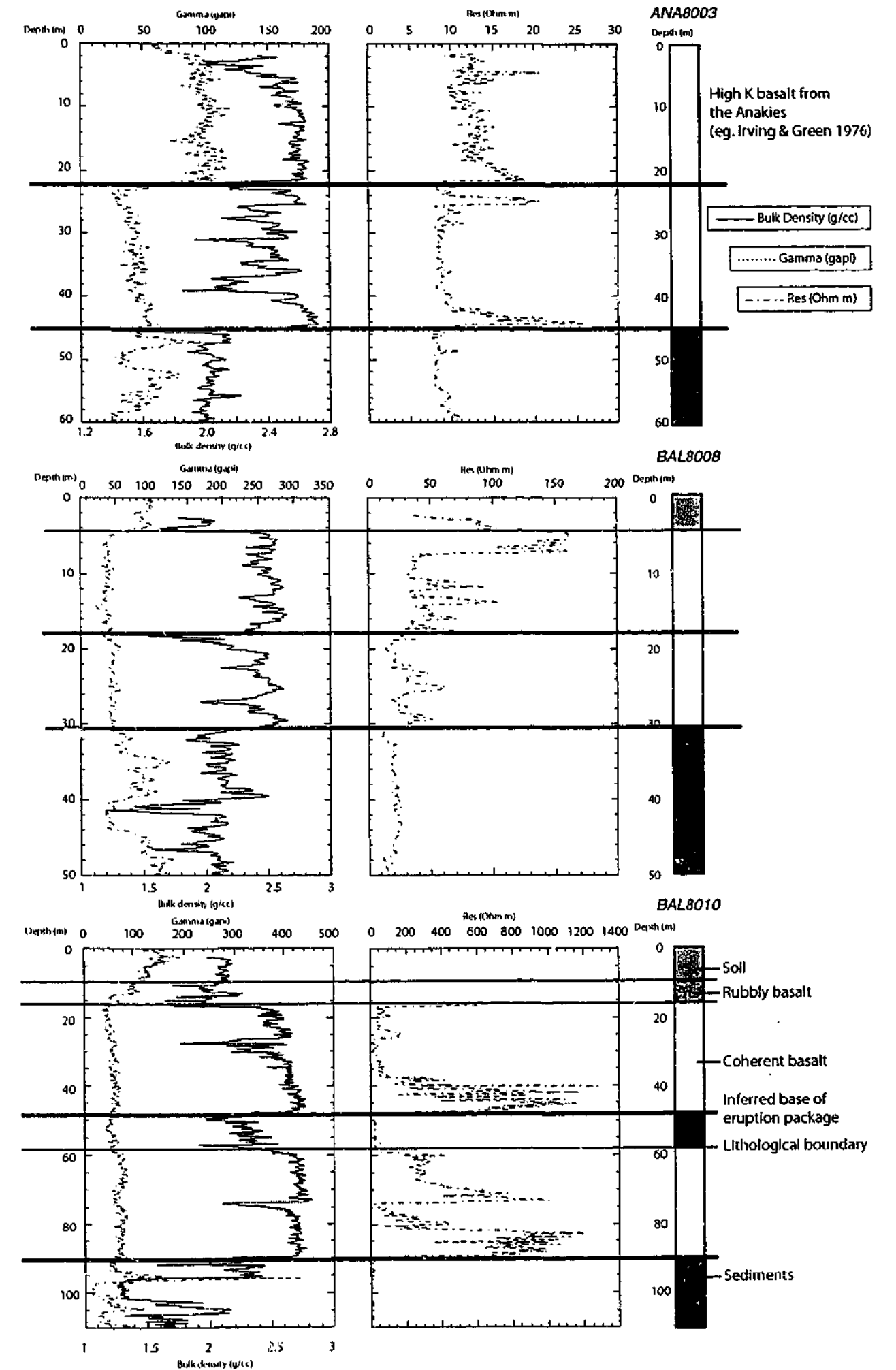
Sample no.	J (NEM)	NRM (S.I)	K (S.I)	Q	F (LF)	F (HF)	LINE-HOLE (G)
TRU50-2	3.27E+03	3.27	6.32E-03	14.31	632	623	1.42
3	1.08E+03	1.08	1.92E-03	15.48	192	182	5.21
4	1.15E+03	1.15	1.90E-03	16.73	190	187	1.58
5	1.33E+03	1.33	3.63E-03	10.15	363	361	0.55
6	5.48E+02	0.55	2.38E-03	6.36	238	234	1.68
7	9.26E+02	0.93	4.18E-03	6.12	418	416	0.48
10	1.84E+03	1.84	3.63E-03	13.97	363	362	0.28
11	2.54E+03	2.54	2.92E-03	24.00	292	290	0.68
12	3.49E+03	3.49	4.24E-03	22.74	424	417	1.65
13	1.38E+02	0.14	5.61E-03	0.68	561	550	1.96
14	1.45E+03	1.45	8.92E-03	4.50	892	881	1.23
15	1.74E+03	1.74	6.06E-03	7.93	606	598	1.32
16	1.19E+03	1.19	2.43E-03	13.53	243	239	1.65
17	1.48E+03	1.48	3.24E-03	12.66	324	322	0.62
18	7.25E+02	0.72	4.11E-03	4.87	411	406	1.22
19	1.42E+03	1.42	3.39E-03	11.61	339	337	0.59
20	3.44E+02	0.34	1.49E-03	6.38	149	144	3.36
21	9.08E+02	0.91	3.44E-03	7.30	344	343	0.29
22	1.55E+03	1.55	1.89E-03	22.70	189	187	1.06
23	7.86E+02	0.79	2.12E-03	10.25	212	210	0.94
24	7.92E+02	0.79	2.33E-03	9.39	233	229	1.72
25	2.32E+03	2.32	2.67E-03	23.99	267	258	3.37

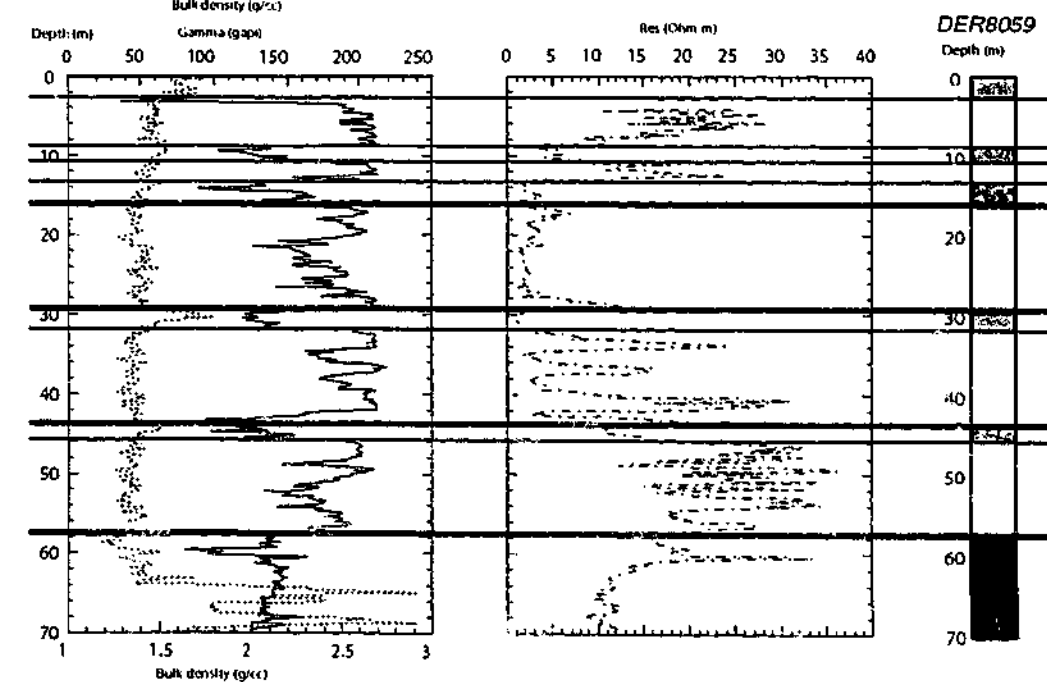
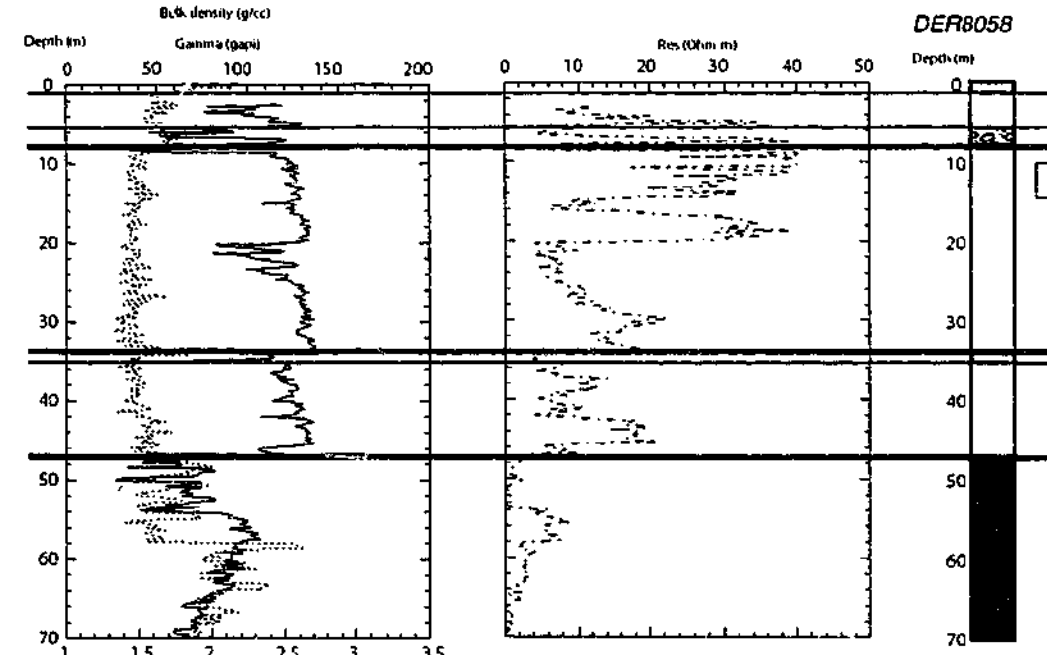
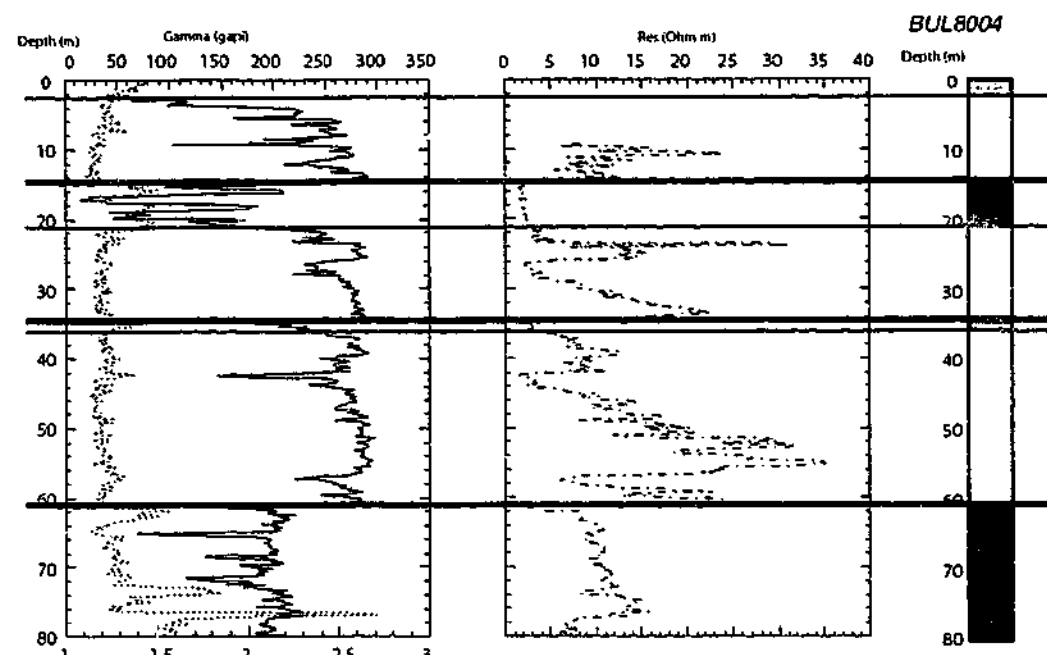
NB: Samples highlighted have been discarded: Q<2

APPENDIX H GEOPHYSICAL WELL LOG INTERPRETATIONS

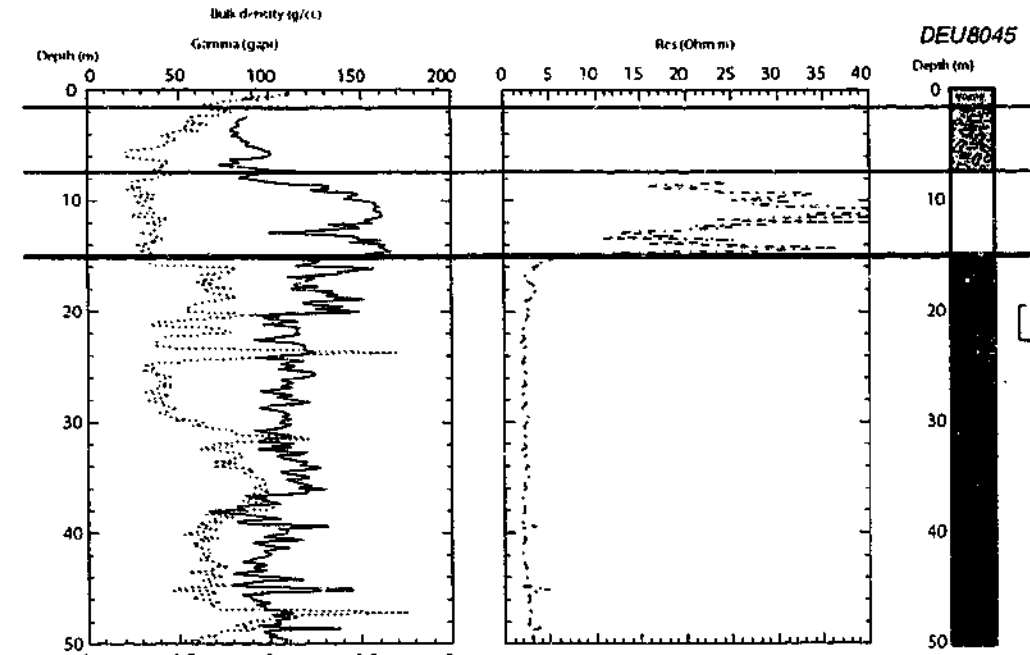
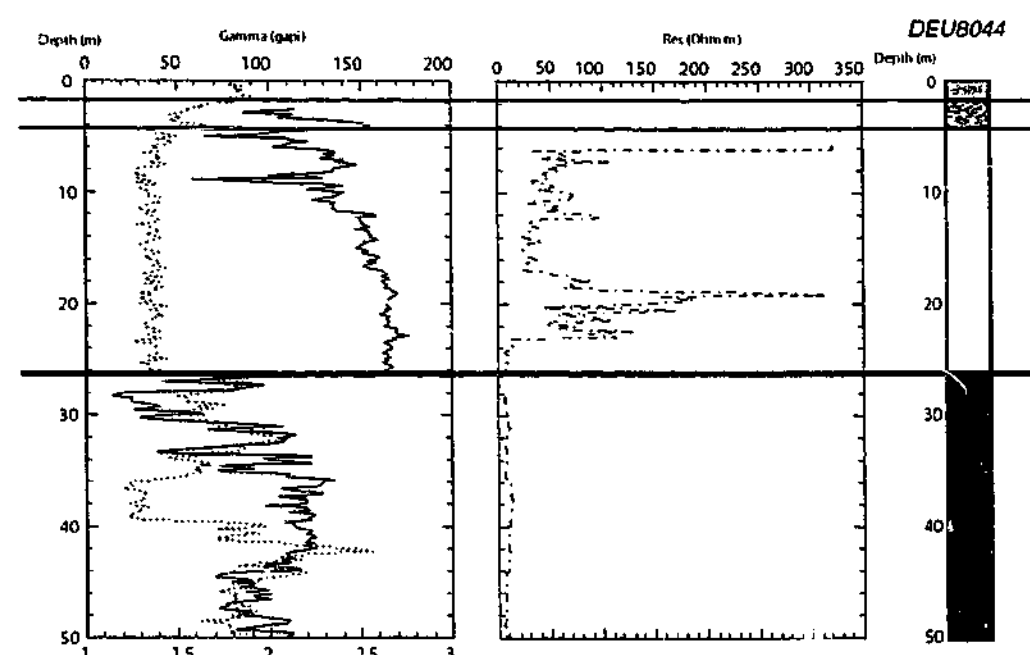
All drill holes used to deduce the palaeotopography of the Werribee Plains prior to basaltic volcanism are listed. The drill holes are classified as either diamond drill holes (DDH) or geophysical wells (GW). The inferred cumulative thickness of interflow sediments is also given. The geophysical well log data is displayed graphically on the following pages, with the interpreted graphic lithological logs adjacent to each. Refer to page 261 for interpretation of symbols.

Drill hole number	Drill hole type	Depth of Red Bluff Sand contact (m)	Present elevation (m)	Paleo elevation (m)	Cumulative interflow distance (m)
ANA8003	GW	45	105	60	
BAL8008	GW	30	120	90	
BAL8010	GW	90	135	45	9
BM22	DDH, GW	20	150	130	
BUL8004	GW	60	25	-35	7
DER7	DDH	105	105	0	
DER8058	GW	45	25	-20	
DER8059	GW	60	60	0	
DEU8044	GW	25	15	-10	
DEU8045	GW	15	5	-10	
DEU8046	GW	0	5	5	
DJE8022	GW	30	145	115	
DJE8023	GW	35	120	85	
GOR8007	GW	70	180	110	5
KOR8003	GW	75	140	65	
KOR14	DDH	65	140	75	
KOR15	DDH	90	120	30	
KOR16	DDH	70	120	50	
MAM8003	GW	60	25	-35	5
MB31	DDH, GW	60	130	70	18
MOO8003	GW	65	125	60	15
MOO8005	GW	70	105	35	12
MOO8006	GW	75	115	40	15
MOU8004	GW	40	105	65	
MOU8006	GW	70	140	70	
MOU8007	GW	50	135	85	14
MOU8009	GW	110	130	20	
PAR8032	GW	65	150	85	13
PAR8034	GW	80	170	90	30
PAR8035	GW	45	140	95	9
PAR8036	GW	70	140	70	10
PAR8037	GW	60	155	95	15
PAR8038	GW	15	100	85	5
PAR8040	GW	85	160	75	17
PAR8041	GW	30	150	120	
PYW7	DDH	85	90	5	
PYW8045	GW	25	70	45	
PYW8047	GW	95	95	0	
TAR12	DDH	75	45	-30	1.5
TAR8031	GW	95	60	-35	
TAR8032	GW	70	40	-30	
TRU50	DDH	75	30	-45	
TRU8004	GW	15	10	-5	
TRU8008	GW	15	10	-5	
TRU8019	GW	55	30	-25	
WER8002	GW	120	65	-55	
WER8004	GW	0	45	45	

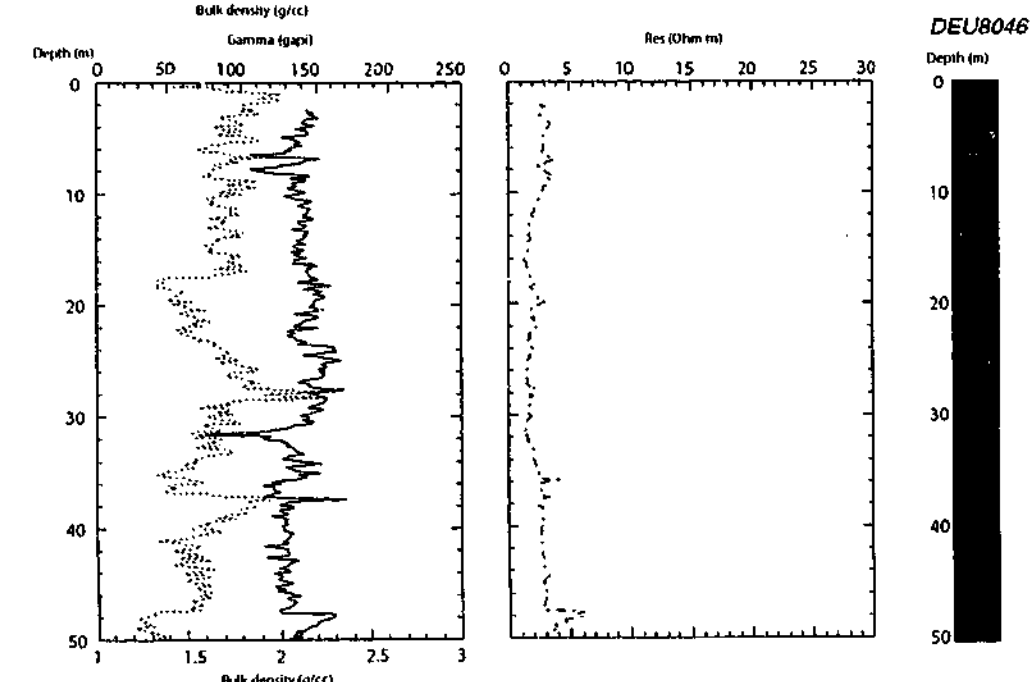


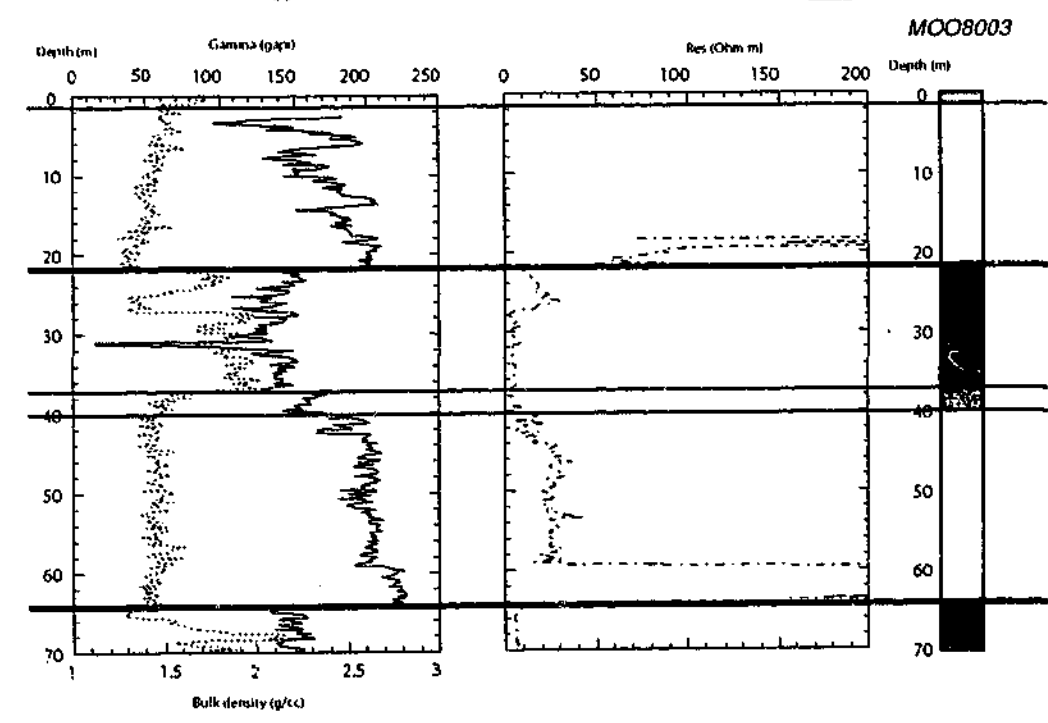
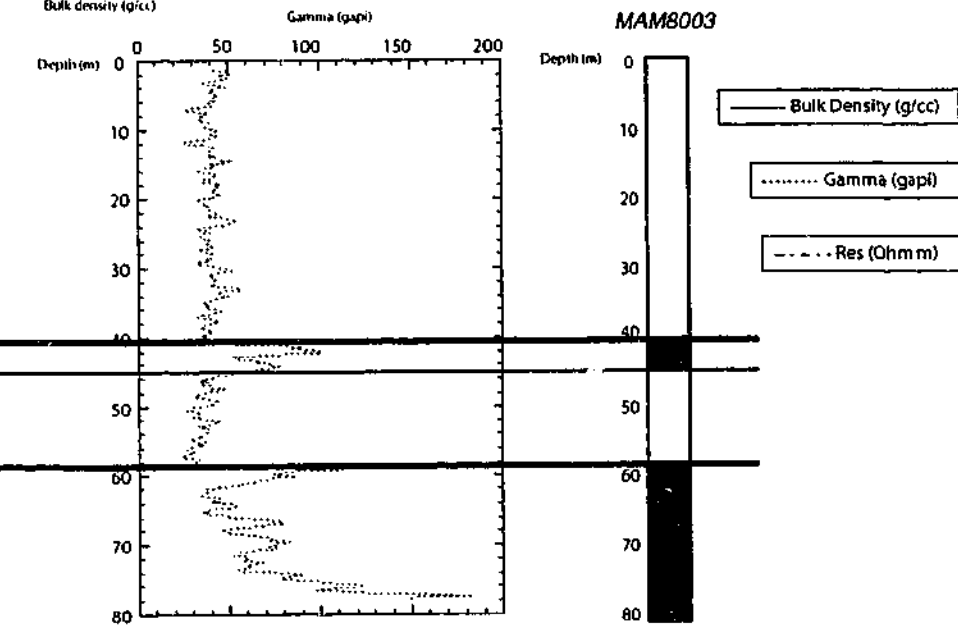
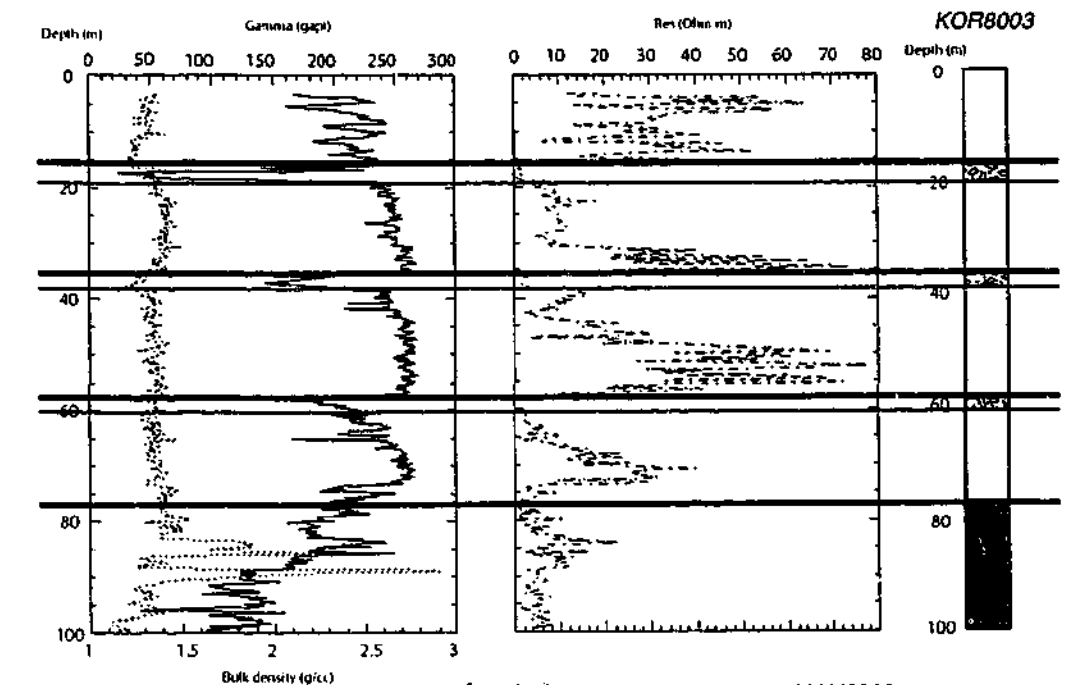
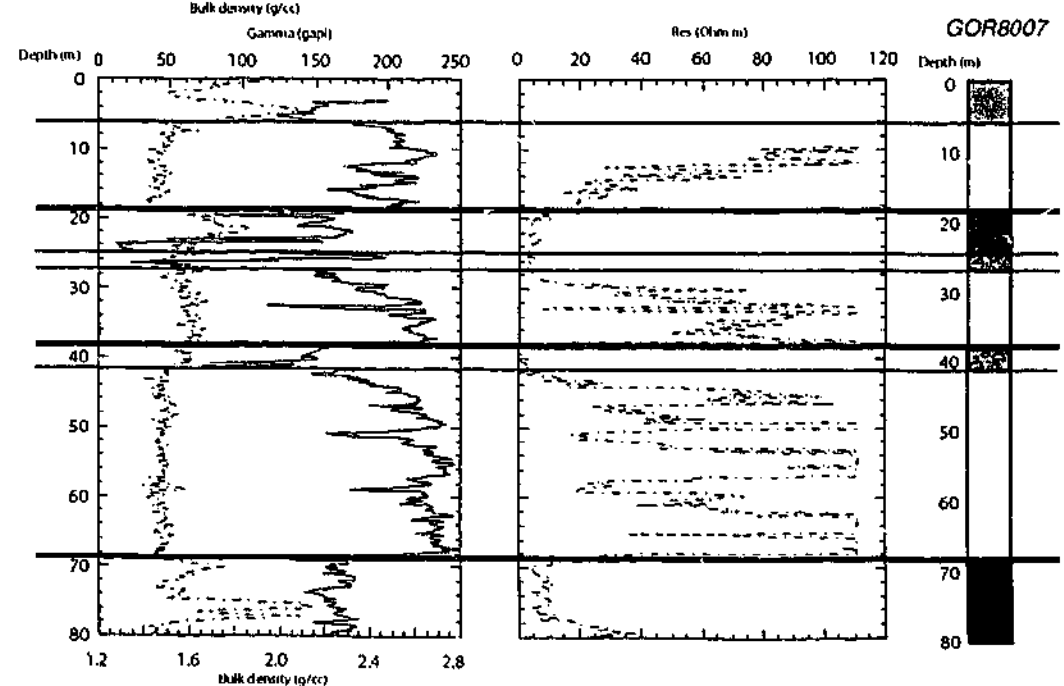
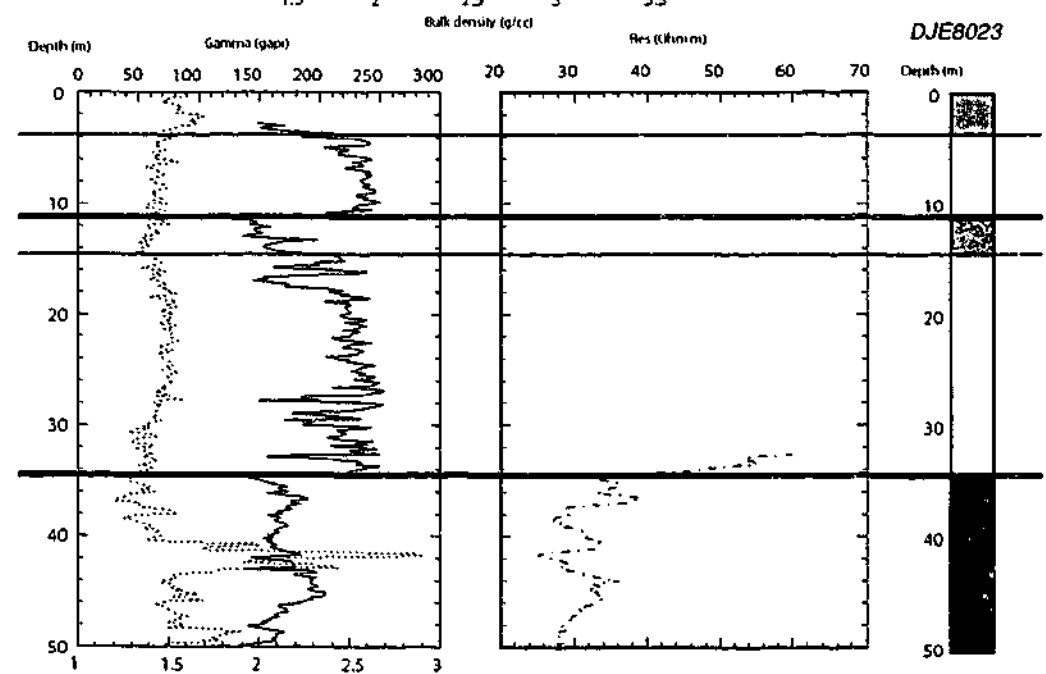
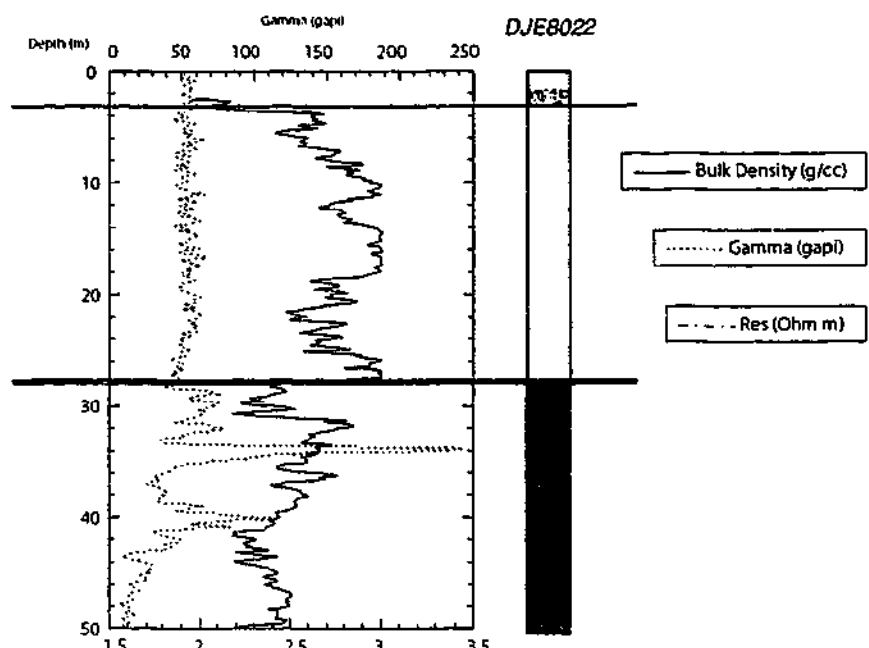


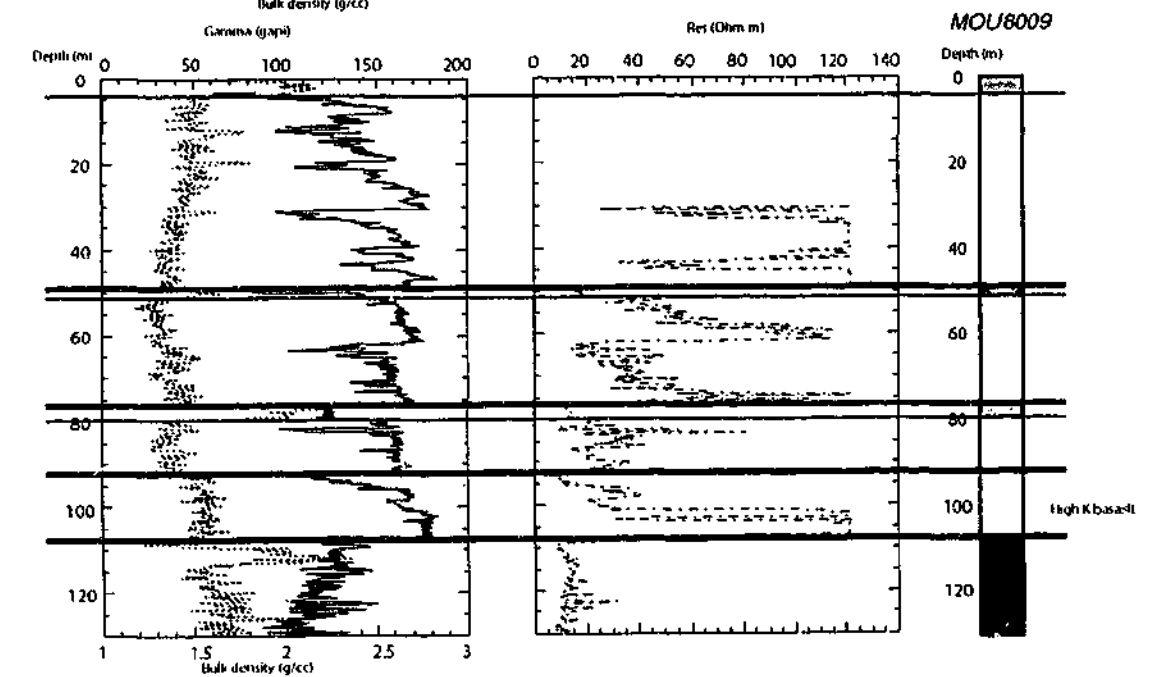
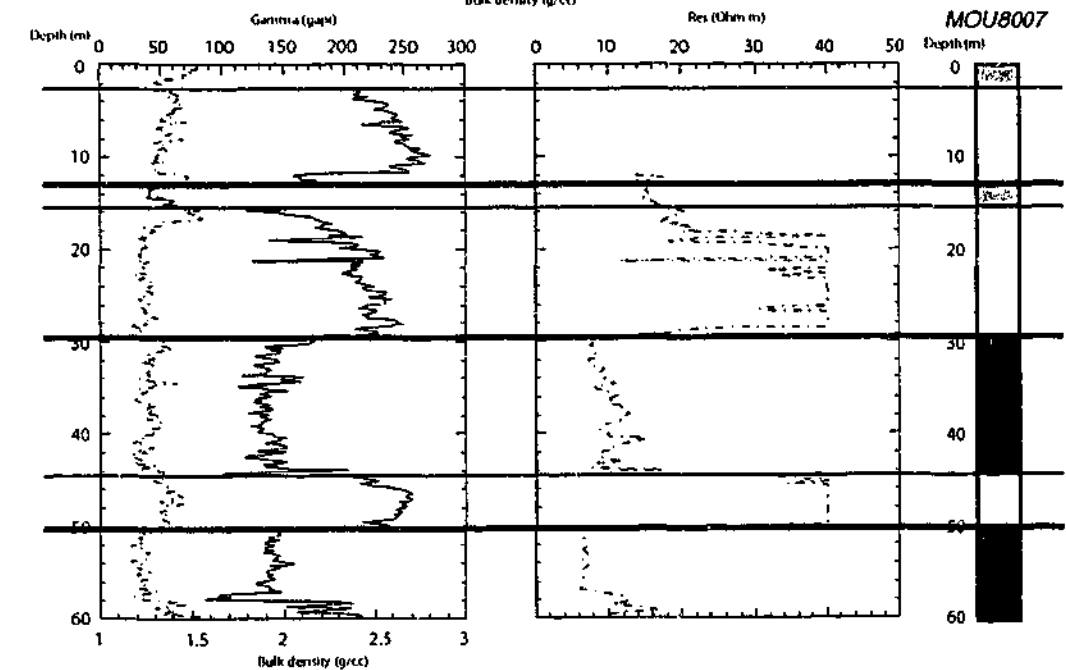
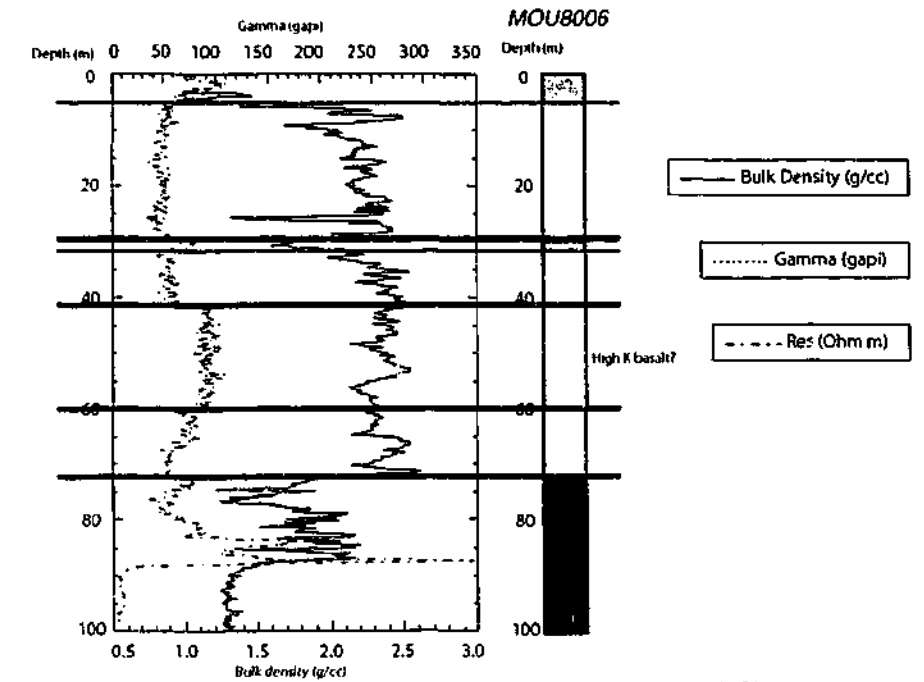
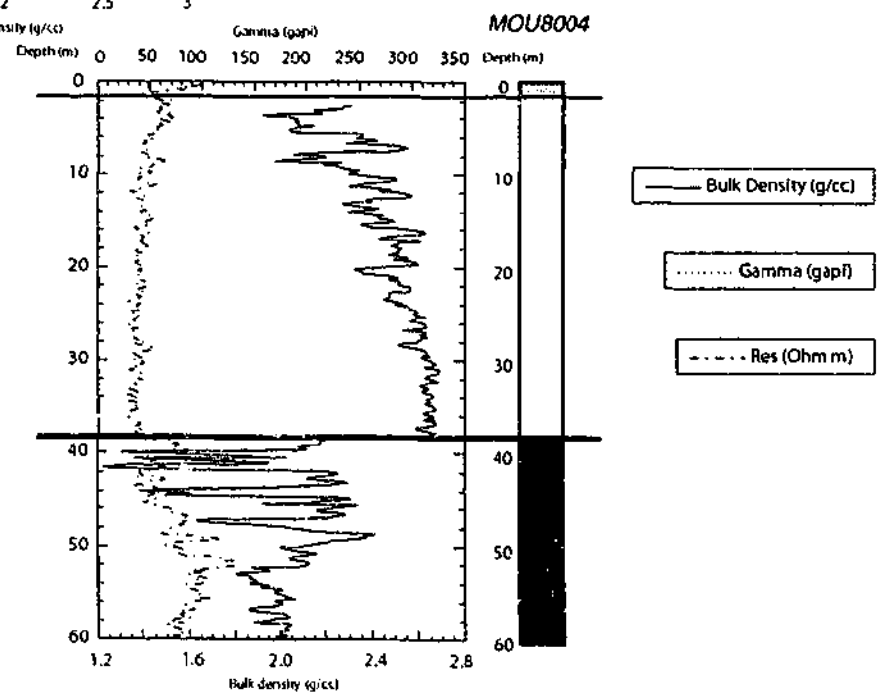
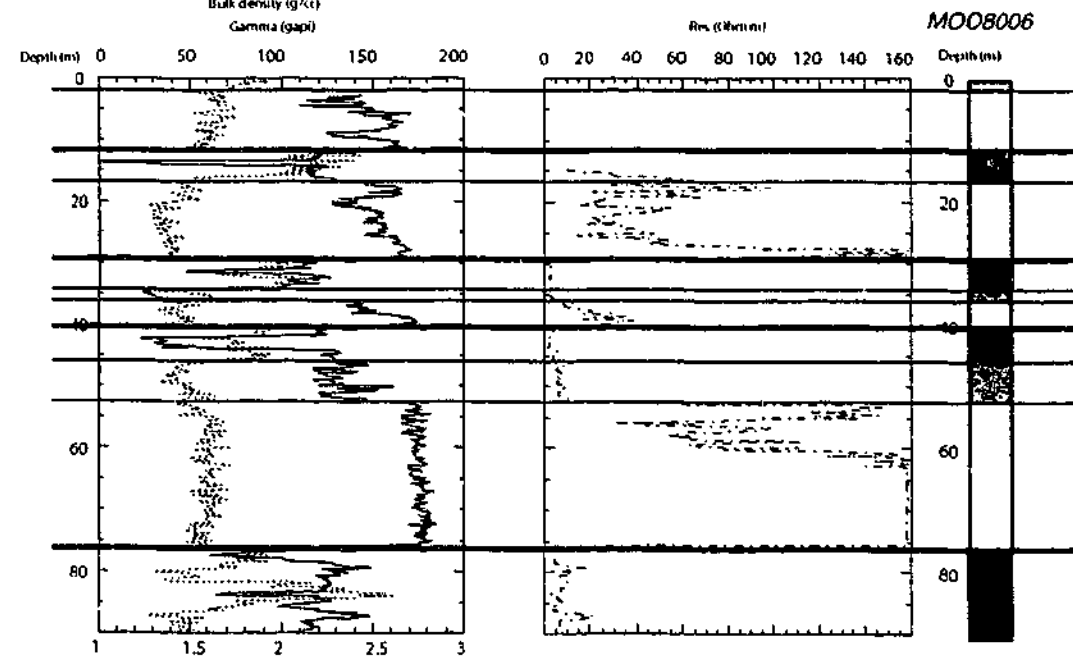
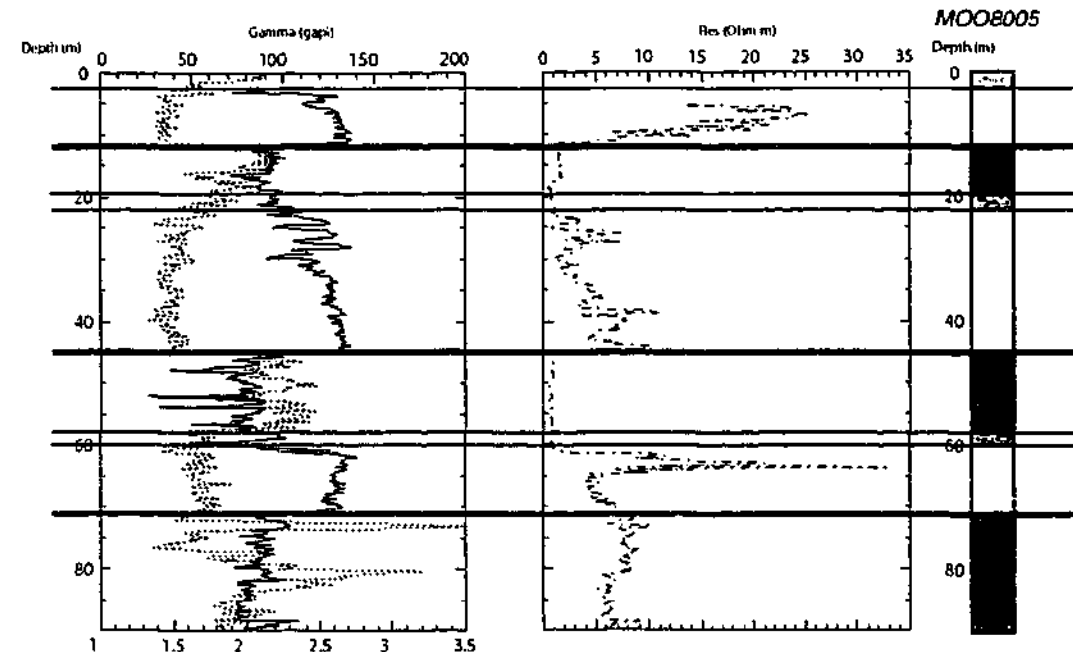
— Bulk Density (g/cc)
 Gamma (gapi)
 - - - Res (Ohm m)

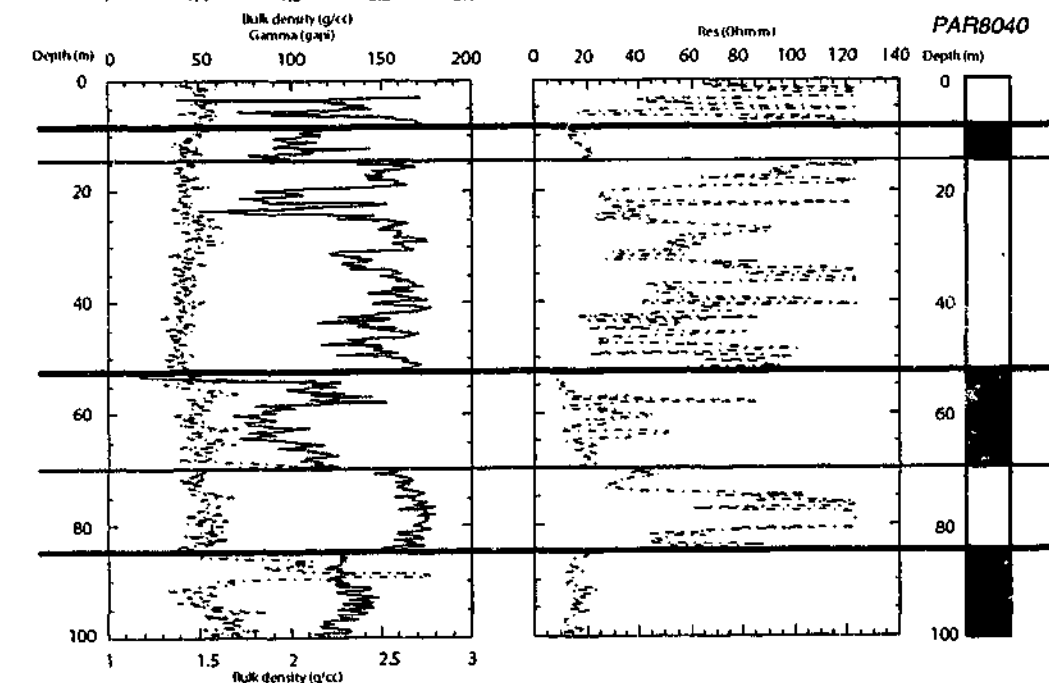
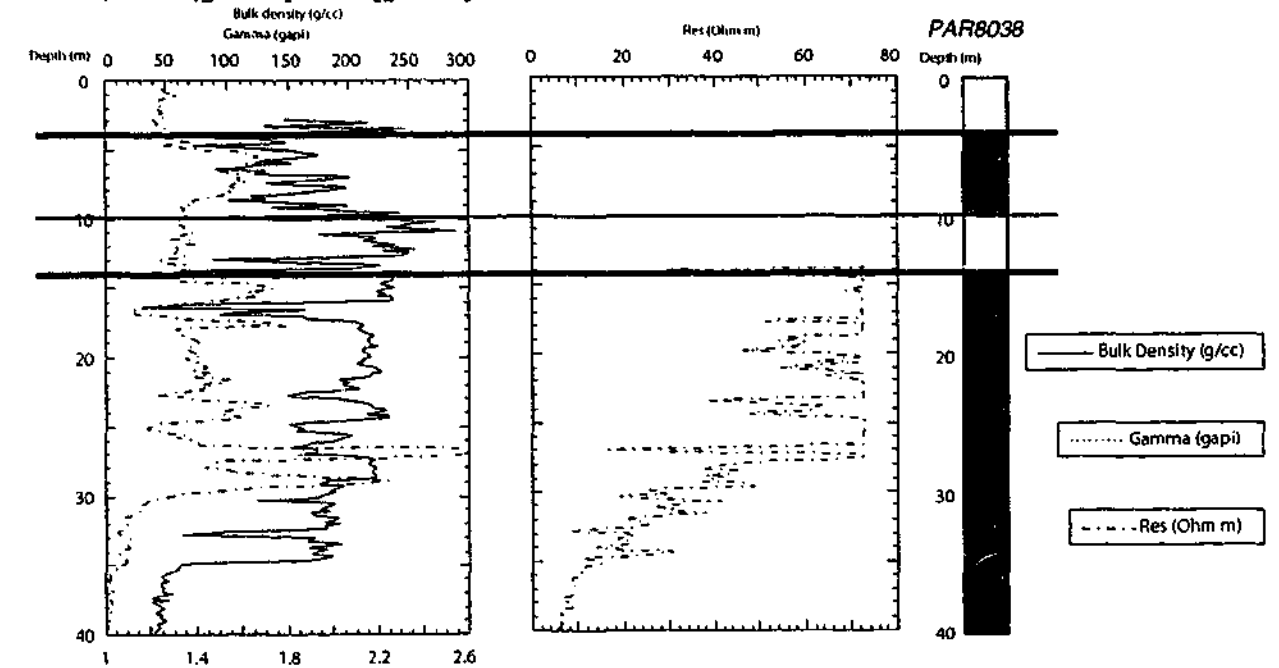
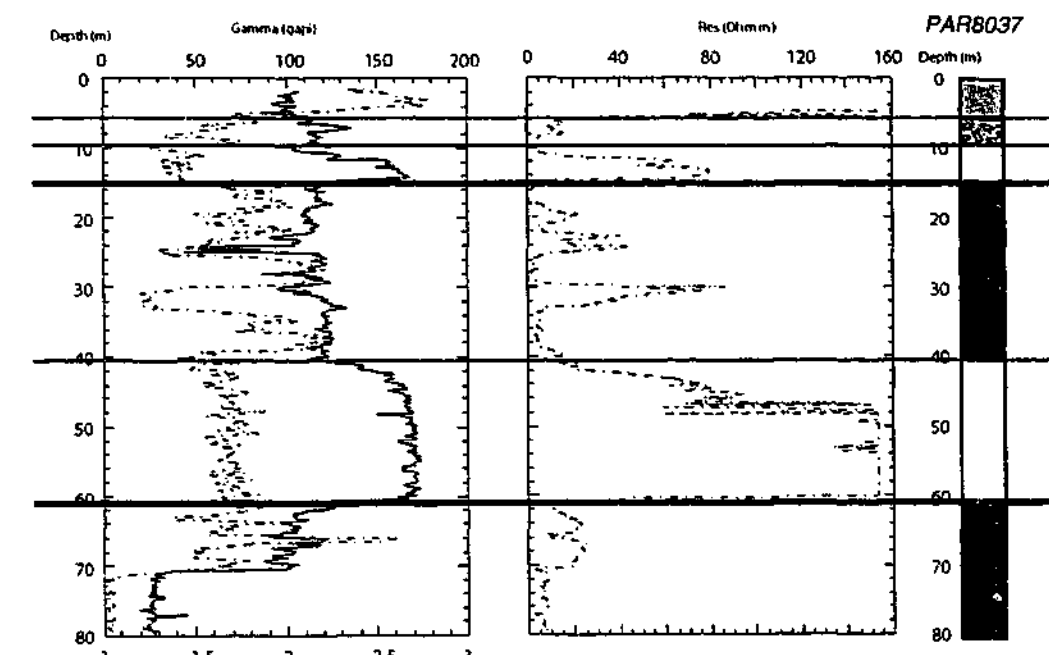
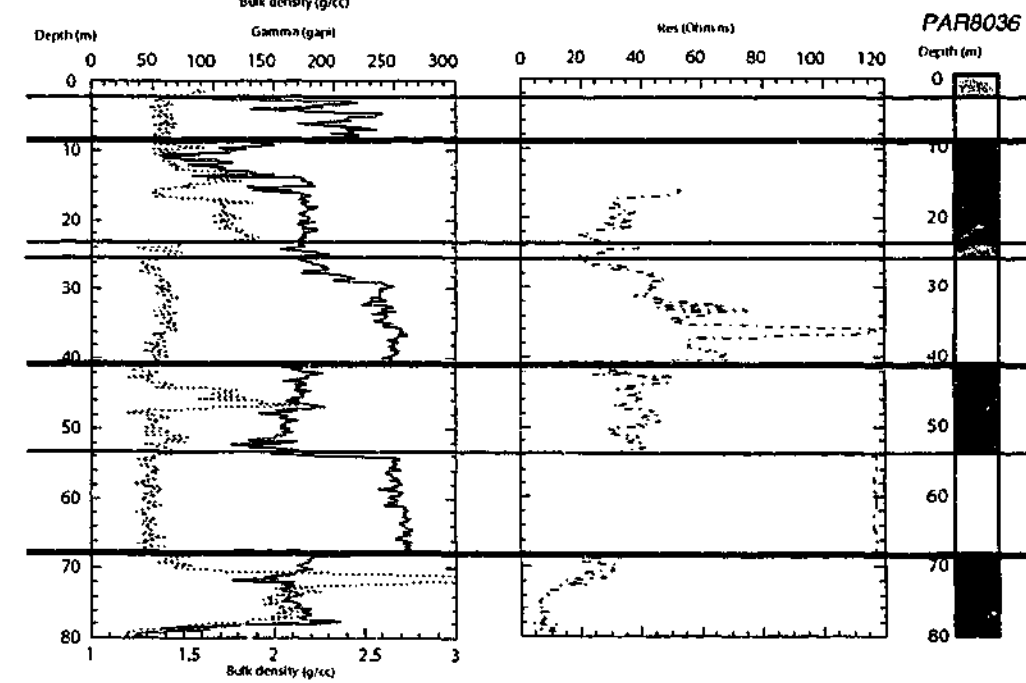
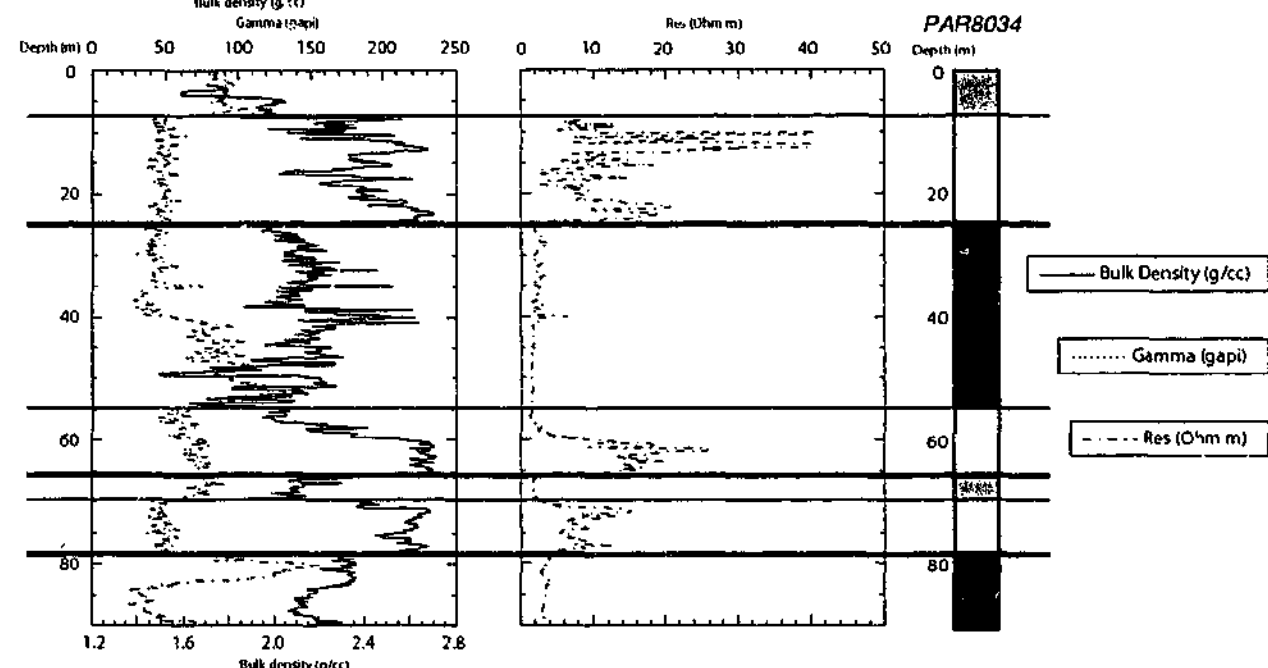
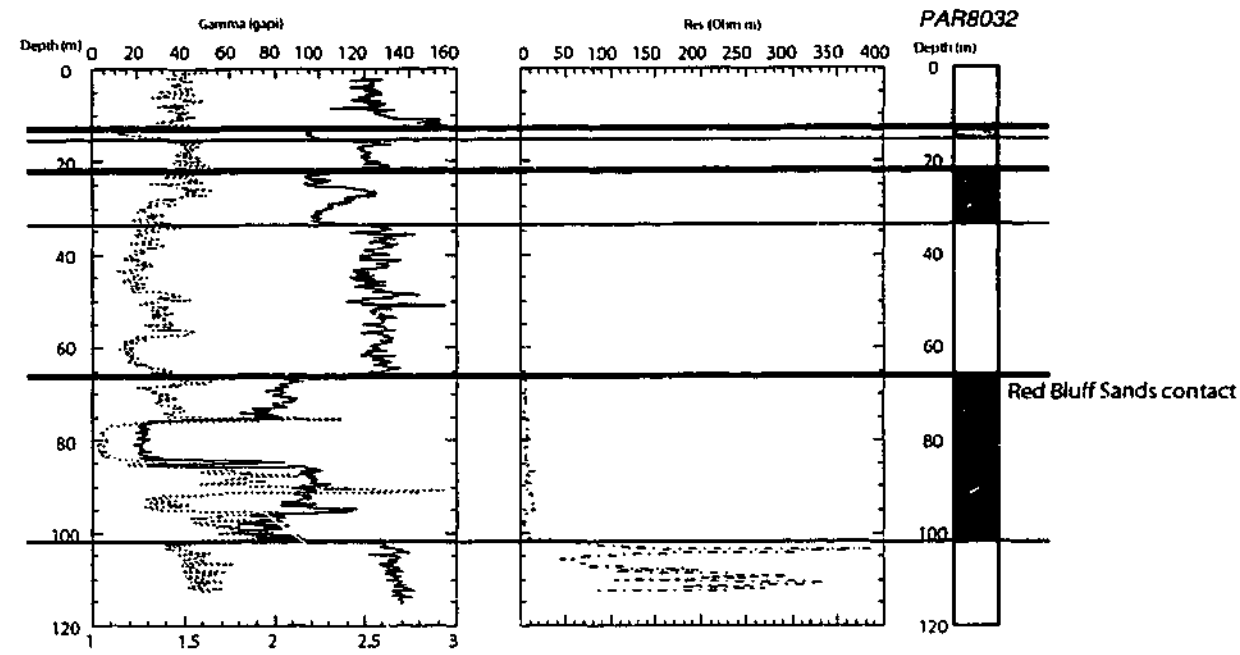


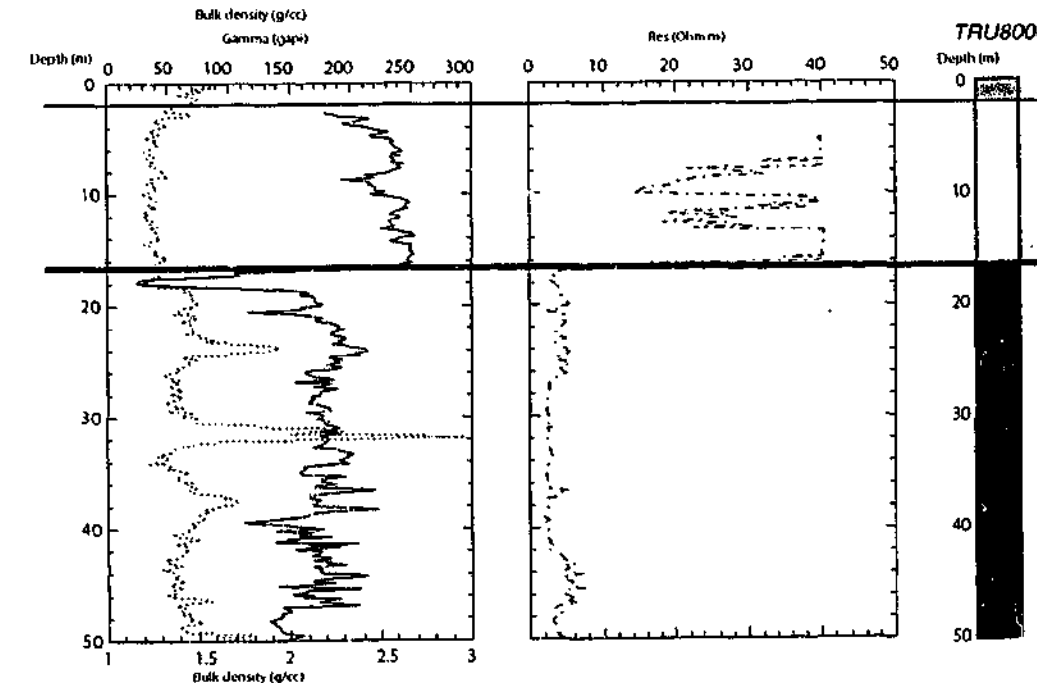
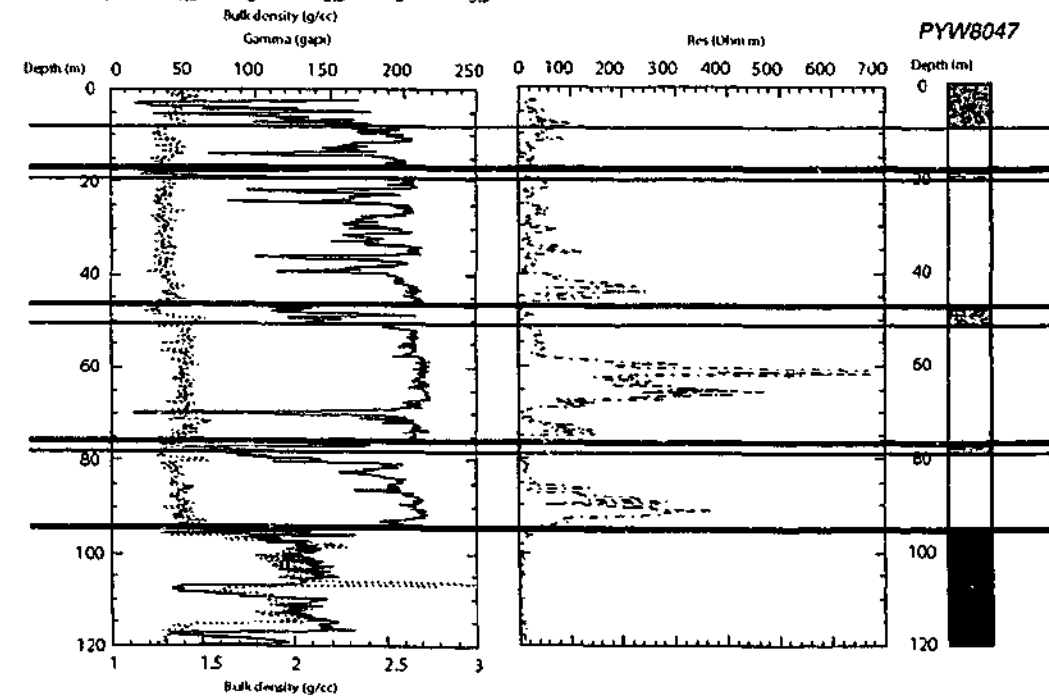
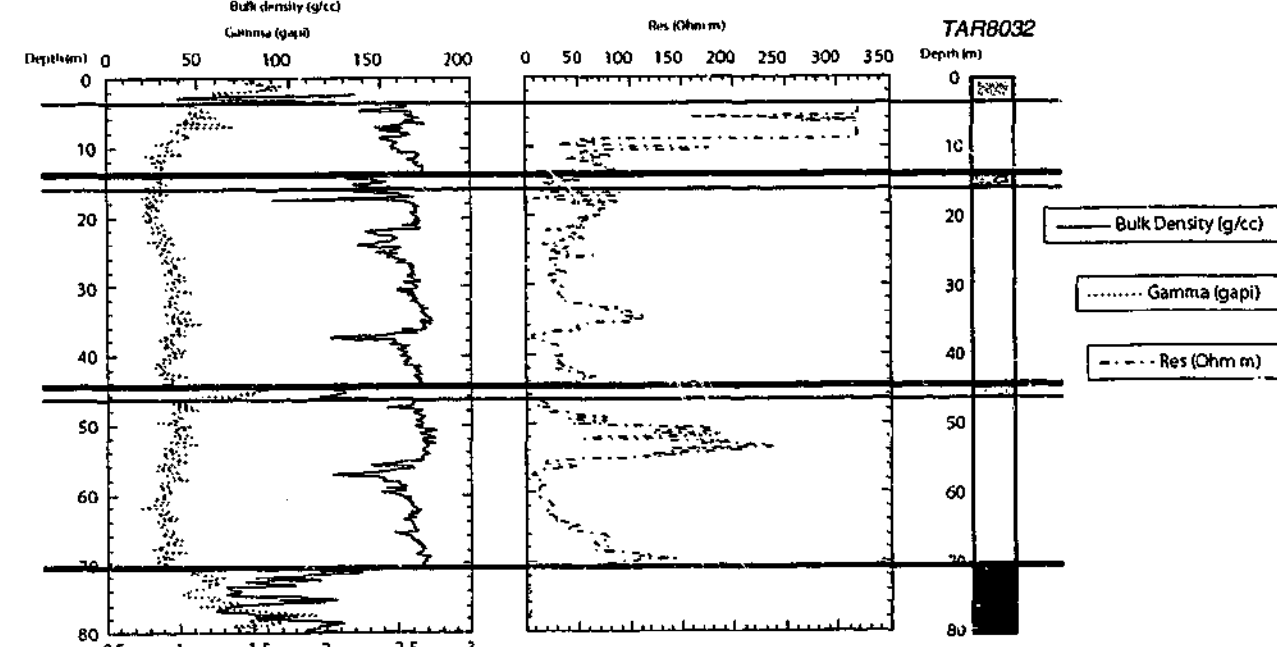
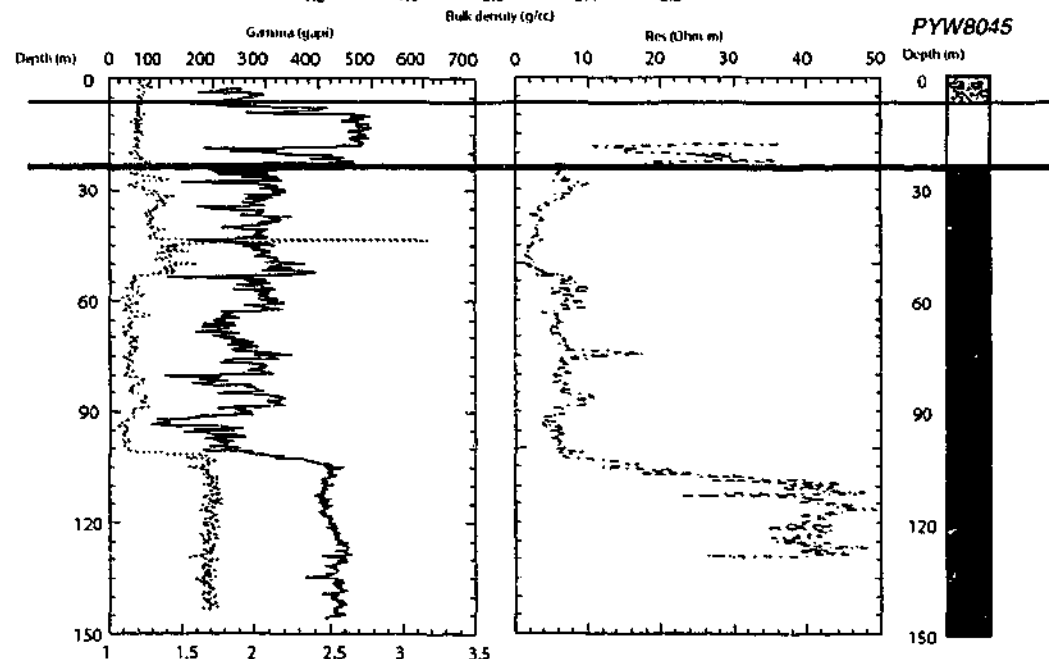
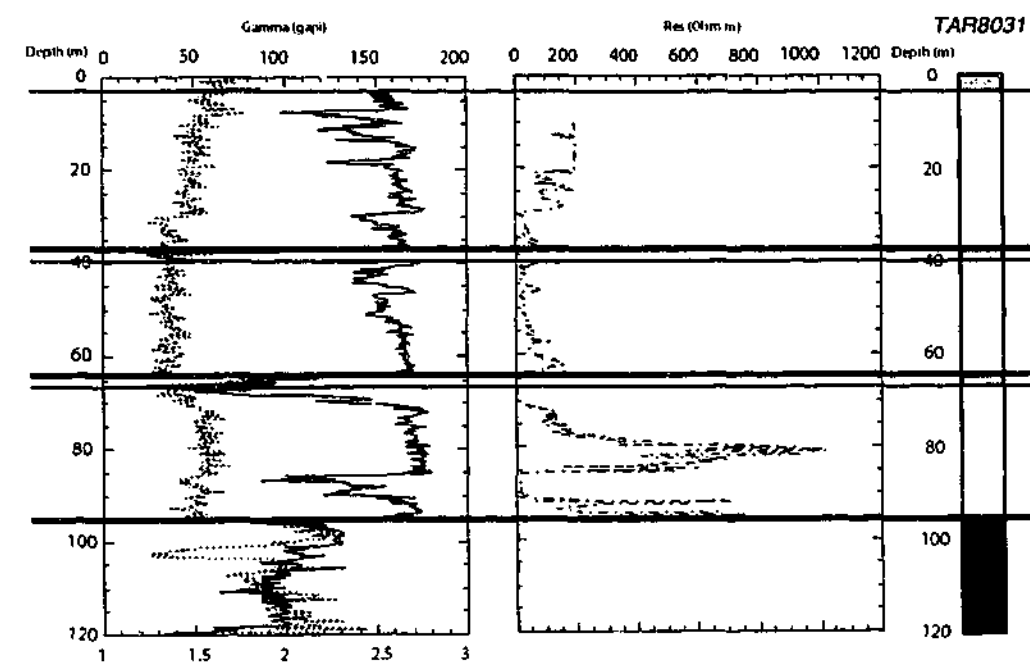
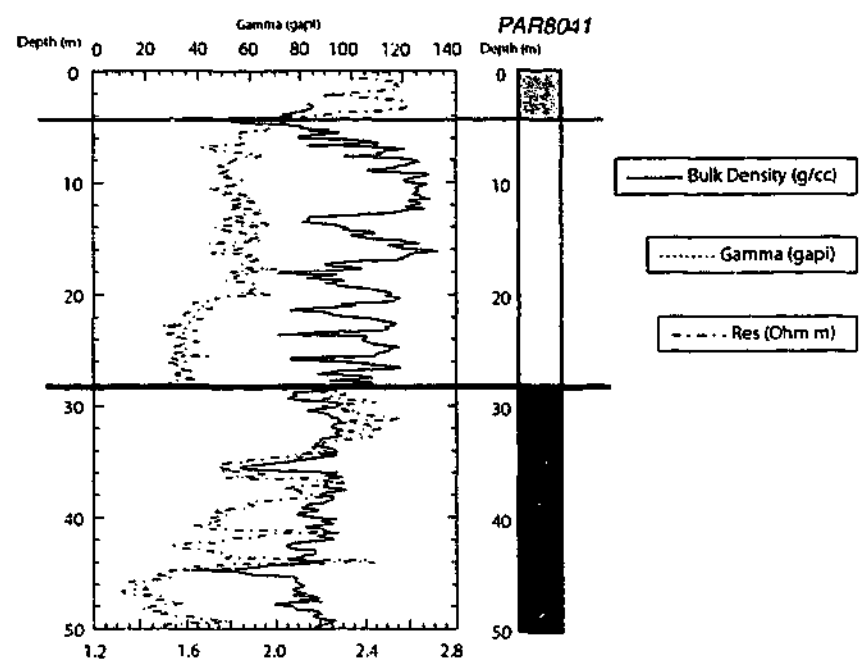
— Bulk Density (g/cc)
 Gamma (gapi)
 - - - Res (Ohm m)

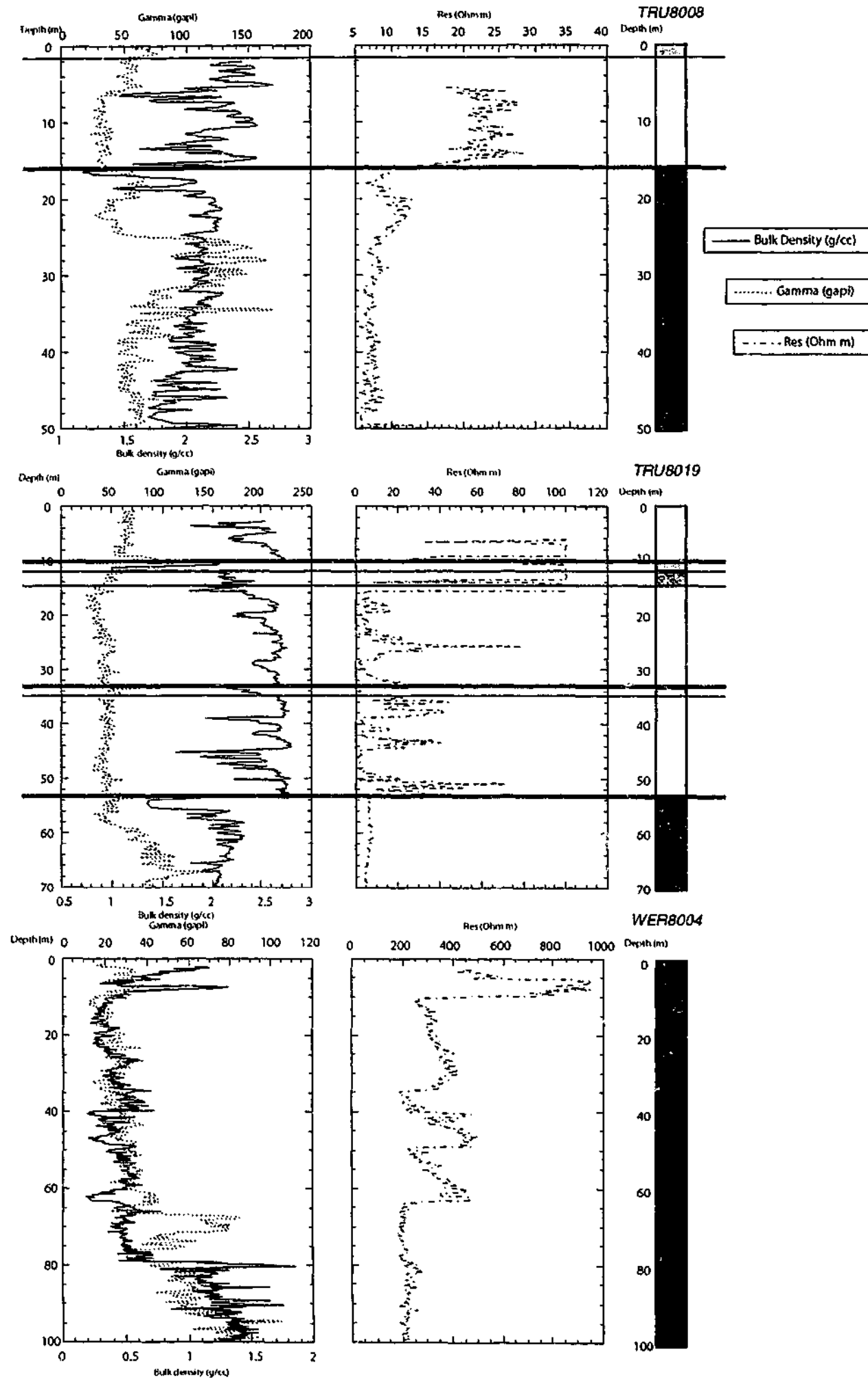












APPENDIX I GEOCHEMICAL DATA FROM THE WERRIBEE PLAINS

Bulk rock XRF results are given along with limited Sr isotope analyses. All rocks have been classified according to the CIPW norm classification scheme (abbreviations: H- hawaiite, TR- transitional, T- tholeiite, QT- quartz tholeiite, BI- basaltic icelandite). Source of data: C.G.- C. Gray unpublished data, M.M.- Mitchell (1990), A.H.- analysed in this study (see Chapter 4).

Depth (m)	CIPW norm.	Data Source	BI		T		TR		H		TR		T		T		BI		TR	
			C.G.	C.G.	C.G.															
SiO2			52.48	48.82	50.92	48.82	48.73	48.04	48.04	48.73	48.73	48.73	51.88	51.88	51.49	51.49	52.11	52.11	50.36	50.36
TiO2			1.69	2.13	1.67	2.13	2.13	2.14	2.14	2.13	2.13	2.13	1.69	1.69	1.66	1.66	1.71	1.71	2.34	2.34
Al2O3			14.78	13.41	14.53	13.41	5.09	4.49	4.49	5.09	5.09	7.89	2.71	2.71	3.49	3.49	3.00	3.00	4.93	4.93
FeO			3.37	5.09	5.63	5.09	5.94	5.47	5.47	5.94	5.94	4.08	7.75	7.20	7.20	7.37	7.37	6.64	6.64	
MnO			6.97	0.16	5.43	0.16	0.16	0.16	0.16	0.16	0.16	0.17	0.16	0.18	0.18	0.16	0.16	0.16	0.16	
MgO			7.42	8.90	7.74	8.90	8.45	8.49	8.49	8.45	8.45	7.02	7.49	7.77	7.77	7.67	7.67	6.95	6.95	
CaO			8.55	8.45	8.69	8.45	3.48	8.29	8.29	8.45	9.21	8.71	8.71	8.76	8.76	8.58	8.58	9.29	9.29	
Na2O			3.21	3.48	3.29	3.48	1.48	3.37	3.37	3.48	3.25	3.25	3.21	3.21	3.23	3.23	3.45	3.45		
K2O			0.74	1.48	0.84	1.48	0.45	1.47	1.47	1.48	1.18	0.78	0.78	0.78	0.58	0.58	1.03	1.03		
P2O5			0.27	0.45	0.28	0.45	0.45	0.45	0.45	0.45	0.30	0.30	0.62	0.62	0.62	0.62	0.62	0.62		
H2O+			0.30	0.71	0.45	0.71	1.04	1.04	1.04	1.04	0.62	0.62	0.44	0.44	0.44	0.44	0.44	0.44		
H2O-			0.30	0.51	0.41	0.51	0.62	0.62	0.62	0.62	0.05	0.05	0.05	0.05	0.05	0.05	0.05	0.05		
CO2			0.04	0.62	0.03	0.62	0.00	0.00	0.00	0.00	0.00	0.00	0.00	0.00	0.00	0.00	0.00	0.00		
S			0.00	0.00	0.00	0.00	0.00	0.00	0.00	0.00	0.00	0.00	0.00	0.00	0.00	0.00	0.00	0.00		
Total			100.29	100.15	100.07	100.15	97.77	97.77	97.77	97.77	100.28	100.28	100.28	100.28	100.28	100.28	100.28	100.28		
Ba			225	489	241	489	460	460	460	460	246	246	246	246	246	246	246	246		
Pb			19	31	24	31	32	32	32	32	26	26	26	26	26	26	26	26		
Sr			342	562	375	562	556	556	556	556	377	377	377	377	377	377	377	377		
Pb			3	7	2	7	3	3	3	3	4	4	4	4	4	4	4	4		
Th			2	6	3	6	3	3	3	3	1	1	1	1	1	1	1	1		
U			2	3	2	3	3	3	3	3	1	1	1	1	1	1	1	1		
Zr			103	164	111	164	39	39	39	144	144	144	144	144	144	144	144	144		
Nb			16	38	19	38	39	39	39	18	18	18	18	18	18	18	18	18		
Y			20	17	20	17	17	17	17	23	23	23	23	23	23	23	23	23		
La			16	29	15	29	27	27	27	15	15	15	15	15	15	15	15	15		
Ce			17	39	23	39	36	36	36	22	22	22	22	22	22	22	22	22		
Sc			20	18	20	18	19	19	19	21	21	21	21	21	21	21	21	21		
V			152	182	166	182	191	191	191	167	167	167	167	167	167	167	167	167		
Cr			256	318	276	318	313	313	313	266	266	266	266	266	266	266	266	266		
Ni			134	224	152	224	212	212	212	135	135	135	135	135	135	135	135	135		
Cu			45	73	52	73	43	43	43	43	43	43	43	43	43	43	43	43		
Zn			109	122	111	122	122	122	122	108	108	108	108	108	108	108	108	108		
Ga			21	21	20	21	21	21	21	21	21	21	21	21	21	21	21	21		
⁸⁷ Sr/ ⁸⁶ Sr			0.70479	0.70474	0.70474	0.70443	0.70436	0.70436	0.70436	0.70474	0.70474	0.70474	0.70474	0.70474	0.70474	0.70474	0.70474	0.70474		

Depth (m)	H		TR		BI		T	BI			H		H
CIPW norm.	C.G.		M.M.		C.G.		C.G.	C.G.			C.G.		C.G.
Data Source	C.G.	M.M.	M.M.	C.G.	C.G.	C.G.	C.G.	C.G.	C.G.	C.G.	C.G.	C.G.	C.G.
SiO2	49.08	49.22	48.89	53.63	53.18	48.36	53.17	53.12	52.62	49.04	47.89	48.60	
TiO2	2.07	2.10	1.91	1.71	1.70	2.56	1.80	1.71	1.71	1.98	2.09	2.10	
Al2O3		13.81	13.59	14.88	14.77	14.16	14.51	14.63	14.59	13.82	13.52	13.82	
Fe2O3	3.61	4.97	4.23	2.73	2.12	5.39	1.96	3.20	2.35	3.13	3.60	2.82	
FeO	7.17	5.72	6.17	7.17	7.59	7.77	7.69	6.67	7.49	7.59	7.11	7.98	
MnO	0.16	0.16	0.15	0.15	0.17	0.21	0.16	0.15	0.16	0.20	0.18	0.17	
MgO	9.05	8.43	8.75	7.27	7.18	4.18	6.65	6.47	7.14	9.01	9.36	8.79	
CaO	9.00	8.59	9.33	8.41	8.41	7.18	8.48	6.98	8.22	8.58	9.12	8.49	
Na2O	3.35	3.42	3.33	2.87	3.18	4.12	3.39	3.49	3.45	3.56	3.49	3.62	
K2O	1.38	1.41	1.28	0.81	0.84	1.89	0.81	1.27	0.71	1.42	1.62	1.53	
P2O5		0.52	0.43	0.26	0.26	1.60	0.30	0.33	0.26	0.45	0.55	0.46	
H2O+		0.94	0.57	0.38	0.43	0.96	0.63	0.94	0.72	0.61	0.68	0.65	
H2O-		0.84	0.35	0.16	0.18	0.57	0.18	0.41	0.26	0.23	0.47	0.37	
CO2		0.20	0.88	0.07	0.14	0.80	0.13	0.43	0.03	0.11	0.29	0.55	
S		0.00	0.00	0.00	0.01	0.01	0.04	0.00	0.01	0.00	0.01	0.00	
Total		100.33	99.86	100.50	100.16	99.76	99.60	99.80	99.72	99.73	99.98	99.95	
Ba				340	673	767	785	653	423	794	976	516	
Rb	32	31	30	31	31	40	28	43	30	30	37	34	
Sr	628	632	574	345	358	559	383	336	347	608	716	594	
Pb		4	5	4	5	6	6	4	4	3	3	5	
Th		4	3	3	3	4	4	5	3	5	4	5	
U		2	1	1	0	1	1	1	0	0	1	0	
Zr				152	143	325	122	220	137	185	185	199	
Nb				17	16	57	20	23	0	0	0	0	
Y		23	22	21	23	44	25	25	27	26	28	24	
La				14	17	55	23	25	20	30	36	31	
Ce				29	27	93	40	34	29	53	51	52	
Sc				20	18	18	19	0	0	0	0	0	
V				163	160	166	160	139	151	157	169	173	
Cr				299	229	44	229	235	284	308	344	308	
Ni				91	87	37	87	110	89	147	164	162	
Cu				29	28	9	28	27	36	48	40	43	
Zn				100	119	144	119	98	101	97	92	103	
Ga		20		21	19	25	19	22	22	21	20	21	
⁸⁷ Sr/ ⁸⁶ Sr		0.70417	0.70468	0.70520	0.70534	0.70501	0.70542	0.70484	0.70522	0.70444	0.70432	0.70428	

Depth (m)	H		H	T	BI	QT	QT	BI	T	T	TR	QT
CIPW norm.	C.G.		C.G.	C.G.	C.G.	C.G.	C.G.	C.G.	C.G.	C.G.	C.G.	C.G.
Data Source	C.G.	C.G.	C.G.	C.G.	C.G.	C.G.	C.G.	C.G.	C.G.	C.G.	C.G.	C.G.
SiO2	48.81	48.90	49.10	49.81	52.06	51.83	51.87	51.94	51.77	50.31	48.87	51.79
TiO2	2.09	2.20	2.10	2.02	1.65	1.64	1.76	1.77	1.69	1.89	2.10	1.69
Al2O3	13.88	13.51	13.66		14.33	14.32	13.67	14.41	13.78		13.61	
Fe2O3	2.91	2.74	2.25	7.20	3.77	3.30	4.02	6.95	3.14	1.92	2.94	3.79
FeO	8.00	8.09	8.50	4.31	6.91	7.21	6.55	4.65	7.24	8.75	7.34	6.74
MnO	0.17	0.18	0.18	0.18	0.17	0.16	0.16	0.17	0.16	0.16	0.16	0.16
MgO	8.90	8.71	8.71	7.75	8.71	8.73	8.04	7.35	8.30	8.39	8.72	7.98
CaO	8.35	8.45	8.52	8.03	8.36	8.47	8.13	8.28	8.25	7.89	8.98	8.32
Na2O	3.57	3.47	3.53	3.20	2.64	2.69	2.63	2.66	3.10	2.99	3.49	3.08
K2O	1.52	1.60	1.51	1.25	0.85	0.75	0.91	0.88	0.79	1.00	1.42	0.79
P2O5	0.45	0.51	0.47		0.26	0.26	0.30	0.28	0.29		0.53	
H2O+	0.51	0.88	0.45		0.49	0.58	0.75	0.53	0.64		0.60	
H2O-	0.33	0.37	0.26		0.15	0.23	0.56	0.28	0.38		0.25	
CO2	0.25	0.21	0.13		0.08	0.16	0.45	0.01	0.06		0.59	
S	0.00	0.30	0.00		0.00	0.02	0.01	0.00	0.01		0.01	
Total	99.54	100.12	99.37		100.43	100.20	99.73	100.16	99.52		99.61	
Ba	787	1252	665		335	639	358	384	445		538	
Rb	33	34	35	29	26	25	24	26	26	24	29	25
Sr	600	605	601	433	366	365	372	388	377	399	593	375
Pb	2	4	3		4	3	2	3	1		0	
Th	5	4	4		4	3	2	4	5		0	
U	1	0	1		0	0	1	0	1		0	
Zr	201	176	189		145	146	153	157	148		214	
Nb	0	51	0		0	0	22	0	22		45	
Y	26	26	25		21	23	22	24	21		21	
La	32	43	34		16	11	18	17	22		31	
Ce	36	61	45		20	18	34	28	29		51	
Sc	0	15	0		0	0	19	0	17		17	
V	166	180	160		152	160	153	161	157		174	
Cr	308	282	243		339	349	288	324	305		303	
Ni	179	176	138		152	151	153	151	154		186	
Cu	41	51	49		45	34	46	41	58		85	
Zn	104	114	96		98	101	109	103	113		108	
Ga	20	20	23		19	18	19	19	19		21	
⁸⁷ Sr/ ⁸⁶ Sr	0.70426	0.70442	0.70447		0.70542	0.70541	0.70535	0.70519	0.70546		0.70433	

APPENDIX K

SURFACE MAGNETIC POLARITY DATA

Unpublished data courtesy of N. Opdyke

Site	Latitude	Longitude	Magnetic polarity
Melton Rd.	37.40.945 'S	144 38.167 'E	Reverse (R)
Near Mt. Kororoit	37.37.479 'S	144 39.600 'E	R
Cobbledick Ford	37.49.304 'S	144 34.723 'E	R
Deer Park Quarry	37.47.445 'S	144 43.913 'E	R
Greig's Rd.	37.44.872 'S	144 34.769 'E	R
Sunshine Quarry	37.44.548 'S	144 49.621 'E	Normal (N)
Sunshine Quarry	37.44.644 'S	144 49.709 'E	N
Metro Quarry	37.40.545 'S	144 40.415 'E	R
Parwan Creek	37.43.754 'S	144 23.594 'E	N

APPENDIX L

LIST OF PUBLICATIONS

Moore, A.G., Cas, R.A.F., Beresford, S.W. & Stone, M. 2000. Geology of an Archaean metakomatiite succession, Tramways, Kambalda Ni province, Western Australia: assessing the extent to which volcanic facies architecture and flow emplacement mechanisms can be reconstructed. *Australian Journal of Earth Sciences* **47**, 659-673.

Moore, A.G. & Cas, R.A.F. 2000. Establishing the stratigraphy of the Werribee Plains, Newer Volcanic Province, Victoria: an interdisciplinary approach. *Geological Society of Australia Abstracts* **62**, 63.

Moore, A.G. & Cas, R.A.F. 2001. Emplacement processes and crystallisation of basaltic lavas: insights from detailed vesicle zonation and petrographic studies. *Abstracts, Cities on Volcanoes 2 Conference, Auckland, New Zealand* 100.

Hare, A.G., Cas, R.A.F. & Musgrave, R.J. 2001. An overview of basaltic volcanism in the Werribee Plains, Newer Volcanic Province, Vic.: products and frequency of eruptions. *Geological Society of Australia Abstracts* **66**, 5.

NB: The first item contains work completed for a BSc (Hons) degree, and was written up and published during my PhD candidature.

Geology of an Archaean metakomatiite succession, Tramways, Kambalda Ni province, Western Australia: assessing the extent to which volcanic facies architecture and flow emplacement mechanisms can be reconstructed

A. G. MOORE,¹ R. A. F. CAS,¹ S. W. BERESFORD¹ AND M. STONE²

¹Department of Earth Sciences, Monash University, Vic. 3800 Australia.

²WMC Resources Ltd, Kambalda, WA 6442, Australia.

The Kambalda Ni province, located in the Archaean Norseman-Wiluna greenstone belt of Western Australia, boasts the largest known concentration of komatiite-associated magmatic Fe-Ni-Cu sulfide deposits. These are found as long, linear massive to disseminated bodies at the base of a thick komatiite sequence. The sulfide bodies are closely associated with, or contained within, trough structures at the contact with the underlying basaltic unit. In this study, the McComish Prospect, located 40 km south of Kambalda at Tramways, was studied to assess the relationships between volcanic facies, mineralisation and trough structures. The rocks in this region have variably experienced four phases of deformation, upper greenschist-lower amphibolite facies metamorphism, granitoid intrusion, and subsequent alteration. Relict igneous textures are locally preserved at McComish, however, enabling the evaluation of existing geological models and interpretations. The McComish trough is considered to be entirely structural in origin and unrelated to primary volcanic processes (e.g. thermal erosion). The association of volcanic textural facies in individual flow units, and the distribution of flow units across the trough is more complex than predicted by prevailing models, suggesting an alternative komatiite lava emplacement mechanism. Results are consistent with the proposal that komatiites did not flow turbulently as widely accepted, nor did they cool by vigorous convection. Alternatively, the lavas were emplaced as inflated, lobate basalt pahoehoe-like flows. Although Fe-Ni-Cu sulfide mineralisation at McComish is most likely volcanic in origin, its present distribution appears to be structurally controlled or modified. The zone of weakly disseminated sulfides at the base of the komatiite sequence is thickened adjacent to a major north-northwest-trending fault on the western margin of the trough. This fault is interpreted to have been a fluid conduit, remobilising the ore during metamorphism and deformation.

KEY WORDS: Archaean, Kambalda, komatiite, nickel sulfides, volcanology.

INTRODUCTION

Many genetic and highly interpretative papers have been written about the volcanology of Archaean komatiite lavas, and the origins of associated nickel sulfide mineralisation in the Yilgarn Craton of Western Australia. Many of these papers give the impression that preservation of original igneous textures and geological relationships are good, and represent a sound basis for the genetic models proposed. In fact, the preservation of textures and geological relationships can be highly variable at even the local scale, due to variable degrees of deformation, metamorphism and alteration. In this paper we document the geology of a metakomatiite succession at the McComish Prospect at Tramways, ~40 km south-southeast of Kambalda (Figure 1). The distribution of preserved primary igneous textures and contacts, the degree of metamorphism and alteration, structural elements, and the extent of mineralisation have all been recorded from diamond drillcore. We have then evaluated the extent to

which original volcanological reconstructions can be made (i.e. the geometry of the komatiite lava flow field, the internal textural variations within flows etc.), the implications these reconstructions have for komatiite lava-flow behaviour, and the most likely origin of the mineralisation.

KOMATIITES AND THE KAMBALDA MODEL

Komatiites are ultramafic volcanic rocks containing 18-32% MgO (Arndt & Nisbet 1982). Eruption temperatures of komatiite lavas ranged from 1400 to 1700°C, the lavas were of very low viscosity (~0.1-1 Pa s), and it is widely assumed that they flowed turbulently (Huppert *et al.* 1984; Huppert & Sparks 1985; Hill *et al.* 1995; Williams *et al.* 1998). The lava is considered to have been focused into 'channels', (either open lava rivers, tubes or constructional lava complexes) forming thick, high-Mg flows (Gresham & Loftus-Hills 1981; Leshner *et al.* 1984; Cowden 1988; Cowden & Roberts 1990; Hill *et al.* 1995), and laminar flowing

overspills of lava from the 'channels' formed thin sheet flows in 'flank' settings.

Dense, immiscible Fe-Ni-Cu sulfide droplets are considered to have been transported by turbulent lava in the 'channels' and settled to the base of the flows as the turbulence eased. At Kambalda this sulfide mineralisation is now often preserved in trough structures, the origin of which has been widely debated. The troughs have been variably interpreted as: (i) thermal erosion channels, formed by melting and assimilation of the substrate by turbulent komatiite lava (Huppert *et al.* 1984; Huppert & Sparks 1985); (ii) pre-existing topographic depressions deepened by thermal erosion ± structural modification (Leshner *et al.* 1984; Groves *et al.* 1986); or (iii) purely structural features, with sulfide bodies in the channel facies being the focus for subsequent deformation (Cowden 1988; Cowden & Roberts 1990). The thin flanking flows are observed to conformably overlie either the footwall metabasalt or sulfidic metasedimentary rocks at Kambalda. Metasedimentary intervals are notably absent in ore-bearing environments (Bavinton 1979; Gresham & Loftus-Hills 1981; Leshner *et al.* 1984). The association of thick flows in the mineralised environments and adjacent, thin barren flows of the komatiite sequence have been described as the channel and flanking sheet-flow facies, respectively (Cowden & Roberts 1990).

These genetic models are largely based on the Archaean komatiite succession of the Kambalda Dome, the type locality for komatiite-hosted Ni sulfide deposits. Unfortunately the simplicity of the models does not reflect the complex geology of the komatiites at Kambalda, which are multiply deformed and metamorphosed to upper greenschist-lower amphibolite facies, often under conditions of high fluid activity (Gresham & Loftus-Hills 1981;

Archibald 1985). Although igneous textures are locally preserved, they are more commonly overprinted by metamorphic textures. This creates difficulties in recognising flow-unit boundaries and flow-unit geometry, as it depends on recognising komatiite textural zones. Detailed relogging of much of the diamond drillcore in the Kambalda province (this study and others in preparation) has shown that most palaeovolcanological reconstructions are too simplistic and have taken little or no account of the effects of structural deformation on stratigraphic and facies architecture.

In addition, the turbulent nature of komatiite lavas has recently been questioned (Cas *et al.* 1999). It has been proposed that continental flood basalts (and by analogy komatiites) need not have been rapid, turbulent flows to travel the vast distances observed (Self *et al.* 1998), as previously interpreted (Shaw & Swanson 1970). Instead, long lava flows are now considered to propagate as inflated, compound sheet flows under laminar-flow conditions by development of an insulating tube system (Self *et al.* 1996, 1997, 1998; Keszthelyi & Self 1998; Kauahikaua *et al.* 1998). If this is correct, current komatiite ore-genesis models and interpretations for the origin of the channel and sheet-flow facies need to be re-evaluated.

GEOLOGICAL SETTING OF THE MCCOMISH PROSPECT, TRAMWAYS

The McComish Prospect, Tramways region, is located in the south-central part of the Norseman-Wiluna greenstone belt, in the Eastern Goldfields Province of the Archaean Yilgarn Craton (Figure 1). The Eastern Goldfields Province consists of a number of terranes (Swager *et al.* 1992) including the Kalgoorlie Terrane. The Kalgoorlie Terrane contains the southern half of the Norseman-Wiluna belt and has been subdivided into six fault-bound tectonostratigraphic domains (Swager *et al.* 1992), one of which is the Kambalda Domain. The rocks in the Kambalda Domain have experienced upper greenschist-lower amphibolite metamorphic conditions and have undergone four phases of deformation (Gresham & Loftus-Hills 1981; Archibald 1985; Swager *et al.* 1992).

The regional stratigraphy of the Kambalda district has been well established in the Kambalda district, where it is moderately well exposed and well known from drillcore from the Kambalda Dome, a folded greenstone sequence intruded by trondhjemite (Gresham & Loftus-Hills 1981; Cowden & Roberts 1990). The stratigraphy consists of a lower basalt unit (Lunnon Basalt) overlain by komatiite (Kambalda Komatiite Formation), another basalt unit (Devon Consols Basalt), the pelitic Kapa Slate and an upper basalt unit (Paringa Basalt). This mafic-ultramafic succession is overlain by the felsic volcanic and volcanoclastic Black Flag Group, which is in turn unconformably overlain by the polymictic sedimentary rocks of the Merougil Group. The Lunnon Basalt and Kambalda Komatiite Formation are of particular interest at Kambalda, as massive Fe-Ni-Cu sulfide bodies are typically found at the contact between the two units. The age of these greenstones is known from the Kapa Slate with a U-Pb SHRIMP age of 2692 ± 4 Ma (Claué-Long *et al.* 1988), interflow sedimentary rocks overlying the basal flow of the

Kambalda Komatiite Formation with a U-Pb SHRIMP age of 2709 ± 4 Ma (J. Claué-Long pers. comm. in Clout 1991) and Re-Os isotopic studies of the komatiites giving an age of 2706 ± 32 Ma for the Kambalda Komatiite Formation (Foster *et al.* 1996).

A brief summary of the regional metamorphic and deformation evolution follows (Archibald 1985; Swager *et al.* 1992; Bennett 1995). The D₁ deformational style is characterised by regionally extensive south to north thrusting and recumbent folding. Open, upright folding and doming is characteristic of D₂, producing structures such as the Kambalda and Widgiemooltha Domes. D₂ structures also include north-northwest-trending upright reverse faults. Late D₂-early D₃ deformation is associated with peak metamorphic conditions ($520 \pm 20^\circ\text{C}$ and 100-400 MPa; Bavinton 1979) and granitoid intrusion. Gold mineralisation is associated with D₃ and D₄, which is associated with reactivation of earlier formed fault systems.

The Tramways region is bound to the north and east by the Tramways thrust (D₁), and the regionally extensive Boulder-Lefroy shear zone (D₁-D₄), respectively. The stratigraphy of the Tramways region has been interpreted to be equivalent to that of the Kambalda Dome (Gresham & Loftus-Hills 1981) (Figure 2), and all the stratigraphic units are present at Tramways except for the Merougil Group of sedimentary rocks. The Tramways succession has been intruded by subvolcanic intrusions of a felsic-intermediate composition. The McComish Prospect is a trough structure situated at the contact between the Lunnon Basalt and the Kambalda Komatiite Formation, containing disseminated Fe-Ni-Cu sulfide mineralisation. The trough is a north-northwest-south-southeast-trending asymmetric structure, which appears to be bound on the western margin by an upright reverse fault (as described later). The area of study has been subdivided into three structural domains, east, west and centre of the trough (Figure 2). The only stratigraphic units present at McComish are the Lunnon Basalt, the Kambalda Komatiite Formation and a limited amount of Devon Consols Basalt. Subvolcanic intrusions were also observed. Previous work at Tramways includes unpublished stratigraphic and structural-metamorphic studies (Archibald 1985), ore-genesis studies (Curl 1997) and a volcanological study of the Kambalda Komatiite Formation (Hollamby 1996).

METHODS

All data were collected from diamond drillcore as there is no surface exposure, nor any underground mine development at McComish. Twelve holes were relogged at centimetre-scale locally, covering an area of approximately 400×600 m (Figure 2), and corresponding to over 3600 m of drillcore. Petrographic examination was undertaken to characterise textural and mineralogical variations. In addition, two drillholes from the Kambalda Dome (KD6068, KD8723) with exceptionally good preservation of primary igneous textures were relogged to establish the scales of textural variation possible in the Kambalda Komatiite Formation. Facies analysis was performed at two scales at McComish: (i) discrete lithofacies were identified and their relationships to each other within a flow unit were studied; and (ii) the relationship between different types of flow units within the trough was also studied. Although there is evidence of structural deformation of the McComish trough, as discussed below, consideration was given as to whether this deformation modified an

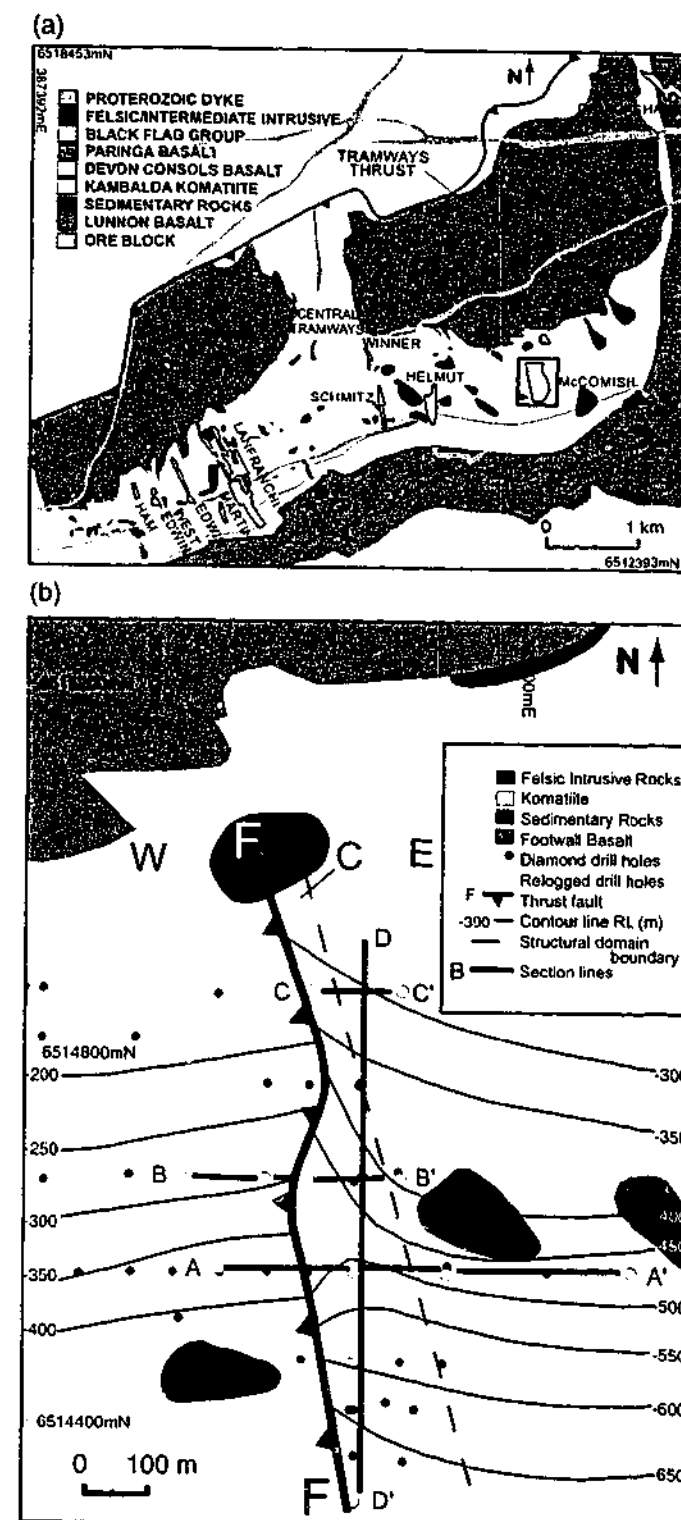


Figure 2 (a) Location of the McComish Prospect in the Tramways region, Kambalda. The boxed area is enlarged in (b). (b) Contour map of the depth to the contact between the Lunnon Basalt and the Kambalda Komatiite Formation, superimposed on the surface geology, to show the geometry of the McComish trough structure. The area is subdivided into Western (W), Central (C) and Eastern (E) domains and the holes relogged for this project are shown as open circles (modified from an unpublished Kambalda Nickel Operations document).

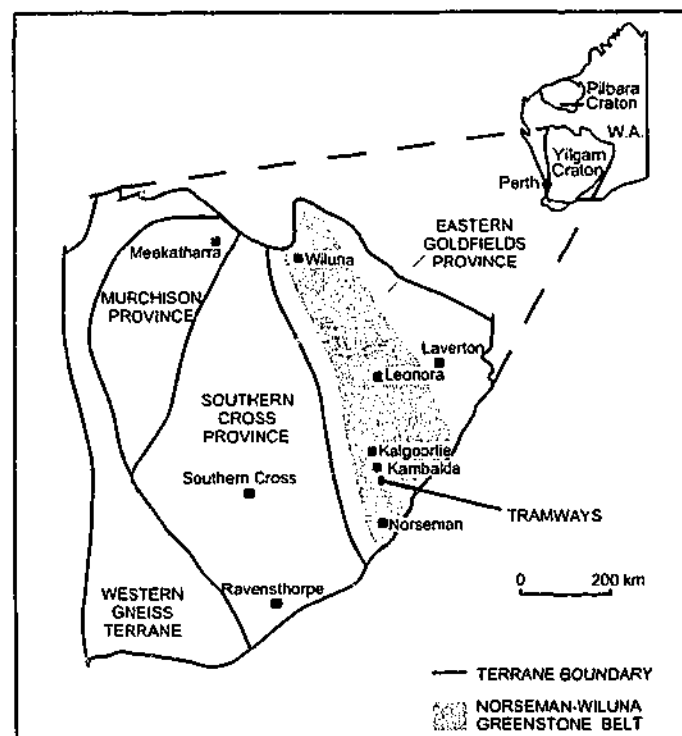


Figure 1 Location of Tramways, part of the Kambalda Ni province, in the Norseman-Wiluna greenstone belt of the Archaean Yilgarn Craton (adapted from Gee *et al.* 1981).

existing volcanic structure or whether the present trough is unrelated to volcanic processes.

OBSERVATIONS AND RESULTS

The Kambalda Komatiite Formation at McComish has been intruded by felsic, xenolith-bearing intrusions. Contact metamorphism of the adjacent komatiite and subsequent fluid interaction has completely obliterated textures locally. Hydraulic brecciation is typically well-developed within these alteration haloes, which range from a few centimetres to ~10 m in thickness. Localised intervals of sheared and brecciated core, in which no primary textures are preserved, are distributed throughout the sequence at McComish. Apart from these localised zones of foliation and cataclastic shearing, the rock fabric is not severely structurally overprinted, and pseudomorphed primary igneous textures are observed within relatively coherent intervals. No cross-cutting relationships were observed between different structural fabrics and it was not possible to distinguish between deformational events in the drillcore, as the orientation of the core was not known.

The Lunnon Basalt is typically foliated and (or) brecciated approaching the contact with the Kambalda

Komatiite Formation, and primary igneous textures are not preserved. The contact has accommodated strain, producing a foliation in both units parallel to the contact. It appears to be concordant and commonly gradational due to modification of textures by overprinting of secondary alteration minerals. The competency contrast and shearing between the two units appears to have provided a preferential conduit for metamorphic fluids along the contact, obliterating primary textures locally. Typical mineral assemblages comprise chlorite, amphibole, large euhedral sulfide phenocrysts, talc and feldspar. Generally each unit is foliated for ~20 cm adjacent to the contact and the base of the Fe-Ni-Cu sulfide mineralisation occurs approximately 10 cm above the foliated zone. Metasedimentary rocks were not observed at the contact between the Lunnon Basalt and the Kambalda Komatiite Formation, nor were any seen throughout the sequence. Rocks that have previously been documented as metasedimentary (Hollamby 1996) are interpreted in this study to be chloritic tectonites and albitised metabasalt. Evidence of thermal and (or) physical erosion was not observed (i.e. no melted substrate, irregular contacts, basalt inclusions, resorption-like embayments or felsic ocelli) at the base of the Kambalda Komatiite Formation, nor throughout the sequence at McComish.

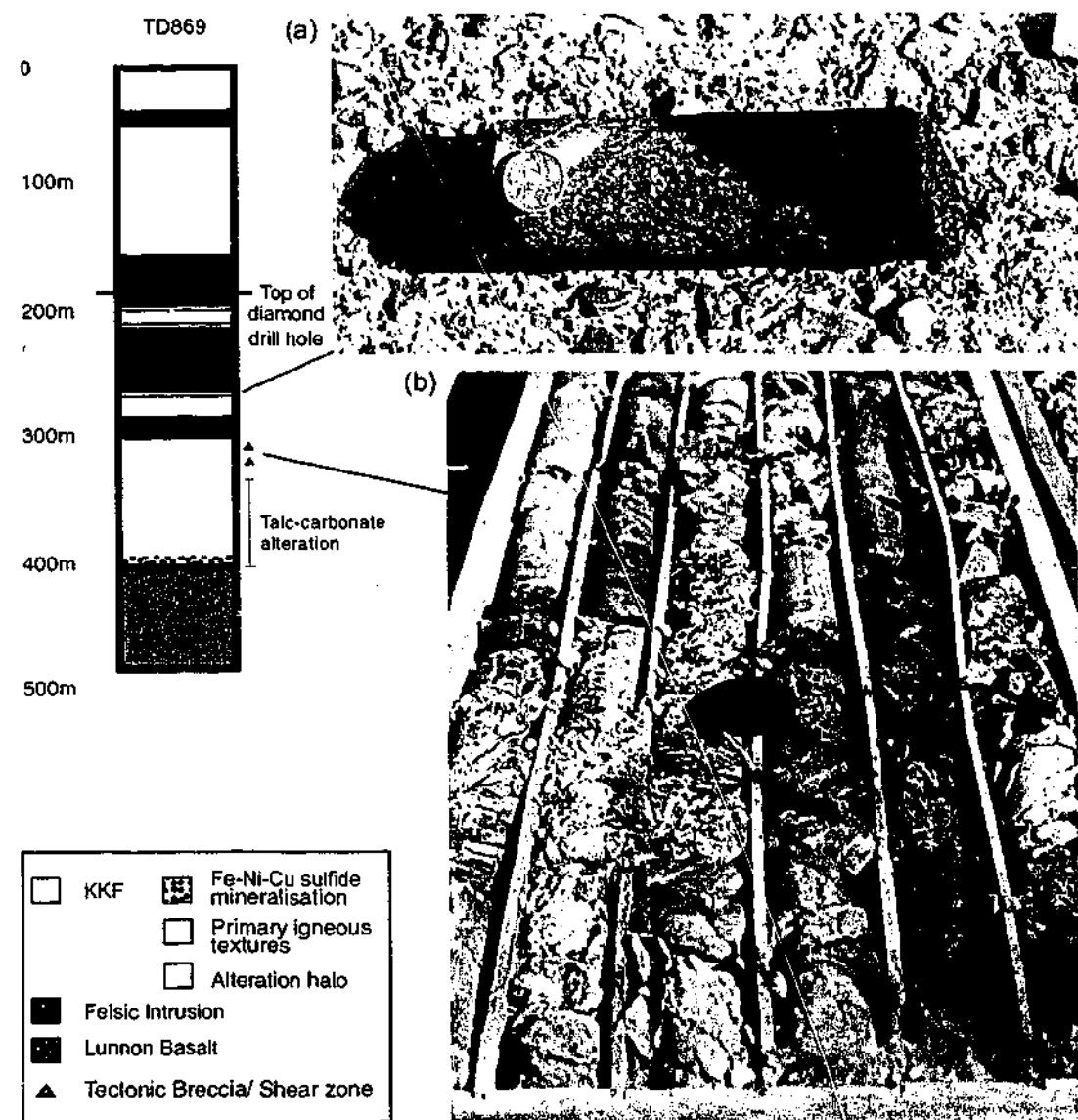


Figure 3 Graphic log showing the degree of textural preservation in a representative drillhole (TD869) from McComish. Relict igneous textures are believed to constitute ~10% of the total Kambalda Komatiite Formation (KKF) viewed in drillcore. (a) Alteration halo within the metakomatiite (right) at the contact with a felsic intrusion (left); TD844, 337.7–338 m. Coin in (a) is 2 cm in diameter; lens cap in (b) is ~5 cm.

Extensive talc-carbonate alteration, particularly toward the base of the Kambalda Komatiite Formation at the McComish Prospect, has resulted in the destruction of the primary mineralogy and almost all of the primary textures on a mesoscopic scale. Abundant porphyroblasts of dolomite and magnesite obscure original textures. Similarly, localised serpentinised domains throughout the Kambalda Ni province have been overprinted by talc-carbonate alteration. Due to the effect of secondary processes discussed above, it is estimated that only ~10% of the total Kambalda Komatiite Formation at McComish contains relict igneous textures (Figure 3) and this level of preservation is typical of the Tramways region (Hollamby 1996). The relict igneous textures are locally well-preserved by secondary minerals pseudomorphing olivine. Chlorite and antigorite are the two most common minerals to have pseudomorphed olivine, and less commonly talc and biotite. Although volume changes may have been associated with metamorphism and alteration, the shapes of the primary igneous grains have been preserved. Finely disseminated magnetite, released during serpentinisation typically occurs at the boundaries of pseudomorphed olivine grains, making their form more visible. Relict olivine was not observed at McComish. The groundmass of the komatiites is composed of various proportions of amphibole, talc, chromite, magnetite and carbonate minerals. The morphology of metamorphic amphiboles is possibly most

similar to primary igneous textures. They can be distinguished from pseudomorphed olivine grains, as they are generally more tabular or plumose in shape, and contain irregular, ragged margins.

Textural facies preserved in the Kambalda Komatiite Formation

Seven lithofacies were identified in the Kambalda Komatiite Formation at McComish, five of which fit into the traditional subdivision of komatiite flows (Pyke *et al.* 1973) (Figure 4). These lithofacies are described below, but first the criteria used to identify flow boundaries at McComish are discussed. Komatiite flow boundaries are generally identified by the presence of flow-top and basal breccias, and (or) chilled margins which are aphanitic grading into random spinifex textural zones (Arndt 1986). Interflow sedimentary rocks are obviously also a good indicator of flow boundaries. The lack of sedimentary rocks at McComish in addition to the effects of polyphase deformation and metamorphism prevent all flow boundaries from being identified. A flow unit can occur at any scale and at any scale is defined by a chilled top and base. Flow-unit boundaries, where preserved, were identified mostly by the presence of platy spinifex textures in spinifex textural zones, which represent downward crystal growth from a chilled surface (Turner *et al.* 1986). Random bladed spinifex textures also represent high degrees of supercooling, although random bladed spinifex grains do not require a chilled surface for nucleation and hence are not always associated with flow (unit) boundaries. Cumulate textural zones are generally poorly preserved due to talc-carbonate alteration, and it is considered that major intervals of talc-carbonate altered core originally represented cumulate textural zones (Gresham & Loftus-Hills 1981). No spinifex zone at the margin of a komatiite has ever been documented as being more than a few metres thick. Since the preserved thickness of the basal komatiites at McComish are at least ~50 m thick, it follows that many, if not all, platy spinifex zones represent flow-unit boundaries.

Within identified flow units, the level of preservation of primary igneous textures ranges from poor to excellent. Centimetre-scale variations in textures were observed in more complete sections (Figure 5), suggesting that the differentiation of a flow (unit) into two zones, the spinifex A zone and cumulate B zone, is too simplistic (Figure 4). Below is a summary of identified textural zones and the complexities in their relationships with each other based on observations both at McComish and the reference drillholes from Kambalda.

RANDOM BLADED SPINIFEX

Individual pseudomorphed olivine blades are commonly 5–10 mm long, but may be up to more than 20 mm in length and 0.5 mm wide (Figure 6a). The blades are not rectangular in shape, but vary from feathery to hollow skeletal grains, typically with pointed ends. It is common for the groundmass between the blades to contain interblades, which are smaller spinifex blades or plates on a micro- to mesoscopic scale. Discrete zones of bladed spinifex range from <5 cm to 1.1 m in thickness. Random bladed spinifex

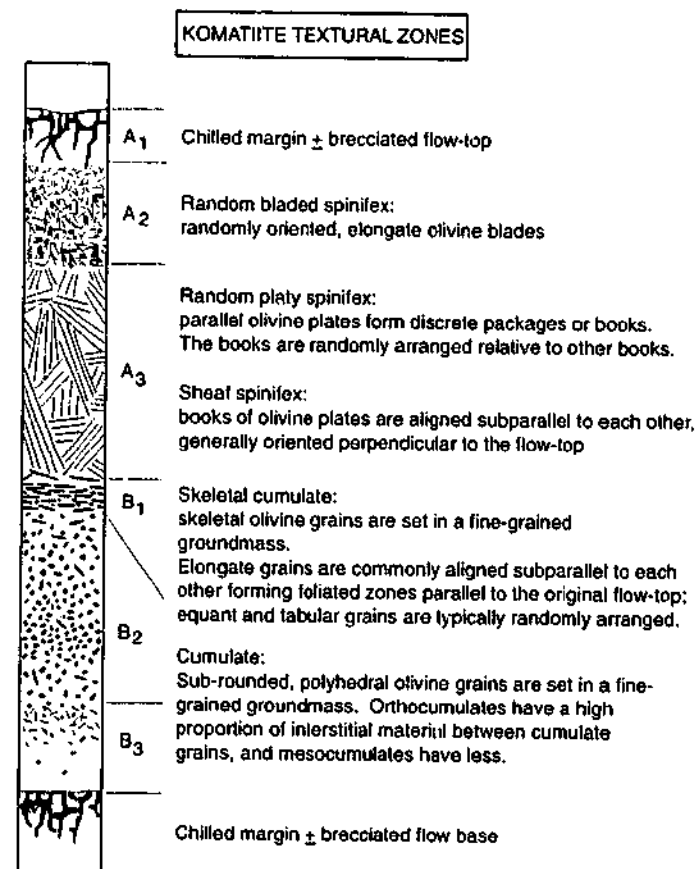


Figure 4 Schematic profile through a hypothetically complete differentiated komatiite lava flow (adapted from Pyke *et al.* 1973 and Hill *et al.* 1990). The flow is subdivided into an A zone consisting of an aphanitic chilled flow top (A1), random spinifex (A2), and sheaf spinifex (A3); all overlying the B zone containing a foliated skeletal cumulate (B1), and an ortho-, meso-, adcumulate zone (B2–B3).

is commonly found at the top and (or) base of a spinifex textural zone at McComish, however it is not always present.

RANDOM PLATY SPINIFEX

The open random arrangement of books of pseudomorphed olivine plates typically results in relatively large triangular interstices, in contrast to sheaf spinifex. These interstices may contain more platy spinifex, even at a microscopic scale. Individual plates are commonly very narrow (<0.1 mm), but may be up to 1.5 mm wide and >20 cm long. Random platy spinifex zones are typically 30–50 cm thick and have been observed to be up to 2 m thick at McComish.

SHEAF SPINIFEX

Pseudomorphed olivine plate dimensions in sheaf spinifex zones are observed to be similar to those in random platy

spinifex, and the maximum thickness of the sheaf spinifex facies at McComish is 1.25 m. Within spinifex textural zones it was observed that spinifex grains do not always coarsen and become oriented parallel with depth (Figure 4), and locally the reverse is evident or the progression is more complex.

SKELETAL CUMULATE

The shapes of pseudomorphs after skeletal olivine grains range from euhedral to tabular hopper crystals to elongate grains. Elongate skeletal cumulate grains are distinguished from spinifex grains by their lower aspect ratio, not their position in a flow. Skeletal cumulates tend to have grains more sparsely distributed than other cumulate rock types, and grains are up to 7–8 mm long and 0.6–3.0 mm wide. Skeletal zones are generally observed to be 20–30 cm thick at McComish, but may be as thin as 2.5–5.0 cm. Skeletal cumulate zones are not simply confined to the interface between the spinifex and orthocumulate zones, as has been

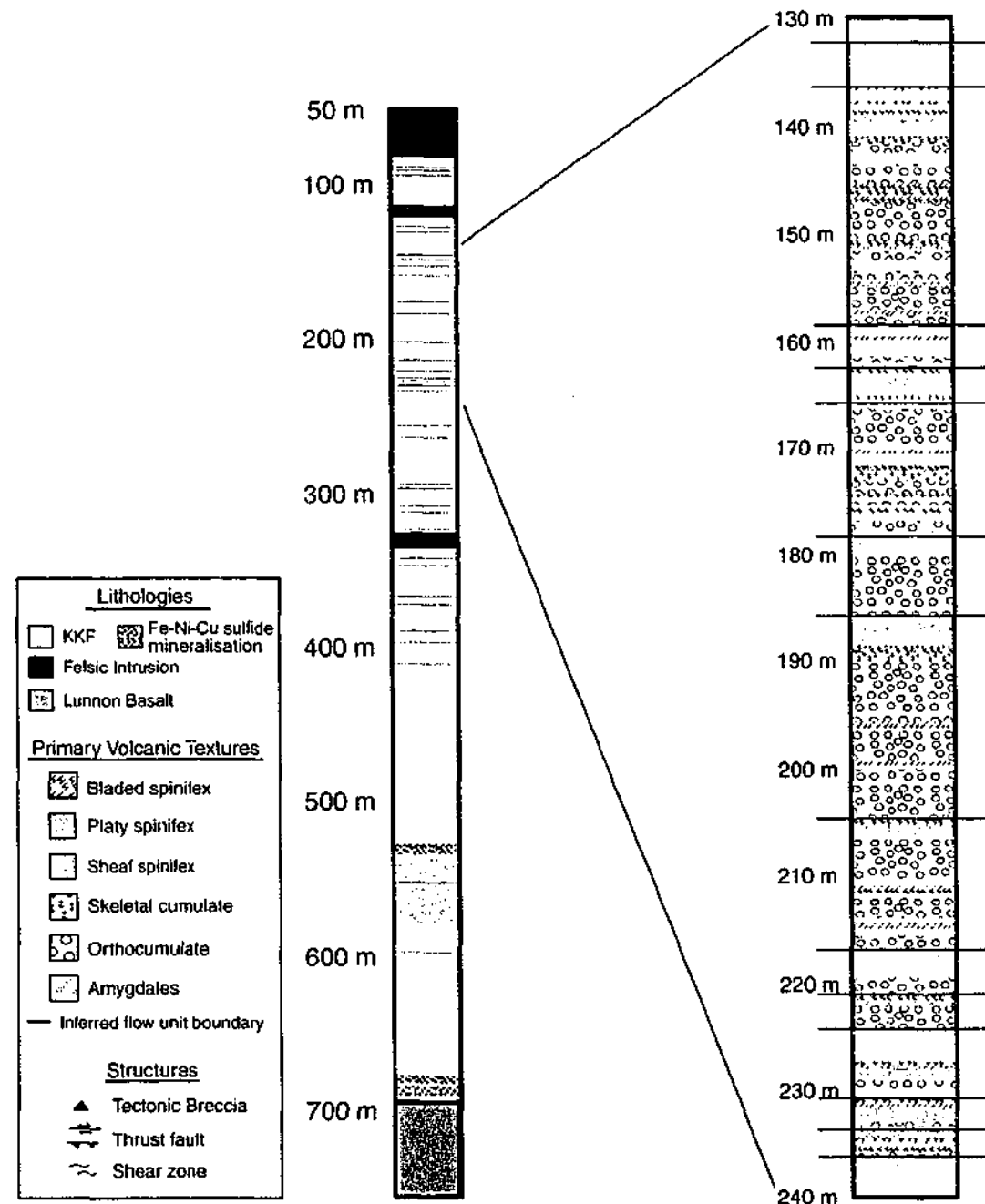


Figure 5 Graphic log of the McComish drillhole with the best preservation of primary igneous textures observed (TD6105) and corresponding legend. A log of the entire hole (left) shows the distribution of flow units in the Kambalda Komatiite Formation (KKF) with approximate flow-unit boundaries identified by the presence of relict platy spinifex. Note the scale of textural variations in the interval 130–240 m shown on the right, and the complexities exhibited.

commonly depicted in generalised zoned komatiite textural models (Figure 4). They also occur: (i) at the base of or within orthocumulate textural zones, locally containing

small patches of random bladed spinifex; and (ii) in some instances platy spinifex zones are separated only by skeletal cumulate. Variations in the morphology and

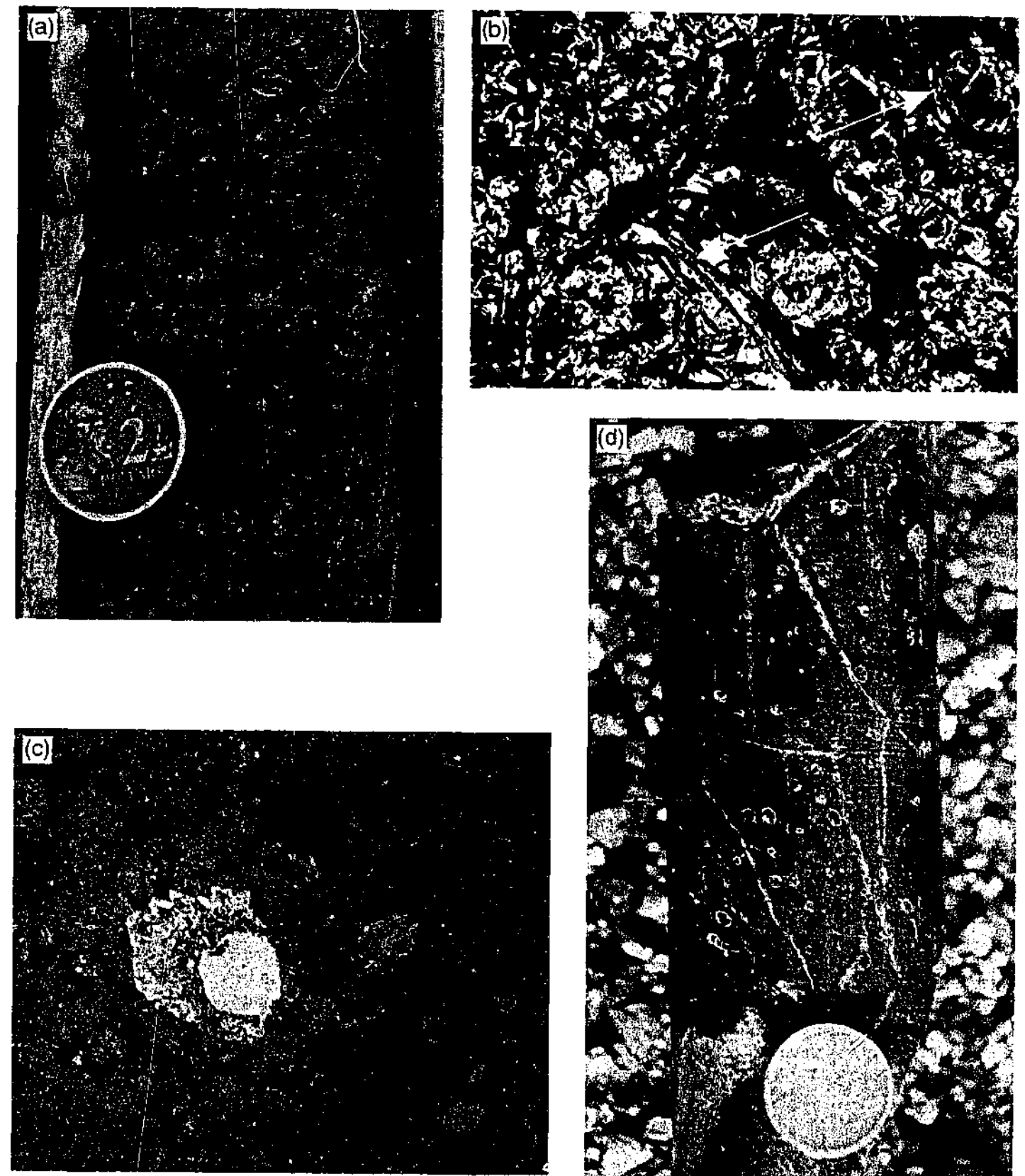


Figure 6 Drillcore samples and textural photomicrographs of relict igneous textures in the Kambalda Komatiite Formation, McComish Prospect (coin is 2 cm in diameter). (a) Random bladed spinifex. Elongate pseudomorphed olivine blades are arranged randomly in a talc-amphibole groundmass (TD864, 237.6–237.7 m). (b) Cumulo-spinifex. Pseudomorphed elongate skeletal olivine blades occur interstitial to more equant relict cumulate grains (right of photo); crossed polars, field of view 1.5 mm (TD6105, 201.8 m). (c) Amygdales. Carbonate porphyroblasts have nucleated on vesicles, the outlines of which are preserved microscopically by oxide minerals; transmitted light; field of view 8 mm (TD891, 485 m). (d) Amygdales. Rounded to slightly elongate vesicles are infilled with chlorite and contain carbonate rims. (TD844, 385.6–385.7 m).

degree of alignment of cumulate grains occurs on a scale of centimetres.

CUMULATE

Ortho- and mesocumulate textures are rarely preserved on a mesoscopic scale at the McComish Prospect, however they are commonly identifiable microscopically. Textures are best-preserved in rocks that did not undergo carbonate alteration, as magnesite porphyroblasts, generally absent in lower Mg spinifex zones, tend to obscure primary textures. Cumulate crystals are consistently 0.50–0.75 mm in diameter, and the thickest preserved zone observed at McComish is ~8 m thick.

CUMULO-SPINIFEX

Cumulo-spinifex is a general term used to describe hybrid textures in komatiites (Moore 1998) and this facies has not been well-documented previously (Barnes *et al.* 1974). Four types of cumulo-spinifex texture were observed in this study, each with a close spatial relationship between cumulate and spinifex grains.

(1) The transition between cumulate and spinifex zones is commonly gradational, with isolated patches of random spinifex blades occurring within the cumulate.

(2a) Within thick cumulate zones, small chloritic patches a few centimetres in diameter occur, containing pseudomorphed spinifex blades that are clearly identifiable microscopically. The patches tend to have clear, well-defined boundaries, and range from irregular in shape to vein-like.

(2b) The contacts of discrete zones of spinifex within thick cumulate zones are more gradational than those in (2a), and cumulate grains have been observed interstitial to the elongate spinifex blades.

(3) Books of platy spinifex have been observed randomly arranged in the interstitial groundmass to euhedral, equant cumulate grains (Barnes *et al.* 1974). This was only observed microscopically (Figure 6b).

The cumulo-spinifex facies is found in localised domains throughout the sequence, at various positions within flow units. Its relationship with other facies may be better constrained in sequences with more complete preservation.

AMYGDALES

Amygdales (i.e. vesicles that have been infilled by secondary materials) were first identified and documented at Kambalda by Beresford *et al.* (2000) and this is the first reported occurrence of them at Tramways. The amygdales are typically spherical, but locally are elongate to irregular in shape. Amygdales are filled with various proportions of carbonate minerals, talc, chlorite, serpentine and Fe–Ni–Cu sulfide. They are not to be confused with ocelli, which by definition are 'rounded feldspathic globules' (Frost & Groves 1989). Some minerals (particularly oxides) form rims on relict vesicles. Dolomite and magnesite porphyroblasts appear to have nucleated on vesicles/amygdales, and in those cases oxide rims provide the only evidence of a vesicle origin (Figure 6c). Sulfidic amygdales are generally more difficult to identify than vesicles infilled with silicate minerals, as the sulfide is more ductile

and more easily deformed than the surrounding silicate rock. In addition, amygdales locally coalesce to form larger, irregular-shaped blebs up to 2 cm in size. Generally amygdales range from millimetres to >1 cm in diameter, with an average of 2–3 mm (Figure 6c, d).

Amygdales are only preserved at McComish within the thicker, higher MgO basal flow units, and tend to occur in definable zones which range from 2 to 24 m in thickness. These zones were observed at McComish to occur at discrete horizons in the cumulate facies, either directly overlying or directly underlying platy spinifex, or in isolation from it. These amygdaloidal zones correspond approximately to the interpreted flow-unit base, top and centre, respectively. The size and distribution of amygdales in any given zone is variable, allowing individual zones to be subdivided into subzones. The abundance of amygdales within these subzones varies from <5% to ~25%.

McComish trough structure

A contour map of the depth to the subsurface contact of the Lunnon Basalt and the Kambalda Komatiite Formation constrains the shape of the trough structure at McComish (Figure 2). Diamond drillcore data provide depths to the contact, and these values were projected to a vertical plane to compensate for irregular angles of drilling. The trough trends north-northwest–south-southeast, is strongly asymmetric, and the western margin is interpreted to be fault-bound. There is up to 200 m vertical displacement of the contact across the inferred fault, over a horizontal distance of <100 m (Figures 7, 8). The fault is not intersected by any of the drillholes relogged in this study. However, one hole (DDH TD923) contains two sheared repetitions of the footwall Lunnon Basalt above the contact, interpreted as thrust wedges produced by splays from the main fault (Figure 8c). Based on detailed structural mapping of the area (Archibald 1985; Bennett 1995) and constraints at McComish, the fault is believed to be a north-northwest-trending, upright, reverse fault produced during D₂ or D₃ deformation. There appears to have been a late strike-slip component due to the inferred truncation of the sub-volcanic intrusions in the trough (Figures 7, 8). The central and eastern portions of the trough are relatively flat and the eastern boundary is difficult to distinguish. The area of study is subdivided into three domains (Figure 2) and the volcanic facies architecture and nickel sulfide distribution are explored in this context.

Two associations of komatiite flows have previously been identified in the basal flows of the Kambalda Komatiite Formation: the channel facies and the flanking sheet-flow facies (Cowden & Roberts 1990) (Table 1). Channel facies flows are characteristically much thicker than the flanking sheet flows. The antithetic relationship between contact sedimentary rocks and contact Fe–Ni–Cu mineralisation in the channel facies has been important in ore genesis models (Leshner *et al.* 1984). Sedimentary rocks were not observed at McComish, hence this relationship could not be evaluated. The only criteria that are useful for facies analysis at McComish are the extent of mineralisation and flow-unit thicknesses. The relationship between trends in these parameters and the trough-like structure are discussed below.

FLOW-UNIT THICKNESS VARIATIONS ACROSS THE TROUGH

The three basal flow units of the Kambalda Komatiite Formation at McComish are 2 to 138 m thick, and the identified flow-unit thicknesses are documented in Table 2. In some instances alteration, felsic intrusions, or lack of primary textures prevent the thicknesses of the three basal flow units from being determined. The values have been considered in terms of their position in the three identified structural domains (Figure 2) in order to interpret any trends in the context of the trough structure. In each of the three structural domains all basal flow units are observed to be more than the thickness defined for flows in the sheet-flow facies (i.e. 10–20 m; Cowden & Roberts 1990). There is no identifiable trend in lateral or vertical variations in thickness. However, the thickest occurrences of the two lowermost flows occur in the western domain, not the central (or trough) domain. Even if it were possible to remove the effects of deformation in modifying the original flow-unit thicknesses, it appears the geometry of the komatiite lava-flow field is far more irregular and complex than previously considered. Flow-unit thicknesses range from <10 m to >100 m over relatively small vertical and lateral distances. This is illustrated in Figures 7 and 8, which are interpretative cross-sections and longitudinal sections through the McComish trough structure (Figure 2). All interpretations are constrained by observations made from diamond drillcore (Figure 7).

Fe–Ni–Cu SULFIDE MINERALISATION

The concentration of sulfides towards the base of the lowermost komatiite flow is termed contact mineralisation and has traditionally been used to distinguish between flows of the channel and flanking sheet-flow facies (Cowden & Roberts 1990) (Table 1). The Fe–Ni–Cu sulfide contact mineralisation at McComish is weakly to strongly disseminated (5–40% sulfides) and no massive or matrix sulfides were observed. Minor sulfides are commonly found higher in the sequence. Within contact mineralisation zones at McComish the sulfide distribution is fairly heterogeneous, and most zones contain barren patches ranging from a few centimetres to metres in thickness. In some cases, the sulfide mineralisation is interstitial to randomly oriented, elongate pseudomorphed olivine grains. In the Kambalda district this style of mineralisation appears to be unique to Tramways (Curl 1997). Locally, irregular-shaped patches of Fe–Ni–Cu sulfides are situated adjacent to talc and (or) carbonate veins, suggesting a genetic relationship between alteration-vein formation and mineralisation.

The thickness of the mineralised zones at McComish does not appear to be consistently related to flow-unit thickness (Figure 9), as predicted by the channel and sheet-flow facies model. However, mineralisation zone thicknesses are far more comparable within each of the structural domains. The drillholes west of the trough are almost barren (mineralisation zones are <5 m thick), the eastern

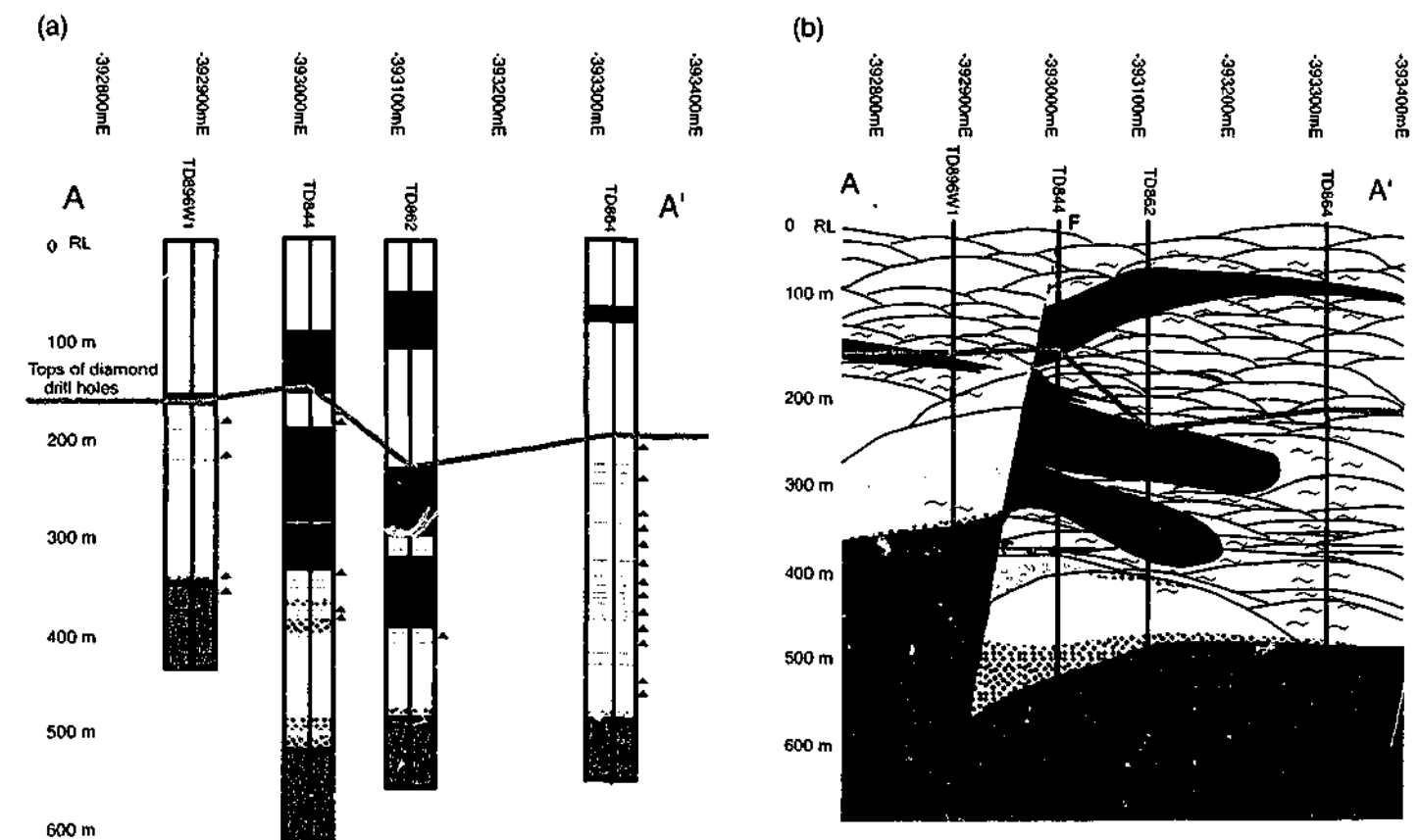


Figure 7 (a) Schematic logs for section A–A' through the McComish trough and (b) corresponding interpretative section A–A'. See Figure 2 for section location and Figure 5 for legend. Interpretations are constrained by drillcore observations below the subhorizontal line; intervals above the line are inferred. Note the distribution of the mineralisation and the variable flow-unit thicknesses. Due to the scale of the section not all relict textures observed are shown, but only inferred flow-unit boundaries (see text). The western margin of the McComish trough is bound by a reverse fault with a strike-slip component.

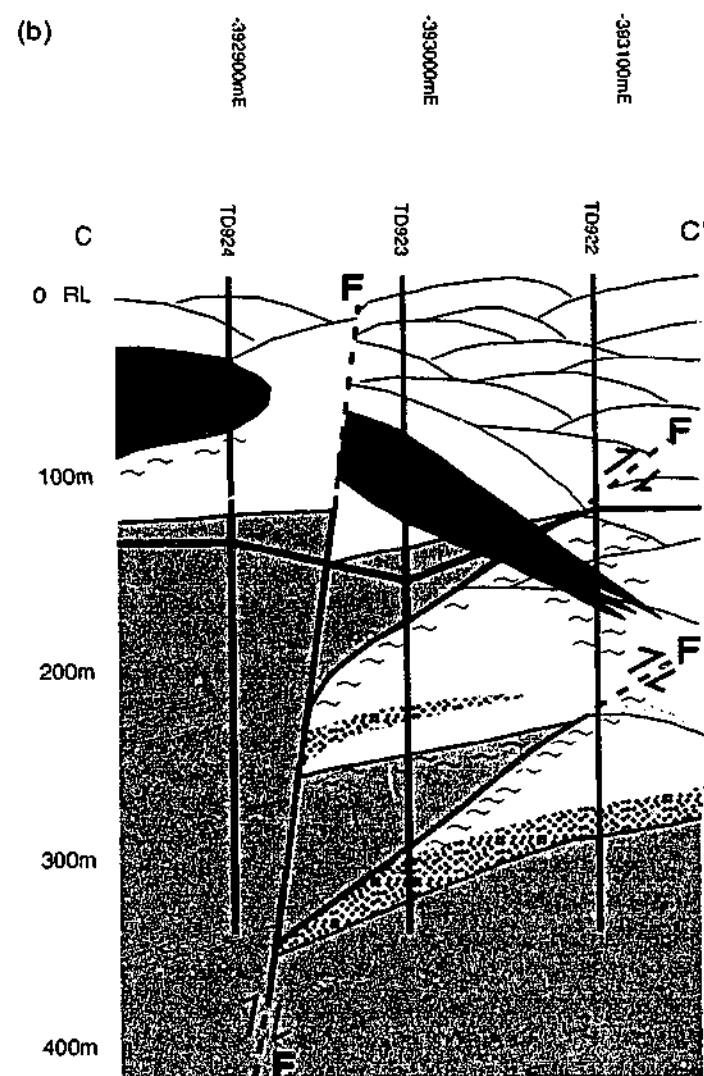


Figure 8 Interpretative sections (a) B-B', (b) C-C' and (c) D-D' through the McComish trough. See Figure 2 for section locations and Figure 5 for legend. Interpretations are based upon drillcore observations below the subhorizontal lines. Note in (b) the repetitions of wedges of the Lunnon Basalt in the komatiite. Note that section D-D' is a longitudinal section.

holes are weakly mineralised (~10 m thick) and the thickest contact mineralisation zones occur in the trough centre (up to >30 m thick), regardless of basal flow-unit thickness. The asymmetric trough structure is defined by an upright reverse fault on the western margin. The height of the mineralisation zones above the base of the komatiite (i.e. mineralisation zone thicknesses) appears to be related to the position of the inferred fault, with the maximum height of mineralisation occurring adjacent to this structure (trough centre), and a progressive decrease in height with increasing distance to the east (Figures 7, 8). To the west of the fault the extent of Fe-Ni-Cu mineralisation is very limited.

DISCUSSION

Clearly the preservation of primary igneous textures in the Kambalda Komatiite Formation at McComish is very limited, and metamorphic and structural effects are more intense than reflected in previous publications on the

Kambalda Ni province. However, this modification is typical of the Kambalda Ni province as a whole and it is therefore unclear how valid previous reconstructions and models are. More detailed studies, documenting in detail the current geological state of the succession are required to gain a better understanding of the secondary processes before original or primary processes can be fully understood. Based on the geology presented, the origin of the McComish trough and associated sulfide mineralisation is explored, by considering observations in terms of current ore-genesis models. The results are then considered in terms of existing komatiite flow emplacement models.

McComish trough structure: implications for the origin of the trough and associated sulfide mineralisation

Various theories have been proposed for the origin of mineralised trough structures in the Kambalda Ni province (Huppert *et al.* 1984; Leshner *et al.* 1984; Huppert & Sparks 1985; Groves *et al.* 1986; Cowden 1988; Cowden & Roberts 1990). Inherent to each theory is the assumption that komatiites flowed turbulently, creating a channel facies (\pm sulfide mineralisation), and that there is a close spatial

relationship between the channel facies and trough structures. It has been established that the McComish trough is a structural feature, produced during D₂ or D₃ deformation. The extent to which the inferred fault modified pre-existing volcanic features (e.g. volcanic 'channels') is explored. No central channel facies and associated flanking sheet-flow facies were identified at McComish: the thicknesses of all basal flow units lie within the range defined for channel facies flows (Cowden & Roberts 1990). There were no thickened basal flow units corresponding to a central 'channel' zone associated with the trough; the flow units are as thick in the flank areas adjacent to the trough as they are in the trough. There is no evidence of a significant pre-existing topographic depression in the Lunnon Basalt prior to komatiite emplacement and structural deformation. There is no evidence of thermal erosion, including the characteristic 're-entrant embayments' (Huppert *et al.* 1984; Leshner *et al.* 1984; Huppert & Sparks 1985). For these reasons the McComish trough is considered to be structural in origin and its present position is unrelated to primary volcanic processes.

Similarly, although it is widely accepted that the Fe-Ni-Cu sulfides are magmatic in origin (Cowden 1988;

Table 1 Distinctive characteristics used to construct a volcanic facies model in the basal flows of the Kambalda Komatiite Formation (Cowden & Roberts 1990) and its application at the McComish prospect.

Distinctive characteristic	Channel facies	Sheet-flow facies	Application to McComish
Extent of Fe-Ni sulfide mineralisation	Mineralised	Barren	Thickness of contact mineralisation zones compared
Flow thickness	Up to 100 m thick	10-20 m thick	Flow-unit thickness inferred and compared
Composition: volatile-free MgO	Up to 45 wt%	16-36 wt%	Not widely sampled and determined
Presence/absence of interflow sedimentary rocks	Rare	Common	Absent
Facies geometry	Lensoidal rock units	Tabular rock units	Undetermined
Cumulate:spinfex ratio	High	Low	Preservation incomplete: meaningless ratios

Table 2 Thicknesses of the three basal flow units identified within the Kambalda Komatiite Formation at McComish, corrected for true thickness.

Hole no.	Flow-unit thickness (m)		
	Basal unit	2nd flow unit from base	3rd flow unit from base
Western domain			
TD5049	59	83	10
TD894	-	-	-
TD896W1	138	-	-
Central domain			
TD923	-	-	-
TD867	-	-	-
TD844	119	24	6
TD891	111	82	10.5
TD6105	96	45	137.5
Eastern domain			
TD922	67	-	-
TD869	78	-	-
TD862	78	11.5	2
TD864	59	9	37.5

Leshner 1989; Naldrett 1989), the present distribution at McComish does not appear to be primarily controlled by volcanic processes. The thicknesses of Fe-Ni-Cu sulfide mineralisation zones are not correlated to flow-unit thicknesses. Instead, the thicknesses of observed disseminated mineralised zones vary consistently across the trough, decreasing with increasing distance from the fault. This suggests structural-metamorphic modification of the original sulfide distribution and further studies are required to determine how the mineralisation was originally related to primary volcanic processes.

It is proposed that primary magmatic sulfides settled towards the base of komatiite flows in narrow linear zones, which were perhaps early lava tubes in the developing flow field (see discussion below), irrespective of flow thickness. The faults that produced trough structures at Kambalda are considered to have 'preferentially nucleated at massive sulfide contacts during peak metamorphic conditions' (Cowden & Archibald 1991). Unequal strain partitioning resulted, due to the competency contrast between massive sulfide and barren altered ultramafic rocks. The inferred north-northwest-trending fault at McComish may have nucleated close to the highest concentration of sulfide. It is proposed that subsequent remobilisation of the sulfide mineralisation by fluids preferentially propagating along the fault modified the original distribution, resulting in thickened disseminated mineralised zones within the central structural domain, adjacent to the fault. It seems reasonable that the western bounding, west-dipping fault acted as a fluid conduit. The close spatial association between the Fe-Ni-Cu sulfide mineralisation and veins in some places at McComish, and the greater than normal height of mineralisation above the base of the host komatiite further supports the possibility of remobilisation of the sulfides. Obviously more detailed studies on the structural and metamorphic controls are required to test this hypothesis, but this would require further drilling or underground development.

Textural variations: implications for komatiite lava flow emplacement mechanisms

Traditionally, it has been considered that komatiites flowed turbulently, at extremely high velocities, fed by very high lava supply rates at vent (Huppert *et al.* 1984; Huppert & Sparks 1985), and entire flows cooled by forced thermal and compositional convection (Huppert *et al.* 1984; Arndt 1986; Turner *et al.* 1986). More recently, it has been proposed that although komatiite lavas were probably turbulent at or near the vent, as the lavas spread out and their surface area increased on eruption they flowed in a more laminar fashion (Cas *et al.* 1999). Komatiite lava flow units are considered to have progressively thickened over extended periods, possibly through endogenous growth beneath a chilled crust (Cas *et al.* 1999), analogous to modern basalt pahoehoe lava flows (Self *et al.* 1998). A network of feeder tubes is considered to have evolved beneath an insulating surface-chilled crust. A continuing supply and (or) pulses of fresh lava were fed to the flow front through this interior tube system, progressively raising the chilled crusts and causing the lava to thicken. Observations at McComish are more consistent with the latter model.

In order to explain the apparently random distribution of flow-unit thicknesses across the McComish trough, it is proposed that a complex network of feeder tubes formed, with maximum inflation occurring at the centre of each tube and solidification at the margins, rather than one central 'channel'. The developing lava tubes are considered to have formed constructional complexes (Hon *et al.* 1994; Self *et al.* 1998; Cas *et al.* 1999) thus accounting for the apparent lack of a significant topographic depression in the Lunnon Basalt prior to the komatiite lava emplacement. It is considered that the emplacement process was relatively continuous, as the absence of significant time breaks between lava pulses permitted no sediments to accumulate at McComish. Progressive inflation of the lava flows (\pm localised structural modification) is considered to explain the extraordinary flow-unit thicknesses observed, unless such very thick units are intrusive in origin (Cas *et al.* 1999). Because the viscosity of komatiites is two to three orders of magnitude less than basalts, komatiite flows should be much thinner than basalt flows. However, the preserved thickness of many of the komatiite lava flow units in the Kambalda Ni province is greater than that typical of most basalts (Cas *et al.* 1999). All the basal units at McComish are in excess of 50 m thick, and it is difficult to envisage emplacement of lava flows at this scale by turbulent lava with crystallisation of entire flows during convection. Similarly, it is difficult to explain the observed textural variations in terms of the emplacement and crystallisation of turbulently flowing komatiite lavas, as discussed below.

SPINIFEX PROGRESSIONS

It was originally proposed that komatiite lavas cooled by convection to account for the high degrees of cooling considered to be required for spinifex growth (Turner *et al.* 1986). Although it is still considered that spinifex formation represents supercooling, the MgO content (Donaldson 1982)

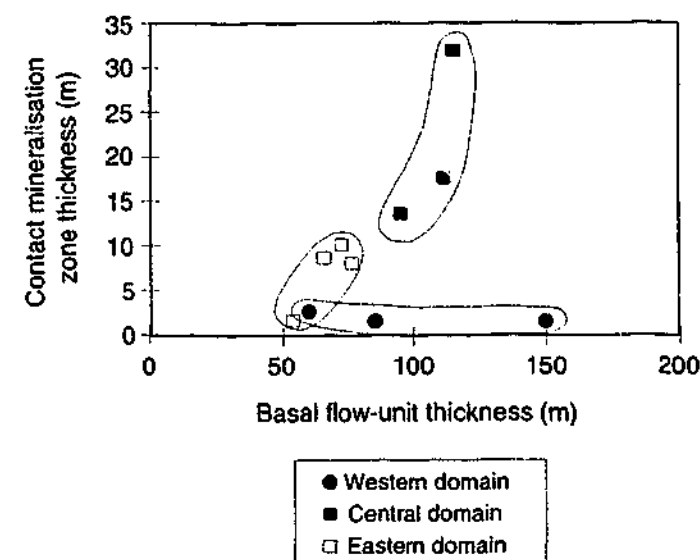


Figure 9 Relationship between the basal flow-unit thickness of the Kambalda Komatiite Formation and contact mineralisation zone thickness. The thickness of mineralised zones appears to be independent of flow-unit thickness and related to the position of the zones relative to the trough.

and the magmatic water content (Grove *et al.* 1997) of the lava are considered to control its development to some extent, and the role of convection is unclear. If convection is not a prerequisite for spinifex growth, olivine spinifex grains will not necessarily become coarser and oriented parallel with depth (a downward progression from random bladed, to random platy, to sheaf spinifex: Figure 4) (Huppert *et al.* 1984). Instead, the spinifex growth orientation and rate is likely to depend on the rate of inflation and drainage of lava from the tube. For example, each fresh injection of lava into the tube may cause lava to be 'plastered' to the tube roof, resulting in random bladed spinifex formation. The thickness of the spinifex zone produced, in addition to the length, morphology and orientation of spinifex crystals within the zone, will depend on the activity of the lava in the tube (e.g. platy spinifex grows downward from a stable crust into stationary molten lava) and convective cooling will be limited. Thus deviations in textural zonation from the hypothetical, differentiated komatiite lava flow (Figure 4) can alternatively be explained through the complex process of endogenous growth of komatiite lava flows.

CUMULATE FACIES: SKELETAL AND ORTHOCUMULATE

It is proposed that during the inflation process, lava beneath the chilled crust also cools and solidifies to some degree prior to the injection of fresh molten material, thus preventing complete homogenisation of the lava within flows (Figure 10). The small-scale repetition of relict skeletal and polyhedral orthocumulate facies (with inter-

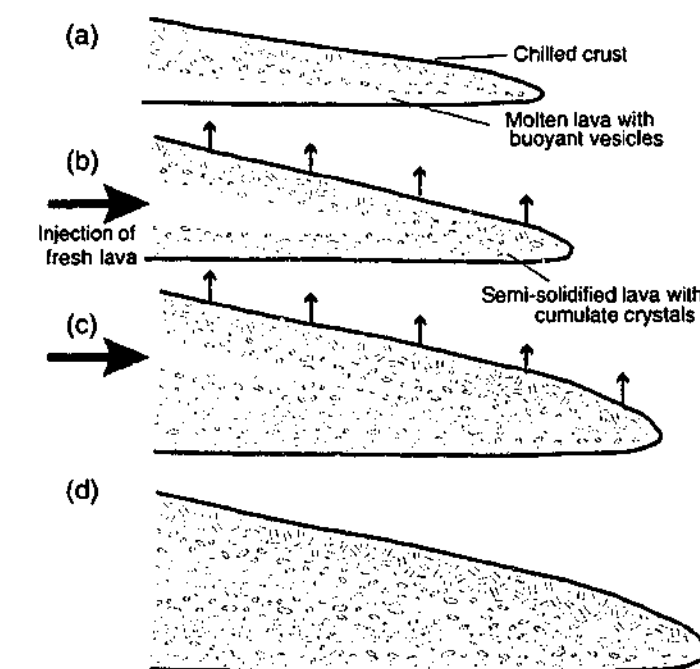


Figure 10 Schematic diagrams showing the progressive inflation of a single flow unit. (a) Spinifex forms beneath the chilled crust and vesicles rising buoyantly through the molten lava are trapped beneath. The lava begins to cool and crystallise cumulus olivine. (b) A fresh injection of lava occurs directly beneath the chilled crust causing the crust to be raised. The partially crystallised lava is now too viscous for vesicles to rise through, although they readily rise through the molten material. (c) The process repeats itself numerous times resulting in (d) the preservation of vesicle horizons at the base, centre and top of flow units.

mittent random spinifex zones) suggests the flow does not convect and differentiate as a large single convective system. This is not consistent with previous models (Silva *et al.* 1997) that have proposed that olivine crystals forming the skeletal and polyhedral cumulate facies are segregated primarily by gravitational settling in a convecting flow.

AMYGDALES

Further evidence for the semi-solidification of lava in inflating lava tubes is the presence of discrete horizons of amygdalites in the centre of flow units and in thick basal zones (Beresford *et al.* 2000). If a flow had differentiated and cooled as a single entity, vesicle horizons would be expected to be confined beneath the spinifex horizon representing the flow top. Alternatively, it is envisaged that the lava flow units are built up gradually through successive pulses or injections of fresh lava beneath an inflating chilled crust. Prior to the injection of fresh material, the residual lava is believed to have cooled enough to be too viscous for the gas bubbles to rise buoyantly through it (Beresford *et al.* 2000) (Figure 10). Multiple amygdale horizons in a single flow unit therefore preserve the process of progressive inflation of a lava tube.

CUMULO-SPINIFEX

It is widely accepted that within flow units the spinifex and cumulate facies formed simultaneously, through forced thermal and compositional convection. An interface is considered to have formed between the textural zones, preventing crystals from passing between them (Turner *et al.* 1986). However, the presence of cumulo-spinifex textures at McComish suggests that there is a closer interaction between the grains during crystallisation than is suggested by the accepted models. Komatiite lavas are considered to have contained cumulate grains upon eruption. Cumulate horizons are produced by gravitational settling of these grains, as well as by subsequent *in situ* crystallisation and settling. As the lavas were cooled beneath chilled crusts, the groundmass is considered to have cooled relatively rapidly, forming mainly glass with some skeletal olivine grains but also containing some suspended cumulate grains. This is a possible way of forming platy spinifex interstitial to cumulate grains, and may account for the gradational boundary observed locally between the spinifex and cumulate textural zones.

SUMMARY

The komatiite lavas of the Kambalda Komatiite Formation are interpreted to have erupted in a subaqueous environment, due to the conformable relationship with the underlying pillowed Lunnon Basalt and the nature of the associated sedimentary rocks (Cowden & Roberts 1990). On eruption, the komatiite lavas are proposed to have initially spread as thin, fluidal sheets, much like basalt pahoehoe lava, but significantly thinner because of the significantly lower viscosity. The lava propagated by lava breakouts from the relatively thin advancing flow front, in the form of toes or sheets with thin 'plastic' skins. These spread laterally and coalesced, forming smooth chilled crusts represented

by spinifex zones. Crust formation is considered to have been virtually instantaneous, due to the high temperature difference between the hot lava and the water it was erupted into. As fresh lava was injected into the insulated interior the crust was raised and the flow unit progressively inflated. All margins lost heat to the surroundings (top, base and sides), resulting in the formation of tubes and lobes. Over extended periods, a network of feeder tubes is believed to have formed beneath actively inflating sheet flows and the lava was focused along discrete pathways (Hon et al. 1994). A laminar flowing lava will cool by conduction rather than convection, thus the entire active flow unit is not necessarily differentiated into an overlying spinifex zone and a relatively homogeneous orthocumulate zone separated by skeletal cumulate (Figure 4).

CONCLUSIONS

Despite having potentially experienced up to four phases of deformation, upper greenschist–lower amphibolite metamorphic grades, and subsequent alteration, the Archaean metakomatiite sequence at McComish contains localised domains of moderately well-preserved relict igneous textures. Observations were interpreted in the context of existing models for komatiite lava emplacement mechanisms and ore genesis. Complexities in the conventional subdivision of komatiite flows into an upper spinifex A zone, and lower cumulate B zone were observed at McComish. The relationships between identified textural facies cannot be accounted for by traditional komatiite crystallisation models involving convective cooling of entire flows. Alternatively, the textural variations are more consistent with progressive inflation of semi-solidified lava feeder tubes beneath solid crusts, sometimes involving multiple pulses of lava. A complex network of feeder tubes is considered to have evolved with maximum inflation occurring at the centre of each tube and solidification of the margins. This more adequately explains the random distribution of basal flow-unit thicknesses across the McComish trough, rather than a central 'channel' produced through turbulent flowing komatiite lava. In addition, endogenous growth of the lavas accounts for the excessive preserved thicknesses observed. It is likely that the initial pulse of magma was enriched in sulfides, which were focused within a lava tube. The present distribution of ore at McComish does not reflect primary volcanic processes but appears to have been modified. The thickness of the observed disseminated mineralised zone varies consistently across the trough, decreasing with increasing distance from the fault, interpreted to define the western margin. It is proposed that the fault acted as a fluid conduit, resulting in remobilisation of the mineralisation during metamorphism and deformation. More detailed structural and metamorphic studies are required to verify this interpretation and to establish the original relationship between the mineralisation and volcanic processes.

ACKNOWLEDGEMENTS

Thanks to Kambalda Nickel Operations, WMC Resources Ltd for the financial and logistical support provided for this

study as an Honours study by AGM, as well as to the Australian Research Council for providing an ARC SPIRT grant to reinvestigate the volcanic and geochemical facies architecture of the komatiites at Kambalda. Thanks to W. Stone for his helpful comments and to journal reviewers M. Barley and P. Morris.

REFERENCES

- ARCHIBALD N. J. 1985. *The stratigraphy and tectonic-metamorphic history of the Kambalda-Tramways area, Western Australia*. Western Mining Corporation, K-Report K/2889 (unpubl.).
- ARNDT N. T. 1986. Differentiation of komatiite flows. *Journal of Petrology* 27, 279–301.
- ARNDT N. T. & NISBET E. G. 1982. What is a komatiite? In: Arndt N. T. & Nisbet E. G. eds. *Komatiites*, pp. 19–28. Allen & Unwin, London.
- BARNES R. G., LEWIS J. D. & GEE R. D. 1974. Archaean ultramafic lavas from Mount Clifford. *Geological Survey of Western Australia Annual Report 1973*, 59–70.
- BAVINTON O. A. 1979. Interflow sedimentary rocks from the Kambalda ultramafic sequence: their geochemistry, metamorphism and genesis. PhD thesis, Australian National University, Canberra (unpubl.).
- BENNETT M. A. 1995. *The structure and timing of gold mineralisation in the Victory area and its relationship to regional deformation in the eastern Goldfields*. Western Mining Corporation internal report (unpubl.).
- BERESFORD S. W., CAS R. A. F., LAMBERT D. D. & STONE W. E. 2000. Vesicles in thick komatiite lava flow. *Journal of the Geological Society of London* 157, 11–14.
- CAS R. A. F., BERESFORD S. W. & SELF S. 1999. The flow front behavior and thickness of active komatiite lavas. *Earth and Planetary Science Letters* 172, 127–139.
- CLAQUE-LONG J. C., COMPSTON W. & COWDEN A. 1988. The age of the Kambalda greenstones resolved by ion-microprobe: implications for Archaean dating methods. *Earth and Planetary Science Letters* 89, 239–259.
- CLOUT J. M. F. 1991. *Geochronology of the Kambalda-Kalgoorlie area: a review*. Western Mining Corporation (Kambalda Nickel Operations) T-Report 187 (unpubl.).
- COWDEN A. 1988. Emplacement of komatiite lava flows and associated nickel sulfides at Kambalda, Western Australia. *Economic Geology* 83, 436–442.
- COWDEN A. & ARCHIBALD N. J. 1991. Massive sulfide fabrics at Kambalda: sensitive records of deformation history. In: *Structural Geology in Mining and Exploration*, pp. 99–102. Department of Geology and Extension Service University of Western Australia Publication 25.
- COWDEN A. & ROBERTS D. E. 1990. Komatiite hosted nickel sulfide deposits, Kambalda. In: Hughes F. E. ed. *Geology of the Mineral Deposits of Australia and Papua New Guinea*, pp. 567–581. Australasian Institute of Mining and Metallurgy, Melbourne.
- CURL E. A. 1997. Predictive geological model for the Helmut Fe-Ni-Cu sulfide deposit, Tramways, Kambalda, WA. BSc (Hons) thesis, Monash University, Melbourne (unpubl.).
- DONALDSON C. H. 1982. Spinifex-textured komatiites: a review of textures, compositions and layering. In: Arndt N. T. & Nisbet E. G. eds. *Komatiites*, pp. 211–244. Allen & Unwin, London.
- FOSTER J. G., LAMBERT D. D., FRICK L. R. & MAAS R. 1996. Re-Os isotopic evidence for genesis of Archaean nickel ores from uncontaminated komatiites. *Nature* 382, 703–706.
- FROST K. M. & GROVES D. I. 1989. Ocellar units at Kambalda: evidence for sediment assimilation by komatiite lavas. In: Jones M. J. & Prendergast M. D. eds. *Magmatic Sulfides—the Zimbabwe Volume*, pp. 207–214. Institution of Mining and Metallurgy, London.
- GEE R. D., BAXTER J. L., WILDE S. A. & WILLIAMS I. R. 1981. Crustal development in the Archaean Yilgarn Block, Western Australia. In: Groves D. I. & Glover J. E. eds. *Archaean Geology—Proceedings Second International Symposium, Perth 1980*, pp. 43–56. Geological Society of Australia Special Publication 7.
- GRESHAM J. J. & LOFTUS-HILLS G. D. 1981. The Geology of the Kambalda Nickel Field, Western Australia. *Economic Geology* 76, 1373–1416.

- GROVE T. L., DE WIT M. J. & DANN J. C. 1997. Komatiites from the Komati type section, Barberton South Africa. In: de Wit M. J. & Ashwal L. D. eds. *Greenstone Belts*, pp. 438–453. Oxford Monographs on Geology and Geophysics 35. Oxford University Press, New York.
- GROVES D. I., KORJAKOSKI E. A., MCNAUGHTON N. J., LESHER C. M. & COWDEN A. 1986. Thermal erosion by komatiites at Kambalda, Western Australia and the genesis of nickel ores. *Nature* 319, 136–138.
- HILL R. E. T., BARNES S. J., GOLE M. J. & DOWLING S. E. 1990. *Physical volcanology of komatiites* (revised edition). Excursion Guidebook, Geological Society of Australia, Western Australian Division, Perth.
- HILL R. E. T., BARNES S. J., GOLE M. J. & DOWLING S. E. 1995. The volcanology of komatiites as deduced from field relationships in the Norseman-Wiluna greenstone belt, Western Australia. *Lithos* 34, 159–188.
- HOLLAMBY J. 1996. The volcanology of the Tramways Arch, Kambalda, Western Australia: a petrographic and textural study of the Silver Lake Member of the Kambalda Komatiite Formation. BSc (Hons) thesis, Monash University, Melbourne (unpubl.).
- HON K., KAUAHIKAUA J., DENLINGER R. & MACKAY K. 1994. Emplacement and inflation of pahoehoe sheet flows: observations and measurements of active lava flows on Kilauea Volcano, Hawaii. *Geological Society of America Bulletin* 106, 351–370.
- HUPPERT H. E. & SPARKS R. S. J. 1985. Komatiites I: eruption and flow. *Journal of Petrology* 26, 694–725.
- HUPPERT H. E., SPARKS R. S. J., TURNER J. S. & ARNDT N. T. 1984. Emplacement and cooling of komatiite lavas. *Nature* 309, 19–22.
- KAUAHIKAUA J., CASHMAN K. V., MATTOX T. N. ET AL. 1998. Observations on basaltic lava streams in tubes from Kilauea Volcano, island of Hawaii. *Journal of Geophysical Research* 103, 27 303–27 323.
- KESZTHELYI L. & SELF S. 1998. Some physical requirements for the emplacement of long basaltic lava flows. *Journal of Geophysical Research* 103, 27 447–27 464.
- LESHER C. M. 1989. Komatiite-associated nickel sulfide deposits. In: Whitney J. A. & Naldrett A. J. eds. *Ore Deposits Associated with Magmas, Reviews in Economic Geology*, pp. 4, 45–101. Society of Economic Geologists.
- LESHER C. M., ARNDT N. T. & GROVES D. I. 1984. Genesis of komatiite-associated nickel sulfide deposits at Kambalda, Western Australia: a distal volcanic model. In: Buchanan D. L. & Jones M. J. eds.

Sulfide Deposits in Mafic and Ultramafic Rocks, pp. 70–80. Institution of Mining and Metallurgy, London.

MOORE A. G. 1998. A volcanic facies model for the McComish Prospect, Tramways, Kambalda, WA. BSc (Hons) thesis, Monash University, Melbourne (unpubl.).

NALDRETT A. J. 1989. *Magmatic Sulfide Deposits*. Oxford University Press, Oxford, New York.

PYKE D. R., NALDRETT A. J. & ECKSTRAND O. R. 1973. Archaean ultramafic flows in Munro Township, Ontario. *Geological Society of America Bulletin* 84, 955–978.

SELF S., KESZTHELYI L. & THORDARSON T. 1998. The importance of pahoehoe. *Annual Review of Earth and Planetary Sciences* 26, 81–110.

SELF S., THORDARSON T., KESZTHELYI L. ET AL. 1996. A new model for the emplacement of Columbia River basalts as large, inflated pahoehoe lava flow fields. *Geophysical Research Letters* 23, 2689–2692.

SELF S., THORDARSON T. & KESZTHELYI L. 1997. Emplacement of continental flood basalt lava flows. In: Mahoney J. J. & Coffin M. eds. *Large Igneous Provinces*, pp. 381–410. American Geophysical Union Geophysical Monograph 100.

SHAW H. & SWANSON D. 1970. Eruption and flow rates of flood basalts. In: *Proceedings 2nd Columbia River Basalt Symposium*, pp. 271–299. Eastern Washington University Press, Cheney.

SILVA K. E., CHEADLE M. J., & NISBET E. G. 1997. The origin of B1 zones in komatiite flows. *Journal of Petrology* 38, 1565–1584.

SWAGER C. P., WITT W. K., GRIFFIN T. J. ET AL. 1992. Late Archaean granite-greenstones of the Kalgoorlie Terrane, Yilgarn Craton, Western Australia. In: Glover J. E. & Ho S. E. eds. *The Archaean: Terrains, Processes and Metallogeny*, pp. 107–122. Geology Department (Key Centre) and University Extension, University of Western Australia Publication 22.

TURNER J. S., HUPPERT H. E. & SPARKS R. S. J. 1986. Komatiites II: Experimental and theoretical investigations of post-emplacement cooling and crystallization. *Journal of Petrology* 27, 397–437.

WILLIAMS D. A., KERR R. C. & LRESHE C. M. 1998. Emplacement and erosion by Archaean komatiite lava flows at Kambalda: revisited. *Journal of Geophysical Research* 103, 27 533–27 549.

Received 10 September 1999; accepted 10 March 2000

AN OVERVIEW OF BASALTIC VOLCANISM IN THE WERRIBEE PLAINS, NEWER
VOLCANIC PROVINCE, VIC: PRODUCTS AND FREQUENCY OF ERUPTIONS

¹Hare, A.G., ¹Cas, R.A.F. & ²Musgrave, R.J.

¹*Department of Earth Sciences, Monash University, Clayton VIC 3800, Australia*

²*Department of Earth Sciences, La Trobe University, Bundoora VIC 3086, Australia*

Although the Newer Volcanic Province (NVP) is classified as an active province, little is known volcanologically about it, including the frequency and volume of eruptions, the distribution of lava types, flow dimensions etc. These parameters are investigated in this study in the Werribee Plains (~2,000 km²) which is located in the east of the late Tertiary- Quaternary intra-plate basaltic NVP. Several small point source eruption centres are considered to have fed the majority of the lava flows exposed at the surface. The eruption centres are scoria cones and low-angle lava shields and are considered to have formed by fissure-fed eruptions in which the magma output was focussed to a point source after a couple of days. Inflated pahoehoe sheet-flows are the most abundant type of lava flow fed from the eruption centres, representing ~50 % of all diamond drill core logged, suggesting a substantial proportion of the lavas were tube-fed. In general the lava flows are relatively thick compared with Hawaiian lavas: pahoehoe sheet-flows average 6.5 m, S-type pahoehoe lobes average 0.6 m, aa flows average 24 m, and ponded lavas average 11 m in thickness. The sequence is up to 120 m thick locally, and can be subdivided into distinct eruption packages (the products of a given eruption), which are generally separated by weathered basalt and/ or paleosols. In order to correlate eruption packages between drill holes a magnetostratigraphy has been identified. Eruptions have occurred infrequently over the span of three different polarity intervals, (tentative age constraints: ~3- 1.4 Ma, although radiometric ages are yet to be determined). Further correlations can be made using the secular variation stratigraphy combined with geochemical data. This study adds to our understanding of volcanism in plains-basalt provinces, which have largely received little attention (compared with ocean island basalt and flood basalt provinces).

Key words: basalt, lava, volcanology, magnetostratigraphy, Newer Volcanic Province.

Establishing the stratigraphy of the Werribee Plains, Newer Volcanic Province, Victoria: an interdisciplinary approach

Moore, A.G. & Cas, R.A.F.

Department of Earth Sciences, Monash University, P.O. Box 28E, Clayton, VIC 3800, Australia.

The Newer Volcanic Province (NVP) of southeastern Australia is an intraplate continental plains-basalt province. The province is east-west trending, extending 330 km west of Melbourne into South Australia, and covers an area of over 15,000 km². Products range in age from 4.6 Ma - ~4.5 ka. The NVP is one of only two volcanic provinces in Australia which is presently classified as active, yet there are aspects of the geology that have not been explored, such as the frequency of past eruptions and the likelihood of future volcanic activity. Conventional mapping techniques are not useful for establishing a stratigraphy in the NVP, because lavas are flat-lying, the topography is flat, weathering has been extensive, and erosional incision is limited. This study involves establishing a stratigraphy for the Werribee Plains in the east of the province by employing a number of different techniques. A network of diamond drill holes (containing up to ~100m basalt thickness) are being logged, and geophysical well logs interpreted to constrain the palaeotopography. Flow unit boundaries have been identified in drill core, and palaeomagnetic studies are being performed on each flow unit. Eruption packages can be correlated between drill holes, based on the polarity of the earth's magnetic field at the time of eruption, which is recorded within the basalts. Within eruption packages separate volcanic facies will be identified by analysing the internal structure of the basalt flow units, including vesicularity trends and petrographic textural zonations. Quarry exposures will act as a guide to the scale of lateral facies variations, and identified facies will be interpreted in terms of physical emplacement processes. Whole rock and trace element geochemistry will further aid in correlating eruption packages, particularly in distinguishing between alkali and tholeiitic basalts. Once a stratigraphy has been established, geochronological studies will provide absolute ages of the products, and the frequency of eruptions.

Keywords: Newer Volcanic Province, basalt, stratigraphy

Emplacement processes and crystallisation of basaltic lavas: insights from detailed vesicle zonation and petrographic studies.

Alison G. Moore* and Raymond A.F. Cas, Monash University, Clayton, Australia.

Keywords basalt, lava, textural zonations, emplacement processes

Much of our present knowledge regarding the morphology and emplacement mechanisms of basalt lavas has been gained from observations of active flows. In this study we interpret the internal textures of basalt flow units in terms of physical emplacement and crystallisation processes. Data has been collected from the Quaternary Newer Volcanic Province of southeastern Australia, from diamond drill core (up to >100 m basalt thickness) and fieldwork in exposed quarry faces. Flow units range in thickness from 1.2 to 27.2 m, and average 8.5 m. Based upon vesicle zonations, examples of both pahoehoe and aa lava flow units have been interpreted to have formed by endogenous growth. The upper vesicular zones (UVZs) generally constitute ~40-60 % of the total flow unit thickness, and may contain multiple small vesicle zones, representing separate injections of volatile-rich lava beneath a chilled crust. The progression in size of vesicles with depth in the UVZ is generally more complicated than has been described previously (e.g. Cashman and Kauahikaua 1997, *Geology* 25, 419-422), reflecting complex emplacement histories of the lavas. Aa lava flow units are characteristically finer-grained than pahoehoe, contain abundant microphenocrysts, and textures are locally very heterogeneous. Inflated P-type pahoehoe lobes, ranging from 6.6 to 11.0 m in thickness, have varied groundmass textures. Within a single flow unit the groundmass texture varies from consistently fine and intergranular, to coarse and ophitic, to a combination of the two. These variations may reflect differences in temperature, hence viscosity, of the erupted material and/or differences in emplacement styles, resulting in different crystallisation histories. Phenocrysts decrease in number and increase in size toward the interior of these flows. This suggests that either the content of the supplied lava has changed over time, or there has been settling of phenocrysts toward the base of the flow unit. Whether this observed textural zonation corresponds with a compositional zonation will be confirmed by geochemical analyses.